**Structural Reliability
Analysis and Prediction**

Structural Reliability Analysis and Prediction

Robert E. Melchers
The University of Newcastle
Australia

André T. Beck
University of São Paulo
Brazil

Third Edition

WILEY

The right of Robert E. Melchers and André T. Beck to be identified as the authors of this work has been asserted in accordance with law.

Wiley also publishes its books in a variety of electronic formats and by print-on-demand. Some content that appears in standard print versions of this book may not be available in other formats.

Contents

@Seismicisolation

@Seismicisolation

Preface

This third edition marks some 18 years since the second edition of this book appeared and what seems like half a lifetime ago—some 31 years—since the first edition was written. It has been extremely gratifying that the book has lasted this long, that it continues to be used by many and that a new edition was welcomed by Wiley.

Since the second edition the subject has consolidated and largely turned to more and more areas of application, including a renewed interest from the geotechnical engineering research community. But also in practice structural reliability increasingly is being applied, particularly for situations where quantitative, data-based risk assessment of non-elementary structural or other systems is required. Overviews of the papers contributed to conferences such as ICASP, ICOSSAR, IFIP, IALCCE and CSM shows much attention paid to applications and relatively little to sorting out some of the remaining really challenging theoretical problems such as how to deal with complex systems with a multitude of random variables or processes, and for which many potential failure modes and combination of such modes may exist. Fortunately, the availability of ever greater computational power has meant that enumeration methods, once thought to be the way forward for dealing with really complex problems, can be cast aside in favour of sheer brute force number crunching. In this sense Chapter 3 and the parts of Chapter 5 dealing with Monte Carlo methods are now more important, for practical problems, than the elegant but simpler FOSM/FOR/SOR methods that allow easier insight into 'what was driving what'.

The present edition follows much of the second edition but updates areas such as Monte Carlo methods, systems reliability, some aspects of load and resistance modelling, code calibration, analysis of existing structures and adds, for the first time, a chapter on optimization in the context of structural reliability. The co-author for this edition, André T. Beck, has contributed much to these changes, as well as to the worked examples provided where relevant for each chapter and collected together in Appendix F. We have had the good fortune to have at hand the many comments and corrections, principally supplied by Dr. Bill Gray during his post-doctoral days at The University of Newcastle. As before, we have had to be selective in our coverage and have had to make difficult decisions about what to include and what leave out.

Now, as 18 years ago, a surf or a beach run at Newcastle's wonderful Pacific Ocean beaches, a surf or a bike ride along the south-eastern Brazilian coast, seem better ways

to spend one's time than revising a book. Our spouses tell us so, our colleagues tell us so, our minds tell us so, but what do we do?

10 February 2017

Robert E. Melchers
Bar Beach, Newcastle

André T. Beck
Florianópolis, SC

Preface to the Second Edition

It is over ten years since the first edition of this book appeared and more than 12 years since the text was written. At the time structural reliability as a discipline was evolving rapidly but was also approaching a degree of maturity. Perhaps it is not surprising, then, that rather little of the first edition now seems out-dated.

This edition differs from the first mainly in matters of detail. The overall layout has been retained but all of the original text has been reviewed. Many sections have been partly rewritten to make them clearer and more complete and many, often small but annoying, errors and mistakes have been corrected. Hopefully not too many new ones have crept in. Many new references have been added and older, now less relevant, ones deleted. This is particularly the case in referring to applications, in which area there has been much progress.

The most significant changes in this edition include the up-dating of the sections dealing with Monte Carlo simulation, the addition of the Nataf transformation in the discussion of FOSM/FORM methods, some comments about asymptotic methods, additional discussion of structural systems subject to multiple loads and a new chapter devoted to the safety checking of existing structures, an area of increasing importance.

Other areas in which there have been rapid developments, such as simulation of random processes and random fields, applications in structural dynamics and fatigue and specialist refinements of theory are all of interest but beyond the scope of an introductory book. Readers might care to refer to the specialist literature, proceedings of conferences such as the ICASP, ICOSSAR and IFIP series and to journals such as Structural Safety, Probabilistic Engineering Mechanics and the Journals of Engineering Mechanics and Structural Engineering of ASCE. Overviews of various aspects of applications of structural reliability are given also in Progress in Structural Engineering and Mechanics. There are, of course, other places to look, but these should form a good starting point for keeping in touch with theoretical developments and applications.

In preparing this edition I had the good furtune to have at hand a range of comments, notes and advice. I am particularly indebted to my immediate colleagues Mark Stewart and Dimitry Val for their critical comments and their assistance with some of the new sections. Former research students have also contributed and I mention in this regard particularly H.Y. Chan, M. Moarefzadeh and X.L. Guan. Naturally, I owe a very significant debt to the international structural reliability community in general and to some key people in particular, including Ove Ditlevsen, Rudiger Rackwitz, Armen Der Kiureghian and Bruce Ellingwood—they, and many others, will know that I appreciate their forebearance and friendship.

The encouragement and generous comments from many sources is deeply appreciated. It has contributed to making the hard slog of revision a little less painful. Sometimes a beach run or a surf seemed a better alternative to spending an hour or so making more corrections to the text… As before, the forebearance of my family is deeply appreciated. Like many academic households they have learnt that academics are their own worst enemies and need occasionally to be dragged away from their Macintoshes to more socially acceptable activities.

August, 1998

Robert E. Melchers
Bar Beach, Newcastle

Preface to the First Edition

The aim of this book is to present a unified view of the techniques and theory for the analysis and prediction of the reliability of structures using probability theory. By reliability, in this context, will be understood not just reliability against extreme events such as structural collapse or facture, but against the violation of any structural engineering requirements which the structure is expected to satisfy.

In practice, two classes of problems may arise. In the first, the reliability of an existing structure at the 'present time' is required to be assessed. In the second, and much more difficult class, the likely reliability of some future, or as yet uncompleted, structure must be predicted. One common example of such a requirement is in structural design codes, which are essentially instruments for the prediction of structural safety and serviceability supported by previous experience and expert opinion. Another example is the reliability assessment of major structures such as large towers, offshore platforms and industrial or nuclear plants for which structural design codes are either not available or not wholly acceptable. In this situation, the prediction of safety both in absolute terms and in terms of its interrelation to project economics is becoming increasingly important. This class of assessment relies on the (usually reasonable but potentially dangerous) assumption that past experience can be extrapolated into the future.

It might be evident from these remarks that the analysis (and prediction) of structural reliability is rather different from the types of analysis normally performed in structural engineering. Concern is less with details of stress calculations, or member behaviour, but rather with the uncertainties in such behaviour and how this interacts with uncertainties in loading and in material strength. Because such uncertainties cannot be directly observed for any one particular structure, there is a much greater level of abstraction and conceptualization in reliability analysis than is conventionally the case for structural analysis or design. Modelling is not only concerned with the proper and appropriate representation of the physics of any structural engineering problem, but also with the need to obtain realistic, sufficiently simple and workable models or representations of both the loads and the material strengths, and also their respective uncertainties. How such modelling might be done and how such models can be used to analyse or predict structural reliability is the central theme of this book.

In one important sense, however, the subject matter has a distinct parallel with conventional structural engineering analysis and its continual refinement; that is, that ultimately concern is with costs. Such costs include not only those of design, construction, supervision and maintenance but also the possible cost of failure (or loss

of serviceability). This theme, although not explicitly pursued throughout the book, is nevertheless a central one, as will become clear in Chapter 2. The assessment or predictions obtained using the methods outlined in this book have direct application in decision-making techniques such as cost-benefit analysis or, more precisely when probability is included, risk-benefit analysis. As will be seen in Chapter 9, one important area of application for the methods presented here is in structural design codes, which, it will be recognized, are essentially particular (if perhaps rather crude and intuitive) forms of risk-benefit methodology.

A number of other recent books have been devoted to the structural reliability theme. This book is distinct from the others in that it has evolved from a short course of lectures for undergraduate students as well as a 30-h graduate course of lectures which the author has given periodically to (mainly) practising structural engineers during the last 8 years. It is also different in that it does not attempt to deal with related topics such as spectral analysis for which excellent introductory texts are already available.

Other features of the present book are its treatment of structural system reliability (Chapter 5) and the discussion of both simulation methods (Chapter 3) and modern second-moment and transformation methods (Chapter 4). Also considered is the important topic of human error and human intervention in the relationship between calculated (or 'nominal') failure probabilities and those observed in populations of real structures (Chapter 2).

The book commences (Chapter 1) by reviewing traditional methods of defining structural safety such as the 'factor of safety', the 'load factor', 'partial factor' formats (i.e. 'limit state design' formats) and the 'return period'. Some consistency aspects of these methods are then presented and their limited use of available data noted, before a simple probabilistic safety measure, the 'safety margin' and the associated failure probability are introduced. This simple one-load one-resistance model is sufficient to introduce the fundamental ideas of structural reliability assessment. Apart from Chapter 2, the rest of the book is concerned with elaborating and illustrating the reliability analysis and prediction theme.

While Chapters 3, 4 and 5 deal with particular calculation techniques for time-independent situations, Chapter 6 is concerned with extending the 'return period' concept introduced in Chapter 1 to more general formulations for time-dependent problems. The three principal methods for introducing time, the time-integrated approach, the discrete time approach and the fully time-dependent approach, are each outlined and examples given. The last approach is considerably more demanding than the other two (classical) methods since it is necessary to introduce elements of stochastic process theory. First-time readers may well decide to skip rather quickly through much of this chapter. Applications to fatigue problems and structural vibrations are briefly discussed from the point of view of probability theory, but again the physics of these problems is outside the scope of the present book.

Modelling of wind and floor loadings is described in Chapter 7 whilst Chapter 8 reviews probability models generally accepted for steel properties. Both load and strength models are then used in Chapter 9. This deals with the theory of structural design codes and code calibration, an important area of application for probabilistic reliability prediction methodology.

It will be assumed throughout that the reader is familiar with modern methods of structural analysis and that he (or she) has a basic background in statistics and

probability. Statistical data analysis is well described in existing texts; a summary of probability theory used is given in Appendix A for convenience.

Further, reasonable competence in applied mathematics is assumed since no meaningful discussion of structural reliability theory can be had without it. The level of presentation, however, should not be beyond the grasp of final-year undergraduate students in engineering. Nevertheless, particularly difficult theoretical sections which might be skipped on a first reading are marked with an asterisk (*).

For teaching purposes, Chapters 1 and 2 could form the basis for a short undergraduate course in structural safety. A graduate course could take up the topics covered in all chapters, with instructors having a bias for second-moment methods skipping over some of the sections in Chapter 3 while those who might wish to concentrate on simulation could spend less time on Chapter 4. For an emphasis on code writing, Chapters 3 and 5 could be deleted and Chapters 4 and 6 cut short.

In all cases it is essential, in the author's view, that the theoretical material be supplemented by examples from experience. One way of achieving this is to discuss particular cases of structural failure in quite some detail, so that students realize that the theory is only one (and perhaps the least important) aspect of structural reliability. Structural reliability assessment is not a substitute for other methods of thinking about safety, nor is it necessarily any better; properly used, however, it has the potential to clarify and expose the issues of importance.

Acknowledgements

December 1985

Robert E. Melchers
Monash University

References

Abdo, R. and Rackwitz, R. (1990) A new beta-point algorithm for large variable problems in time-invariant and time-variant reliability problems, *Proc. 3rd IFIP WG7.5 Working Conf. on Reliability and Optimization of Structural Systems*, Der Kiureghian, A. and Thoft-Christensen, P. (Eds) Springer, 112.

Abramowitz, M. and Stegun, I.A. (Eds) (1966) *Handbook of Mathematical Functions*, Applied Mathematics Series No. 55, National Bureau of Standards, Washington, DC.

Agarwal, H., Mozumder, C.K., Renaud, J.E. and Watson, L.T. (2007) An inverse-measure-based unilevel architecture for reliability-based design. *Structural and Multidisciplinary Optimization*, **33**: 217–227.

Agarwal, H., Renaud, J., Lee, J. and Watson, L. (2004) A unilevel method for reliability based design optimization, *45th AIAA/ASME/ASCE/AHS/ASC Structures, Structural Dynamics and Materials Conference*, Palm Springs, CA, Apr. 19–22.

Ahammed, M. and Melchers, R.E. (1997) Probabilistic Analysis of Underground Pipelines Subject to Combined Stresses and Corrosion, *Engineering Structures*, **19** (12): 988–994.

Ahammed, M. and Melchers, R.E. (2006) Gradient and parameter sensitivity estimation for systems evaluated using Monte Carlo analysis, *Reliability Engineering and System Safety* **91** (5): 594–601.

Akgul, F. and Frangopol, D.M. (2005) Lifetime performance analysis of existing reinforced concrete bridges, II: Application, *J. Infrastructure Systems*, **11** (2): 129–141.

Albrecht, P. and Naeemi, A. (1984) *Performance of Weathering Steel in Bridges*, NCHRP Report 272, Washington, DC.

Allen, D.E. (1968), Discussion of Turkstra, C.J., Choice of failure probabilities, *J. Structural Div.*, ASCE, **94**: 2169–2173.

Allen, D.E. (1970) Probabilistic study of reinforced concrete in bending, *J. Amer. Concrete Inst.*, **67** (12) 989–993.

Allen, D.E. (1975) Limit states design—a probabilistic study, *Can. J. Civil Eng.*, **2** (1): 36–49.

Allen, D.E. (1981a) Criteria for design safety factors and quality assurance expenditure, *Structural Safety and Reliability*, Moan, T., and Shinozuka, M., (Eds), Elsevier, Amsterdam, 667–678.

Allen, D.E. (1981b) Limit states design: what do we really want?, *Can. J. Civil Eng.*, **8**: 40–50.

Allen, D.E. (1991) Limit states criteria for structural evaluation of existing buildings, *Can. J. Civil Eng.*, **18**: 995–1004.

Alpsten, G.A. (1972) Variations in mechanical and cross-sectional properties of steel, *Proc. Int. Conf. on Planning and Design of Tall Buildings*, Vol. Ib, Lehigh University, Bethlehem, 775–805.

Andrieu, C., Lemaire, M. and Sudret, B., (2002) The PHI2 Method: a way to Assess Time-variant Reliability Using Time-invariant Reliability Tools, Proc. European Safety and Reliability Conference ESREL'02, ISdF, Lyon, 472–479.

Ang, A.H-S. and De Leon, D. (1997) Determination of optimal target reliabilities for design and upgrading of structures, *Structural Safety*, **19** (1): 91–103.

Ang A.H.-S. and Lee J.-C. (2001) Cost optimal design of R/C buildings, *Reliability Engineering and System Safety*, **73**, 233–238.

Ang, A.H.-S. and Tang, W.H. (1975) *Probability Concepts in Engineering Planning and Design, Vol. I, Basic Principles*, John Wiley, New York.

Ang, G.L., Ang, A.H.-S. and Tang, W.S. (1989) Kernel method in importance sampling density estimation, *Proc. 5th International Conference on Structural Safety and Reliability*, A.H.-S. Ang, M. Shinozuka and G.I. Schuëller (Eds), ASCE, New York, 1193–1200.

Ang, G.L., Ang, A.H.-S. and Tang, W.S. (1991) Multi-dimensional kernel method in importance sampling, *Proc. 6th International Conference on Applications of Statistics and Probability in Civil Engineering*, L. Esteva and S.E. Ruiz (Eds), CERRA, 289–295.

Angst, U., Elsener, B., Jamali, A. and Adey, B. (2012) Concrete cover cracking owing to reinforcement corrosion—theoretical considerations and practical experience, *Materials and Corrosion*, **63** (12): 1069–1077.

Angst, U., Elsener, B., Larsen, C. and Vennesland, O. (2009) Critical chloride content in reinforced concrete—A review, *Cement and Concrete Research*, **39**: 1122–1138.

Aoues, Y. and Chateauneuf, A. (2008) Reliability-based optimization of structural systems by adaptive target safety—Application to RC frames, *Structural Safety*, **30**: 144–161.

Aoues, Y. and Chateauneuf, A. (2010) Benchmark study of numerical methods for reliability-based design optimization. *Structural and Multidisciplinary Optimization*, **41**: 277–294.

Arnold, R.J. (1981) *The Geometry of Random Fields*, John Wiley & Sons, New York.

Arora, J.S. (2012) *Introduction to Optimum Design*, 3rd Edition, Elsevier, London.

Arora, J.S. (Ed.) (2007) *Optimization of Structural and Mechanical Systems*, World Scientific Publishing.

ASCE (1982) Fatigue reliability (a series of papers), (Committee on Fatigue and Fracture Reliability), *J. Structural Div.*, ASCE, **108** (ST1): 3–88.

ASCE (2013) *Report Card for America's Infrastructure*, American Society of Civil Engineers, Washington, DC.

Au, S.K. (2005) Reliability-based design sensitivity by efficient simulation, *Computers & Structures*, **83**: 1048–1061.

Au, S.K. and Beck, J.L. (2001) Estimation of small failure probabilities in high dimensions by subset simulation, *Prob. Eng. Mech.* **16** (4): 263–277.

Au, S.K. and Beck, J.L. (2003) Subset simulation and its application to seismic risk based on dynamic analysis, *J. Eng. Mech.* ASCE **129** (8): 1–17.

Au, S.K., Ching, J. and Beck, J.L. (2007) Application of subset simulation methods to reliability benchmark problems. *Structural Safety*, **29**: 183–193.

Augusti, G. (1980) Probabilistic methods in plastic structural analysis, *Nuclear Engineering and Design*, **57**: 403–415.

Augusti, G. and Baratta, A. (1972) Limit analysis of structures with stochastic strength variations, *J. Structural Mechanics*, **1** (1): 43–62.

Augusti, G. and Baratta, A. (1973) Theory of probability and limit analysis of structures under multiparameter loading, *Foundations of Plasticity*, Sawczuk, A. (Ed), Noordhoff, Leyden, 347–364.

Augusti, G., Baratta, A. and Casciati, F. (1984) *Probabilistic Methods in Structural Engineering*, Chapman and Hall, London.

Augusti, G. and Ciampoli, M. (2008) Performance-based design in risk assessment and reduction, *Probabilistic Engineering Mechanics*, **23** (4): 496–508.

Aven, T. and Vinnem, J.E. (2005) On the use of risk acceptance criteria in the offshore oil and gas industry, *Reliability Engineering & System Safety*, **90** (1): 15–24.

Ayyub, B.M. and Chia, C.-Y. (1991) Generalized conditional expectation for structural reliability assessment, *Structural Safety*, **11** (2): 131–146.

Ayyab, B.M. and Haldar, A. (1984) Practical structural reliability techniques, *J. Structural Engineering*, ASCE, **110** (8): 1707–1724.

Ayyub, B.M. and Lai, K.-L. (1990) Structural reliability assessment using Latin hypercube sampling, *Proc. Intl. Conf. Structural Safety and Reliability*, Ang, A. H.-S., Shinozuka, M. and Schuëller, G.I. (Eds), ASCE, New York, 1177–1184.

Ba-abbad, M., Nikolaidis, E. and Kapania, R. (2006) A new approach for system reliability–based design optimization, *AIAA J.*, **44** (5): 1087–1096.

Baboian, R. (1995) Environmental conditions affecting transport infrastructure, *Materials Performance*, **34** (9): 48–52.

Baker, M.J. (1969) Variations in the mechanical properties of structural steels, *Final Report, Symposium on Concepts of Safety of Structures and Methods of Design*, IABSE, London, 165–174.

Baker, M.J. (1976) Evaluation of partial safety factors for Level I codes—example of application of methods to reinforced concrete beams, *Bulletin d'Information No. 112*, Comité Européen due Béton, Paris, 190–211.

Baker, M.J. (1985) The reliability concept as an aid to decision making in offshore engineering, *Behaviour of Offshore Structures*, Elsevier, Amsterdam, 75–94.

Baker, M.J. and Wyatt, T. (1979) Methods of reliability analysis for jacket platforms, *Proc. Second Intl. Conf. on Behaviour of Offshore Structures*, British Hydromechanics Research Association, Cranfield, 499–520.

Baratta, A. (1995) Discussion on Wang, et al. (1994), *Structural Safety*, **17** (2): 111–115.

Barbato, M., Petrini, F., Unnikrishnan, V.U. and Ciampoli, M. (2013) Performance-Based Hurricane Engineering (PBHE) framework, *Structural Safety*, **45**: 24–35.

Bartlett, F.M. (1997) Precision of in-place concrete strengths predicted using core strength correction factors obtained by weighted regression analysis, *Structural Safety*, **19** (4): 397–410.

Bartlett, F.M. and McGregor, J.G. (1996) Statistical analysis of the compressive strength of concrete in structures, *ACI Materials Journal*, **93** (2): 158–168.

Basler, B. (1961) Untersuchungen über den Sicherheitsbegriff von Bauwerken, *Schweiz. Arch.*, **27** (4): 133–160.

Batts, M.B., Russell, L.R. and Simiu, B. (1980) Hurricane wind speed in the United States, *J. Structural Div.*, ASCE, **106** (ST10): 2001–2016.

Beck, A.T. (2003) *Reliability Analysis of Degrading Uncertain Structures—with Applications to Fatigue and Fracture Under Random Loading*, Ph.D. Thesis, Dept. of Civil & Environmental Engineering, University of Newcastle, Australia.

Beck, A.T. (2008) The random barrier-crossing problem, *Probabilistic Engineering Mechanics*, **23**: 134–145.

Beck, A.T. (2013) Structural Optimization under Uncertainties: Understanding the Role of Expected Consequences of Failure, (In) *Civil and Structural Engineering Computational Methods*, Tsompanakis, Y., Iványi, P. and Topping, B.H.V. (Eds.), Saxe-Coburg Publications, Stirlingshire, Scotland.

Beck, A.T. and Gomes, W.J.S. (2012) A comparison of deterministic, reliability-based and risk-based structural optimization under uncertainty, *Probabilistic Engineering Mechanics*, **28**: 18–29.

Beck, A.T., Gomes, W.J.S., Lopez, R.H. and Miguel, L.F.F. (2015) A comparison between robust and risk-based optimization under uncertainty, *Struct. Multidisc. Optim.* **52**: 479–492.

Beck, A.T. and Melchers, R.E. (2004a) On the Ensemble Crossing Rate Approach to Time Variant Reliability Analysis of Uncertain Structures, *Probabilistic Engineering Mechanics*, **19**: 9–19.

Beck, A.T. and Melchers, R.E. (2004b) Overload failure of structural components under random crack propagation and loading – a random process approach, *Structural Safety*, **26**: 471–488.

Beck, A.T. and Melchers, R.E. (2005) Barrier failure dominance in time variant reliability analysis, *Probabilistic Engineering Mechanics*, **20**: 79–85.

Beck, A.T. and Silva Jr., C.R.A. (2016) Strategies for finding the design point under bounded random variables, *Structural Safety*, **58**: 79–93.

Beet, J., Ginsbourger, D., Li, L., Picheny, V. and Vazquez, E. (2012) Sequential design of computer experiments for the estimation of a probability of failure, *Stats. and Comp.*, **22** (3): 773–193.

Belyaev, Y.K. (1968) On the number of exists across the boundary of a region by a vector stochastic process, *Theory Prob. Appl.*, **13** (2): 320–324.

Belyaev, Y.K. and Nosko, V.P. (1969) Characteristics of excursions above a high level for a Gaussian process and its envelope, *Theory Prob. Appl.*, **14**: 296–309.

Benjamin, J.R. (1968) Probabilistic structural analysis and design, *Journal of the Structural Division*, ASCE, **94**: 1665–1679.

Benjamin, J. R. (1970) Reliability studies in reinforced concrete design, *Structural Reliability and Codified Design*, Lind, N. C. (Ed), SM Study No. 3, University of Waterloo, Waterloo, Ontario.

Benjamin, J. R. and Cornell, C. A. (1970) *Probability, Statistics and Decisions for Civil Engineers*, McGraw-Hill, New York.

Bennett, R.M. and Ang. A. H.-S. (1983) *Investigation of Methods for Structural Systems Reliability*, Structural Research Series No. 510, University of Illinois, Urbana, IL.

Beveridge, G.S.G. and Schechter, R.S. (1970) *Optimization: Theory and Practice*, McGraw-Hill, New York.

Beyer, H.G. and Sendhoff, B. (2007) Robust optimization—A comprehensive survey, *Computer Methods in Applied Mechanics and Engineering*, **196**: 3190–3218.

Bichon, B.J., Eldred, M.S., Swiler, L.P., Mahadevan, S. and McFarland, J.M. (2008) Efficient global reliability analysis for nonlinear implicit performance functions, *AIAA Journal*, **46** (10): 2459–2468.

Birge, J.R. and Louveaux, F. (1997) *Introduction to Stochastic Programming*, New York, Springer.

Birnbaum, Z.W. (1950) Effect of linear truncation on a multinormal population, *Annals of Mathematical Statistics*, **21**: 272–279.

Bitner-Gregersen, E.M. and Toffoli, A. (2011) On the probability of occurrence of rogue waves, *Nat. Hazards Earth Syst. Sci.*, **12**: 751–762.

Bjerager, P. (1988) Probability integration by directional simulation, *J. Engineering Mechanics*, ASCE, **114** (8): 1285–1302.

Bjerager, P. (1990) On computational methods for structural reliability analysis, *Structural Safety*, **9** (2): 79–96.

Bjerager, P. and Krenk, S. (1989) Parametric sensitivity in first order reliability theory, *J. Engineering Mechanics*, ASCE, **115** (7): 1577–1582.

Bjorhovde, R., Galambos, T.V. and Ravindra, M.K. (1978) LRFD criteria for steel beam-columns, *J. Structural Div.*, ASCE, **104** (ST9): 1371–1387.

Blockley, D.I. (1980) *The Nature of Structural Design and Safety*, Ellis Horwood, Chichester.

Blockley, D.I. (1992) (Ed) *Engineering Safety*, McGraw-Hill, London.

Bolotin, V.V., Babkin, A.A. and Belousov, I.L. (1998) Probabilistic model of early fatigue crack growth, *Prob. Engineering Mechanics*, **13** (3): 227–232.

Bonferroni, C.E. (1936) Teoria statistica classi e calcolo della proababilità, *Pubbl. R. Ist. Super Sci. Econ. Comm.*, Florence, **8**: 1–63.

Borgman, L.E. (1963) Risk criteria, *J. Waterways Harbours Div.*, ASCE, **89** (WW3) 1–35.

Borgman, L.E. (1967) Spectral analysis of ocean wave forces on piling, *J. Waterways Harbors Div.*, ASCE, **93** (WW2): 129–156.

Bosshard, W. (1975) *On Stochastic Load Combinations*, Technical Report No. 20, Department of Civil Engineering, Stanford University, CA.

Bosshard, W. (1979) Structural safety—A matter of decision and control, *IABSE Surveys*, No. S-9/1979, 1–27.

Bourinet, J.-M., Deheeger, F. and Lemaire, M. (2011) Assessing small failure probabilities by combined sub-set simulation and support vector machines, *Structural Safety*, **33** (6) 343–353.

Bournonville, M., Dahuke, J. and Darwin, D. (2004) Statistical analysis of the mechanical properties and weight of reinforcing bars, Structural Engineering and Materials Laboratory Report 04-1, The University of Kansas.

Box, G.E.P. and Muller, M.E. (1958) A note on the generation of normal deviates, *Ann. Math. Stat.*, **29**, 610–611.

Box, G.E.P. and Tiao, G.C. (1973) *Bayesian Inference in Statistical Analysis*, Addison-Wesley Publishing Co., Reading, MA.

Breitung, K. (1984) Asymptotic approximations for multinormal integrals, *J. Engineering Mechanics*, ASCE, **110** (3) 357–366.

Breitung, K. (1988) Asymptotic approximations for the outcrossing rates of stationary Gaussian vector processes, *Stochastic Processes and their Applications*, **29**, 195–207.

Breitung, K. (1989) Asymptotic approximations for probability integrals, *Prob. Engineering Mechanics*, **4** (4) 187–190.

Breitung, K. (1991) Probability approximations by log likelihood maximization, *J. Engineering Mechanics*, ASCE, **117** (3) 457–477.

Breitung, K. (1994) *Asymptotic Approximations for Probability Integrals*, Springer-Verlag, Berlin.

Breitung, K. and Hohenbichler, M. (1989) Asymptotic approximations for multivariate integrals with application to multinormal probabilities, *J. Multivariate Analysis*, **30**, 80–97.

Breitung, K. and Rackwitz, R. (1982) Non-linear combination load processes, *J. Structural Mechanics*, **10** (2) 145–166.

Broding, W.C., Diederich, F.W. and Parker, P.S. (1964) Structural optimization and design based on a reliability design criterion, *J. Spacecraft*, **1** (1) 56–61.

Brown, C.B., Elms, D.G. and Melchers, R.E. (2008) Assessing and achieving structural safety, *Proc. Institution of Civil Engineers, Structures & Buildings*, **161** (SB1) 219–230.

Bucher, C. (2009) Asymptotic sampling for high-dimensional reliability analysis, *Prob. Eng. Mech.*, **24**: 504–510.

Bucher, C.G. (1988) Adaptive sampling – an iterative fast Monte Carlo procedure, *Structural Safety*, **5** (2) 119–126.

Bucher, C.G. and Bourgund, U. (1990) A fast and efficient response surface approach for structural reliability problems, *Structural Safety*, **7**, 57–66.

Bucher, C.G., Chen, Y.M. and Schuëller, G.I. (1988) Time variant reliability analysis utilizing response surface approach, *Proc. 2nd IFIP Conference on Reliability and Optimization of Structural Systems*, Thoft-Christensen, P. (Ed), Springer, 1–14.

Bucher, C.G. and Most, T. (2008) A comparison of approximate response functions in structural reliability analysis, *Prob. Eng. Mech.*, **23** (2–3) 154–163.

Byers, W.G., Marley, M.J., Mohammadi, J. Nielsen, R.J. and Sarkani, S. (1997) Fatigue reliability reassessment procedures: state-of-the-art paper, *J. Structural Engineering*, ASCE, **123** (3) 271–276.

Byfield M.P. and Nethercot D.A. (1998) An analysis of the true bending strength of steel beams, *Proc. Inst. Civil Engrs., Structures and Building*, **128** (2) 188–197.

Casciati, F. and Faravelli, L. (1991) *Fragility Analysis of Complex Structural Systems*, Research Studies Press, Taunton, England.

Castillo, E. (2012) *Extreme Value Theory in Engineering*, Elsevier, London.

Castillo, E. and Sarabia, J.M. (1992) Engineering analysis of extreme value data: selection of models, *Journal of Waterway, Port, Coastal, and Ocean Engineering*, **118** (2) 129–146.

CEB (1976) *Common Unified Rules for Different Types of Construction and Material* (3rd draft), Bulletin d'Information No. 116-E, Comité Européen du Béton, Paris.

Chalk, P.L. and Corotis, R.B. (1980) Probability model for design live loads, *J. Structural Div.*, ASCE, **106** (ST10) 2107–2033.

Chaves I.A. and Melchers R.E. (2014) External corrosion of carbon steel pipeline weld zones, *Int. J. Offshore and Polar Engrg.* **24** (1) 68–74.

Chen, X. and Lind, N.C. (1983) Fast probability integration by three-parameter normal tail approximation, *Structural Safety*, **1** (4) 269–276.

Chen, Y.M. (1989) Reliability of structural systems subjected to time variant loads, *Z. angew. Math. Mech.*, **69**, T64–T66

Chen, Y.M., Schuëller, G.I. and Bourgund, U. (1988) Reliability of large structural systems under time varying loads, *Proc. 5th ASCE Speciality Conference on Probabilistic Methods in Civil Engineering*, Spanos, P.D. (Ed), ASCE, 420–423.

Cheng, G., Xu L, Jiang, L. (2006) A sequential approximate programming strategy for reliability-based structural optimization, *Computers and Structures*, **84**, 1353–1367.

Choi, E.C.C. (1991) Extraordinary live load in office buildings, *J. Structural Engineering*, ASCE, **117** (11) 3216–3227.

Choi, E.C.C. (1992) Live load in office buildings: lifetime maximum load and the influence of room use, *Proc. Institution of Civil Engineers, Structures and Buildings*, **94** (3) 307–314.

Chou, K.C. and Corotis, R.B. (1984) Conditioned Gaussian probability density, *J. Engineering Mechanics*, ASCE, **110** (1) 115–119.

Ciampoli, M. and Petrini, F. (2011) Performance-based design of structures under Aeolian hazard, *Proceedings of the 11th International Conference on Applications of Statistics and Probability in Civil Engineering*, pp. 899–906.

Ciampoli, M., Petrini, F. and Augusti, G. (2011) Performance-based wind engineering: Towards a general procedure, *Structural Safety*, **33** (6) 367–378.

Cibula, B. (1971) *The Structure of Building Control – An International Comparison*, Current Paper No. CP28/71, Building Research Station, Garston, UK.

CIRIA (1977) *Rationalization of Safety and Serviceability Factors in Structural Codes*, Report No. 63, Construction Industry Research and Information Association, London.

CIRIA (2014) *Engaging with risk*, Report C747, Construction Industry Research and information Association, London.

Clough, R.W. and Penzien, J. (1975) *Dynamics of Structures*, McGraw-Hill, New York.

Coles, S. (2001) *An Introduction to the Modelling of Extreme Values*, Springer, New York.

Comanescu, I., Melchers, R.E. and Taxén, C. (2016) Corrosion and durability of offshore steel water injection pipelines, *Ships and Offshore Structures*, **11** (4) 424–437.

Comerford, J.B. and Blockley, D.I. (1993) Managing safety and hazard through dependability, *Structural Safety*, **12** (1) 21–33.

Cook, N.J. (1983) Note on directional and seasonal assessment of extreme winds for design, *J. Wind Engg. Indust. Aerodyn.*, **12**, 365–372.

Cooper, P.B., Galambos, T.V. and Ravindra, M.K. (1978) LRFD criteria for plate girders, *J. Structural Div.*, ASCE, **104** (ST9) 1389–1407.

Cornell, C.A. (1967) Bounds on the reliability of structural systems, *J. Structural Div.*, ASCE, **93** (ST1) 171–200.

Cornell, C.A. (1969a) A probability based structural code, *J. Amer. Concrete Inst.*, **66** (12) 974–985.

Cornell, C.A. (1969b) Bayesian Statistical Decision Theory and Reliability-Based Design, *Proceedings of the Int. Conference on Structural Safety and Reliability*, Washington DC, 47–66.

Corotis, R.B. and Doshi, V.A. (1977) Probability models for live load survey results, *J. Structural Div.*, ASCE, **103** (ST6) 1257–1274.

Corotis R.B. and Nafday, A.M. (1989) Structural system reliability using linear programming and simulation, *J. Structural Engineering*, ASCE, **115** (10) 2435–2447.

Cramer, H. and Leadbetter, M.R. (1967) *Stationary and Related Stochastic Processes*, John Wiley & Sons, New York.

Crandall, S.H. and Mark, W.D. (1963) *Random Vibration in Mechanical Systems*, Academic Press, New York.

Crespo-Minguillon, C. and Casas, J.R. (1997) A comprehensive traffic load model for bridge safety checking, *Structural Safety*, **19** (4) 339–359.

Cressie, N. (1993) *Statistics for spatial data*, Wiley, New York.

CSA (1974) *Steel Structures for Buildings—Limit States Design*, CSA Standard No. S16.1-1974, Canadian Standards Association.

Culver, C.G. (1976) *Survey Results for Fire Loads and Live Loads in Office Buildings*, NBS Building Science Series Report No. 85, Center for Building Technology, National Bureau of Standards, Washington, DC.

Curnow, R.N. and Dunnett, C.W. (1962) The numerical evaluation of certain multivariate normal integrals, *Ann. Math. Stat.*, **33** (2) 571–579.

Dahlquist, G. and Björck, A. (1974), *Numerical Methods*, Prentice-Hall, Englewood Cliffs, NJ.

Daley, D.J. (1974) Computation of bi- and tri-variate normal integrals, *Appl. Stat.*, **23** (3) 435–438.

Dandola, J.C. and Basar, N.S. (1980) Probabilistic structural analysis of ship hull longitudinal strength, Ship Structure Committee, Report SSC-301, U.S. Coast Guard, Washington D.C.

Daniels, H.E. (1945) The statistical theory of the strength of bundles of threads, *Proc. Royal Soc., Ser. A*, **183**, 405–435.

Davenport, A.G. (1961) The application of statistical concepts to the wind loading of structures, *Proc. Inst. Civil Engrs.*, **19**, 449–472.

Davenport, A.G. (1967) Gust loading factors, *J. Structural Div.*, ASCE, **93** (ST3) 11–34.

Davenport, A.G. (1983) The reliability and synthesis of aerodynamic and meteorological data for wind loading, *Reliability Theory and Its Application in Structural and Soil Mechanics*, Thoft-Christensen, P. (Ed), NATO Advanced Study Institute Series E, No. 70, Martinus Nijhoff, The Hague, 314–335.

Davenport, A.G. (1987) Proposed new international (ISO) wind load standard. High winds and building codes, *Proc. WERC/NSF Wind Engineering Symposium*, Kansas City, MI., 373–388.

Davis, P.J. and Rabinowitz, P. (1975), *Methods of Numerical Integration*, Academic Press, New York.

Dawson, D.A. and Sankoff, D. (1967) An inequality for probabilities, *Proc. Amer. Math. Soc.*, **18**, 504–507.

de Finetti, B. (1974) *Theory of Probability*, John Wiley & Sons, New York.

de Neufville, R. and Stafford, J.H. (1971) *Systems Analysis for Engineers and Managers*, McGraw-Hill, New York.

Deák, I. (1980) Fast procedures for generating stationary normal vectors, *J. Stat. Comput. Simul.*, **10**, 225–242.

Deák, I. (1980) Three digit accurate multiple normal probabilities, *Numerische Mathematik*, **35**, 369–380.

Der Kiureghian, A. (1990) Bayesian analysis of model uncertainty in structural reliability, *Proc. 3rd IFIP WG7.5 Conf. Reliability and Optimization of Structural Systems*, Der Kiureghian, A. and Thoft-Christensen, P. (Eds), Springer, Berlin, 211–221.

Der Kiureghian, A. and Dakessian, T. (1998) Multiple design points in first and second-order reliability, *Structural Safety*, **20** (1) 37–50.

Der Kiureghian, A. and De Stafeno, M. (1991) Efficient algorithm for second-order reliability analysis, *J. Engineering Mechanics*, ASCE, **117** (12) 2904–2923.

Der Kiureghian, A. and Ditlevsen, O.(2009) Aleatory or epistemic? Does it matter? *Structural Safety*, **31**: 105–112.

Der Kiureghian, A., Lin, H.-Z. and Hwang, S.-J. (1987) Second order reliability approximations, *J. Engineering Mechanics*, ASCE, **113** (8) 1208–1225.

Der Kiureghian, A. and Liu, P.-L. (1986) Structural reliability under incomplete probability information, *J. Engineering Mechanics*, ASCE, **112** (1) 85–104.

Der Kiureghian, A. and Taylor, R.L. (1983) Numerical Methods in Structural Reliability, *Proc. 4th Int. Conf. on Applications of Statistics and Probability in Soil and Structural Engineering*, Augusti, G., Borri, A. and Vannuchi, G. (Eds), Pitagora Editrice, Bologna, 769–775.

Der Kiureghian, A., Zhang, Y. and Li, C.-C. (1994) Inverse reliability problem, *J. Engineering Mechanics*, ASCE, **120** (5) 1154–1159.

Dewdney, A.K. (1997) *Yes, We Have No Neutrons: An Eye-Opening Tour through the Twists and Turns of Bad Science*, Wiley, New York.

Diamantidis, D. (Ed.) (2001) Probabilistic Assessment of Existing Structures, Report 32, *Joint Committee on Structural Safety*, RILEM Publications, Cachan, France.

Diamantidis, D. and P. Bazzurro (2007) Safety acceptance criteria for existing structures, *Workshop on Risk Acceptance and Risk Communication*, March 26–27, Stanford University CA, USA.

Didonato, A.R., Jarnagin, M.P. and Hageman, R.K. (1980) Computation of the integral of the bivariate normal distribution over convex polygons, *SIAM J. Sci. Stat. Comput.*, **1** (2) 179–186.

Ditlevsen, O. (1973) *Structural Reliability and the Invariance Problem*, Solid Mechanics Report No. 22, University of Waterloo, Ontario.

Ditlevsen, O. (1979a) Generalized second moment reliability index, *J. Structural Mechanics*, **7** (4) 435–451.

Ditlevsen, O. (1979b) Narrow reliability bounds for structural systems, *J. Structural Mechanics*, **7** (4) 453–472.

Ditlevsen, O. (1981a) Principle of normal tail approximation, *J Engineering Mechanics Div.*, ASCE, **107** (EM6) 1191–1208.

Ditlevsen, O. (1981b) *Uncertainty Modeling*, McGraw-Hill, New York.

Ditlevsen, O. (1982a) The fate of reliability measures as absolutes, *Nucl. Eng. Des.*, **71**, 439–440.

Ditlevsen, O. (1982b) Systems reliability bounding by conditioning, *J. Engineering Mechanics Div.*, ASCE, **108** (EM5) 708–718.

Ditlevsen, O. (1983a) Fundamental postulate in structural safety, *J. Engineering Mechanics Div.*, ASCE, **109** (4) 1096–1102.

Ditlevsen, O. (1983b) Gaussian outcrossings from safe convex polyhedrons, *J. Engineering Mechanics Div.*, ASCE, **109** (1) 127–148.

Ditlevsen, O. (1988) Probabilistic statics of discretized ideal plastic frames, *J. Engineering Mechanics*, ASCE, **144** (12) 2093–2114.

Ditlevsen, O. (1997) Structural reliability codes for probabilistic design – a debate paper based on elementary reliability and decision analysis concepts, *Structural Safety*, **19** (3) 253–270.

Ditlevsen, O. and Arnbjerg-Nielsen, T. (1989) Decision rules in re-evaluation of existing structures, *Proceedings of DABI Symposium on Re-evaluation of Concrete Structures*, Rostram, S. and Braestrup, M.W. (Eds), Danish Concrete Institute, Copenhagen, 239–248.

Ditlevsen, O. and Arnbjerg-Nielsen, T. (1992) Effectivity factor method in structural reliability, *Reliability and Optimization of Structural Systems*, Rackwitz, R. and Thoft-Christensen, P. (Eds), Springer, Berlin, 171–179.

Ditlevsen, O. and Bjerager, P. (1984) Reliability of highly redundant plastic structures, *J. Engineering Mechanics*, ASCE, **110** (5) 671–693.

Ditlevsen, O. and Bjerager, P. (1986) Methods of structural systems reliability, *Structural Safety*, **3** (3 & 4) 195–229.

Ditlevsen, O. and Bjerager, P. (1989) Plastic reliability analysis by directional simulation, *J. Engineering Mechanics*, ASCE, **115** (6) 1347–1362.

Ditlevsen, O. and Friis-Hansen, P. (2005) Life quality time allocation index – an equilibrium economy consistent version of the current Life Quality Index, *Structural Safety*, **27** (3) 262–275.

Ditlevsen, O., Hasofer, A.M., Bjerager, P. and Olesen, R. (1988) Directional simulation in Gaussian processes, *Prob. Engineering Mechanics*, **3** (4) 207–217.

Ditlevsen, O. and Madsen, H.O. (1980) Discussion of 'Optimal Reliability Analysis by Fast Convolution', *J. Engineering Mechanics Div.*, ASCE, **106** (EM3) 579–583.

Ditlevsen, O. and Madsen, H.O. (1983) Transient load modeling: clipped normal processes, *J. Engineering Mechanics Div.*, ASCE, **109** (2) 495–515.

Ditlevsen, O. and Madsen, H.O. (1996) *Structural Reliability Methods*, John Wiley & Sons, Chichester.

Ditlevsen, O., Melchers, R.E. and Gluver, H. (1990) General multi-dimensional probability integration by directional simulation, *Computers & Structures*, **36** (2) 355–368.

Ditlevsen, O., Olesen, R. and Mohr, G. (1987) Solution of a class of load combination problems by directional simulation, *Structural Safety*, **4**, 95–109.

Divgi, D.R. (1979) Calculation of univariate and bivariate normal probability functions, *Annals of Statistics*, **7**, 903–910.

Dolinsky, K. (1983) First order second-moment approximation in reliability of structural systems: critical review and alternative approach, *Structural Safety*, **1** (3) 211–231.

Dorman, C.L. (1983) Extreme wind gusts in Australia, excluding tropical cyclones, *Civ. Engg. Trans. Inst. Engrs. Aust.*, **CE25**, 96–106.

Drezner, Z. (1978) Computation of the bivariate normal integral, *Math. Comput.*, **32** (141) 277–279.

Drury, C.G. and Fox, J.G. (Eds) (1975) *Human Reliability in Quality Control*, Taylor and Francis, London.

Drysdale, R.G. (1973) Variation of concrete strength in existing buildings, *Mag. Concrete Research*, **25** (85) 201–207.

Du, X. and Chen, W. (2004) Sequential Optimization and Reliability Assessment Method for Efficient Probabilistic Design, *J. Mech. Des.*, ASME, **126** (2) 225–233.

Dubourg, V., Sudret, B. and Deheeger, F. (2013) Meta-model-based importance sampling for structural reliability analysis, *Prob. Engrg. Mech.* **33**: 47–57.

Dunker, K.R. and Rabbat, B.G. (1993) Why America's bridges are crumbling, *Sci. American*, March, 66–72.

Dunnett, C.W. and Sobel, M. (1955) Approximations to the probability integral and certain percentage points of a multivariate analogue of Students t-distribution, *Biometrika*, **42**, 258–260.

Duprat, F., Sellier, A., Xuan Son Nguyen, Pons, G. (2010) The gradient projection algorithm with error control for structural reliability, *Engineering Structures*, **32** (11) 3725–3733.

Echard, B., Gayton, N. and Lemaire, M. (2011) AK-MCS: An active learning reliability method combining Kriging and Monte Carlo simulation, *Struct. Safety*, **33** (2): 145–154.

El-Tawil, K., Lemaire, M. and Muzeau, J.-P. (1992) Reliability method to solve mechanical problems with implicit limit functions, *Reliability and Optimization of Structural Systems*, Rackwitz, R. and Thoft-Christensen, P. (Eds), Springer, Berlin, 181–190.

Eldred, M.S. and Bichon, B.J. (2006) Second-order reliability formulations in DAKOTA/UQ, *Proc. 47th AIAA/ASME/ASCE/AHS/ASC Structures, Structural Dynamics, and Materials Conference*, 1–4 May, Newport, RI. Paper AIAA 2006-1828.

Elderton, W.P. and Johnson, M.L. (1969) *Systems of Frequency Curves*, Cambridge University Press, New York.

Ellingwood, B. (1983) Probability-based loading criteria for codified design, *4th Intl. Conf. on Applications of Statistics and Probability in Soil and Structural Engineering*, Augusti, G., Borri, A. and Vannuchi, G. (Eds), Pitagora Editrice, Bologna, 237–248.

Ellingwood, B. and Culver, C. (1977) Analysis of live loads in office buildings, *J. Structural Div.*, ASCE, **103** (ST8) 1551–1560.

Ellingwood, B., Galambos, T.V., MacGregor, J.C. and Cornell, C.A. (1980) *Development of a Probability Based Load Criteria for American National Standard A58*, NBS Special Publication No. 577, National Bureau of Standards, US Department of Commerce, Washington, DC. [*See also*: Galambos T.V., Ellingwood, B., MacGregor, J.G. and Cornell, C.A. (1982) Probability-based load criteria: assessment of current design practice, *J. Structural Engineering*, ASCE, **108** 959–977, *and*: Ellingwood, B., MacGregor, J.G., Galambos, T.V. and Cornell, C.A. (1982) Probability-based load criteria: load factors and load combinations, *J. Structural Engineering*, ASCE, **108** 978–997.]

Ellingwood, B.R. (1977) Statistical analysis of R.C. beam-column interaction *J. Structural Div.*, ASCE, **103** (ST7) 1377–1388.

Ellingwood, B.R. (1994) Probability-based codified design: past accomplishments and future challenges, *Structural Safety*, **13** (3) 159–176.

Ellingwood, B.R. (1996) Reliability-based condition assessment and LRFD for existing structures, *Structural Safety*, **18** (2+3) 67–80.

Ellingwood, B.R. (1997) Probability-based LRFD for engineered wood construction, *Structural Safety*, **19** (1) 53–65.

Ellingwood B.R. (2005) Risk-informed condition assessment of civil infrastructure, state of practice and research issues, *J. Structural and Infrastructure Engineering*, **1**(1) 7–18.

EMSA (2015) *Risk Acceptance Criteria and Risk Based Damage Stability. Final Report, part 1: Risk Acceptance Criteria*, European Maritime Safety Agency, DV-GL, Hovik, Norway.

Enevoldsen, I. and Sørensen, J.D. (1993) Reliability-based optimization of series system of parallel systems. *J. Struct. Eng.* **119** (14) 1069–1084.

Enevoldsen, I. and Sørensen, J.D. (1994) Reliability-based optimization in structural engineering, *Structural Safety*, **15**: 169–196.

Engelund, S. and Rackwitz, R. (1993) A benchmark study on importance sampling techniques in structural reliability, *Structural Safety*, **12** (4) 255–276.

Engelund, S., Rackwitz, R. and Lange, C. (1995) Approximations of first-passage times for differentiable processes based on higher-order threshold crossings, *Probabilistic Engineering Mechanics*, **10**, 53–60.

Enright, M.P. and Frangopol, D.M. (1998) Service-life prediction of deteriorating concrete bridges, *J. Structural Engineering*, ASCE, **124** (3) 309–317.

Entroy, H.C. (1960) *The Variation of Works Test Cubes*, Research Report No. 10, Cement and Concrete Association, UK.

Er, G.K. (1998) A method for multi-parameter PDF estimation of random variables, *Structural Safety*, **20** (1) 25–36.

Faber, M.H., Kroon, I.B. and Sørensen, J.B. (1996) Sensitivities in structural maintenance planning, *Rel. Engg. Syst. Safety*, **51**, 317–329.

Faber, M.H., Val, D.V. and Stewart, M.G. (2000) Proof load testing for bridge assessment and upgrading, *Engineering Structures*, **22**: 1677–1689.

Faravelli, L. (1989) Response-surface approach for reliability analysis, *J. Engineering Mechanics*, ASCE, **115** (12) 2763–2781.

Feller, W. (1957) *An Introduction to Probability Theory and its Applications*, Vol. **1** (2nd Edn), John Wiley & Sons, New York.

Feng, Y. (1989) A method for computing structural system reliability with high accuracy, *Computers & Structures*, **33**, 1–5.

Feng, Y.S. and Moses, F. (1986) A method of structural optimization based on structural system reliability. *J. Struct. Mech.* **14** (4) 437–553.

Ferry-Borges. J. (1954) *O Dimensionamento de Estruturas*, Publication 54, Ministry of Public Works, National Laboratory of Civil Engineering, Lisbon, Portugal.

Ferry-Borges, J. and Castenheta, M. (1971), *Structural Safety*, Laboratoria Nacional de Engenhera Civil, Lisbon.

Fiessler, B. (1979) *Das Programmsystem FORM zur Berechnung der Versagens-wahrscheinlichkeit von Komponenten von Tragsystemen*, Berichte zur Zuverlässigkeitstheorie der Bauwerke, No. 43, Technical University Munich.

Fiessler, B., Hawranek, R. and Rackwitz, R. (1976) *Numerische Methoden für probabilistische Bemessungsverfahren und Sicherheitsnachweise*, Berichte zur Sicherheitstheorie der Bauwerke No. 14, Technical University Munich.

Fiessler, B., Neumann, H.-J. and Rackwitz, R. (1979) Quadratic limit states in structural reliability, *J. Engineering Mechanics*, ASCE, **105** (4) 661–676.

Fishburn, P.C. (1964) *Decision and Value Theory*, John Wiley & Sons, New York.

Fisher, J.W., Galambos, T.V., Kulak, G.L. and Ravindra, M.K. (1978) Load and resistance factor design criteria for connectors, *J. Structural Div.*, ASCE, **104** (ST9) 1427–1441.

Fisher, J.W. and Struik, J.H.A. (1974) *Guide to Design Criteria for Bolted and Riveted Joints*, John Wiley, New York.

Flint, A.R., Smith, B.W., Baker, M.J. and Manners, W. (1981) The derivation of safety factors for design of highway bridges, *Design of Steel Bridges*, Granada Publishing, UK.

Forristall, G. (2000) Wave crests distributions: observations and second order theory, *J. Phys. Ocean.*, **30**: 1931–1943.

Foschi, R.O. (1999) Reliability applications in wood design, *Progress in Structural Engineering and Mechanics*, **2** (2).

Fougeres, A.-L., Nolan, J. and Rootzen, H., Models for dependent extremes using stable mixtures, *Scandinavian J. of Statistics*, 2009, **36**, 42–59.

Frangopol, D.M. (1985a) Sensitivity studies in reliability based analysis of redundant structures, *Structural Safety*, **3** (1) 13–22.

Frangopol, D.M. (1985b) Structural optimization using reliability concepts, *Journal of Structural Engineering*, **111** (11) 2288–2301.

Frangopol, D.M. (1998) Probablistic structural optimization, *Progress in Structural Engineering and Materials* **1** (2) 223–230.

Frangopol, D.M. and Hearn, G. (1996) (Eds) *Structural Reliability in Bridge Engineering: Design, Inspection, Assessment, Rehabilitation and Management*, McGraw-Hill, New York.

Frangopol, D.M., Lin, K.-Y. and Estes, A.C. (1997) Reliability of reinforced concrete girders under corrosion attack, *J. Structural Engineering*, ASCE, **123** (3) 286–297.

Frangopol, D.M., Milner, D., Ide, Y., Durmus, A.K. Iwaki, I. and Spacone, E. (1997) Reliability of reinforced concrete columns under random loads, *Reliability and Optimization of Structural Systems*, Frangopol, D.M., Corotis, R.B. and Rackwitz, R. (Eds), Pergamon, 141–148.

Freeman, H. (1963) *An Introduction to Statistical Inference*, Addison-Wesley, Reading, MA.

Freudenthal, A.M. (1956) Safety and the probability of structural failure, *Trans. ASCE*, **121**, 1337–1397.

Freudenthal, A. M. (1961) Safety, reliability and structural design, *J. Structural Div.*, ASCE, **87** (ST3) 1–16.

Freudenthal, A.M. (1964) Die Sicherheit der Baukonstruktionen, *Acta Tech. Hung.*, **46**, 417–446.

Freudenthal, A.M. (1975) Structural safety, reliability and risk assessment, *Reliability Approach in Structural Engineering*, Freudenthal, A. M., et al. (Eds), Maruzen, Tokyo.

Freudenthal, A.M., Garrelts, J.M. and Shinozuka, M. (1966) The analysis of structural safety, *J. Structural Div.*, ASCE, **92** (ST1) 267–325.

Fu, G. and Tang, J. (1995) Risk-based proof-load requirements for bridge evaluation, *J. Structural Engineering*, ASCE, **121** (3) 542–556.

Fujino, Y. (1996) Seismic, structural, economic and societal impacts of the Great Hanshin earthquake, *Applications of Statistics and Probability*, Lemaire, M., Favre, J.-L. and Mebarki, A. (Eds), Balkema, Rotterdam, 1387–1394.

Fujino, Y. and Lind, N.C. (1977) Proof-load factors and reliability, *J. Structural Divn.*, ASCE, **103** (ST4) 853–870.

Galambos, J. (1987) *The Asymptotic Theory of Extreme Order Statistics*, 2nd Ed, Krieger, Malabar, FL.

Galambos, T.V. and Ellingwood, B. (1986) Serviceability limit states: deflection, *J. Structural Engineering*, ASCE, **112** (1), 67–84.

Galambos, T.V. and Ravindra, M.K. (1978) Properties of steel for use in LRFD, *J. Structural Div.*, ASCE, **104** (ST9) 1459–1468.

Garson, R.C. (1980) Failure mode correlation in weakest-link systems, *J. Structural Div.*, ASCE, **106** (ST8) 1797–1810.

Gasper, B. Teixeira, A.P. and Guedes Soares, C. (2014) Assessment of the efficiency of Kriging surrogate models for structural reliability analysis, *Prob. Engrg. Mech.* **37**: 24–34.

Gauther, P. (2010) *Timber Frame Engineering in Limit States Design*, TFE Publishing, Vancouver.

Gaver, D.P. and Jacobs, P. (1981) On combination of random loads, *J. Appl. Maths.*, SIAM, **40** (3) 454–466.

Ghobarah, A. (2001) Performance-based design in earthquake engineering: state of development, *Engineering Structures*, **23**: 878–884.

Ghosn, M. and Moses, F. (1985a) Markov renewal model for maximum bridge loading, *J. Engineering Mechanics*, ASCE, **111** (9) 1093–1104.

Ghosn, M. and Moses, F. (1985b) Reliability calibration of bridge design code, *J. Structural Engineering*, ASCE, **112** (4) 745–763.

Gjorv, O.E. (2009) *Durability design of concrete structures in severe environments*, London, Taylor & Francis.

Glanville, J.I., Hatzinikolas, M.A. and Ben-Omran, H.A. (1996) *Engineered Masonry Design: Limit States Design*, Winston House, Winnepeg.

Gollwitzer, S. and Rackwitz, R. (1983) Equivalent components in first-order system reliability, *Reliab. Engg.*, **5**, 99–115.

Gomes, L. and Vickery, B.J. (1976) Tropical cyclone gust speeds along the northern Australian coast, *Civ. Engg. Trans. Inst. Engrs. Aust.*, **CE18** (2) 40–48.

Gomes, W.J.S. and Beck, A.T. (2014a) Optimal inspection and design of onshore pipelines under external corrosion process, *Structural Safety*, **47**: 48–58.

Gomes, W.J.S. and Beck, A.T. (2014b) Optimal inspection planning and repair under random crack propagation, *Engineering Structures*, **69**: 285–296.

Gomes, W.J.S. and Beck, A.T. (2016) The Design Space Root Finding method for efficient risk optimization by simulation. *Probabilistic Engineering Mechanics*, **44**: 99–110.

Gomes, W.J.S., Beck, A.T. and Haukaas, T. (2013) Optimal inspection planning for onshore pipelines subject to external corrosion, *Reliability Engineering & Systems Safety*, **118**: 18–27.

Gorman, M.R. (1979) *Reliability of Structural Systems*, Report No. 79-2, Department of Civil Engineering, Case Western Reserve University, OH.

Gorman, M.R. (1981) Automatic generation of collapse mode equations, *J. Structural Div.*, ASCE, **107** (ST7) 1350–1354.

Gorman, M.R. (1984) Structural resistance moments by quadrature, *Structural Safety*, **2**, 73–81.

Grandhi, R.V. and Wang, L. (1997) Structural failure probability calculations using nonlinear approximations, *Reliability and Optimization of Structural Systems*, Frangopol, D.M., Corotis, R.B. and Rackwitz, R. (Eds), Pergamon, Oxford, 165–172.

Grandori, G. (1991) Paradigms and falsification in earthquake engineering, *Meccanica*, **26**, 17–21.

Grant, L.H., Mizra, S.A. and MacGregor, J.G. (1978) Monte Carlo study of strength of concrete columns, *J. Amer. Concrete Inst.*, **75** (8) 348–358.

Grausland, H. and Lind, N.C. (1986) A normal probability integral and some applications, *Structural Safety*, **4**, 31–40.

Greig, G.L. (1992) An assessment of high-order bounds for structural reliability, *Structural Safety*, **11**, 213–225.

Grigoriu, M. (1975) *On the Maximum of the Sum of Random Process Load Models*, Internal Project Working Document No. 1, Department of Civil Engineering, Massachusetts Institute of Technology, Cambridge, MA.

Grigoriu, M. (1982) Methods for approximate reliability analysis, *Structural Safety*, **1** (2) 155–165.

Grigoriu, M. (1983) Approximate analysis of complex reliability problems, *Structural Safety*, **1** (4) 277–288.

Grigoriu, M. (1984) Crossings of non-Gaussian translation processes, *J. Engineering Mechanics Div.*, ASCE, **110** (6) 610–620.

Grimmelt, M.J. and Schuëller, G.I. (1982) Benchmark study on methods to determine collapse failure probabilities of redundant structures, *Structural Safety*, **1**, 93–106.

Grimmelt, M.J., Schuëller, G.I. and Murotsu, Y. (1983) On the evaluation of collapse probabilities, Proc. 4th ASCE-EMD *Speciality Conf. on Recent Advances in Engineering Mechanics*, Vol. II, ASCE, 859–862.

Guan, X.L. and Melchers, R.E. (1998) A load space formulation for probabilistic finite element analysis of structural reliability, *Prob. Engineering Mechanics.* **14**, 73–81.

Guedes-Soares, C. and Garbatov, Y. (1996) Fatigue reliability of the ship hull girder accounting for inspection and repair, *Reliability Engineering and System Safety*, **51**, 341–351.

Guedes-Soares, C., Garbatov, Y., Zayed, A., Wang, G., Melchers, R.E., Paik, J.K. and Cui, W. (2006) Non-linear corrosion model for immersed steel plates accounting for environmental factors, *Transactions 2005 Society of Naval Architects and Marine Engineers* **113**: 306–329.

Guenard, Y.F. (1984) *Application of System Reliability Analysis to Offshore Structures*, Report No. RMS-1, Department of Civil Engineering, Stanford University.

Guiffre, N. and Pinto, P.E. (1976) *Discretisation from a Level II Method*, Bulletin d'Information No. 112, Comité Européen du Béton, Paris, 158–189.

Gumbel, E.J. (1958) *Statistics of Extremes*, Columbia University Press, New York.

Gupta, S.S. (1963) Probability integrals of multivariate normal and multivariate t, *Ann. Math. Stat.*, **34**, 792–828.

Gurney, K. (1997) *An Introduction to Neural Networks*, Routledge, London.

Haftka, R.T., Gürdal, Z. and Kamat, M.P. (1990) *Elements of Structural Optimization*, 2nd Ed., Springer.

Hagen, J. (Ed) (1983) *Deterrence Reconsidered*, Sage Publications.

Hagen, O. and Tvedt, L. (1991) Vector process out-crossing as a parallel system sensitivity measure, *Journal of Engineering Mechanics*, **117** (10) 2201–2220.

Hall, W.B. (1988) Reliability of service-proven structures, *J. Structural Engineering*, ASCE, **114** (3) 608–624.

Hall, W.B. and Tsai, M. (1989) Load testing, structural reliability and test evaluation, *Structural Safety*, **6**, 285–302.

Hallam, M.G., Heaf, N.J. and Wootton, L.R. (1978) *Dynamics of Marine Structures*, (2nd Edn), CIRIA Underwater Engineering Group, London.

Hammersley, J.M. and Handscomb, D.C. (1964) *Monte Carlo Methods*, John Wiley & Sons, New York.

Harbitz, A. (1983) Efficient and accurate probability of failure calculation by use of the importance sampling technique, Proc. 4th Int. Conf. on *Applications of Statistics and Probability in Soil and Structural Engineering*, Augusti, G., Borri, A. and Vannuchi, O. (Eds), Pitagora Editrice, Bologna, 825–836.

Harbitz, A. (1986) An efficient sampling method for probability of failure calculation, *Structural Safety*, **3** (2) 109–115.

Harris, D.H., and Chaney, F.B. (1969) *Human Factors in Quality Assurance*, John Wiley & Sons, New York.

Harris, M.E., Corotis, R.B. and Bova, C.J. (1981) Area dependent processes for structural live loads, *J. Structural Div.*, ASCE, **107** (ST5) 857–872.

Harris, R.I. (1971) The Nature of Wind, *The Modern Design of Wind Sensitive Structures*, Construction Industry Research and Information Association, London.

Harris, R.I. (1996) Gumbel revisited—a new look at extreme value statistics applied to wind speeds, *J. Wind Engg. Indust. Aerodyn.*, **59**, 1–22.

Hasofer, A.M. (1974) The upcrossing rate of a class of stochastic processes, *Studies in Probability and Statistics*, Williams, E. J. (Ed), North-Holland, Amsterdam, 151–159.

Hasofer, A.M. (1984) Objective probabilities for unique objects, *Risk, Structural Engineering and Human Error*, M. Grigoriu (Ed), University of Waterloo Press, Waterloo, Ontario, 1–16.

Hasofer, A.M., Ditlevsen, O. and Oleson, R. (1987) Vector outcrossing probabilities by Monte Carlo, DCAMM Report No. 349, Technical University of Denmark.

Hasofer, A.M. and Lind, N.C. (1974) Exact and Invariant Second-moment Code Format, *J. Engineering Mechanics Div.*, ASCE, **100** (EM1) 111–121.

Hasselmann, K., et al. (1973) Measurements of the wind wave growth and swell decay during the Joint North Sea Wave Project (JONSWAP), Ergänzungsheft zur (supplementary volume to) *Deutsche Hydrographischen Zeitschrift*, **A(8)** No. 12.

Hastings, C., Jr., (1955) *Approximations for Digital Computers*, Princeton University Press, Princeton, NJ.

Haugen, E.B. (1968) *Probabilistic Approaches to Design*, John Wiley & Sons.

Haukaas, T. and Der Kiureghian, A. (2006) Strategies for finding the design point in non-linear finite element reliability analysis, *Probab. Eng. Mech.* **21**: 133–47.

Haver, S. and Andersen, J. (2000) Freak waves: rare realizations of a typical population or typical realizations of a rare population?, *Proc. 10th Int. Conf. Offshore and Polar Engrg.*, Seattle, USA, Int. Society of Offshore and Polar Engineers, Cupertino, CA.

Hawrenek, R. and Rackwitz, R. (1976) Reliability calculation for steel columns, *Bulletin d'Information No. 112*, Comité Européen du Béton, Paris, 125–157.

Hearn, G. (1996) Deterioration modeling for highway bridges, *Structural Reliability in Bridge Engineering: Design, Inspection, Assessment, Rehabilitation and Management*, Frangopol, D.M. and Hearn, G. (Eds) McGraw-Hill, New York, 60–71.

Henley, E.J. and Kumamoto, H. (1981) *Reliability Engineering and Risk Assessment*, Prentice-Hall, Englewood Cliffs, NJ.

Hess, P.E., Bruchman, D. Assakkaf, I.A. and Ayyub, B.M. (2002) Uncertainties in material and geometric strength and load variables, *Naval Engineers J.*, **114** (2) 139–166.

Heyman, J. (1971) *Plastic Design of Frames*, Vol. **2**, Cambridge University Press.

Hilton, H.H. and Feigen, M. (1960) Minimum Weight Analysis Based on Structural Reliability, *Journal of the Aerospace Sciences*, **27**: 641–653.

Hoffman, P.C. and Weyers, R.E. (1994) Probabilistic durability analysis of reinforced concrete bridge decks, *Probabilistic Mechanics and Structural Reliability: Proceedings of the Seventh Speciality Conference*, Frangopol, D.M. and Grigoriu, M. (Eds) ASCE, 290–293.

Hohenbichler, M. (1980) *Abschätzungen für die versagenswahrscheinlichkeiten von Seriensystemen*, Research Report, Technical University, Munich.

Hohenbichler, M., Gollwitzer, S., Kruse, W. and Rackwitz, R. (1987) New light on first- and second-order reliability methods, *Structural Safety*, **4**, 267–284.

Hohenbichler, M. and Rackwitz, R. (1981) Non-normal dependent vectors in structural safety, *J. Engineering Mechanics Div.*, ASCE, **107** (EM6) 1227–1237.

Hohenbichler, M. and Rackwitz, R. (1983a) First-order concepts in systems reliability, *Structural Safety*, **1** (3) 177–188.

Hohenbichler, M. and Rackwitz, R. (1983b) Reliability of parallel systems under imposed uniform strain, *J. Engineering Mechanics Div.*, ASCE, **109** (3) 896–907.

Hohenbichler, M. and Rackwitz, R. (1986a) Sensitivity and importance measures in structural reliability, *Civil Engineering Systems*, **3** (4) 203–209.

Hohenbichler, M. and Rackwitz, R. (1986b) Asymptotic outcrossing rate of Gaussian vector process into intersection of failure domains, *Prob. Engineering Mechanics*, **1** (3) 177–179.

Hohenbichler, M. and Rackwitz, R. (1988) Improvement of second-order reliability estimation by importance sampling, *J. Engineering Mechanics*, ASCE, **114** (12): 2195–2199.

Holmes, J.D. (1990) Directional effects on extreme winds loads, *Civ. Engg. Trans. Inst. Engrs. Aust.*, **CE32**, 45–50.

Holmes, J.D. (1998) Wind loading of structures—application of probabilistic methods, *Progress in Structural Engineering and Mechanics*, **1** (2) 193–199.

Holmes, J.D. (2007) *Wind Loading on Structures*, Second Edition, Taylor & Francis, Abingdon.

Holmes, P. Chaplin, J.R., and Tickell, R.G (1983). Wave loading and structure response, *Design of Offshore Structures*, Thomas Telford, London, 3–12.

Holmes, J.D. and Pham, L. (1994) Wind-induced dynamic response and the safety index, *Proc. 6th Int. Conf. on Structural Safety and Reliability*, Balkema, Rotterdam, 1707–1709.

Holmes, P. and Tickell, R.G. (1979) Full scale wave loading on cylinders, *Proc. Second Int. Conf. on Behaviour of Offshore Structures*, London, Vol. 3, British Hydromechanics Research Association, Cranfield, 746–761.

Horne, M.R. and Price, P.H. (1977) Commentary on the level 2 procedure, *Rationalization of Safety and Serviceability Factors in Structural Codes*, Report No. 63, Construction Industry Research and Information Association, London, 209–226.

HSE (1992) *The tolerability of risk from nuclear power stations*, Health and Safety Executive, London.

Hueste, M.B.D., Chompreda, P., Trejo, D., Cline, D.B.H. and Keating, P.B. (2003) *Mechanical properties of high strength concrete for prestressed concrete bridge girders*, Report FHWA/TX-04/0-2101-2, Texas Transportation Institute, College Station, TX.

Hunter, D. (1976) An upper bound for the probability of a union, *J. Appl. Prob.*, **13**, 597–603.

Hunter, D. (1977) Approximate percentage points of statistics expressible as maxima, *TIMS Stud. Management Sci.*, **7**, 25–36.

Huntington, D.E. and Lyrintzis, C.S. (1998) Improvements to and limitations of Latin hypercube sampling, *Prob. Engrg. Mech*, **13** (4) 245–253.

Hurtado, J.E. and Alvarez, D.A. (2001) Neural-network-based reliability analysis: a comparative study, *Comp. Methods in App. Mech. and Engrg.*, **191** (1–2) 113–132.

Ibrahim, Y. (1992) Comparison between failure sequence and failure path for brittle systems, *Computers & Structures*, **42** (1) 79–85.

Ingles, O.G. (1979) Human factors and error in civil engineering, *Proc. 3rd Intl. Conf. on Applications of Statistics and Probability in Soil Structural Engineering*, Sydney, 402–417.

ISE (1980) *Appraisal of Existing Structures*, The Institution of Structural Engineers, London.

ISO 31000 (2009) *Risk management – Risk Assessment Techniques*, International Standards Office, Geneva.

ISO 13824 (2009) *Bases for the design of structures – general principles on risk assessment of systems involving structures*, International Standards Office, Geneva.

JCSS (2000) *Probabilistic Model Code, Part 3: Material Properties*, Danish Technical University, Lyngby.

JCSS (2001) *Probabilistic Model Code, Part 2: Load Models*, Danish Technical University, Lyngby. (http://www.jcss.byg.dtu.dk/About_JCSS).

JCSS (2006) *Probabilistic Model Code, Part 2.15: Wave Load*, Danish Technical University, Lyngby. (http://www.jcss.byg.dtu.dk/About_JCSS).

JCSS (2008) *Risk Assessment in Engineering – Principles, System Representation & Risk Criteria*, Joint Committee on Structural Safety, Danish Technical University, Lyngby, ISBN 978-3-909386-78-9.

Jeffrey, R. (2004) *Subjective Probability: The Real Thing*, Cambridge University Press, Cambridge.

Jensen, H.A. (2006) Structural optimization of non-linear systems under stochastic excitation, *Probabilistic Engineering Mechanics*, **21**: 397–409.

Jensen, H.A., Mayorga, F. and Valdebenito, M.A. (2015) Reliability sensitivity estimation of nonlinear structural systems under stochastic excitation: A simulation-based approach, *Computer Methods in Applied Mechanics and Engineering*, **289**: 1–23.

Jensen, H.A., Valdebenito, M.A. and Schuëller, G.I. (2008) An efficient reliability-based optimization scheme for uncertain linear systems subject to general Gaussian excitation, *Computer Methods in Applied Mechanics and Engineering*, **198**: 72–87.

Jensen, H.A., Valdebenito, M.A., Schuëller, G.I. and Kusanovic, D.S. (2009) Reliability-based optimization of stochastic systems using line search, *Computer Methods in Applied Mechanics and Engineering*, **198**: 3915–3924.

Jia, G. and Taflanidis, A.A. (2013) Non-parametric stochastic subset optimization for optimal-reliability design problems, *Computers & Structures*, **126**: 86–99.

Jia, G., Taflanidis, A.A. and Beck, J.L. (2015) Non-parametric stochastic subset optimization for design problems with reliability constraints, *Structural and Multidisciplinary Optimization*, **52** (6) 1185–1204.

Johnson, A.I. (1953) Strength, Safety and Economical Dimensions of Structures, Division of Building Statistics and Structural Engineering Bulletin 12, Royal Institute of Technology, Stockholm, Sweden.

Johnson, A.I. (1971) *Strength, safety and economical dimensions of structures*, 2nd ed., Nat. Swedish Building Research Inst., Stockholm.

Johnson, N.L. and Kotz, S. (1972) *Distributions in Statistics: Continuous Multivariate Distributions*, John Wiley & Sons, New York.

Johnston, B.G. and Opila, F. (1941) Compression and tension tests of structural alloys, *ASTM Proc.*, **41**, 552–570.

Jonkman, S.N., van Gelder, P.H. and Vrijling, J.K. (2003) An overview of quantitative risk measures for loss of life and economic damage, *Journal of Hazardous Materials*, **A99**: 1–30.

Joos, D.W., Sabri, Z.A. and Hussein, A.A. (1979) Analysis of gross error rates in operation of commercial nuclear power stations, *Nucl. Engg. Des.*, **52**, 265–300.

Julian, O.G. (1957) Synopsis of first progress report of Committee on Safety Factors, *J. Structural Div.*, ASCE, **83** (ST4) 1316.1–1316.22.

Juocevicius, V. and Kadzys, A. (2009) *Structural safety under extreme construction loads, (In) Safety, Reliability and Risk Analysis: Theory, Methods and Applications*, (In) Martorell, S., Guedes Soares C. and Barnett, J. (Eds.), Taylor & Francis, London, 1677–1683.

Kahn, H. (1956) Use of different Monte Carlo sampling techniques, *Proc. Symp. on Monte Carlo Methods*, H.A. Meyer (Ed), John Wiley & Sons, New York, 149–190.

Kaimal, J.C., Wyngaard, J.C., Izumi, Y. and Cote, O.R. (1972) Spectral characteristics of surface layer turbulence, *Q. J. Royal Meteorol. Soc.*, **98**, 563–589.

Kall, P. and Wallace, S.W. (1994) *Stochastic programming*, John Wiley & Sons, New York.

Kameda, H. and Koike, T. (1975) Reliability analysis of deteriorating structures, *Reliability Approach in Structural Engineering*, Maruzen Co., Tokyo, 61–76.

Kanda, J. and Ellingwood, B. (1991) Formulation of load factors based on optimum reliability, *Structural Safety*, **9**: 197–210.

Karadeniz, H. (2001) Uncertainty modeling in the fatigue reliability calculation of offshore structures, *Reliability Engineering & System Safety*, **74**(3): 323–336.

Karadeniz, H., van Manen, S. and Vrouwenvelder, A. (1984) *Probabilistic Reliability Analysis for the Fatigue Limit State of Offshore Structures*, Bull. Tech. Bur. Veritas, 203–219.

Karamchandani, A. and Cornell, C.A. (1991a) Sensitivity estimation within first and second order reliability methods, *Structural Safety*, **11** (1) 59–74.

Karamchandani, A., Bjerager, P. and Cornell, C.A. (1989) Adaptive importance sampling, *Proc. 5th Intl. Conf. Structural Safety and Reliability*, San Francisco, Ang, A.-H., Shinozuka, M. and Schuëller, G.I. (Eds), ASCE, 855–862.

Karamchandani, A. and Cornell, C.A. (1991b) Adaptive hybrid conditional expectation approaches for reliability estimation, *Structural Safety*, **11** (2) 95–107.

Kareem, A. (1988) Effect of parametric uncertainties on wind excited structural response, *J. Wind Engg. Indust. Aerodyn.*, **30**, 233–241.

Karshenas, S. and Ayoub, H. (1994) Analysis of concrete construction live loads on newly poured slabs, *J. Structural Engineering*, ASCE, **120** (5) 1525–1542.

Katsuki, S. and Frangopol, D.M. (1994) Hyperspace division method for structural reliability, *J. Engineering Mechanics*, ASCE, **120** (11) 2405–2427.

Kaymaz, I. (2005) Application of Kriging method to structural reliability problems, *Struct. Safety*, **27** (2) 133–151.

Kecman, V. (2001) *Learning and Soft Computing—Support Vector machines, Neural Networks, Fuzzy Logic Systems*, MIT Press, Cambridge, MA.

Kim, S.-H. and Na, S.-W. (1997) Response surface method using vector projected sampling points, *Structural Safety*, **19** (1) 3–19.

Kim, S.H. and Wen, Y.K. (1990) Optimization of structures under stochastic loads, *Structural Safety*, **7**: 177–190

Knappe, O.W., Schuëller, G.I. and Wittmann, F.H. (1975) On the probability of failure of a reinforced concrete beam in flexure, *Proc. 2nd Int. Conf. on Applications of Statistics and Probability in Soil Structural Engineering*, Aachen, 153–170.

Knoll, F. (1985) Quality, Whose Job?, Introductory Report, *Symp. on Safety and Quality Assurance of Civil Engineering Structures*, Tokyo, Report No. 50, IABSE, London, 59–64.

Kolisko, J. Hunka, P. and Jung, K. (2012) A statistical analysis of the modulus of elasticity and compressive strength of concrete C45/55 for pre-stressed precast beams, *J. Civil Engrg. and Architecture*, **6** (11) 1571–1579.

Konig, G.L., Hosser, D. and Manser, R. (1985) *Superimposed loads in carparks*, CIB Commission W81.

Kounias, E.G. (1968) Bounds for the probability of a union, with applications, *Amer. Math. Stat.*, **39** (6) 2154–2158.

Koutsourelakis, P.S., Pradlwarter, H.J. and Schueller, G.I. (2004) Reliability of structures in high dimensions, Part I: algorithms and application, *Probab. Engrg. Mech.* **19**: 409-417.

Köylüoglu, H.U. and Nielsen, S.R.K. (1994) New approximations for SORM integrals, *Structural Safety*, **13** (4) 235–246.

Kupfer, J. and Rackwitz, R. (1980) Models for human error and control in structural reliability, *Final Report, 11th Congr.* IABSE, London, 1019–1024.

Kuschel, N. and Rackwitz, R. (2000) Optimal design under time-variant reliability constraints, *Structural Safety*, **22** (2)113–127.

Kyburg, H. (1978) Subjective probability: Criticisms, reflections, and problems, *J. of Philosophical Logic*, **7**: 157-180.

Lacaze, S., Brevault, L., Missoum, S. and Balesdent, M. (2015) Probability of failure sensitivity with respect to decision variables, *Struct Multidisc Optim.* **52**: 375–381.

Laird, D.A., Drysdale, R.G., Stubbs, D.W. and Sturgeon, G.R. (2005) The new CSA S302.1-04 Design of masonry structures, *Proc. 10th Canadian Masonry Symposium*, Banff, Alberta, 8–12 June, University of Calgary.

Larrabee, R.D. and Cornell, C.A. (1979) Upcrossing rate solution for load combinations, *J. Structural Div.*, ASCE, **105** (ST1) 125–132.

Larrabee, R.D. and Cornell, C.A. (1981) Combination of various load processes, *J. Structural Div.*, ASCE, **107** (ST1) 223–239.

Lay, M.G. (1979) Implications of probabilistic methods in steel structures, *Proc. 3rd Int. Conf. on Applications of Statistics and Probability in Soil and Structural Engineering*, Vol. 3, Sydney, 145–156.

Leadbetter, M.R., Lindgren, G. and Rootzen, H. (1983) *Extremes and related properties of random sequences and processes*, Springer, New York.

Lee, J., Yang. S. and Ruy, W. (2002) A comparative study on reliability index and target performance based probabilistic structural design optimization, *Computer & Structures*, **257**: 269–280.

Legerer, F. (1970) Code theory—a new branch of engineering science, *Structural Reliability and Codified Design*, Lind, N.C. (Ed), SM Study No. 3, University of Waterloo, Ontario, 113–127.

Leicester, R.H. and Beresford, R.D. (1977) A probabilistic model for serviceability specifications, *Proc. 6th Australasian Conf. on the Mechanics and Structures of Materials,* Christchurch, 407–413.

Leira, B.J. Evaluation of risk-type integrals by system reliability methods, *Structural Safety*, **17** (4) 239–254.

Lemaire, M. (2009) *Structural Reliability*, Wiley-ISTE, London, 261–263.

Lemaire, M., Mohamed, A. and Flores-Macias, O. (1997) The use of finite element codes for the reliability of structural system, *Reliability and Optimization of Structural Systems*, Frangopol, D.M., Corotis, R.B. and Rackwitz, R. (Eds), Pergamon, Oxford, 223–230.

Leonel, E.D., Beck, A.T. and Venturini, W.S. (2011) On the performance of response surface and direct coupling approaches in solution of random crack propagation problems, *Structural Safety*, **33**: 261–274.

Li, C.-C. and Der Kiureghian, A. (1993) Optimal discretization of random fields, *J. Engineering Mechanics*, ASCE, **119** (6) 1136–1154.

Li, C.Q. (2003) Life-cycle modeling of corrosion-affected concrete structures: Propagation, *J. Struct. Engrg.* **129** (6) 753–761.

Li, C.Q. and Melchers, R.E. (1992) Reliability analysis of creep and shrinkage effects, *J. Structural Engineering*, ASCE, **118** (9) 2323–2337.

Liang. J., Mourelatos, Z.P. and Nikolaidis, E. (2007) A single-loop approach for system reliability-based design optimization, *J. Mech. Des.*, **129** (12) 1215–1224.

Liang. J., Mourelatos, Z.P. and Tu, J. (2004) A single-loop method for reliability-based design optimization, In: *Proceedings of ASME design engineering technical conferences*, paper C2004/DAC-57255.

Lighthill, J. (1978) *Waves in Fluids*, Cambridge University Press, New York.

Lin, T.S. and Corotis, R.B. (1985) Reliability of ductile systems with random strengths, *J. Structural Engineering*, ASCE, **111** (6) 1306–1325.

Lin, Y.K. (1970) First excursion failure of randomly excited structures, II, *AIAA J.*, **8** (10) 1888–1890.

Lind, N.C. (1969) Deterministic formats for the probabilistic design of structures, *An Introduction to Structural Optimization*, SM Study No. 1, Kachaturian, N. (Ed), University of Waterloo, Ontario, 121–142.

Lind, N.C. (1972) *Theory of Codified Structural Design*, University of Waterloo, Ontario.

Lind, N.C. (1976a) Approximate analysis and economics of structures, *J. Structural Div.*, ASCE, **102** (ST6) 1177–1196.

Lind, N.C. (1976b) *Application to Design of Level I Codes*, Bulletin d'Information No. 112, Comité Européen du Béton, Paris, 73–89.

Lind, N.C. (1976c) Approximate analysis and economics of structures, *J. Struct. Div.* ASCE, **102** (6) 1177–1196.

Lind, N.C. (1977) Formulation of probabilistic design, *J. Engineering Mechanics Div.*, ASCE, **103** (EM2) 273–284.

Lind, N.C. (1979) Optimal reliability analysis by fast convolution, *J. Engineering Mechanics Div.*, ASCE, **105** (EM3) 447–452.

Lind, N.C. (1983) Models of human error in structural reliability, *Structural Safety*, **1** (3) 167–175.

Lind, N.C. (1996) Validation of probabilistic models, *Civil Engg. Systems*, **13** (3) 175–183.

Lind, N.C. and Davenport, A.G. (1972) Towards practical application of structural reliability theory, *Probabilistic Design of Reinforced Concrete Buildings*, Special Publication No. 31, American Concrete Institute.

Lindley, D.V. (1972) *Bayesian Statistics, A Review*, Society of Industrial and Applied Mathematics.

Liu, P.-L. and Der Kiureghian, A. (1986) Multivariate distribution models with prescribed marginals and covariances, *Prob. Engineering Mechanics*, **1** (2) 105–112.

Liu, P.-L. and Der Kiureghian, A. (1991a) Finite element reliability of geometrically nonlinear uncertain structures, *J. Engineering Mechanics*, ASCE, **117** (8) 1806–1825.

Liu, P.-L, and Der Kiureghian, A. (1991b) Optimization algorithms for structural reliability, *Structural Safety*, **9**: 161–177.

Liu, S.C., Neghabat, F. and Dougherty, M.R. (1976) Optimal aseismic design of building and equipment, *J. Engrg. Mech.* ASCE, **102** (3), 395–414.

Liu, Y.W. and Moses, F. (1994) A sequential response surface method and its application in the reliability analysis of aircraft structural systems, *Structural Safety*, **16** (1+2) 39–46.

Longuet-Higgins, M.S. (1952) On the statistical distribution of the heights of sea waves, *J. Marine Sci.*, **11**, 245–266.

Lopez, R.H. and Beck, A.T. (2012) Reliability-based design optimization strategies based on FORM: a review. *Journal of the Brazilian Society of Mechanical Sciences and Engineering*, **34**: 506–514.

Luthans, F. (2010) *Organizational Behaviour* (12th Edn) McGraw-Hill, New York.

Lyse, I. and Keyser, C.C. (1934) Effect of size and shape of test specimens upon the observed physical properties of structural steel, *ASTM, Proc.*, **34**, Part II, 202–210.

Ma, H.-F. and Ang, A. H.-S. (1981) *Reliability Analysis of Redundant Ductile Structural Systems*, Structural Research Series No. 494, Department of Civil Engineering, University of Illinois, Urbana.

MacGregor, J.G. (1976) Safety and limit states design for reinforced concrete, *Can. J. Civil Engg.*, **3** (4) 484–513.

Madsen, H.O. (1982) *Deterministic and Probabilistic Models for Damage Accumulation due to Time Varying Loading*, DIALOG 5-82, Danish Engineering Academy, Lyngby, Denmark.

Madsen, H.O. (1987) Model updating in reliability analysis, *Proc. 5th Int. Conf. on Applications of Statistics and Probability in Soil and Structural Engineering*, Vancouver, 564–577.

Madsen, H.O. (1988) Omission sensitivity factors, *Structural Safety*, **5**, 35–45.

Madsen, H.O. and Bazant, Z.P. (1983) Uncertainty analysis of creep and shrinkage effects in concrete structures, *ACI Journal*, **80** (2) 116–127.

Madsen, H.O. and Egeland, T. (1989) Structural reliability—models and applications, *Int. Stat. Rev.*, **57** (3) 185–203.

Madsen, H.O., Kilcup, R. and Cornell, C.A. (1979) Mean upcrossing rate for stochastic load processes, *Probabilistic Mechanics and Structural Reliability*, ASCE, New York, 54–58.

Madsen, H.O., Krenk, S. and Lind, N.C. (1986) *Methods of Structural Safety*. Prentice Hall, Englewood Cliffs.

Madsen, H.O. and Turkstra, C. (1979) *Residential floor loads—a theoretical and field study*, Report No. ST79-9, Department of Civil Engineering, McGill University.

Madsen, H.O. and Zadeh, M. (1987) Reliability of plates under combined loading, *Proc. Marine Struct. Rel. Symp., SNAME*, Arlington, Virginia, 185–191.

Maes, M.A. (1996) Ignorance factors using model expansion, *J. Engineering Mechanics*, ASCE, **122** (1) 39–45.

Maes, M.A., Breitung, K. and Dupois, D.J. (1993) Asymptotic importance sampling, *Structural Safety*, **12** (3) 167–186.

Mann, N.R., Schafer, R.E. and Singpurwalla, N.D. (1974) *Methods for Statistical Analysis of Reliability and Life Data*, John Wiley, New York.

Marsaglia, G. (1968) Random numbers fall mainly in the planes, *Proc. Nat. Acad. Sci. USA.* **61**, 25–28.

Matheron, G. (1973) The intrinsic random functions, and their applications, *Adv. Appl. Prob.*, **5**: 439–468.

Matheron, G. (1989) *Estimating and Choosing*, Springer, Berlin.

Matousek, M. and Schneider, J. (1976) *Untersuchungen zur Struktur des Sicherheitsproblems bei Bauwerken*, Bericht No. 59, Institut für Baustatik und Konstruktion, Eidgenössiche Technische Hochschule, Zurich.

Matthies, H.G., Brenner, C.E., Bucher, C.G. and Guedes Soares, C. (1997) Uncertainties in probabilistic numerical analysis of structures and solids—Stochastic finite elements, *Structural Safety*, **19** (3) 283–336.

Mayer, H. (1926) *Die Sicherheit der Bauwerke*, Springer, Berlin.

Maymon, G. (1993) Probability of failure of structures without a closed-form failure function, *Computers & Structures*, **49** (2) 301–313.

McGuire, R.K. and Cornell, C.A. (1974) Live load effects in office buildings, *J. Structural Div.*, ASCE, **100** (ST7) 1351–1366.

Meister, S. (1966) Human factors in reliability, *Reliability Handbook*, Ireson, W.G. (Ed), McGraw-Hill, New York.

Melbourne, W.H. (1977) Probability distributions associated with the windloading of structures, *Civ. Engg. Trans. Inst. Engrs. Aust.*, **CE19** (1) 58–67.

Melbourne, W.H. (1998) Comfort criteria for wind-induced motion in structures, *Structural Engg. Intl.*, **8** (1) 40–44.

Melchers, R.E. (1977) Influence of organization on project implementation, *J. Construction Div.*, ASCE, **103** (CO4) 611–625.

Melchers, R.E. (1978) The influence of control processes in structural engineering, *Proc. Inst. Civil Engrs.*, **65**, Part **2**, 791–807.

Melchers, R.E. (1979) Selection of control levels for maximum utility of structures, *Proc. 3rd Int. Conf. on Applications of Statistics and Probability in Soil and Structural Engineering*, Sydney, 839–849.

Melchers, R.E. (1980) Societal options for assurance of structural performance, *Final Report, 11th Congr. IABSE*, London, 983–988.

Melchers, R.E. (1981) *On Bounds and Approximations in Structural Systems Reliability*, Research Report No. 1/1981, Department of Civil Engineering, Monash University, Australia.

Melchers, R.E. (1983a) Reliability of parallel structural systems, *J. Structural Div.*, ASCE, **109** (11) 2651–2665.

Melchers, R.E. (1983b) Static theorem approach to the reliability of parallel plastic structures, *Proc. 4th Int. Conf. on Applications of Statistics and Probability in Soil and Structural Engineering*, Vol. 2, Augusti, G., Borri, A., and Vannuchi, G. (Eds), Pitagora Editrice, Bologna, 1313–1324.

Melchers, R.E. (1984) *Efficient Monte-Carlo Probability Integration*, Research Report No. 7/1984. Department of Civil Engineering, Monash University, Australia.

Melchers, R.E. (1989a) Improved importance sampling for structural reliability calculation, *Proc. 5th International Conference on Structural Safety and Reliability*, Ang, A. H.-S. Shinozuka, M. and Schuëller, G.I. (Eds), ASCE, New York, 1185–1192.

Melchers. R.E. (1989b) Discussion to Bucher (1988) *Structural Safety*, **6** (1) 65–66.

Melchers, R.E. (1990a) Search-based importance sampling, *Structural Safety*, **9** (2) 117–128.

Melchers, R.E. (1990b) Radial importance sampling for structural reliability, *J. Engineering Mechanics*, ASCE, **116** (1) 189–203.

Melchers, R.E. (1991) Simulation in time-invariant and time-variant reliability problems, *Proc. 4th IFIP Conference on Reliability and Optimization of Structural Systems*, Rackwitz, R. and Thoft-Christensen P. (Eds), Springer, Berlin, 39–82.

Melchers, R.E. (1992) Load space formulation of time dependent structural reliability, *J. Engineering Mechanics*, ASCE, **118** (5) 853–870.

Melchers, R.E. (1993) Society, tolerable risk and the ALARP principle, *Probabilistic Risk and Hazard Assessment*, Melchers, R.E. and Stewart, M.G. (Eds), Balkema, Rotterdam, 243–252.

@Seismicisolation

Melchers, R.E. (1994), Structural System Reliability Assessment using Directional Simulation, *Structural Safety*, **16** (1 & 2) 23–39.

Melchers, R.E. (1995a) Human errors in structural reliability, *Probabilistic Structural Mechanics Handbook*, C. (Raj) Sundararajan (Ed), Chapman and Hall, New York, 211–237.

Melchers, R.E. (1995b) Load space reliability formulation for Poisson pulse processes, *J. Engineering Mechanics*, ASCE, **121** (7) 779–784.

Melchers, R.E. (1997) Modeling of marine corrosion of steel specimens, *Corrosion Testing in Natural Waters*; Second Volume, Kain, R.M. and Young, W.T. (Eds), ASTM STP 1300, Philadelphia, 20–33.

Melchers, R.E. (1998a) Load path dependence in directional simulation in load space, *Proc. 8th IFIP WG7.5 Conf. Reliability and Optimization of Structural Systems*, Krakow, Poland.

Melchers, R.E. (1998b) Corrosion Uncertainty Modelling for Steel Structures, *J. Const. Steel Res.*

Melchers, R.E. (2001) On the ALARP approach to risk management, *Reliability Engineering and System Safety*, **71**: 201–208.

Melchers, R.E. (2008a) Reliability of aged land-based structures, (In) *Condition Assessment of Aged Structures*, Paik, J.K. and Melchers, R.E. (Eds.), Woodhead Publishing Ltd, Cambridge, 352–363.

Melchers, R.E. (2008b) Chapter 4, Corrosion wastage in aged structures, (In) *Condition Assessment of Aged Structures*, Paik, J.K. and Melchers, R.E. (Eds.), Woodhead Publishing Ltd, Cambridge, 77–106.

Melchers, R.E. (2013) Human intervention and the safety of complex structural systems, *Civil Engineering and Environmental Systems*, **30** (3–4) 211–220.

Melchers, R.E. (2014a) Bi-modal trend in the long-term corrosion of aluminium alloys, *Corrosion Science*, **82**: 239–247.

Melchers, R.E. (2014b) Long-term immersion corrosion of steels in seawaters with elevated nutrient concentration, *Corrosion Science*, **81**: 110–116.

Melchers, R.E. (2015a) Bi-modal trends in the long-term corrosion of copper and copper alloys, *Corrosion Science*, **95**: 51–61.

Melchers, R.E. (2015b) Chapter 23: Progression of pitting corrosion and structural reliability of welded steel pipelines, (in) *Oil and Gas Pipelines: Integrity and Safety Handbook*, edited by R. Winston Revie, John Wiley & Sons, Hoboken, 327–341.

Melchers, R.E., Baker, M.J. and Moses, F. (1983) Evaluation of experience, *Quality Assurance within the Building Process*, Report No. 47, IABSE, 21–38.

Melchers R.E. and Chaves I.A. (2016) A study of initiation and active reinforcement corrosion in conventional reinforced concrete, *Proc. Australasian Corrosion Conference*, Auckland, NZ, Australasian Corrosion Association, Melbourne, Paper 52.

Melchers, R.E. and Chaves, I.A. (2017) A comparative study of chlorides and longer-term reinforcement corrosion. *Materials and Corrosion*, **68** DOI: 10.1002/maco.201609310.

Melchers, R.E. and Jeffrey, R.J. (2014) Corrosion of steel piling in seawater harbours, *Proc. Instn. of Civil Engineers, Maritime Engineering*, **167,** MA4, 159–172.

Melchers, R.E. and Li, C.Q. (1994) Discussion of Engelund, S. and Rackwitz, R. (1993), *Structural Safety*, **14** (4) 299–302.

Melchers, R.E. and Li, C.Q. (2006). Phenomenological modeling of corrosion loss of steel reinforcement in marine environments, *ACI Materials Journal*, **103** (1) 25–32.

Melchers, R.E. and Li, C.Q. (2009a). Reinforcement corrosion in concrete exposed to the North Sea for over 60 years, *Corrosion*, **65** (8) 554–566.

Melchers, R.E. and Li, C.Q. (2009b). Reinforcement corrosion initiation and activation times in concrete structures exposed to severe marine environments, *Cement and Concrete Research*, **39**: 1068–1076.

Melchers, R.E., Li, C.Q. and Lawanwisut, W. (2008) Probabilistic modelling of structural deterioration of reinforced concrete beams under saline environment corrosion, *Structural Safety*, **30** (5) 447–460.

Melchers, R.E. and Tang, L.K. (1983) *Reliability of Structural Systems with Stochastically Dominant Modes*, Research Report No. 2/1983, Department of Civil Engineering, Monash University, Australia.

Melchers, R.E. and Tang, L.K. (1984) Dominant failure modes in stochastic structural systems, *Structural Safety*, **2**, 127–143.

Melchers, R.E. and Tang, L.K. (1985a) Failure modes in complex stochastic systems, *Proc. 4th Int. Conf. on Structural Safety and Reliability*, Vol. 1, Kobe, Japan, 97–106.

Melchers, R.E. and Tang, L.K. (1985b) Reliability analysis of multi-member structures, *NUMETA'85, Proc. Int. Conf. on Numerical Methods in Engineering Theory and Applications*, A. A. Balkema, 763–772.

Menzies, J.B. (1996) Bridge safety targets and needs for performance feedback, *Structural Reliability in Bridge Engineering: Design, Inspection, Assessment, Rehabilitation and Management*, Frangopol, D.M. and Hearn, G. (Eds), McGraw-Hill, New York, 156–161.

Mettem, C.J. and Tietz, S. (1999) Demystifying Limit States Design in timber: Practice update, *The Structural Engineer*, **77** (15) 13-18.

Micic, T.V., Chryssanthopoulos, M.K. and Baker, M.J. (1995) Reliability analysis for highway bridge deck assessment, *Structural Safety*, **17** (3) 135–150.

Milton, R.C. (1972) Computer evaluation of the multivariate normal integral, *Technometrics*, **14** (4) 881–889.

Mirza, S.A. (1996) Reliability-based design of reinforced concrete columns, *Structural Safety*, **18** (2&3) 179–194.

Mirza, S.A., Hatzinikolas, M. and McGregor, J.G. (1979) Statistical descriptions of strength of concrete, *J. Structural Division*, ASCE, **105** (ST6) 1021–1037.

Mirza, S.A. and MacGregor, J.G. (1979a) Variations in dimensions of reinforced concrete members, *J. Structural Div.*, ASCE, **105** (ST4) 751–766.

Mirza, S.A. and MacGregor, J.G. (1979b) Variability of mechanical properties of reinforcing bars, *J. Structural Div.*, ASCE, **105** (**ST5**) 921–937.

Mitchell, G.R. and Woodgate, R.W. (1971a) *Floor Loading in Office Buildings—The Results of a Survey*, Building Research Current Paper 3/71, Building Research Station, Department of the Environment, Watford, UK.

Mitchell, G.R. and Woodgate, R.W. (1971b) *Floor Loading in Retail premises—the Results of a Survey*, Building Research Current Paper 24/71, Building Research Station, Department of the Environment, Watford, UK.

Mitchell, G.R. and Woodgate, R.W. (1977) *Floor Loading in Domestic Premises—the Results of a Survey*, Building Research Current Paper 2/77, Building Research Station, Department of the Environment, Watford, UK.

Mitteau, J.-C. (1996) Error estimates for FORM and SORM computations of failure probability, *Proc. Speciality Conf. Probabilistic Mechanics and Structural Reliability*, Worcester, MA, ASCE, 562–565.

Moarefzadeh, M.R. and Melchers, R.E. (1996a) Sample-specific linearization in reliability analysis of off-shore structures, *Structural Safety*, **18** (2 & 3) 101–122.

Moarefzadeh, M.R. and Melchers, R.E. (1996b) *Non-linear wave theory in reliability analysis of off-shore structures*, Research Report No. 139.7.1996, Department of Civil Engineering and Surveying, The University of Newcastle, Australia.

Moarefzadeh, M.R. and Melchers, R.E. (1996c) Directional simulation applied to idealized off-shore structures, Proc. 7th IFIP WG 7.5 Conference on *Reliability and Optimization of Structural Systems*, (Eds) D.M. Frangopol, R.B. Corotis and R. Rackwitz, Springer Verlag, 247–254.

Mori, Y. and Ellingwood, B.R. (1993a) Time-dependent system reliability analysis by adaptive importance sampling, *Structural Safety*, **12** (1) 59–73.

Mori, Y. and Ellingwood, B.R. (1993b) Reliability-based service-life assessment of aging concrete structures, *J. Structural Engineering*, ASCE, **119** (5) 1600–1621.

Morison, J.R., O'Brien, M.P. Johnston, J.W. and Schaaf, S.A. (1950) The force exerted by surface waves on piles, *Pet. Trans.*, AIME, **189**, 149–154.

Moses, F. (1969) Approaches to structural reliability and optimization, in: *An Introduction to Structural Optimization*, Cohn, M.Z. (Ed.), Solid Mechanics Division, University of Waterloo, Study No. 1, 81-120.

Moses, F. (1974) Reliability of structural systems, *J. Structural Div.*, ASCE, **100** (ST9) 1813–1820.

Moses, F. (1977) Structural system reliability and optimization, *Computers & Structures*, **7**: 283–290.

Moses, F. (1982) System reliability development in structural engineering, *Structural Safety*, **1** (1) 3–13.

Moses, F. (1996) Bridge evaluation based on reliability, *Structural Reliability in Bridge Engineering: Design, Inspection, Assessment, Rehabilitation and Management*, Frangopol, D.M. and Hearn, G. (Eds), McGraw-Hill, New York, 42–53.

Moses, F. and Kinser, D. E. (1967) Analysis of structural reliability, *J. Structural Div.*, ASCE, **93** (ST5) 147–164.

Moses, F., Lebet, J. and Bez, R. (1994) Applications of field testing to bridge evaluation, *J. Structural Engineering*, ASCE, **120**, 1745–1762.

Moses, F. and Stevenson, J.D. (1970) Reliability-based structural design, *J. Structural Division*, ASCE, **96** (ST2) 221–244.

Murdock, L.J. (1953) The control of concrete quality, *Proc. Inst. Civil Eng.*, **2**, Part **1**, (4) 426–453.

Murotsu, Y., Okada, H. and Matsuzaki, S. (1985) Reliability analysis of frame structures under combined load effects, *Proc. 4th Int. Conf. on Structural Safety and Reliability*, Kobe, Vol. **1**, 117–128.

Murotsu, Y., Okada, H., Taguchi, K., Grimmelt, M. and Yonezawa, M. (1984) Automatic generation of stochastically dominant failure modes of frame structures, *Structural Safety*, **2**, 17–25.

Murotsu, Y., Okada, H., Yonesawa, M. and Kishi, M. (1983) Identification of Stochastically Dominant Failure Models in Frame Structures, *Proc. 4th Int. Conf. on Applications of Statistics and Probability in Soil and Structural Engineering*, Augusti, G., Borri, A., and Vannuchi, O. (Eds), Pitagora Editrice, Bologna, 1325–1338.

@Seismicisolation

Murotsu, Y., Yonesawa, M., Oba, F. and Niwa, K. (1977) Methods for reliability analysis and optimal design of structural systems, *Proc. 12th Int. Symp. on Space Technology and Science*, Tokyo, 1047–1054.

Myers, R.H. (1971) *Response Surface Methodology*, Allyn and Bacon, New York.

Nadolski, V. and Sykora, M. (2015) Model uncertainties in resistance of steel members, (In) Safety and Reliability of Complex Engineering Systems, ESREL2015, (Eds.) Podofillina, L., Sudret, B., Stojadinovic, B., Zio. E. and Kroger, W., Taylor & Francis, London, pp. 4189–4195.

Naess, A., Leira, B.J. and Batsevych, O. (2009) System reliability analysis by enhanced Monte Carlo simulation, *Struct Safety*, **31**: 349–355.

Naess A, Leira B.J., Batsevych O (2012). Reliability analysis of large structural systems, *Prob. Eng. Mechanics* **28**: 164-168.

Nakken, O. and Valsgard, S. (1995) *Life Cycle Costs of Ships Hulls*, Paper Series No. 94-P003, Det Norske Veritas Classification AS.

Nataf, A. (1962) Determination des Distributions dont les Marges sont Donnees, *Comptes Rendus de l'Academie des Sciences*, **225**, 42–43.

NBS (1953) *Probability Tables for the Analysis of Extreme Value Data*, Applied Mathematics Series No. 22, National Bureau of Standards, Washington, DC.

NBS (1959) *Tables of the Bivariate Normal Probability Distribution and Related Functions*, Applied Mathematics Series No. 50, National Bureau of Standards, Washington, DC.

Nessim, M.A. and Jordaan, I.J. (1983) Decision-making for error control in structural engineering, *Proc. 4th Int. Conf. on Applications of Statistics and Probability in Soil and Structural Engineering*, Augusti, G., Borri, A. and Vannuchi, O. (Eds), Pitagora Editrice, Bologna, 713–727.

Newland, D.E. (1984) *An Introduction to Random Vibrations and Spectral Analysis* (2nd Edn) Longman.

Nguyen, T.H., Song, J. and Paulino, G.H. (2010) Single-Loop system reliability-based design optimization using matrix-based system reliability method: Theory and applications, *Journal of Mechanical Design*, **132**: 011005-1-11.

Nocedal, J. and Wright, S. (2006) *Numerical Optimization*, 2nd Edition, Springer, New York.

Nowak, A.S. (1979) Effects of human error on structural safety, *J. Amer. Concrete Inst.*, **76** (9) 959–972.

Nowak, A.S. (1986) (Ed), *Modeling Human Error in Structural Design and Construction*, ASCE, New York.

Nowak, A.S. (1993) Live load model for highway bridges, *Structural Safety*, **13** (1 & 2) 53–66.

Nowak, A.S. and Carr, R.I. (1985) Sensitivity analysis of structural errors, *J. Structural Engineering*, ASCE, **111** (8) 1734–1746.

Nowak, A.S. and Lind, N.C. (1979) Practical bridge code calibration, *J. Structural Div.*, ASCE, **105** (ST12) 2497–2510.

Nowak, A.S., Rakoczy, A.M. and Szeliga, E.K. (2012) *Revised Statistical Resistance Models for R/C Structural Components*, Report ACI SP-284-6, American Concrete Institute, Detroit, pp. 1–16.

Nowak, A.S. and Tharmabala, T. (1988) Bridge reliability evaluation using load tests, *J. Structural Engineering*, ASCE, **114** (10) 2268–2279.

NRCC (1977) *National Building Code of Canada*, National Research Council of Canada, Ottawa.

NSW DEP (2011) *Planning Guidelines for hazardous development*, NSW Department of Planning and Environment, Sydney.

OHBDC (1983) *Ontario Highway Bridge Design Code*, Ontario Ministry of Transport, Canada.

Okasha, N.M. (2016) An improved weighted average simulation approach for solving reliability-based analysis and design optimization problems, *Structural Safety*, **60**: 47–55.

Okasha, N.M. and Frangopol, D.M. (2009) Lifetime-oriented multi-objective optimization of structural maintenance considering system reliability, redundancy and life-cycle cost using GA, *Structural Safety*, **31**: 460–474.

Olagnon, M. and Prevosto, M., (Eds.) (2008) *Rogue Waves 2008 Workshop*, Proceedings, IFREMER, Brest.

Olsson, A., Sandberg, G. and Dahlblom, O. (2003) On Latin hypercube sampling for structural reliability analysis, *Structural Safety*, **25**: 47–68.

Orcesi, A.D. and Frangopol, D.M. (2011) Use of lifetime functions in the optimization of nondestructive inspection strategies for bridges, *J. Struct. Engrg.* **137** (4) 531–539.

Osborne, A.F. (1957) *Applied Imagination: Principles and Practices of Creative Thinking*, Scribners, New York.

Ostlund, L. (1993) Load combination in codes, *Structural Safety*, **13** (1 & 2) 83–92.

Oswald, G.F. and Schuëller, G.I. (1983) On the reliability of deteriorating structures, *Proc. 4th Int. Conf. on Applications of Statistics and Probability in Soil and Structural Engineering*, Augusti, G., Borri, A. and Vannuchi, O. (Eds), Pitagora Editrice, Bologna, 597–608.

Otway, H.J., Battat, M.E., Lohrding, R.K., Turner, R.D. and Cubitt, R.L. (1970) *A Risk Analysis of the Omega West Reactor*, Report No. LA 4449, Los Alamos Scientific Laboratory, University of California, Los Alamos, CA.

Owen, D.B. (1956) Tables for computing bivariate normal probabilities, *Ann. Math. Stat.*, **27**, 1075–1090.

Owen, D.B. (1980) A Table of Normal Integrals. Communications in Statistics, *Simulation and Computation B*, **9** (2), 389–419.

Paik. J.K. and Melchers, R.E. (Eds.) (2008) *Condition Assessment of Aged Structures*, Woodhead Publishing, Cambridge.

Paloheimo, E. and Hannus, M. (1974) Structural design based on weighted fractiles, *J. Structural Div.*, ASCE, **100** (ST7) 1367–1378.

Pandey, M.D. (1998) An effective approximation to evaluate multinormal integrals, *Structural Safety*, **20** (1) 51–67.

Pandey, M.D. and Nathwani, J.S. (2004) Life quality index for the estimation of societal willingness-to-pay for safety, *Structural Safety*, **26** (2) 181–199.

Papoulis, A. (1965) *Probability, Random Variables and Stochastic Processes*, McGraw-Hill, New York.

Parkinson, D.B. (1980) Computer solution for the reliability index, *Engineering Structures*, **2**, 57–62.

Parzen, E. (1962) *Stochastic Processes*, Holden-Day.

Pearce, H.T. and Wen, Y.K. (1984) Stochastic combination of load effects, *Journal of Structural Engineering*, **110** (7) 1613–1629.

Pearson, E.S. and Johnson, N.L. (1968) *Tables of the Incomplete Beta Function* (2nd Edn), Cambridge University Press.

Pedroni, N. and Zio, E. (2009) Functional failure analysis of a thermal-hydraulic passive system by means of line sampling, *Reliab. Engrg. System Safety*, **94**: 1764–1781.

Petrini, F. and Ciampoli, M. (2012) Performance-based wind design of tall buildings, *Structure and Infrastructure Engineering*, **8** (10) 954–966.

Petroski, H. (1992) *To Engineer Is Human: The Role of Failure in Successful Design*, 1st Vintage Books, New York.

Petroski, H. (2012) *To Forgive Design: Understanding Failure*, Harvard University Press, Cambridge, MA.

Pham, L. (1985) Load combinations and probabilistic load models for limit state codes, *Civ. Engg. Trans. Inst. Engrs. Aust.*, **CE27**, 62–67.

Pham, L., Holmes, J.D. and Leicester, R.H. (1983) Safety indices for wind loading in Australia, *J. Wind Engg. Indust. Aerodyn.*, **14**, 3–14.

Philpot, T.A., Rosowsky, D.V. and Fridley, K.J. (1993) Serviceability design in LRFD for wood, *J. Structural Div.*, ASCE, **119** (12), 3649–3667.

Piak, J.K., Kim, S.K., Yang, S.H. and Thayamballi, A.K. (1997) Ultimate strength reliability of corroded ship hulls, *Trans. Royal Inst. Naval Arch.*, **137**, 1–14.

Pier, J.-C., and Cornell, C.A. (1973) Spatial and temporal variability of live loads, *J. Structural Div.*, ASCE, **99** (ST5) 903–922.

Pierson, W.J. and Moskowitz, L. (1964) A proposed spectral form for fully developed wind seas based on the similarity theory of S. A. Kitaigorodskii, *J. Geophys. Res.*, **69** (24) 5181–5190.

Popper, K.R. (1959) *The Logic of Scientific Discovery*, Basic Books, New York.

Pradlwarter, H.J., Pellissetti, M.F., Schenk. C.A., Schueller, G.I., Kreis, A., Fransen, S., Calvi, A. and Klein, M. (2005) Realistic and efficient reliability estimation for aerospace structures, *Comput. Meth. Appl. Mech. Eng.* **194**: 1597–1617.

Pradlwarter, H.J. Schueller, G.I., Koutsourelakis, P.S. and Charmpis, D.C. (2007) Application of line sampling simulation method to reliability benchmark problems, *Structural Safety*, **29**: 208–221.

Press, W.H., Teukolsky, S.A., Vetterling, W.T. and Flannery, B.P. (2007), *Numerical Recipes: The Art of Scientific Computing* (3rd ed.), Cambridge University Press, New York.

Prest, A.R. and Turvey, R. (1965) Cost Benefit Analysis: A Survey, *Econ. J.*, 685–735.

Provan, J. (ed.) (1987) *Probabilistic Fracture Mechanics and Reliability*, Martinus Nijhoff, Dordrecht, The Netherlands.

Pugsley, A.G. (1962) *Safety of Structures*, Edward Arnold, London.

Pugsley, A.G. (1973) The prediction of proneness to structural accidents, *Structural Engineer*, **51** (6) 195–196.

Pugsley, A. et al., (1955) Report on structural safety, *Structural Engineer*, **33** (5) 141–149.

Rackwitz, R. (1976) *Practical Probabilistic Approach to Design*, Bulletin d'Information No. 112, Comité Européen du Béton, Paris.

Rackwitz, R. (1977) *Note on the Treatment of Errors in Structural Reliability*, Berichte zur Sicherheitstheorie der Bauwerke, SFB 96, Vol. 21, Technical University, Munich.

Rackwitz, R. (1984) Failure rates for general systems including structural components, *Reliab. Engg.*, **9**, 229–242.

Rackwitz, R. (1985a) Reliability of systems under renewal pulse loading, *J. Engineering Mechanics*, ASCE, **111** (9) 1175–1184.

Rackwitz, R. (1985b) Predictive distribution of strength under control, *Materiaux et Construction*, **16** (94) 259–267.

Rackwitz, R. (1993) On the combination of non-stationary rectangular wave renewal processes, *Structural Safety*, **13** (1+2) 21–28.

Rackwitz, R. (1996) Static properties of reinforcing steel, *Working Notes, JCSS Probabilistic Model Code*, Part 3: Resistance Models, Second draft.

Rackwitz, R. (2001) Optimizing systematically renewed structures, *Reliability Engineering and System Safety*, **73**, 269–279.

Rackwitz, R. (2002) Optimization and risk acceptability based on the Life Quality Index, *Structural Safety*, **24**: 297–331.

Rackwitz, R. (2004) *Life quality index revisited, Structural Safety*, **26**: 443–451.

Rackwitz, R. and Fiessler, B. (1978) Structural reliability under combined random load sequences, *Computers and Structures*, **9**, 489–494.

Rackwitz, R. and Joanni, A. (2009) Risk acceptance and maintenance optimization of aging civil engineering infrastructures, *Structural Safety*, **31**: 251–259.

Rajashekhar, M.R. and Ellingwood, B.R. (1993) A new look at the response surface approach for reliability analysis, *Structural Safety*, **12** (3) 205–220 (see also Discussion (1994), *Structural Safety*, **16** (3) 227–230).

Rakoczy, A.M. and Nowak, A.S. (2013) Resistance model of lightweight concrete members, *Materials Journal*, ACI, **110** (1): 99-108.

Ramachandran, K. (1984) Systems bounds: A critical study, *Civil Engg. Systems*, **1**, 123–128.

Rand Corporation (1955) *A Million Random Digits with 1,000,000 Normal Deviates*, Free Press, New York.

Rao, N.R.N., Lohrman, M. and Tall, L. (1966) The effect of strain rate on the yield stress of structural steels, *ASTM, J. Mater.*, **1** (1) 241–262.

Rao, S.S. (2009) *Engineering Optimization: Theory and Practice*, 4th Edition, Wiley, New York.

Rashki, M., Miri, M. and Moghaddam, M.A. (2012) A new efficient simulation method to approximate the probability of failure and most probable point, *Structural Safety*, **39**: 22–29.

Rashki, M., Miri, M. and Moghaddam, MA. (2014a) A simulation-based method for reliability based design optimization problems with highly nonlinear constraints, *Autom Constr.*, **47**: 24–36.

Rashki, M., Miri, M. and Moghaddam, M.A. (2014b) Closure to "A new efficient simulation method to approximate the probability of failure and most probable point". *Structural Safety*, **46**: 15–16.

Ravindra, M.K. and Galambos, T.V. (1978) Load and resistance factor design for steel, *J. Structural Div.*, ASCE, **104** (ST9) 1337–1353.

Ravindra, M.K., Heany, A.C., and Lind, N.C. (1969) Probabilistic evaluation of safety factors, *Symp. on Concepts of Safety of Structures and Methods of Design*, Final Report, IABSE, London, 36–46.

Reason, J. (1990) *Human Error*, Cambridge University Press, Cambridge.

Rebelo, C., Lopes, N., Simões da Silva, L., Nethercot, D. and Vila Real, P.M.M. (2009) Statistical evaluation of the lateral–torsional buckling resistance of steel I-beams, Part 1: Variability of the Eurocode 3 resistance model, *J. Construct. Steel Res.* **65** (4) 818–831.

Reid, S.G. (1997) Probability-based patterned live load for design, *Structural Safety*, **19** (1) 37–52.

Reid, S.G. and Caprani, C.C. (2014) Influence on bridge reliability of uncertainty in estimated traffic load effects, (In) Deodatis, G., Ellingwood, B.R. and Frangopol, D.M. (Eds.) *Safety, Reliability, Risk and Life-Cycle Performance of Structures and Infrastructures*, Taylor & Francis, London, 3787–3793.

Reid, S.G. and Turkstra, C.J. (1980) *Serviceability Limit States—Probabilistic Description*, Report No. ST80-1, McGill University, Montreal.

Rice; S.O. (1944) Mathematical analysis of random noise, *Bell System Tech. J.*, **23**, 282–332; (1945), **24**, 46–156. Reprinted in Wax, N. (1954) *Selected Papers on Noise and Stochastic Processes*, Dover Publications.

Riera, J.D. and Rocha, M.M. (1997) Implications of phenomenological uncertainty in engineering reliability assessments, *Proc. Int. Conf. on Structural Safety and Reliability*, Kobe.

Ritter, M.A. and Nowak, A.S. (1994) LRFD provisions for wood bridges, *Structures Congress 12*, American Society of Civil Engineers, Vol. **1**, 549–554.

Rockafellar, R.T. and Royset, J.O. (2010) On buffered failure probability in design and optimization of structures, *Rel. Eng. & System Safety*, **95**: 499–510.

Romero, V.J., Swiler, L.P. and Giunta, A.A. (2004) Construction of response surfaces based on progressive-lattice-sampling experimental designs with applications to uncertainty propagation, *Struct. Safety*, **26** (2) 201–219.

Rosenblatt, M. (1952) Remarks on a multivariate transformation, *Ann. Math. Stat.*, **23**, 470–472.

Rosenblueth, E. (1976a) Optimum design for infrequent disturbances, *J. Struct. Div.* ASCE **102** (9) 1807–1825.

Rosenblueth, E. (1976b) Towards optimum design through building codes, *J. Struct. Div.* ASCE, **102** (3) 591–607.

Rosenblueth, E. (1985a) Discussion of Ditlevsen, O., Fundamental postulate in structural safety, *J. Engineering Mechanics*, ASCE, **111** (1) 109.

Rosenblueth, E. (1985b) On computing normal reliabilities, *Structural Safety*, **2** (3) 165–167.

Rowe, W. D. (1977) *An Anatomy of Risk*, John Wiley & Sons, New York.

Royal Society Study Group (1991) *Risk: analysis, perception and management*, The Royal Society, London.

Royset, J.O., Der Kiureghian, A. and Polak, E. (2001) Reliability-Based Optimal Design of Series Structural Systems, *J. Eng. Mech.* **127** (6), 607–614.

Royset, J.O. and Polak, E. (2004) Reliability-based optimal design using sample average approximations, *Prob. Eng. Mech.* **19**: 331–343.

Rubinstein, R. Y. (1981) *Simulation and the Monte Carlo Method*, John Wiley & Sons, New York.

Rüsch, H. and Rackwitz, R. (1972) The significance of the concept of probability of failure as applied to the theory of structural safety, *Development—Design—Construction*, Held und Francke Bauaktiengesellschaft, Munich.

Rüsch, H., Sell, R. and Rackwitz, R. (1969) *Statistical Analysis of Concrete Strength*, Deutscher Ausschuss für Stahlbeton, No. 206, Berlin (in German).

Russell, L.R. and Schuëller, G.I. (1974) Probabilistic models for Texas Gulf coast hurricane occurrences, *J. Pet. Tech.*, **279–288**.

Ruszczynski, A. and Shapiro, A. (2003) *Stochastic Programming*, Elsevier, New York.

Rzhanitzyn, R. (1957) It is Necessary to Improve the Standards of Design of Building Structures, *A Statistical Method of Design of Building Structures*, Allan, D. E. (transl.), Technical Translation No. 1368, National Research Council of Canada, Ottawa.

Santner, T.J., Williams, B.J. and Notz, W.I. (2003) *The Design and Analysis of Computer Experiments*, Springer, New York.

Santos, S.R. and Beck, A.T. (2015) A benchmark study on intelligent sampling techniques in Monte Carlo Simulation, *Latin American Journal of Solids and Structures*, **12**: 624–648.

Santos, S.R., Matioli, L.C. and Beck, A.T. (2012) New Optimization Algorithms for Structural Reliability, *Computer Modeling in Engineering & Sciences*, **83**: 23-55.

Sarpkaya, T. and Isaacson, M. (1981) *Mechanics of Wave Forces on Offshore Structures*, Van Nostrand Reinhold, New York.

Schall, G., Faber, M.H. and Rackwitz, R. (1991) The ergodicity assumption for sea states in the reliability estimation of offshore structures, *Journal of Offshore Mechanics and Arctic Engineering*, **113**: 241–246.

Schijve, J. (1979) Four lectures on fatigue crack growth, *Engg. Fract. Mech.*, **11**, 167–221.

Schittkowskii, K. (1980) *Nonlinear Programming Codes: Information, Tests, Performance*, Lecture Notes in Economics and Mathematical Systems No. 183, Springer, Berlin.

Schneider, J. (1981) Organization and management of structural safety during design, construction and operation of structures, *Structural Safety and Reliability*, Moan, T. and Shinozuka, M. (Eds), Elsevier, Amsterdam, 467–482.

Schneider, J. (Ed) (1983) *Quality Assurance within the Building Process*, Report No. 47, IABSE, *London.*

Schuëller, G.I. (1981) *Einführung in die Sicherheit und Zuverlässigkeit von Tragwerken*, W. Ernst, Berlin.

Schuëller, G.I. (Ed) (1997) A state-of-the-art report on computational stochastic mechanics, *Prob. Engineering Mechanics*, **12** (4) 203–321.

Schuëller. G.I. (2007) On the treatment of uncertainties in structural mechanics and analysis, *Comput. Struct.* **85**: 235–243.

Schuëller, G.I. and Bucher, C.G. (1991) Computational stochastic structural analysis—a contribution to the software development for the reliability assessment of structures under dynamic loading, *Prob. Engineering Mechanics*, **6** (3–4) 134–138.

Schuëller, G.I. and Choi, H.S. (1977) Offshore platform risk based on a reliability function model, *Proc. 9th Offshore Technology Conf.*, Houston, 473–482.

Schuëller, G.I., Hirtz, H. and Booz, G. (1983) The effect of uncertainties in wind load estimation on reliability assessments, *J. Wind Engg. Indust. Aerodyn.*, **14**, 15–26.

Schuëller, G.I. and Jensen, H.A. (2009) Computational methods in optimization considering uncertainties—an overview, *Computer Methods in Applied Mechanics and Engineering*, **198**: 2–13.

Schuëller, G.I., Pradlwarter, H.J. and Bucher, C.G. (1991) Efficient computational procedures for reliability estimates of MDOF systems, *J. Nonlinear Mechanics*, **26** (6) 961–974.

Schueremans, L. (2001) Probabilistic Evaluation of Structural Unreinforced Masonry, *Doctor of Civil Engineering dissertation*, Katholieke Universiteit Leuven, Belgium.

Schueremans. L. and van Gemert, D. (2004) Assessing the safety of existing structures: Reliability based assessment framework, examples and applications, *J. Civil Engineering and Management*, **10** (2) 131–141.

Schwarz, R. F. (1980) *Beitrag zur Bestimmung der Zuverlässigkeit nichtlinearer Strukturen unter Berücksichtigung kombinierter Stochastischer Einwirkungen*, Doctoral Thesis, Technical University, Munich.

SEAOC (1995) *Vision 2000, Performance based seismic engineering of buildings*, Vols. I and II: Conceptual framework. Sacramento (CA), Structural Engineers Association of California.

Segal, I.E. (1938) Fiducial distribution of several parameters with applications to a normal system, *Proc. Cambridge Philosophical Society*, **34**, 41–47.

Sentler, L. (1974) *A Live Load Survey in Office Buildings and Hotels*, Division of Building Technology, Lund Institute of Technology, Lund.

Sentler, L. (1975) *A Stochastic Model for Live Loads on Floors in Buildings*, Report 60, Division of Building Technology, Lund Institute of Technology, Lund.

Sentler, L. (1976) *Live Load Surveys, a Review with Discussions*, Report 78, Division of Building Technology, Lund Institute of Technology, Lund.

Sexsmith, R.G. and Lind, N.C. (1977) Policies for selection of target safety levels, *Proc. Second Int. Conf. on Structural Safety and Reliability*, Technical University Munich, Werner, Düsseldorf, 149–162.

Shao, S.F. and Murotsu, Y. (1991) Reliability evaluation of methods for systems with complex limit states, *Proc. 4th IFIP Conference on Reliability and Optimization of Structural Systems*, Rackwitz, R. and Thoft-Christensen P. (Eds), Springer, Berlin, 325–338.

Shellard, H.C. (1958) Extreme wind speeds over Great Britain and Northern Ireland, *Meteorol. Mag.*, **87**, 257–265.

Sheppard, W.F. (1900) On the calculation of the double integral expressing normal correlation, *Trans. Camb. Phil. Soc.*, **19**, 23–66.

Shinozuka, M. (1983) Basic analysis of structural safety, *J. Structural Div.*, ASCE, **109** (3) 721–740.

Shinozuka, M. (1987) Stochastic fields and their digital simulation, *Stochastic Methods in Structural Dynamics*, Schuëller, G.I. and Shinozuka, M. (Eds), Martinus Nijhoff, The Hague.

Shiraishi, N. and Futura, H. (1989) Evaluation of lifetime risk of structures—recent advances of structural reliability in Japan, *Structural Safety and Reliability*, Ang, A. H-S, Shinozuka, M. and Schuëller, G.I. (Eds), ASCE, New York, **3**, 1903–1910.

Shiryaev, A.N., 1996, *Probability*, Second Edition, Springer, New York.

Shooman, M.L. (1968) *Probabilistic Reliability: An Engineering Approach*, McGraw-Hill, New York.

Shreider, Y.A. (Ed) (1966) *The Monte Carlo Method*, Pergamon Press, Oxford.

Sibley, P.G. and Walker, A.C. (1977) Structural accidents and their causes, *Proc. Inst. Civil Engrs.*, **62**, Part 1, 191–208.

Sichani, M.T., Nielsen, S.R.K. and Bucher, C. (2011a) Applications of asymptotic sampling on high dimensional structural dynamic problems, *Struct. Safety*, **33**: 305–316.

Sichani, M.T., Nielsen, S.R.K. and Bucher, C. (2011b) Efficient estimation of first passage probability of high-dimensional nonlinear systems, *Prob. Eng. Mech*, **26**: 539–549.

Sigurdsson, G. Sørensen, J.O. and Thoft-Christensen, P. (1985) *Development of Applicable Methods for Evaluating the Safety of Offshore Structures (Part 1)*, Report No. 8501, Institute of Building Technology and Structural Engineering, Aalborg University Centre, Aalborg, Denmark.

Silk, M.G., Stoneham, A.M. and Temple, J.A. (1987) *The Reliability of Non-destructive Inspection*, Adam Hilger, Bristol.

Silvestri, S., Gasperini, G., Trombetti, T. and Ceccoli, C. (2008) Statistical analysis towards the identification of accurate probability distribution model for the compressive strength of concrete, (in) *Proc. 14th World Congress on Earthquake Engineering*, 12–17 Oct. 2008, Beijing, China.

Simiu, E., Bietry, J. and Filliben, J.J. (1978) Sampling errors in estimation of extreme winds, *J. Structural Div.*, ASCE, **104** (ST3) 491–501.

Simiu, E. and Filliben, J.J. (1980) Weibull distributions and extreme wind speeds, *J. Structural Div.*, ASCE, **106** (ST12) 491–501.

Simiu, E. and Scanlan, R.U. (1978) *Wind Effects on Structures, An Introduction to Wind Engineering*, John Wiley & Sons, New York.

Simões da Silva, L., Rebelo, C., Nethercot, D., Marques, L., Simões, R. and Vila Real, P.M.M. (2009) Statistical evaluation of the lateral-torsional buckling resistance of steel I-beams, Part 2: Variability of steel properties, *J. Construct. Steel Res.* **65** (4) 832–849.

Simpson, R.H. and Riehl, H. (1981) *The Hurricane and its Impact*, Louisiana State University Press.

Skov, K. (1976) *The Calibration Procedure Applied by the NKB Safety Committee*, Bulletin d'Information No. 112, Comité Européen du Béton, Paris, 108–124.

Slepian, D. (1962) The one-sided barrier problem in Gaussian noise, *Bell Syst Tech. J.*, **41** (2) 463–501.

Sobczyk, K. and Spencer, B. F. (1992) *Random Fatigue: From Data to Theory*, Academic Press, New York.

Sokolnikoff, I.S and Redheffer, R. M. (1958) *Mathematics of Physics and Modern Engineering*, McGraw-Hill, New York.

Solari, G. (1993) Gust buffeting I. Peak wind velocity and equivalent pressure, *J. Struct. Engrg*, ASCE, **119** (2) 365–382.

Song, J., and Der Kiureghian, A. (2003) Bounds on system reliability by Linear Programming, *J. Eng. Mech.* **129** (6), 627–636.

Song, J., and Kang, W.-H. (2009) System reliability and sensitivity under statistical dependence by matrix-based system reliability method, *Struct. Safety*, **31** (2), 148–156.

Sørensen, J.D. and Enevoldsen, I. (1993) Sensitivity weaknesses in application of some statistical distributions in First Order Reliability Methods, *Structural Safety*, **12** (4) 315–325.

Sørensen, J.D. and Faber, M.H. (1991) Optimal inspection and repair strategies for structural systems, *Proc. 4th IFIP Conference on Reliability and Optimization of Structural Systems*, Rackwitz, R. and Thoft-Christensen, P. (Eds), Springer, Berlin, 383–394.

Spall, J.C. (2003) *Introduction to Stochastic Search and Optimization*, Wiley Interscience, New York.

Steenbergen, R.D.J.M. and Vrouwenvelder, A.C.W.M. (2010) Safety philosophy for existing structures and partial factors for traffic loads on bridges, *Heron*, **55** (2) 123–140.

Stevenson, J. and Moses, F. (1970) Reliability analysis of frame structures, *J. Structural Div.*, ASCE, **96** (ST11) 2409–2427.

Stewart, M.G. (1991) Safe load tables: a design aid in the prevention of human error, *Structural Safety*, **10**, 269–282.

Stewart, M.G. (1995) Workmanship and its influence on probabilistic models of concrete compressive strength, *ACI Materials Journal*, **92** (4) 361–372.

Stewart, M.G. (1996a) Optimization of serviceability load combinations for structural steel beam design, *Structural Safety*, **18** (2–3) 225–238.

Stewart, M.G. (1996b) Serviceability reliability analysis of reinforced concrete structures, *J. Structural Engineering*, ASCE, **122** (7) 794–803.

Stewart, M.G. (1997) Concrete workmanship and its influence on serviceability reliability, *ACI Materials Journal*, **94** (6) 1–10.

Stewart, M.G. (1998) Reliability-based bridge design and assessment, *Progress in Structural Engineering and Mechanics*, **1** (2) 214–222.

Stewart, M.G. (2001) Effect of construction and service loads on reliability of existing RC structures, *J. Struct. Engrg*, ASCE, **127** (10) 1232–1236.

Stewart, M.G. and Melchers, R.E. (1988) Simulation of human error in a design loading task, *Structural Safety*, **5** (4) 285–297.

Stewart, M.G. and Melchers, R.E. (1989a) Checking models in structural design, *J. Structural Engineering*, ASCE, **116** (ST6) 1309–1324.

Stewart, M.G. and Melchers, R.E. (1989b) Error control in member design, *Structural Safety*, **6** (1) 11–24.

Stewart, M.G. and Melchers, R.E. (1997) *Probabilistic Risk Assessment of Engineering Systems*, Chapman & Hall, London.

Stewart, M.G. and Rosowsky, D.V. (1998) Time-dependent reliability of deteriorating reinforced concrete bridge decks, *Structural Safety*, **20** (1) 91–109.

Stewart, M.G. and Val, D.V. (1998) Effect of proof and prior service loading on bridge reliability, *Proc. Australasian Structural Engineering Conf.*, Auckland, New Zealand.

Stewart, M.G. and Val, D.V. (2003) Multiple limit states and expected failure costs for deteriorating reinforced concrete bridges, *J. Bridge Engrg.* **8** (6) 405–415.

Strauss, A., Bergmeister, K., Hoffmann, S., Pukl, R. and Navak, D. (2008) Advanced life-cycle analysis of existing concrete bridges, *J. Materials in Civil Engrg.* **20** (1) 9–19.

Stroud, A.H. (1971) *Appropriate Calculation of Multiple Integrals*, Prentice-Hall, Englewood Cliffs.

Tabsh, S.W. and Aswad, A. (1995) Statistical properties of plant-produced high strength concrete in compression, *PCI Journal*, **40** (4) 72–76.

Taflanidis, A.A. and Beck, J.L. (2008a) Stochastic subset optimization for optimal reliability problems, *Prob. Eng. Mech.* **23** (2–3) 324–338.

Taflanidis, A.A. and Beck, J.L. (2008b) An efficient framework for optimal robust stochastic system design using stochastic simulation, *Computer Methods in Applied Mechanics and Engineering*, **198**: 88–101.

Taflanidi, A.A. and Beck, J.L. (2009) Stochastic Subset Optimization for reliability optimization and sensitivity analysis in system design, *Computers & Structures*, **87**: 318–331.

Tall, L. (Ed) (1964) *Structural Steel Design*, Ronald Press, New York.

Tall, L. and Alpsten, G.A. (1969) On the scatter of yield strength and residual stresses in steel members, *Symp. on Concepts of Safety of Structures and Methods of Design*, Final Reports, IABSE, London, 151–163.

Tallis, G.M. (1961) The moment generating function of the truncated multi-normal distribution, *J. Royal Statistical Society*, Series B, **23**, 223–229.

Tang, L.K. and Melchers, R.E. (1987a) Improved approximations for multi-normal integral, *Structural Safety*, **4**, 81–93.

Tang, L.K. and Melchers, R.E. (1987b) Dominant mechanisms in stochastic plastic frames, *Reliability Engineering*, **18**, (2) 101–116.

Tang, L.K. and Melchers, R.E. (1988) Incremental formulation for structural reliability analysis, *Civil Engg. Systems*, **5**, 153–158.

Tang, W.H. (1973) Probabilistic updating in reliability analysis, *J. Testing and Evaluation*, ASTM, **1**(6) 459-467.

Terada, S. and Takahashi, T. (1988) Failure-conditioned reliability index, *J. Structural Engineering*, ASCE, **114** (4) 943–952.

Terza, J.V. and Welland, U. (1991) A comparison of bivariate normal algorithms, *J. Statist. Comput. Simul.* **39**, 115–127.

Thoft-Christensen, P., Jensen, F.M., Middleton, C. and Blackmore, A. (1996) Revised rules for concrete bridges, *International Symposium on the Safety of Bridges*, Institution of Civil Engineers and Highways Agency, London, UK, **4-5** July, 1–12.

Thoft-Christensen, P. and Murotsu, Y. (1986) *Application of Structural System Reliability Theory*, Springer, Berlin.

Thoft-Christensen, P. and Sørensen, J.D. (1982) *Calculation of Failure Probabilities of Ductile Structures by the Unzipping Method*, Report No. 8208, Institute for Building Technology and Structural Engineering, Aalborg University Centre, Aalborg, Denmark.

Thoft-Christensen, P. and Sørensen, J.D. (1987) Optimal strategies for inspection and repair of structural systems, *Civil Engineering Systems*, **4**, 94–100.

Thom, H.C.S. (1968) New distributions of extreme winds in the United States, *J. Structural Div.*, ASCE, **94** (ST7) 1787–1802.

Tichy. M, (1994) First-order third-moment reliability method, *Structural Safety*, **16** (4) 189–200.

Tickell, R.G. (1977) Continuous random wave loading on structural members, *Structural Engineer*, **55** (5) 209–222.

Tribus, M. (1969) *Rational Descriptions, Decisions and Designs* (2nd Edn), Macmillan, New York.

Tu, J., Choi, K.K. and Park, Y.H. (1999) A new study on reliability-based design optimization, *Journal of Mechanical Design*, **121** (4) 557–564.

Turkstra, C.J. (1970) *Theory of Structural Design Decisions Study No. 2*, Solid Mechanics Division, University of Waterloo, Waterloo, Ontario.

Turkstra, C.J. and Daley, M.J. (1978) Two-moment structural safety analysis, *Can. J. Civil Engg.*, **5**, 414–426.

Turkstra, C.J. and Madsen, H.O. (1980) Load combinations in codified structural design, *J. Structural Div.*, ASCE, **106** (ST12) 2527–2543.

Tvedt, L. (1985) *On the Probability Content of a Parabolic Failure Set in a Space of Independent Standard Normal Distributed Random Variables*, Veritas Report, Det Norske Veritas, Hovik.

Tvedt, L. (1990) Distribution of quadratic forms in normal space—application to structural reliability, *J. Engineering Mechanics*, ASCE, **116** (6) 1183–1197.

Val, D.V. (2004) Effect of different limit states on life-cycle cost of RC structures in corrosive environments, *J. Infrastructure Systems*, **11** (4) 231–240.

Val, D.V. (2007) Deterioration of strength of RC beams due to corrosion and its influence on beam reliability, *J. Struct. Engrg.*, **133** (9) 1297–1306.

Val, D.V. and Melchers, R.E. (1997) Reliability of deteriorating RC slab bridges, *J. Structural Engineering*, ASCE, **123** (12) 1638–1644.

Val, D.V., Stewart, M.G. and Melchers, R.E. (1998a) Assessment of existing RC structures: statistical and reliability issues, *Proc. Second International RILEM Conference on the Rehabilitation of Structures*, Melbourne.

Val, D.V., Stewart, M.G. and Melchers, R.E. (1998b) Effect of reinforcement corrosion on reliability of highway bridges, *Engineering Structures* , **20** (11) 1010–1019.

Valdebenito, M.A. and Schuëller, G.I. (2011) Efficient strategies for reliability-based optimization involving non-linear, dynamical structures, *Computers & Structures*, **89**: 1797–1811.

Vanmarcke, E.H. (1973) Matrix formulation of reliability analysis and reliability-based design, *Computers and Structures*, **3**, 757–770.

Vanmarcke, E.H. (1975) On the distribution of the first-passage time for normal stationary processes, *J. Applied Mech.*, ASME, **42**, 215–220.

Vanmarcke, E.H. (1983) *Random Fields*, Massachusetts Institute of Technology Press, Cambridge, MA.

Vanmarcke, E., Shinozuka, M., Nakagiri, S., Schuëller, G.I. and Grigoriu, M. (1986) Random fields and stochastic finite elements, *Structural Safety*, **3**, 143–166.

Veneziano, D. (1974) *Contributions to Second Moment Reliability*, Research Report No. R74-33, Department of Civil Engineering, Cambridge, MA.

Veneziano, D. (1976) *Basic Principles and Methods of Structural Safety*, Bulletin d'Information No. 112, Comité Européen du Béton, Paris, 212–288.

Veneziano, D. Casciati, F. and Faravelli, L. (1983) Methods of seismic fragility for complicated systems, *Proc. Second Conf. on the Safety of Nuclear Installations* (CSNI), Specialist meeting on Probabilistic Methods in Seismic Risk Assessment for NPP, Livermore, California.

Veneziano, D., Galeota, D. and Giammatteo, M.M. (1984) Analysis of bridge proof-load data I: Model and statistical procedures, *Structural Safety*, **2**, 91–104.

Veneziano, D., Grigoriu, M. and Cornell, C.A. (1977) Vector-process models for system reliability, *J. Engineering Mechanics Div.*, ASCE, **103**, (EM3) 441–460.

Vrouwenvelder, A.C.M. (1983) *Monte Carlo Importance Sampling—Application to Structural Reliability Analysis*, TNO-IBBC, Report No. B-83-529/62.6.0402, Rijswijk, Netherlands.

Vrouwenvelder, A.C.M. (1997) The JCSS probabilistic model code, *Structural Safety*, **19** (3) 245–251.

Vrouwenvelder, A.C.M. and Waarts, P.H. (1992) *Traffic Flow Models*, TNO Report No. B-91-0293, TNO Building and Construction Research, Delft.

Vu, K.A. and Stewart, M.G. (2005) Predicting the likelihood and extent of reinforced concrete corrosion-induced cracking, *Journal of Structural Engineering, ASCE*, **131** (11): 1681–1689.

Wadsworth, G.P. and Bryan, J.G. (1974) *Applications of Probability and Random Variables* (2nd Edn.), McGraw-Hill, New York.

Walker, A.C. (1981) Study and analysis of the first 120 failure cases, *Structural Failures in Buildings*, Institution of Structural Engineers, 15–39.

Wang, W., Corotis, R.B. and Ramirez, M.R. (1995) Limit states of load-path-dependent structures in basic variable space, *J. Engineering Mechanics*, ASCE, **121** (2) 299–308.

Wang, W., Ramirez, M.R. and Corotis, R.B. (1994) Reliability analysis of rigid-plastic structures by the static approach, *Structural Safety*, **15** (3) 209–235.

Wang, Y., Mallahzadeh, M.K., Abu Hussain, M.K., Mohd Zaki, Ni.I. and Hajafian, G. (2013) Probabilistic modelling of extreme offshore structural response due to random wave loading, *Proc. Offshore Mechanics and Arctic Engineering Conf.*, Vol. 2B: Structures, Safety and Reliability, Nantes, France, paper 10905. (ISBN 978-0-7918-5533-1).

Warner, R.F. and Kabaila, A.P. (1968) Monte Carlo study of structural safety, *J. Structural Div.*, ASCE, **94** (ST12) 2847–2859.

Warr, P.B. (1971) *Psychology at Work*, Penguin Books, Harmondsworth.

Watwood, V.B. (1979) Mechanism generation for limit analysis of frames, *J. Structural Div.*, ASCE, **109** (ST1) 1–15.

Waugh, C. B. (1977) *Approximate Models for Stochastic Load Combination*, Report No. R77-1, 562, Department of Civil Engineering, Massachusetts Institute of Technology, Cambridge, MA.

Weibull, W. (1939) A statistical theory of the strength of materials, *Proc. Roy. Swed. Inst. Engg. Res.*, **15**.

Weigel, R.L. (1964) *Oceanographical Engineering*, Prentice-Hall, Englewood Cliffs, NJ.

Wen, Y.-K. (1977a) Statistical combination of extreme loads, *J. Structural Div.*, ASCE, **103** (ST5) 1079–1093.

Wen, Y.-K. (1977b) Probability of extreme load combination, *J. Structural Div.*, ASCE, **104** (ST10) 1675–1676.

Wen, Y.-K. (1981) A clustering model for correlated load processes, *J. Structural Div.*, ASCE, **107** (ST5) 965–983.

Wen, Y.-K. (1983) Wind direction and structural reliability: I, *J. Structural Engineering*, ASCE, **109**, 1028–1041.

Wen, Y.-K. (1984) Wind direction and structural reliability: II, *J. Structural Engineering*, ASCE, **110**, 1253–1264.

Wen, Y.-K. (1990) *Structural Load Modeling and Combination for Performance and Safety Evaluation*, Elsevier Science Publishers, Amsterdam.

Wen, Y.-K. and Chen, H.C. (1987) On fast integration for time variant structural reliability, *Prob. Engineering Mechanics*, **2** (3) 156–162.

Wen, Y.-K. and Kang Y.J. (2001a) Minimum building life-cycle cost design criteria i: methodology, *Journal of Structural Engineering*, ASCE, **127** (3) 330–337.

Wen, Y.-K. and Kang Y.J. (2001b) Minimum building life-cycle cost design criteria II: Applications, *Journal of Structural Engineering*, ASCE, **127** (3) 338–346.

Wickham, A. (1985) Reliability analysis techniques for structures with time-dependent strength parameters, *Proc. 4th Int. Conf. on Structural Safety and Reliability*, Kobe, Vol. **3**, 543–552.

Winterstein, S. and Bjerager, P. (1987) The use of higher moments in reliability estimation, *Proc. 5th Intl. Conf. Applications Stats. and Probability*, Vancouver, 1027–1036.

Wirsching, P. (1998) Fatigue reliability, *Progress in Structural Engineering and Materials*, **1** (2) 200–206.

Wu, B. (2013) Reliability *Analysis of Dynamic Systems*, Academic Press, Amsterdam.

Wu, Y.-T., Millwater, H.R. and Cruse, T.A. (1990) Advanced probabilistic structural analysis method for implicit performance functions, *AIAA Journal*, **28** (9) 1663–1669.

Wu., Y.-T., Shah, C.R. and Deb Baruah, A.K. (2002) Progressive advanced-mean-value method for CDF and reliability analysis, *Int. J. Materials and Product Techn.*, **17** (5–6) 303–318.

Xiao, Q. and Mahadevan, S. (1994) Fast failure mode identification for ductile structural system reliability, *Structural Safety*, **13** (4) 207–226.

Xiaopeng, L., Zhenzhou, L. and Xin, X. (2014) Discussion of paper: "A new efficient simulation method to approximate the probability of failure and most probable point": M. Rashki, M. Miri and M.A. Moghaddam, *Structural Safety*, 39 (2012) 22–29, *Structural Safety*, **46**: 13–14.

Yang, J.-N. (1975) Approximation to first passage probability, *J. Engineering Mechanics Div.*, ASCE, **101** (EM4) 361–372.

Yang, R.J., Chuang, C., Gu, L. and Li, G. (2005) Experience with approximate reliability based optimization methods II: an exhaust system problem. *Structural and Multidisciplinary Optimization*, **29**: 488–497.

Yang, R.J. and Gu, L. (2004) Experience with approximate reliability based optimization methods, *Structural and Multidisciplinary Optimization*, **26** (1–2) 152–159.

Yi, P. and Cheng, G.D. (2008) Further study on efficiency of sequential approximate programming strategy for probabilistic structural design optimization, *Structural and Multidisciplinary Optimization*, **35**: 509–522.

Yi, P., Cheng, G.D. and Jiang, L. (2008) A Sequential approximate programming strategy for performance measure based probabilistic structural design optimization, *Structural Safety*, **30**: 91–109.

Youn, B.D. and Choi, K.K. (2004a) Selecting Probabilistic Approaches for Reliability Based Design Optimization, *AIAA Journal*, **124**: 131–42.

Youn, B.D. and Choi, K.K. (2004b) An investigation of nonlinearity of reliability-based design optimization approaches, *Journal of Mechanical Design*, **126**: 403–411.

Youn, B.D., Choi, K.K. and Park, Y.H. (2003) Hybrid analysis method for reliability-based design optimisation, *Journal of Mechanical Design*, **125**: 221–32.

Yu, L., Das, P.K. and Zheng, Y. (2009) A response surface approach to fatigue reliability of ship structures, *Ships and Offshore Structures*, **4**(3): 253–259.

Yuan, X. and Lu, Z. (2014) Efficient approach for reliability-based optimization based on weighted importance sampling approach, *Rel. Eng. & System Safety*, **132**: 107–114.

Yura, J.A., Galambos, T.V. and Ravindra, M.K. (1978) The bending resistance of steel beams, *J. Structural Div.*, ASCE, **104** (ST9) 1355–1370.

Zang, C., Friswell, M.I. and Mottershead, J.E. (2005) A review of robust optimal design and its application in dynamics, *Comput. & Struct.* **83**: 315–326.

Zaremba, S.K. (1968) The mathematical basis of Monte-Carlo and quasi-Monte-Carlo methods, *SIAM Rev.*, **10** (3) 303–314.

Zhang, J. and Ellingwood, B. (1995) Error measure for reliability studies using reduced variable set, *J. Engineering Mechanics*, ASCE, **121** (8) 935–937.

Zhang, Y.C. (1993) High-order reliability bounds for series systems and application to structural systems. *Comput. & Struct.* **46**: 381–386.

Zimmerman, J.J., Corotis, R.B. and Ellis, J.H. (1992) Collapse mechanism identification using a system-based objective, *Structural Safety*, **11** (3 & 4) 157–171.

Zio, E. (2011) *The Monte Carlo Simulation Method for System Reliability and Risk Analysis*, Springer-Verlag, London.

1

Measures of Structural Reliability

1.1 Introduction

The manner in which an engineering structure will respond to loading depends on the type and magnitude of the applied load and the structural strength and stiffness. Whether the response is considered satisfactory depends on the requirements that must be satisfied. These include safety of the structure against collapse, limitations on damage, or on deflections or other criteria. Each such requirement may be termed a limit state. The 'violation' of a limit state can then be defined as the attainment of an undesirable condition for the structure. Some typical limit states are given in Table 1.1.

Table 1.1 Typical limit states for structures.

Limit state type	Description	Examples
Ultimate (safety)	Collapse of all or part of structure	Tipping or sliding, rupture, progressive collapse, plastic mechanism, instability, corrosion, fatigue, deterioration, fire.
Damage (often included in above)		Excessive or premature cracking, deformation or permanent inelastic deformation.
Serviceability	Disruption of normal use	Excessive deflections, vibrations, local damage, etc.

From observation it is known that very few structures collapse, or require major repairs, etc., so that the violation of the most serious limit states is a relatively rare occurrence. When violation of a limit state does occur, the consequences may be extreme, as exemplified by the spectacular collapses of structures such as the Tay Bridge (wind loading), Ronan Point Flats (gas explosion), Kielland Offshore Platform (local strength problems), Kobe earthquake (ductility), etc.

The study of structural reliability is concerned with the *calculation* and *prediction* of the probability of limit state violation for an engineered structural system at any stage during its life. In particular, the study of structural safety is concerned with the violation of the ultimate or safety limit states for the structure. More generally, the study of structural reliability is concerned with the violation of performance measures (of which ultimate or safety limit states are a subset). This broader definition allows the scope of application to move from structural criteria as specified in traditional design codes

(Chapter 9) to broader-based performance requirements for structures, such as might be used in design optimization processes (Chapter 11).

In the simplest case, the probability of occurrence of an event such as limit state violation is a numerical measure of the chance of its occurrence. This measure either may be obtained from measurements of the long-term frequency of occurrence of the event for generally similar structures, or it may be simply a subjective estimate of the numerical value. In practice it is seldom possible to observe for a sufficiently long period of time, and a combination of subjective estimates and frequency observations for structural components and properties may be used to predict the probability of limit state violation for the structure.

In probabilistic assessments any uncertainty about a variable (expressed, as will be seen, in terms of its probability density function) is taken into account explicitly. This is not the case in traditional ways of measuring safety, such as the 'factor of safety' or 'load factor'. These are 'deterministic' measures, since the variables describing the structure, its strength and the applied loads are assumed to take on known (if conservative) values about which there is assumed to be no uncertainty. Precisely because of their traditional and really quite central position in structural engineering, it is appropriate to review the deterministic safety measures prior to developing probabilistic safety measures.

1.2 Deterministic Measures of Limit State Violation

1.2.1 Factor of Safety

The traditional method to define structural safety is through a 'factor of safety', usually associated with elastic stress analysis and which requires that:

$$\sigma_i(\varepsilon) \leq \sigma_{p\,i} \tag{1.1}$$

where $\sigma_i(\varepsilon)$ is the ith applied stress component calculated to act at the generic point ε in the structure, and σ_{pi} is the permissible stress for the ith stress component.

The permissible stresses σ_{pi} are usually defined in structural design codes. They are derived from material strengths (ultimate moment, yield point moment, squash load, etc.), expressed in stress terms σ_{ui} but reduced through a factor F:

$$\sigma_{pi} = \sigma_{ui}/F \tag{1.2}$$

where F is the 'factor of safety'. The factor F may be selected on the basis of experimental observations, previous practical experience, economic and, perhaps, political considerations. Usually, its selection is the responsibility of a code committee.

According to (1.1), failure of the structure should occur when any stressed part of it reaches the local permissible stress. Whether failure actually does occur depends entirely on how well $\sigma_i(\varepsilon)$ represents the actual stress in the real structure at ε and how well σ_{pi} represents actual material failure. It is well known that observed stresses do not always correspond well to the stresses calculated by linear elastic structural analysis (as commonly used in design). Stress redistribution, stress concentration and changes due to boundary effects and the physical size effect of members all contribute to the discrepancies.

Similarly, the permissible stresses that, commonly, are associated with linear elastic stress analysis are not infrequently obtained by linear scaling down, from well beyond the linear region, of the ultimate strengths obtained from tests. From the point of view of structural safety, this does not matter very much, provided that the designer recognizes that his calculations may well be quite fictitious and provided that (1.1) is a conservative safety measure.

By combining expressions (1.1) and (1.2) the condition of 'limit state violation' can be written as

$$\frac{\sigma_{ui}(\varepsilon)}{F} \le \sigma_i(\varepsilon) \quad \text{or} \quad \frac{\sigma_{ui}(\varepsilon)}{F} \Big/ \sigma_i(\varepsilon) \le 1 \tag{1.3}$$

Expressions (1.3) are 'limit state equations' when the inequality sign is replaced by an equality. These equations can be given also in terms of stress resultants, obtained by appropriate integration:

$$\frac{R_i(\varepsilon)}{F} \le S_i(\varepsilon) \quad \text{or} \quad \frac{R_i(\varepsilon)}{F} \Big/ S_i(\varepsilon) \le 1 \quad \text{for all } i \tag{1.4}$$

where R_i is the ith resistance at location ε and S_i is the ith stress resultant (internal action). In general, the stress resultant S_i are made up of the effects of one or more applied loads Q_j; typically

$$S_i = S_{iD} + S_{iL} + S_{iW}$$

where D is the dead load, L is the live load and W is the wind load.

The term 'safety factor' also has been used in another sense, namely in relation to overturning, sliding, etc., of structures as a whole, or as in geomechanics (dam failure, embankment slip, etc.). In this application, expressions (1.3) are still valid provided that the stresses σ_{ui} and σ_i are interpreted appropriately.

1.2.2   Load Factor

The 'load factor' λ is a special kind of safety factor developed for use originally in the plastic theory of structures. It is the theoretical factor by which a set of loads acting on the structure must be multiplied, just enough to cause the structure to collapse. Commonly, the loads are taken as those acting on the structure during service load conditions. The strength of the structure is determined from the idealized plastic material strength properties for structural members [Heyman, 1971].

For a given collapse mode (i.e. for a given ultimate 'limit state'), the structure is considered to have 'failed' or collapsed when the plastic resistances R_{pi} are related to the factored loads λQ_j by

$$W_R(\mathbf{R}_R) \le W_Q(\lambda \mathbf{Q}) \tag{1.5}$$

where $\mathbf{R}_P$ is the vector of all plastic resistances (e.g. plastic moments) and $\mathbf{Q}$ is the vector of all applied loads. Also, $W_R(\ )$ is the internal work function and $W_Q(\ )$ the external work function, both described by the plastic collapse mode being considered.

If proportional loading is assumed, as is usual, the load factor can be taken out of parentheses. Also the loads Q_j usually consist of several components, such as dead, live,

wind, etc. Thus (1.5) may be written in the form of a limit state equation:

$$\frac{W_R(R_{pi})}{\lambda W_Q(Q_D + Q_L + \ldots)} = 1$$

with 'failure' denoted by the left-hand side being less than unity.

Clearly there is much similarity in formulation between the factor of safety and the load factor as measures of structural safety. What *is* different is the reference level at which the two measures operate: the first at the level of working loads and at the 'member' level; the second at the level of collapse loads and at the 'structure level'.

1.2.3 Partial Factor ('Limit State Design')

A development of the above two measures of safety is the so-called 'partial factor' approach. For limit state i it can be expressed at the level of stress resultants (i.e. member design level) as

$$\phi_i R_i \leq \gamma_{Di} S_{Di} + \gamma_{Li} S_{Li} + \ldots \tag{1.6}$$

where R is the member resistance, ϕ is the partial factor on R and S_D, S_L are the dead and live load effects respectively with associated partial factors γ_D, γ_L. Expression (1.6) was originally developed during the 1960s for reinforced concrete codes. It enabled the live and wind loads to have greater 'partial' factors than the dead load, in view of the former's greater uncertainty, and it allowed a measure of workmanship variability and uncertainty about resistance modelling to be associated with the resistance R [MacGregor, 1976]. This extension of earlier safety formats had considerable appeal since it allowed better representation of the factors and uncertainties associated with loadings and resistances.

For a plastic collapse analysis at the structure level, formulation (1.6) becomes

$$W_R(\phi\mathbf{R}) \leq W_Q(\gamma_D \mathbf{Q}_D + \gamma_L \mathbf{Q}_L + \ldots)$$

where $\mathbf{R}$ and $\mathbf{Q}$ are vectors of resistance and loads respectively. Clearly the partial factors (ϕ, γ) in this expression will be different from those of expression (1.6).

Example 1.1 The simple portal frame of Figure 1.1(a) is subject to loads Q_1 and Q_2. If the relative moments of inertia of the members are known, the elastic bending moment diagram can be found as in Fig 1.1(b). The 'limit states' for bending capacity are then

section 2: $$\phi M_{C2} = \gamma_1 \frac{3l}{16} Q_1 + \gamma_2 \frac{3l}{16} Q_2$$

sections 1 and 3: $$\phi M_{C1,3} = \gamma_1 \frac{l}{16} Q_1 + \gamma_2 \frac{l}{16} Q_2$$

where ϕ, γ_1 and γ_2 are partial factors described by a structural design code. The M_{Ci} are the ultimate moment capacities required at sections $i (i = 1, 2, 3)$ for the structure to be considered 'just safe'.

If the frame is to be designed or analysed assuming rigid-plastic theory, the relative distribution of the plastic moments M_{pi} around the frame must be known or assumed.
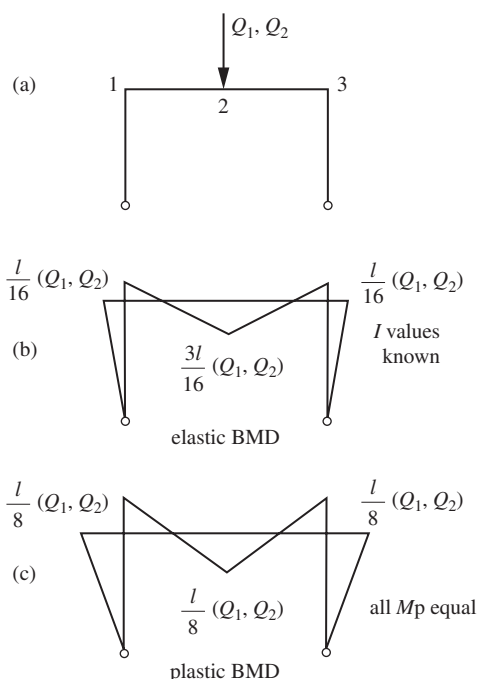
Figure 1.1 Bending moment diagrams for Example 1.1.

If they all are equal, the plastic bending moment diagram of [Figure 1.1(c) is obtained and only one limit state equation is needed for sections 1–3:]

$$\phi_p M_{pi} = \gamma_{p1} \frac{l}{8} Q_1 + \gamma_{p2} \frac{l}{8} Q_2$$

where now M_{pi} is the required plastic moment capacity at sections 1, 2 and 3 and where ϕ_p, γ_{p1} and γ_{p2} are now code-prescribed partial factors for plastic structural systems.

1.2.4 A Deficiency in Some Safety Measures: Lack of Invariance

From Example 1.1, it will be evident that the partial factors ϕ and $\gamma_i (i = 1, \ldots)$ in (1.6) depend on the limit state being considered. Hence they depend on the definitions of R, S_D and S_L. However, even for a given limit state, these definitions are not necessarily unique, and therefore the partial factors may not be unique either. This phenomenon is termed the 'lack of invariance' of the safety measure. It arises because there are different ways in which the relationships between resistances and loads may be defined. Some examples of this are given below. Ideally, the safety measure should not depend on the way in which the loads and resistances are defined.

Example 1.2 The structure shown in Figure 1.2 is supported on two columns. The capacity of column B is $R = 24$ in compression. The safety of the structure can be measured in three different ways using the traditional 'factor of safety' F:
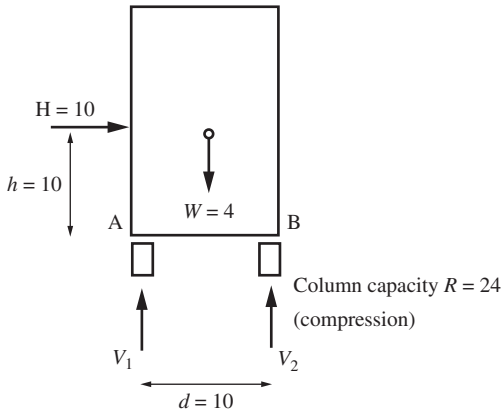
Figure 1.2 Example 1.2: Structure subject to overturning under lateral load H and with vertical load W and supported by two columns applying vertical forces V_1 and V_2.

(a) *Overturning resistance about A*

$$F_1 = \frac{resisting\ moment\ about\ A}{overturning\ moment\ about\ A} = \frac{dR}{Hh + Wd/2} = \frac{10 \times 24}{10 \times 10 + 4 \times 5} = 2.0$$

(b) *Capacity of column B*

$$F_2 = \frac{compression\ resistance\ of\ column\ B}{compressive\ load\ on\ column\ B} = \frac{R}{Hh/d + W/2} = 2.0$$

(c) *Net capacity of column B* (resistance minus load effect of W)

$$F_3 = \frac{net\ compression\ resistance\ of\ column\ B}{net\ compressive\ load\ on\ column\ B} = \frac{R - W/2}{Hh/d} = 2.2$$

All three of these factors of safety $F_i (i = 1, 2, 3)$ for column B apply to the same structure and the same loading, so that the difference in the values of F_i is due entirely what is considered to represent the resistance of the structure and what is considered to be the applied load. In general such a difference in outcomes is not helpful for the unique definition of a factor of safety. However, for some special cases of the partial factors the outcomes can be made the same. Thus it is easily verified that the calculations give the identical result $F_1 = F_2 = F_3 = 1.0$ if a partial safety factor $\phi = \frac{1}{2}$ is applied to the resistance R, thus:

$$F_1 = \frac{d\phi R}{Hh + Wd/2}, \quad F_2 = \frac{\phi R}{Hh/d + W/2} \quad F_3 = \frac{\phi R - W/2}{Hh/d}$$

Similarly, the result $F_1 = F_2 = F_3 = 1.0$ would be achieved if the loads H and W were factored by $\gamma = 2$. More generally, any choice of combination of ϕ and γ could be appropriate, provided that $F_i = 1$. This can be expressed as:

$$F_1 = \frac{d\phi R}{\gamma(Hh + Wd/2)}, \quad F_2 = \frac{\phi R}{\gamma(Hh/d + W/2)}, \quad F_3 = \frac{\phi R - \gamma W/2}{\gamma Hh/d}$$

with $F_1 = F_2 = F_3 = 1$

A different way of defining a measure of safety is the 'safety margin'. It measures the excess of resistance compared with the stress resultant (or loading); thus:

$$Z = R - S \tag{1.7}$$

For the present example, the safety margins are

$$Z_1 = dR - (Hh + Wd/2) \tag{1.7a}$$
$$Z_2 = R - (Hh/d + W/2) \tag{1.7b}$$

and

$$Z_3 = R - W/2 - Hh/d \tag{1.7c}$$

It is readily verified that when $Z = 0$, i.e. at the point of failure, these three expressions are equivalent. This shows that the safety margin concept of safety is 'invariant' with respect to the limit state functions (1.7a–c).

Example 1.3   [adapted from Ditlevsen, 1973]   The reinforced concrete beam shown in Figure 1.3(a) has a moment capacity R when it is subject to an axial force N and a moment M applied at the beam centroid $\xi = 0$. Both N and M are composed of the effects of a dead load and a live load: $N = N_D + N_L$ and $M = M_D + M_L$. The moment capacity calculated about $\xi = a$ is $R_1 = R + aN$, from simple statics. (Note that the actual moment capacity of the beam is not changed!) Also, at $\xi = a$, the applied moment is given by $M_1 = M + aN$. The state 'just safe' can now be defined for given moment capacity R, and given axial force N, by the factor of safety as:

$$F_0 = \frac{R}{M} \qquad \text{at } \xi = 0 \tag{1.8a}$$

$$F_1 = \frac{R_1}{M_1} = \frac{R + aN}{M + aN} \qquad \text{at } \xi = a \tag{1.8b}$$

In this format $F_1 = F_0$ is true only when $\xi = a = 0$. This means that the factor of safety depends on the convention chosen for the origin of the applied actions and of the resistance. If, as in Example 1.2, R is replaced by the factored term ϕR, such that $F_0 = 1$, then it follows readily that F_1 is also unity. Hence, provided that 'partial factor' ϕ is chosen in such a way that the 'factor of safety' F is unity, the origin chosen to define R, N and M is immaterial. A similar result holds if N and M are replaced by γN and γM, where γ is an appropriately chosen partial factor on the loading.
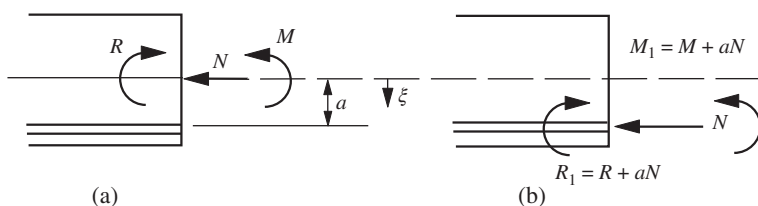
Figure 1.3 Reinforced concrete beam: Example 1.3.

@Seismicisolation

The state 'just safe' can be written also in the partial factor format of (1.6). Indeed, noting that $M = M_D + M_L$ and $N = N_D + N_L$, at $\xi = 0$ it follows that

$$\phi R = \gamma_D M_D + \gamma_L M_L \tag{1.9a}$$

and at $\xi = a$, treating, as before, $R_1 = R + aN$ as the resistance to bending,

$$\phi(R + aN_D + aN_L) = \gamma_D(M_D + aN_D) + \gamma_L(M_L + aN_L) \tag{1.9b}$$

Subtracting (1.9a) from (1.9b) and dividing out by a leaves

$$(\phi - \gamma_D)N_D + (\phi - \gamma_L)N_L = 0 \tag{1.10}$$

Since in general N_D, $N_L > 0$, it follows that (1.10) will be satisfied only if either $\gamma_D \leq \phi \leq \gamma_L$ or $\gamma_L \leq \phi \leq \gamma_D$. Except for $\phi = \gamma_D = \gamma_L = 1$ these expressions are both inconsistent with the conventional interpretation that $\phi \leq 1$ (to reduce the calculated resistance) and γ_D, $\gamma_L \geq 1$ (to increase the loads or applied stresses).

The reason for this result should be clear. In (1.9b) the term $(aN_D + aN_L)$ on the left-hand side was treated as a resistance, per se, whereas it is strictly a resistance effect caused directly by the applied loading (note that it is not affected by workmanship, material strength, etc., as is R). The key to an invariant safety measure is thus at hand. Partial factors such as ϕ should be applied directly to resistances only, and partial factors such as γ to loads only, and the direct application of (1.6) to a mixed variable $R_1 = R + aN$ is not correct.

It is important to note that the safety margin Z (Equation 1.7) is invariant for both definitions of resistance in this example. In the first case $Z_0 = R - M$, while in the second case $Z_1 = (R + aN) - (M + aN) = R - M$.

1.2.5 Invariant Safety Measures

As can be seen from the above examples, one form of invariant safety measure is obtained if the resistances R_i and the loads Q_j acting on the structure are so factored that the ratio between any relevant pair $\phi_i R_i$ and $\gamma_j Q_j$ is unity at the point of limit state violation. In simple terms, this requires that all variables be reduced to a common base before being compared. This is the case for the permissible stress measure of structural safety expressed by equation (1.3). Another and important form of invariant safety measure is the safety margin $Z = R - S$ defined in equation (1.7). It will be used extensively in the sections to follow because of its invariant properties.

Some readers may recognize a parallel between the above discussion and the decision criteria in cost-benefit analysis. The safety margin corresponds to the 'net present value' criterion and the problem of safety factor invariance to the 'numerator-denominator' problem [e.g. Prest and Turvey, 1965].

1.3 A Partial Probabilistic Safety Measure of Limit State Violation—The Return Period

In the historical development of engineering design, loads due to natural phenomena such as winds, waves, storms, floods, earthquakes, etc. were recognized quite early as

having randomness in time as well as in space. The randomness in time was considered in terms of the 'return period'. The return period is defined as the average (or expected) time between two successive statistically independent events. Of course, the actual time T between events is a random variable.

In most practical applications an 'event' constitutes the exceedance of a certain threshold, for example as associated with loading (e.g. wind velocity > 100 m/s). Such an event may be used to define a 'design load' and the design of the structure itself is then usually considered deterministically, i.e. using conventional design procedures. Hence this approach is only a partially probabilistic method.

The return period may be defined as follows. For independent samples from a population (i.e. for a Bernoulli trial sequence), the trial T on which the first occurrence of an event takes place is given by the geometric distribution (A.23), which states that the probability that the first occurrence occurs on the t th trial is:

$$P(T = t) = p \ (1 - p)^{t-1} \qquad t = 1, 2, \dots \tag{1.11}$$

where p is the probability of occurrence of the event (e.g. $X > x$) in any one trial and $1 - p$ is the probability that the event does not occur. If trials are now interpreted as time intervals, during each of which only the occurrence of events $X > x$ is recorded, the first occurrence of an event becomes the 'first occurrence time', given by expression (1.11). The 'mean recurrence time' or the 'return period' is then the expected value of T (see A. 10):

$$E(T) = \overline{T} = \sum_{t=1}^{\infty} tp(1-p)^{t-1} = p[1 + 2(1-p) + 3(1-p)^2 + \dots]$$

$$= \frac{p}{[1 - (1 - p)]^2} \qquad \text{for } (1 - p) < 1.0$$

$$= \frac{1}{p} \qquad \text{or} \qquad = [1 - F_x(x)]^{-1} \tag{1.12}$$

where $F_X(x) = P(X \le x)$ is the cumulative distribution function of X.

Thus the return period $\overline{T}$ is equal to the reciprocal of the probability of the occurrence of the event in any one (or a single) time interval. For most engineering problems, the chosen time interval is one year, so that p is the probability of occurrence of the event $X > x$ in any one year (e.g. the probability that a load > x will occur (at least once) during the year). Then $\overline{T}$ is the number of years, on average, between events.

Because the exceedance events that occur during a time period (e.g. during a year) are associated with the end of that period, $\overline{T}$ is dependent on the time period chosen [Borgman, 1963]. This is illustrated in Figure 1.4, where four exceedance events, A, B, C and D are shown occurring after an arbitrary initial event 0. The mean recurrence time $\overline{T}_1$ for the actual observations is shown in Figure 1.4(a) and is given by the average of the distance (i.e. time) between the events, i.e. by $\overline{T}_1 \approx 1.5$ years.

In Figure 1.4(b) with the time period taken as 1 year, and the events counted at the end of each time period, it follows easily that $\overline{T}_2 = 7/4 = 1.75$ years. Similarly, for $\overline{T}_3 = 2$ years. However, when a 4-year time period is used (Figure 1.4(d)) two of the
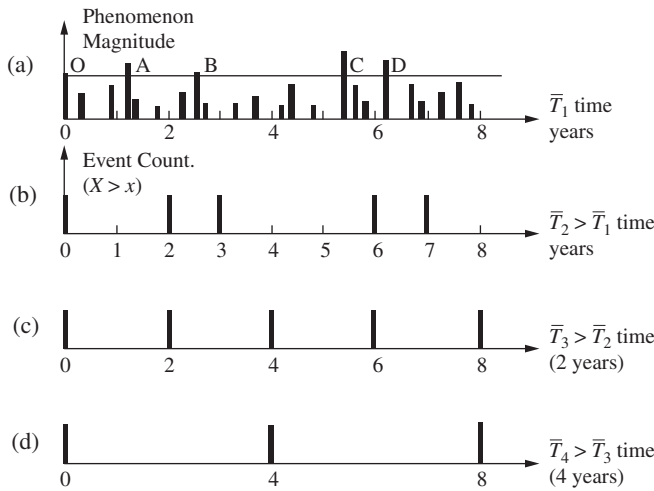
Figure 1.4 Idealizations of actual load phenomenon for the 'return period' concept.

events in each period are counted as one at the end of the period, and $\overline{T}_4$ in this case becomes 4 years.

This somewhat artificial example shows three things. Firstly, that the return period depends, as noted, on the definition of the time scale, and secondly that the possible occurrence of more than one event within a time period is ignored. This means that, where event occurrence is relatively frequent compared with the time period employed, the return period measure is not accurate.

The third and a most important point is that the probability distribution of the magnitude of X (i.e. the phenomenon being considered) is not considered. Only magnitudes $X > x$ are counted. This means that the return period is a probabilistic measure in terms of time only, but not in terms of the magnitude of the loading and its interaction with the resistance.

It should be clear that in practice the events may not be independent, as postulated, particularly if the events occur rather frequently. Fortunately, the return period concept is used mainly for rather rare events (i.e. the level X is quite high), and it is then reasonable to assume event independence. Time scale dependence is then also not a significant issue. Chapter 6 gives a much more detailed discussion.

Example 1.4 For a structure subject to a '50-year wind' of 60 km/h velocity:

(a) the return period for a 60-km/h wind = $\overline{T}$ = 50 years
(b) the probability of exceeding 60 km/h in any one year is

$$p = 1/\overline{T} = 1/50 = 2\%;$$

(c) the probability of exceeding the design wind velocity (i.e. $V > 60$) for the first time during the fourth year, is (geometric distribution A.23):

$$P_T(T = 4) = (0.02)(0.98)^3 = 0.01882$$

(d) the probability of exceeding the design wind velocity in only one of the years in a 4-year period is given by the binomial distribution (A.17):

$$P_X(x = 1) = \binom{4}{1}(0.02)(0.98)^3 = \frac{4 \times 3 \times 2 \times 1}{1(3 \times 2 \times 1)}(0.02)(0.98)^3 = 0.0753$$

(e) the probability of exceeding the design wind velocity (i.e. $V > 60$) during any of the years in a 4 year period is given by the geometric distribution (A.23):

$$P_T(T \leq 4) = \sum_{t=1}^{4} P_T(T = t) = \sum_{t=1}^{4}(0.02)(0.98)^{t-1}$$
$$= 0.02 + 0.0196 + 0.01921 + 0.01883$$
$$= 0.0776$$

or alternatively,

$$P_T(T \leq 4) = 1 - [P(V < 60)]^4 = 1 - (1 - 0.02)^4 = 0.0776$$

Note that the period 4 years can be generalized to 'design life' t_L and the question rephrased to 'the probability of exceeding the design velocity within the design life':

$$P_T(T \leq t_L) = \sum_{t=1}^{t_L} P_T(T = t) \quad \text{or} \quad = 1 - (1 - p)^{t_L} \tag{1.13}$$

Some typical values for the relationship between the exceedance probability $P_T(T \leq t_L)$ the return period $\overline{T} = 1/p$ and the design life t_L are given in Table 1.2 [Borgman, 1963].

(f) the probability of exceeding the design wind velocity within the return period is

$$P_T(T \leq \overline{T}) = 1 - [P(V < 60)]^{\overline{T}}$$

but $P(V < 60) = 1 - P(V \geq 60) = 1 - p$ where $p = 1/\overline{T}$. Hence

$$P_T(T \leq \overline{T}) = 1 - (1 - p)^{\overline{T}}$$
$$= 1 - \left(1 - \overline{T}p + \frac{\overline{T}(\overline{T} - 1)}{2!}p^2 - \dots\right)$$
$$\approx 1 - \exp(-\overline{T}p) \quad \text{for large } \overline{T} \text{ (i.e. small } p)$$
$$\approx 1 - \exp(-1) = 1 - 0.3679 = 0.6321$$

Note that even for smaller $\overline{T}$, this result is a good approximation; thus, for $\overline{T} = 5$,

$$P_T(T \leq 5) = 1 - \left(1 - \frac{1}{5}\right)^5 = 0.6723$$

This shows that there is a chance of about 2 in 3 that the exceedance event will occur within a design life equal to the return period.

Table 1.2 Return period $\overline{T}$ as function of design life t_L and exceedance probability P_T ($T \leq t_L$).

	Return period $\overline{T}$ for the following exceedance probabilities (see 1.13)								
Design life t_L	0.02	0.05	0.10	0.15	0.20	0.30	0.40	0.50	0.70
1	50	20	10	7	5	3	3	2	1
2	99	39	19	13	9	6	4	3	2
3	149	59	29	29	14	9	6	5	3
4	198	78	38	25	18	12	8	6	4
5	248	98	48	31	23	15	10	8	5
6	297	117	57	37	27	17	12	9	6
7	347	137	67	44	32	20	14	11	6
8	396	156	76	50	36	23	16	12	7
9	446	176	86	56	41	26	18	13	8
10	495	195	95	62	45	29	20	15	9
12	594	234	114	74	54	34	24	18	10
14	693	273	133	87	63	40	28	21	12
16	792	312	152	99	72	45	32	24	14
18	892	351	171	111	81	51	36	26	15
20	990	390	190	124	90	57	40	29	17
25	1238	488	238	154	113	71	49	37	21
30	1485	585	285	185	135	85	59	44	25
35	1733	683	333	216	157	99	69	51	30
40	1981	780	380	247	180	113	79	58	34
45	2228	878	428	277	202	127	89	65	38
50	2475	975	475	308	225	141	98	73	42

1.4 Probabilistic Measure of Limit State Violation

1.4.1 Introduction

The return period concept considers only the probability that a loading exceeds a set limit and assumes such exceedances (or 'level crossings' – see Chapter 6) to be randomly distributed in time. This is a useful improvement over deterministic descriptions of loading but ignores the fact that, even at a given point in time, the actual value of the loading is uncertain. This is illustrated in Figure 1.5 for floor loading.

The histogram of Figure 1.5 shows, for example, that the probability that the floor loading lies between 0.6 and 0.7 kPa is about 7%. Such information is obtained from actual surveys of floor loads (see Chapter 7), and can be represented by the probability density function $f_Q(q)$. (Recall that $f_Q(\ )$ denotes the probability that the load Q will take on a value between q and $q + \Delta q$ as $\Delta q \to 0$ - see also Section A.3.) The load Q can be converted to a load effect S by conventional structural analysis procedures. Using the same transformation(s), the probability density function $f_S(\ )$ can be obtained also,

No. obs   = 625
Max. val. = 2.22 kN/m²
            (45.4 1b/ft²)
Min. val. = 0 kN/m²
Mean   = 0.44 kN/m²
            (9.0 1b/ft²)
Std. dev. = 0.27 kN/m²
            (5.5 1b/ft²)
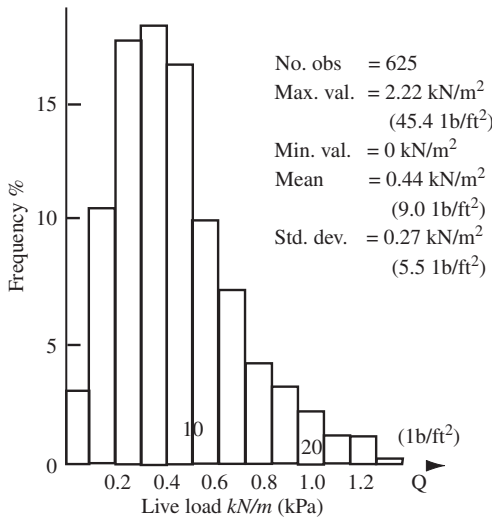
Figure 1.5 Histogram of private office live loads [after Culver, 1976].

if necessary, using methods such as outlined in Section A.10. However, details of this need not be of concern for the present.

Resistance, geometric and workmanship variables and many others may be described similarly in probabilistic terms. For example, a typical resistance histogram and the inferred probability distribution for the yield strength of steel are shown in Figure 1.6. Naturally, material strengths such as steel yield strength can be converted to member resistance R by multiplying by section properties (such as A, the cross-sectional area). Then it is possible to determine a probability density function $f_R(\ )$.

In general, the loads applied to a structure fluctuate with time and are of uncertain value at any one point in time. This is carried over directly to the load effects (or internal actions) S. Somewhat similarly the structural resistance R will be a function of time
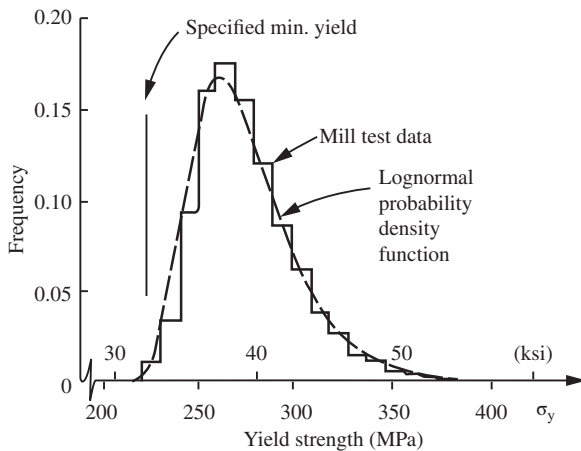
Figure 1.6 Histogram and inferred distribution for structural steel yield strength [adapted from Alpsten, 1972 with permission of ASCE].
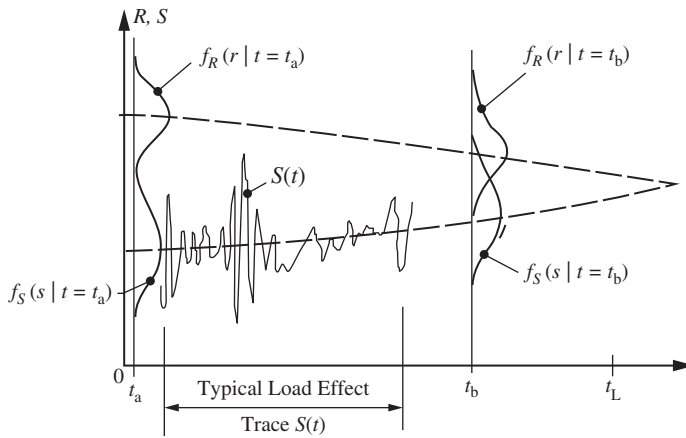
Figure 1.7 Schematic time-dependent reliability problem.

(but not usually a fluctuating one) owing to fatigue, deterioration and similar actions. Loads have a tendency to increase, and resistances to decrease, with time. It is likely also that the uncertainty in both quantities increases with time, particularly if they have to be predicted. This means that the probability density functions $f_S(\ )$ and $f_R(\ )$ become wider and flatter with time and that the mean values of S and R also change with time. As a result, the general reliability problem can be represented as in Figure 1.7.

The safety limit state will be violated whenever, at any time t,

$$R(t) - S(t) < 0 \qquad \text{or} \qquad \frac{R(t)}{S(t)} < 1 \tag{1.14}$$

The probability that this occurs for any one (single) load application (or load cycle) is the probability of limit state violation, or simply the probability of failure p_f. Roughly, it may be represented by, but is not actually equal to, the amount of overlap of the probability density functions f_R and f_S in Figure 1.7. Since this overlap may vary with time, p_f also may be a function of time.

To make the problem more tractable, it is convenient for many situations to assume that Q and R are 'time-invariant', that is they are not functions of time. An example of this is the case when the load Q is applied to the structure only once and the probability of limit state violation is sought for that particular load application only.

However, if the load is applied many times (e.g. a single time-varying load might be considered this way) and R is taken as constant, then the maximum value of that load (within a given time interval $[0, T]$) is of interest if it is assumed that the structure will fail under the (once-only) application of this maximum load. One way to properly represent this maximum load is through the use of an extreme value distribution, such as the Gumbel (EV-I) or Frechet (EV-II) distributions (see Appendix A). If this is done, the effect of time may be ignored in the reliability calculations. This approach is not satisfactory when more than one load is involved or when the resistance changes with time. Discussion of these matters and the more general reliability problem is deferred to Chapter 6.

1.4.2 The Basic Reliability Problem

The basic structural reliability problem considers only one load effect S resisted by one resistance R. Each is described by a known probability density function, $f_S(\ )$ and

$f_R(\ )$ respectively. As noted, S may be obtained from the applied loading Q through a structural analysis (either deterministic or with random components). It is important that R and S be expressed in the same units.

For convenience, but without loss of generality, only the safety of a structural element will be considered here and, as usual, that structural element will be considered to have failed if its resistance R is less than the stress resultant S acting on it. The probability p_f of failure of the structural element can then be stated in any of the following ways:

$$p_f = P(R \le S) \tag{1.15a}$$

$$= P(R - S \le 0) \tag{1.15b}$$

$$= P\left(\frac{R}{S} \le 1\right) \tag{1.15c}$$

$$= P(\ln R - \ln S \le 1) \tag{1.15d}$$

or in general

$$= P[G(R,\ S) \le 0] \tag{1.15e}$$

where $G(\ )$ is termed the 'limit state function' and the probability of failure is identical with the probability of limit state violation. Equations (1.15) could, of course, also have been written in terms of R and Q for the structure as a whole.

Quite general (marginal) density functions f_R and f_S for R and S respectively are shown in Figure 1.8 together with the joint (bivariate) density function $f_{RS}(r, s)$ (see also Section A.6). For any infinitesimal element ($\Delta r\ \Delta s$), the latter represents the probability that R takes on a value between r and $r + \Delta r$ and S a value between s and $s + \Delta s$ as Δr and Δs each approach zero. In Figure 1.8, Equations (1.15) are represented by the hatched failure domain D, so that the failure probability may be written as:

$$p_f = P(R - S \le 0) = \int_D \int f_{RS}(r, s)\, dr\, ds \tag{1.16}$$
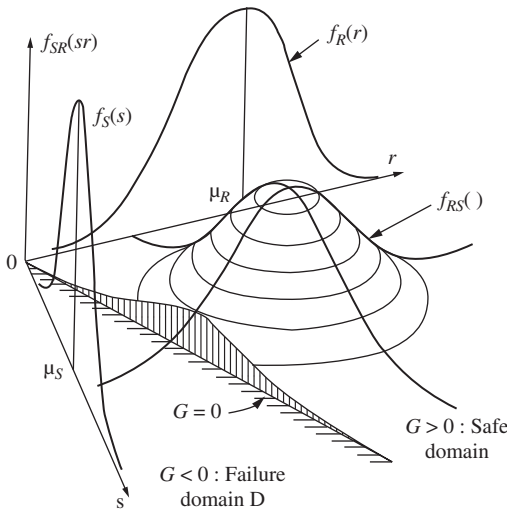
Figure 1.8 Space of the two random variable (r, s) and the joint density function $f_{RS}(r, s)$, the marginal density functions f_R and f_S and the failure domain D.

When R and S are independent, $f_{RS}(r, s) = f_R(r)f_S(s)$ (see A.6.3), and (1.16) becomes:

$$p_f = P(R - S \leq 0) = \int_{-\infty}^{\infty} \int_{-\infty}^{S \geq r} f_R(r)f_S(s)\, dr\, ds \tag{1.17}$$

Noting that for any random variable X, the cumulative distribution function is given by (A.8):

$$F_X(x) = P(X \leq x) = \int_{-\infty}^{x} f_X(y)\, dy$$

provided $x \geq y$, it follows that for the common, but special, case when R and S are independent, (1.17) can be written in the single integral form:

$$p_f = P(R - S \leq 0) = \int_{-\infty}^{\infty} F_R(x)f_S(x)\, dx \tag{1.18}$$

This is also known as a 'convolution integral' with meaning easily explained by reference to Figure 1.9. $F_R(x)$ is the probability that $R \leq x$ or the probability that the actual resistance R of the member is less than some value x. This represents failure if the loading is $\geq x$. The probability that this is the case is given by the term $f_S(x)$ that represents the probability that the load effect S acting in the member has a value between x and $x + \Delta x$ in the limit as $\Delta x \to 0$. By considering all possible values of x, i.e. by taking the integral over all x, the total failure probability is obtained. This is also seen in Figure 1.10 where the (marginal) density functions f_R and f_S have been drawn along the same axis.

Through integration of $f_R(\ )$ in (1.17), the order of integration was reduced by one. This is convenient and useful, but not general. It was only possible because R was assumed independent of S. In general, dependence between variables should be considered. This more complex situation is discussed further is Section 1.5 and Chapters 3 and 4.

For the present, restricting attention to simpler formulations, an alternative to expression (1.18) is:

$$p_f = \int_{-\infty}^{\infty} [1 - F_S(x)]f_R(x)dx \tag{1.19}$$

This can be seen to be simply the 'sum' of the failure probabilities over all the cases of resistance for which the load exceeds the resistance.
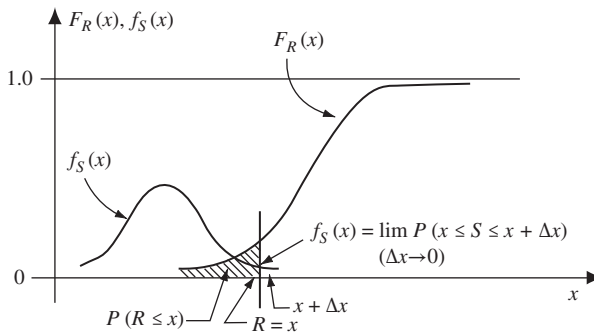
Figure 1.9 Basic $R - S$ problem: $F_R(\ )f_S(\ )$ representation.
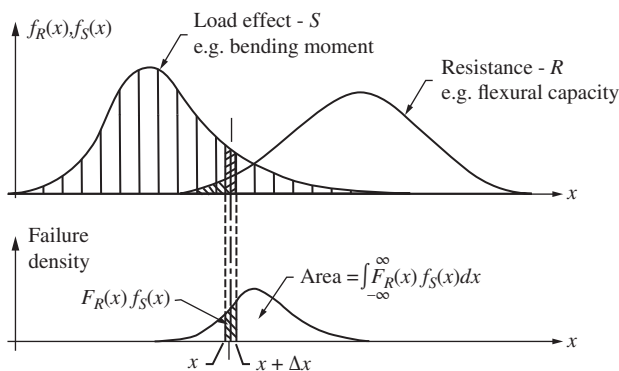
Figure 1.10 Basic $R - S$ problem: $f_R(\ )f_S(\ )$ representation.

The lower limit of integration shown in Expressions (1.17) to (1.19) may not be totally satisfactory, since a 'negative' resistance usually is physically not possible. The lower integration limit therefore strictly should be zero, although this may be inconvenient and slightly inaccurate if R or S or both are modelled by distributions unlimited in the lower tail (such as the Normal or Gaussian distribution). The inaccuracy arises strictly from the modelling of R and/or S, and not from the theory involved with (1.17) to (1.19). This important point is sometimes overlooked in discussions about appropriate distributions to represent random variables.

1.4.3 Special Case: Normal Random Variables

For a few distributions of R and S it is possible to integrate the convolution integral (1.18) analytically. The most notable example is when both R and S are normal random variables with means μ_R and μ_S and variances σ_R^2 and σ_S^2 respectively. The safety margin $Z = R - S$ then has a mean and variance given by well-known rules for addition (subtraction) of normal random variables:

$$\mu_Z = \mu_R - \mu_S \tag{1.20a}$$
$$\sigma_Z^2 = \sigma_R^2 + \sigma_S^2 \tag{1.20b}$$

Equation (1.15b) then becomes

$$p_f = P(R - S \leq 0) = P(Z \leq 0) = \Phi\left(\frac{0 - \mu_Z}{\sigma_Z}\right) \tag{1.21}$$

where $\Phi(\ )$ is the standard normal distribution function (zero mean and unit variance) extensively tabulated in statistics texts (see also Appendix D). The random variable $Z = R - S$ is shown in Figure 1.11, in which the failure region $Z \leq 0$ is shown shaded. Using (1.20) and (1.21) it follows that [Cornell, 1969a]

$$p_f = \Phi\left[\frac{-(\mu_R - \mu_S)}{(\sigma_S^2 + \sigma_R^2)^{1/2}}\right] = \Phi(-\beta) \tag{1.22}$$

where $\beta = \mu_Z/\sigma_Z$ is defined as the 'safety index' (1.21).

@Seismicisolation
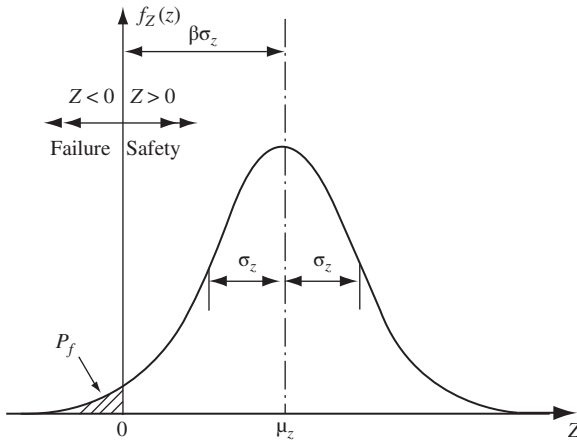
Figure 1.11 Distribution of safety margin $Z = R - S$.

If either of the standard deviations σ_S or σ_R or both is increased, the term in square brackets in (1.22), will become smaller and hence p_f will increase, as might be expected. Similarly if the difference between the mean of the load effect and the mean of the resistance is reduced, p_f increases. These observations may be deduced also from Figure 1.7, taking the amount of overlap of $f_R(\ )$ and $f_S(\ )$ as a rough indicator of p_f at any point in time.

Example 1.5 A simply supported timber beam of length 5 m is loaded with a central load Q having mean $\mu_Q = 3$ kN and variance $\sigma_Q^2 = 1$ (kN)^2. The bending strength of similar beams has been found to have a mean strength $\mu_R = 10$ kNm with a coefficient of variation (COV) of 0.15. It is desired to evaluate the probability of failure.

Assume that the beam self-weight and any variation in the length of the beam can be ignored. From basic structural theory, the applied moment (the load effect S) at the centre of the beam (due to the load Q) is given by $S = (QL)/4$. Since $L = 5$ it follows that the mean load effect and the variance of S are:

$$\mu_S = \frac{5}{4}\mu_Q = \frac{5}{4} \times 3 = 3.75 \text{ kNm} \tag{see A.160}$$

$$\sigma_S^2 = \left(\frac{5}{4}\right)^2 \sigma_Q^2 = \frac{25}{16} \times 1 = 1.56 \text{ (kNm)}^2 \tag{see A.162}$$

Also, the mean resistance and its variance are:

$$\mu_R = 10 \text{ kNm}$$
$$\sigma_R^2 = [(COV)\mu_R]^2 = (0.15 \times 10)^2 = 2.25 \text{ (kNm)}^2$$

Hence

$$\mu_Z = \mu_R - \mu_S = 10 - 3.75 = 6.25$$
$$\sigma_Z^2 = \sigma_R^2 + \sigma_S^2 = 2.25 + 1.56 = 3.81$$

@Seismicisolation

Therefore $\beta = \dfrac{\mu_Z}{\sigma_Z} = \dfrac{6.25}{1.95} = 3.20$ and from (1.21) and Appendix D

$$p_f = \Phi(-3.20) = 7 \times 10^{-4}.$$

1.4.4 Safety Factors and Characteristic Values

The traditional deterministic measures of limit state violation, namely the factor of safety and the load factor, can be related directly to the probability p_f of limit state violation. Analytically this is demonstrated most easily for the basic 'one-resistance one-load-effect' case, when R and S (or Q) are each normally distributed.

Consider a convenient simple safety measure sometimes referred to as the 'central' safety factor λ_0 and defined as

$$\lambda_0 = \frac{\mu_R}{\mu_S} \quad \text{or} \quad = \frac{\mu_R}{\mu_Q} \tag{1.23}$$

This definition does not accord with conventional usage, since generally some upper range value of applied load or stress is compared with some lower range value of strength of material. Such values might be termed 'characteristic' values, reflecting that in conventional usage (e.g. in design) the load or strength is described only by this value. Thus the characteristic yield strength of steel bars is the strength that most (say 95%) bars will exceed. There is a finite (but small) probability that some bars will have a lower strength.

For resistances, the design or 'characteristic' values are defined on the low side of the mean resistance (see Figure 1.12):

$$R_k = \mu_R(1 - k_R V_R) \tag{1.24}$$

where R_k is the characteristic resistance, μ_R the mean resistance, V_R the coefficient of variation for R and k_R a constant. This description is based on the Normal distribution. R_k is the value of resistance below which only, say 5% of samples will fail. Also, for the standardized Normal distribution function (see Section A.5.7), it follows that

$$0.05 = \Phi\left(-\frac{R_k - \mu_R}{\sigma_R}\right)$$

and for a 5% 'one-sided tail', $k_{0.05} = 1.645 = (\mu_R - R_k)/\sigma_R$ (e.g. see Appendix D). Expression (1.24) now follows directly, noting that the standard deviation can be expressed as $\sigma_R = \mu_R V_R$.
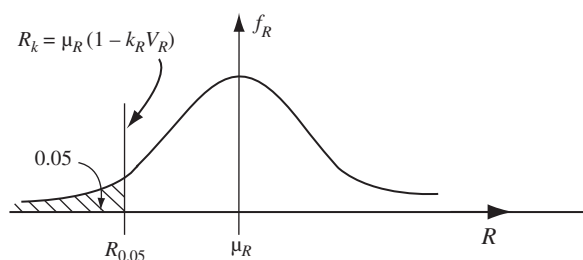
Figure 1.12 Definition of characteristic resistance.
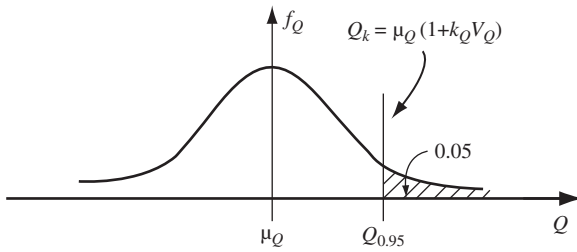
Figure 1.13 Definition of characteristic load.

Similarly, for the load effect the characteristic value is estimated on the high side of the mean:

$$S_k = \mu_S(1 + k_S V_S) \tag{1.25}$$

where S_k is the characteristic load effect (a design value), μ_S the mean load effect, V_S the coefficient of variation for S and k_S is a constant. If design values are defined, for example, as not being exceeded 95% of the time a load effect is applied, then $k_S = 1.645$ if S is Normally distributed (see Figure 1.13). Where loads (actions) are used, Q replaces S in (1.25).

In codified design, the percentiles used (such as 5% and 95% above) either are explicitly specified or may be deduced from the characteristic value specified in existing codes or documents. Other percentile characteristic values can be obtained in the manner indicated above for Normal distributions, and also for non-Normal distributions. Example 1.6 below shows a typical calculation, while Table 1.3 summarizes 5 and 95

Table 1.3 5% and 95% values for X_k / μ_X.

Distribution type	q %	X_k/μ_X for the following coefficients of variation				
		0.1	0.2	0.3	0.4	0.5
Normal	5	0.8355	0.6710	0.5065	0.3421	0.1176
	95	1.164	1.329	1.493	1.658	1.822
Lognormal	5	0.8445	0.7080	0.5910	0.4927	0.4112
	95	1.172	1.358	1.552	1.750	1.945
Gumbel	5	0.8694	0.7389	0.6083	0.4778	0.3472
	95	1.187	1.373	1.560	1.746	1.933
Frechet	5	0.8802	0.7809	0.6999	0.6344	0.5818
	95	1.187	1.367	1.534	1.681	1.809
Weibull	5	0.8169	0.6470	0.4979	0.3736	0.2747
	95	1.142	1.305	1.489	1.689	1.903
Gamma	5	0.8414	0.6953	0.5608[a]	0 4355[a]	0.3416
	95	1.170	1.350	1.541[a]	1.752[a]	1.938

a)   Note that values are for $V_X = 0.302$ and 0.408 respectively, since the Gamma distribution usually only allows discrete values of $V_X^2 (= k)$ (see Section A.5.6).

percentile values for some common distributions. Similar results may be derived for other percentile values.

In some situations it may be appropriate to use the mean of the extreme value distribution to define a design load value. The precise choice is rather arbitrary and need not be of specific concern provided it is consistent. The important point is that the characteristic values are derived values and are convenient and useful for practical design rules but they have no fundamental meaning.

Using the characteristic values for the basic variables, it is now possible to define the so-called 'characteristic safety factor' λ_k:

$$\lambda_k = \frac{R_k}{S_k} \quad \text{or} \quad = \frac{R_k}{Q_k} \tag{1.26}$$

which corresponds closely to the conventional understanding of the factor of safety if the characteristic values are taken to correspond to the usual design values.

A relationship can be established between the characteristic safety factor λ_k (and the central λ_0) and the probability p_f of limit state violation. Obviously this relationship will depend on the probability distributions for R and S, so that no general result can be given. Again, a particularly simple but quite useful case is when both R and S are described by Normal distributions. From (1.22), the probability of failure is

$$p_f = \Phi \left[\frac{-(\mu_R - \mu_S)}{(V_R^2 \mu_R^2 + V_S^2 \mu_S^2)^{1/2}} \right] \tag{1.27}$$

and dividing through by μ_S

$$p_f = \Phi \left[\frac{-(\lambda_0 - 1)}{(V_R^2 \lambda_0^2 + V_S^2)^{1/2}} \right] = \Phi(-\beta) \text{ say} \tag{1.28}$$

where λ_0 is given by (1.23) and β is the 'safety index' as before. It follows that

$$\lambda_0 = \frac{1 + \beta(V_R^2 + V_S^2 - \beta^2 V_R^2 V_S^2)^{1/2}}{1 - \beta^2 V_R^2} \tag{1.29}$$

Also (1.24)–(1.26) give

$$\lambda_k = \frac{1 - k_R V_R}{1 + k_S V_S} \, \lambda_0 \tag{1.30}$$

so that a relationship between p_f, λ_0 and λ_k for given V_R, V_S, k_R and k_S follows immediately. Some typical relationships obtained by numerical integration are given in Figure 1.14.

Expressions (1.29) and (1.30) indicate that the factors λ_0 and λ_k depend on the variability or uncertainty associated with R and S; with greater V_R and V_S requiring greater factors if the failure probability p_f is to be kept constant (Figure 1.14). This demonstrates again the deficiencies of the deterministic measures of limit state violation. They ignore much information that may be available about uncertainties in structural strengths or applied loads.
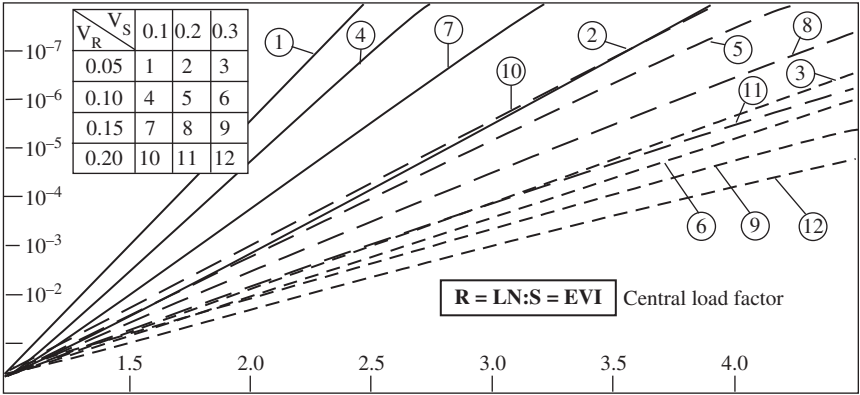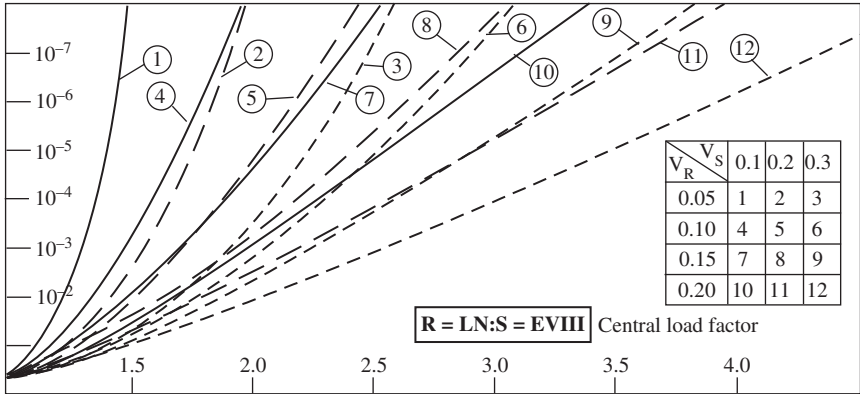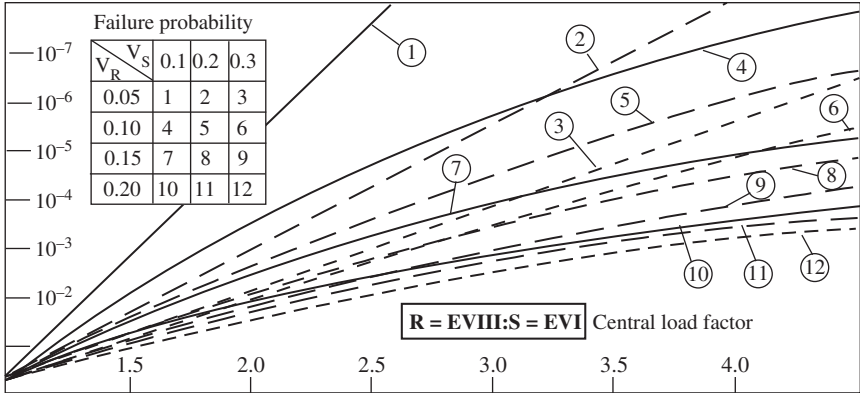
Figure 1.14 Failure probability p_f versus central safety factor λ_0 for lognormal (LN) and extreme value (EV-) distributions and different coefficients of variation.

Example 1.6   For a random variable S with $\mu_S = 60$, $V_S = 0.2$, the 95 percentile for the Gumbel (EV-I) distribution, for example, may be determined as follows (see A.77)

$$0.95 = F_Y(y) = \exp[-e^{-\alpha(y-u)}]$$

where, from (A.79), $\alpha^2 = \pi^2/6\,\sigma_Y^2$ and, from (A.78), $u = \mu_Y - \gamma/\alpha$ with $\gamma = 0.57722$.

Now $\sigma_Y = \sigma_S = 0.2 \times 60 = 12$, $\mu_Y = \mu_S = 60$, so that $\alpha = (\pi/\sqrt{6})/12 = 0.1069$ and $u = 60 - 0.57722/0.1069 = 54.60$. Hence

$$0.95 = \exp[-e^{-0.1069(S-54.60)}]$$

or

$$S_{0.95} = 82.38$$

Alternatively, Table 1.3 shows that, for the Gumbel distribution, $S_{0.95}/\mu_S = 1.373$. Thus the 95 percentile value of S is $S_{0.95} = 1.373\mu_S = 82.38$.

1.4.5   Numerical Integration of the Convolution Integral

As noted above, closed-form integration of Expressions (1.16) or (1.18) is only possible for some special cases. One of these cases, when both R and S are normally distributed, has already been considered (see Section 1.4.3). When both R and S are lognormal, and failure is defined as $Z = R/S < 1$, an exactly parallel result is obtained (see Example 1.7 below).

In general, however, to evaluate (1.16) or (1.18) for non-normal distributions, recourse must be made to numerical integration. The simplest approach, using the trapezoidal rule, is often quite effective [e.g. Dahlquist and Bjorck, 1974; Davis and Rabinowitz, 1975]. Step sizes around $x = 0.2\sigma_R$ have proved sufficiently accurate together with an integration range of about $\pm\ 5\ \sigma_Z$ instead of $\pm\infty$ [Ferry-Borges and Castenheta, 1971].

Some typical results obtained by numerical integration are given in Figure 1.14. Other, and similar, results have been given by Freudenthal (1964) and Ferry-Borges and Castenheta (1971).

Example 1.7   As an exercise for readers, use the probability density function (A.61) for the lognormal variable $Z = R/S$, where R and S are each lognormal, to show that

$$p_f = \Phi(-\beta_1) = \Phi\left\{-\frac{\ln\left\{\dfrac{\mu_R}{\mu_S}[(1+V_S^2)/(1+V_R^2)]^{1/2}\right\}}{\{\ln[(1+V_R^2)(1+V_S^2)]\}^{1/2}}\right\}$$

Also show that this simplifies to

$$p_f = \Phi(-\beta_1) \approx \Phi\left\{-\frac{\ln(\mu_R/\mu_S)}{(V_R^2+V_S^2)^{1/2}}\right\} \qquad \text{for}\ \ V_R < 0.3,\ V_S < 0.3$$

Finally, show that the expression for the central safety factor $\lambda_0 = \mu_R / \mu_S$ simplifies to

$$\lambda_0 \approx \exp[\beta_1 (V_R^2 + V_S^2)^{1/2}]$$

1.5 Generalized Reliability Problem

For many problems the simple formulations (1.15a)–(1.15e) are not entirely adequate, since it may not be possible to reduce the structural reliability problem to a simple R versus S formulation with R and S independent random variables.

In general, R is a function of material properties and element or structure dimensions, while S is a function of applied loads Q, material densities and perhaps dimensions of the structure, each of which may be a random variable. Also, R and S may not be independent, such as when some loads act to oppose failure (e.g. overturning) or when the same dimensions affect both R and S. In this case it is not valid to use the convolution integral (1.18). It is also not valid when there is more than one applied stress resultant acting at a section, or more than one factor contributing to the resistance of the structure. A more general formulation is required. The first step is to define the variables involved in the generalized reliability problem.

1.5.1 Basic Variables

The fundamental variables that define and characterize the behaviour and safety of a structure may be termed the 'basic' variables. Usually they are the variables employed in conventional structural analysis and design. Typical examples are dimensions, densities or unit weights, materials, loads, material strengths. The compressive strength of concrete would be considered a basic variable even though it can be related to more fundamental variables such as cement content, water-to-cement ratio, aggregate size, grading and strength, etc. However, structural engineers do not normally use these latter variables in strength or safety calculations.

It is very convenient to choose the basic variables such that they are independent. However, this may not always be possible. Thus the compressive and tensile strengths and the elastic modulus of concrete are related; yet in a particular analysis they might each be treated as a basic variable. Dependence between basic variables usually adds some complexity to a reliability analysis. It is important that the dependence structure between dependent variables be known and expressible in some form. Usually this will be through a correlation matrix; however, as noted in Appendix A, this can at best provide only limited information.

The probability distributions to be assigned to the basic variables depend on the knowledge that is available. If it can be assumed that past observations and experience for similar structures can be used, validly, for the structure under consideration the probability distributions might be inferred directly from such observed data. More generally, subjective information may be employed or some combination of techniques may be required. Thus, in practice some subjective influence is nearly always present, since only seldom are sufficient data available to identify unambiguously only one distribution as the most appropriate.

Sometimes physical reasoning may be used to suggest an appropriate probability distribution. Thus, where a basic variable consists of the sum of many other variables

(which are not explicitly considered), the central limit theorem (see Section A.5.8) can be invoked to suppose that a normal distribution (see Section A.5.7) is appropriate. This reasoning would be appropriate for the compressive strength of concrete (many component strengths) and for the dead load of a beam or slab (again many components of weight and several dimensions). In another example, the maximum wind velocity per year might be represented by the Gumbel (EV-I) distribution (see Section A.5.11), as this is based on an underlying wind phenomenon that, at any instantaneous point in time can be considered described as essentially Normal in probability distribution (see Chapter 7).

   The parameters of the distribution may be estimated from the data using one of the usual methods, e.g. methods of moments, maximum likelihood, or order statistics. These are well described in standard statistics texts and will not be considered here [e.g. Ang and Tang, 1975]. However, it must be emphasized that such techniques should not be used blindly. Critical examination of the data for trends and outliers is always necessary, and the reasons for these phenomena should be established. It is quite possible for such behaviour to be the result of data recording and storage procedures rather than the behaviour of the variable itself.

   Finally, when model parameters have been selected, the model should be compared with the data if at all possible. A graphical plot on appropriate probability paper is often very revealing, but analytical 'goodness of fit' tests (e.g. Kolmogorov-Smirnov test) can be used also.

   It may not be possible, always, to describe each basic variable by an appropriate probability distribution. The required information may not be available. In such circumstances a 'point estimate' of the value of the basic variable might be used, i.e. the best estimate, given the known information. If some uncertainty information about the variable is also available, it might be appropriate to represent it by an estimate of its mean and its variance only. This is then known as a 'second moment' representation. One way in which such a representation might be interpreted is that in the absence of more precise data, the variable might be assumed to have a normal distribution (as this is completely described by the mean and variance, i.e. the first two moments (see Section A.5.7)). However, other probability distributions might be more appropriate, even if only the first two moments are known or can be determined.

1.5.2 Generalized Limit State Equations

With the basic variables and their probability distributions established, the next step is to replace the simple $R - S$ form of limit state function with a generalized version, expressed directly in terms of basic variables.

   Let the vector $\mathbf{X}$ represent all the basic variables involved in the problem. Then the resistance R can be expressed as $R = G_R(\mathbf{X})$ and the loading or load effect as $S = G_S(\mathbf{X})$. Since the functions G_R and G_S may be non-linear, the cumulative distribution function $F_R(\ )$, for example, must be obtained by multiple integration over the relevant basic variables (see A.155):

$$F_R(r) = \int_r \dots \int f_{\mathbf{X}}(x) dx$$

A similar expression would apply for S and $F_S(\ )$. These could then be used in (1.18) or (1.19). Fortunately, it is seldom necessary to follow this somewhat complex and

piecemeal approach. Instead it is noted that in (1.l5e) the limit state function $G(R, S)$ itself can be generalized. When the functions $G_R(\mathbf{X})$ and $G_S(\mathbf{X})$ are used in $G(R, S)$, the resulting limit state function can be written simply as $G(\mathbf{X})$, where $\mathbf{X}$ is the vector of all relevant basic variables and $G(\ )$ is some function expressing the relationship between the limit state and the basic variables. The limit state equation $G(\mathbf{x}) = 0$ now defines the boundary between the satisfactory or 'safe' domain $G > 0$ and the unsatisfactory or 'unsafe' domain $G \leq 0$ in n-dimensional basic variable space. Usually the limit state equation(s) is derived from the physics of the problem. (Note that $\mathbf{X}$ is the vector of random variables and that $\mathbf{X} = \mathbf{x}$ defines a particular 'point' $\mathbf{x}$ in the basic variable space.)

Where some loads may influence resistance (e.g. in overturning situations (see Figure 1.2)) care should be taken that $G(\mathbf{X})$ is defined properly. Again by analogy with the simple case of Figure 1.2 a useful rule is that any basic variable adding resistance to the limit state should have a positive gradient, that is: $\partial G / \partial X_i > 0$.

Example 1.8   Consider a simple pin-ended strut supporting one end of a simply supported beam of length L_1, loaded at midpoint by a load Q. The actual load on the strut is thus $QL_1 / 2$. The strength of the strut is governed by its length L_2, its radius r of gyration, its cross-sectional area A and either the yield strength σ_Y of the steel or some combination of axial load capacity and bending capacity, usually expressed by an interaction rule in structural design codes. Such rules are based, usually, on experimental observations and are then modified for code users by adding conservative assumptions and factors of safety. It is apparent, therefore, that code rules must be used with great caution in reliability analyses. A better approach is to use the original data and/or original relationships for ultimate strength.

For the squash load limit state, it follows easily that the relevant limit state equation is:

$$G_1(\mathbf{X}) = \sigma_Y A - \frac{QL_1}{2}$$

Here usually all the variables may be considered to be random variables, although some might be considered closely deterministic, for example the variable A since usually there is little uncertainty about its value.

For the interaction case, the limit state equation is:

$$G_2(\mathbf{X}) = FN\left(\sigma_Y A, \frac{L_2}{r}\right) - \frac{QL_1}{2}$$

where $FN(\ )$ is an appropriate interaction equation for ultimate strength of pin-ended struts.

1.5.3   Generalized Reliability Problem Formulation

With the limit state function expressed as $G(\mathbf{X})$, the generalization of (1.16) becomes:

$$p_f = P[G(\mathbf{X}) \leq 0] = \int \ldots \int_{G(\mathbf{X}) \leq 0} f_{\mathbf{X}}(\mathbf{x}) d\mathbf{x} \qquad (1.31)$$

Here $f_{\mathbf{X}}(\mathbf{x})$ is the joint probability density function for the n-dimensional vector $\mathbf{X}$ of basic variables. Note that the resistance R and load effect S are not shown in the formulation — they are implicit in $\mathbf{X}$. Moreover, even if $\mathbf{X}$ were dissected, R and S

may not show up explicitly and may be represented by the variables of which they are composed. If the basic variables are all independent, formulation (1.31) is simplified, with (see A.117):

$$f_{\mathbf{X}}(\mathbf{x}) = \prod_{i=1}^{n} f_{X_i}(x_i) = f_{X_1}(x_1).f_{X_2}(x_2).f_{X_3}(x_3) \ldots \tag{1.32}$$

Here $f_{X_i}(x_i)$ is the 'marginal' probability density function for the basic variable X_i.

The region of integration $G(\mathbf{X}) \leq 0$ in (1.31) denotes the (hyper-)space in which limit state violation occurs. It is directly analogous to the failure domain D shown in Figure 1.8. Except for some special cases, the integration of (1.31) over the failure domain $G(\mathbf{X}) \leq 0$ cannot be performed analytically. However, the solution of (1.31) can be made more tractable by simplification or by numerical treatment (or both) of (i) the integration process, (ii) the integrand $f_{\mathbf{X}}( )$ and (iii) the definition of the failure domain. Each approach has been explored in the literature. Two dominant approaches have emerged:

(a) using numerical approximations such as simulation to perform the multidimensional integration required in (1.31)—the so-called 'Monte Carlo' methods;
(b) sidestepping the integration process completely by transforming $f_{\mathbf{X}}(\mathbf{x})$ in (1.31) to a multi-Normal probability density function and using some remarkable properties which may then be used to determine, approximately, the probability of failure—the so-called 'First Order Second Moment' methods and developments thereof.

These methods are described in more detail in Chapters 3 and 4 respectively. Some special results are given also in Appendix C.

1.5.4   Conditional Reliability Problems*

The probability estimate given by (1.31) becomes conditional when complete statistical information about the random variables $\mathbf{X}$ is not available. For example, the means or the variances might be estimated or not known with precision. In this case the probability expressed by (1.31) is a 'point estimate', given a particular set of assumptions about the probability distributions for $\mathbf{X}$. If the relevant statistical parameters are denoted $\boldsymbol{\theta}$ and are considered as random variables, the probability estimate becomes a conditional estimate and is a function of $\boldsymbol{\theta}$. Further, the limit state function now will be a function of $\boldsymbol{\theta}$ as well, i.e. $G(\mathbf{x}, \boldsymbol{\theta}) = 0$ and the joint probability function in $\mathbf{X}$ will be a function of $\boldsymbol{\theta}$ also, thus $f_{\mathbf{X}|\boldsymbol{\theta}}( )$. It should be noted that the nature of the uncertainties for the basic random variables $\mathbf{X}$ are different from the uncertainties in $\boldsymbol{\theta}$, the first expressing inherent variability (see Chapter 2) and the latter expressing uncertainty, which can be influenced by the collection of additional data (and perhaps by the use of alternative probability models). The net result is that the probability can now be expressed as a conditional probability estimate:

$$p_f(\boldsymbol{\theta}) = \int_{G(\mathbf{x},\boldsymbol{\theta}) \leq 0} f_{\mathbf{x}|\boldsymbol{\theta}}(\mathbf{x}\,|\,\boldsymbol{\theta})d\mathbf{x} \tag{1.33}$$

Of course, for decision-making an unconditional probability estimate is required. This can be done by invoking the total probability theorem (see A.6). For the present

this can be done by taking the expected value of the conditional probability estimate [Der Kiureghian, 1990]:

$$p_f = E[p_f(\boldsymbol{\theta})] = \int_{\theta} p_f(\boldsymbol{\theta}) f_{\boldsymbol{\Theta}}(\boldsymbol{\theta}) d\boldsymbol{\theta} \tag{1.34}$$

where $E[\ ]$ is the expectation operator and $f_{\boldsymbol{\Theta}}(\boldsymbol{\theta})$ is the joint probability density function of the parameters $\boldsymbol{\theta}$. Substitution of (1.33) into (1.34) then yields the unconditional probability estimate.

In passing it is noted that the integral of $f_{\mathbf{X}|\boldsymbol{\Theta}}(\ )$ over $\boldsymbol{\theta}$ sometimes is referred to, in the present context, as a 'predictive' distribution (since it takes into account uncertainties in $\boldsymbol{\theta}$), defined as:

$$f_{\mathbf{X}}(\mathbf{x}) = \int_{\theta} f_{\mathbf{X}|\boldsymbol{\Theta}}(\mathbf{x}\,|\,\boldsymbol{\theta}) f_{\boldsymbol{\Theta}}(\boldsymbol{\theta}) d\boldsymbol{\theta} \tag{1.35}$$

Methods to solve for these integrals are the subject of discussion in Chapters 3 and 4 and are relevant also to Bayesian updating in Chapter 10.

Another way in which the probability estimate (1.31) can be conditional is if the limit state function is given a more general interpretation. Consider, for convenience, the indicator function $I(\ )$ defined such that (Figure 1.15(a)):

$$\begin{aligned} I(x) &= 0 && \text{if } x \leq 0 \\ &= 1 && \text{if } x > 0 \end{aligned} \tag{1.36}$$

It follows that $I[G(\mathbf{X})]$ may then be interpreted as a 'utility function' with the failure state $G(\mathbf{X}) \leq 0$ having a 'utility' of zero, and the safe state $G(\mathbf{X}) > 0$ having unit 'utility'.

In practice, such as in problems involving serviceability considerations, the distinction between full utility and zero utility may not always be clear cut, and values between zero and unity may be appropriate (see Figure 1.15). Thus it may be that utility depends inversely on concrete crack size, with no cracks having a utility of 1, cracks < 0.1 mm a utility of 0.5 and greater cracks zero utility. Clearly many other possibilities and applications exist [e.g. Reid and Turkstra, 1980; Stewart, 1996b; Augusti and Ciampoli, 2008; Barbato *et al.*, 2013].

If now $J(x)$ denotes the above more general interpretation of the indicator function (see Figure 1.15(b)) and $J^c(\ ) = 1 - J(\ )$ defines the complement of J, the generalization of (1.31) becomes:

$$p_f = P\{J^c[G(\mathbf{X})]\} = \iint_{\mathbf{X}} \{J^c[G(\mathbf{x})] f_{\mathbf{x}}(\mathbf{x})\} \, d\mathbf{x} \tag{1.37}$$

As might be imagined, evaluation of (1.34) is not necessarily a simple matter.
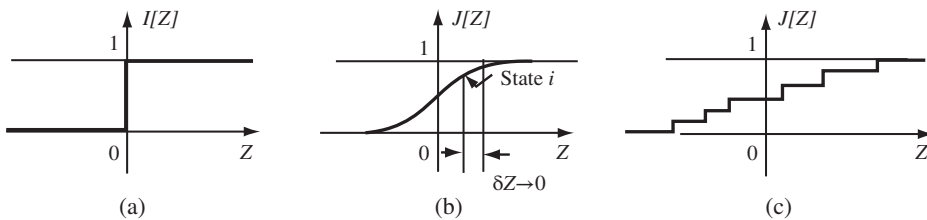
Figure 1.15 Limit state violation indicators.

If J (or J^c) is defined as a probability distribution function (see A.8), then (1.37) may be interpreted also as a total probability (see A.6) with (1.31) providing only the conditional probability of failure for a given realization of the limit state function. This more general interpretation is useful in structural reliability problems that are part of more general risk and reliability studies. For these, a range of possible limit state functions, not all structural, might arise. A good example is that of Probabilistic Safety Analysis (PSA) for nuclear facilities such as power stations or Probabilistic Risk Analysis (PRA) for other potentially hazardous facilities. In the case of nuclear power stations suffering a 'loss of coolant accident' (LOCA), the ability of the reactor block and its building to contain the resulting run-away reaction and its products is critical. The conditional probability of failure under a LOCA can be estimated for a defined external event such as for a level of (earthquake-induced) ground shaking. Repeating this for other levels of ground shaking and using the probability density for these levels together with the conditional probabilities of plant failure in the theorem of total probability allows the total probability of failure to be estimated. Similarly the occurrence of a LOCA may by the result of failure of critical pipework, and this may depend on the relative dynamic response of the reactor block and the reactor building under earthquake conditions (and others). More details of integrating structural reliability estimates as conditional events in larger risk assessments are discussed elsewhere [e.g. Stewart and Melchers, 1997].

1.6   Conclusion

Various ways in which structural reliability may be defined have been reviewed in this chapter. To do so it was necessary to introduce the concept of 'limit states'. This was seen to be a formalization of the possibly multiple criteria under which the structure can be considered to have 'failed' or have reached an unsatisfactory state.

Traditional measures of limit state violation were reviewed, including the factor of safety, the load factor and possible 'limit state design' concepts. It was shown that care is required in their definition; otherwise the safety measure might depend on how safety is defined, i.e. the formulation might not be 'invariant'.

Another common measure, the return period, was reviewed prior to the introduction of a fully probabilistic measure of limit state violation. Several aspects of this were then outlined and generalizations given.

2

Structural Reliability Assessment

2.1 Introduction

Before proceeding to elaborate the concepts introduced in Chapter 1, it is necessary to address fundamental questions about the meaning of the calculated probability of limit state violation (whether for ultimate limit states or otherwise). Specifically, what does the calculated probability p_f mean? Can it be related to observed rates of failure for real structures? How can knowledge of p_f help in achieving better (safer?) or more economical structures? And how does it relate to failure probabilities for other constructed or existing facilities? Surprising as it may seem, a degree of controversy and disagreement still remains about these important questions.

It will be helpful to examine the meaning of some terms. 'Probability' has already been used in Chapter 1. It denotes the chance that a particular, predefined event occurs. Classically, the probability of event occurrence was considered to be obtainable only from many repeated observations of the process that led to the event, the so-called 'frequentist' (or objective) definition. Obviously, the events must be observed. The observation process itself immediately adds an element of subjectivity, even to an otherwise frequentist meaning, in much the same way that observations in, say, physics are always partly subjective [de Finetti, 1974; Popper, 1959; Blockley, 1980; Jeffrey, 2004]. This aspect is sometimes (erroneously) ignored, and relative frequency data assumed to be purely 'objective' information.

An alternative interpretation is that probability expresses a 'degree of belief' about the occurrence of an event, rather than the actual (but unknown) frequency. It is therefore a 'subjective' or 'personal' probability. This interpretation is much wider than the relative frequency definition, and in its extreme form could be based on no previous data or experience of any sort to express degree of belief. Subjective probabilities are often referred to as 'Bayesian' probabilities, reflecting the tract on probability theory expressing these ideas, written by the Rev. Thomas Bayes in the early 1700s and since developed by many others. It is sometimes noted that a subjective probability estimate reflects the degree of ignorance about the phenomenon under consideration. There is a large literature on subjective probabilities [e.g. as summarized in Lindley, 1972; Jeffrey, 2004]. Reconciliation of the various interpretations of the meaning of probability still has interesting practical and sometimes quite controversial issues, although the latter are more philosophical than practical in nature [e.g. Fishburn, 1964; Kyburg, 1978; Hasofer, 1984; Lind, 1996; CIRIA 2014].

In socio-technical contexts the possibility of no information is rather rare, particularly for infrastructure applications. In most situations some relevant or related frequentist information is available to form a basis for subjective probability estimates. Generally, as more frequentist data become available the subjective probability estimates will tend to be adjusted so as to be in broad agreement with such data. The manipulation of subjective estimates and use of compatible data to amend and improve the estimates may be achieved through Bayes' theorem (A.7).

The term 'reliability' is commonly defined as the complement of the probability of failure $(= 1 - p_f)$, but more properly it is the probability of safety (or proper performance) of the structure over a given period of time.

'Risk' has two meanings. In the context of structural engineering, the first meaning is equivalent to the probability of structural failure from all possible causes, both from violation of predefined limit states and from other causes.

The second interpretation of 'risk' refers to the magnitude of the 'failure' condition, usually expressed in money terms and is commonly used in connection with insurance. This meaning will not be used herein.

'Structural failure' might be considered to be the occurrence of one or more types of undesirable structural responses including the violation of predefined limit states. Thus collapse of all or part of a structure, major cracking and excessive deflection are some possible forms of failure (see Table 1.1).

Fortunately, in practice structures fail only rarely in a serious manner, but when they do it is often due to causes not related directly to the predicted nominal loading or strength probability distributions considered in Chapter 1. Other factors such as human error, negligence, poor workmanship or neglected loadings are most often involved [Melchers et al., 1983; Brown et al., 2008]. To a large extent these factors are foreseeable and predictable. In fact, their occurrence might be considered as the occurrence of 'imaginable' events. Obviously, they must be accounted for in any analysis of structural reliability that attempts to replicate or predict reality with some degree of confidence. However, not all possible reasons for structural failure are always imaginable [Ditlevsen, 1982a; Brown et al., 2008]. Events that must once have been 'unimaginable' have led to structural failure; examples include the collapse of the Tay Bridge (1879) due (mainly) to underestimation of wind loading in storm conditions, and the Tacoma Narrows Bridge (1940) due to wind excitation of the deck. Even in these cases, there is some evidence to suggest that the phenomena involved were not totally 'unimaginable' before the accidents occurred. They were, however, apparently unimaginable to those involved with the projects [Sibley and Walker, 1977; Petroski, 1992; 2012]. In this respect, hindsight is not helpful.

Making estimates of failure probabilities for truly unimaginable events obviously is impossible. However, for imaginable events designers and others need to take care to ensure that they are aware of the state of the art of their specialization. Further, it is suggested that the public is more likely to accept the consequences of truly unimaginable events than it is likely to accept those of imaginable (and therefore foreseeable) events.

The theory needed to carry out a structural reliability analysis for imaginable events is the topic of this book. To do so, it will be necessary to consider the various types of such uncertainty that must be taken into account. These are considered in Section 2.2. Some uncertainties will be describable in terms of probability density functions. Others

may only be describable in less precise ways, such as by 'point' estimates of probabilities (see also Example 2.3). For the most part, the latter type of uncertainty will not be considered herein, although how it might be incorporated into a reliability assessment is described in Section 2.3. There are other, complementary, views of how this might be done [Schuëller, 2007].

Reliability analysis considering only a subset of uncertainties will result in a probability estimate that herein will be termed a 'nominal' or 'formal' measure. The meaning of such a measure is considered in Section 2.5, together with the implications of using such a measure for deriving rules such as those given in structural design codes.

Finally, some criteria that may be used to decide the acceptability of calculated reliabilities are discussed in Section 2.4.

2.2   Uncertainties in Reliability Assessment

2.2.1   Identification of Uncertainties

The uncertainties considered in Chapter 1 were the load acting on a structural element and its resistance. More generally, a range of uncertainties may need to be considered. These might include various environmental conditions, workmanship and human error, and prediction of future events.

Identification of uncertainties for complex systems may be difficult. Usually it is advantageous to use a systematic scheme to help to enumerate all operational and environmental loading states and, for each, to consider possible combinations of error or malfunction. This is essentially 'event-tree analysis' [Henley and Kumamoto, 1981; Stewart and Melchers, 1997]. Rather similarly, the systematic development of all possible forms of hazard to which a structure might be subjected has been termed 'hazard scenario analysis' even for structural systems [Schneider, 1981]. More generally, techniques such as 'brain storming' originally developed by Osborn (1957) and since much developed, may be of use. Various other techniques are available in the risk assessment literature [e.g. Stewart and Melchers, 1997]. Essentially all amount to a critical analysis of the problem to be analysed, consideration of all imaginable consequences and all imaginable possibilities and retaining only those with some finite probability of occurrence. Further, all techniques rely on having available expert opinion and up-to-date information on which to base assessments.

There are various ways in which the types of uncertainty might be classified in the wider context. Derived largely from the nuclear industry, one distinction is between what have been called 'epistemic' uncertainties and 'aleatory' uncertainties. The first refers to those uncertainties arising from lack of or gaps in knowledge. To reduce epistemic uncertainty requires more investigation of the basic phenomenon or issue so as to improve understanding. On the other hand, 'aleatory' uncertainty covers uncertainties intrinsic to the component or system being considered and thus might be reduced with gathering of additional data or information, improved numerical or other modelling and better parameter estimation. While much has been made of the difference between these two broad classes of uncertainty, it is clear both represent incomplete states of knowledge, whether it is in understanding or in data. In this respect, the difference is more philosophical than practical [Der Kiureghian and Ditlevsen, 2009].
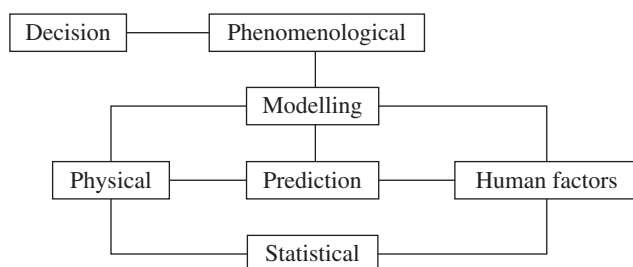
Figure 2.1 Uncertainties in reliability assessment.

A more practical breakdown of uncertainties is shown schematically in Figure 2.1. Each of the uncertainty classifications shown will now be discussed. Extra attention is given to human factors as these have been found to be particularly important.

2.2.2 Phenomenological Uncertainty

As already noted, sometimes an apparently 'unimaginable' phenomenon occurs to cause structural failure. The Tacoma Narrows Bridge noted earlier was apparently one such case. It was also of a design that departed considerably from earlier suspension bridge designs.

Phenomenological uncertainty may be considered to arise whenever the form of construction or the design technique generates uncertainty about any aspect of the possible behaviour of the structure under construction, service and extreme conditions. Therefore it is of particular importance for novel projects, or those which attempt to extend the 'state of the art' [Pugsley, 1962]. Evidently, only subjective estimates of the effect of this type of uncertainty can be given.

2.2.3 Decision Uncertainty

Decision uncertainty arises in connection with the decision as to whether a particular phenomenon has occurred. In terms of limit states, it is concerned purely with the decision as to whether a limit state violation has occurred.

A typical example concerns crack widths or deflections. It is unlikely, in general, that a slight increase in either will suddenly render the structure unsafe or unserviceable. At most, it is a question of relative loss of structural usefulness. One way in which decision uncertainty might be formulated has already been suggested in Section 1.5.4 using the indicator function $J(\ )$. This might also be taken as a measure of utility (see Figure 1.15). Decision uncertainty might be formulated also in terms of a probability density function for the (uncertain) criterion.

2.2.4 Modelling Uncertainty

Modelling uncertainty is associated with the use of one (or more) simplified relationship between the basic variables to represent the 'real' relationship or phenomenon of interest. In its simplest form, modelling uncertainty concerns the uncertainty in representation of physical behaviour, such as through the limit state equations. Modelling uncertainty is often simply due to lack of knowledge. It can be reduced with research or increased availability of data.
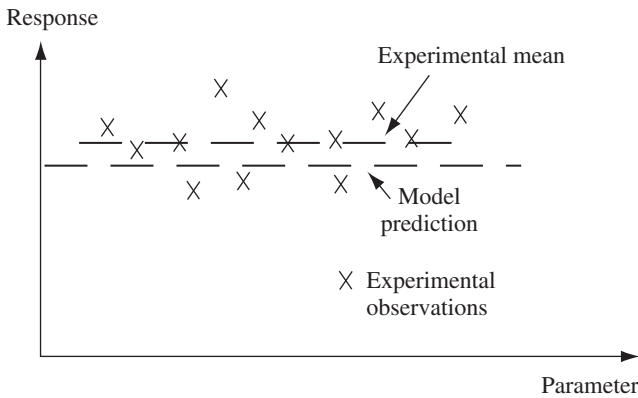
Response

Figure 2.2 Modelling error (schematic).

Modelling uncertainty can be incorporated into a reliability analysis by introducing a modelling variable X_m, say, to represent the ratio between actual and predicted model response or output (see Figure 2.2). Here X_m may be represented by a probability density function or simply as a mean and standard deviation (i.e. a second moment representation). This is a convenient approach where both the model and the actual phenomenon are measured by the same type of variables (e.g. deflection, or crack width). However, if structural system capacity or behaviour is modelled by individual member capacity or behaviour, say (as is implicit in permissible stress design philosophy), there usually will be a considerable amount of variability, depending on the type and the degree of static indeterminacy of the structure. It would be preferable in this case to include the structural system analysis more formally in the reliability analysis (see Chapter 5).

A special case of model uncertainty relates to the treatment of human errors and human intervention effects. If sufficient information about these effects is known, allowance could, in principle, be made for them in the modelling. Because of their special nature, a separate and detailed discussion of human factors is given in Section 2.2.8 below.

2.2.5 Prediction Uncertainty

Many problems in structural reliability assessment involve the prediction of some future state of affairs—in this case the prediction of the reliability of some structure at some time $t > 0$ in the future.

An estimate of structural reliability depends on the state of knowledge available to the analyst(s). As new knowledge related to the structure becomes available, the estimate will become more refined, with, usually but not necessarily, a concomitant reduction in uncertainty. This applies particularly during the construction phase of a project, when information about actual strengths of materials, workmanship, etc., becomes available to replace estimates based on the past performances of, and the experiences with, similar structures. When the structure is placed in service, its response to initial loading (or perhaps to 'proof loading') will constitute further information from which the reliability estimate may be revised.

It will be clear, therefore, that a probability estimate is not only a function of the properties of the structure, but also a reflection of the analyst's knowledge of the structure and the forces and influences likely to act on it. Similarly, if a reliability estimate for a particular structural lifetime is required, the analyst's uncertainty in the prediction of the lifetime (as well as the loadings that might be expected during that time) enter into the uncertainty of the reliability estimate (see Chapter 6).

2.2.6   Physical Uncertainty

Physical uncertainty is that identified with the inherent random nature of a basic variable. Examples include:

(1) variation in steel yield strength,
(2) variability of wind loading,
(3) variability of actual floor loading, and
(4) physical dimensions of a structural component.

Physical uncertainty might be reduced with greater availability of data or, in some cases, such as with steel yield strength, with greater effort in quality control. However, usually it cannot be eliminated, as is evident for natural phenomena such as wind loading, snow loading or earthquake loading.

Generally, the physical uncertainty for any basic variable is not known a priori and must be estimated from observations of the variable or assessed subjectively (see Section 1.5.1).

2.2.7   Statistical Uncertainty

Statistical estimators such as the sample mean and higher moments can be determined from available data and then used to suggest an appropriate probability density function and associated parameters. Generally the observations of the variable do not represent it perfectly, and as a result there may be bias in the data as recorded. In addition, different sample data sets will usually produce different statistical estimators. This causes statistical uncertainty. The process of using sample statistic estimators to infer (subjectively) a probability distribution for a variable is described in many standard texts [e.g. Benjamin and Cornell, 1970] and is not be considered here.

Statistical uncertainty can be incorporated in a reliability analysis by letting parameters such as the mean and variance (and other parameters which describe the probability distribution) themselves be random variables (see Section 1.5.4). Alternatively, the reliability analysis might be repeated using different values of the parameters to indicate sensitivity. If this is done often enough, quantitative estimates of sensitivity can be obtained (see Chapters 3, 4).

Example 2.1   Consider cylinder test results for a concrete of specified nominal strength as delivered by a number of concrete suppliers. To achieve the required nominal strength, some suppliers, with lesser control or quality, will aim for a higher mean strength to counter the greater variability of their product. There will also be variability due to between-batch variability for any one supplier, and variability due to the casting and testing of the test cylinders.

It is clear that the probability distribution that can be developed for concrete cylinder strength will depend on the manner in which each of these uncertainties contributes to the strength being measured. Evidently, if one supplier is changed, or deleted, the recorded histogram and hence the inferred probability distribution function for concrete strengths would be expected to change. Ideally, sampling should be on homogenous samples (i.e. those for which there is no *evidence* of non-homogeneity), with other factors separately sampled and perhaps included in a combined distribution model if required. Thus, restricting attention to only two different suppliers, the probability density function for concrete strength, irrespective of supplier, is given by

$$f_c(\ ) = q_1 f_1(\ ) + q_2 f_2(\ )$$

with

$$q_1 + q_2 = 1$$

where q_1, q_2 represent the respective contributions of suppliers 1 and 2, having concrete strength probability distribution f_1 and f_2 respectively. Clearly, a change in q_1 or in q_2 changes f_c.

2.2.8 Uncertainties Due to Human Factors

The uncertainties resulting from human involvement in the design, construction, use, etc., of structures may, for convenience, be considered as due to the effects of (i) human errors and (ii) human intervention. In practice, there is likely to be some interaction between these.

2.2.8.1 Human Error
Human errors can be divided, roughly, into errors V due to natural variation in task performance and gross errors E, G (see Table 2.1). As shown, gross error might be considered again in two categories: those errors which occur in the normal processes of design,

Table 2.1 Classification of human errors.

Error type	Human variability V	Human error E	Gross human error G
Failure process	In a mode of behaviour against which the structure was designed		In a mode of behaviour against which the structure was *not* designed
Mechanism of error	One or more errors during design, documentation, construction and/or use of the structure		Engineer's ignorance or oversight of fundamental behaviour. Profession's ignorance of fundamental behaviour
Possibility of analytic representation	High	Medium	Low

Adapted from Baker and Wyatt (1979).

documentation, construction and use of the structure within accepted procedures, and those which are a direct result of ignorance or oversight of fundamental structural or service requirements.

The relative importance of these types of errors can be gauged from Tables 2.2 and 2.3, which summarize the findings of Matousek and Schneider (1976) and Walker (1981). Other surveys suggest similar findings [Melchers et al., 1983; Nowak, 1986; Melchers, 1995a; Brown et al., 2008]. Note that unimaginable events, as interpreted from the information in Tables 2.2 and 2.3, constitute a rather low percentage of error factors.

The overriding conclusion from these surveys is that human error is involved in the majority of cases of recorded failure. Human error must, it seems, be considered if a reliability assessment is to relate to reality.

Unfortunately, understanding of human error is limited, and much of that understanding is qualitative [Reason, 1990; Blockley, 1992; Brown et al., 2008]. It is known that humans perform best at an appropriate level of arousal, as indicated schematically in Figure 2.3 [e.g. Warr, 1971]. If the level of arousal is too high or too low, performance deteriorates, although at the extremes there are rather vague barriers due to legal sanctions (see Section 2.2.8.2 below). Further, different persons operate at different arousal levels and, even at peak arousal, their performance will vary (cf. IQ tests).

Table 2.2 Error factors in observed failure cases.

Factor	%
Ignorance, carelessness, negligence	35
Forgetfulness, errors, mistakes	9
Reliance upon others without sufficient control	6
Underestimation of influences	13
Insufficient knowledge	25
Objectively unknown situations (unimaginable?)	4
Remaining	8

Adapted from Matousek and Schneider (1976).

Table 2.3 Prime 'causes' of failure.

Cause	%
Inadequate appreciation of loading conditions or structural behaviour	43
Mistakes in drawings or calculations	7
Inadequate information in contract documents or instructions	4
Contravention of requirements in contract documents or instructions	9
Inadequate execution of erection procedure	13
Unforeseeable misuse, abuse and/or sabotage, catastrophe, deterioration	7
Random variation in loading, structure, materials, workmanship etc.	10
Others	7

Adapted from Walker (1981).
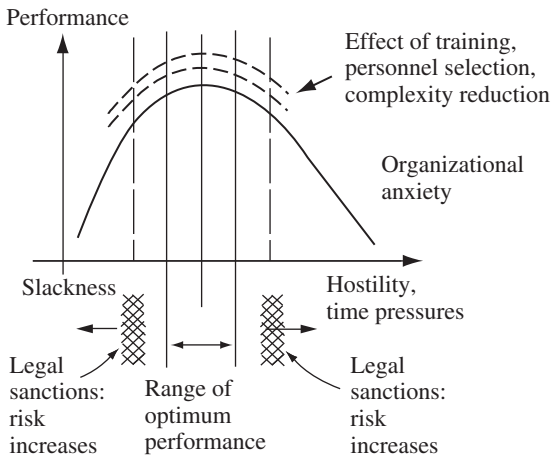
Figure 2.3 Human performance function [Melchers, 1980].

In his classic discussion of the problem, Pugsley (1973) considered that the main factors which affect 'proneness to structural accidents' are:

(1) new or unusual materials,
(2) new or unusual methods of construction,
(3) new or unusual types of structure,
(4) experience and organisation of design and construction teams,
(5) research and development background,
(6) financial climate,
(7) industrial climate, and
(8) political climate.

Evidently, these factors will have an influence on individual arousal and hence performance; they will also affect other aspects of human behaviour, such as human interaction, a matter also observed more generally in the management, psychology and sociology literature [e.g. Luthans, 2010].

Because of its complexity, human behaviour cannot yet be related to all the various factors that influence it. However, some specific empirical results for operator error in the nuclear, aircraft and chemical process industries, for example, are available [Joos et al., 1979; Harris and Chaney, 1969; Drury and Fox, 1975]. Typical rates for human error in psycho-motor tasks (such as monitoring or active control of a process) are of the order of 10^{-2} per stimulus, but with quite wide variations [e.g. Meister, 1966].

Preliminary investigation of typical (micro-)tasks used in detail structural design has found that errors occur in numerical desk-top calculator computation at a rate of about 0.02 per mathematical step. As the mean length of computation involves about two mathematical steps, the average error per calculation is about 0.04 [Melchers, 1995a]. Somewhat similar error rates were found to occur in 'table look-up' tasks and for 'table interpolation' tasks.

Such errors, while indicative of those that may occur in detail design may not be very significant by themselves. What needs to be considered is the effect that an error may have on the structure as built, and this depends largely on error magnitude [Nowak and
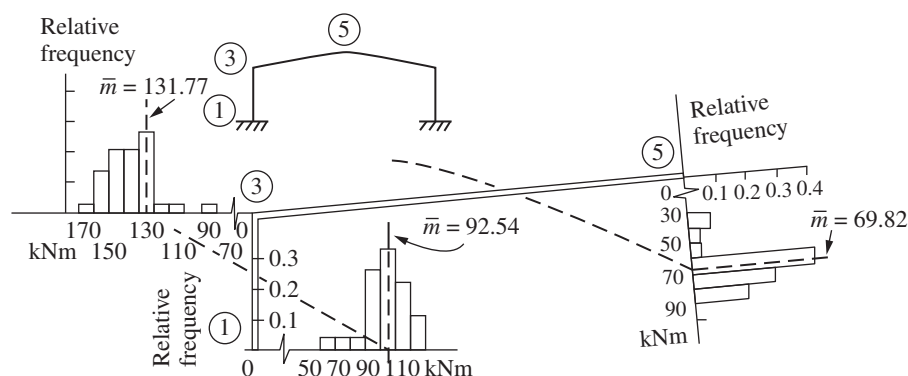
Figure 2.4 Typical histogram of bending moments from analysis of loading.

Carr, 1985]. It has also been suggested that usually more than one gross error needs to be committed before a structure is likely to fail [Lind, 1983].

For these reasons, and because errors may be detected, the integrated effect of the quality of performance in several micro-tasks, of error occurrence and of error detection is of interest. The output from the performance of a 'macro-task' such as design loading calculation has been studied and tends to show rather less variation than that observed for micro-tasks. For example, Figure 2.4 shows the histograms obtained for the calculated required moment capacity at three locations of a steel portal frame subject to wind and live and dead load. Designers participating in the study were required to decide on the loads acting on the various surfaces, and these were then converted to actions [Stewart and Melchers, 1988]. It is seen that most designers tend to err on the conservative side, but that some low results were recorded. Examination of individual responses showed that much of the variation was due to differences in assumed unit wind loads as a result of using 'shortcuts' in following structural design code requirements.

The available studies are not sufficient to give definitive information about the direct effect of human error on structural resistance [Brown et al. 2008]. It is evident, however, that human error will usually increase the uncertainty in the resistance of structures or structural members above that conveyed by uncertainty in material strength and geometric properties alone.

2.2.8.2   Human Intervention

There is little doubt that many existing and quite adequate structures remain in service despite (many minor) errors committed during their design and construction. One important reason for this is that structural design is, in general, rather conservative, producing structures, such as highway bridges, with significantly greater capacity than predicted by theory [e.g. Frangopol and Hearn, 1996]. The other important reason is that, apart from committing errors, humans also intervene in the processes of design, documentation and construction [Bosshard, 1979; Knoll, 1985] and, to some extent, also in the use and in the control of the use of a structure [Melchers, 2013]. Some forms of intervention are institutionalized, e.g. design checking to obtain building approval, and sanctions for violations of the law (contract, criminal or tort). Intervention may also be informal, such as may result from the observation that 'something is wrong'.

Safety factors or other nominal measures of safety can cater for some degree of human variability. However, it is unlikely that merely strengthening a structure against

Table 2.4 Human intervention strategies.

Facilitative measures	Control measures
Education	Self-checking
Good work environment	External checking and inspection
Complexity reduction	Legal (or other) sanctions
Personnel selection	

well-understood hazards, as would be achieved by increasing factors of safety, will be effective in obviating the effects of gross human error (see Table 2.2). Some form of positive action is required; a number of strategies are shown in Table 2.4. Brief comments about each of these follow but, as will be obvious, detailed discussion is beyond the scope of this book.

(i) Education
Education is widely recognized as important, particularly continuing professional education. Some of this occurs quite informally 'on the job', and through the technical press. Of particular interest in this regard would be balanced accounts of failure or poor performance of structures; yet it is precisely this information that has been difficult to obtain. Proposals for data banks have been made many times and tried so far with little longer-term success.

(ii) Work Environment
Work environment is recognized as an important factor in the effectiveness of the people working within an organization [e.g. Luthans, 2010]. Thus an open-minded goal-oriented environment is probably more likely to aid identification of all appropriate uncertainties. There are many examples in the literature where organizational problems created work environments which contributed to structural failure [Melchers, 1977].

(iii) Complexity Reduction
The simplification of complex tasks is a recognized strategy for error reduction. However, oversimplification can lead to boredom with concomitant increase in error rate. Some design (and other) processes lend themselves to extensive computerization, and this, together with the use of checklists and standardization, may well reduce certain types of error [Stewart, 1991]. However, different types of error are likely to arise in their place. A related development is that of 'expert systems', computer-based storage of available expert information.

A possible problem associated with standardization is that an undetected error may become 'institutionalized', with possible widespread effects, such as has occurred with so-called 'system built' housing and some high-rise apartment projects.

(iv) Personnel Selection
The effectiveness of a design or construction team will depend on the skills and abilities of the team members. In practice various constraints (such as seniority, lack of experience, existing staff commitments) may exist to prevent completely appropriate personnel selection. Conventional management theory lays considerable stress on having appropriate personnel [e.g. Luthans, 2010].

(v) Self-checking

Self-checking of a task appears to occur to some degree in all human actions. Together with checking by subsequent individuals or organizations in the design and construction processes, self-checking has been identified as an important factor in structural engineering. In design, for example, a designer is reasonably likely to spot significant errors that he has committed. This happens mainly when the member being designed is not of the 'right' proportions, or the reinforcement is somehow not as expected. Obviously not all errors will be detected since some experience is necessary to make the necessary judgements, but it is clear that the large errors are more likely to be detected than small errors [Stewart and Melchers, 1989a, b].

(vi) External Checking and Inspection

From the point of view of ensuring societal safety levels, external controls such as checking and inspection, and legal sanctions (see below) are often held to be far more powerful strategies to control human error than the ones described so far [CIRIA, 1977; Melchers, 1980; Brown et al., 2008]. Such procedures are well recognized in structural engineering. According to the studies by Matousek and Schneider (1976), only about 15% of errors would not be detected either by existing control arrangements working with greater care or through additional control measures. This last would, according to their estimate, have been required in about half the cases of failure they studied.

A typical model for checking effectiveness is a 'filter' that removes part of the error [Rackwitz, 1977]. Thus, if x_i represents the error rate in design calculations before checking, the error rate after checking might be given by

$$x_{i+1} = (1 - \gamma_i)x_i \tag{2.1}$$

where γ_i is the probability of error detection. Values of γ_i for inspection of electrical and other small components in factory production are in the range 0.3–0.9 with 0.75 for simple visual tasks under good conditions and with trained inspectors [Drury and Fox, 1975]. Preliminary data for checking of structural designs suggest an efficiency of about 0.7–0.8.

Search theory suggests that the detection probability increases with the time t spent on checking according to an exponential relationship [Kupfer and Rackwitz, 1980; Nessim and Jordaan, 1983], but Stewart and Melchers (1989a) found that a 'learning curve' of the form

$$\gamma = 1 - \exp[-\alpha(t - t_0)] \qquad t > t_0 \text{ (familiarization time)} \tag{2.2}$$

or

$$\gamma = \frac{1}{1 + A \, \exp(-Bt^{1/2})} \tag{2.3}$$

better fits empirical data. Here α is a parameter that depends on the degree of detailed examination and on the size of the task. A and B are constants with a similar function. All constants are dependent on the person performing the checking task. The checking time t could be replaced by the cost of checking, with appropriate new constants. In each case the checking function is preceded by a learning function required for the checker to familiarize himself with the material to be checked.

Some data are available to suggest that checking efficiency increases with error size but tends to level off to about 85% for large errors [Stewart and Melchers, 1989a].

(vii) Legal Sanctions

The doctrine that legal sanctions deter is firmly entrenched, it usually being taken for granted that fear of sanctions acts as a motivator and inhibitor of human conduct [Hagen, 1983]. There is evidence to suggest that sanctions may well be effective for 'premeditated' crime but that in general the effect is likely to be most pronounced on those least likely to be involved. It is reasonable to suggest that few engineers premeditate to perpetrate errors, so that the most likely result of excessive threat of legal sanction is inefficiency, over-caution and conservatism in the execution of work.

The available research on deterrence relates mainly to cases for which the boundary between lawful and unlawful behaviour or action, is relatively clearly defined. Except, perhaps, for negligence and deliberate malpractice, this does not appear to be the case for human errors.

2.2.8.3 Modelling of Human Error and Intervention

Human error may be incorporated in a reliability analysis as follows. If the human error phenomenon can be represented by a (perhaps subjective) random variable for which a probability density function can be postulated, it can be incorporated directly in the analysis for p_f, i.e. it becomes another basic variable (see Section 1.5.1). This is often possible for the type V and E errors of Table 2.1. Otherwise, a point estimate of the value of the phenomenon may be used to represent it.

Let R_m denote the structural resistance R when modified for human error E. In practice further modification may occur as a result of the possible effect of human intervention. The probability density function for R_m will then be further modified, in the lower tail region, to R_I, as shown in Figure 2.5. The discussion above suggests that an appropriate form is:

$$f_{R_I}(r) = K(r)f_{R_M}(r) \qquad r \leq r_d \tag{2.4}$$

with

$$K(r) = \exp[A(r - r_d)]$$

where r_d is a so-called 'discrimination' level, the value of the resistance for which errors typically are first noted, and A is a constant. The pdf must be modified also in the region $r > r_d$ to ensure that the area under the probability density function for R remains unity.
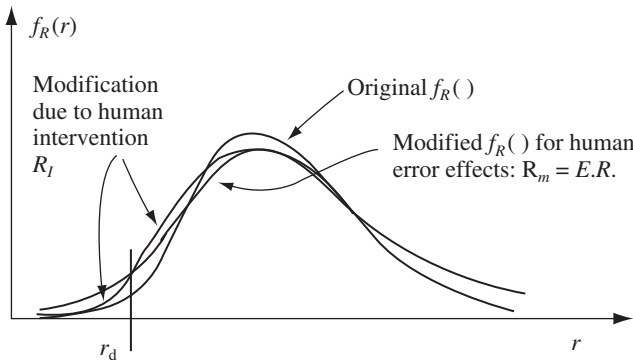
Figure 2.5 Modification of resistance probability density function for human error and human intervention effects.

Values of A can be estimated from data for checking and inspection effectiveness. A reasonable first choice might be to assume that, with R_d selected at one standard deviation, the reduction in the distribution at two standard deviations below the mean is, say, 90%. This would correspond in general terms to the initial estimates of checking effectiveness.

Example 2.2 The resistance R when modified for human error E, a random variable, becomes ER. The error term E may involve bias ($\mu_E \neq 1.0$) and will have a probability density function $f_E(\ )$ that, in the absence of contrary information, might be taken as normal. This is in agreement with the theory of errors and the central limit theorem (see Section A.5.8) since E is likely to be the result of a number of error processes.

An alternative formulation for modified resistance is $R + E$, with, $\mu_E = 0$ for zero bias. If R is $N(100, 20)$ and E is $N(0,10)$, the distribution of the modified R in this case is (see A.56 and A.57) given by $N(100, \sigma)$, where $\sigma = (20^2 + 10^2)^{1/2}$.

2.2.8.4 Quality Assurance

The various approaches to the reduction of gross human error described in the previous section should not be seen in isolation. In any engineering project they should be viewed as complementary techniques to achieve a desired goal. Usually this is the achievement of a safe and satisfactory project of sufficiently low cost and sufficiently high utility over the required design life. Use of the above techniques together with (i) establishment of appropriate managerial and organization structures, (ii) establishment of systems for material compliance testing, etc., and (iii) the selection of appropriate nominal safety measures may be given the umbrella title of quality assurance (QA). In the broadest sense, this is concerned with the management, coordination and monitoring of all stages of a project so as to achieve a desired set of objectives. International documents now exist to convey these ideas more generally [e.g. ISO 31000, 2009].

In the particular context of a building or construction project the QA functions must be applied to each of the various phases of conceptualization, design and analysis, documentation, construction, use and maintenance. It follows that for structural systems formalized methods of QA must take into account the need to meet the structural design objectives of structural safety, serviceability and durability. In common with other (non-structural) projects, a useful approach to achieve this is the institution of a 'safety' plan. This is based on a detailed 'hazard scenario' analysis. The safety plan is then used to lay down the requirements to be met by the QA procedures. In the case of structural engineering these would include [Schneider, 1981; ISO 13824, 2009]:

(1) proper definition of functions,
(2) definition of tasks, responsibilities, duties,
(3) adequate information flow,
(4) structural design brief,
(5) control plans and check lists,
(6) documentation of accepted risks and supervision plan,
(7) inspection and maintenance plan, and
(8) user instructions.

In addition it would be necessary to have adequate and systematic feedback of information to management at all stages of the project.

It is known from practical experience that there is a danger that excessive formalization of QA procedures will lead to unacceptable and self-defeating generation of paperwork. An appropriate level of QA is needed, tailored to each project and preferably designed in consultation with all concerned. This probably will mean that, for minor projects, only a very modest QA system is necessary. For major projects with complex QA procedures, there are the threats of complacency and unthinking adherence to instituted QA procedures.

In principle it is possible to arrive at an optimal set of QA measures using cost-benefit (-risk) analysis. The principles for this are considered in Section 2.4.2 below. In practice such an approach may be difficult, partly because of the lack of appropriate models for human error effects, partly because of the lack of models for the effect of QA measures and partly because of the difficulty of assigning costs associated with QA measures [Schneider, 1983].

2.2.8.5 Hazard Management

Following on from the ideas of QA, it is clear that those responsible for projects should concentrate not only on reducing risk but also on managing the hazards (or consequences) associated with significant risks. This means that reduction of consequences should be seen as part of the management of a project. In part this will depend also on the level of confidence to be had in the possible outcomes in the event of an accident. Moreover, with increased favourable experience with a facility, usually there is an increased level of confidence about the 'dependability' of the performance of the facility, irrespective of whether this is wholly justified or not [Comerford and Blockley, 1993].

Hazard management is particularly important in 'low probability–high consequence' situations. Typically these are situations where the risk is judged to be extremely low but if the event does occur the consequences are likely to be devastating. Nuclear accidents could be of this type. Earthquake events in intra-plate regions and other traditionally low-risk areas are another. Moreover, even if the immediate hazards from an event cannot be completely controlled or significantly reduced, the situation after the event might be managed appropriately. For example, following the January 1994 Kobe (Great Hanshin) earthquake in Japan, it has been realized that controlling the immediate consequences of a rare earthquake (building collapses etc.) may not be practical, as this would involve very high (and politically unacceptable) up-grading costs for the existing infrastructure. However, appropriate systems should be in place to control the subsequent hazards, that is, those associated with rescue and emergency operations and disease control.

It should be clear that the estimation of the probability of failure of a system is only one part of the overall process of risk assessment and risk-based decision-making. The next three sections deal with various aspects of this problem.

2.3 Integrated Risk Assessment

2.3.1 Calculation of the Probability of Failure

The probability estimates considered this far, and in particular in Chapter 1, rest on the notion that the uncertainty associated with a basic variable can be represented by a

probability density function. In Section 1.5.1 it was pointed out that this is not always the case, and that point estimates may need to be used for likely values of basic variables. Similarly, it may not always be possible to calculate probabilities in the manner suggested in Chapter 1, owing to lack of information. Again, point estimates may need to be used instead. For example, the observed failure rate per metre of high-pressure piping of given diameter is of this type, since no information is given about the type or extent of damage. The failure rate of electrical components (which will either fail or not fail) is another example, as are failure probability estimates due to human error.

A comprehensive estimate of failure probability must be able to incorporate both types of probability information. Assuming that the events described by point estimates are independent of those described by probability density functions, the combined (subjective) estimate of the structure failure probability is given by [CIRIA, 1977; Melchers, 1978] (see A.2).

$$p_f = (1 - p_E)p_0 + p_E p_1 \approx p_{fv} + p_{fu} \tag{2.5}$$

where p_E is the probability of human error occurrence, p_0 is the (conditional) probability of system failure without human error occurrence and p_1 is the (conditional) probability of system failure, given the occurrence of human error.

In the simplified form of expression (2.5), p_{fv} represents the failure probability as a function of random variables with probability distributions and p_{fu} the failure probability as a function of events for which only point estimates of probability are available. Where the independence assumption is not valid, the more general form with (+) replaced by the union ($\cup$) should be used. However, there are then seldom sufficient data to make evaluation possible.

There are considerable differences of opinion as to the validity of (2.5). Some hold that p_{fv} represents essentially 'objective' information and as such should not be combined with the largely 'subjective' probability p_{fu} on the grounds that subjective probabilities express a 'degree of belief' not compatible with objective or frequentist probabilities. There are schools of thought advocating that other methods of combining objective and subjective information be used. Various frameworks for dealing with such apparently disparate information types have been proposed. Probably the most popular is 'fuzzy set theory'. However, despite its advocacy over many years, it has not gained practical acceptance, nor has it been shown to be able to deal, conclusively, with problems that cannot be dealt with, satisfactorily, using (perhaps subjective) probability theory.

In common with most fields in which risk analysis is applied, the view taken here is that all probabilities are 'subjective' or 'Bayesian' to some degree (see Section 2.1). With this interpretation, the term p_{fv} can be evaluated with the aid of the total probability theorem (A.6):

$$p_{fv} = \sum_{i=1}^{n} p_{fi} p_i = \sum_{i=1}^{n} P(F \mid N_i) P(N_i) \tag{2.6}$$

where $p_{fi} = P(F \mid N_i)$ is the probability of failure given that the ith 'state of nature' N_i occurs and $p_i = P(N_i)$ is the probability of occurrence of the ith state of nature, with $\sum_{i=1}^{n} p_i = 1$. The state of nature refers to the set of conditions, qualifications, assumptions and state of knowledge which is implicit in the evaluation of $P(F)$; this may include

assumptions (and hence predictions) about human error, workmanship, etc., as well as, for example, an estimate of how well the calculation p_{fi} represents the actual failure probability [e.g. Tribus, 1969]. Expression (2.6) assumes independence of N_i; appropriate selection of the set $\{N_i\}$ may be required to achieve this.

The term p_{fu} in expression (2.5) is simply the sum of all point estimate probabilities of failure not otherwise accounted for. In general, the events included in the term p_{fu} are those for which the probability of occurrence is not well understood, so that questions of dependence or correlation are of little relevance. As understanding grows about these events, they will be expressed more easily in probabilistic terms. Hence it would be expected that p_{fu} will reduce, and that p_{fv} will increase. Conversely, poorly understood problems would be represented mainly by p_{fu}.

Example 2.3 It is estimated that the probability of accidental traffic overload (event N_1) for a small bridge is 0.01. When that occurs, the conditional probability $P(F|N_1)$ of failure of the bridge, estimated using the method of Chapter 1, is 0.1. Under normal loading conditions the probability of failure is 0.002. In addition, it is possible for flooding to occur (event N_2) independently of the traffic loads applied to the bridge; the probability that this occurs at a magnitude sufficient to cause failure is estimated at 0.005. All probabilities are for a 50-year life. Assuming that overload and flooding are unlikely to occur simultaneously, the predicted probability of failure is then estimated as follows:

$$P(F|N_1) = 0.1 \qquad P(N_1) = 0.01$$

$$P(F|N_2) = 0.002 \qquad P(N_2) = 1 - P(N_1) = 0.99$$

$$p_{fu} = 0.005$$

Substituting into (2.5) and (2.6), there is obtained

$$p_f = (0.1)(0.01) + (0.002)(0.99) + 0.005 = 0.008$$

2.3.2   Analysis and Prediction

The determination of the probability of failure can be carried out from two viewpoints: (i) analysis of a given state of affairs, and (ii) prediction of failure probability for some time period in the future.

For analysis, the probability density functions of all random variables are presumed known for the time at which the analysis is required; these may, of course, have been obtained from direct observation or from subjective estimates. Similarly, any point estimates for random variables or events are assumed to be known or obtainable for the time at which the analysis is required. Using such information in expression (2.5), together with the techniques described in this book, will allow an estimate of the current probability of failure to be obtained. If it is assumed that there are no changes to be expected with time in any of the parameters, then the calculated probability estimate may also be used to describe the probability of failure for future times.

More generally, however, it would be expected that probability density functions for some of or all the random variables will change with time (see Figure 1.7). The problem of prediction of probability of failure is thus one of predicting the future probabilistic descriptions of the relevant random variables. Not only may means and variances

change with time, but the type of probability density function also may change. Similar comments apply to variables with point estimates of probability—these may change, or might be expected to change, with time.

For a project in the planning stage, the predicted failure probability for the completed structure will be quite uncertain, since details of actual loadings, material strengths, etc., will not be well defined. Hence coefficients of variation typically are rather large. This is relevant, for example, in structural design code calibration work (see Chapter 9). When construction is under way, details of actual material suppliers become available and this should, generally, allow a reduction in coefficients of variation for material strengths, and better estimates of workmanship variability. Similarly, when the structure is put into service, better definition of loading uncertainties should be possible.

The difference between analysis and prediction can be seen, now, to be a matter of the amount and type of information available to the analyst. In the case of prediction, the information may be more subjective and tentative than that available for the analysis of an existing structural system, but the basic process is the same.

2.3.3 Comparison to Failure Data

From the above it follows directly that as better estimates of the various properties and assumptions become available, the (subjective) probability prediction can be refined. It would be expected that, in the limit, the probability of failure so estimated would approach the probability of failure for similar structures; this assumes that subjective estimates tend to approximate objective (frequentist) data as the information available improves, which, of course, may not always be correct [Jeffrey, 2004].

With time, and with engineering research and with practical experience with actual structures over many years, the proportion of the structural behavioural phenomena that are unknown or poorly understood decreases [Shiraishi and Futura, 1989]. Such changes need not always be gradual and may have major changes: for example, as a result of structural failure. Overall the net result is that with time and practical experience the likelihood of structural failure from unknown or poorly understood phenomena tends to decrease. This also should decrease the probability of failure from human error, although it is possible that the proportion of failures caused by human error will increase as technical uncertainties decrease (Figure 2.6).
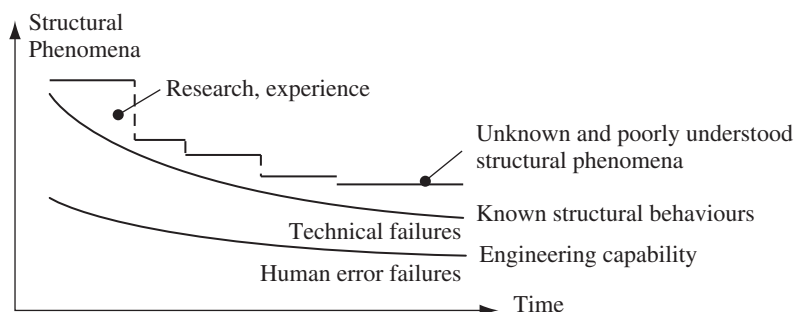
Figure 2.6 Schematic representation of the development of understanding of structural phenomena with time and research and the reduction of probability of failure from related technical failure, and the possible increase in the proportion of failures from human error.

Further, it might be expected that with the inclusion of all relevant variables and with perfect probabilistic modelling of all the variables and the appropriate limit states, the estimated failure probability would approach the failure rate that might be observed for sufficient large samples of nominally identical structures. While this is true in principle, in practice this is unlikely to be closely achieved. Apart from severe problems with historical records and observed rates of failure (see Section 2.4), the failure probability estimate for a particular structure is based on past experience with, at best, similar structures and with probability distributions for materials, sizes and loadings (etc.) subjectively selected. Although frequentist data for these may be available from historical records for other structures, the validity of their application to the structure being considered still requires (subjective) judgement. In particular, fundamental probability theory dictates that probability distributions must be derived from data drawn from homogeneous populations. Also, for model development, the accuracy of design, the standard of workmanship and the effectiveness of inspection and control must be estimated.

It follows that the quality of a structural reliability estimate is very much a function of the data and modelling used to derive it but that it may not agree closely with observed rates of failure for real structures (assuming that such rates can actually be observed).

Comparison of estimated probabilities of failure for a given structure to observations about failure rates in practice (and between estimates for different structures) requires the utmost care. As noted in Section 2.2, there are few failure statistics of sufficient richness and depth to make useful comparisons for practical structural configurations, type, method of construction, and, most importantly, the design code used for the structural design [Rüsch and Rackwitz, 1972]. This latter point is illustrated in failure statistics for building damage and collapse as a result of the January 1994 Kobe (Great Hanshin) earthquake [Fujino, 1996]. Figure 2.7 shows clearly that the level of damage for buildings could be related to the period of original construction. In turn this could be related directly to the design code in force during that period. It was concluded that structural damage for buildings designed to the most recent design code was significantly less than for earlier, less stringent, codes. Evidently, such changes in design requirements will affect 'observed' rates of failure and hence complicate comparisons to computed estimates. Similar observations have been made elsewhere.
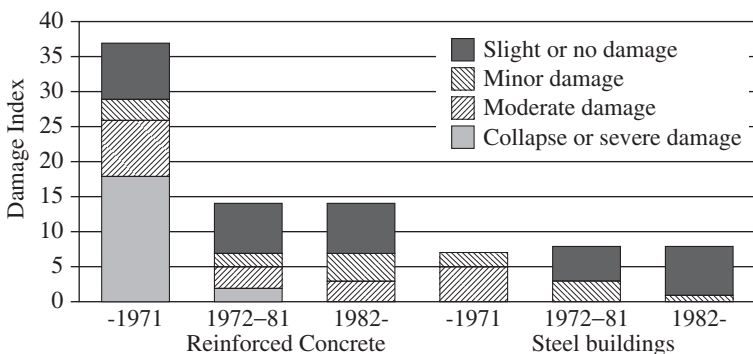
Figure 2.7 Damage level for buildings in Kobe, Japan, as a function of year of construction [based on data reported by Fujino, 1996].

2.3.4 Validation—a Philosophical Issue

At first sight the above situation may appear to be rather unsatisfactory. It implies that different analysts can obtain different estimates of the probability of structural failure, depending on the models they care to use. Moreover, it renders the notion of a probability estimate as unscientific in the sense that the outcome is not open to the test of falsification [Popper, 1959]. For example, consider the statement that 'a given level of seismic activity has a return period of 500 years'. To test whether this statement is scientifically reliable, it must first be established that it is 'scientific'. Unfortunately, it fails on this score as there is no practical way that it could be shown to be false. To do so would require observation over a period much longer than 500 years [Grandori, 1991]. It is clear that the statement cannot be verified either.

In structural engineering in particular, the situation is even more difficult, since there is no population of identical structures that can be observed under identical conditions. Moreover, practicalities dictate that structures are not allowed to simply wear out and fail. They are, usually, maintained and repaired as required. This means that the notion of a 'design life' remains largely a theoretical one, seldom reached for the original structure. It also means that even if it was reached, the information obtained would be worthless as being much too old for use with theory for the design of new structures [Lind, 1996].

Since 'scientific' validity cannot be ensured for the outcomes predicted by reliability analyses, it is more useful to focus on the reliability of the procedures themselves [Ditlevsen, 1983a, 1997; Grandori, 1991]. This may require specification of formalized procedures to use for risk assessments, as is common in the nuclear industry and as advocated also for codified structural design (see Chapter 9). Alternatively, reliability estimation procedures can be tested for validity against artificially generated data sets, a subset of which is used as input for them [Lind, 1996]. Such approaches for development of models have extensive application in other areas, for example in the development of models for stream flow and in weather prediction.

In summary, methods to estimate structural failure probability cannot have scientific status. The justification and the acceptance of these methods do not stem from them being able, necessarily, to provide correct descriptions of reality. On the contrary, it stems from the fact that they can give reliable, consistent and satisfactory solutions for practical problems [Matheron, 1989]. In this sense they are engineering rather than scientific tools.

2.3.5 The Tail Sensitivity 'Problem'

The tail sensitivity 'problem' has some history in structural reliability analysis but arises simply from the observation that the probability distribution assigned to any one basic variable can have a marked influence on the calculated failure probability. This can be seen, for example, in Figure 1.14, by comparing curves with similar coefficients of variation V_R and V_S for different probability functions. The reason for the difference lies, of course, in the shape and extent of the overlap of the probability density functions shown in Figure 1.10. This dependency of p_f on the assumptions made for the probability density functions is sometimes considered to be an obstacle in providing meaningful estimates of p_f. However, in view of the discussion in the previous section, it is evident that the tail sensitivity problem is merely a reflection of the various uncertainties

@Seismicisolation

that arise in quantifying the probability density functions for the variables in a reliability analysis. Further, if p_f is seen only as a 'nominal' or 'formal' measure of structural failure probability as will be discussed in Section 2.5, it will have as its purpose only comparison between probability estimates for structures, rather than as an absolute value. In this comparative sense the tail sensitivity problem becomes essentially inconsequential, as no absolute frequentist meaning is now directly attached to such a measure.

Of course, the tail sensitivity problem is of major importance if the aim of the structural reliability analysis is to estimate realistic probabilities. In this case considerable attention must be paid to using the best available probabilistic models, in particular those that best model the relevant extremes ('tails') of the probability density functions. Generally this means that the 'tails' of the models must be good fits for the higher values of the loads and for the lower values of the resistances (*cf*. Figure 1.10).

2.4   Criteria for Risk Acceptability

When a reliability assessment has been performed, it must be decided whether the probability of limit state violation (i.e. the probability of structural system failure) assessed by (2.5) is acceptable. There is no easy answer to such a question, even if the assessed failure probability represented a 'perfect' estimate. But as has been discussed above, the estimated failure probability associated with a project is very much a function of the understanding of the issues, modelling and data—it follows that any comparison to acceptance criteria must take at least some account of the context within which the estimate of the probability of failure is made. This also has important implications in the context of setting probabilistically consistent requirements in design codes (see Chapter 9).

In general, acceptance criteria have been formulated mainly as 'risk acceptance' criteria (or, sometimes, as 'risk tolerance' criteria). Moreover, they have been framed both using 'risk' in the context of probability of occurrence of limit state(s) violation and in the context of probability of occurrence of associated consequences.

Two criteria for making decisions about risk acceptance will be outlined below. More complete discussions are available [e.g. Royal Society Study Group, 1991; Stewart and Melchers, 1997; CIRIA, 2014; EMSA, 2015].

2.4.1   Acceptable Risk Criterion

2.4.1.1   Risks in Society
One criterion is to compare the calculated probability of structural failure with other risks in society and from these to infer 'acceptable' or 'tolerable' risks for structures [e.g. Stewart and Melchers, 1997; CIRIA 2014]. Table 2.5 shows a summary of selected risks in society, based largely on historical data but unlikely to have changed much with time. It is seen that there is a difference of about one order of magnitude between the so-called 'voluntary' risks and the 'involuntary' (or background) risks, and that the risks depend on the degree of exposure to a hazard (i.e. on the potential consequences). Generally, people are confident in their use of engineered structures, in the expectation that they will not fail. Hence the probability of structural failure may be related to involuntary risk. However, opinion about this varies. Some broad indicators of tolerable risk levels have been suggested also (Table 2.6).

Table 2.5 Selected risks in society (indicative).

Activity	Approximate death rate[a] ($\times 10^{-9}$ deaths/h exposure)	Typical exposure[b] (h/year)	Typical risk of death ($\times 10^{-6}$ / year) (rounded)
Alpine climbing	30 000–40 000	50	1500–2000
Boating	1500	80	120
Swimming	3500	50	170
Cigarette smoking	2500	400	1000
Air travel	1200	20	24
Car travel	700	300	200
Train travel	80	200	15
Coal mining (UK)	210	1500	300
Construction work	70–200	2200	150–440
Manufacturing	20	2000	40
Building fires[c]	1–3	8000	8–24
Structural failures[c]	0.02	6000	0.1

a) Adapted from Allen (1968) and CIRIA (1977).
b) For those involved in each activity (estimated values).
c) Exposure for average person (estimated).

Table 2.6 Broad indicators of tolerable risks [based on Otway et al. 1970].

Risk of death per person per year.	Characteristic response
10^{-3}	uncommon accidents; immediate action is taken to reduce the hazard
10^{-4}	people spend money, especially public money to control the hazard (e.g. traffic signs, police, laws);
10^{-5}	mothers warn their children of the hazard (e.g. fire, drowning, firearms, poisons), also air travel avoidance
10^{-6}	not of great concern to average person; aware of hazard, but not of personal nature; act of God.

Typical failure rates for building structures and for bridges based on historical data are given in Tables 2.7 and 2.8 respectively. For comparison purposes, the rates have been adjusted, where necessary, in an attempt to extract the limit state of 'collapse', this being the closest to that likely to lead to fatalities and hence to allow a degree of comparison to Table 2.5.

For a number of reasons the rates given in the tables must be viewed with caution. There is some evidence and much qualitative conceptual support that 'collapse' failures account for only about 10–20% of all cases of failure. Many failures of lesser magnitude involve serviceability limit state violation [Melchers et al., 1983]. Further, many of the 'collapse' failure cases occurred during construction. It is not always clear whether the structure failed under 'normal' loading or whether temporary works failed. Also, the

Table 2.7 Typical 'collapse' failure rates for building structures.

Structure type	Data cover	Number of structures (estimated)	Average life (years)	Estimated lifetime p_f
Apartment floors	Denmark	5×10^6	30	3×10^{-7}
Mixed housing	The Netherlands (1967–1968)	2.5×10^6	-	5×10^{-4}
Controlled domestic housing	Australia (New South Wales)	145 500	-	10^{-5}
Mixed housing	Canada	5×10^6	50	10^{-3}
Engineered structures	Canada	-	-	10^{-4}

Sources: Allen, 1981a; Ingles, 1979; Melchers, 1979.

Table 2.8 Typical 'collapse' failure rates for bridges.

Bridge type	Data cover	Number of structures (estimated)	Average life (years)	Estimated lifetime p_f
Steel railway	USA (< 1900)	-	40	10^{-3}
Large suspension	World (1900-1960)	55	40	3×10^{-3}
Cantilever and suspended span	USA	-	-	1.5×10^{-3}
Bridges	USA	-	-	10^{-3}
Bridges	Australia	-	-	10^{-2}

Sources: Pugsley, 1962; Ingles, 1979.

probability of failure during construction may not always be considered in a reliability assessment. It would be quite erroneous to compare failure statistics including construction with predictions excluding construction.

A further matter to be taken into account is subjectivity in deciding whether a structure has 'failed'. This may very well depend on the consequences, with large consequence failure gaining much publicity and being subject to major inquiries, etc. However, a failure with little consequence may never be recorded. It is likely that the rather higher rates of failure for bridges in Table 2.8 are due to this effect. It may also be due to phenomenological uncertainty (see Section 2.2.2) associated with novel forms of construction.

2.4.1.2 Acceptable or Tolerable Risk Levels

From the risks that are encountered in society, various bodies, including regulators of hazardous industries, such as nuclear facilities, chemical plants etc. have developed 'acceptable' or 'tolerable' risk levels. Generally these are related to consequences, most typically death of 'passers-by' and operatives [e.g. Henley and Kumamoto, 1981; Royal Society Study Group, 1991; Stewart and Melchers, 1997; NSW DEP, 2011; EMSA, 2015]. Although not yet applied to structural engineering, they provide a broad indication of the risk levels that might need to be met also for engineered structures.

It may not be possible, always, to comply completely or closely with regulatory risk criteria (however defined). One approach developed in other areas dealing with risk situations is the concept of 'As Low As Reasonably Practical (or Achievable)', the ALARP (or ALARA) principle [HSE, 1992]. It considers that (i) there is an upper limit to the risk, that is, greater risk cannot be tolerated in any circumstances and (ii) a lower limit below which risk is of no practical interest. Between these two limits lies the region in which the risks must be reduced to a level which is as low as 'reasonably practical', such as through spending money to reduce the risk imposed by the facility. Although this approach has a certain intuitive and practical appeal, there are considerable associated theoretical and philosophical difficulties. These include the question of definition of terms and their interpretation, openness of decision processes, comparability between facilities and serious questions about morality of actions of individuals, companies and governments acting on behalf (usually) of its citizens [Royal Society Study Group, 1991; Melchers, 2001; Jonkman, et al., 2003]. Instead of risk criteria (e.g. Tables 2.7 and 2.8) costs, direct and indirect may be more appropriate to derive ALARP criteria, particularly for high-cost construction such as offshore structures [Aven and Vinnem, 2005].

2.4.2 Socio-economic Criterion

If failure consequences are to be taken into account, a more general criterion for assessing acceptability of structural failure probability is cost-benefit (-risk) analysis given by the net present value criterion as:

$$\max(B - C_T) = \max(B - C_I - C_{QA} - C_C - C_{INS} - C_M - p_f C_F) \qquad (2.7)$$

where B is the total benefit of project, C_T is the total cost of project, $C_I(\lambda)$ is the initial cost of project, $C_{QA}(e) = \sum_{i=1}^{n} C_{QAi}(e)$ is the cost of n quality assurance (QA) measures, $C_c(e)$ is the cost of corrective actions in response to QA measures, $C_{INS}(\lambda, e)$ is the cost of insurance, $C_M(e)$ is the cost of maintenance, $p_f(\lambda, e)$ is the probability of failure of the project, C_F is the cost associated with failure, λ is the nominal factor of safety and e is the vector of QA efforts (such as expenditure on QA). All costs and the benefit B must be discounted to allow for the effect of time as in standard cost-benefit analysis [e.g. de Neufville and Stafford, 1971]. Formulation (2.7) also can be rewritten as a minimization problem in costs, since the benefit B generally is neither a function of the degree e of QA nor of the nominal safety factor λ.

Both p_f and C_F depend on the mode(s) of failure being considered. The value of C_F is uncertain. It depends on how much damage is likely to be caused, how many lives lost, etc. Hence C_F might be modelled as a random variable, although appropriate data are scarce. In addition, the long-term effects of project failure should be included in C_F. The evaluation of C_F may well vary for different parties involved in the ownership, use and responsibility for the structural project, at various stages during its life, so that (2.7) is strictly a multi-objective optimization problem with C_F varying for different interest groups.

Before the maximization of (2.7) can be carried out, relationships between $p_f(\lambda, e)$ and e and between the costs $C_{QA}(e)$, $C_c(e)$, $C_{INS}(e)$ and $C_M(e)$ and e must be established. Models such as these outlined in Section 2.2.8 may be of some help here, particularly for $C_{QA}( )$. The cost of insurance should, in theory, vary inversely with the amount of QA, although this does not appear to be the case in practice [CIRIA, 1977] except in a

special sense in the French decennial form of insurance and building control [Cibula, 1971]. Maintenance costs would be expected to decrease with *e*.

In principle it is possible to use expression (2.7) to derive the optimal probability of failure for a structure, given a certain level of quality assurance. Assuming a constant benefit *B* and minimizing the total cost, the variation of the various costs is shown in Figure 2.8. Evidently, a minimum $dC_T/dp_f = 0$ exists, and it is clear that this minimum is highly sensitive to changes in the slopes of the cost curves. Nevertheless, it has been estimated that the optimal probability of failure for buildings is about 10^{-4} per year, and 10^{-3} per year for bridges [Rüsch and Rackwitz, 1972]. These estimates appear to have been determined under the (questionable) assumption that the cost C_F of failure is negligible and that human error effects may be ignored. For this reason these values probably are better regarded as nominal failure probabilities rather than more realistic ones (see Section 2.5 below).

Appropriate levels of QA efforts can be determined similarly. The result depends strongly on the effectiveness and unit costs of each QA measure, as well as on the ratio C_F/C_I. Typical values for the latter are 30–75 for beam elements and 350–700 for columns supporting one floor to 90–1800 for columns supporting ten floors [CIRIA, 1977]. Unless C_F/C_I is very high (which is not normally the case), optimal total cost is only achieved with high QA effectiveness; otherwise $C_{QA}(e) > p_f C_F$. The full implications of this for practical quality control schemes are not always fully realized.

Finally, it must be noted that increased investment in structural safety, whether in terms of C_{QA} or C_I may not be as effective in terms of benefit gained, as additional
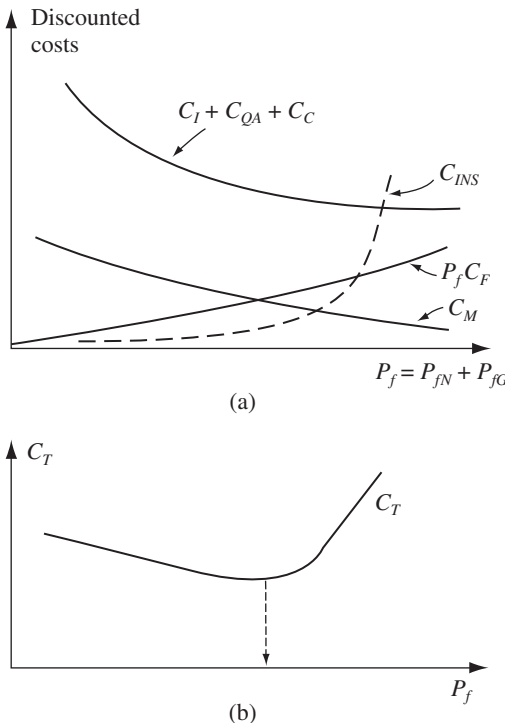
Figure 2.8 (a) Component costs and (b) total costs as a function of p_f.

expenditure in, say, road safety or medical research. The allocation of resources between competing sectors of the economy is essentially a socio-political matter. An appropriate framework for structural engineering decisions may well be to assume that C_T is fixed and that any optimization must be a matter of allocating available resources within this constraint.

A more general decision framework than risk-benefit analysis is utility theory. However, formulation of appropriate utility functions is often difficult. Some initial studies in this area have been reported [Augusti et al., 1984]. Even more generally, there has been interest in relating structural risks and consequences to 'quality of life' in a more general sense, exemplified by a (rather arbitrarily defined and society-dependent) Life Quality Index [Rackwitz, 2002; Pandey and Nathwani, 2004; Ditlevsen and Friis-Hansen, 2005].

2.5 Nominal Probability of Failure

2.5.1 General

The discussions in Sections 2.2 and 2.3 indicated the importance of accurate modelling, and in particular the inclusion of human error and human intervention effects in determining a good estimate of structural failure probability. When these matters are ignored, and also sometimes when approximations have been made in the calculations, the corresponding failure probability becomes a nominal one, p_{fN} (*cf*. Section 2.1). It is pertinent to question whether such a probability measure has any useful meaning. This question is relevant since p_{fN} has been used in a comparative sense, with a lower value preferred to a higher one. A particular application is in code calibration work (see Chapter 9). More generally, the possibility of the use of p_{fN} as a surrogate for p_f in decision-making usually is discussed with the proviso that it should not be interpreted as a relative frequency, but rather as a 'formal' failure probability measure, interpreted as a 'degree of belief' [e.g. Ditlevsen, 1983a; 1997].

As noted in Section 2.1, the interpretation of probability as a degree of belief is an acceptable one, consistent with Bayesian statistics. However, whether p_{fN} can be used to make valid comparisons of structural safety needs to be examined. For p_{fN} to be used as a surrogate for p_f and hence to be used validly to compare two alternatives, 1 and 2, it is required that:

$$\frac{p_{f1}}{p_{f2}} \approx \frac{p_{fN1}}{p_{fN2}} \tag{2.8}$$

The validity of this statement can be examined on at least two (somewhat interrelated) grounds:

(1) axiomatic definition,
(2) influence of gross and other errors on design.

2.5.2 Axiomatic Definition

In Expression (2.8) the p_{fi} $(i = 1,2)$ may be replaced by the sum p_{fNi} of the nominal failure probabilities and a term p_{fGi} expressing the contribution of uncertainties not absorbed

by p_{fNi}. The latter are mainly due to (gross) human error, while p_{fNi} includes mainly physical and statistical uncertainties. Then,

$$\frac{p_{f1}}{p_{f2}} \approx \frac{p_{fN1} + p_{fG1}}{p_{fN2} + p_{fG2}} \tag{2.9}$$

which reduces to (2.8) only if $p_{fGi} = kp_{fNi}$, $i = 1,2$ and k is a constant.

In view of the discussion in Section 2.2.8, this condition is unlikely to be true in general. A special case arises when the components being compared are essentially similar and therefore perhaps also subject to similar human and other errors. This may well be true for certain types of structural components, particularly in building structures. In this case $p_{fN1}/p_{fN1} = p_{f1}/p_{f2} = 1$ (impartiality).

2.5.3 Influence of Gross and Other Errors

One argument to suggest that p_{fN} is an adequate measure of structural safety is to show that the choice of design (e.g. its safety factors, or p_{fN}) is unaffected by the knowledge that (gross) human and other errors might occur (i.e. by the knowledge of p_{fG}). This question has been addressed in the literature using a rather more rigorous approach than that given here [e.g. Baker and Wyatt, 1979; Ditlevsen, 1983a].

Consider the total cost C_T (in present value) as in (2.7) and let the failure probability p_f be represented, as before, by $p_{fN} + p_{fG}$ with $p_{fG} > p_{fN}$ (see Section 2.3.8.1). Then (2.7) can be written in simplified form as

$$C_T = C_I(p_{fN}) + (p_{fN} + p_{fG})C_F \tag{2.10}$$

where the initial cost C_I (in present value) depends, reasonably, only on the nominal probability p_{fN} of failure.

For a very low likelihood of failure, the initial cost would be expected to be very high, reducing progressively less as p_{fN} increases, as shown in Figure 2.9.

The cost of C_F failure would usually contain a term representing reconstruction costs, assumed here for convenience equal to the initial cost $C_I(p_{fN})$ plus a term C_S representing other or consequential costs. Two extreme cases may be considered: $C_F = C_S(\ )$ and $C_F = C_I$. These are shown in Figures 2.9(b) and 2.9(c) respectively.

In the first case it is seen that changing the value of p_{fG} has no effect on the optimal value p_{fN} (at A) since this merely moves the line LL' parallel to itself, provided that p_{fG} is independent of p_{fN}, a reasonable first approximation. In the second case, changing the value of p_{fG} has only a small effect on the optimal value of p_{fN} (at B).

The true cost of failure will lie somewhere between the two extremes shown in Figures 2.9(b) and 2.9(c); note also that the actual values of $p_{fN}C_S$ and $p_{fN}C_I$ respectively, do not change the conclusion.

In reality p_{fG} is likely to be positively correlated to p_{fN}. One example is in the design against earthquakes, where an increase in ductility capacity would reduce p_{fN} for the structure and also its sensitivity to (gross) human error [Rosenblueth, 1985a]. It is easily verified that this makes little difference to the conclusion.

Although p_{fN} is insensitive to p_{fG}, clearly C_T and $p_f = p_{fN} + p_{fG}$ are not. This is important in comparing alternatives. Consider two members with the same $C_I(p_{fN})$ curve and the same C_F. It follows that p_{fN} will be the same for each (see Figure 2.9), but the costs C_T and the failure probabilities p_f will depend on the relative p_{fG} values.

(a)

(b)

(c)
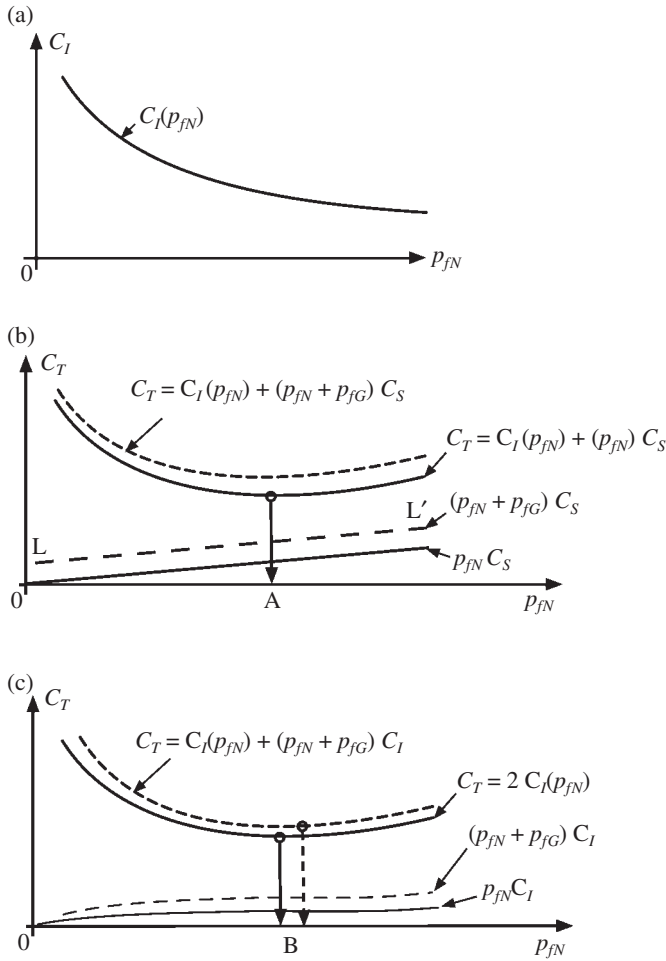
Figure 2.9 (a) Initial Cost curve; (b) optimal p_{fN} for $C_F = C_S$ = constant: (c) optimal p_{fN} for $C_F = C_I$.

Clearly the members with the lowest cost C_T (and hence also lowest p_f) will be preferred. The value of p_{fN} is non-informative for this choice, unless the values of p_{fG} are identical for each member. This corresponds to the conclusion reached in the previous section.

2.5.4 Practical Implications

It is clear that the use of p_{fN} as a surrogate for p_f strictly is only acceptable in a comparative sense if the failure probability component, due to the influence of human error and other effects not included in p_{fN}, affect each of the alternatives in a manner roughly proportional to p_{fN}.

For practical purposes, however, p_{fN} can be accepted as a measure of a more accurately determined probability of failure if it is interpreted in the same sense that factors of

safety and load factors traditionally have been used, as a purely nominal measure. This is then an axiomatic definition. Note that the conventional factor of safety and the partial factors also do not consider human error and related effects.

When p_{fN} is not used in a comparative manner between components but as a measure of the safety of a structure (however defined) against more general societal risk criteria, the argument of Section 2.5.3 shows that knowledge of gross and other error effects may well have a significant influence on total cost, particularly if action is taken to control risks through QA measures. Importantly, however, such influences do not change the most appropriate value for the nominal measure p_{fN} very much, if at all. For this reason it is rational to use nominal safety measures (such as p_{fN}) for design and risk assessment and in design codes to obtain structural sizes.

2.5.5 Target Values for Nominal Failure Probability

Just as in traditional design codes, a factor of safety having a value of about 1.7–2.0 appears to be appropriate, depending on the structure, materials, consequences, etc., the nominal probability of failure might be expected similarly to have a 'target' value. As will be seen in Chapter 9, for structural design-code-writing purposes it is often convenient and appropriate to back-calculate this target value from existing practice, and to use a similar value for a modified or new code. However, proposals for determining target values of p_{fN} have been given on purely empirical grounds and these will now be reviewed briefly.

One proposal is to have a nominal failure probability given by [CIRIA, 1977]:

$$p_{fN}^* = 10^{-4} \mu t_L n^{-1} \tag{2.11}$$

where t_L is the structural design life in years), n is the average number of people within or near the structure during the period of use and μ is a social criteria factor (see Table 2.9).

A somewhat different proposal is (Allen, 1981a):

$$p_{fN}^* = 10^{-5} A W^{-1} t_L n^{-1/2} \tag{2.12}$$

where t_L and n have the same meaning as in (2.11) and where A and W are 'activity' and 'warning' factors respectively (Table 2.10). Of course, they are selected as plausible but entirely arbitrary numbers. The use of $n^{-1/2}$ in (2.11) rather than n^{-1} clearly suggests the influence of utility theory notions in which the rate of risk aversion decreases with the number of fatalities [de Neufville and Stafford, 1971; Rowe, 1977].

Table 2.9 Social criteria factor.

Nature of structure	μ
Places of public assembly, dams	0.005
Domestic, office, trade, industry	0.05
Bridges	0.5
Towers, masts, off-shore structures	5

Source: CIRIA, 1977.

Table 2.10 Activity and warning factors.

Activity factor	A	Warning factor	W
Post-disaster activity	0.3	Fail-safe condition	0.01
Normal activities: buildings	1.0	Gradual failure with some warning likely	0.1
bridges	3.0		
High exposure structures (construction, offshore)	10.0	Gradual failure hidden from view	0.3
		Sudden failure without previous warning	1.0

Source: Allen, 1981a.

Comparison of these two approaches without specific information is not possible. Both lack accounting for injuries and other economic costs of failure. These and *n* are extremely difficult to predict, so that both (2.11) and (2.12) must be considered to be indicative only, perhaps to be used with expert guidance.

In general it is difficult to give useful, abstract, values for p_{fN}^* without reference to the context of the reliability estimation calculations (i.e. the various assumptions for modelling, statistical distributions, etc.). As noted above, it is more usual to back-calculate p_{fN}^* from existing, acceptable structural systems (see Chapter 9). Such calculations often indicate that p_{fN}^* can be defined by β^* values in the range 3.0–3.5 (i.e. p_{fN}^* in the range $10^{-3} - 10^{-4}$) over the lifetime of the structure for failure under extreme loading conditions (but not human error, etc.). How to deal with acceptance criteria for existing structures is discussed in Chapter 10.

2.6 Hierarchy of Structural Reliability Measures

The discussion in Chapter 1 and in this chapter may be summarized conveniently in terms of various 'levels' at which safety (or more generally limit state violation) can be defined (Table 2.11).

The lowest, and simplest level, Level 1, corresponds to the partial factor approach of Section 1.2.3. It is a non-probabilistic generalized version of the traditional safety factor and load factor formats. It is the format most commonly used for limit state design codes and thus for applied engineering design work at the present time. How this format relates to Level 2 procedures was sketched in Section 1.4.4 and will be discussed in more detail in Chapter 9.

Level 2 procedures deal with nominal probabilities based on the use of the normal distribution and some simple mathematical forms for the limit state function. These are described in more detail in Chapter 4.

Level 3 procedures attempt to obtain the best estimate of the probability of failure, using accurate probability models as well as the use of human error and intervention data if available. Structural system effects, and the influence of time may be of importance. Various parts of Chapters 3, 4, 5 and 6 deal with these aspects.

@Seismicisolation

Table 2.11 Hierarchy of structural reliability measures.

Level	Calculation methods	Probability distributions	Limit state functions	Uncertainty data	Result
1: code level methods	(Calibration to existing code rules using level 2 or 3)	Not used	Linear functions (usually)	Arbitrary factors	Partial factors
2: 'Second moment methods'	Second moment algebra	Normal distributions only	Linear, or approximated as linear	May be included as second moment data	'Nominal' failure probability p_{fN}
3: 'exact methods'	Trans- formation	Related to equivalent Normal distributions	Linear, or approximated as linear	May be included as random variables	Failure probability p_f
	Numerical integration and simulation	Fully used	Any form		
4: decision methods	Any of the above, plus economic data				Minimum cost, or maximum benefit

2.7 Conclusion

The combined and interrelated effects of human error (gross and otherwise) and human intervention have been shown to be major considerations in the estimation of the probability of structural failure. Better understanding of these factors, coupled with appropriate data from similar structures and design and construction practices, should allow better predictions of failure probability to be made; as noted repeatedly, all such estimates must be seen as subjective or nominal to at least some degree.

For any particular structure the applicability of probability models for basic variables and the conditions under which the evaluation is valid can be judged only subjectively. Measures of failure probability do not, therefore, have an absolute objective relative frequency interpretation. However, when high-quality models of the structural system, load models and resistance models (including human error effects) are used, estimates of structural failure probability may approach estimates of frequency of structural failure obtained from properly analysed and carefully dissected data.

Nominal measures of failure probability can be used as surrogates for more accurately determined measures if the effects of human error in particular are assumed to be similar for similar situations or structural components. Such nominal measures are particularly useful for design-code-writing purposes.

Finally, as might be expected intuitively, careful examination of the basis for the theory of structural reliability reinforces the notion that QA measures must be used to control both the total probability of failure (including the effects of gross errors) and the total discounted cost of a structural engineering project.

@Seismicisolation

3

Integration and Simulation Methods

3.1 Introduction

The previous chapters have given an overview of the basic principles of structural reliability theory. This and the next chapter will discuss in more detail the computational aspects of the problem. As was noted in Section 1.5.3 there are essentially three ways in which the multi-dimensional integration required in (1.31):

$$p_f = P\left[G(\mathbf{X}) \leq 0\right] = \int \ldots \int_{G(\mathbf{X}) \leq 0} f_{\mathbf{X}}(\mathbf{x}) \ d\mathbf{x} \tag{1.31}$$

might be performed:

  (i) direct integration (possible only in some special cases);
 (ii) numerical integration, such as through using the Monte Carlo technique; and
(iii) obviating the integration through transforming the integrand to a multi-normal joint probability density function for which some special results are available immediately (*cf.* section 1.4.3).

   In this chapter the first two of these approaches to solving (1.31) will be explored. Chapter 4 deals with the third type of approach.

3.2 Direct and Numerical Integration

Analytical integration of the convolution integral (1.18) or of the integral from (1.31) is possible only for some special cases of limited practical interest. A numerical solution of the convolution integral (1.18) is obtained easily through the use of the trapezoidal rule (see Section 1.4.5). This approach has been found to give satisfactory results, mainly because any underestimation of the exact integrand around the mean is compensated by slight but extensive overestimation elsewhere [Dahlquist and Björck, 1974]. However, more refined methods, such as Simpson's rule, or the methods based on polynomials, such as Laguerre-Gauss or Gauss-Hermite quadrature formulae may be more appropriate [e.g. Davis and Rabinowitz, 1975]. Standard routines for such numerical integration are available on most computer systems.

When the load effect S and the resistance R in the convolution integral (1.18) are not independent, or there are more than two variables, the probability of failure must be obtained from the general formulation (1.31). Again, the computation of this integral in all but very special cases cannot be achieved in closed form. In addition, numerical integration is not always feasible owing to the growth of round-off errors and excessive computation times. Moreover, computational demands increase rapidly with dimension n of the integration space. Typically, the practical limit for numerical integration is considered to be around $n \leq 5$. Even then, the integration region is confined to one of the following simpler regions: hypercube, n-dimensional solid sphere, or the surface thereof, n-dimensional simplex (generalization of triangle and tetrahedron) and the semi-infinite half-space [Davis and Rabinowitz, 1975; Stroud, 1971; Johnson and Kotz, 1972]. These references might be consulted for more details and for algorithms.

In the special case when the limit state function is a linear function

$$G(\mathbf{x}) = Z = a_1 x_1 + a_2 x_2 + \ldots + a_n x_n \tag{3.1}$$

with a_i known constants and with any number n of random variables x_i $(i = 1, \ldots, n)$, it is possible to reduce the multiple integral (1.31) to a series of single integrals [Stevenson and Moses, 1970]. However, the evaluation still requires extensive numerical work or rather drastic simplifications. In a similar vein, it has been suggested that it may be possible to invoke the divergence theorems of Stokes and Gauss to convert two- and three-dimensional integrals to one- and two-dimensional contour and surface integrals, respectively [Shinozuka, 1983].

As noted already in Section 1.4.3, when the load effect S and the resistance R are each described by normal distributions, the safety margin $Z = R - S$ also is normal. In this case the (two-dimensional) integration of the probability integral (1.31) can be achieved essentially through the special property of the normal distribution $\Phi(\ )$ (see A 5.7).

More generally, when the random variables x_i $(i = 1, \ldots, n)$ in the linear function (3.1) are all normally distributed random variables, the function $G(\mathbf{x})$ itself will be normally distributed with mean μ_Z and variance σ_Z (as given by (A 160) and (A 162) respectively). If the function is now recognized as the limit state function $G(\mathbf{x}) = 0$ for a structural reliability problem, it follows that the integration of (1.31) can be by-passed, in a manner directly analogous to that given in Section 1.4.3. Also, dependence between the random variables X_i presents no difficulties as follows from (A 162). This special case forms the starting point for the discussion in Chapter 4.

In practice, limit state functions usually are of more general form than linear functions. Similarly, the random variables x_i $(i = 1, \ldots, n)$ are unlikely all to be normally distributed random variables. Hence methods must be available to deal with these requirements. Integration methods would be suitable, at least in principle. However, because of the rapidly increasing computational demands as the number of dimensions increases, numerical integration of the classic variety has not found great favour in reliability computations. Instead, resort has had to be made to methods developed for other large integrations problems (e.g. Kahn, 1956) and described already in texts (e.g. Stroud, 1971) dealing with numerical integration. These methods are the simulation or Monte Carlo methods. They form a class of approximate numerical solutions to the

probability integral (1.31) applicable to problems for which the limit state function $G(\mathbf{x}) = 0$ may have any form, and for which the probabilistic description of the random variables X_i is unrestricted. The present chapter is devoted to these methods.

3.3 Monte Carlo Simulation

3.3.1 Introduction

As the name implies, Monte Carlo simulation techniques involve 'sampling' at 'random' to simulate artificially a large number of experiments and to observe the result. In the case of analysis for structural reliability, this means, in the simplest approach, sampling each random variable X_i randomly to give a sample value $\hat{x}_i$. The limit state function $G(\mathbf{x}) = 0$ is then checked using the sample set of values $\hat{x}_i$. If the limit state function is violated (i.e. $G(\hat{\mathbf{x}}) \leq 0$), the structure or structural element has 'failed'. The experiment is repeated many times, each time with a randomly chosen vector $\hat{\mathbf{x}}$ of $\hat{x}_i$ values. If N trials are conducted, the probability of failure is given approximately by

$$p_f \approx \frac{n\left(G(\hat{x}_i) \leq 0\right)}{N} \tag{3.2}$$

where $n(G(\hat{x}_i) \leq 0)$ is the number of trials n for which $(G(\hat{x}_i) \leq 0)$. Obviously the number N of trials required is related to the desired accuracy for p_f.

It is clear that in the Monte Carlo method a game of chance is constructed from known probabilistic properties in order to solve the problem many times over, and from that to deduce the required result (i.e. the failure probability).

In principle, Monte Carlo methods are only worth exploiting when the number of trials or simulations is less than the number of integration points required in numerical integration. This is achieved for higher dimensions by replacing the systematic selection of points by 'random' selection, under the assumption that the points so selected will be in some way unbiased in their representation of the function being integrated.

To apply Monte Carlo techniques to structural reliability problems it is necessary:

(a) to develop systematic methods for numerical 'sampling' of the basic variables $\mathbf{X}$;
(b) to select an appropriate economical and reliable simulation technique or 'sampling strategy';
(c) to consider the effect of the complexity of calculating $G(\hat{x}_i)$ and the number of basic variables on the simulation technique used;
(d) for a given simulation technique to be able to determine the amount of 'sampling' required to obtain a reasonable estimate of p_f.

It may be necessary also to deal with dependence between all or some of the basic variables. All these matters will be considered in the sections to follow.

3.3.2 Generation of Uniformly Distributed Random Numbers

In a physical experiment it might be possible to select a sample value of each basic variable by means of some arbitrary random selection process, such as putting a sequence

of numbers in a lot and selecting one. Provided that the lot size is large and the interval between numbers small, the probability distribution for these numbers would be the 'uniform' or 'rectangular' distribution ((A.73) or (A.74)), given by

$$
\begin{aligned}
F_R(r) = P(R \leq r) &= r \qquad \text{for } 0 \leq r \leq 1 \\
f_R(r) &= 1 \\
&= 0 \qquad\qquad \text{elsewhere}
\end{aligned}
\tag{3.3}
$$

It is possible to generate uniformly distributed random numbers through automated roulettes or the noise properties of electronic circuits. These generators tend to be slow and non-reproducible, so that an 'experiment' can never be checked. Tables of random numbers [e.g. Rand Corporation, 1955] (see Appendix E) can be stored in computer systems, but their recovery for use is also very slow.

The most common practical approach is to employ a 'pseudo' random number generator (PRNG) such as is available on virtually all computer systems. They are termed 'pseudo' since they use a formula to generate a sequence of numbers. Although this sequence is reproducible and repeats after (normally) a long cycle interval, for most practical purposes, it is indistinguishable from a sequence of strictly true random numbers [Rubinstein, 1981]. The production of a reproducible sequence has an advantage in certain problems and in research work (since it permits checking of any computational sequence). If required, reproducibility can be destroyed simply by changing (randomly) the 'seed number' required as input for most PRNGs. A simple device is to use the local time as a seed value.

There are some mathematical reservations about the terminology 'random sampling'. As soon as a table of 'random numbers' or a PRNG is used, the sequence of numbers is determined, and so no longer is truly random. It follows that 'tests of randomness' are therefore strictly misnomers; these tests usually are applied only for a one-dimensional sequence, and may not guarantee 'randomness' in more dimensions [e.g. Deák, 1980]. To avoid the philosophical difficulties, it has been suggested that Monte Carlo methods using PRNGs be dubbed 'quasi Monte Carlo' methods and that the only justification for the use of sequences of pseudo-random numbers is the equi-distribution (or uniform distribution) property implied by their use. In essence, the numbers so selected give a reasonable guarantee of accuracy in the computations [Zaremba, 1968].

Example 3.1   A simple random number generator can be made as follows. Take a die and let the "six" denote an invalid sample. Also take a coin and let 'heads' be 5 and 'tails' be 0. Then tossing the die and the coin repeatedly will produce (apart from invalid samples) a series of digits between 1 and 10, which should be random (if the die and coin are unbiased). 'Lotto' results can also be used as random number generators.

3.3.3 Generation of Random Variates

Basic variables only seldom have a uniform distribution. A sample value for a basic variable with a given (nonuniform) distribution is called a 'random variate' and can be obtained by a number of mathematical techniques. The most general of these is the
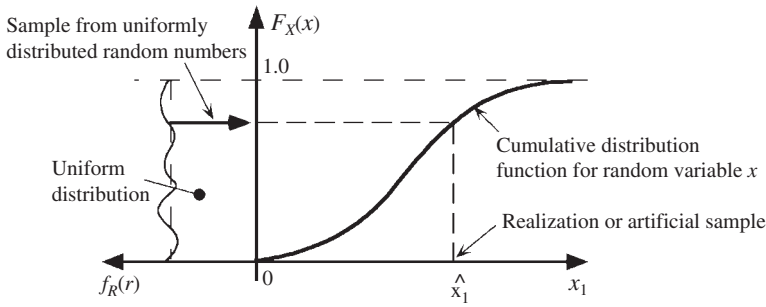
Figure 3.1 Inverse transform method for generation of random variates.

'inverse transform' method. Consider the basic variable X_i for which the cumulative distribution function $F_{X_i}(x_i)$ must, by definition, lie in the range (0,1), shown in Figure 3.1. The inverse transform technique is to generate a uniformly distributed random number $r_i (0 \leq r_i \leq 1)$ and equate this to as $F_{X_i}(x_i)$:

$$F_{X_i}(x_i) = r_i \qquad \text{or} \qquad x_i = F_{X_i}^{-1}(r_i) \tag{3.4}$$

This uniquely fixes the sample value $x_i = \hat{x}_i$, provided that an analytic expression for the inverse $F_{x_i}^{-1}(r_i)$ exists (as it does for the Weibull, exponential, Gumbell and rectangular distributions among others). In these cases the inverse transform method is likely to be the most efficient technique. The technique can also be applied to basic variables whose cumulative distribution function has been obtained from direct observation.

Specialized techniques for generating random variates from specific distributions often are computationally more efficient than the inverse transform method. Most computer systems have standard subroutines available. One such procedure is due to Box and Muller (1958). It produces a pair of 'exact' independent standardized normal variates, u_1 and u_2, given by

$$u_1 = \left(-2 \ln r_1\right)^{\frac{1}{2}} \sin 2 \pi r_2 \tag{3.5a}$$

$$u_2 = \left(-2 \ln r_1\right)^{\frac{1}{2}} \cos 2 \pi r_2 \tag{3.5b}$$

where r_1, r_2 are realizations of uniformly distributed independent random variables **R** in the interval (0,1). Lognormal distributed random variables v_i may be obtained directly from expressions (3.19) since, for **V** lognormal distributed, $v_i = \ln u_i$.

Example 3.2 Generate a vector of standard Normal random variates **u** drawn from a standard Normal distribution (i.e. N(0,1)). Use Eqn. (3.5) to generate them from a vector of random numbers **r**. For this example let these be the first 10 random numbers in each of the two columns in Appendix E. Show that even for this small number the mean of standard Normal random variates **u** is about zero, and the standard deviation is about unity. This working can be done most easily using the following Table. Columns 1 and 3 show the random variables from Appendix E.

(1)	(2)	(3)	(4)	(5)	(6)	(7)
r_1	$-\ln(r_1)$	r_2	$\sin 2\pi\, r_2$	$\cos 2\pi\, r_2$	u_1	u_2
0.9311	0.0714	0.4537	0.2868	−0.9580	0.1084	−0.3620
0.7163	0.3336	0.1827	0.9119	0.4104	0.7449	0.3352
0.4626	0.7709	0.2765	0.9861	−0.1657	1.218	−0.2057
0.7895	0.2364	0.6939	−0.9385	−0.3452	−0.6453	−0.2374
0.8184	0.2004	0.8189	−0.9077	0.4195	−0.6185	0.2859
0.3008	1.2013	0.9415	−0.3593	0.9332	−0.5569	1.4464
0.3989	0.9190	0.4967	0.0207	−0.9998	0.0281	−1.3554
0.0563	2.8771	0.2097	0.9681	0.2505	2.3223	0.6009
0.1470	1.9173	0.4575	0.2638	−0.9646	0.5166	−1.8888
0.2036	1.5916	0.4950	0.0314	−0.9995	0.0707	−2.2497

Columns (6) and (7) are obtained from Eqn. (3.5): $\left\{\begin{matrix} u_1 \\ u_2 \end{matrix}\right\} = \left(-2\ln r_1\right)^{1/2} \left\{\begin{matrix} \sin 2\pi r_2 \\ \cos 2\pi r_2 \end{matrix}\right\}$.

Note the sin() and cos() terms are in radians. The mean of just these 20 values of u_i ($i = 1, \dots, 20$) is −0.02207 and the standard deviation is 1.0798. This is close to the theoretical requirement of (0,1).

3.3.4   Direct Sampling ('Crude' Monte Carlo)

The technique sketched in Section 3.3.1 is the simplest Monte Carlo approach for reliability problems but not the most efficient. The basis for its application is as follows. The probability of limit state violation (1.31) may be expressed as:

$$p_f = J = \int \dots \int I\left[G(x) \leq 0\right] f_X(\mathbf{x})d\mathbf{x} \tag{3.6}$$

where $I[\ ]$ is an 'indicator function' which equals 1 if $[\ ]$ is 'true' and 0 if $[\ ]$ is 'false'. Thus the indicator function identifies the integration domain. Comparison with (A.10) shows that (3.20) represents the expected value of $I[\ ]$. If x_j represents the jth vector of random observations from $f_X(\ )$, it follows directly from sample statistics that

$$p_f \approx J_1 = \frac{1}{N}\sum_{j=1}^{N} I\left[G(\hat{x}_j) \leq 0\right] \tag{3.7}$$

is an unbiased estimator of J. Thus expression (3.7) provides a direct estimate of p_f.

In exploiting this procedure, three matters are of interest: how to extract most information from the simulation points, how many simulation points are needed for a given accuracy, or conversely, how to improve the sampling technique to obtain greater accuracy for the same or fewer sample points. These matters will be considered below.

Before proceeding, however, it is noted that one way the results of the above sampling technique may be represented is as a cumulative distribution function $F_G(g)$ (see Figure 3.2). Obviously, much of the range of $F_G(g)$ is of little interest, since the structure or member is (usually) amply safe. To estimate the failure probability the region for which $G(\ ) \leq 0$, which represents 'failure', is clearly of most interest.

@Seismicisolation
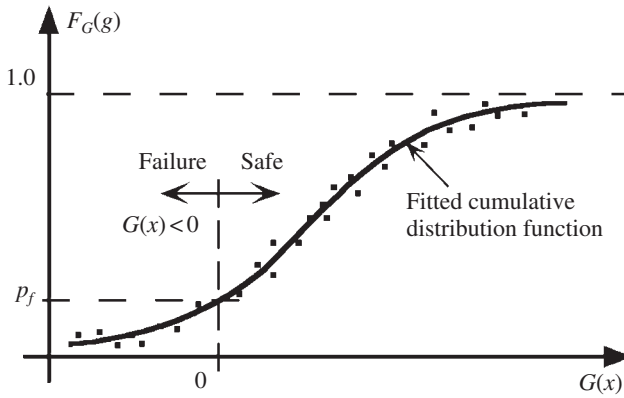
Figure 3.2 Use of fitted cumulative distribution function to estimate p_f.

The estimate of p_f in equation (3.7) may be improved by fitting an appropriate distribution function through the points for which $G(\ ) \leq 0$, i.e. the left-hand tail in Figure 3.6. However, the choice of an appropriate distribution function may be difficult. Distributions that could be of use for this purpose are the Johnson and Pearson distribution systems [Elderton and Johnson, 1969]. However, it is possible that the parameters of the distribution function are rather sensitive to extreme results in the region $G(\ ) \leq 0$. In that case, the choice of distribution function parameters may not stabilize until N is quite large [Moses and Kinser, 1967]. Rather than fitting a single distribution to the sample points, it is possible to fit a sequence of distributions and to optimize the parameters to give a 'best fit' to the sample points [Grigoriu, 1983].

3.3.5 Number of Samples Required

An estimate of the number of simulations required for a given confidence level may be made as follows. Since $G(\mathbf{X})$ is a random variable in $\mathbf{X}$, the indicator function $I[G(\mathbf{X}) \leq 0]$ is also a random variable, albeit with only two possible outcomes. It follows from the central limit theorem that the distribution of J_1 given by the sum of independent sample functions (3.7) approaches a normal distribution as $N \to \infty$. The mean of this distribution is (*cf.* A.160):

$$E(J_1) = \sum_{i=1}^{N} \frac{1}{N} E[I(G \leq 0)] = E[I(G \leq 0)] \tag{3.8}$$

which is equal to J (see 3.7), while the variance is given by (cf. A.161):

$$\sigma_{J_1}^2 = \sum_{i=1}^{N} \frac{1}{N^2} \mathrm{var}\,[I(G \leq 0)] = \frac{\sigma_{I(G \leq 0)}^2}{N} \tag{3.9}$$

This shows that the standard deviation of J_1 and hence of the Monte Carlo estimate (3.7) varies directly with the standard deviation of $I(\ )$ and inversely with $N^{1/2}$. These observations are important in determining the number of simulations required for a particular level of confidence. To actually calculate confidence levels, an estimate of $\sigma_I(\ )$

is required. Using (A.11), the variance is given by;

$$\text{var}[I(\ )] = \int \dots \int [I(G \leq 0]^2 \ d\mathbf{x} - J^2 \tag{3.10}$$

so that the sample variance is given by:

$$S^2_{I(G \leq 0)} = \frac{1}{N-1}\left(\left\{\sum_{j=1}^{N} I^2\left[G\left(\hat{x}_j\right) \leq 0\right]\right\} - N\left\{\frac{1}{N}\sum_{j=1}^{N} I\left[G\left(\hat{x}_j\right) \leq 0\right]\right\}^2\right) \tag{3.11}$$

where the last { } term is simply the mean (3.8) or, by (3.7) the estimate J_1 for p_f.

On the basis that the central limit theorem applies, the following confidence statement can be given for the number (J_1) of trails in which 'failure' occurs:

$$P\left(-k\sigma < J_1 - \mu < +k\sigma\right) = C \tag{3.12}$$

where μ is the expected value of J_1 given by (3.8) and σ is given by (3.9). For confidence interval $C = 95\%$, $k = 1.96$, as can be verified from standard normal tables (see Appendix C). As σ is not known, it may be estimated from (3.24b). However, this is not very helpful at the beginning of a Monte Carlo study.

Shooman (1968) has suggested that σ and μ in (3.25) can be approximated by the binomial parameters $\sigma = (Nqp)^{1/2}$ and $\mu = Np$ μ, with $q = 1 - p$, (cf. (A.20) and (A.21)) provided that $Np \geq 5$ when $p \leq 0.5$. If these are substituted in (3.25), there is obtained:

$$P\left[-k(Nqp)^{1/2} < J_1 - np < +k(Nqp)^{1/2}\right] = C \tag{3.13}$$

If the error between the actual value of J_1 and the observed is denoted by $\varepsilon = (J_1 - Np)/Np$ and this is substituted into (3.13), it follows easily that $\varepsilon = k[(1 - p)/Np]^{1/2}$. Thus, if $N = 100\,000$ samples, and $p = p_f = 10^{-3}$ (expected), the error in (J_1) and hence p_f will be less than 20% with 95% confidence (as then $k = 1.96$).

Broding et al. (1964) suggested that a first estimate of the number N of simulations for a given confidence level C in the failure probability p_f can be obtained from:

$$N > \frac{-\ln(1-C)}{p_f} \tag{3.14}$$

Thus, for a 95% confidence level and $p_f = 10^{-3}$, the required number of simulations is more than 3000. The actual number of variates to be calculated is, of course, N times the number of independent basic variables. Others have suggested that the number of simulations may need to be of the order of 10 000 to 20 000 for approximately 95% confidence limit, depending on the function being evaluated [Mann et al., 1974].

The above 'rules', while often useful, do not tell the analyst much about the accuracy being achieved in any particular Monte Carlo analysis. A useful tool for this purpose is to plot (or print-out) progressive results of the estimate of p_f and its estimated variance as obtained from (3.7) and (3.11) respectively. Typically such plots (see Figure 3.3) will show that these measures are reduced as the number of samples is increased and that a degree of stability is reached at a sufficiently high number of samples. However, the rate of convergence and its stability depend to some extent on the quality of the random
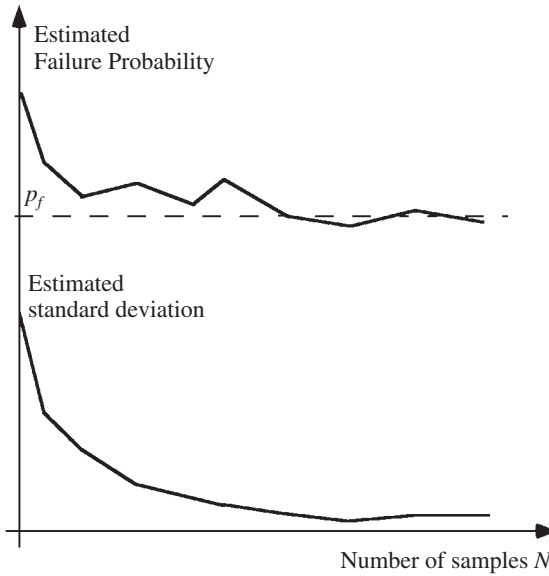
Figure 3.3 Typical convergence of probability estimate with increasing sample size (schematic).

number generator being used. Hence it is possible for apparent stability to be attained under some (unfavourable) circumstances.

Example 3.3   The stress resultant S acting on a member in tension has statistical properties estimated to be $N(10.0, 1.25)$. The resistance R is estimated to be $N(13.0, 1.5)$. What probability of failure is estimated using the 'crude' Monte Carlo method, if R and S are independent?

Using integral (1.16), both R and S need to be simulated. For convenience, only ten random sample variates $\hat{r}$ and another ten random sample variates $\hat{s}$ are given below, but generally more samples will be required. For a sample for R, say, select a random number, say, $\hat{u}_1 = 0.9311$ from a table of random numbers (e.g. Appendix E). Then following (3.4) and Figure 3.1, $\hat{x}_1 = \Phi^{-1}(\hat{u}_1) = +1.49$ from standardized Normal tables such as given in Appendix D. The sample value $\hat{r}$ then follows directly (cf. Section A.5.7):

$$\hat{x}_1 = 1.49 = \frac{\hat{r}_1 - \mu_R}{\sigma_R} = \frac{\hat{r}_1 - 10}{1.25} \quad \text{or} \quad \hat{r}_1 = 15.24 \tag{3.15}$$

Similar calculations for another nine $\hat{r}_i$ $(i = 2, \dots, 10)$ values and for ten $\hat{s}$ can be made using the next 19 values in Appendix E. The $\hat{s}$ values follow from $\hat{x} = (\hat{s} - \mu_S)/\sigma_S$. In particular, using the eleventh random number in Appendix E, $\hat{s}_1$ can be found to be 10.53. Thus $\hat{r}_1 > \hat{s}_1$.

It will be left to the reader to show that, in this case, only one of the sample pairs $(\hat{r}_i, \hat{s}_i)$ led to a failure (i.e. $\hat{r}_1 \leq \hat{s}_1$) so that $p_f \approx 0.1$. Obviously more sampling is required. Since both R and S are Normally distributed, the exact result is directly obtainable from expression (1.22):

$$p_f = \Phi\left[\frac{-(13 - 10)}{(1.5^2 + 1.25^2)^{1/2}}\right] = \Phi(-1.54) = 0.0618 \tag{3.16}$$

Example 3.4 If the single integral form (1.18) is to be used in a Monte Carlo analysis, it may be seen from comparison to (3.6) that, in essence, $I[\ ]$ is replaced by $F_R(x)$. This means that the value for $F_R(\ )$ averaged over all samples, is to be estimated. The samples $\hat{x}_i$ themselves are drawn from the probability distribution given by $f_S(\ )$. This is done using the inverse transform technique (3.4) to give $\hat{x}_i = F_S^{-1}(\hat{u}_i)$ where $\hat{u}_i$ is a random number.

With data as in Example 3.3, the calculation procedure is as follows. Select a random number from Appendix E, $\hat{u}_1 = 0.9311$, say. Then the sample value $\hat{x}_1$ is obtained from $\hat{x}_1 = F_S^{-1}(\hat{u}_1)$. In the present case, since $S = N(,)$, this relationship becomes $\hat{x}_1 = \Phi^{-1}(\hat{u}_1) = \Phi^{-1}(0.9311) = +1.49$ where $\hat{x}_1$ is a standardized Normal sample variate. Since $\hat{x}_1 = (\hat{s}_1 - \mu_S)/\sigma_S$ it follows that $\hat{s}_1 = 11.86$. With this sample value, $F_R(\hat{s}_1)$ is evaluated, first by calculating the reduced variate, $\hat{v}_1$, say, with $\hat{v}_1 = (\hat{s}_1 - \mu_R)/\sigma_R = -0.76$, and then determining $F_R(\hat{s}_1) = \Phi(\hat{v}_1) = 0.2237$. Similar results can be obtained for nine more samples, using the next nine random numbers in Appendix E, say. These will be found to be (0.0631, 0.0188, 0.0918, 0.1075, 0.0075, 0.0136, 0.0005, 0.0021, 0.0036). The sum of the ten $F_R(\hat{s}_i)$ samples is 0.532, so that $p_f \approx (1/10) \times 0.532 = 0.0532$. This is 14% in error compared with the correct result of 0.0618, a reasonable result considering that only ten samples were used. Clearly the size of the error will depend on the selection of random numbers, and the number of samples.

3.3.6 Variance Reduction

From expression (3.9) it is seen that the variance σ_I^2 directly affects the variance of J_1 and that the number of samples N inversely affects the variance of J_1. This means that the standard deviation of $\hat{J}$ and hence of the Monte Carlo estimate (3.21) decreases in proportion to $N^{-1/2}$. By comparison, for one-dimensional integration, the error in standard deviation reduces as N^{-2} for the trapezoidal rule and N^{-4} for Simpson's rule [Dahlquist and Bjorck, 1974]. Obviously the slow convergence of the 'crude' Monte Carlo method is a significant disadvantage for its practical application. It also was one of the reasons for efforts to develop simplified methods such as those outlined in Chapter 4. The other approach is to try to find ways to reduce the variance σ_I^2 for the estimate of the probability of failure J (3.9). These are the so-called 'variance reduction' techniques [Rubinstein, 1981].

Apart from increasing the number of samples, variance reduction can be achieved only by using additional (a priori) information about the problem to be solved. For example, from Figure 1.10 it is evident that only sampling in the region of overlap between $f_R(\ )$ and $f_S(\ )$ is likely to prove more interesting than sampling elsewhere. This observation, generalized, forms the basis for 'importance sampling', a powerful technique that is considered further in Section 3.4 below.

A number of other variance reduction techniques with roughly similar strategies exist. In each case information about the problem is used to limit the simulation to particular regions, ideally to regions of significant interest for their contributions to the estimate of J (3.8), but often rather arbitrarily chosen regions. A good overview of the various strategies for variance reduction in general Monte Carlo work is given by Rubinstein (1981) and by Warner and Kabaila (1968) in relation to some techniques for structural reliability calculations.

@Seismicisolation

3.3.7   Stratified and Latin Hypercube Sampling

Stratified and Latin Hypercube sampling use the common idea that the sampling space be divided into strata (or hypercubes) and that only a few of the many possible samples be selected in each strata (or hypercube) for inclusion in the estimation of the integral J. The samples used from within each strata (or hypercube) can be randomly selected from those that would otherwise be used, or, for example, the mean or central point might be used as the one representative value. The evaluation of J then uses these selected values, weighted by their probability of occurrence. Latin hypercube sampling considers all the random variables, whereas stratified sampling might be done in only one (say) dimension [Rubinstein, 1981; Olsson et al., 2003].

   For convenience, consider the special case in which all the random variables $x_i (i = 1, \ldots, n)$ are each divided into the same number of strata, say N. It is convenient also to make the divisions such that the probability of x_i falling in each stratum is $1/N$. Now, select a representative value for each stratum and for each random variable. In principle more values could be selected, but this also can be achieved by using a greater number of strata. To now estimate J the procedure is to use just one of the (N) representative values for each random variable x_i (that is, selected from one of the strata) in a combination with a selected representative value from each of the other random variables. This collection of representative values forms a sample set. The process is repeated, selecting from the remaining representative values, thereby forming another sample set, and so on. In the end there will be N sample sets. These can be interpreted directly as the number N of sample vectors selected in Monte Carlo sampling and thus can be used directly in (3.2), with evaluations of the limit state function using the present sample sets, to estimate J (and thus p_f). Latin hypercube sampling can be combined also with other variance reduction techniques, such as importance sampling [Olsson et al., 2003], although it is generally considered to be most suitable for small-scale simulation problems [Huntington and Lyrintzis, 1998].

3.4   Importance Sampling

3.4.1   Theory of Importance Sampling

The multiple integral (1.31) can be written as in (3.6) using the indicator function $I[\ ]$, or, equivalently, as:

$$J = \int \ldots \int I[G(\mathbf{x}) \leq 0] \frac{f_{\mathbf{X}}(\mathbf{x})}{h_{\mathbf{V}}(\mathbf{x})} h_{\mathbf{V}}(\mathbf{x}) d\mathbf{x} \tag{3.17}$$

where $h_{\mathbf{V}}(\mathbf{v})$ is termed the 'importance-sampling' probability density function. Its definition is considered in detail below. Again by comparison with (A.10), expression (3.17) can be written as an expected value:

$$J = E \left\{ I[G(\mathbf{v}) \leq 0] \frac{f_{\mathbf{X}}(\mathbf{v})}{h_{\mathbf{V}}(\mathbf{v})} \right\} = E \left(\frac{If}{h} \right), \text{ say} \tag{3.18}$$

where $\mathbf{V}$ is any random vector with probability density function $h_{\mathbf{V}}(\mathbf{v})$. Obviously it is required that $h_{\mathbf{V}}(\mathbf{v})$ exists for all valid $\mathbf{v}$ and that $f_X(\mathbf{v}) \neq 0$. Comparison with Section 3.3.4 shows that $I[\ ]$ there is here replaced by $I[\ ] f/h$.

An unbiased estimate of J is given by (*cf.* 3.21):

$$p_f \approx J_2 = \frac{1}{N} \sum_{j=1}^{N} \left\{ I[G(\hat{\mathbf{v}}_j) \leq 0] \frac{f_x(\hat{\mathbf{v}}_j)}{h_{\mathbf{V}}(\hat{\mathbf{v}}_j)} \right\} \tag{3.19}$$

where $\hat{\mathbf{v}}_j$ is a vector of sample values taken from the importance sampling function $h_{\mathbf{V}}(\ )$.

It should be clear that $h_{\mathbf{V}}(\ )$ describes what might be termed the 'topographic' distribution of sample values of $\mathbf{V}$ in x space. How this distribution should be chosen is quite important. By direct analogy with (3.9) and (3.10), the variance of J_2 is given by:

$$\mathrm{var}(J_2) = \mathrm{var}\left(\frac{If}{h}\right) \Big/ N \tag{3.20}$$

where

$$\mathrm{var}\left(\frac{If}{h}\right) = \int \dots \int \left\{ I[\ ] \frac{f_X(\mathbf{x})}{h_{\mathbf{V}}(\mathbf{x})} \right\}^2 h_{\mathbf{V}}(\mathbf{x}) d\mathbf{x} - J^2 \tag{3.21}$$

Clearly (3.21) should be minimized so as to minimize $\mathrm{var}(J_2)$. If the function $h_{\mathbf{V}}(\ )$ is selected as

$$h_{\mathbf{V}}(\mathbf{v}) = \frac{\left| I[\ ] f_X(\mathbf{v}) \right|}{\int \dots \int \left| I[\ ] f_X(\mathbf{v}) \right| d\mathbf{v}} \tag{3.22}$$

then upon substitution into (3.21) it is easily found that

$$\mathrm{var}\left(\frac{If}{h}\right) = \left(\int \dots \int \left| I[\ ] f_X(\mathbf{v}) \right| d\mathbf{v} \right)^2 - J^2 \tag{3.23}$$

If the integrand $I[\ ] f_X(\mathbf{v})$ does not change sign, the multiple integral is identical with J and $\mathrm{var}(I.f/h) = 0$. In this case the optimal function $h_{\mathbf{V}}(\ )$ is obtained from (3.22) as:

$$h_{\mathbf{V}}(\mathbf{v}) = \frac{I[G(\mathbf{v}) \leq 0] f_X(\mathbf{x})}{J} \tag{3.24}$$

At first sight this expression is not very helpful since the very integral to be determined, J, is needed. However, progress can be made even if only an approximate value can be estimated for. Then the variance can be reduced using (3.21) or (3.23). Evidently, it is desirable that $h_{\mathbf{V}}(\ )$ should have the form of the integrand of (3.6), divided by the estimate for J. It should be clear that the variance is reduced if $h_{\mathbf{V}}(\mathbf{v})/I[\ ] f_X(\mathbf{v}) \approx \text{constant} < 1$ [Shreider, 1966].

If the integrand does change sign, then the addition of a sufficiently large constant may adapt it to the above form. A weaker result when the integrand does change sign also can be given [Kahn, 1956; Rubinstein, 1981].

@Seismicisolation

From (3.23) it follows that a good choice of $h_V(\ )$ can actually produce zero variance in the estimate for J for the special case of non-negative integrand. This may seem to be a surprising result. However, it demonstrates that the more effort is put into obtaining a close initial estimate of J in equation (3.24), the better the Monte Carlo result will be. Conversely, and importantly, the variance is likely to be increased by using a very poor choice of $h_V(\ )$ [Kahn, 1956].

3.4.2 Importance Sampling Functions

While in general the derivation of optimal $h_V(\ )$ functions is difficult, appropriate functions often may be selected on a priori grounds. Thus, in the n-dimensional reliability problem, the region of most interest is the hyperzone $G(\mathbf{x}) \leq 0$ and, more particularly, the region of greatest probability density within that zone. This is the region just to the right of the point $\mathbf{x}^*$ shown for a two-variable problem in Figure 3.4. In general the region cannot be identified easily as there are no simple criteria with which to work. However, a surrogate for identifying the region of interest is to identify the point $\mathbf{x}^*$. In this case the point $\mathbf{x}^*$ is the point having the largest ordinate $f_X(\mathbf{x})$ on the limit state function. This point is known also as the point of 'maximum likelihood'. For most probability density functions $f_X(\mathbf{x})$, the point $\mathbf{x}^*$ may be found by the direct application of numerical maximization techniques. In some cases, such as when $f_X(\mathbf{x})$ has a rectangular distribution, no unique maximum point $\mathbf{x}^*$ may exist. This is not as critical as it may seem at first, since p_f is usually quite small, and therefore the region of $f_X(\mathbf{x})$ satisfying $G(\mathbf{X}) < 0$ also is small. In consequence, the choices for location of an appropriate point $\mathbf{x}^*$ are limited and may be made rather arbitrarily within $G(\mathbf{X}) < 0$, although a point close to the maximum mass location of $f_X(\mathbf{x})$ is likely to be preferable.

Once $\mathbf{x}^*$ is identified, one approach for choosing $h_V(\ )$ is simply to use the distribution $f_X(\mathbf{x})$ shifted so that its mean is at $\mathbf{x}^*$ [Harbitz, 1983]. However, a more appropriate distribution for $h_V(\ )$ is considered to be $h_V(\ ) = \Phi_n(\mathbf{v}, \mathbf{C}_V)$, where $\mathbf{C}_V$ is a strictly diagonal matrix of σ_i^2 and with the mean of $\mathbf{V}$ placed at $\mathbf{x}^*$. Such a distribution will produce
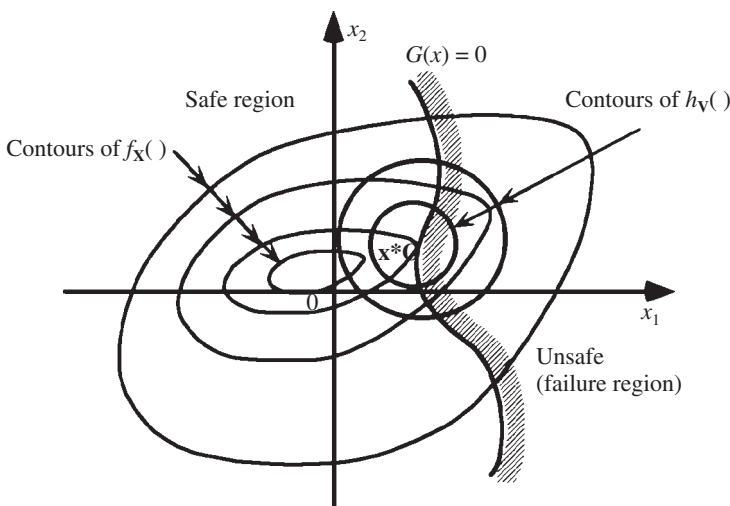
Figure 3.4 Importance sampling function $h_v(\ )$ in x space.

sample points unbiased with respect to each variable. It also will give greater sampling density in the neighbourhood of the region where it is of most significance. The choice of $\mathbf{x}^*$ as the locating point for $h_V(\ )$ has the obvious advantage that it gives a systematic procedure for its selection. As can be seen from Figure 3.4 for two-variable problems, the shape or format of the limit state function $G(\mathbf{X}) = 0$ is of little importance, since with $h_V(\ )$ centred at $\mathbf{x}^*$, a wide region is included in the sample space. This means that problems with non-linear regions are handled as easily as those with linear limit state functions. Similarly, the format of $f_{\mathbf{X}}(\mathbf{x})$ is of little significance, and dependence between the X_i, such as indicated schematically in Figure 3.4, does not affect the procedure.

It is also seen that, unless $G(\mathbf{X}) = 0$ is a very non-linear function, the 'success' rate for sample points selected from $h_V(\ )$ is about 50%, i.e. there is an approximately equal likelihood of any sample point falling in either the safe or the unsafe region. It follows directly that for a given level of confidence, far fewer sample points are required using $h_V(\ )$ as shown, than using the 'crude' Monte Carlo method with $f_{\mathbf{X}}(\mathbf{x})$ as sampling distribution [Melchers, 1984; Enguland and Rackwitz, 1993].

An approximate measure of the relative efficiencies of the two methods can be obtained by considering the number of sample points required to obtain a given number of points (say 100) in the 'failure' region. Assuming a 'success' rate of 50%, for a linear limit state function with $h_V(\ )$ centred on the 'design' point $\mathbf{x}^*$, on average some 200 points need to be generated with importance sampling. By contrast, if p is the probability of a sample point based on $f_{\mathbf{X}}(\mathbf{x})$ falling in the 'failure' region, then $100/p$ sample points, on average, need to be generated. Hence, if p is of the order of $10^{-3} - 10^{-5}$, as may be typical, $10^5 - 10^7$ sample points are required for the 'crude' Monte Carlo method. Similar results can be obtained for confidence levels, for example, using (3.12) with $p = 0.5$ being the 'success rate'. An important observation is that, since $h_V(\ )$ can be selected by the analyst, it can have independent components $\mathbf{V}$. Unlike the 'crude' Monte Carlo technique, for which the generation of correlated or dependent random variables $\mathbf{X}$ may be required (since $f_{\mathbf{X}}(\mathbf{x})$ is the sampling function!), no such requirement exists for importance sampling. Because of the complexity of obtaining dependent random variables (see Appendix B), this is sufficient reason in itself to use importance sampling instead of 'crude' Monte Carlo.

Example 3.5 Example 3.4 will now be repeated using importance sampling. With R being N(13, 1.5) and S being N(10, 1.25), a reasonable choice for the importance sampling function is N(11.5, 1.3). Hence, the random numbers $\hat{u}_i$(identical with those used in the earlier examples, to enable comparison) are transformed to sample values $\hat{x}_i$ through the inverse Normal transformation. The first four lines of calculation are shown in Table 3.1. The sampling function is then evaluated as $\phi(\hat{y}_i)$ where $\hat{y}_i = (\hat{x}_i - \mu_V)/\sigma_V$. The function $F_R f_S / h_V$ takes the place of $I[\ ] f_X / h_V$ in equation (3.17). For ten samples, it will be found that $p_f \approx (1/10) \times 0.478 = 0.0478$.

Experimentation with sample size and $l_V(\ )$ will show that sensible selection of $h_V(\ )$ is required if rapid convergence is to be achieved. As a general rule, the standard deviation σ_{V_i} for variable X_i should increase the further x_i^* lies from μ_{X_i} [Melchers, 1984].

3.4.3 Observations About Importance Sampling Functions

The importance sampling function suggested in the previous section has been shown to be very effective and robust when applied to a range of possible shapes of the limit state function [Engelund and Rackwitz, 1993; Melchers and Li, 1994]. Nevertheless, there are

Table 3.1 Example 3.5: Importance sampling.

$\hat{u}_i$	$\hat{x}_i = F_i^{-1}(\hat{u}_i)$ $= \Phi^{-1}(\hat{u}_i)$	$\hat{v}_i =$ $1.3\hat{x}_i + 11.5$	$h_V(\hat{v}_i)$ $= \phi(\hat{y}_i)$	$F_R(\hat{v}_i)$		$f_S(\hat{v}_i)$		$\dfrac{F_R(\hat{v}_i)f_S(\hat{v}_i)}{h_V(\hat{v}_i)}$
				$\hat{r}_i =$ $\dfrac{\hat{v}_i - 13}{1.5}$	$F_R(\hat{v}_i) =$ $\Phi(\hat{r}_i)$	$\hat{s}_i =$ $\dfrac{\hat{v}_i - 10}{1.25}$	$f_S(\hat{v}_i) =$ $\dfrac{1}{\sigma_S}\phi(\hat{s}_i)^{a)}$	
0.9311	+1.49	13.44	0.1315	0.29	0.6141	2.75	0.0073	0.0340
0.7163	+0.57	12.24	0.3391	−0.51	0.3050	1.79	0.6432	0.0578
0.4626	−0.09	11.38	0.3973	−1.08	0.1401	1.10	0.1743	0.0614
0.7895	+0.80	12.54	0.2897	−0.31	0.3783	2.03	0.0406	0.0530

a) Obtained from $\phi(s) = [1/(2\pi)]^{1/2} \exp\left(-\frac{1}{2}s^2\right)$ or from a table of standard normal probability distribution functions.
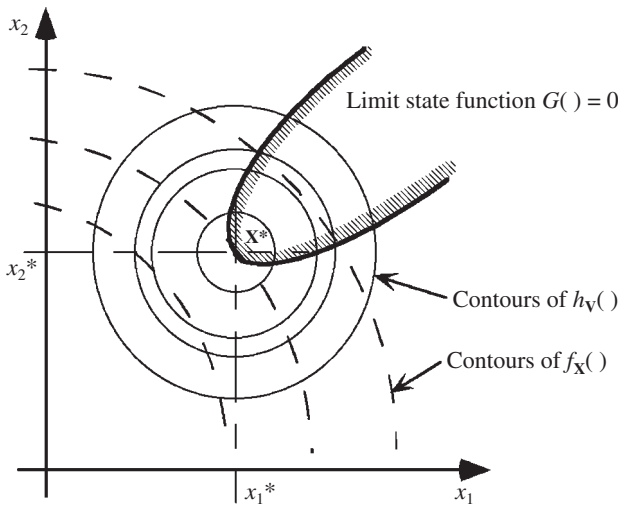
Figure 3.5 Highly concave limit state function in two dimensions showing obvious inefficiency of the importance sampling density.

some matters which must be considered as possible limitations. These are [Melchers, 1991]:

(1) $h_V(\ )$ may not be well-chosen, such as being too 'flat' or being skewed;
(2) extremely concave limit state functions may lead to low sampling efficiency (see Figure 3.5);
(3) a unique point of maximum likelihood $\mathbf{x}^*$ may not be identifiable (e.g. Figure 3.6):
   (a) when $f_X(\ )$ has a 'flat' contour region;
   (b) when the limit state function $G(\ ) = 0$ coincides with a contour of $f_X(\ )$ in a region of interest; or
   (c) when the limit state function $G(\ ) = 0$ is non-smooth (e.g. ripple-like) and has a number of candidate locations for $\mathbf{x}^*$;
(4) there may be more than one point of local maximum likelihood such as when $f_X(\ )$ is not uni-modal.
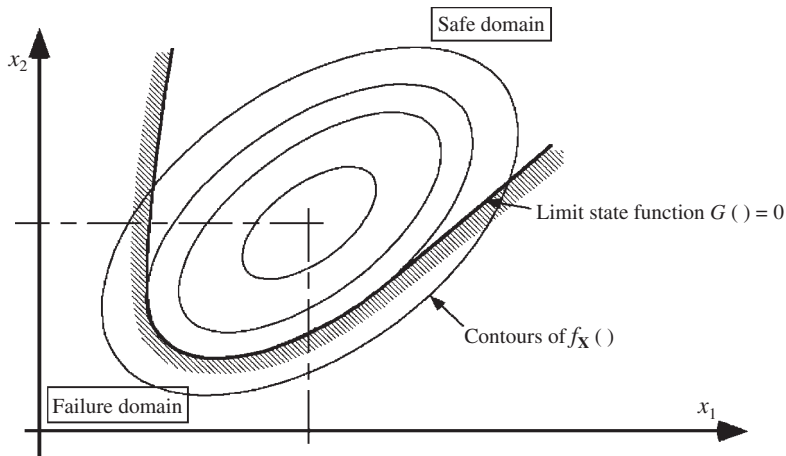
Figure 3.6 Situations in which $\mathbf{X}^*$ is not unique.
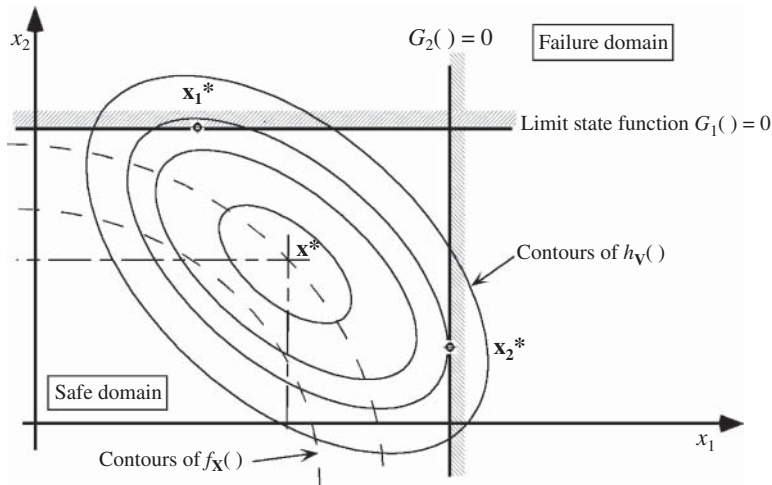
Figure 3.7 Poor choice of $h_v(\ )$ for case with two candidate points of maximum likelihood.

Examples of these matters can be found in the literature. For example, Figure 3.7 shows a case where $h_{\mathbf{V}}(\ )$ was centred at a point midway between the two points of maximum likelihood. This case would be better treated with a multi-modal $h_{\mathbf{V}}(\ )$ as discussed in Chapter 5 for structural systems with multiple limit state functions [Melchers, 1991]. It is important to note that not all the above issues are confined only to importance sampling. Thus points (2), (3) and (4) also produce difficulties for the FOSM methods considered in Chapter 4.

Generally, the $h_{\mathbf{V}}(\ )$ should attempt to mirror as closely as possible the shape of the failure domain. Thus when the limit state function forms a surface which is close to spherical, or partly so, an appropriate $h_{\mathbf{V}}(\ )$ could be obtained by using a multi-normal probability density function centred at or near the origin of the 'spherical' limit state system and censoring all samples which would lie in the safe domain. In two dimensions

@Seismicisolation

the resulting $h_V(\ )$ is then like a doughnut with a hole in the middle. However, this rather special problem is better handled by directional simulation (see Section 3.5 below).

The above examples reinforce the comment [Kahn, 1956] that the choice of $h_V(\ )$ involves a certain amount of intuition or 'art'. This is not particularly satisfactory for problems in high-dimensional spaces and which therefore cannot be visualized. Various suggestions have been made to develop procedures to obtain an 'optimal' $h_V(\ )$ for a given problem without the need for visualization. The more important and realistic of these are considered in the next section.

3.4.4 Improved Sampling Functions

As noted in Section 3.4.1 the importance sampling process becomes more efficient as the sampling function $h_V(\ )$ becomes more closely proportional to $f_X(\ )$ in the failure region. Various suggestions have been made to attempt to optimize $h_V(\ )$ in some way.

One simple observation is that it may be possible to 'censor' part of the region included by $h_V(\ )$, that is, sampling is prevented in a region for which it is clear there will be no contribution to the estimate of the failure probability. In Figure 3.8, the region $f_X(\ ) > f_X(\mathbf{x}^*)$ can be censored for samples taken from $h_V(\ )$ centred at $\mathbf{x}^*$ as points in this region cannot make a contribution [Melchers, 1989]. An exactly parallel case [Harbitz, 1986] exists in the standardized Normal space $\mathbf{y}$ with the censored region described by the circle having radius β, the safety index – see Chapter 4.

Another possibility for improving the importance sampling function is to select a trial $h_V(\ )$ and to perform some initial sampling. From this information, $h_V(\ )$ could be modified in some way in an attempt to improve the rate of convergence to the probability estimate. One proposal is to let $h_V(\ )$ be a composite of k elementary pre-selected sampling densities $h_{V_j}(\ )$:

$$h_V(\mathbf{x}) = \sum_{j=1}^{k} w_j h_{V_j}(\mathbf{x}) \tag{3.25}$$
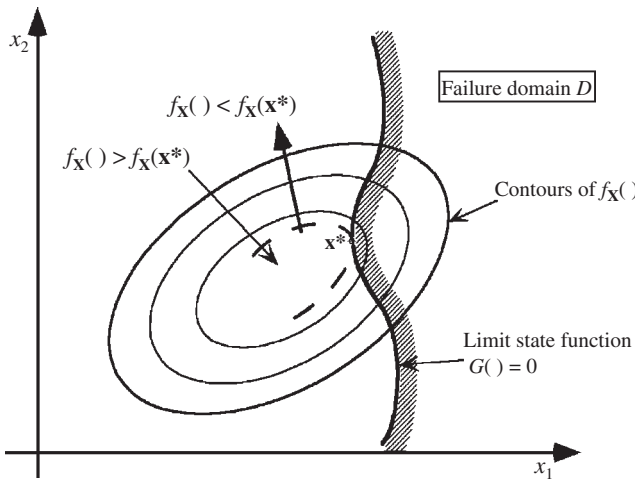
Figure 3.8 Censored region $f_X(\ ) > f_X(\mathbf{x}^*)$ for importance sampling about $\mathbf{x}^*$.

where $w_j, j = 1, \ldots, k$ are weights whose values are selected to let $h_V(\ )$ approach as closely as possible the shape of $f_X(\ )$ within the failure region. If the $h_{Vj}(\ )$ are selected as components of $f_X(\ )$ but with smaller standard deviation, and each centred at some initial sample point $\hat{\mathbf{x}}_j^*$, the weights w_j can be chosen as (Karamchandani et al., 1989):

$$w_j = \frac{f_X\left(\hat{\mathbf{x}}_j\right)}{\sum_{r=1}^{k} f_X\left(\hat{\mathbf{x}}_r\right)} \tag{3.26}$$

where $\hat{\mathbf{x}}_j$ is a sample vector. This means that the weights w_j are proportional to the contribution the sample vector $\hat{\mathbf{x}}_j$ makes to the (current) estimate of the probability. Once the weights are established from preliminary sampling, further sampling can be done and the process repeated to establish new weightings and a better estimate of the failure probability. To prevent clustering of newly obtained sampling densities $h_{Vj}(\ )$ around previously obtained densities, sampling points located closer than some distance d_0 from the centre of the current sampling densities $h_{Vj}(\ )$ might be ignored.

A slightly different approach is to modify $h_V(\ )$ by changing the weights w_j in (3.25) so as to minimize the variance in the estimate of the failure probability p_f [Ang et al., 1989; 1991]. This can be done with a limited amount of Monte Carlo sampling to estimate p_f for setting the weights (or 'kernels'). With an a priori choice for the form of each $h_{Vj}(\ )$, sampling from the constructed sampling density function $h_V(\ )$ obtained from (3.25) will allow refinement of the estimate for p_f.

In both techniques the location of the initial $h_{Vj}(\ )$ is based on the samples $\hat{\mathbf{x}}_j$ obtained from an initial sampling scheme (either Monte Carlo or some importance sampling). This means that the effectiveness of further sampling in developing an improved sampling density function depends very much on the initial samples and therefore on the sampling distribution from which they were drawn. Moreover, it has been assumed that convergence is assured. In addition, assumptions need to be made a priori about appropriate initial or component sampling densities. More ambitious schemes, in which the sampling densities are modified as more information becomes available with additional sampling have been proposed to address these matters.

It has been proposed also that the form of $h_V(\ )$ can be based on asymptotic notions (see Section 4.5.3) about the shape and gradient of $f_X(\ )$ in the region of interest [Maes et al., 1993]. This approach is useful for very low probability situations and with explicit limit state functions.

3.4.5 Search or Adaptive Techniques

It has been suggested above that for any one limit state function the 'best' location for the importance sampling probability density is the point of maximum likelihood (or the design point). Usually, this point is not known and will require a prior analysis to locate it, particularly for problems of high dimensionality. An alternative approach is to seek out the point using a search algorithm with the constraint that the point must lie along the limit state. This would then fix the desired location of $h_V(\ )$. It is possible also to modify $h_V(\ )$, depending on the information being obtained during the search process.

The process commences with the selection of the initial location (described by a mean vector) and the form (described by a covariance matrix) of $h_V(\ )$. A limited amount of

sampling is then carried out. The samples which fall into the failure domain are used to estimate the conditional mean vector μ_X and the covariance matrix $\mathbf{C_X}$. These are then used to update the original mean vector and covariance matrix and hence used to relocate $h_V(\ )$ and to change its form [Bucher, 1988]. Alternatively, for those sample points in the failure domain, the sample point which has the largest value of $f_X(\ )$ can be chosen as the best point to which to relocate $h_V(\ )$ [Melchers, 1989].

One approach for selecting the starting location is to select any point in a region in which the failure probability is likely to be large [Karamchandani et al. 1989]. This selection can be refined by evaluating $G(\ )$ at the selected point and also at a (any other) selected point in the safe domain. A better estimate for the point is then obtained by linear interpolation between the two points, to estimate the point at which $G(\ ) = 0$ [Melchers, 1989]. As with all search techniques, there is the possibility that the search will converge to a sub-optimal point (i.e. there may be several points of local maximum likelihood – see Figure 3.6).

Whether sub-optimal points should be considered depends on the contribution the associated probability is likely to make to the overall probability estimate. If the contribution is likely to be small, convergence to sub-optimal points can be guarded against to some extent [e.g. Der Kiureghian and Dakessian, 1998]. In general, to do so requires good physical understanding of the problem being solved so as to allow selection of appropriate starting points. It is also a good strategy to use different starting points.

Where the contribution of local points of maximum likelihood is not necessarily small, as may arise in structural systems when there are several limit state functions to be considered, a multimodal sampling function is appropriate. This is discussed further in Chapter 5.

If all the sample points available at any time are used for estimating the failure probability, (3.17) becomes [Melchers, 1990a]:

$$p_f = J_3 = \sum_{j=1}^{N_1} \left\{ \frac{I\left[_1\hat{\mathbf{v}}_j\right] f_X\left(_1\hat{\mathbf{v}}_j\right)}{N_1 h_V\left(_1\hat{\mathbf{v}}_j\right)} \right\} + \sum_{j=N_1+1}^{N_2} \left\{ \frac{I\left[_2\hat{\mathbf{v}}_j\right] f_X\left(_2\hat{\mathbf{v}}_j\right)}{N_2 h_V\left(_2\hat{\mathbf{v}}_j\right)} \right\} + \dots \text{etc.} \qquad (3.27)$$

where $_1h_V(\ )$ is the initial importance sampling function from which are drawn N_1 samples, $_2h_V(\ )$ is the modified sampling function from which are drawn the next set of samples $(N_2 - N_1)$, etc. and $I[_kh_V]$ is shorthand for $I\left[\cup_{k=1}^{m}\left\{G_i\left(_k\hat{\mathbf{v}}_j\right) \leq 0\right\}\right]$ which applies for m limit state functions. If there are n importance sampling distributions used in a search sampling sequence, the total number of samples is given by $N = N_n$.

Evidently, the variance of $I[\ ] f_X/_kh_V$ for each term in (3.27) directly affects the variance of J_3. While the individual sampling densities clearly are not independent, it is intuitively obvious that convergence will occur and that minimizing the variance for each term will minimize the overall variance in the limit as $N \rightarrow \infty$.

3.4.6 Sensitivity

If the effect of changing one (or more) variables on the failure probability is required to be evaluated, running two Monte Carlo assessments, with and without the change and comparing them, is unlikely to be very helpful. This is because the change is obtained by subtracting the outputs, while the variance for the change is obtained by adding

the two variances, so that the result sought might have a very large uncertainty. The problem can be circumvented by employing the same set of random numbers for both probability estimates. The total variance is then significantly less than for independent calculations, since the probability estimates are now (highly) correlated. This type of sampling is sometimes known as 'correlated' sampling [Rubinstein, 1981].

If the limit state function is analytic, the differentials $\partial G/\partial X_i$ will give the sensitivity of $G(\mathbf{X})$ to a (unit) change in X_i, but values so obtained will not be comparable unless the variances of the X_i are closely similar and the X_i are independent random variables. For independent variables, an approximate comparable measure of the sensitivity of $G(\mathbf{X})$ to a change in X_i is given by $c_i \approx (\sigma_{X_i}^{-1}) \ \partial G(\ )/\partial X_i$. This might be compared with the sensitivity coefficients α_i to be discussed in Section 4.3.3 for the First Order Second Moment (FOSM) method. This comparison also provides a way of estimating sensitivities in Monte Carlo analysis by finding an equivalent FOSM problem and then using its simple approach for sensitivity estimation to estimate the sensitivities for the original Monte Carlo problem [Ahammed and Melchers, 2006].

In importance sampling the sensitivity of p_f to changes in the random variables can be estimated as follows. The unchanged p_f would be obtained from (3.6), and the probability estimate for the modified problem (with random variable x_i, say, changed) would be given by:

$$p_f + \Delta p_i = \int_D f_{\mathbf{X}+\Delta X_i}(\mathbf{x})d\mathbf{x} = \int_X I[\mathbf{x}] \frac{f_{\mathbf{X}+\Delta X_i}(\mathbf{x})}{h_{\mathbf{X}}(\mathbf{x})} \ h_{\mathbf{X}}(\mathbf{x})d\mathbf{x} \tag{3.28}$$

$$\approx \frac{1}{N} \sum_{j=1}^{N} I[\hat{\mathbf{x}}_j] \frac{f_{\mathbf{X}+\Delta X_i}(\hat{\mathbf{x}}_j)}{h_{\mathbf{X}}(\hat{\mathbf{x}}_j)} \tag{3.29}$$

where the same sample set $\hat{\mathbf{x}}_j$ is used for evaluating (3.29). The computational effort to obtain results for (3.29) is rather small since the $I[\hat{\mathbf{x}}_j]$ terms would have been obtained already as part of the process of estimating p_f using (3.7). This assumes that the sample space is essentially unchanged by the change to $\mathbf{X} + \Delta X_i$. The same approach holds for a change of a parameter θ_i from the original parameter set $\boldsymbol{\theta}$ [Melchers, 1991]. The sensitivity is now given by:

$$S_i = [(p_f + \Delta p_i) - p_f]/\Delta x_i \tag{3.30}$$

and similarly for θ_i.

It is also possible to obtain the sensitivity S_i to a parameter θ_i (in $\mathbf{X}$ or $f_{\mathbf{X}}$ or both) by writing [Karamchandani and Cornell, 1991a]:

$$S_i = \frac{\partial p_f}{\partial \theta_i} = \frac{\partial}{\partial \theta_i} \int I[\mathbf{x}] f_{\mathbf{X}}(\mathbf{x})d\mathbf{x} \tag{3.31}$$

3.5 Directional Simulation*

3.5.1 Basic Notions

So far in this book the problem of estimating the probability of failure has been formulated exclusively in the Cartesian coordinate system. The idea of using a polar

@Seismicisolation

coordinate system arose from the specialized work of Deák (1980) in evaluating the multi-variate standard Normal distribution function. This led to simulation in the polar coordinate standard Normal (**y**) space and was given the name 'directional simulation' [Ditlevsen et al., 1987].

It will be convenient for the present to restrict discussion to the special case of the standard Normal space, denoted the (**y**) space here. The basic notion of directional simulation will be outlined in this section. The next section describes the application of importance sampling. In Section 3.5.3 discussion reverts to simulation in the original (**x**) space.

In the **y** space let the n-dimensional Gaussian vector **Y** be expressed as $\mathbf{Y} = R\mathbf{A}\,(R \geq 0)$, where **A** is an independent random vector of direction cosines. It represents directions in the **y**-space. In the simplest case **A** is uniformly distributed $f_{\mathbf{A}}(\ )$ on the n-dimensional unit (hyper-)sphere Ω_n. It follows from elementary probability theory [Benjamin and Cornell, 1970] that the radial distance R is such that R^2 is chi-square distributed with n degrees of freedom. If R is independent of **A**, then, by conditioning on $\mathbf{A} = \mathbf{a}$ the probability integral (1.31) can be re-written as [Bjerager, 1988]:

$$p_f = \int_{\mathbf{a}} P\left[g(R\mathbf{A}) \leq 0 | \mathbf{A} = \mathbf{a}\right] . f_{\mathbf{A}}(\mathbf{a}) d\mathbf{a} \tag{3.32}$$

where $f_{\mathbf{A}}(\ )$ is the (constant) density of **A** on the unit (hyper-)sphere and $g(\ ) = 0$ is the limit state function in **y**-space. Simulation using (3.32) now proceeds by generating randomly a standard Normal unit vector $\hat{\mathbf{a}}_j$ and moving along the outward direction of this vector until the limit state function is encountered at $R = r$ (see Figure 3.9), i.e. until $g(r\ \hat{\mathbf{a}}_j) = 0$. From this expression r may be determined. Often this must be done by trial and error. For a particular 'radius' r the associated estimate of the failure probability is the probability content beyond the (n-dimensional) hypersphere of radius r. It is given by:

$$p_j = P[g(r\ \hat{\mathbf{a}}_j) \leq 0] = 1 - \chi_n^2(r) \tag{3.33}$$
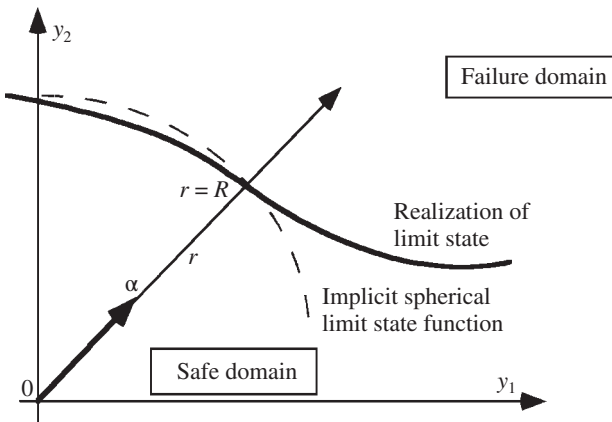
Figure 3.9 A radial sample in direction $\mathbf{A} = \mathbf{a}$ and its intersection with the limit state at $r = R$, showing also the implicit spherical limit state function.

where $\chi_n^2(\ )$ denotes the chi-squared distribution function with n degrees of freedom (see Section A.5.6). Repeating this for N samples drawn from $\mathbf{A}$ allows the unbiased estimator of the failure probability to be written as

$$p_f \approx E\left(\hat{p}_f\right) = \frac{1}{N} \sum_{j=1}^{N} \hat{p}_j \tag{3.34}$$

and the estimate of the standard deviation as

$$D\left[p_f\right]^2 \approx \frac{1}{N(N-1)} \sum_{j=1}^{N} \left(\hat{p}_j - E\left[\hat{p}_f\right]\right)^2 \tag{3.35}$$

The chief advantage of the above formulation is that $\chi_n^2(\ )$ can be evaluated analytically or by looking up standard tables, thus effectively reducing the order of integration by one dimension. Moreover, the directional simulation approach is particularly useful for limit state surfaces which are nearly spherical (in standard Normal space $\mathbf{y}$) as in this case all or most directional samples $\hat{\mathbf{a}}_j$ will contribute to (3.34). For this type of problem the amount of sampling required may be reduced considerably compared to importance sampling in Cartesian coordinates – one such case of practical importance is discussed in Section 3.5.4. Further, for the (very) special case of a single (hyper-)spherical limit state surface in standard Normal space, only one directional sample is required (to fix the radius) and (3.33) would give the 'exact' result immediately. (The parallel situation to importance sampling should be evident – compare with Section 3.4.1). However, the technique is not very efficient for one or few planar limit states [Engelund and Rackwitz, 1993].

Some practical points are:

(1) a sample outcome $\hat{\mathbf{a}}_j$ of $\mathbf{A}$ can be obtained by generating a sample $\hat{\mathbf{u}}_j$ of $\mathbf{U}$ and then using $\hat{\mathbf{a}}_j = \hat{\mathbf{u}}_j/\|\hat{\mathbf{u}}_j\|$ where $\|\hat{\mathbf{u}}_j\|$ is the norm and $\hat{\mathbf{u}}_j$ is a sample vector with each component drawn from the uniform distribution (Ditlevsen, et al. 1988);

(2) sampling efficiency can be improved through the use of anti-thetic variables for samples $\hat{\mathbf{a}}_j$ (and $-\hat{\mathbf{a}}_j$) (Rubenstein, 1981);

(3) the solution to $g(r\hat{\mathbf{a}}_j) = 0$ may be multi-valued, as sketched in Figure 3.10 (Bjerager, 1988; Engelund and Rackwitz, 1993), so that care is required in specifying the limit state function; and

(4) the limit state function need not be known explicitly to solve for $g(r\,\hat{\mathbf{a}}_j) = 0$. However, if an explicit form is required, use can be made of response surfaces (see Chapter 5).

3.5.2 Directional Simulation with Importance Sampling

Still operating in the $\mathbf{y}$ space, importance sampling can be applied with direction simulation to modify the uniform density on the unit sphere $f_{\mathbf{A}}(\ )$ if particularly interesting directions $\mathbf{A}$ can be identified. Following the same principle as in (3.17), expression (3.32) is modified to

$$p_f = \int_{\mathbf{b}} P\left[g(R\mathbf{B}) \leq 0 \,|\, \mathbf{B} = \mathbf{b}\right] \frac{f_{\mathbf{A}}(\mathbf{b})}{h_{\mathbf{B}}(\mathbf{b})} h_{\mathbf{B}}(\mathbf{b}) d\mathbf{b} \tag{3.36}$$
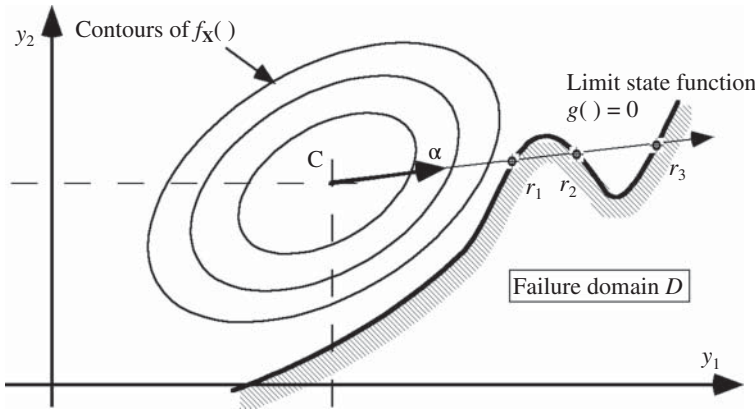
Figure 3.10 Multi-valued solutions for $g(r\,\hat{\mathbf{a}}_j) = 0$ in standard normal space.

where $h_{\mathbf{B}}(\mathbf{b})$ is the importance sampling probability density function on the unit sphere. For any sample $\hat{\mathbf{b}}_j$ generated from $h_{\mathbf{B}}(\mathbf{b})$, the corresponding sample value of the failure probability is

$$p_j = P\left[g(R\ \hat{\mathbf{b}}_j) \leq 0\right] \frac{f_{\mathbf{A}}(\hat{\mathbf{b}}_j)}{h_{\mathbf{B}}(\hat{\mathbf{b}}_j)} \tag{3.37}$$

which may be used in (3.33), (3.34) and (3.35) above. Evidently, $h_{\mathbf{B}}(\mathbf{b})$ must be non-zero.

As before, in principle the ideal sampling density function would predict p_f immediately. In practice some knowledge of the characteristics of the problem may help to obtain a suitable choice for $h_{\mathbf{B}}(\mathbf{b})$. Some assistance can be derived in the standard Normal space $\mathbf{y}$ from identification of the design points (see Figure 3.4 and Chapter 4). Ideal sampling densities are available for only some idealized cases, including a plane in n-dimensional space [Bjerager, 1988]. More generally, a composite sampling density may be defined as

$$h_{\mathbf{B}}^c(\mathbf{b}) = (1-q).f_{\mathbf{A}}(\mathbf{b}) + q.f_{\mathbf{B}}(\mathbf{b}) \qquad 0 \leq q \leq 1 \tag{3.38}$$

An example is given in Figure 3.11 for the two-dimensional standard Normal space. The value selected for q is arbitrary. However, the extreme values $q = 0$ and $q = 1$ correspond to one or other of the component sampling densities having no influence, and this should provide considerable information about the form of the limit state surface. The technique has been applied to the reliability analysis of ideal plastic frames [Ditlevsen and Bjerager, 1989].

3.5.3 Generalized Directional Simulation

Directional simulation can be formulated also in the original ($\mathbf{x}$) space, although the advantage of being able to apply the chi-squared distribution is lost.

Consider now an $\mathbf{x}$ space and a corresponding polar coordinate system so selected that both are centred at a convenient location such as the point $\mathbf{c} = \mu_{X(\text{original})}$ where $\mu_{X(\text{original})}$ represents the vector of the means of the random variables X_i in $\mathbf{x}$ space. It will
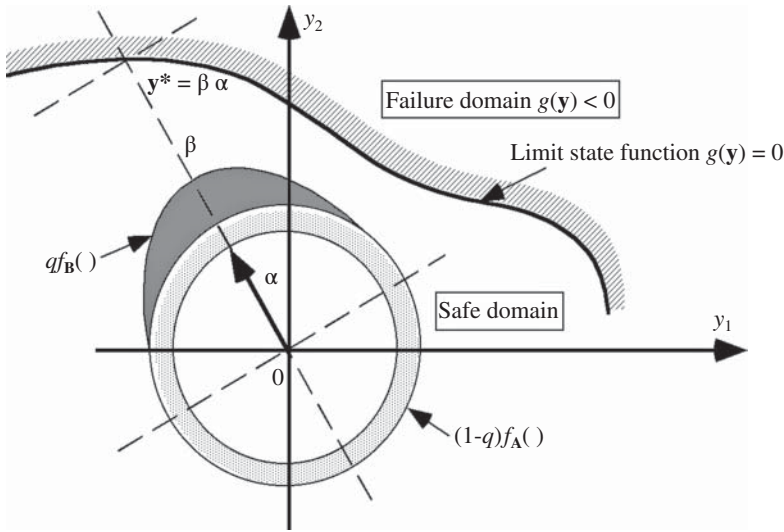
Figure 3.11 Composite sampling function $h_{\mathbf{B}}^c(\mathbf{b})$.

be advantageous also to consider re-scaling the various random variables X_i such that their units of measurement are approximately consistent – this will assist with obtaining reasonable sampling functions [Ditlevsen et al., 1990].

The probability integral (3.17) can now be written in polar coordinates as

$$p_f = \int \cdots \int_{\mathbf{A}} \int_{\mathbf{R}} I[\ ]\, f_{\mathbf{X}}(r\mathbf{a})\ r^{(n-1)} dr\ d\mathbf{a} \tag{3.39}$$

where $\mathbf{A}$ is the random directional unit vector (i.e. the direction cosines), $R \geq 0$ is the radius, a random variable with n degrees of freedom and defined such that $\mathbf{X} = R.\mathbf{A}$ and $\mathbf{A} = \mathbf{X}/\|\mathbf{X}\|, R = \|\mathbf{X}\|$. As for directional simulation in the standard Normal space, R is not necessarily independent of $\mathbf{A}$. With E_j defined as the expectation operator over j, (3.39) may be written in a form directly suitable for sampling over $\mathbf{A}$ and R:

$$p_f = E_{\mathbf{A}}\, E_R \left\{ I[\ ]\, r^{(n-1)} \right\} \tag{3.40}$$

or, for sampling only over $\mathbf{A}$ and integration along R:

$$p_f = S_A E_{\mathbf{A}} \left\{ \int_R I[\ ]\, f_{X|\mathbf{A}}(r\mathbf{a}|\mathbf{a}) r^{(n-1)} dr \right\} \tag{3.41}$$

where S_A is the surface area of the n-dimensional unit hypersphere and $f_{\mathbf{X}|\mathbf{A}}(\ )$ is the probability density function in $\mathbf{X}$, conditioned on $\mathbf{A} = \mathbf{a}$ in the radial direction. Comparing (3.41) with (3.33) and (3.34) shows that the chi-squared component has been replaced by the integral { } in (3.41).

Importance sampling may be added to the above. Thus if

$$h_{\mathbf{Z}}(r.\mathbf{a}) = h_{\mathbf{A}}(a).h_{R|\mathbf{A}}(r\,|\,\mathbf{a}) \tag{3.42}$$

is an importance sampling density function such that $\mathbf{Z} = R.\mathbf{A}$ and if $h_{R|\mathbf{A}}(\ )$ is the sampling density function for the radial direction and $h_{\mathbf{A}}(\ )$ is the sampling density function on the unit sphere, as before, then expressions (3.40) and (3.41) become,

respectively [Melchers, 1990b]:

$$p_f = S_A E_{\mathbf{A}} E_R \left\{ I[\ ] h_{\mathbf{A}}(\mathbf{a}) \frac{f_{\mathbf{X}}(r\mathbf{a}) r^{(n-1)}}{h_{R|\mathbf{A}}(r|\mathbf{a})} \right\} \tag{3.43}$$

with radial integration by simulation and

$$p_f = S_A E_{\mathbf{A}} \left\{ \int_R I[\ ] \frac{f_{\mathbf{X}|\mathbf{A}}(r\mathbf{a}|\mathbf{a}) r^{(n-1)} dr}{h_{\mathbf{A}}(\mathbf{a})} \right\} \tag{3.44}$$

with explicit analytical radial integration.

Note that each of the importance sampling function $h_{\mathbf{A}}(\ )$ and $h_{R|\mathbf{A}}(\ )$ can be given appropriate properties, depending on the understanding the analyst has of the problem. The special case for a uniform (i.e. constant) probability density over the unit sphere corresponds simply to $h_{\mathbf{A}} = 1/S_A$ where S_A is the 'surface area' of the n-dimensional unit sphere [Melchers, 1990b]. Also, in considering the importance sampling function $h_{R|\mathbf{A}}(\ )$ in the radial direction it might be noted that the limit state function usually is some considerable distance from the mean or from the point $\mathbf{c} = \mu_{\mathbf{X}(\text{original})}$. This suggests that $h_{R|\mathbf{A}}(\ )$ could have a form which is rather low in value within the safe region and increasing with the probability of encountering a limit state as r increases.

A comparison of directional simulation in the standardized Normal space $\mathbf{y}$ (as in Section 3.5.1) (after transformation of the problem from the original space, see Chapter 4 and Appendix B) with directional simulation directly in the original space $\mathbf{x}$ shows that, for a simple problem, the results are comparable in accuracy and efficiency [Ditlevsen et al., 1990].

3.5.4   Directional Simulation in the Load Space

Rather than formulating the problem in the polar coordinate space for all the random variables and processes, it is possible for many problems to separate the loads from the resistances and to use the load (process) space for directional simulation. This way of using directional simulation has been applied mainly to structural systems (see Chapter 5) and for situations where the loads must be represented as processes (see Chapter 6). In the following the basic concept is described, together with the manner in which the structural strength of the structure can be developed. Applications to systems and to load processes are considered in Chapters 5 and 6.

3.5.4.1   Basic Concept

Consider the m-dimensional space of load processes $\mathbf{Q}(t)$ and let this be the space in which directional simulation will be performed. Typically it will be of low order, since there are usually only a few loads acting on a structure. In the case of only one load, there will be only one axis and the following discussion degenerates to the formulation (1.18) and to Figure 1.9 as discussed in Chapter 1.

Let the structural resistance in the load space be described by $\mathbf{R} = \mathbf{R}(\mathbf{X})$ where each component of $\mathbf{R}$ corresponds directly with one component of $\mathbf{Q}$. The joint probability density function of $\mathbf{R}$ is given by $f_{\mathbf{R}}(\ )$. The n-dimensional vector $\mathbf{X}$ contains random material strengths, dimensions, etc. and also could contain any uncertainties in the specification of the load processes. It then follows that the conventional limit state
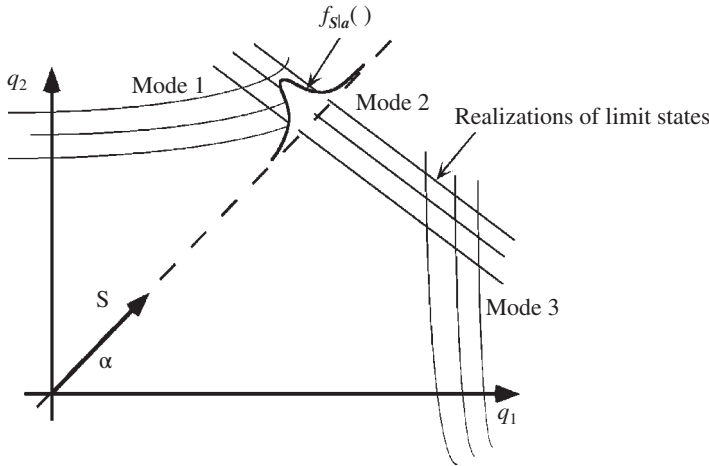
Figure 3.12 Two-dimensional load space showing a typical directional simulation and the probabilistic description of limit states and some realizations.

function $G(\mathbf{x}) = 0$ is represented as a probabilistic 'boundary' in the load process space (see Figure 3.12).

It follows from (1.18) and (3.32) that the probability of failure now can be expressed as [Corotis and Nafday, 1989]:

$$p_f = \int_{\text{unit sphere}} f_{\mathbf{A}}(\mathbf{a}) \int_0^\infty F_{\mathbf{R}|\mathbf{a}}(s\,|\,\mathbf{a}) f_{s|\mathbf{a}}(s\,|\,\mathbf{a}) ds\, d\mathbf{a} \qquad (3.45)$$

where $f_{S|\mathbf{A}}(\;)$ is the conditional probability density function for the m-dimensional load (process) vector $\mathbf{Q}(t)$ and $F_{\mathbf{R}|\mathbf{A}}(\;)$ is the conditional cumulative probability distribution function for the structural resistance $\mathbf{R} = \mathbf{R}(\mathbf{X})$, both for a given radial direction $\mathbf{A} = \mathbf{a}$. Also $\mathbf{R} = S.\mathbf{A} + \mathbf{c}$ where $\mathbf{c}$ is the point selected as the origin for directional simulation (see previous section) and S is a (scalar) radial distance representing the (conditional) structural strength in the radial direction, with conditional pdf $f_{S|\mathbf{A}}(\;)$. As before, it is possible to apply importance sampling notions to make $\mathbf{A}$ have preferred orientations.

Since $F_{R|\mathbf{A}}(s\,|\,\mathbf{a}) = P[R < s]\,|_{\mathbf{A}=\mathbf{a}} = p_f(s\,|\,\mathbf{a})$ a more direct expression is [Melchers, 1992]:

$$p_f = \int_{\text{unit sphere}} f_{\mathbf{A}}(\mathbf{a}) \left[\int_S p_f(s\,|\,\mathbf{a}) . f_{S|\mathbf{A}}(s\,|\,\mathbf{a}) ds \right] d\mathbf{a} \qquad (3.46)$$

where now $p_f(s\,|\,\mathbf{a})$ is a conditional failure probability. This term can be evaluated for each radial direction using any of the methods for evaluating the basic probability integral (1.18), including (i) direct integration (see Section 1.4.5 and the early part of the present Chapter), (ii) simulation methods (as in Sections 3.3 and 3.4) and first order second moment (FOSM) and first order reliability (FOR) methods (as described in detail in Chapter 4).

Expression (3.46) forms the basis for directional simulation in the load space, with either one or both integrals replaced by an expectation operator, as was done in the previous section [Ditlevsen et al., 1990; Melchers, 1992]. To make (3.46) operational, the two terms in the second integrand must be available: the conditional failure probability $p_f(s\,|\,\mathbf{a})$ and the variation of structural strength $f_{S|\mathbf{A}}(\;)$, both a function of the distance s along the radial sampling direction.

The conditional failure probability $p_f(s|\mathbf{a})$ is the probability that the structure will fail for a given value $S(\mathbf{X}) = s$ of the structural strength along the direction $\mathbf{A} = \mathbf{a}$. This is now a one-dimensional problem. Hence the result can be obtained readily from the convolution integral (1.18) with fixed strength. The necessary loading probability density function $f_{Q|A}( )$ can be obtained from the complete loading probability description $f_{\mathbf{Q}(t)}(\mathbf{q})$ by taking the conditional function for the sample direction $\mathbf{A} = \mathbf{a}$.

As was noted in Section 1.4.1 (and as discussed in more detail in Chapter 6) this way of handling the problem applies strictly only for one load system applied only once. It is therefore useful as an estimator of structure failure probability when the structure is first loaded or under extreme loading (with an appropriate choice of load pdf – see Section 1.4.1). Multiple loadings, unless they are fully dependent, require consideration as load processes (see Chapter 6).

3.5.4.2 Variation of Strength with Radial Direction

Both expressions (3.45) and (3.46) require the evaluation of $f_{S|A}( )$ [or $F_{S|A}( )$], the variation of structural strength with distance along the radial direction (Figure 3.13).

If the limit state expression $G(\mathbf{x}) = 0$ is known explicitly, $f_{S|A}( )$ can be evaluated by multiple integration along the radial direction S, that is, for a given $\mathbf{A} = \mathbf{a}$ [Melchers, 1992]. Alternatively, the first two moments of S can be estimated from the first two moments of the random variables $\mathbf{X}$ which contribute to it. The relationships which are needed are $\mathbf{R} = \mathbf{R}(\mathbf{X})$ and $\mathbf{R} = S.\mathbf{A} + \mathbf{c}$ from which it follows that $S = S(\mathbf{X})|\mathbf{A} = \mathbf{a}$. Hence:

$$\boldsymbol{\mu}_S = E[S] \approx S(\boldsymbol{\mu}_X)|_{\mathbf{A}=\mathbf{a}} \tag{3.47}$$

$$\text{var}(S) \approx \sum_i^n \sum_j^n c_i c_j \ \text{cov}(X_i, X_j)|_{\mathbf{A}=\mathbf{a}} \tag{3.48}$$

where $c_i \equiv \frac{\partial S(\mathbf{x})}{\partial X_i}|_{\mu_x, \mathbf{a}}$ and $\text{cov}(X_i, X_i) = \text{var}(X_i)$ and $\text{cov}(X_i, X_j) = 0$ ($i \neq j$) if X_i and X_j are independent. Then $f_{S|A}( )$ and $F_{S|A}( )$ can be determined immediately. The situation becomes more complex if there are several limit state functions (see Chapter 5).
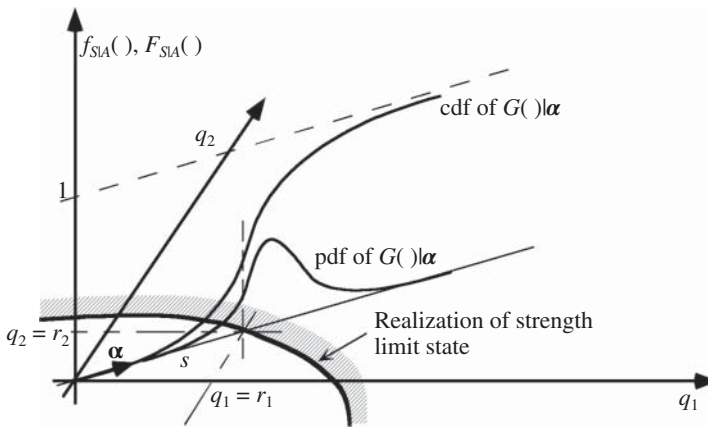
Figure 3.13 Schematic directional simulation in the load space showing variation of structural strength along a sample radial direction.

For some problems, such as those involving a finite element routine for the structural analysis, the limit state functions are not known explicitly. In this case so-called response surfaces may be used as surrogates for the actual limit state function(s) (see Chapter 5). Then, for directional simulation, $F_{S|A}(\ )$ can be obtained for any $\mathbf{A} = \mathbf{a}$ and any $S = s$ by considering the structure subject to a deterministic loading $\mathbf{q} = \mathbf{r}(\mathbf{x})$ at various points along the radial sample direction S and noting that $p_f(s)_{|\mathbf{a}} = \Pr(S < s)_{|\mathbf{a}} = F_{S|\mathbf{a}}(s)$ for any $\mathbf{A} = \mathbf{a}$. From this, $F_{S|A}(\ )$ may be constructed through evaluation at different points s along the radial direction $\mathbf{A} = \mathbf{a}$. By differentiation (numerically perhaps) $f_{S|A}(\ )$ can be obtained.

Finally, a third possibility is to use simulation along $\mathbf{A} = \mathbf{a}$ to estimate $f_{S|A}(\ )$ and $f_{\mathbf{R}|\mathbf{A}}(\ )$ directly [Melchers, 1992]. However, this is computationally expensive, and is essentially equivalent to finding a solution by 'crude' Monte Carlo simulation. This possibility should therefore be avoided if possible.

As already noted, an important assumption underlying the above technique of directional simulation in the load space is that the limit state is independent of the realizations of the load (processes). In other words, the limit state function is assumed to be 'load-path independent'. This is an important assumption, particularly for structural systems since for these the ultimate limit state function(s) may be dependent on violations of other limit states. In other words, they are functionally dependent on previous realizations. More detailed comments and discussion are given in Chapter 5.

3.5.4.3   Line Sampling

A variation of the above is so-called 'line' sampling. It seeks to find the direction $\boldsymbol{\alpha}$ of a radial line from the origin in the space of the random variables $\mathbf{x}$ that points to the region that contributes the most to the failure probability [Koutsourelakis et al., 2004]. In 2-dimensional space (Figure 3.9) the point $\hat{\mathbf{x}}$ on the limit state function could be considered as the point to represent such a region. Other possibilities are the region with the highest rate of change (gradient) in the $\boldsymbol{\alpha}$ direction or (less accurately) the centre of mass of much of the failure region [Pradlwarter et al., 2005]. Once such a line is identified, the approach is to generate a series of points, randomly, within the identified failure domain and use these in conventional Monte Carlo to estimate the failure probability, allowing, as in importance sampling, for the bias in those points. To generate those points, Markov Chain Monte Carlo simulation based on a user-supplied probability density function has been proposed [Pradlwarter et al., 2005]. This increases the computational effort. A further possibility is to transform the problem to the standard Normal space and then use some of the approximate techniques described in Chapter 4. An application of line sampling to a fracture mechanics problem has been described by Pedroni and Zio (2009) and to several bench-mark problems by Pradlwarter et al. (2007).

3.6   Practical Aspects of Monte Carlo Simulation

3.6.1   Conditional Expectation

In cases where at least one of the random variables in $\mathbf{X}$ in (1.31) is an independent random variable, the Monte Carlo process can be made more efficient by reducing the

order of integration. To illustrate this approach for one random variable, select the independent random variable with the largest uncertainty (variance). Let this be X_1 for the discussion to follow. Expression (1.31) can then be rewritten as:

$$p_f = \int_{G(\mathbf{x}) \leq 0} \int_n f_{\mathbf{X}}(\mathbf{x})\, d\mathbf{x} = \int_{G(\mathbf{x}') \leq 0} \int_{n-1} F_{X_1}(\mathbf{u}) f_{\mathbf{X}'}(\mathbf{u}) d\mathbf{u} \tag{3.49}$$

where $\mathbf{X}'$ represents the reduced vector of random variables. This form may be used as a basis for a Monte Carlo technique known as 'conditional expectation'. The unbiased estimator for (3.49) is given by

$$p_f \approx \frac{1}{N} \sum_{j=1}^{N} F_{X_1}(\hat{x}_{1j}) \tag{3.50}$$

where, for the jth trial, $\hat{x}_{1j}$ is the jth value of $\mathbf{X}'$, obtained from the limit state equation $G(\mathbf{X}) = 0$ when it is solved for x_1 with all other random variables $X_i, (i = 1, \ldots, n-1)$ represented by the vector of generated sample values $\hat{x}_j$. Hence, the simulation procedure generates a sample $\hat{x}_j$, which satisfies the limit state equation. This is then used to determine an estimate $\hat{p}_{f_j} = F_{X_1}(\hat{x}_{1j})$ of the failure probability. By repeating this process N times an estimate of p_f is obtained through (3.50). Expression (3.50) can be shown to have a smaller variance than the equivalent 'crude' formulation [Ayyab and Haldar, 1984; Ayyub and Chia, 1991; Karamchandani and Cornell, 1991b].

It is possible to continue the conditional expectation process by sequentially conditioning on more of the variables [Au and Beck, 2001]. This has been termed 'subset' simulation. One potential issue is that it entails the non-insignificant task of sampling from conditional probability densities. While successive Markov Chain Monte Carlo simulations have been proposed as a way of dealing with this (Au and Beck, 2003), it is clear that the computational requirements are much increased. See also Au et al. (2007).

Several other techniques have been proposed to deal with very large systems. Asymptotic Sampling [Bucher, 2009; Sichani et al., 2011a, 2011b] is based on the asymptotic behavior of failure probabilities as the standard deviation of the random variables tends to zero. Enhanced Sampling [Naess et al., 2009, 2012] uses the asymptotic behaviour of failure probabilities as the limit states are moved further and further away from the mean of random vector $\mathbf{X}$. These techniques have been explored and compared by Santos and Beck (2015).

Some additional variance reduction may be achieved through 'anti-thetic' variates in which variates in sample sequences are given negative correlation. This variance reduction technique, as are several others, is discussed in the literature [Rubinstein, 1981].

3.6.2 Generalized Limit State Function – Response Surfaces

Considerable computational problems may arise if $G(\mathbf{X})$ is at all complex to calculate. This might occur, for example, with a finite element analysis or for iterative calculation of non-linear material or structural behaviour. If the number of basic variables is relatively small, some typical calculations for $G(\mathbf{X})$ might be performed so as to cover the range of values of $\mathbf{X}$ likely to be obtained by simulation. These values may then be used as interpolation points for $G(\mathbf{X})$ each time that a sample vector $\hat{\mathbf{x}}$ is generated. This procedure is only feasible if $G(\mathbf{X})$ is reasonably regular. It is sometimes referred to as the 'response surface' technique. This is discussed in Chapter 5.

3.6.3 Systematic Selection of Random Variables

It is important to note that random sampling is not always required for every variable. If, as would be usual for structural reliability, the samples can be taken sequentially, say $\hat{x}_1, \hat{x}_2, \hat{x}_3$, etc., for $G(\mathbf{x})$, then the sampling for X_1, say, could be done systematically, rather than randomly. For example, the interval over which the sampling would be done for X_1 could be divided into n equal intervals. For each interval represented by the point i, (which might be taken as the centre of the interval), the probability density function would be simply $f_{X_1}(x_i)$. In a conventional random sampling of X_1, using N samples, it would be expected that N/n values of X_1 would occur in the i-th interval. Hence N/n values, each equal to $f_{X_1}(x_i)$ could be employed. The results are not biased if the first N/n values for X_1 are systematically set at $f_{X_1}(x_1)$, the next N/n at $f_{X_1}(x_2)$, etc., with $x_1 < x_2 < x_{3,}$ etc. [Kahn, 1956].

3.6.4 Applications

A common criticism of the Monte Carlo method is that it is a crude and time-consuming method of solution. Unfortunately for some practical applications where Monte Carlo techniques have been used in the past these criticisms are well founded, but this need not be the case in general, and it is increasingly less so, largely as a result in the dramatic reductions in computation times, even for desk-top computers. Numerous applications also show that time-saving refinements such as importance sampling are widely used. The only real remaining challenges lie in probability estimation for very complex problems with very large numbers of random variables or complex limit state functions, described, for example, by finite element routines. The other area in which there are still constraints is where complete time-dependent simulation of load processes is required – see Chapter 6).

Applications of the Monte Carlo technique to a large variety of problems have been described, for example, in the classical works of Kahn (1956), Hammersley and Handscomb (1964) and Rubinstein (1981). Some typical early structural engineering applications were described by Moses and Kinser (1967), and Knappe et al. (1975). Warner and Kabaila (1968) reported on various ways of applying the Monte Carlo technique (but not importance sampling) to an idealized reinforced concrete member. These are still educational sources of information. Application of some other variance reduction techniques, such as Latin hypercube sampling, have been described now by many authors [e.g. Ayyub and Lai, 1990; Zio, 2011].

The effectiveness and efficiency of the techniques is always an issue. There have been few detailed investigations, but a useful comparison of some of the simulation methods for a range of single limit state applications has been given by Engelund and Rackwitz (1993). Their conclusions suggest that for single limit state problems the most robust and efficient approach is importance sampling (Section 3.4). This is supported by some simpler comparisons that also showed the effectiveness of directional simulation and the much lower effectiveness of conditional expectation and Latin Hypercube sampling (Huntington and Lyrintzis, 1998; Lemaire, 2009).

@Seismicisolation

3.7   Conclusion

Much of this chapter has been devoted to the use of the Monte Carlo technique to enable integration of the convolution integral. The 'crude', the 'importance sampling' and 'directional' simulation methods were considered in some detail. Other possibilities as well as some practical matters were noted.

4

Second-Moment and Transformation Methods

4.1 Introduction

Rather than use approximate (and numerical) methods to perform the integration required in the reliability integral (1.31) to check or to analyse or to assess the safety of a structure, in this chapter the probability density function $f_X(\ )$ in the integrand will be simplified. The first part of this chapter will consider the special case of reliability estimation (checking) in which each variable is represented only by its first two moments i.e. by its mean and standard deviation. This is known as the 'second-moment' level of representation. Higher moments, which might describe skew and flatness of the distribution, are ignored. As noted earlier, a convenient way in which the second-moment representation might be interpreted is that each random variable is represented by the Normal (or Gaussian) distribution. (This continuous probability distribution is described completely by its first two moments – see Section A.5.7). As was seen in Section 1.4.3 when both R and S are Normal distributed, integration of (1.18) is completely obviated; further, as already suggested in Section 3.2, the multiple integral (1.31) may also be tractable when $f_X(\ )$ is multi-Normal.

Because of their inherent simplicity, the so-called 'second-moment' methods have become very popular. Early works by Mayer (1926), Freudenthal (1956), Rzhanitzyn (1957) and Basler (1961) contained second-moment concepts. Not until the late 1960s, however, was the time ripe for the ideas to gain a measure of acceptance, prompted by the work of Cornell (1969a).

From the original second-moment ideas have grown a number of extensions and refinements. Of these, the most important is that it is now possible, with iterative techniques, to approximate the actual probability distributions in $f_X(\ )$ with Normal probability distributions and still to obtain good estimates of the failure probability. These matters are considered later in this chapter.

4.2 Second-Moment Concepts

In Section 1.4.3 it was shown that when resistance R and load effect S are each second-moment random variables (i.e. such as having Normal distributions), the limit state equation is the 'safety margin' $Z = R - S$ and the probability of failure p_f is

$$p_f = \Phi(-\beta) \quad \beta = \frac{\mu_Z}{\sigma_Z} \tag{4.1}$$

where β is the 'safety index' and $\Phi(\ )$ the standard Normal distribution function. The function $\Phi(\ )$ is tabulated in Appendix D, and approximate expressions are given in Section A.5.7.

Evidently, Eq. (4.1) yields the exact probability of failure p_f when both R and S are Normal distributed. However, p_f defined in this way is only a 'nominal' failure probability when R and S have distributions other than Normal. Conceptually it is probably better in this case not to refer to probabilities at all, but simply to β, the 'safety index'. It also is known as the 'reliability index'.

As shown in Figure 1.11, β is a measure (in standard deviation σ_Z units) of the distance that the mean, σ_Z is away from the origin $Z = 0$. This point marks the boundary of the 'failure' region. Hence β is a direct (if imprecise) measure of the safety of the structural element and greater β represents greater safety, or lower nominal failure probability p_{fN}.

For convenience, and for clarity, in what follows the notation p_{fN} is used to refer to the nominal probability estimate, i.e. that calculated using second-moment (and other) approximations.

The above ideas are readily extended in the case where the limit state function is a random function consisting of more than two basic random variables:

$$G(\mathbf{X}) = Z(\mathbf{X}) = a_o + a_1 X_1 + a_2 X_2 + \ldots + a_n X_n \tag{4.2}$$

then $G(\mathbf{X}) = Z(\mathbf{X})$ is Normal distributed and (A.160) and (A.161) provide μ_Z and σ_Z from which β and p_{fN} again can be evaluated using (4.1).

In general, however, the limit state function $G(\mathbf{x}) = 0$ is not linear. In this case, the first two moments of $G(\mathbf{X})$ are not readily obtainable. The most suitable approach is to linearize $G(\mathbf{x}) = 0$. This can be done by using expressions (A.178) and (A.179) which then give approximate moments by expanding $G(\mathbf{x}) = 0$ as a first-order Taylor series expansion about some point $\mathbf{x}^*$. Approximations that linearize $G(\mathbf{x}) = 0$ will be denoted 'first-order' methods.

The first-order Taylor series expansion which linearizes $G(\mathbf{x}) = 0$ at $\mathbf{x}^*$ might be denoted $G_L(\mathbf{x}) = 0$ (Figure 4.1). Expansion about the mean, μ_Z is common in probability theory, but there is no rationale for doing so in general; it will be shown later that there is indeed a better choice for the present problem. In anticipation, it can be said that this better choice $\mathbf{x}^*$ is the point of maximum likelihood (or most probable point MPP) on the limit state function. At this stage, it is sufficient to note that the choice of expansion point directly affects the estimate of β. This is demonstrated in the following example.

Example 4.1 The first two moments of Z linearized about $\mathbf{x}^*$ rather than μ_X are given by [*cf.* (A.178) and (A.179)] $\mu_Z \approx G(x^*)$ and $\sigma_Z^2 \approx \Sigma (\partial G/\partial X_i)^2 \big|_{x^*} \sigma_{x_i}^2$ respectively.

Now, if $G(\mathbf{X})$ is defined as $G(\mathbf{X}) = X_1 X_2 - X_3$ with the random variables X_i being independent and with $\sigma_{X_1} = \sigma_{X_2} = \sigma_{X_3} = \sigma_X$, then $\partial G/\partial X_1 = X_2$, $\partial G/\partial X_2 = X_1$ and $\partial G/\partial X_3 = -1$. Then (A.178) and (A.179) evaluated at the means μ_{X_i} become

$$\mu_Z \big|_{\mu_\mathbf{x}} \approx \mu_{X_1} \mu_{X_2} - \mu_{X_3}$$

$$\sigma_Z^2 \big|_{\mu_\mathbf{x}} \approx \mu_{X_2}^2 \sigma_{X_1}^2 + \mu_{X_1}^2 \sigma_{X_2}^2 + \sigma_{X_3}^2 = \sigma_X^2 \left(\mu_{X_1}^2 + \mu_{X_2}^2 + 1 \right)$$
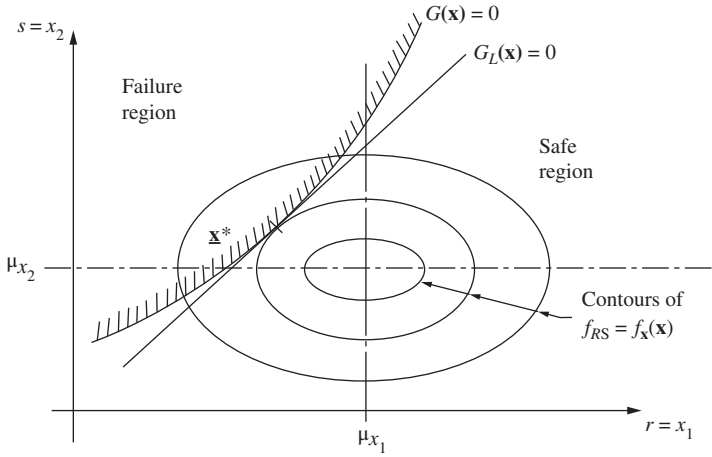
Figure 4.1 Limit state surface $G(\mathbf{x}) = 0$ and its linearized version $G_L(\mathbf{x}) = 0$ in the (2-D) space of the basic variables. Here the linearization is at point $\mathbf{x}^*$. (It is known also as the 'checking point' and is clearly the most probable point – MPP).

However, if the expansion point was taken as $x_1^* = \mu_{X_1}/2$, $x_2^* = \mu_{X_2}$, $x_3^* = \mu_{X_3}$ then the corresponding terms become

$$\mu_Z\big|_{\mu_{\mathbf{x}}} \approx \frac{\mu_{X_1}}{2}\mu_{X_2} - \mu_{X_3}$$

and

$$\sigma_Z^2\big|_{\mu_{\mathbf{x}}} \approx \mu_{X_2}^2\sigma_{X_1}^2 + \left(\frac{\mu_{X_1}}{2}\right)^2\sigma_{X_2}^2 + \sigma_{X_3}^2 = \sigma_X^2\left(\frac{\mu_{X_1}^2}{4} + \mu_{X_2}^2 + 1\right)$$

It follows readily using (4.1) that:

$$\beta\big|_{\mu_{\mathbf{x}}} = \frac{\mu_{X_1}\mu_{X_2} - \mu_{X_3}}{\sigma_X\left(\mu_{X_1}^2 + \mu_{X_2}^2 + 1\right)^{1/2}}$$

and

$$\beta\big|_{x^*} = \frac{\frac{1}{2}\mu_{X_1}\mu_{X_2} - \mu_{X_3}}{\sigma_X\left(\frac{1}{4}\mu_{X_1}^2 + \mu_{X_2}^2 + 1\right)^{1/2}}$$

These are clearly not equivalent, thus demonstrating the dependence of β on the selection of the expansion point. Fundamentally, this is not a desirable situation.

4.3 First-Order Second-Moment (FOSM) Theory

4.3.1 The Hasofer–Lind Transformation

The desirability of a safety measure being invariant was noted in Chapter 1. How this can be achieved for the reliability index β will be discussed below. A useful

(but not essential) first step is to transform all variables to their standardized form $N(0, 1)$ (Normal distribution with zero mean and unit variance) using the well-known transformation:

$$Y_i = \frac{X_i - \mu_{X_i}}{\sigma_{X_i}} \tag{4.3}$$

where Y_i has $\mu_{Y_i} = 0$ and $\sigma_{Y_i} = 1$. As a result of applying this transformation to each basic variable X_i, the unit of measurement in any direction in the **y** space will be $\sigma_{Y_i} = 1$ in any direction. In this space, the joint probability density function $f_{\mathbf{Y}}(\mathbf{y})$ is the standardized multi-variate Normal (see Section A.5.7); thus many well-known properties of this distribution can be applied [Hasofer and Lind, 1974]. Of course, the limit state function also must be transformed and is given by $g(\mathbf{y}) = 0$.

The transformation (4.3) can be performed without complication if the Normal random variables X_i are all uncorrelated (i.e. linearly independent) random variables. If this is not the case, an intermediate step is required to find a random variable set $\mathbf{X}'$ that is uncorrelated, and this new set can then be transformed according to (4.3). The procedure for finding the uncorrelated set $\mathbf{X}'$ (including means and variances) from the correlated set $\mathbf{X}$ is essentially that of finding the eigenvalues and eigenvectors (characteristic values and vectors). Details are given in Appendix B. As an approximation, weak correlation (e.g. $\rho < 0.2$) usually can be ignored and the variables treated as independent, whereas strong correlations (e.g. $\rho > 0.8$) usually can be treated as fully dependent, with one of the two correlated variables replaced by the other.

4.3.2 Linear Limit State Function

For simplicity of illustration consider now the important special case in which the limit state function is linear, i.e. $G(\mathbf{X}) = X_1 - X_2$, shown as $G_L(\mathbf{x}) = 0$ in Figure 4.1. The transformation (4.3) changes the joint probability density function $f_{\mathbf{X}}(\mathbf{x})$ shown in Figure 4.1 to $f_{\mathbf{Y}}(\mathbf{y})$ shown in Figure 4.2 in the transformed $\mathbf{y} = (y_1, y_2)$ space. The joint probability
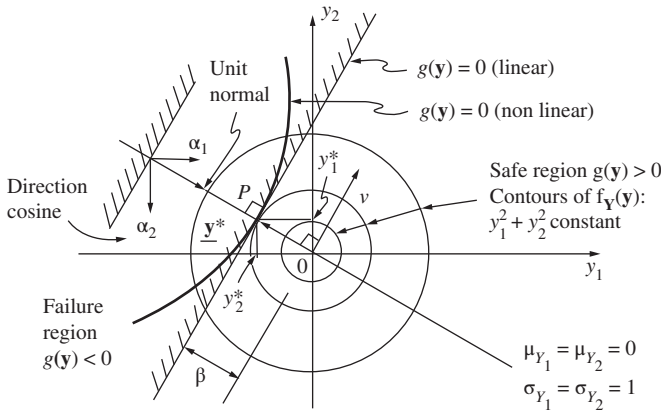
Figure 4.2 Probability density function contours and original (non-linear) and linearized limit state surfaces in the standard Normal space. The linearized version of $g(\mathbf{y})$ is shown linearized at $\mathbf{y}^*$.
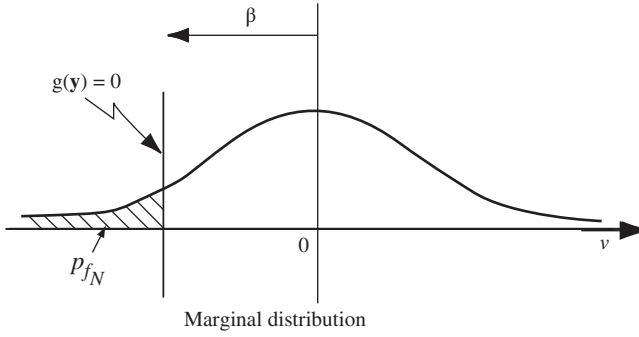
Figure 4.3 Marginal distribution in the space of the standardized Normal variables.

function $f_{\mathbf{Y}}(\mathbf{y})$ is now a bivariate Normal distribution $\Phi_2(\mathbf{y})$, symmetrical about the origin. As noted in Section 1.4.2, the probability of failure is given by the integral of $\Phi_2(\mathbf{y})$ over the transformed failure region $g(\mathbf{Y}) < 0$, shown part shaded. This can be obtained from the results for the standardized bivariate Normal given in Appendices A and C. It is given more directly, however, by integrating in the direction v $(-\infty < v < +\infty)$, shown in Figure 4.2, to obtain the marginal distribution (Figure 4.3).

By well-known properties of the bivariate Normal distribution the marginal distribution is also Normal, and hence the shaded area in Figure 4.3 represents the failure probability $p_f = \Phi(-\beta)$, where β is as shown (note that $\sigma = 1$ in the β direction since the normalized $\mathbf{y}$ space is being used). The direct correspondence between Figure 4.3 and Figure 1.11 should be noted.

The distance β shown in Figure 4.2 is perpendicular to the v axis and hence is perpendicular to $g(\mathbf{y}) = 0$. It clearly corresponds to the shortest distance from the origin in the $\mathbf{y}$ space to the limit state surface $g(\mathbf{y}) = 0$.

More generally, there will be many basic random variables $\mathbf{X} = \{X_i\}$, $i = 1, \ldots, n$, describing a structural reliability problem. In the case of complex structures, n could be very large indeed. Evidently this will create a problem for integration methods (see Chapter 3). However, this 'curse of dimensionality' is not so critical for the First-Order Second-Moment method since the concepts described above carry over directly to an n-dimensional standardized Normal space $\mathbf{y}$ with a (hyper-)plane limit state. In this case the shortest distance and hence the safety index is given by:

$$\beta = \min\left(\sum_{i=1}^{n} y_i^2 \right)^{1/2} = \min\left(\mathbf{y}^T \cdot \mathbf{y} \right)^{1/2}$$

$$\text{subject to} \quad g(\mathbf{y}) = 0 \tag{4.4}$$

where the y_i represent the coordinates of any point on the limit state surface.

The particular point for which (4.4) is satisfied, i.e. the point on the limit state surface perpendicular to β, in n-dimensional space, is variously called the 'checking' or 'design' point $\mathbf{y}^*$. Evidently this point is the projection of the origin on the limit state surface. It should be obvious from Figures 4.2 and 4.3 that the greatest contribution to the total probability content in the failure region is that made by the probability content in the zone close to $\mathbf{y}^*$. Further, as earlier foreshadowed, $\mathbf{y}^*$ represents the point of greatest

probability density or the point of 'maximum likelihood' on the very edge of the failure domain. This observation was used already in Chapter 3 and is particularly important for the various discussions to follow in the present chapter and in Chapters 5 and 11.

Note that $\mathbf{y}^*$ also is known as the 'most probable point' MPP. In addition, strictly speaking, $\mathbf{y}^*$ should be referred to as a 'checking' point since what is being performed here is essentially a safety checking analysis. There is no design involved, and thus the nomenclature 'design point' is misleading.

A direct relationship between the checking point $\mathbf{y}^*$ and β can be established as follows. From the geometry of surfaces [e.g. Sokolnikoff and Redheffer, 1958] the outward normal vector to a hyperplane given by $g(\mathbf{y}) = 0$, has components given by

$$c_i = \lambda \frac{\partial g}{\partial y_i} \tag{4.5a}$$

where λ is an arbitrary constant. The total length of the outward normal is

$$l = \left(\sum_i c_i^2 \right)^{1/2} \tag{4.5b}$$

and the direction cosines α_i of the unit outward normal are then

$$\alpha_i = \frac{c_i}{l} \tag{4.5c}$$

With α_i, known, it follows that the coordinates of the checking point are

$$y_i^* = y_i = -\alpha_i \, \beta \tag{4.6}$$

where the negative sign arises because the α_i are components of the outward normal as defined in conventional mathematical notation [i.e. positive with increasing g( )]. Figure 4.2 shows the geometry for the two-dimensional case $\mathbf{y} = (y_1, y_2)$.

For a linear limit state function (i.e. a hyperplane in $\mathbf{y}$ space) the direction cosines α_i do not change with position along the limit state function, so that it is easy to find a set of co-ordinates y^* satisfying both equation (4.4) and equation (4.6). This will be demonstrated in Example 4.3.

The equation for the hyperplane $g(\mathbf{y}) = 0$ can be written as

$$g(\mathbf{y}) = \beta + \sum_{i=1}^{n} \alpha_i y_i = 0 \tag{4.7}$$

The validity of (4.7) can be verified by applying (4.5); it can be deduced also directly from Figure 4.2 for the two-dimensional case.

The linear function in $\mathbf{X}$ space corresponding to (4.7) is obtained by applying (4.3)

$$G(\mathbf{x}) = \beta - \sum_{i=1}^{n} \frac{\alpha_i}{\sigma_{X_i}} \mu_{X_i} + \sum_{i=1}^{n} \frac{\alpha_i}{\sigma_{X_i}} x_i \tag{4.8a}$$

or

$$G(\mathbf{x}) = b_0 + \sum_{i=1}^{n} b_i x_i \tag{4.8b}$$

which is again a linear function. Also, β can be determined directly from the coordinates of the checking point y^* using (4.7):

$$\beta = -\sum_{i=1}^{n} y_i^* \alpha_i = -\mathbf{y}^{*T} \alpha \tag{4.9}$$

Example 4.2 For a linear limit state function, $Z(\mathbf{X}) = G(\mathbf{X})$, such as given by (4.8b), β may be estimated in $\mathbf{x}$ space using (4.1) and (4.8a):

$$\mu_G = b_0 + \sum_{i=1}^{n} b_i \mu_{X_i} = \beta$$

and

$$\sigma_G = \left(\sum_{i=1}^{n} b_i^2 \sigma_{X_i}^2 \right)^{1/2} = \left(\sum_{i=1}^{n} \left(\frac{\alpha_i}{\sigma_{X_i}} \right)^2 \sigma_{X_i}^2 \right)^{1/2} = 1$$

so that $\beta_{\mathbf{X}} = \mu_G / \sigma_G = \beta$. Using (4.7) it follows easily that $\mu_g = \mu_G = \beta$ and $\sigma_g = \sigma_G = 1$. Hence β does not depend on the space used. This independence is true if (and only if) $G(\mathbf{X})$ is a linear function. The safety index β derived in this manner is sometimes referred to as the 'geometric' safety index, for obvious reasons.

4.3.3 Sensitivity Factors and Gradient Projection

The direction cosines α_i given by (4.5c) represent the sensitivity of the standardized limit state function $g(\mathbf{y})$ at $\mathbf{y}^*$ to changes in $\mathbf{y}$ [Hohenbichler and Rackwitz, 1986a; Bjerager and Krenk, 1989]. This sensitivity has an important practical implication. Thus if the sensitivity α_i to y_i, say, is low there is little need to be very accurate about the determination of y_i. Also it would signal that, if necessary, y_i might well be treated as a deterministic rather than a random variable. This reduces the dimensionality of the space of random variables.

The corresponding expressions in the original $\mathbf{x}$ space, for $\mathbf{X}$ independent, are obtained by using (4.3) in (4.5a):

$$c_i = \lambda \sigma_i \frac{\partial G}{\partial x_i} \tag{4.10}$$

with (4.5b) and (4.5c) as before. For those X_i that are not independent, the direction cosines α_i have no direct physical meaning. This is because of the transformation to independent standardized $\mathbf{y}$ space, even if the $\mathbf{X}$ are (partly) dependent.

Expression (4.10) shows that the c_i are components of what can be considered to be the 'gradient' of the function G at the limit state surface $G = 0$. For this reason, the minimization in (4.10) is sometimes referred to as the 'gradient projection method' for finding the checking point $\mathbf{y}^*$ and hence the minimum distance β in standard Normal space.

The idea of sensitivity factors can be extended also to so-called 'omission sensitivity', that is, the effect on β when a random variable is replaced by a deterministic number [Madsen, 1988; Madsen and Egeland, 1989] and to the converse, when a deterministic number is replaced by a random variable, so-called 'ignorance sensitivity' [Der Kiureghian et al., 1994; Maes, 1996].

@Seismicisolation
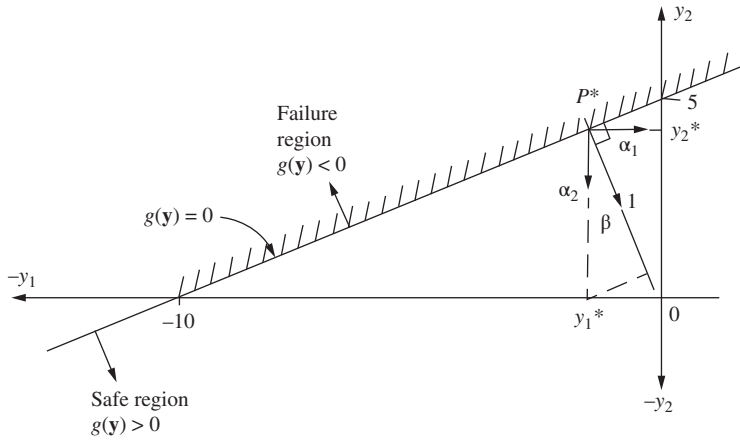
Figure 4.4 Linear limit state function in two-dimensional **y** space.

Example 4.3 Consider a limit state function $g(\mathbf{y})$ in two-dimensional Normal space $\mathbf{y} = (y_1, y_2)$ given by $g(\mathbf{y}) = y_1 - 2y_2 + 10 = 0$. This meets the requirement that $g(\mathbf{y}) > 0$ for the safe state and $g(\mathbf{y}) < 0$ for the failure state. The limit state is shown in Figure 4.4. Evidently, the checking point is point P^*, which is the projection of the origin onto $g(\mathbf{y}) = 0$, with perpendicular OP^*. It follows from (4.5) that:

$$c_1 = \lambda \frac{\partial g}{\partial y_1} = \lambda(1) = \lambda$$

$$c_2 = \lambda(-2) = -2\lambda$$

$$l = \left[\lambda^2 + (-2\lambda)^2\right]^{1/2} = \sqrt{5}\,\lambda$$

so that $\alpha_1 = 1/\sqrt{5}$ and $\alpha_2 = -2/\sqrt{5}$. These direction cosines (sensitivity factors) are valid anywhere along the linear limit state function (see Figure 4.4). They represent the normal to the limit state function surface. Note again that the direction of the normal is governed by the definition of $g(\mathbf{y}) = 0$ and the mathematics of planar surfaces.

The checking point $\mathbf{y}^*$ is now given by (4.6) as $\mathbf{y}^* = \left(-\beta/\sqrt{5},\ 2\beta/\sqrt{5}\right)$. Also $\mathbf{y}^*$ must satisfy $g(\mathbf{y}^*) = 0$, so that

$$-\frac{\beta}{\sqrt{5}} - 2\left(\frac{2\beta}{\sqrt{5}}\right) + 10 = 0$$

from which $\beta = 2\sqrt{5}$, as is easily verified on Figure 4.4. Also, it is clear from Figure 4.4, expression (4.6) and (α_1, α_2) that changes to y_2 have greater impact on β than do changes to y_1. For this special linear problem, of course, it would have been just as correct simply to put $\beta = \mu_g/\sigma_g = [(0) - (2)(0) + 10]/[1^2 + (2)^2(1)^2]^{1/2} = 10/\sqrt{5} = 2\sqrt{5}$.

4.3.4 Non-Linear Limit State Function—General Case

As was noted in Section 4.2, when the limit state function is non-linear, the first two moments of $G(\mathbf{X})$ in **x** space, and therefore the first two moments of $g(\mathbf{Y})$ in **y** space, can

no longer be obtained exactly. This is because non-linear combination of the implicit (standardized) Normal distributions does not lead to a Normal distribution for $G(\mathbf{X})$ or $g(\mathbf{Y})$ (see Appendix A). The approach suggested in Section 4.2 was to linearize $G(\mathbf{X})$ using (A.178) and (A.179) even though β then depends on the choice of the linearization or expansion point used in the Taylor series expansion, as was shown in Example 4.1.

It was noted in Section 4.3.2 that the 'checking point' in $\mathbf{y}$ space (e.g. point $\mathbf{y}^*$ in Figure 4.2) represents the point of greatest probability density or maximum likelihood (i.e. the most probable point MPP) and that it makes the most significant contribution to the nominal failure probability p_{fN} $[= \Phi(-\beta)]$. It is, therefore, an intuitively appealing linearization point. Indeed this was shown already in Figure 4.2.

The concepts and method used for the case of a linear limit state equation can be used also when $g(\mathbf{Y})$ is non-linear. Again the shortest distance β from the origin to $\mathbf{y}^*$ must be found, subject to $g(\mathbf{y}^*) = 0$. How well a linear limit state function $g(\mathbf{y}) = 0$ approximates a non-linear function $g(\mathbf{Y})$ in terms of the nominal probability p_{fN} of failure depends on the shape of $g(\mathbf{y}) = 0$; if it is concave towards the origin, p_{fN} is underestimated by the hyperplane approximation. Similarly, a convex function implies overestimation, as evident in Figure 4.2.

In most cases the point $\mathbf{y}^*$ is not known a priori and must be determined to estimate β. It should be clear from the above that the problem of finding β is equivalent to finding the shortest distance from the origin to $\mathbf{y}^*$ in $\mathbf{y}$ space, subject to $g(\mathbf{y}) = 0$ and that this is strictly a minimization problem [Flint et al., 1981; Shinozuka, 1983]. There are several ways in which a solution may be found; the classical calculus of variations method will be considered in this section. Its application reveals some useful properties.

The minimization problem (4.4) is subject to the constraint $g(\mathbf{y}) = 0$. Introducing a Lagrangian multiplier λ, the problem becomes:

$$\min(\Delta) = \left(\mathbf{y}^T \cdot \mathbf{y} \right)^{1/2} + \lambda g(\mathbf{y}) \tag{4.11}$$

For a stationary point, $\partial\Delta/\partial y_i = 0$ for all i, and $\partial\Delta/\partial\lambda = 0$:

$$\frac{\partial\Delta}{\partial y_1} = y_1 \left(\mathbf{y}^T \cdot \mathbf{y} \right)^{-1/2} + \lambda \frac{\partial g}{\partial y_1} = 0$$

$$\frac{\partial\Delta}{\partial y_2} = y_2 \left(\mathbf{y}^T \cdot \mathbf{y} \right)^{-1/2} + \lambda \frac{\partial g}{\partial y_2} = 0, \tag{4.12}$$

$$\text{and } \frac{\partial\Delta}{\partial\lambda} = g(\mathbf{y}) = 0$$

which may be written compactly as:

$$0 = \delta^{-1}\mathbf{y} + \lambda \mathbf{g}_Y \tag{4.13a}$$

$$0 = g(\mathbf{y}) \tag{4.13b}$$

where $\mathbf{g}_Y = \left(\partial g/\partial y_1, \partial g/\partial y_2, \dots \right)$ and the distance $\delta[cf.\ (4.4)]$ is given by $\delta = \left(\mathbf{y}^T \cdot \mathbf{y} \right)^{1/2}$. Expression (4.13b) is satisfied by definition, and (4.13a) immediately produces the coordinates for the stationary point $\mathbf{y}^S$ as [Horne and Price, 1977]:

$$\mathbf{y}^S = -\lambda\ \mathbf{g}_Y \delta \tag{4.l4}$$

Whether the point represents a minimum, maximum or a 'saddle point' depends on the nature of $g(\mathbf{y}) = 0$. No general statement can be made, although for a given function $g(\mathbf{y}) = 0$ standard tests can be applied [e.g. Ditlevsen, 1981a, b]. If $g(\mathbf{y}) = 0$ is linear, or regular and convex towards the origin, the stationary point is clearly a minimum point [Lind, 1979]. Since many limit state functions depart only slightly from linearity, it is assumed in what follows in this section that the vector $\mathbf{y}^S$ does indeed locate the minimum point.

Let the minimum distance δ corresponding to $\mathbf{y}^S$ be δ^S. Substituting (4.14) into (4.4) with $\mathbf{y}^S$ replacing $\mathbf{y}$ and δ^S replacing β, it is easily shown that $\lambda = \pm\left(\mathbf{g}_Y^T \cdot \mathbf{g}_Y\right)^{-1/2}$ and hence, from (4.14), that

$$\delta^S = \frac{-\left(\mathbf{y}^S\right)^T \cdot \mathbf{g}_y}{\left(\mathbf{g}_Y^T \cdot \mathbf{g}_Y\right)^{1/2}} = \frac{-\sum_{i=1}^{n} y_i^S \left(\partial g/\partial y_i\right)}{\left[\sum_{i=1}^{n} \left(\partial g/\partial y_i\right)^2\right]^{1/2}} \tag{4.15}$$

It will now be shown that δ^S is equal to β and that β is therefore the minimum distance from the origin to the limit state function $g(\mathbf{y}) = 0$, provided that β is measured to the checking point $\mathbf{y}^S = \mathbf{y}^*$ and that $g(\mathbf{y}) = 0$ is linearized at $\mathbf{y}^*$. Let the limit state function $g(\mathbf{y}) = 0$ be linearized at $\mathbf{y}^*$ by means of a Taylor series expansion (i.e. in first-order terms only). This approximation provides a tangent (hyper-)plane $g_L(\mathbf{y}) = 0$ to the function $g(\mathbf{y}) = 0$ at $\mathbf{y}^*$:

$$g_L(\mathbf{y}) \approx g(\mathbf{y}^*) + \sum_{i=1}^{n} \left(y_i - y_i^*\right)\frac{\partial g}{\partial y_i} = 0 \tag{4.16}$$

Since $\mathbf{y}^*$ is on the limit state, the term $g(\mathbf{y}^*) = 0$. Further, using rules (A.160) and (A.161) for addition of first- and second-moment functions and remembering that $\mu_{Y_i} = 0$, $\sigma_{Y_i} = 1$ it follows that

$$\mu_{g_L}(\mathbf{y}) = -\sum_{i=1}^{n} y_i^* \frac{\partial g}{\partial y_i} = -\mathbf{y}^{*T} \cdot \mathbf{g}_Y \tag{4.17}$$

and

$$\sigma_{g_L}^2(\mathbf{y}) = \sum_{i=1}^{n} \left(\frac{\partial g}{\partial y_i}\right)^2 = \mathbf{g}_Y^T \cdot \mathbf{g}_Y \tag{4.18}$$

Since $\beta = \mu_{G_L}/\sigma_{G_L}$ (see 4.1) it follows that:

$$\beta = \frac{\mu_{g_L}}{\sigma_{g_L}} = \frac{-\sum_{i=1}^{n} y_i^* \left(\partial g/\partial y_i\right)}{\left[\sum_{i=1}^{n} \left(\partial g/\partial y_i\right)^2\right]^{1/2}} = \frac{-\mathbf{y}^{*T} \cdot \mathbf{g}^Y}{\left(\mathbf{g}_Y^T \cdot \mathbf{g}_Y\right)^{1/2}} = -\mathbf{y}^{*T}\, \boldsymbol{\alpha} \tag{4.19}$$

which, noting (4.5), is identical to (4.9), as might be expected. It should be evident also that expression (4.19) is equivalent to δ^S, given by expression (4.15), if $\mathbf{y}^* = \mathbf{y}^S$. Hence

$\mathbf{y}^*$ is the point that minimizes the distance from the origin to the non-linear limit state function $g(\mathbf{y}) = 0$, and is also its expansion (linearization) point.

It follows immediately that once the point $\mathbf{y}^*$ has been located, the nonlinear limit state function may be replaced by its linearized equivalent and the method of Section 4.3.2 applied.

Finally, since β is the minimum distance from the origin of the rotationally symmetric standardized Normal probability density function $f_Y(\ )$ in $\mathbf{y}$ space, it is easily verified that $\mathbf{y}^*$ represents the point of maximum likelihood. This might be compared with the choice $\mathbf{x}^*$ in Section 3.4.2.

Example 4.4   For the two-dimensional problem of Figure 4.5, let the limit state function be

$$g(\mathbf{y}) = -\frac{4}{25}(y_1 - 1)^2 - y_2 + 4 = 0$$

The distance to be minimized is then $\delta = (y_1^2 + y_2^2)^{1/2}$ subject to $g(\mathbf{y}) = 0$. With λ denoting the Lagrangian multiplier, the modified function Δ is then [*cf.* (4.11)]

$$\min(\Delta) = (y_1^2 + y_2^2)^{1/2} + \lambda\left[-\frac{4}{25}(y_1 - 1)^2 - y_2 + 4\right]$$

for which

$$\frac{\partial\Delta}{\partial y_1} = y_1(y_1^2 + y_2^2)^{-1/2} - \lambda\frac{8}{25}(y_1 - 1) = 0 \tag{4.20a}$$

$$\frac{\partial\Delta}{\partial y_2} = y_2(y_1^2 + y_2^2)^{-1/2} - \lambda = 0 \tag{4.20b}$$

$$\frac{\partial\Delta}{\partial\lambda} = -\frac{4}{25}(y_1 - 1)^2 - y_2 + 4 = 0 \tag{4.20c}$$
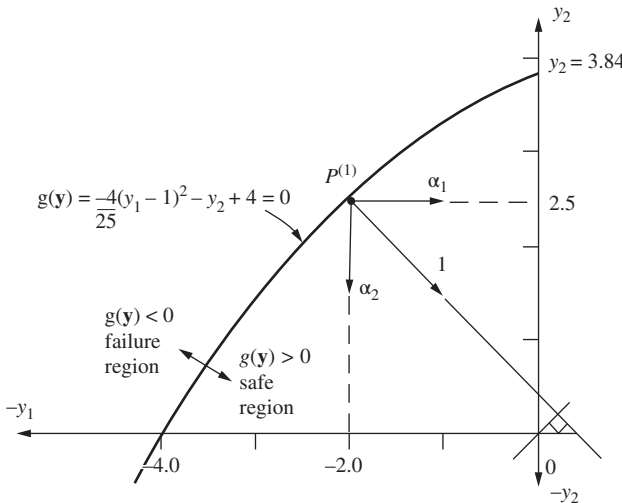
Figure 4.5 Non-linear limit state function in two-dimensional basic variable space [note point $P^{(1)}$ refers to Example 4.5].

Eliminating λ from (4.20a) and (4.20b) gives

$$y_2 = \frac{25y_1}{8\left(y_1 - 1\right)} \tag{4.20d}$$

which together with (4.20c) leaves, upon eliminating y_2,

$$-\frac{4}{25}\left(y_1 - 1\right)^2 + 4 = \frac{25y_1}{8\left(y_1 - 1\right)} \tag{4.20e}$$

This equation is cubic in y_1. A trial and error solution shows that $y_1 = 2.36$ satisfies (4.20e) and that $y_2 = +2.19$ from (4.20d). The safety index is then estimated as $\beta = \left(y_1^2 + y_2^2\right)^{1/2} = 3.22$, and the coordinates of the checking point are given by $\mathbf{y}^* = (-2.36, \ 2.19)^T$. It is readily verified that the checking (stationary) point does indeed give a minimum value of β.

For problems with a greater number of basic variables the solution of the system of simultaneous equations requires numerical evaluation. A more formal verification that the calculated β is a minimum is then desired.

4.3.5 Non-Linear Limit State Function—Numerical Solution

For some situations, principally those with a large number of basic variables or having complex limit state equations, a numerical approach may be preferred. When the constraint is linear, the problem of finding β, given by (4.4), is essentially a quadratic programming problem, for which efficient computer algorithms exist.

If the constraint $g\left(\mathbf{y}\right) = 0$ is not a linear function and a vector $\mathbf{y}^{(1)}$ can be found which satisfies $g\left(\mathbf{y}^{(1)}\right) = 0$, then there are some efficient algorithms available. In principle Lagrangian multipliers could be used to convert the problem into an unconstrained optimization problem as was done in the previous section and then solved by one of the many efficient algorithms available for this purpose. If a vector $\mathbf{y}^{(1)}$ to satisfy $g\left(\mathbf{y}^{(1)}\right) = 0$ cannot be found, the solution of (4.4) requires minimization under non-linear inequality constraints. Again, a range of algorithms is available for solution [e.g. Beveridge and Schechter, 1970; Schittkowski, 1980]. Alternatively, an iterative solution scheme can be considered, as described below. For obvious reasons it is also known sometimes as the 'modified' gradient projection method or the Hasofer-Lind-Rackwitz-Fiessler (HLRF) algorithm (*cf.* Section 4.3.3).

4.3.6 Non-Linear Limit State Function—HLRF Algorithm

The HLRF algorithm is an iterative solution scheme. First, a trial checking point $\mathbf{y}^{(1)}$ is chosen and equation (4.4) and the limit state expression checked. If $\mathbf{y}^{(1)}$ is poorly chosen, the condition of perpendicularity between the tangent (hyper-)plane at $\mathbf{y}^{(1)}$ and the β direction will not be satisfied. How a new trial checking point $\mathbf{y}^{(1)}$ should be chosen to converge eventually to the correct solution of (4.4) is now of interest.

Let $\mathbf{y}^{(m)}$ be the mth approximation to the vector representing the local perpendicular to $g\left(\mathbf{y}\right) = 0$ from the origin. A better approximation $\mathbf{y}^{(m+1)}$ is sought. The relationship between $\mathbf{y}^{(m+1)}$ and $\mathbf{y}^{(m)}$ can be obtained from a first-order Taylor series expansion of $g\left(\mathbf{y}^{(m+1)}\right) = 0$ about $\mathbf{y}^{(m)}$ (i.e. a linear approximation) [Hasofer and Lind, 1974]. Using

index notation,

$$g_L\left(y_1^{(m+1)},\ldots,y_n^{(m+1)}\right) \approx g\left(y_1^{(m)},\ldots,y_n^{(m)}\right)$$

$$+ \sum_{i=1}^{n}\left(y_i^{(m+1)} - y_i^{(m)}\right)\frac{\partial g\left(y_1^{(m)},\ldots,y_n^{(m)}\right)}{\partial y_i} = 0 \qquad (4.21)$$

or, in matrix notation (*cf.* 4.16),

$$g_L\left(\mathbf{y}^{(m+1)}\right) \approx g\left(\mathbf{y}^{(m)}\right) + \left(\mathbf{y}^{(m+1)} - \mathbf{y}^{(m)}\right)^T \cdot \mathbf{g}_Y = 0 \qquad (4.22)$$

This expression represents a hyperplane $g_L(\mathbf{y}) = 0$ approximating the hypersurface $g(\mathbf{y}) = 0$ in $\mathbf{y}$ space, for which, at point $m + 1$, the linearized limit state function must be satisfied, i.e. $g_L\left(\mathbf{y}^{(m+1)}\right) = 0$. However, for the earlier trial point $\mathbf{y}^{(m)}$ the direction cosines are $\alpha^{(m)}$ which together with the trial value of $\beta^{(m)}$ are given by (4.6):

$$y^{(m)} = -\alpha^{(m)}\beta^{(m)} \qquad (4.23)$$

in which, from (4.5)

$$\alpha^{(m)} = \frac{\mathbf{g}_Y^{(m)}}{l} \qquad (4.5c)$$

and

$$l = \left(\mathbf{g}_Y^{(m)T} \cdot \mathbf{g}_Y^{(m)}\right)^{1/2} \qquad (4.5b)$$

Substituting (4.23) for $\mathbf{y}^{(m)}$ in (4.22), using (4.5) and rearranging produces the following recurrence relationship:

$$\mathbf{y}^{(m+1)} = -\alpha^{(m)}\left[\beta^{(m)} + \frac{g\left(\mathbf{y}^{(m)}\right)}{l}\right] \qquad (4.24)$$

In practice the iteration proceeds by assuming a starting point $\mathbf{y}^{(1)}$, evaluating the gradients $\mathbf{g}_{Y_i} = \partial g\left(\mathbf{y}^{(m)}\right)/\partial y_i$ and also evaluating $\beta^{(m)} = \left[\sum_{i=1}^{n}\left(y_i^{(m)}\right)^2\right]^{1/2}$ and then substituting into (4.24) to obtain a new trial checking point and β estimate. This is continued until convergence on $y_i^{(m)}$ or β is reached.

Comparison of (4.24) and (4.6) shows the essential similarity between the procedures. It also shows that the term in the square brackets of (4.24) is essentially a correction term to allow for the fact that $g(\mathbf{y})$ is not zero.

In parallel to the discussion in Section 4.3, there is no guarantee that the repeated use of (4.24) does indeed converge to a minimum value of β; again either an appeal to intuition or a more formal check is required.

The above may be formalized to the following algorithm:

(a) Standardize basic random variables $\mathbf{X}$ to the independent standardized normal variables $\mathbf{Y}$, using (4.3) and Appendix B if necessary.

(b) Transform $G(\mathbf{x}) = 0$ to $g(\mathbf{y}) = 0$.
(c) Select initial checking point $(x^{(1)}, y^{(1)})$.
(d) Compute $\beta^{(1)} = \left[\mathbf{y}^{(1)^T} \cdot \mathbf{y}^{(1)} \right]^{1/2}$; let $m = 1$.
(e) Compute direction cosines $\alpha^{(m)}$ using (4.5).
(f) Compute $g(\mathbf{y}^{(m)})$.
(g) Compute $\mathbf{y}^{(m+1)}$ using (4.24).
(h) Compute $\beta^{(m+1)} = \left(\mathbf{y}^{(m+1)T} \cdot \mathbf{y}^{(m+1)} \right)^{1/2}$.
(i) Check whether $\mathbf{y}^{(m+1)}$ and/or $\beta^{(m+1)}$ have stabilized; if not go to (e) and increase m by unity.

This (the HLRF) algorithm has been programmed, sometimes using slightly different logic [Fiessler et al., 1976; Fiessler, 1979; Ellingwood et al., 1980].

It is possible to transform the recurrence relationship (4.24) into the space of the original variables $\mathbf{X}$; this has the advantage that transformation to the $\mathbf{y}$ space is not required. Substituting $x_i = y_i \sigma_{X_i} - \mu_{X_i}$ into equation (4.24) yields [Parkinson, 1980]

$$\mathbf{X}^{(m+1)} - \mu_{\mathbf{X}} = -\mathbf{C}\mathbf{G}_X^{(m)} \frac{\left(\mathbf{X}^{(m)} - \mu_{\mathbf{X}} \right)^T \cdot \mathbf{G}_X^{(m)}}{\mathbf{G}_X^{(m)T} \mathbf{C} \mathbf{G}_X^{(m)}} \tag{4.25}$$

where $\mathbf{G}_X^{(m)} = \left(\frac{\partial G}{\partial x_1}, \frac{\partial G}{\partial x_2}, \dots, \frac{\partial G}{\partial x_n} \right)^T \Big|_{x=\mu_x^{(m)}}$, $\mathbf{X}$ is the vector of random variables in the original x space, $\mu_{\mathbf{X}}$ is the vector of means and $\mathbf{C}$ is the covariance matrix for $\mathbf{X}$. (If the X_i are independent, $c_{ii} = \sigma_i^2, c_{ij} = 0$ for $i \neq j$; see Section A.11.1.)

Example 4.5   Example 4.4 will now be reworked, this time using the above algorithm. The geometry of the problem is shown in Figure 4.5.

Let the trial solution for the checking point be $P^{(1)}$ given by $\mathbf{y}^{(1)} = (-2.0, 2.5)^T$ which does not quite satisfy $g(\mathbf{y}) = 0$ (this would require $y_2^{(1)} = 2.56$, as is easily verified). Then

$$\frac{\partial g}{\partial y_1} = \frac{-4}{25} 2 (y_1 - 1) = \frac{24}{25} = +0.96 \quad \frac{\partial g}{\partial y_2} = -1 \quad \text{and} \quad \alpha_i = \frac{\partial g}{\partial y_1} \Big/ l$$

where

$$l = \left[(0.96)^2 + (-1)^2 \right]^{1/2} = 1.386$$
$$\beta = \left(y_1^2 + y_2^2 \right)^{1/2} = \left(2^2 + 2.5^2 \right)^{1/2} = 3.20$$
$$g(\mathbf{y}) = \frac{-4}{25}(-2 - 1)^2 - (2.5) + 4 = +0.06$$

so that

$$\begin{bmatrix} y_1 \\ y_2 \end{bmatrix}^{(2)} = \frac{-1}{1.386} \begin{bmatrix} +0.96 \\ -1 \end{bmatrix} \left(3.20 + \frac{+0.06}{1.386} \right) = \begin{bmatrix} -2.22 \\ 2.309 \end{bmatrix}$$

which, with two iterations, will converge closely to the results given in Example 4.4.

@Seismicisolation
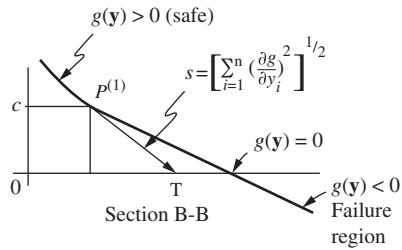
Figure 4.6 One cycle of iterative solution scheme.

4.3.7 Geometric Interpretation of Iterative Solution Scheme

The iteration scheme has its limitations. Expression (4.24) can be written as

$$\mathbf{y}^{(m+1)} = -\alpha^{(m)}\beta^{(m+1)} \tag{4.26}$$

where $\beta^{(m+1)}$ denotes the term [ ] in (4.24) and consists of $\beta^{(m)}$ plus a correction term, and $\alpha^{(m)}$ is a vector.

Consider now the two-dimensional space $\mathbf{y} = (y_1, y_2)$ shown in Figure 4.6 [after Fiessler, 1979], with the limit state surface as shown, together with a contour $g(\mathbf{y}) = c$ in the safe domain. Assume that the initial trial $\mathbf{y}^{(1)}$ values are given by point $P^{(1)}$, for which $\beta = \beta^{(1)}$. The linear approximation to $g(y)$ at $P^{(1)}$ is given by line AA. The direction cosines α_i evaluated at $P^{(1)}$ give the direction of the vector $(P^{(1)}, T)$ normal to AA; the gradient $\partial g / \partial \mathbf{y}$ gives the slope in the direction of the vector, as shown by section BB. The true slope of the vector $(P^{(1)}, T)$ is given by

$$S = \left[\sum_{i=1}^{n} \left(\frac{\partial g}{\partial y_i} \right)^2 \right]^{1/2}$$

and hence the horizontal projection in section BB is given by c/S, which is the second (i.e. the correction) term in [ ] in equation (4.24). This term then gives the vector length $\beta^{(1)} + P^{(1)}T$ and multiplication by $\alpha_i^{(1)}$ fixes the new trial $y^{(2)}$ as OU parallel to $(P^{(1)}, T)$ in Figure 4.6.

The iteration procedure of the HLRF algorithm can fail in certain circumstances. One case is illustrated in Figure 4.7. For a highly non-linear limit state function it is possible to alternate between successive approximation points i and $i + 1$ [Fiessler, 1979]. Thus, starting at $P^{(1)}$, the local gradient perpendicular to the tangent AA at $g(\mathbf{y}^{(1)}) = c_2$ leads to point T (given by $g(\mathbf{y}) = 0$). The new checking point U is then defined by the parallel TU to AA and the perpendicular $\beta^{(2)}$ from O. This is point $P^{(2)} \equiv U$. However, for the situation shown, starting at $P^{(2)}$ for the next iteration, the new point $P^{(3)}$ is found to be at $P^{(1)}$. Obviously a breakdown situation exists because of the non-linear nature of
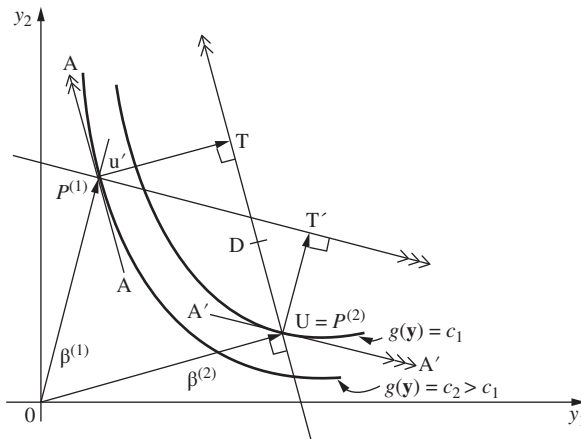
Figure 4.7 Breakdown of iteration through oscillation.

$g(\mathbf{y}) = 0$. The difficulty is easily overcome. Rather than selecting $P^{(2)}$ on TU at U, some lesser correction, such as point D, might be chosen for $\beta^{(2)}$.

A second breakdown case is when the trial checking point lies close to a stationary point which is not a minimum. As noted in Section 4.3.6, the iteration procedure can only search for local stationary points and cannot distinguish between maxima, minima or saddle points [Ditlevsen and Madsen, 1980]. The problem can only be overcome by selecting different starting points and common sense appraisal of results.

The HLRF algorithm iteration procedure above can also break down when the transformation to standardized Normal space is strongly non-linear, and/or when the failure domain vanishes. Examples of this, also involving bounded uniform variables, and comparison to other algorithms for finding the checking point, are available [Beck and Silva Jr., 2016].

4.3.8 Interpretation of First-Order Second-Moment (FOSM) Theory

When the limit state function is non-linear the theory discussed so far is 'first-order' in the sense that a linear approximation for the limit state function is used to estimate the failure probability. This involved using the probability content of the failure region near the (single) 'checking' point as the best estimate. This approach is sometimes referred to as a 'single-check-point' method.

Unfortunately, an ambiguity of interpretation of the probability represented by the safety index β can arise when the limit state function is nonlinear (see Figure 4.8). For the linear limit state bb, containing P_1 as checking point, the failure probability for normal variables is given exactly by $p_f = \Phi(-\beta)$. However, the point P_1 is also the checking point for the non-linear limit state functions aa and cc. In terms of first-order theory, each of these limit states has an identical value of β, and hence an identical nominal failure probability $P_{fN} = \Phi(-\beta)$; yet it is quite clear from Figure 4.8 that the actual probability contents of the respective failure regions are not identical. Similarly, the limit state dd represents what is probably a lower failure probability still; yet its safety index β_1 is less than β. Evidently β as defined so far lacks a sense

Figure 4.8 Inconsistency between β and p_{fN} for different forms of limit state functions.
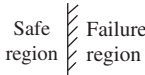
of 'comparativeness' or an 'ordering property' with respect to the implied probability content for non-linear limit states [Ditlevsen, 1979a].

A further point is that no limitation has been placed on the direction of β in **y** space so that, for some other checking point P_2, the probability content for the linear limit state ee should be identical with that implied for the linear limit state bb when both limit states are at the same distance β from the origin.

A measure of comparativeness can be introduced by defining a formal probability density function $f_Y(y)$ in the reduced variable space. The probability content associated with each limit state can then be calculated formally and compared. It is not difficult to see that such a formal density function must give greater reliability (i.e. lower probability of failure) with greater values of β. This means that it must allow for the shape of the limit state function. It also means that it must be rotationally symmetric, i.e. independent of θ. It appears that the only function that can satisfy all requirements is the n-dimensional standardized Normal density function with independent variables:

$$\phi_n(\mathbf{y}) = \prod_{i=1}^{n} \left[\frac{1}{(2\pi)^{1/2}} \exp\left(-\frac{1}{2} y_i^2 \right) \right] \tag{4.27}$$

The safety index β associated with a given limit state (hyper-)surface with safe domain D_k, say, is then obtained by integrating $\phi_n(\mathbf{y})$ over the domain D_k to give the β value for the safe state as:

$$\Phi\left[\beta(k)\right] = \int_{D_k} \phi_n(\mathbf{y}) \, d\mathbf{y} \tag{4.28}$$

where $\Phi(\ )$ is the standardized Normal distribution function. It follows that

$$\beta(k) = \Phi^{-1} \int_{D_k} \phi_n(\mathbf{y}) \, d\mathbf{y} \tag{4.29}$$

is a more general definition of the safety index, now a function of the shape of the limit state function for safe domain D_k. As known from Chapter 3, the calculation of the integral (4.29) generally is not straightforward, owing to the nature of the shape of the domain D_k of integration. Some specific cases are considered below.

4.3.9 General Limit State Functions—Probability Bounds

So far attention has been focussed on a single limit state function – one that is a linear function or one that does not depart significantly from linearity, at least in the original **X** space. While such limit state functions are common in many practical problems, it is appropriate to consider what will happen once the limit state function becomes highly non-linear or becomes a piecewise function or (equivalently) there are a number of (linear) limit states governing the problem. It is appropriate to do this by focussing, conceptually mainly at this time, on bounds to the probability estimate.

To allow the development of bounds on p_f consider the ϕ_n in expression (4.29). It is the n-dimensional standardized Normal density function. Then, p_f will be a function of $\beta(k)$ for a given non-linear limit state function k: $g(\mathbf{y}) = 0$.

If the limit state function $g(\mathbf{y}) = 0$ is linear, and **y** is n-dimensional standard Normal, it follows directly from Section 4.3.2 that $p_f = \Phi(-\beta)$. If $g(\mathbf{y}) = 0$ is convex to the origin this result is a lower bound on p_f. If $g(\mathbf{y}) = 0$ is concave to the origin it is an upper bound on p_f. This last case can be illustrated as follows.

Recall that β in the standardized Normal variable space **y** of FOSM theory measures the distance to the point on the limit state function closest to the origin. Then an upper bound on p_f is given by the probability content outside a (hyper-)spherical limit state function with radius β, centred at the origin of **y** space:

$$g(\mathbf{y}) = \beta^2 - \sum_{i=1}^{n} y_i^2 = 0 \tag{4.30}$$

Since the Y_i are Normal distributed and independent, $\sum_{i=1}^{n} y_i^2$ has a chi-squared distribution χ_n with n degrees of freedom (see Section A.5.6) [Benjamin and Cornell, 1970]. The probability of failure is then $p_f = 1 - \chi_n(\beta^2)$, which is shown in Figure 4.9 as a function of n [Lind, 1977]. When $n = 1$ the probability content is twice that given by a single linear limit state surface, as is readily verified.

A number of more complex approximations for general limit state functions have been proposed; these include the use of piecewise spherical sectors [Veneziano, 1974], the use of quadratic expressions centred about the checking point [Fiessler et al., 1979; Horne and Price, 1977] and the use of (linear) tangents at various predefined locations on $g(\mathbf{y}) = 0$ (the so-called 'polyhedral approximation') [Ditlevsen, 1997b]. For obvious reasons, these methods are also known as 'multiple-check-point methods'. Piecewise linear limit state functions may be evaluated using the system bounds and other methods to be discussed in Chapter 5.

4.4 The First-Order Reliability (FOR) Method

4.4.1 Simple Transformations

In the discussion so far, only the first two moments of each random variable have been considered in the calculation of the failure probability. However, if information about probability distributions is available for some or all of the basic variables it would be sensible to incorporate it in the reliability analysis if possible. One way of doing this is to transform non-Normal distributions into equivalent Normal distributions
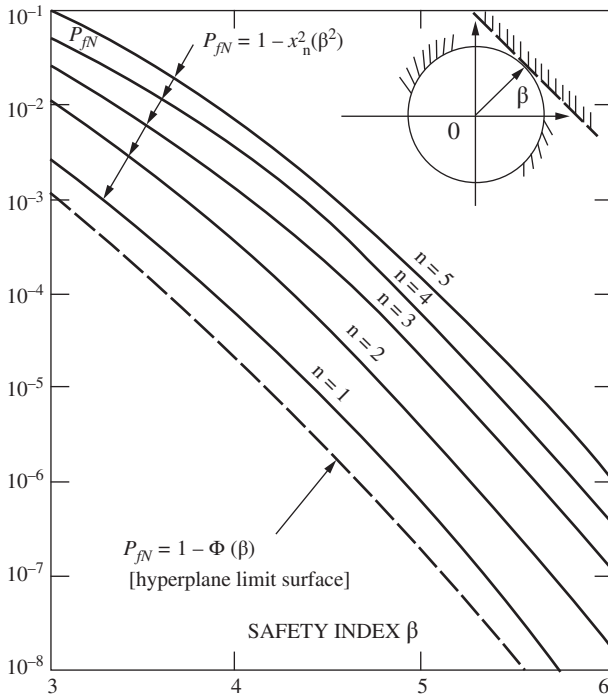
Figure 4.9 Safety index β and p_{fN} for hyperspherical limit state surface.

[Paloheimo and Hannus, 1974]. For example, if the random variable X has a Lognormal distribution with mean μ_X and variance σ_X^2, the transformation to an equivalent variable U is given by $U = \ln X$, with $\mu_U \approx \ln \mu_X$ and $\sigma_U^2 \approx V_X^2$ for $V_X < 0.3$ where V_X is the coefficient of variation (see A 5.9). If U is then converted to the standardized Normal random variable Y, then $Y = (U - \mu_U)/\sigma_U$. This may be approximated by $Y = [\ln (X/\mu_X)]/V_X$. It follows that the original variable X can be represented in terms of the standard Normal variable Y and the first two moments μ_x and $\sigma_x = \mu_x V_x$ as $X \approx \mu_X \exp (Y V_X)$. This can be done for other non-Normal random variables as well.

Evidently, if the random variables are transformed, the limit state function $G(\mathbf{X}) = 0$ also must be transformed to the **y** space. Usually the transformation yields a non-linear $g(\mathbf{y}) = 0$ function.

In general the transformation from non-Normal distributed variables to equivalent standardized Normal variables is not as elementary as suggested so far. However, once it has been done the resulting Normal equivalents can be used directly in second-moment calculation procedures.

In the next section a general approach for transforming independent non-Normal basic variables to equivalent Normal variables will be described. It will be seen that the transformation is best made about the 'checking point' already introduced in FOSM theory. Additional requirements for dealing with dependent variables will then be described. The algorithm for the transformation method is outlined also and an example is given.

Historically the transformation approach was developed as an extension of the FOSM method, and is therefore still sometimes called the 'advanced' or 'extended' FOSM method. It is better to adopt the term First Order Reliability (FOR) method (or sometimes called FORM), since limit state functions are still linearized (hence of 'first order'), but probability distributions are no longer approximated only by their first and second moments.

Exercise   Show that if X has an extreme type I distribution, it can be given in terms of the standardized Normal random variable Y as

$$x = \frac{-\ln\left\{-\ln\left[\Phi\left(y\right)\right]\right\} - 0.5772}{1.2825}\sigma_x + \mu_x$$

4.4.2   The Normal Tail Transformation

The transformation of an independent basic random variable X of non-Normal distribution to an equivalent standardized Normal distributed random variable Y is shown schematically in Figure 4.10 and mathematically can be expressed as

$$p = F_X\left(x\right) = \Phi\left(y\right) \quad \text{or} \quad y = \Phi^{-1}\left[F_X\left(x\right)\right] \tag{4.31}$$

where p is some probability content associated with $X = x$, and hence with $Y = y$; $F_X(\ )$ is the marginal cumulative distribution function of X and $\Phi(\ )$ is the cumulative distribution function for the standardized Normal random variable Y. The transformation is shown by the lines abcde in Figure 4.11.

As in the previous section, an equivalent Normal variable U with cumulative distribution function $F_U(\ )$ might be introduced to represent X; (see Figure 4.11). Evidently, many choices for U can be made, depending on the selection of μ_U and σ_U. What constitutes an appropriate choice will now be discussed. Consider the first-order Taylor series expansion of (4.31) about some point x^e:

$$y \approx \Phi^{-1}\left[F_X\left(x^e\right)\right] + \frac{\partial}{\partial x}\left\{\Phi^{-1}\left[F_X\left(x\right)\right]\right\}\Big|_{x^e}\left(x - x^e\right) \tag{4.32}$$

By letting $\Phi^{-1}\left[F_X\left(x\right)\right] = T$ it can be shown that the term $(\partial/\partial x)\{\}$ in (4.32) is given by

$$\frac{\partial}{\partial x}\{\ \} = \frac{\partial T}{\partial x} = \frac{f_X\left(x\right)}{\phi\left(T\right)} = \frac{f_X\left(x\right)}{\phi\left\{\Phi^{-1}\left[F_X\left(x\right)\right]\right\}} \tag{4.33}$$
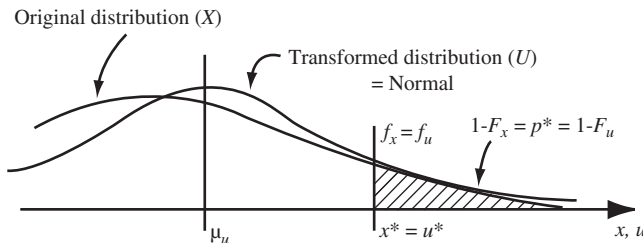
Figure 4.10 Original and transformed probability density functions.
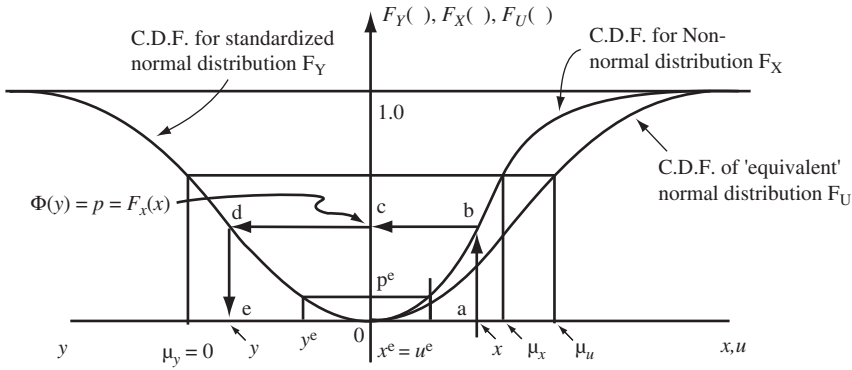
Figure 4.11 Relationships between original non-Normal X, standardized Normal Y and equivalent Normal U cumulative distribution functions.

Upon substituting (4.33) into (4.31) and rearranging, it follows that

$$y \approx \frac{x - \left\{ x^e - \Phi^{-1}\left[F_X\left(x^e\right)\right] \phi\left\{\Phi^{-1}\left[F_X\left(x^e\right)\right]\right\} / f_X\left(x^e\right)\right\}}{\phi\left\{\Phi^{-1}\left[F_X\left(x^e\right)\right]\right\} / f_X\left(x^e\right)} \tag{4.34}$$

which may be written as

$$y = \frac{u - \mu_U}{\sigma_U} \tag{4.35}$$

if

$$u = x \tag{4.36}$$

with

$$\mu_U = x^e - y^e \sigma_U \tag{4.37}$$

$$\sigma_U = \frac{\phi\left(y^e\right)}{f_X\left(x^e\right)} \tag{4.38}$$

and

$$y^e = \Phi^{-1}\left[F_X\left(x^e\right)\right] \tag{4.39}$$

This shows that it is possible to express the transformation (4.31) in terms of a new random variable U, Normal distributed, with mean μ_U and standard deviation σ_U given by (4.37) and (4.38) above. Using (4.31), (4.35) and (4.36) it follows easily that $F_X\left(x^e\right) = F_U\left(x^e\right)$ and using (4.38) with (4.35), (4.36) and (A.146) that $f_X\left(x^e\right) = f_U\left(x^e\right)$. Thus the probability density and the cumulative distribution function (i.e. the tail probability) for the equivalent Normal random variable U should both be set equal to those of the original non-Normal random variable X. This is shown in Figures 4.10 and 4.11. It is the so-called 'Normal tail approximation' [Ditlevsen, 1981a]. It may be carried out for each random variable X_i separately, provided that the expansion point $\mathbf{x}^e$ is known.

The fact that the expansion point $\mathbf{x}^e$ is identical with the checking point $\mathbf{x}^*$ is shown as follows. Since $\beta = \min(\mathbf{y}^T \cdot \mathbf{y})^{1/2}$ from (4.4) and since each component of $\mathbf{y}$ is given by (4.31), it follows that β is a function of the location of the expansion point $\mathbf{x}^e$. For β to be stationary, it is necessary that

$$0 = \frac{\partial \beta}{\partial x_i^e} = \frac{\partial}{\partial x_i^e} \left\{ \sum_{i=1}^{n} \left[y_i \left(x_i^e \right) \right]^2 \right\}^{1/2} \quad \text{for all } i \tag{4.40}$$

Noting that the Y_i are independent, it is convenient to drop the subscript from y_i, x_i and x_i^e. Hence (4.40) becomes

$$0 = \frac{1}{\beta} y \left(x^e \right) \frac{\partial y \left(x^e \right)}{\partial x^e}$$

from which $\partial y \left(x^e \right) \ \partial x^e = 0$ since, in general, $y \left(x^e \right) \neq 0$. Using $\mathbf{y}$ obtained from expression (4.32) and differentiating by parts,

$$0 = \frac{\partial y \left(\right)}{\partial x^e} = \frac{\partial}{\partial x^e} \left\{ \Phi^{-1} \left[F_X \left(x^e \right) \right] \right\} + \frac{\partial^2}{\partial (x^e)^2} \left\{ \Phi^{-1} \left[F_X \left(x \right) \right] \right\} \left(x - x^e \right)$$
$$- \frac{\partial}{\partial x^e} \left\{ \Phi^{-1} \left[F_X \left(x \right) \right] \right\} \tag{4.41}$$

Since generally neither the first nor the second derivative terms are zero, it follows that, for β to be a stationary value, it is necessary that $\mathbf{x} = \mathbf{x}^e$. It was shown in Section 4.3.4 that a stationary value of β is achieved if $\mathbf{x} = \mathbf{x}^*$ (the 'checking point') so that the expansion point considered thus far is identical with the checking point; $\mathbf{x}^e = \mathbf{x}^*$ [*cf.* Lind, 1977].

Because each non-Normal random variable is individually approximated by a Normal distribution at the checking point, the latter may not correspond exactly to the point of maximum joint probability density [Horne and Price, 1977]. Any resulting error in β or p_f, is thought to be small.

Refinements to the above approach, and which appear to improve computational efficiency, have been suggested [e.g. Chen and Lind, 1983; Tichy, 1994]. One approach is to relax the relationships (4.37) and (4.38) and introduce the additional requirement that the slopes of the probability density functions at the design point must be the same. It is evident that, provided that the approximating distributions are valid probability distributions, there is scope for a variety of Normal tail approximations.

The above considerations immediately suggest an iterative procedure for finding the checking point $\mathbf{x}^*$ and hence the safety index β [Rackwitz and Fiessler, 1978]. In practical problems the basic variables may not be independent, as assumed so far. Attention will be given in the next section to transformations from dependent to independent random variables. Once this has been done the iterative procedure will be considered in detail.

4.4.3   Transformations to Independent Normal Basic Variables

The simple 'Normal tail' approximation described above is a useful introduction to more general transformations. If the joint probability density function $f_X(\mathbf{x})$ is completely

described, the notion of the Normal tail approximation can be extended to more than one dimension, and hence to obtain a set of independent Normal random variables that may then be used with FOSM reliability estimation methods. This approach is discussed in the context of the Rosenblatt transformation (see Appendix B) in Section 4.4.3.1 below.

In practice, the necessary data to allow $f_{\mathbf{X}}(\mathbf{x})$ to be described completely may not be available. If only marginal probability distributions and correlation data are available, even for non-Normal random variables, the Nataf transformation may be applied to give a set of independent Normal random variables for use with FOSM methods. Unlike the Rosenblatt transformation, the Nataf transformation is approximate. It is discussed in Section 4.4.3.2.

4.4.3.1 Rosenblatt Transformation

Consider a vector of uniformly distributed random variables, denoted $\mathbf{R}$. Let these be the intermediaries between the random variables in the original space, represented by the vector $\mathbf{X}$, and the standardized Normal variables, represented by the vector $\mathbf{Y}$. Provided the necessary data for the joint probability distribution function $F_{\mathbf{X}}(\mathbf{x})$ and its conditional distributions $F_i(x_i|x_1, \ldots, x_{i-1})$ is available, the Rosenblatt transformation (see Appendix B) in n-dimensional space becomes:

$$
\begin{aligned}
\Phi\left(y_1\right) &= r_1 = F_1\left(x_1\right) \\
\Phi\left(y_2\right) &= r_2 = F_2\left(x_2 | x_1\right) \\
&\vdots \\
\Phi\left(y_n\right) &= r_n = F_n\left(x_n | x_1, \ldots, x_{n-1}\right)
\end{aligned}
\tag{4.42}
$$

where $\Phi(\ )$ is the standard Normal cumulative distribution function for $\mathbf{Y}$ and $F_i\left(x_i | x_1, \ldots, x_{i-1}\right)$ the conditional cumulative distribution function for the random variable X_i as given by (B.4). The component random variables y_i can be obtained from (4.42) by successive inversion:

$$
\begin{aligned}
y_1 &= \Phi^{-1}\left[F_1\left(x_1\right)\right] \\
y_2 &= \Phi^{-1}\left[F_2\left(x_2 | x_1\right)\right] \\
&\vdots \\
y_n &= \Phi^{-1}\left[F_n\left(x_n | x_1, \ldots, x_{n-1}\right)\right]
\end{aligned}
\tag{4.43}
$$

In general the valuation will need to be done numerically. Similarly, the inverse transformation is obtained from

$$
\begin{aligned}
x_1 &= F_1^{-1}\left[\Phi\left(y_1\right)\right] \\
x_2 &= F_2^{-1}\left[\Phi\left(y_2\right) \Big| x_1\right] \\
&\vdots \\
y_n &= F_n^{-1}\left[\Phi\left(y_n\right) \Big| x_1, \ldots, x_{n-1}\right]
\end{aligned}
\tag{4.44}
$$

If the X_i are independent random variables, all the conditions in (4.42) to (4.44) disappear, and the transformation is essentially identical with that discussed in the previous

section and given by (4.31). This means that, for the present case also, the expansion point is identical with the checking point.

Before the above transformations can be incorporated into an iteration algorithm, it is necessary to determine the transformation of the limit state function from $G(\mathbf{x}) = 0$ to $g(\mathbf{y}) = 0$. A probability density function defined in the $\mathbf{x}$ space is transformed to the $\mathbf{y}$ space according to identity (A.150). This transformation also holds for the relationship between any (continuous) functions in $\mathbf{X}$ and $\mathbf{Y}$; in particular it also holds for $G(\mathbf{X})$:

$$G(\mathbf{x}) = g(\mathbf{y})\,|\mathbf{J}| \tag{4.45}$$

where the Jacobian $\mathbf{J}$ has elements $J_{ij} = \partial y_i/\partial x_j$; (see A.151). The differential may be evaluated by substituting for y_i using (4.43), and then noting that, from (4.42), $\partial y_i = \left[\phi(y_1)\right]^{-1}\partial F_i\left(x_1 \mid x_1, \ldots, x_{i-1}\right)$, so that

$$\frac{\partial y_i}{\partial x_j} = \frac{1}{\phi(y_i)}\frac{\partial F_i\left(x_i \mid x_1, \ldots, x_{i-1}\right)}{\partial x_j} \tag{4.46}$$

Evidently, if $i < j$, $\partial F_i/\partial x_j = 0$, so that $\mathbf{J}$ is lower triangular. This allows the inverse $\mathbf{J}^{-1}$ to be obtained from $\mathbf{J}$ by back-substitution.

The components α_i of the gradient of $g(\mathbf{Y})$ are given by (4.5), but this is not easily evaluated since usually no explicit expression for $g(\mathbf{Y})$ is available. However, it follows easily that

$$\frac{\partial G(\mathbf{x})}{\partial x_j} = \sum_{i=1}^{n}\frac{\partial g(\mathbf{y})}{\partial y_i}\frac{\partial y_i}{\partial x_j} \tag{4.47}$$

so that

$$\begin{bmatrix} \dfrac{\partial G(\mathbf{x})}{\partial x_1} \\[2mm] \vdots \\[2mm] \vdots \\[2mm] \dfrac{\partial G(\mathbf{x})}{\partial x_n} \end{bmatrix} = [J]\begin{bmatrix} \dfrac{\partial g(\mathbf{y})}{\partial y_1} \\[2mm] \vdots \\[2mm] \vdots \\[2mm] \dfrac{\partial g(\mathbf{y})}{\partial y_n} \end{bmatrix} \tag{4.48}$$

from which the components of the gradient $\partial g/\partial y_i$ can be computed by matrix inversion. This allows the direction cosines α_i to be evaluated. However, the earlier interpretation of α_i as sensitivity factors (see Section 4.3.3) is not now necessarily valid. This is because the y_i have, in general, no direct physical meaning (unless the basic variables are independent).

4.4.3.2 Nataf Transformation

In some cases only the marginal cumulative distribution functions $F_{X_i}(\ )$, $i = 1, \ldots, n$ and the correlation matrix $\mathbf{P} = \{\rho_{ij}\}$ are available instead of the complete joint cumulative distribution function $F_{\mathbf{X}}(\mathbf{x})$. It is now not possible to apply the Rosenblatt transformation since the conditional distributions required in (4.43) are not available. However, some of the above ideas can be used in part to 'create' an approximation,

based on a joint Normal distribution, to the complete distribution $F_X(x)$. As will be seen, this has the advantage that it generates immediately the random variables formulated in the n-dimensional standard Normal variable space y.

Consider the marginal transformation from the random variables $X = (X_1, \ldots, X_n)$ in x space to the standardized Normal random variables $Y = (Y_1, \ldots, Y_n)$ in y space, given by

$$Y_i = \Phi^{-1}\left[F_{X_i}(X_i)\right], \qquad i = 1, \ldots, n \tag{4.49}$$

where, as before, $\Phi()$ is the standard Normal cumulative distribution function. It is now assumed that $Y = (Y_1, \ldots, Y_n)$ is jointly Normal, with n-dimensional standard Normal probability density function $\phi_n(y, P')$ having zero means, unit standard deviations and correlation matrix $P' = \{\rho'_{ij}\}$. The Nataf (1962) approximation for the joint probability density function $f_X()$ is then given by:

$$f_X(x) = \phi_n\left(y, \ P'\right).|J| \tag{4.50}$$

where the Jacobian $|J|$ is necessary due to the usual rules for transformation of random variables (A.150) and is defined by:

$$|J| = \frac{\partial(y_1, \ldots, y_n)}{\partial(x_1, \ldots, x_n)} = \frac{f_{X_1}(x_1).f_{X_2}(x_2)\cdots f_{X_n}(x_n)}{\phi(y_1)\,\phi(y_2)\cdots\phi(y_n)} \tag{4.51}$$

Thus $f_X()$ is forced to be a unique n-dimension joint density function defined by (4.50). The only matter left for resolution is the definition of the correlation matrix $P' = \{\rho'_{ij}\}$ in (4.50). It would be expected that this should be related to the correlation matrix $P = \{\rho_{ij}\}$ in x space.

For convenience, introduce the Normalized random variables $Z_i = (X_i - \mu_{X_i})/\sigma_{X_i}$. Then for any two random variables the correlation between the X_i can be stated as (see A.123, A.124):

$$\rho_{ij} = \frac{\text{cov}\left[X_i X_j\right]}{\sigma_{X_i}\sigma_{X_j}} = E\left[Z_i Z_j\right] = \int_{-\infty}^{\infty}\int_{-\infty}^{\infty} z_i z_j \phi_2\left(y_i, y_j; \rho'_{ij}\right) dy_i dy_j \tag{4.52}$$

with y_i and y_j dummy variables. From this expression the terms in the correlation matrix $P' = \{\rho'_{ij}\}$ can be determined for each pair of marginal distributions with known $P = \{\rho_{ij}\}$. Clearly it will be an iterative (and rather tedious) process, as the unknown is contained within the double integral, but readily programmable. To ease the burden, Liu and Der Kiureghian (1986) have produced empirical, approximate expressions for the ratio

$$R = \frac{\rho'_{ij}}{\rho_{ij}} \tag{4.53}$$

for which some results are given in Appendix B for a range of combinations of marginal distributions. Suffice to note here that with the clear exception of combinations involving the shifted Exponential distribution, it is generally the case that $0.9 \leq R \leq 1.1$. In view of the fact that the correlation structure can, in practice, only

seldom be determined with high precision, this suggests that for many problems it is sufficient to take the correlation structure $\mathbf{P}' = \{\rho'_{ij}\}$ for the standardized variables $\mathbf{Y}$ as $\mathbf{P} = \{\rho_{ij}\}$ [*cf*. Der Kiureghian and Liu, 1986]. Restrictions on the use of the Nataf transformation are given in Appendix B.

Once $\mathbf{P}' = \{\rho'_{ij}\}$ has been obtained, the complete description of the 'created' (approximate) probability density function $f_\mathbf{X}(\ )$ is available in (4.50). In principle this could be used in the Rosenblatt transformation to obtain a set of equivalent independent Normal random variables for use in FOSM analysis. In practice it is simpler to go directly to one of the FOSM solution schemes, to determine β, such as the iterative scheme of Section 4.3.5. This is possible since $f_\mathbf{X}(\ )$ is a (transformed) Normal distribution as can be seen from (4.50). The only additional requirement over what was done previously is the need to evaluate $|\mathbf{J}|$. The resulting distribution may be transformed to an independent standardized distribution $\phi_n(\mathbf{z}', \mathbf{I})$ through a simple orthogonal transformation (see Appendix B).

Example 4.6 Let two random variables X_1 and X_2 have identical exponential marginals with means 1.0 and correlation coefficient $\rho_{12} = \rho = 0.25$. It follows from Section A.5.5 that the standard deviations also are unity and from expressions (A.35) and (A.36) that

$$F_{X_i} = 1 - \exp\left(-x_i\right)$$

and

$$f_{X_i} = \exp\left(-x_i\right)$$

To obtain the approximate probability density according to the Nataf transformation, expression (4.50) must be applied. This requires knowledge of $\rho' = R.\rho$. From Table B.2, for both marginals Exponential distributed, $R = 1.229 - 0.367\rho + 0.153\rho^2 = 1.148$, so that $\rho' = 0.287$.

The term $\phi_n(\ )$ in (4.50) becomes (see A.125)

$$\phi_2\left(\mathbf{y}, \rho'\right) = \frac{1}{2\ \pi\sigma_1\sigma_2\left(1 - \rho'^2\right)^{1/2}} \exp\left[\frac{-\frac{1}{2}(h^2 + k^2 - 2\rho'hk)}{\left(1 - \rho'^2\right)}\right]$$

with $h = \dfrac{x_1 - \mu_{X_1}}{\sigma_{X_1}} = y_1$ since the mean and standard deviation are each unity. A similar result holds for X_2. Substituting $\rho' = 0.287$ and the mean and standard deviation values produces

$$\phi_2\left(\mathbf{y}, \rho'\right) = 0.166 \exp\left[0.545\left(y_1^2 + y_2^2\right) - 0.574y_1y_2\right]$$

To complete the probability density function the Jacobian is required:

$$|\mathbf{J}| = \frac{f_{X_1}\left(x_1\right).\ f_{X_2}\left(x_2\right)}{\phi\left(y_1\right).\ \phi\left(y_2\right)}$$

with the two terms in the numerator given by $f_{X_i} = \exp\left(-x_i\right)$ and the terms in the denominator obtained from the standard Normal distribution $N(0, 1)$ as $\phi\left(y_i\right) = \frac{1}{\sqrt{2\pi}} \exp\left(-\frac{1}{2}y_i^2\right)$ (see Section A.5.7). It follows readily that

$$|\mathbf{J}| = \frac{\exp\left(-x_1\right).\exp\left(-x_2\right)}{0.159 \exp\left(-0.5y_1^2\right)\exp\left(-0.5y_2^2\right)}$$

and substituting into (4.50) that

$$f_{\mathbf{X}}\left(\mathbf{x}\right) = 0.104 \exp\left(-x_1 - x_2\right)\exp\left[-0.045\left(y_1^2 + y_2^2\right) + 0.313y_1y_2\right]$$

with $y_i = \Phi^{-1}\left[1 - \exp\left(-x_i\right)\right]$ [*cf.* expression (4.49)].

4.4.4   Algorithm for First-Order Reliability (FOR) Method

The algorithm given in Section 4.3.6 for determining the design point in FOSM theory can now be generalized to FOR [Hohenbichler and Rackwitz, 1981]. For illustration the Rosenblatt transformation will be assumed.

(1) Select an initial checking point vector $\mathbf{x}^* = \mathbf{x}^{(1)}$ where $\mathbf{x}^{(1)}$ might be $\mu_{\mathbf{X}}$.
(2) Use the transformation (4.43) to obtain $\mathbf{y}^{(1)}$; this transformation will be of the simple form (4.31) for any of the components of $\mathbf{X}$ that are independent random variables.
(3) Use expressions (4.45) and (4.46) to obtain the Jacobian $\mathbf{J}$ and its inverse $\mathbf{J}^{-1}$.
(4) Compute the direction cosines α_i according to equations (4.5) and (4.48), the current value of $g(\mathbf{y}^{(1)})$ and the current estimate of β according to $\beta = -\mathbf{y}^{*T} \cdot \alpha$ (see 4.9) where α is the vector of direction cosines.
(5) A new estimate of the co-ordinates of the checking point in $\mathbf{y}$ space is then given by expression (4.24) using the current β value.
(6) The co-ordinates in $\mathbf{x}$ space of the current estimate of the checking point are then given by the reverse transformation (4.44).

Repeat steps (2)–(6) until $\mathbf{x}^*$ (or $\mathbf{y}^*$) and β stabilize in value.

It is evident that this algorithm is essentially a generalization of that given in Section 4.3.6 with the more complex transformation (4.43) and the inverse (4.44) used in steps (2) and (6).

Example 4.7   The following example is adapted from Dolinsky (1983) and Hohenbichler and Rackwitz (1981). It is one of the few cases that can be treated wholly analytically using the Rosenblatt transformation.

Consider the problem in which the limit state function is $G\left(\mathbf{x}\right) = 6 - 2x_1 - x_2 = 0$ (e.g. the random variables X_1, X_2 are actions) with $\mathbf{X}$ being rather highly correlated and having the joint probability density function

$$f_{\mathbf{X}}\left(\mathbf{x}\right) = \left(ab - 1 + ax_1 + bx_2 + x_1x_2\right)\exp\left(-ax_1 - bx_2 - x_1x_2\right) \quad \text{for} \quad \left(x_1, x_2\right) \geq 0$$
$$= 0, \quad \text{otherwise.}$$

By appropriate integration (see Section A.6), it follows that the marginal probability density functions for X_1 and X_2 are

$$f_{X_1}(x_1) = a \exp(-ax_1), \qquad \text{for } x_1 \geq 0$$
$$f_{X_2}(x_2) = b \exp(-bx_2), \qquad \text{for } x_2 \geq 0$$

while the joint cumulative distribution function is

$$F_{\mathbf{X}}(\mathbf{x}) = 1 - \exp(-ax_1) - \exp(-bx_2) + \exp(-ax_1 - bx_2 - x_1x_2) \quad \text{for } (x_1, x_2) \geq 0$$
$$= 0, \qquad \text{otherwise.}$$

Substituting into the first and second lines of the Rosenblatt transformation (4.42) produces

$$\Phi(y_1) = F_1(x_1) = \int_0^{x_1} f_{X_1}(t)\, dt = 1 - \exp(-ax_1), \qquad \text{for } x_1 \geq 0 \tag{4.54}$$

$$\Phi(y_2) = F_2(x_2 \mid x_1) = \frac{\int_0^{x_2} f_{\mathbf{X}}(x_1, w)\, dw}{f_{X_1}(x_1)}$$

$$= 1 - \left(1 + \frac{x_2}{a}\right) \exp(-bx_2 - x_1 x_2) \tag{4.55}$$

The limit state function becomes

$$G(\mathbf{X}) = 6 - 2F_1^{-1}\left[\Phi(y_1)\right] - F_2^{-1}\left[\Phi(y_2 \mid x_1)\right] = 0$$

This expression can only be evaluated numerically. For example, if $a = 1$, $b = 2$ and $x_1 = 1$, then (4.81) becomes $\Phi(y_1) = 1 - \exp(-1) = 0.6321$ or $y_1 = 0.34$. Then, in (4.55), $\Phi(y_2) = 1 - (1 + x_2)\exp(-2x_2 - x_1x_2)$, but $x_2 = 4$ for $G(\mathbf{x}) = 0$, so that $\Phi(y_2) = 1 - 5\exp(-12) = 0.999969$ or $y_2 \approx 4.01$. This marks point A on Figure 4.12(a). The complete curve can be constructed in a similar manner by taking other values of x_1.

Noting (4.46), the Jacobian (A.151) is evaluated using (4.54) and (4.55) as:

$$\mathbf{J} = \begin{bmatrix} \dfrac{1}{\phi(y_1)} \dfrac{a}{\exp(ax_1)} & 0 \\[4mm] \dfrac{1}{\phi(y_2)} \dfrac{(1 + x_2/a)\, x_2}{\exp(bx_2 + x_1x_2)} & \dfrac{1}{\phi(y_2)} \dfrac{-1/a + (b + x_1)(1 + x_2/a)}{\exp(bx_2 + x_1x_2)} \end{bmatrix} \tag{4.56}$$

from which it follows by back-substitution that

$$\mathbf{J}^{-1} = \begin{bmatrix} \phi(y_1) \dfrac{\exp(ax_1)}{a} & 0 \\[4mm] -\phi(y_1) \dfrac{(1 + x_2/a)\, x_2 \exp(ax_1)}{1/a - (b + x_1)(1 + x_2/a)\, a} & -\phi(y_2) \dfrac{\exp(bx_2 + x_1x_2)}{1/a - (b + x_1)(1 + x_2/a)} \end{bmatrix}$$

$$\tag{4.57}$$

With $a = 1$, $b = 2$, the algorithm can now be used as follows.
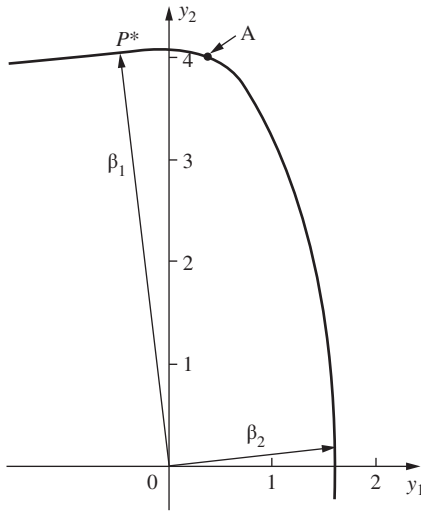
(a)
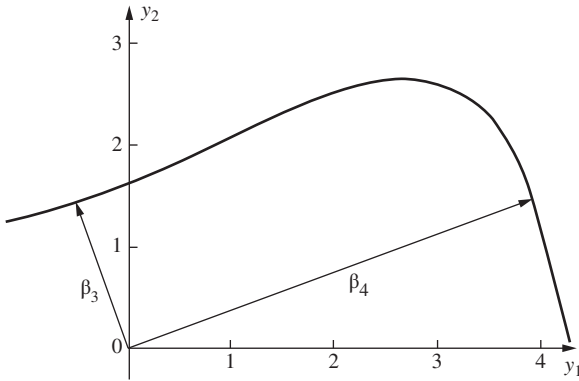
(b)

Figure 4.12 Local stationary points for Example 4.7: (a) original order of dependent basic variables; (b) interchanged order.

(1) Let a trial design point be, arbitrarily, $x_1 = 1$, $x_2 = 4$, which it was seen corresponds to the point A in Figure 4.12(a).

(2) From (4.54) it follows that $\phi\left(y_1\right) = 1 - \exp\left(-1\right)$, or $y_1 = 0.34$ and, from (4.55) that $\Phi\left(y_2\right) = 1 - (1 + 4)\exp\left(-12\right)$ or $y_2 = 4.01$. Hence $\mathbf{y} = [0.34, \ 4.01]^T$.

(3) From (4.56) and (4.57):

$$\mathbf{J} = \begin{bmatrix} 0.977 & 0 \\ 0.917 & 0.642 \end{bmatrix}$$

$$\mathbf{J}^{-1} = \begin{bmatrix} 1.024 & 0 \\ 1.462 & 31.289 \end{bmatrix}$$

(4) (a) The direction cosines are [see (4.5) and (4.48)]

$$
\begin{bmatrix} c_1 \\ c_2 \end{bmatrix} = \begin{bmatrix} \dfrac{\partial g}{\partial y_1} \\ \dfrac{\partial g}{\partial y_2} \end{bmatrix} = \mathbf{J}^{-1} \begin{bmatrix} \dfrac{\partial G(\mathbf{x})}{\partial x_1} \\ \vdots \\ \vdots \\ \dfrac{\partial G(\mathbf{x})}{\partial x_n} \end{bmatrix} = \begin{bmatrix} 1.024 & 0 \\ 1.462 & 31.829 \end{bmatrix} \begin{bmatrix} -2 \\ -1 \end{bmatrix} = \begin{bmatrix} -2.048 \\ -34.21 \end{bmatrix}
$$

so that $l \approx 34.27$, $\alpha_1 = -0.060$, $\alpha_2 = -0.998$.

(b) By the original choice of values for x_1 and x_2 it is seen that the limit state function is identically satisfied for this cycle, i.e. $g(\mathbf{y}) = G(\mathbf{x}) = 0$.

(c) Calculate β:

$$
\beta = \left(\mathbf{y}^T \cdot \mathbf{y} \right)^{1/2} = \left(0.34^2 + 4.01^2 \right)^{1/2} = 4.02
$$

(5) From (4.24) the new estimates for $\mathbf{y}$ are

$$
\begin{bmatrix} y_1 \\ y_2 \end{bmatrix} = - \begin{bmatrix} -0.060 \\ -0.998 \end{bmatrix} (4.02 - 0) = \begin{bmatrix} 0.24 \\ 4.02 \end{bmatrix}
$$

which, by inspection of Figure 4.13(a), is obviously a better estimate of the (apparent) checking point P^*.

(6) From (4.54) inverted according to (4.44), the second estimate for x_1 is

$$
x_1 = F_1^{-1} \left[\Phi(y_1) \right] = -\ln\left[1 - \Phi(0.24) \right] = 0.903
$$

and from (4.55)

$$
1 - \Phi(y_2) = (1 + x_2) \exp\left[-(2 + x_1) x_2 \right]
$$

i.e.

$$
0.262 \times 10^{-4} = (1 + x_2) \exp\left[-2.903 x_2 \right]
$$

or $x_2 = 4.2$ obtained by trial and error.

The algorithm should now be repeated until y or x stabilizes. This should then give β_1 as shown in Figure 4.12(a).

4.4.5 Observations

Without actually using the algorithm, it is evident that if a rather different starting point was chosen in the above example, say $\mathbf{y} = (1.5, 1.3)^T$, the algorithm would converge to β_2 in Figure 4.12(a), with $\beta_2 < \beta_1$. This shows again that the algorithm provides only stationary points and that, for each of these, the respective β (and hence p_f) must be checked [Dolinsky, 1983].

This difficulty does not arise if a numerical algorithm for seeking the point of maximum likelihood (or the MPP) is used instead of the iteration algorithm (which identifies only stationary points). Such an approach was outlined in Section 4.3.5 for a second-moment problem with non-linear limit state function [*cf.* Beck and

Silva Jr., 2016]. The present problem is essentially similar but has a highly non-linear limit state function, owing to the format of the joint cumulative distribution function used.

Difficulties may arise also with sensitivities (see Section 4.3.3) for β when there are random variables modelled by asymmetrical distributions such as the exponential or extreme value distributions, with β tending to increase with increased variance (rather than the reverse) [Sørensen and Enevoldsen, 1993].

A further problem can arise. The Rosenblatt transformation (4.42) can be given in $n!$ different ways, depending on how the basic variables are arranged. The importance of this can be demonstrated as follows. If the order x_1, x_2 in (4.42) is interchanged, then

$$
\begin{aligned}
\Phi\left(y_1\right) &= F_2\left(x_2\right) \\
\Phi\left(y_2\right) &= F_1\left(x_1 \middle| x_2\right)
\end{aligned}
\tag{4.58}
$$

and for $a = 1, b = 2$ as before

$$
\begin{aligned}
\Phi\left(y_1\right) &= 1 - \exp\left(-2x_2\right) \\
\Phi\left(y_2\right) &= 1 - \left(1 + \frac{x_1}{2}\right)\exp\left(-x_1 - x_1 x_2\right)
\end{aligned}
\tag{4.59}
$$

Using a similar procedure as before, the limit state function $G\left(\mathbf{x}\right) = 0$ is transformed to that shown in Figure 4.12(b). Again two stationary points exist. Let the respective distances from the origin be marked as β_3 and β_4. Then it is easily verified that $\beta_3 < \beta_2 < \beta_4$. This demonstrates that in principle *all n!* possible combinations of arrangement of $\mathbf{X}$ in (4.42) must be considered if the critical (i.e. lowest) is to be identified [Dolinsky, 1983]. In practice some prior knowledge of the problem may be advantageous in selecting an appropriate ordering of variables.

The above example represents an unusually severe test for the FOR method. In most practical situations, highly correlated exponential distributions, as used here, are unlikely to occur.

4.4.6   Asymptotic Formulation

It should be evident that the use of the simple transformation of Section 4.4.1 and the Rosenblatt and the Nataf transformations essentially are attempts to find a new surface, in the standard normal space, which closely matches the surface of the actual joint probability density function. This new surface then facilitates estimating the probability content under (an appropriate part of) the surface, in a manner simpler than was possible under the original PDF. For a simple one-dimensional situation this new surface is shown in Figure 4.10 as the transformed distribution.

The idea of using an approximating surface can be extended mathematically by seeking functions which are asymptotic to the true surface such that the error in the approximation is minimized. Specifically, (1.31) can be rewritten as

$$
p_f = \int_D f_{\mathbf{X}}\left(\mathbf{x}\right) d\mathbf{x} = \int_D \exp\left\{\ln\left[f_{\mathbf{X}}\left(\mathbf{x}\right)\right]\right\} \; d\mathbf{x}
\tag{4.60}
$$

where D is the failure domain. If, as is usually the case, the probability content enclosed by D is small, the probability density function $f_{\mathbf{X}}(\,)$ is also small everywhere in D and the

{ } term is negative. Defining now a 'scaling factor' $\beta_0 = \sqrt{-\max_D \ln\left[f_X(x)\right]}$ and letting $h(x) = \ln\left[f_X(x)\right] / \beta_0^2$ allows the integral (4.60) to be rewritten as:

$$p_f = \int_D \exp\left[\beta_0^2 h(x)\right] dx \qquad (4.61)$$

The integral in (4.61) may be compared to the following integral of the Laplace type [Breitung and Hohenbichler, 1989]:

$$p_f(\beta) = \int_D \exp\left[\beta^2 h(x)\right] dx \qquad (4.62)$$

for which solution schemes exist. Expression (4.62) approximates (4.61) asymptotically as $\beta \to \infty$ but provides good approximations with $\beta = \beta_0$, where β_0 is the scaling factor corresponding to the point of maximum likelihood (see above) on the failure domain boundary.

These results carry-over to the space of the original random variables provided the log likelihood function of the joint probability distribution is used, with the approximation point (*cf*. 'checking point') at the point of maximum log likelihood [Breitung, 1991]. The reader is referred to the specialized literature for detailed discussion of this approach.

4.5   Second-Order Reliability (SOR) Methods

4.5.1   Basic Concept

From the above discussions it should be clear that approximating the limit state surface by a linear surface (through a Taylor series expansion) may not be satisfactory if the limit state surface has significant curvature. Even for linear limit state functions in the original space, a non-linear limit state may be the result when the reliability problem is transformed from the original space to the standard Normal space. That this can occur is shown very clearly in Figure 4.12 of Example 4.7.

Since the use of a linear approximation for the limit state surface becomes less accurate as the limit state function becomes more curved, it would be expected that limit state curvature has a role in defining any simple surface used to approximate a non-linear limit state function. Various ways of doing this have been proposed. In the context of second-moment approaches and developments thereof, methods to deal with the non-linearity of the limit state function have been termed 'second order' methods [Fiessler et al., 1979; Hohenbichler, et al., 1987]. The most common approach has been to attempt to fit a parabolic, quadratic or higher order surface to the actual surface, centred on the checking point. This requires some decision about the extent to which the approximation is valid away from the checking point. Figure 4.13 shows the relationship between a first order (linear) approximation and a second order (parabolic) approximation at the checking point in standard Normal space [Der Kiureghian, et al., 1987].

4.5.2   Evaluation Through Sampling

There are no easy ways to estimate the probability content enclosed by a quadratic surface. Essentially two approaches for estimating it have been proposed. The first relies on
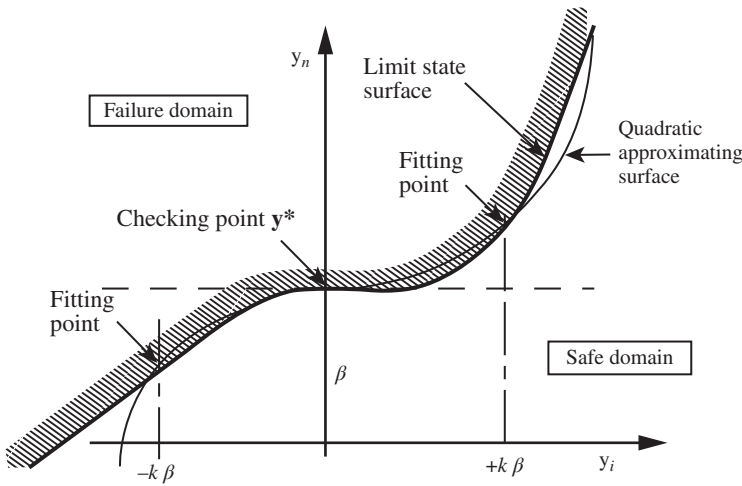
Figure 4.13 Second order approximation to actual limit state surface at checking point **y*** in **y** space, showing also first order (linear) approximation.

sampling the space between the linear approximation and the quadratic approximation to estimate the probability content between these two approximations to the limit state surface. The majority of the probability content is estimated using First Order theory [Hohenbichler and Rackwitz, 1988]. Alternatively, the FOR result for a linear limit state can be taken as the starting point for simulation about the design point to estimate the error in failure probability between that given by the linear limit state approximation and the actual limit state [e.g. Mitteau, 1996].

4.5.3 Evaluation Through Asymptotic Approximation

An alternative approach to evaluating the probability content for the Second Order approach uses asymptotic concepts. In the space of independent standard Normal random variables (the **y** space), and for a limit state function which is not too highly non-linear, the failure probability can be estimated from a determination of the limit state surface curvatures K_i at the design point $\mathbf{y}^*$ and then applying the asymptotic expression [Breitung, 1984]:

$$p_f \approx \Phi(-\beta) \sum_{j=1}^{k} \left[\prod_{i=1}^{n-1} \left(1 - \beta \cdot \kappa_i \right) \right]^{-1/2} \tag{4.63}$$

where $\kappa_i = -\left[\frac{\partial^2 y_n}{\partial y_i^2} \right]$ is the ith principal curvature of the limit state surface $g(\mathbf{y}^*) = 0$ at $\mathbf{y}^*$.

Evidently, the (known) limit state function must be continuous and twice differentiable in the neighbourhood of $\mathbf{y}^*$. Also, this approach can deal, directly, only with a single design point.

The error in the asymptotic approximation (4.63) is not defined, in general, but it appears that, roughly, the approximation improves as the limit state becomes 'flatter', i.e. as $\beta \to \infty$, in which case the first order result is approached (i.e. that with a linear limit state function). Evidently, (4.63) has a singularity if $\beta_i = 1/\kappa_i$ so that (4.63) gives rather

poor results for high curvature limit states. Derivations and more formal discussions are available [Breitung, 1984, 1994; Ditlevsen and Madsen, 1996].

The use of (4.63) requires computation of the curvatures, which can be demanding for large problems with a large number of basic variables or where the limit state function is complex. The curvatures could be approximated iteratively using the gradients of the limit state function using a gradient-based algorithm. This can then find both the checking point and the principal curvatures [Der Kiureghian and De Stafeno, 1991]. A number of algorithms for finding the checking point(s) have been reviewed and proposed [Abdo and Rackwitz, 1990; Liu and Der Kiureghian, 1991a; Haukaas and Der Kiureghian, 2006; Santos et al., 2012; Beck and Silva Jr., 2016].

Rather than using curvatures, an alternative approach is to return to the idea of Figure 4.13 and to fit a quadratic surface through the checking point $\mathbf{y}^*$ and a set of points on the limit state surface. The location of the points is arbitrary. They may be selected to lie along the axes of a standardized Normal space in which one axis coincides with the checking point (which must be obtainable) and the points may be located a distance $\beta_i K_i$ away from the checking point, with $\beta_i K_i$ around 3 for $\beta_i > 3$ and $K_i = 1$ for lower β_i values [Der Kiureghian et al., 1987]. Because there is no attempt to match the curvature at the checking point, this approach tends to allow for smoothing of localized irregularities and for limit state surfaces which are not close to a quadratic shape in the region of interest.

It will become evident that this approach is not unlike the response surface approach (see Section 5.5.4), except that, compared to the situation discussed there, the original limit state surface is known for the present situation. Improved versions of (4.63) have been proposed, including removal of the limitation on accuracy for higher values of β [Tvedt, 1985, 1990; Hohenbichler and Rackwitz, 1988]. However, this comes at the expense of more complexity. A simpler version, using an accurate polynomial based expansion of the gradient of the probability density function around the checking point, appears promising [Köylüoglu and Nielsen, 1994].

4.6   Application of FOSM/FOR/SOR Methods

The FOSM method in particular has proved very popular with those wishing to obtain probability statements about particular problems with relative ease. The procedure to determine the safety index β is straightforward even for non-linear limit state functions. Once experience has been gained with the FOSM method, its extension to non-normal random variables, known as the First Order Reliability (FOR) method (sometimes FORM), is a natural step to incorporate distributional probability information. As was discussed in relation to Example 4.7 it is only in rather extreme situations that difficulties arise or that the linearization of the transformed limit state equation leads to grossly inaccurate results. Applications of the FOSM/FOR methods can be found aplenty in the literature, although mainly for problems with relatively simple or with only a few limit state functions. How to deal with more complex systems will be discussed in Chapter 5.

Both the FOSM and the FOR methods require the use of derivatives of the limit state function. For the simple examples given in this chapter, explicit expressions could be obtained for derivatives. More generally, however, such as when the limit state

function is complex and/or dependent on structural behaviour analysis, resort may have to be made to numerical procedures. This will have a significant effect on the amount of computation necessary as the number of basic variables increases.

The concept of using a second-moment (SM) representation to approximate a non-Normal distribution function can be extended and improved by also using approximating higher moments. One such approach uses a weighted system of second-moment cumulative distribution functions to represent the non-Normal distribution and to modify the limit state function accordingly [Grigoriu, 1982]. Winterstein and Bjerager (1987) suggested also exploiting the information contained in the third and fourth moments: in this way the deviations in the distribution tails obtained with fewer moments are reduced significantly. Further, it is possible to bypass the use of the Rosenblatt transformation by the use of Hermite polynomials. Such methods are beyond the scope of this book.

Finally it is possible also to specify safety indices other than β. A useful overview of most of these has been given by Turkstra and Daly (1978). None has found wide acceptance.

4.7 Mean Value Methods

As mentioned in Sections 4.2 and 4.3.2, the natural and theoretically consistent point for linearizing non-linear limit state functions (in standard Normal space $\mathbf{y}$) is the checking point (or point of maximum likelihood or the most probable point – MPP) $\mathbf{y}^*$ on the limit state function. This also was shown (Section 4.3.4) to be the natural point for the Normal tail approximation of non-Normal random variables in the FOR approach. However, it is clear that in both cases the point $\mathbf{y}^*$ is not known at the outset. Typically an iterative (or other) process is required to seek $\mathbf{y}^*$. This may be complicated by the need to also seek the appropriate Normal tail approximation most consistent with the current estimate of $\mathbf{y}^*$. The net result is that the computational demands increase in progressing from linear limit state functions through non-linear limit state functions to non-Normal distributions. If the reliability analysis is then also to be embedded in a structural analysis program, for example, a finite element analysis, or an optimization scheme (see Chapter 11), the total computational costs become very high. Although not originally developed for such applications, there is a simplified, approximate, reliability analysis, known as (Advanced) Mean Value reliability analysis [Wu et al. 1990] that sometimes can be used to help reduce high computational costs.

As noted, usually the checking point is not known at the beginning of the analysis. On the other hand, the mean point μ_Y is always known a priori. It does not need to be sought by numerical or other means, irrespective of whether second-moment or Normal or non-Normal random variables are involved. Using the mean value of the relevant random variables as the expansion point makes it easy, using Taylors series expansion, as before, to determine an equivalent linearized limit state function. It also makes the computation of β or the equivalent probabilities very easy, through single evaluations of the limit state functions and of their gradients at the mean values. However, generally the β value so obtained will not have the same value as that obtained from the theory and the various algorithms described in Sections 4.3–4.5 [Wu et al., 2002].

It has been claimed that mean value methods provide reasonable results for many practical applications such as reliability analyses. They can have acceptable accuracy when the limit state functions are nearly linear (not 'excessively non-linear') and when the probability density functions for the random variables are approximately Normal. However, the accuracy can be poor in other situations. This cannot be estimated without additional analyses to obtain estimates of the errors involved. Algorithms for this are available [e.g. Eldred and Bichon, 2006].

4.8   Conclusion

The discussion in this chapter commenced with the FOSM method. It was shown that for linear limit state functions the failure probability can be obtained directly from the safety or reliability index β. If the limit state function is non-linear, β can still be defined, but only with respect to an approximating tangent (hyper-)plane. In each case β represents the shortest distance from the origin in standardized Normal space to the (hyper-)plane. It is therefore perpendicular to the hyperplane. The corresponding point on the hyperplane was termed the 'checking' point (also sometimes known as the 'design' point). This point is the point of greatest probability density (or point of maximum likelihood or the most probable point) within the space encompassed by the failure region. This point may be found by direct minimization using a Lagrangian multiplier formulation, by numerical maximization or by iteration to find a saddle point.

When more than second-moment information is available for some or all of the basic variables, the FOSM method of determining a nominal failure probability, or β, may still be used, provided that each basic variable is first transformed to an equivalent Normal random variable. The procedure for doing this has been termed the First Order Reliability (FOR) method (sometimes called the FORM method). The transformation may be based on the Rosenblatt transformation if sufficient information is available or on the Nataf transformation if only marginal and correlation information is available (see Appendix B). In the special case when all basic variables are independent, these transformations degenerate into transformation of each variable independently.

A brief discussion was given of Second Order Reliability (SOR) methods (sometimes called SORM), including the formulation based on using an asymptotic surface approximation of the joint probability density function in the region of the point of maximum likelihood. Such methods are inherently more complex and may require numerical methods such as importance sampling for solution.

Finally, some remarks were made about the approximate mean value methods. These may be useful where the computational demands imposed by the theoretically more rigorous FOR and SOR methods are too great, such as in iterative design or optimization schemes.

5

Reliability of Structural Systems

5.1 Introduction

This chapter is concerned with structures for which more than one limit state must be considered. Even in simple struc tures composed of just one element, various limit states such as bending action, shear, buckling, axial stress, deflection, etc., may apply. Most structures are, in addition, composed of many members or elements. Such a composition will be referred to as a 'structural system'.

The reliability of a structural system is likely to be a function of the reliability of its members, for the following reasons:

(a) Load effects (stress resultants) on different members may be obtained from one or more common loads;
(b) Loads and resistances may not be independent (e.g. dead loads may be related to member size, and strength may be related to previously applied loadings);
(c) Correlation of member properties such as member strength and stiffness may exist between different locations in the structure;
(d) Construction practices may influence member properties for a group of members.

Furthermore, there may exist limit states for the structure as a whole rather than its elements (e.g. overall deflection, foundation settlement, residual stiffness) and the configuration of the structure itself may be of importance. It is likely, therefore, that the reliability assessment of structural systems will involve the need to consider multiple and perhaps correlated limit states.

In this chapter only time-invariant random loading will be considered. This means, as previously discussed in Section 1.4.1, that the structural reliability problem is reduced to one for which the probability of failure is sought under the maximum (but uncertain) loading applied (once only) to the system sometime during its life $[0, t_L]$. Where there is more than one load applied to the structural system, this approach remains valid if the loads are all fully dependent, so that there is in essence only one independent load parameter. This is often assumed to be the case, for example, in conventional rigid-plastic theory. This approach is valid also if each of the loads is applied only once and in a known order since then the sequence of structural response can be traced with certainty. Thus in both cases the statistical properties assigned to the load(s) represent the uncertainty about the actual maximum value which is applied. When these assumptions about loading do not hold, it is necessary to turn to the time-dependent reliability

assessment, as discussed in Chapter 6. Emphasis in the present chapter, therefore, is on structural system response.

The basic structural system reliability estimation problem will be formulated in the next section. This section will describe also the fundamental structural system idealizations and essential approaches to problem solution. Monte Carlo solutions are considered in Section 5.3 and bounding methods, using the First-Order Second-Moment (FOSM) or First-Order Reliability (FOR) methods, are discussed in Section 5.4. This will lead to response surface methods in Section 5.5. Sequential methods of analysis for large complex structures are described in Section 5.6.

5.2 Systems Reliability Fundamentals

5.2.1 Structural System Modelling

The analysis of realistic structural systems even within a deterministic framework can be a considerable task. Usually it is facilitated by simplifications and idealizations in each of (i) applied loads and load sequencing (load modelling), (ii) structural system and its components and connections between components (system modelling), and (iii) material response and strength characteristics (material modelling). Criteria for limit state violation also need to be specified—in conventional design usually a permissible stress criterion as adopted (see Section 1.2.1) but other criteria may have greater validity.

5.2.1.1 Load Modelling

The discussion in the previous chapters has been confined, largely, to extreme value loading, that is, the probability of failure has been estimated using the probability distribution for the uncertain extreme loading which might be applied to the structure sometime during its life (see Section 1.4.4). As already noted, this idealization assumes that there is only one such load possible and that the structure is, therefore, essentially loaded only once. Of course, a realistic load process with time is more like that shown in Figure 1.7 for a single time-dependent load. If the entire time-dependent load pattern is considered, it is conceivable that some part of the structure might reach a (local) limit state before an overall structural limit state is reached. Therefore, it is possible that the failure mode of a structure will depend on the exact loading sequence. Clearly, if the loading is a random process this means that there are an infinity of possible load realizations and hence failure possibilities—an impossible situation for analysis. The possibility of more than one loading process acting on the structural system only adds to the complexity.

This issue has been termed 'load-path dependence' in the literature, indicating that in many cases the estimated failure probability may depend on the path traced out by the (stochastic) vector of the applied load processes [Ditlevsen and Bjerager, 1986; Wang et al. 1995]. This may be important for some structures. A simple example is shown in Figure 5.1(a). It has a column loaded by a vertical force V and a horizontal force H. If the column were loaded first with a given value of vertical force followed by an increasing horizontal force H, the load path would be V-H as shown. As H is increased, eventually the point marked 'Failure' would be reached on the failure envelope for the column (as given in elementary texts for reinforced concrete design). However, the alternate load path H-V is not feasible for the same failure point since the failure envelope would be reached already for a lower value of H, before V even could be applied.
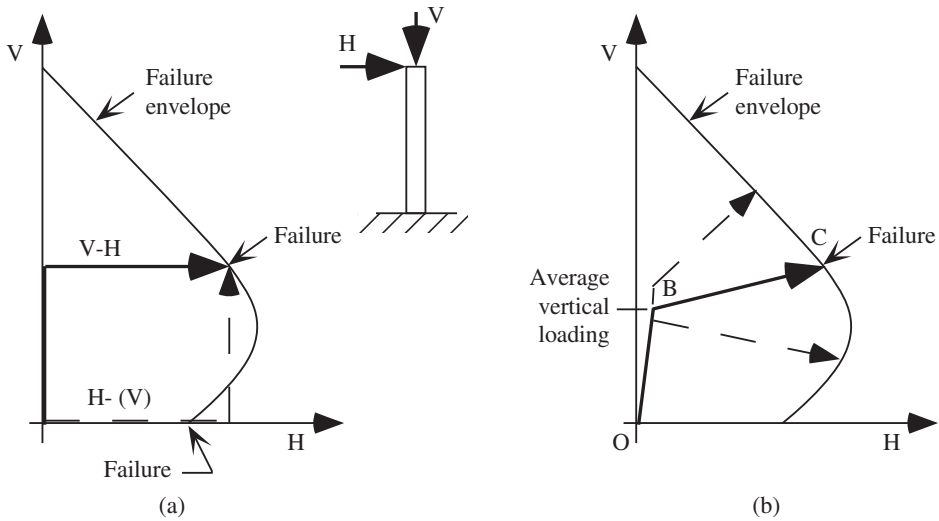
Figure 5.1 (a) Simple example of load path dependence—horizontal load applied before vertical load produces a different failure mode than an attempt to apply the loads in the reverse order. (b) Typical internal action path OBC within many realistic structures.

Despite the above observations, it is likely that for many practical structures the load-path issue is not as critical as appears at first sight [Melchers, 1998a]. In part this is due to the combination effect of internal actions at critical locations fixing the internal action path to something like OBC in Figure 5.1(b), with OB being due to self-weight and sustained live loading and only BC being due to extreme loading. In part also the apparent insensitivity to external load-paths is due to many realistic structural systems being designed deliberately (according to accepted design codes) to fail in ductile failure modes rather than brittle ones. In this sense the behaviour of many structures tends to approach plastic behaviour for which the well-known rigid-plastic theory provides a good approximation of structural system behaviour [Ditlevsen, 1988]. Fortunately, the capacity of simple ideal rigid-plastic systems does not depend on the load-path. For these the deformation of the system at failure is governed only by the 'normality flow-rule' (see also Section 5.2.2.3 below).

The matter of load-path dependence has not had much consideration in structural system reliability work. In many cases the loads have been idealized as time-independent random variables (i.e. as uncertain extreme loads applied once only during a specified time period). This approach will be used also in the present chapter where appropriate. A more general formulation (but subject to restrictions about the modelling of the structural system and member properties) is described in Chapter 6.

5.2.1.2 Material Modelling

Because of the complexity of actual material behaviour, material behaviour in structural engineering usually is idealized. When combined with cross-sectional properties, member response relationships such as those shown in Figure 5.2 can be hypothesized.

Elastic behaviour (Figure 5.2(a)) corresponds to the maximum permissible stress concept of Section 1.2.1. With this idealization, failure at any one location within the
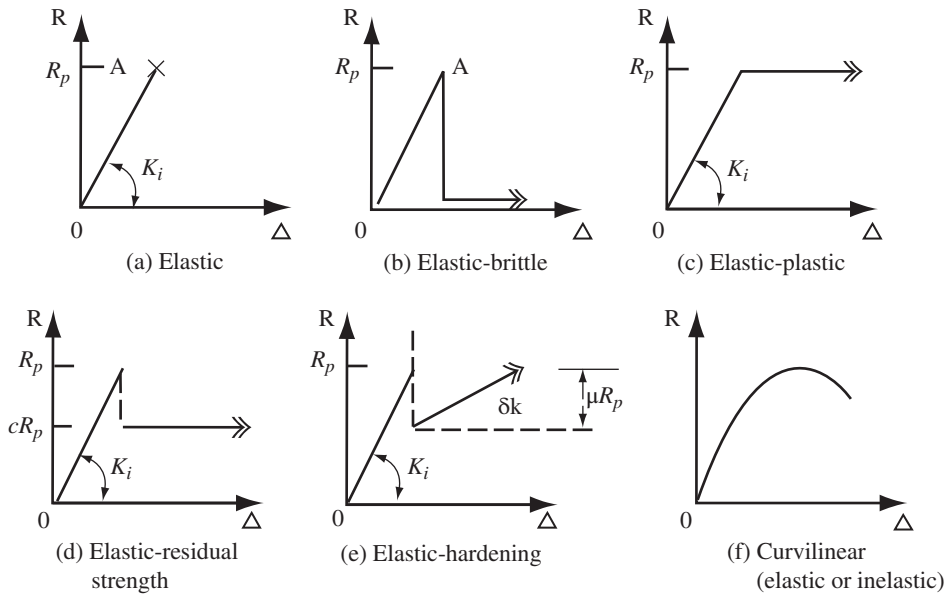
Figure 5.2 Various strength-deformation (R-Δ) relationships.

structure, or of any one element, is considered to be identical with structural system failure. Although clearly unrealistic for most structures, it is nevertheless a convenient idealization.

When one load (or one fully dependent load system) acts on a structure, the location of the peak stress or stress resultant can be identified from an appropriate analysis, such as an elastic stress analysis. For this, the use of deterministic elastic properties and dimensions is often adequate owing to the very low coefficient of variation associated with these variables (see Chapter 8). Typically, the location of the peak stress (resultant) will depend on the magnitude of the load (system), and several candidate locations or members may need to be considered. For large structures, such identification may not be easy by inspection alone.

Brittle failure of a member does not always imply structural failure owing to redundancy of the structure. The actual member behaviour therefore can be better idealized as 'elastic-brittle' indicating that deformation at zero capacity is possible for a member, even after the peak capacity has been reached (Figure 5.2(b)).

Elastic-plastic member behaviour (Figure 5.2(c)) allows individual members or particular regions within a structure to sustain the maximum stress resultant as deformation occurs. When the elastic member stiffness K_i approaches infinity, this behaviour is the well-known idealized 'rigid-plastic' behaviour. A generalization of both elastic-brittle and elastic-plastic behaviour is elastic-residual strength behaviour (Figure 5.2(d)) and a further generalization is elastic-hardening (or softening) behaviour (Figure 5.2(e)). The latter may be seen as an approximation to general behaviour including post-buckling effects. Even without introducing reliability concepts, the analysis of structures with these latter behaviours is complex. Of course, general non-linear (curvilinear) strength-deformation relationships (Figure 5.2(f)) present even more difficulty.

5.2.1.3 System Modelling

Even in conventional deterministic structural analysis, the actual structural system is simplified for analysis. For example, in framed structures the members are idealized by their centroids, the connections are idealized as points, and critical sections for strength or stress checking are taken only at a finite number of pre-defined points in the frame. Similarly, the loads are modelled as point loads or limited forms of continuous loads. When the loads are not point loads, the critical points for safety checking may vary with load combination and intensity.

Structural system failure (as distinct from individual member or material failure) may be defined in a number of different ways, including:

(a) maximum permissible stress reached anywhere ($\sigma(x) = \sigma_{\text{max}}$);
(b) (plastic) collapse mechanism formed (i.e. zero structural stiffness attained: $|\mathbf{K}| = 0$);
(c) limiting structural stiffness attained ($|\mathbf{K}| = K_{\text{limit}}$);
(d) maximum deflection attained ($\Delta = \Delta_{\text{limit}}$);
(e) total accumulated damage reaches a limit (e.g. as in fatigue).

Structural failure modes that consist of the combined effects of two or more member (or cross-section) failure events, such as for statically indeterminate structures, are of particular interest in the determination of structural systems reliability.

When all the different failure modes for the structural system have been identified, the various events (member or cross-sectional failures) contributing to these failure modes may be enumerated systematically using the 'fault-tree' concept. An example of a fault tree is shown in Figure 5.3(b) for the elementary structure of Figure 5.3(a).

The procedure is to take each structural system failure event and to decompose it into contributing sub-events, which themselves are decomposed in turn. The lowest sub-events in the tree correspond, for structures, to failure of individual members or cross-sections. At this level (if not earlier) local limit state equations can be written. Fault-tree methodology has found most application in general, rather than structural systems, reliability analysis but clearly is applicable also to structural reliability [Henley and Kumamoto, 1981; Stewart and Melchers, 1997]. These methods also suggest possibilities for simplification of the structural system, such as restricting the number of
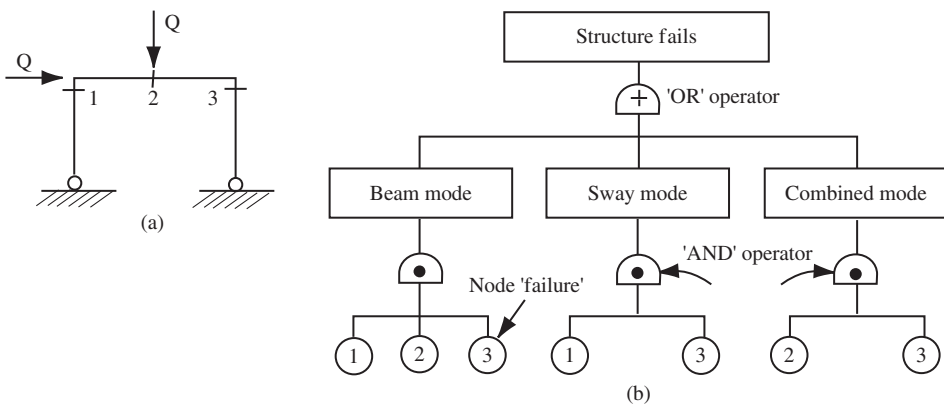

Figure 5.3 Fault tree representation.

potential failure modes, that is, the number of limit states that are developed for the structural system.

For the particular case of rigid-plastic structural systems the traditional approach for failure mode identification is that of combination of elementary mechanisms. These can be obtained systematically, for example using an algorithm proposed by Watwood (1979). An alternative is to use an algorithm that determines all the collapse mechanisms (elementary and combinations) such as proposed by Gorman (1981).

Evidently, these various aspects of system modelling introduce a subjective element to the reliability analysis of structural systems. One way of handling this aspect is to introduce a modelling error. Thus it may be appropriate to represent a real system with an idealization such as rigid-plastic behaviour [e.g., Ditlevsen and Arnbjerg-Nielsen, 1992].

For simplicity, discussion in much of this chapter will be confined to framed structures such as trusses and rigid frames. These are essentially 'one-dimensional systems'. For two-dimensional systems such as plates, slabs and shells, and for three-dimensional continua such as earth embankments and dams the same general principles apply although the actual problem formulation and execution might be more complex.

5.2.2   Solution Approaches

For the reliability analysis of multi-member structures (or structures which can be idealized as such) there are, in principle at least, two complementary approaches that can be adopted [Bennett and Ang, 1983]. These are the 'failure modes' approach and the 'survival' modes approach.

5.2.2.1   Failure Mode Approach

The failure mode approach is based on the identification of all possible failure modes for the structure. A common example is the collapse mechanism technique for ideal plastic structures. Each mode of failure for the structure will normally consist of a sequence of member 'failures' (i.e. the reaching of an appropriate member limit state) sufficient to cause the structure as a whole to reach a limit state such as (a)–(e) above. The possible ways in which this might occur can be represented by an 'event tree' (Figure 5.4) or as a 'failure graph' (Figure 5.5). Each branch of the failure graph represents the failure of a member of the structure, and any complete forward path through the branches starting from the 'intact structure' node and concluding at the 'failure' node represents a possible sequence of member failures. This information is also conveyed in the event tree.

Since failure through any one failure path implies failure of the structure, the event 'structural failure' F_S is the union of all m possible failure modes:

$$p_f = P(F_S) = P(F_1 \cup F_2 \cup \ldots \cup F_m) \tag{5.1}$$

where F_i is the event 'failure in the i th mode'. For each such mode, a sufficient number of members (or structural 'nodes') must fail; thus

$$P(F_i) = P(F_{1i} \cap F_{2i} \cap \ldots \cap F_{ni}) \tag{5.2}$$

where F_{ji} is the event 'failure of the j th member in the i th failure mode' and n_i represent the number of members required to form the i th failure mode. For the simple example of Figure 5.3(a), there are $m = 3$ failure modes, and $n_1 = 3$, $n_2 = 2$, $n_3 = 2$.
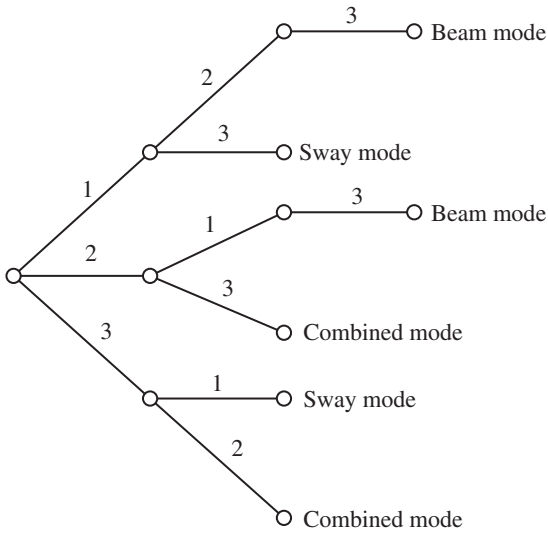
Figure 5.4 Event-tree representation for structure of Figure 5.3(a).
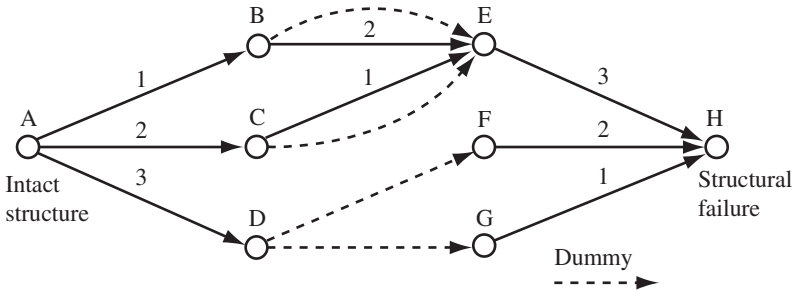
Figure 5.5 Failure-graph representation for structure of Figure 5.3(a).

5.2.2.2 Survival Mode Approach

The survival mode approach is based on identifying various states (or modes) under which the structure survives. For the structure of Figure 5.3(a), each of A, B, C, D, E, F, G (but not H!) in the failure graph Figure 5.5 represents such a state (see also Figure 5.4). For each survival mode the structure has partially failed but is still capable of supporting the load (i.e. it is still statically and geometrically stable).

Survival of the structure requires survival in at least one survival mode, or

$$p_s = P(S_S) = P\left(S_1 \cup S_2 \cup \ldots \cup S_k\right) \tag{5.3}$$

where S_S is the event 'structural survival' and S_i the event 'structural survival in mode i', $i = 1, \ldots, k$, with k not equal to the final node index.

From (A.5) it follows that

$$p_f = P(\bar{S}_1 \cap \bar{S}_2 \cap \ldots \bar{S}_k) \tag{5.4}$$

@Seismicisolation

where $\overline{S}_i$ is the event 'structure does not survive in survival mode i'. Clearly, to attain survival in any particular survival mode all the members contributing to that survival mode must survive. For example, survival in mode B of Figure 5.4 requires member 3 to survive.

It follows that failure to survive in a given survival mode is equivalent to failure of a sufficient number of the contributing members, or

$$P(\overline{S}_i) = P\left(F_{1i} \cup F_{2i} \cup \dots \cup F_{\ell_i\, i}\right) \tag{5.5}$$

where F_{ji} is the event 'failure of the *j* th member in the *i* th survival mode' and where ℓ_i represent the number of members required to ensure survival of the *i* th survival mode. Some results have been given for structural systems composed of ideal rigid-plastic members [Bennet and Ang, 1983].

The survival mode approach has received much less attention in the literature than the failure modes approach, perhaps in part owing to difficulties in conceptualization of survival modes and in formulating the limit state equations and in part owing to the difficulty of generating a truly lower bound stress field to satisfy the requirements for the survival mode. For this reason, it will not be explored further herein.

5.2.2.3   Upper and Lower Bounds—Plastic Theory

It follows directly from (5.1) and (5.5) that any estimate of the probability of structural system failure based on failure modes will be un-conservative (i.e. tend to underestimate p_f) unless all possible failure modes have been included in the analysis; conversely, the failure probability based on the survival mode approach (5.4) will be conservative (i.e. tend to overestimate p_f) unless all possible survival modes have been incorporated in the analysis.

When these statements are applied to rigid-plastic structures, statements analogous to the well-known bounding theorems of ideal plastic (limit analysis) materials are obtained [Augusti and Baratta, 1972; Augusti, 1980; Baratta, 1995]. Thus, if the intensity of all the loads acting on a structure depends on only one factor $w \geq 0$ the probability of the plastic collapse event $\{E_k\}$ for the *k* th collapse mode can be written as $\text{Prob}\{E_k\} = P_k(w)$. Evidently, if there are *n* failure modes possible for the structure, then $P(w) = \text{Prob}\{E\} = \text{Prob}\{E_1 \cup E_2 \cup \dots E_n\}$ denotes the probability of failure for the structural system as a whole (*cf*. 5.5). If the set of size γ denotes a subset of the total plastic collapse event set of size *n* then the application of such a subset of failure modes will imply failure of the system. However, the probability of such a subset occurring is lower than that of the complete set, or

$$P_\gamma(w) \leq P(w) \tag{5.6}$$

This is the first bounding theorem (kinetic theorem). It is rather obvious and is widely used in an intuitive way.

In classical plastic limit analysis a dual approach is the 'static' or equilibrium approach, stating that a structure does not fail if there exists at least one statically admissible stress field, that is, a stress field in equilibrium with the applied loads and which nowhere violates the local yield conditions of the material. Suppose now that there exist at least one such stress field.

If *D* denotes the event that none of a set of stress fields which are investigated turns out to be admissible, then by the static theorem this implies failure of the system.

The probability of this occurring can be written as $\text{Prob}\{D\} = P_\psi(w)$. It then follows immediately that

$$P(w) \leq P_\psi(w) \tag{5.7}$$

which is the second bounding theorem of probabilistic limit analysis (static theorem). Its application has not been extensively explored, but see Augusti (1980), Ditlevsen and Bjerager (1984), Melchers (1983b) and Wang et al. (1995) for examples.

5.2.3 Idealizations of Structural Systems

Structural systems or their sub-systems may be idealized into two simple categories: series and parallel. Some structural systems will consist of combinations of these, and others still will be more complex, containing conditional aspects as well. The idealizations are discussed below, together with some simple results.

5.2.3.1 Series Systems

In a series system, typified by a chain, and also called a 'weakest link' system, attainment of any one element limit state constitutes failure of the structure (Figure 5.5). For this idealization the precise material properties of the elements or members do not matter. If the members are brittle, failure is caused by member fracture; if the members have a plastic deformation capacity, failure is by excessive yielding. It is evident that a statically determinate structure is a series system since the failure of any one of its members implies failure of the structure. Each member is therefore a possible failure mode. It follows that the system failure probability for a weakest link structure composed of m members is [Freudenthal, 1961; Freudenthal et al., 1966]:

$$p_f = P\left(F_1 \cup F_2 \cup F_3 \cup \ldots \cup F_m\right) \tag{5.8}$$

Comparison with (5.1) shows that the series systems formulation (5.8) is of the 'failure mode' type.

If each failure mode $F_i(i = 1, m)$ is represented by a limit state equation $G_i(\mathbf{x}) = 0$ in basic variable space, the direct extension of the fundamental reliability problem (1.31) is

$$p_f = \int_{D \in \mathbf{X}} \ldots \int f_{\mathbf{X}}(\mathbf{x}) \, d\mathbf{x} \tag{5.9}$$
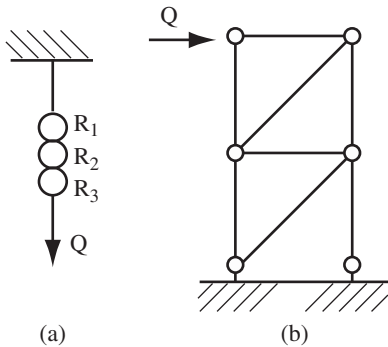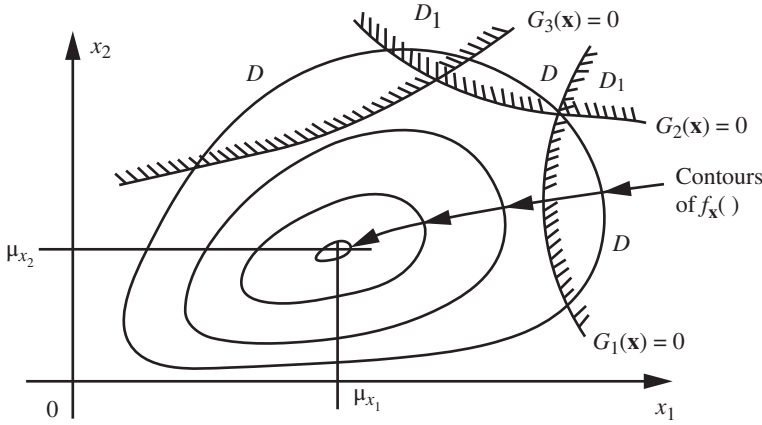

Figure 5.6 Example series systems.

Figure 5.7 Basic structural system reliability problem in two dimensions showing failure domain D (and D_1).

where $\mathbf{X}$ represents the vector of all basic random variables (loads, strengths of members, member properties, sizes, etc.) and D (and D_1) is the domain in $\mathbf{X}$ defining failure of the system. This is defined in terms of the various failure modes as $G_i(\mathbf{X}) \leq 0$. In two-dimensional $\mathbf{x}$ space, expression (5.9) is defined in Figure 5.7 with D and $G_i(\mathbf{X}) \leq 0$ shown shaded.

Let the safe (or survival) region be denoted $\overline{D}$. Evidently, it is the complement of the failure regions shown as D and D_1 in Figure 5.7. $\overline{D}$ is given by

$$\overline{D}: \quad \overline{F}_1 \cap \overline{F}_2 \cap \ldots \cap \overline{F}_m \tag{5.10}$$

where $\overline{F}_i$ is defined as 'survival in mode i' or $G_i(\mathbf{X}) \geq 0$. The probability of survival is then

$$p_s = P\left(\bigcap_{i=1}^{m} \overline{F}_i\right) = \int_{\overline{D}} \ldots \int f_{\mathbf{X}}(\mathbf{x}) d\mathbf{x} \tag{5.11}$$

clearly indicating that this formulation is equivalent to the 'survival mode' approach of Section 5.2.2.

A particularly simple result can be derived immediately without recourse to the integrations required by (5.9) or (5.11) above. For the chain of Figure 5.6 the load effect S in each link of the chain is identical with the load Q. If $F_{R_i}(r)$ is the cumulative distribution function for the strength of the i th link, then the cumulative distribution function $F_R()$ for the chain as a whole is given by

$$F_R(r) = P(R \leq r) = 1 - P(R > r)$$
$$= 1 - P\left(R_1 > r_1 \cap R_2 > r_2 \cap \ldots \cap R_m > r_m\right)$$

which, for independent strength properties, becomes

$$F_R(r) = P(R \leq r) = 1 - [1 - F_{R_1}(r_1)].[1 - F_{R_2}(r_2)] \ldots$$
$$= 1 - \prod_{i=1}^{m} \left[1 - F_{R_i}(r_i)\right] \tag{5.12}$$

This expression forms the basis for the probability distribution of the mechanical resistance of perfectly brittle materials [Weibull, 1939]. When each R_i is identically and normally distributed, the distribution of R as m approaches infinity is given by the type III extreme value distribution for the smallest value (see section A.5.13).

The series system model is appropriate for a redundant structure such as a redundant truss or framework if there are only a small number of members and these members are brittle. In this case, failure of one member will usually lead to a redistribution of internal actions which then triggers failure in another member, and so on. In this case the probability of failure for the whole structural system is well approximated by the probability of failure of the first (brittle) member(s) [Moses and Stevenson, 1970]. However, this is not a good approximation when there is a large number of redundant brittle members since then the reserve strength can be quite significant.

Example 5.1   Consider the chain (series system) shown in Figure 5.6(a) consisting of three links of strength $R_i(i = 1, 2, 3)$ described only by the first two moments (μ_i, σ_i) as $(110, 20)$, $(140, 10)$ and $(68, 5)$. The cumulative distribution function for the load capacity $F_Q(\ )$ can then be expressed as follows and the probability of failure for a given value of a deterministic load of $Q = 50$ may be determined, and the rest follows.

For a given value of applied load $Q = q$, say, the probability that the capacity of the system will be less than this value is given by:

$$\text{Prob}[Q < q] = \text{Prob}\left[(R_1 < q) \cup (R_2 < q) \cup (R_3 < q)\right]$$

which becomes, for independent links in the chain:

$$F_Q(q) = P(R_1 - q < 0) + P(R_2 - q < 0) + P(R_3 - q < 0)$$

For a given value $Q = q$ the probability of failure then becomes, using second-moment theory and Appendix D:

$$p_f = F_Q(q) = \Phi\left(\frac{q - \mu_1}{\sigma_1}\right) + \Phi\left(\frac{q - \mu_2}{\sigma_2}\right) + \Phi\left(\frac{q - \mu_3}{\sigma_3}\right)$$

or

$$p_f = \Phi\left(\frac{50 - 110}{20}\right) + \Phi\left(\frac{50 - 120}{10}\right) + \Phi\left(\frac{50 - 68}{5}\right)$$

$$p_f = \Phi(-3) + \Phi(-7) + \Phi(-3.5) = (0.135 + 0.0233 + \text{neg1.}) \times 10^{-2} = 0.16 \times 10^{-2}$$

5.2.3.2   Parallel Systems—General

When the elements in a structural system (or subsystem) behave in such a way or are so interconnected that the reaching of the limit state in any one or more elements does not necessarily mean failure of the whole system, the system is said to be a 'parallel' or 'redundant' system. Two simple parallel systems are shown in Figure 5.8.

Redundancy in systems may be of two types. 'Active redundancy' occurs when the redundant member(s) participates in structural behaviour even at low loading. 'Passive (or stand-by or fail-safe) redundancy' occurs when the redundant member(s) does not participate in structural behaviour until the structure has suffered a sufficient degree of degradation or failure of its members.
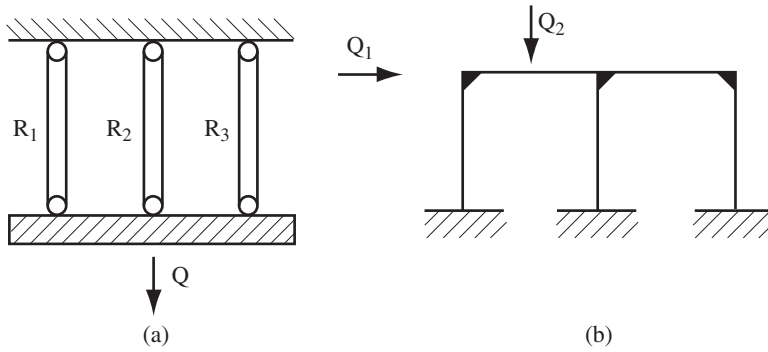
Figure 5.8 Simple parallel systems: (a) parallel members (b) rigid-plastic frame.

Whether active redundancy is beneficial depends on the behaviour characteristics of the members or elements and how failure is defined. For ideal plastic systems, the 'static theorem' guarantees that active redundancy cannot reduce the reliability of a structural system [Augusti and Barratta, 1973]. Hence it is beneficial.

With active redundancy, the failure probability of an n component parallel (sub-)system is given by

$$p_f = P(F_S) = P(F_1 \cap F_2 \cap \ldots \cap F_n) \tag{5.13}$$

where F_i is the event 'failure of the i th component'. It follows immediately that (5.13) is equivalent to (5.4), and can be represented in **x** space by

$$p_f = \int_{D_1 \in X} \ldots \int f_{\mathbf{X}}(\mathbf{x}) \, d\mathbf{x} \tag{5.14}$$

as shown in Figure 5.7 for the intersection domains D_1.

In contrast with the situation for series systems, a parallel system can fail only when all its contributory components have reached their limit states. This means that the behavioural characteristics of the system components are of considerable importance in defining 'system failure'. This is illustrated in Example 5.2.

Example 5.2 Consider the idealized parallel system (Figure 5.9) in which all the elements are brittle, with different fracture strains ε_f. The maximum load Q that can be supported at any particular strain level ε is given by

$$R_{sys} = \max_{\varepsilon} \left[R_1(\varepsilon) + R_2(\varepsilon) + R_3(\varepsilon) \right] \tag{5.15}$$

where $R_i = A_i \sigma_i(\varepsilon)$ for $i = 1, 2, 3$. Here A_i represents cross-sectional area and σ_i represents stress.

Since each resistance R_i ($i = 1, 2, 3$) is a random variable, it is not easy to apply expression (5.15) since each possible state $\varepsilon_{f1}, \varepsilon_{f2}$ and ε_{f3} must be considered as a possible state of maximum capacity. This means that all possible combinations of failed and surviving members must be considered:

$$R_{sys} = \max \left\{ [R_1(\varepsilon_{f2}) + R_2(\varepsilon_{f2}) + R_3(\varepsilon_{f2})], \ [R_1(\varepsilon_{f1}) + R_3(\varepsilon_{f1})], \ R_3(\varepsilon_{f3}) \right\} \tag{5.16}$$
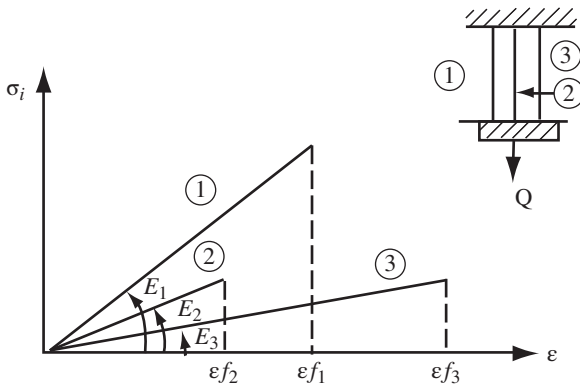
Figure 5.9 Brittle material behaviour in parallel system.

and when R_{sys} is known, the failure probability for the system is

$$p_f = P(R_{sys} - Q < 0) \tag{5.17}$$

In order to evaluate (5.17) the probability density or cumulative distribution function for R_{sys} must be known. By comparison to (5.13), it is obtained from (5.16) as [Hohenbichler and Rackwitz, 1983b]

$$
\begin{aligned}
F_{R_{sys}}(r) &= P\left\{ \max_{\varepsilon_{fi}} \left[\sum_{i=1}^{n} R_i(\varepsilon_{fi}) \right] \le r \right\} \\
&= P\left\{ \bigcap_{\varepsilon_{fi}} \left[\sum_{i=1}^{n} R_i(\varepsilon_{fi}) - r \le 0 \right] \right\}
\end{aligned} \tag{5.18}
$$

In general, evaluating this type of expression is not straightforward. When all [ ] terms can be approximated as, or converted to, standard Normal, the methods described in Appendix C may be employed.

A special case of practical importance occurs when the elastic modulii E_i of the brittle members in Figure 5.9 are identical. In this case it can be shown that the probability distribution for R_{sys} approaches a Normal distribution as n approaches infinity [Daniels, 1945].

5.2.3.3 Parallel Systems—Ideal Plastic

In parallel systems of low redundancy and with brittle elements, failure of one element often is sufficient to cause failure of the system. Unless the failed element contributed very little to the system strength immediately prior to its failure, the load redistribution caused by it usually leads to overloading of other elements in sequence (causing so-called 'progressive collapse'). This has led to the common assumption that, with brittle members, failure of the most highly stressed member even for a parallel system is tantamount to failure of the system.

The situation is completely different for ideal plastic structures, such as rigid frames (Figure 5.8(b)), for which each collapse or failure mode (i.e. limit state) can be

represented by an equation of the following type:

$$\sum_i Q_i \Delta_i - \sum_j M_j \theta_j = 0 \tag{5.19}$$

where Q_i $(i = 1, \dots)$ are the external loads, Δ_i are the deflections corresponding to Q_i (a function of θ_j and dimensions), M_j is the plastic moment resistance at section $j = 1, \dots$ and θ_j is the plastic rotation at section j. Expression (5.19) clearly is of the 'parallel' type since each resistance M_j must be mobilized to develop the total resistance against the loading Q_i.

Collectively, a set of failure mode equations, each like (5.19), constitutes a series system since the structure will fail when any one failure mode (collapse mode) occurs. It follows that plastic moment capacities M_j may occur in more than one failure mode expression. This means that the structural capacities obtained from different failure modes may be correlated. (Note that this is quite distinct from any correlation that may exist between individual M_j values.)

Example 5.3   Consider the parallel member system shown in Figure 5.8(a). Let there be n members with each member assumed to take an equal proportion of the load and each member assumed to have ideal rigid-plastic behaviour. Let the plastic resistance R_i, $i = 1, \dots, n$, of each member be identical and be a Normal distributed random variable with mean value $\mu_i = \mu$ and standard deviation $\sigma_i = \sigma$. For independent members, the total load capacity for the system is then given by

$$R_S = \sum_{i=1}^{n} R_i \tag{5.20}$$

and from (A.160) and (A.162) it follows that the mean and variance are

$$\mu_S = \sum_{i=1}^{n} \mu_i = n\mu \qquad \sigma_S^2 = \sum_{i=1}^{n} \sigma_i^2 = n\sigma^2 \tag{5.21}$$

for equal member mean and member variance. It follows readily that the standard deviation of the total capacity is given by $\sigma_S = \sqrt{n}\,\sigma$. This shows that the variance of the total system capacity increases with the number of members if their strengths are independent. Of course, the total capacity also increases with increased number of members. Hence another way of expressing this is to rewrite the result in terms of the coefficient of variation $V_i = \sigma_i / \mu_i$. The equivalent expression is then

$$V_S = \frac{1}{\sqrt{n}} V \tag{5.22}$$

If the strengths of the members are not independent, the expressions in (5.21) must be replaced with (A.160) and (A.161) or (A.162) with an appropriate value for the covariance. In the special case when there is complete dependence between member strength, such as when they are all taken from the one piece of homogeneous material, $\rho_{ij} = 1$ in (A.162). It is easily shown that in this case the variance in (5.21) becomes $\sigma_S = n\sigma$ and that (5.22) becomes $V_S = V$, i.e. there is no advantage in increasing the number of members.

It is left as an exercise for the reader to show that if the problem were rephrased to seek the effect of increasing the number of independent members while holding the system capacity to a given mean value, the system standard deviation would be given by $\sigma_S = \sigma/\sqrt{n}$. This and the previous result (5.22) show that the random variability of the overall strength of the system decreases indefinitely as the number of independent redundant members in parallel increases. In other words, the effects of individual high or low member strengths tends to vanish. This is an important result [Moses, 1974].

Example 5.4 The rigid-plastic portal frame shown in Figure 5.10 is loaded by two random variable loads, H and V, and has random variable moment capacities M_i, $i = 1, \ldots, 4$. The limit state equations are defined by the four plastic collapse modes shown in Figure 5.10(a-d):

$$
\begin{array}{llllllll}
\text{mode a:} & M_1 & & +2M_3 & +2M_4 & -H & -V & = 0 \\
\text{mode b:} & & +M_2 & +2M_3 & +M_4 & & -V & = 0 \\
\text{mode c:} & M_1 & +M_2 & & +M_4 & -H & & = 0 \\
\text{mode d:} & M_1 & +2M_2 & +2M_3 & & -H & +V & = 0
\end{array}
\tag{5.23}
$$

Let each random variable $X_i = (M_1, M_2, \ldots, H, V)$ be Normal distributed, with properties $\mu_{X_i} = (1.0, 1.0, 1.0, 1.0, 1.0, 1.0)$ and $\sigma_{X_i} = (0.15, 0.15, 0.15, 0.15, 0.17, 0.50)$. The β index for each collapse mode can be obtained using the FOSM concepts of Chapter 4. These give, for mode a:

$$
G(\mathbf{X}) = M_1 + 2M_3 + 2M_4 - H - V
$$

so that

$$
\mu_G = 1 + 2 + 2 - 1 - 1 = 3
$$

and

$$
\sigma_G^2 = (0.15)^2 + 2^2(0.15)^2 + 2^2(0.15)^2 + (0.17)^2 + (0.5)^2 = 0.4814
$$

Thus

$$
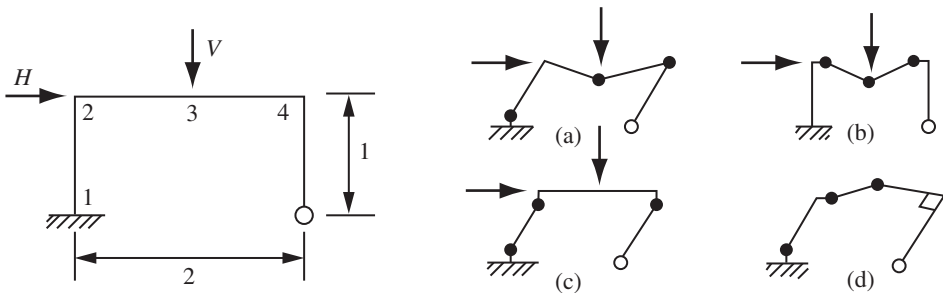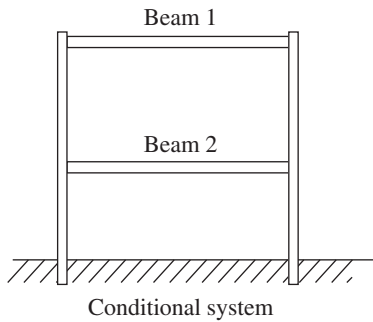\beta_a = \frac{\mu_G}{\sigma_G} = \frac{3}{\sqrt{0.4814}} = 4.32.
$$

Figure 5.10 Rigid frame and collapse modes: Example 5.4.

Figure 5.11 Conditional system.

The β indices for modes b, c and d may be determined similarly; $\beta_b = 4.83$, $\beta_c = 6.44$ and $\beta_d = 7.21$. Since the same plastic moments are involved in a number of collapse modes, the limit state expressions and hence the safety indices are not independent. How these results for individual failure modes can be combined is considered in Example 5.6.

5.2.3.4 Combined and Conditional Systems

A real structural system usually requires both series and parallel subsystems for its complete specification. For example, a redundant structure having brittle members may not fail if one of the brittle elements fails. Conversely, it might be possible for the system to fail before all the brittle members have failed. The combination of member and sub-system failure is important in specifying limit states for a structure. For complex structures this is not a simple task, in part due to the redistribution of internal actions within the structure as members fail and in part because the loading usually also changes with time and with structural response (e.g. if the structure deflects). The graph-theoretical cut-set (series system) and tie-set (parallel) representation used extensively in classical reliability theory is therefore not particularly helpful in a structural reliability context. When the loads can be represented as random variables and the precise order of member failure is not critical, recourse can be made to methods such as those discussed in Section 5.6.

The modelling of a real structural system also may require the use of conditional (sub-) systems. The latter arises if the failure of one independent element or group of elements affects the likelihood of failure of other elements or element groups. For example, in Figure 5.11, if the upper beam collapses, it may affect the performance and reliability of the lower beam (since the lower beam may be damaged and will be subject to extra load) [Benjamin, 1970]. In this situation, the failure probabilities of the structural elements are dependent on the behaviour of the structure under extreme events. Provided that the sequence of events can be enumerated, it is evident that a structure with conditional events can be reduced to one containing both 'series' and 'parallel' element groups or sub-systems.

Example 5.5   Consider a single-span three-girder bridge. Investigations show that it will fail if any two adjacent girders G_i fail, or if any deck panel D fails or if either (or both) of its abutments A_j fail. The abutments could fail through failure of its two bored

piles P_k or through overturning O. This set of scenarios can be expressed as

$$p_f = P\left[(G_1 \cap G_2) \cup (G_2 \cap G_3) \cup D \cup A_1 \cup A_2\right]$$

where

$$D = \underset{i}{\cup} D_i$$

and

$$A_j = (P_{1j} \cap P_{2j}) \cup O_j$$

with obvious notation.

5.3 Monte Carlo Techniques for Systems

5.3.1 General Remarks

The following section builds directly on the discussion of Monte Carlo techniques given in Chapter 3. The concepts described there can be used to deal with the calculation of systems reliability. Section 5.3.2 extends the importance sampling approach of Section 3.4 to structural systems for which failure is defined by multiple limit state functions. The discussion includes comments about search-type techniques (Section 3.4.5) in cases where the points of maximum likelihood are not known initially.

In Section 5.3.3 brief comments are made about the extension of directional simulation (Section 3.5) to systems, and in Section 5.3.4 a more detailed description is given of the extension of directional simulation in the load space (Section 3.5.4) to structural systems. The latter approach appears to be particularly suited for systems as distinct from the original directional simulation approach. In this context some comments are made also about the use of finite element and other complex structural analyses techniques.

5.3.2 Importance Sampling

5.3.2.1 Series Systems
The probability of failure represented by (5.9) can be rewritten as:

$$p_f = \int \dots \int I[\ ] f_{\mathbf{X}}(\mathbf{x}) d\mathbf{x} \tag{5.24}$$

where the indicator function I[ ] for a series system is generalized from (1.33) and (3.6) to

$$
\begin{aligned}
I\left[\overset{m}{\underset{i=1}{\cup}} G_i(x) \le 0\right] &= 1 \quad \text{if [ ] is true} \\
&= 0 \quad \text{if [ ] is false}
\end{aligned}
\tag{5.25}
$$

where $G_i(\mathbf{x}) = 0$ represents the i th (known) limit state function, $i = 1, \dots, m$.

For a two-dimensional $\mathbf{x}$ space, $I[\ ]$ represents the integration domain abcd of Figure 5.12(a), i.e. a sample point $\hat{\mathbf{x}}$ lies in the failure region if any one $G_i(\mathbf{x}) \le 0$. This formulation is directly applicable if the 'crude' Monte Carlo approach is used. It is also immediately applicable in the case of importance sampling.
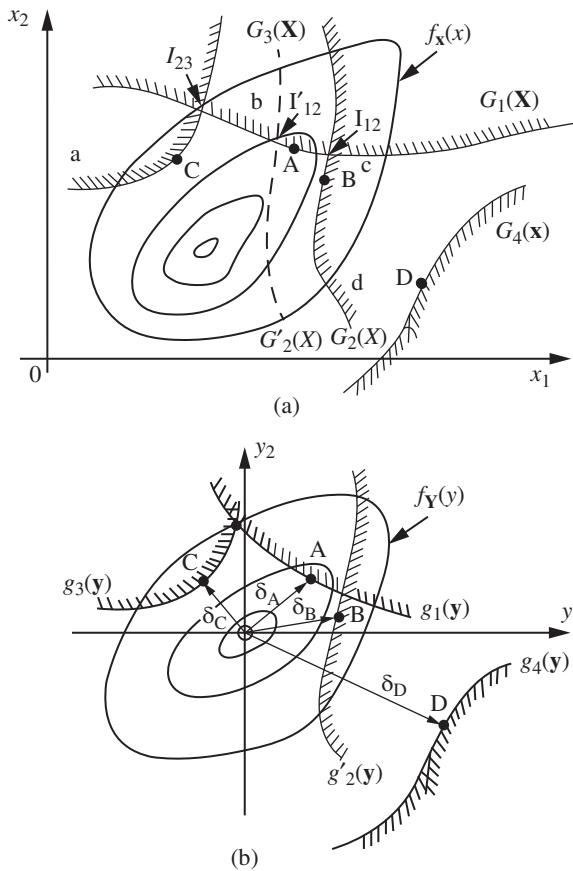
Figure 5.12 Two variable system problems: (a) original space; (b) hypothetical standardized space, with failure regions shown hatched.

The integration of (5.24) using importance sampling was described by (3.17) for one limit state function. Where there are m different limit state functions as in a structural system, it is unlikely to be sufficient to use a uni-modal sampling density function. Very large errors can be introduced this way [Melchers, 1991]. Instead, a useful approach is to use the multi-modal sampling function [Melchers, 1984, 1990a]:

$$h_{\mathbf{V}}( ) = a_1 h_{\mathbf{V}1}( ) + a_2 h_{\mathbf{V}2}( ) + a_3 h_{\mathbf{V}3}( ) + \ldots + a_m h_{\mathbf{V}m}( ) \tag{5.26}$$

with

$$\sum_{i}^{m} a_i = 1$$

where the a_i are weighting coefficients. Each component $h_{\mathbf{V}i}( )$ is selected for the i th limit state in the same way as for an individual limit state, with most interest being the regions contributing the greatest probability density for the limit state. Points such as A, B, C and D in Figure 5.12(a) represent the points of maximum likelihood (probability density),

and these may be used as surrogates for these regions (see Section 3.4.6.2). They have the advantage of being obtainable systematically, such as through search techniques (see below) or approximate FOSM analysis [Melchers, 1989a].

   Normally, not all limit states will be of equal importance for a reliability analysis. This can be taken into account by appropriate selection of the weighting coefficients a_i. In particular, the calculations will be simplified if those limit states which contribute in only a minor way to p_f can be identified. One way in which this can be done is with reference to FOSM concepts. The suggested algorithm runs as follows [Melchers, 1984, 1990a].

(a) For each limit state i determine $\mathbf{x}_i^*$, the point in n -dimensional $\mathbf{x}$ space having the highest probability density $f_{\mathbf{X}}( )$ consistent with $G_i(\mathbf{X}) \leq 0$.

(b) For each $\mathbf{x}_i^*$, calculate $\delta_i = \left[\sum_{j=1}^{n} (y_j^*)_i^2 \right]^{1/2}$ with $(\mathbf{y}^*)_i$ given by $y_j^* = \left(x_j^* - \mu_{Xj} \right) / \sigma_{Xj}$ (i.e.

   a 'standardized' space such as shown in Figure 5.12(b) might be visualized in which the relative importance of each limit state function is considered).

(c) Ignore all limit state functions for which $\delta_i > \delta_L$ where δ_L is some arbitrarily chosen limit. As a first-order approximation, the error in p_f associated with any limit state which is ignored in this way is given by $p_{\text{error}} \approx \Phi(-\delta_L)$.

(d) For the remaining k limit states, use (5.26) as the sampling function in (5.24) with a_i chosen on the basis of the δ_i values.

   The total number of sample points required in this approach if M points are to fall in the failure region is 2kM, which is considerably less than M/p_f required for 'crude' Monte Carlo' simulation, unless k is extremely (and impracticably) large.

   When the limit states are closely clustered over all or part of the region of integration, one sampling function $h_{\mathbf{V}}( )$ may be used for such limit states considered as a group. Such an approach might be invoked when the distance Δ_{ij} between any two 'checking points' i and j in the hypothesized 'standardized' space, given, in $k = 1, \dots , n$ space, by

$$\Delta_{ij} = \left[\sum_{k=1}^{n} \left(y_{ki}^* - y_{kj}^* \right)^2 \right]^{1/2} \tag{5.27}$$

is less than some criterion Δ_C, say. In this expression y_{ik}^* represents the k th component for the i th checking point. The suggested coordinates for $h_{\mathbf{V}}( )$ would be the mean of x_i^*, x_j^*. This concept is readily extendable to situations with more than two-limit-state 'checking points' in a cluster. A suggested criterion Δ_C might be one standard deviation in $\mathbf{Y}$ space.

5.3.2.2 Parallel Systems
For parallel systems the probability content associated with the intersection of two or more (i.e. k) limit states is given by (5.14), which may be rewritten in the form (5.24) but with $I[\ ]$ defined as

$$I \left[\bigcap_{i=1}^{k} G_i(\mathbf{x}) \leq 0 \right] \tag{5.28}$$

Typically, the regions of most interest are those that are bounded by the appropriate limit state functions and are near their intersection. Again, appropriate surrogates for these regions and which are systematically determinable are the co-ordinates of the intersection(s) of the appropriate limit state functions, such as points I_{12}, I_{23} in the two-dimensional space of Figure 5.12(a). It follows readily that the procedure of the previous section applies but now with I_{ij}, etc., instead of points A, B, etc. for the points of maximum likelihood consistent with (5.28). Since the sampling efficiency may be quite low (e.g. at point I_{23} Figure 5.12(a)), rather more sample points may need to be used.

The point I_{ij} is obtained, of course, directly by equating limit state functions:

$$G_i(\mathbf{x}) = G_j(\mathbf{x}) = 0 \tag{5.29}$$

for a two-dimensional intersection in n (hyper-)space. In general, if the dimension of the intersection is less than that of the (hyper-)space $\mathbf{x}$, then I_{ij} refers to what can be imagined as a 'crease' (or fold) in that space (or a (hyper-)crease in $\mathbf{x}$ space), and the 'checking' point $\mathbf{x}^*$ will then lie along the (hyper-)crease. If the dimension of the intersection equals that of the (hyper-)space, $\mathbf{x}^*$ will be at the 'vertex' formed by the intersection of the limit state functions. In two dimensions this reduces to the points I_{ij} in Figure 5.12(a).

It is important to note, however, that $\mathbf{x}^*$ may not lie at I_{ij}, or along a crease. This may occur where the limit state functions involved in the interaction are significantly different in their contribution to p_f. Consider, for example, limit state $G_2(\mathbf{x})$ translated to the left in Figure 5.12(a), i.e., to the location marked $G_2'(\mathbf{x})$. It is immediately evident that the intersection $G_2'(\mathbf{x}) \cap G_1(\mathbf{x})$ has its greatest probability density at A, and not at I_{12}'. The extension to multidimensional space is obvious: the implication is that the (hyper-)creases are likely points of greatest probability density, and hence good surrogates for the region of interest, but other locations may need to be checked. This may be accomplished using search-type techniques to locate the points of maximum probability density as indicated in Section 3.4.5.

5.3.2.3 Search-Type Approaches in Importance Sampling

Knowledge of the points of maximum likelihood is particularly important in conventional importance sampling (see Section 3.4.1). This implies that the limit state functions must be known before the sampling functions can be selected in a sensible manner. In many problems, however, the system limit state functions $G_i(\mathbf{x}) = 0$ are not known a priori.

The limit state functions and the points of maximum likelihood may be found by application of a generalization of the search-type approaches (see Section 3.4.5) but now to systems described by multiple limit state functions. Usually this will require multiple starting points for the search process. In principle, if there are m limit state functions with candidate points of maximum likelihood, at least m starting points will need to be employed. If one of these starting points then converges to an already determined point of maximum likelihood, another starting point will need to be used. However, there can be no guarantee that all critical points of maximum likelihood will be identified [Bucher, 1988; Melchers, 1989b, 1990a]. The parallel to search-type optimization routines will be obvious.

5.3.2.4 Failure Modes Identification in Importance Sampling

In some problems it may be desired to identify the most common failure modes for a structure, given that the modes of failure for individual members and the failure criteria for the structure have been specified. In principle, this can be done by proper accounting of Monte Carlo results. However, experience shows that rather large samples are required to discriminate between all important modes of failure, particularly when the structural failure probabilities are very low, as is usual for structural reliability. In this case only a few samples tend to fall in the failure regions.

Alternatively, the important limit states can be identified, perhaps, using a preliminary 'crude' sampling strategy on the whole basic variable space. One approach is to use $f_X(\ )$ (or some simplified form of it) as the sampling distribution $h_V(\ )$ but with very much larger coefficients of variation. This tends to spread the region over which sample points are taken and results in rather more samples in the various failure regions [Vrouwenvelder, 1983]. However, as the procedure falls somewhere between crude sampling and good-quality importance sampling, its efficiency is still quite low. For rigid-plastic structural systems a completely different approach is to use a separate algorithm for system failure mode identification (see Section 5.2.1.3).

5.3.3 Directional Simulation

For directional simulation in the **x** space or in the **y** space the discussions of Section 3.5.3 carry over directly with the more general interpretation of the limit state function now defined as the (series) collection of m individual limit states: $\bigcup_{i=1}^{m} G_i(\ ) \leq 0$. With this function describing the system limit state set, there is only one important difference between what is considered in Section 3.5.3 and what is required for the treatment of structural systems. Specifically, for a given individual directional sample, it is likely that several limit state functions will be encountered. As evident (see, for example, Figure 5.7) the governing limit state function is the limit state function first encountered when moving from the safe domain to the unsafe domain. This is implicit in the union expression for the limit states.

Evidently, if the limit states for the structural system are of the general form shown in Figure 5.7, the technique is likely to be more efficient than is the case for linear or near-linear limit state functions for individual elements or members (see Section 3.5.3).

In practical problems the limit state functions may not be explicit, and search techniques may need to be used along the individual directional sample. Such techniques need to be able to differentiate between the various limit state functions that may intersect the directional 'ray'. An application of the technique, and an exposition of some of the details of numerical solution, has been given by Ditlevsen and Bjerager (1989).

5.3.4 Directional Simulation in the Load Space

The theory for directional simulation in the load space follows directly from Section 3.5.4. The only complication is that the procedures for deriving the variation of strength with radial direction will need to be modified to allow for the existence of multiple limit state functions describing the strength of the structural system. Thus, use of either expression (3.45) or (3.46) requires the evaluation of the variation of structural strength with distance along the radial direction, expressed through the probability density function $f_{S|A}(\ )$ or the cumulative distribution function $F_{S|A}(\ )$ (see Figure 3.13).
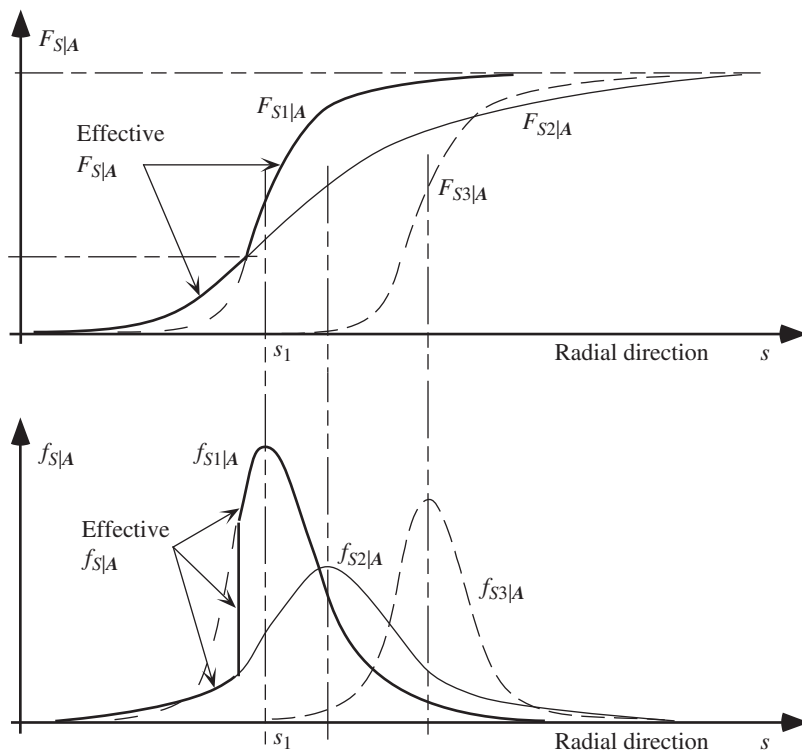
Figure 5.13 Resulting cdf $F_{S|A}(\ )$ and pdf $f_{S|A}(\ )$ in radial direction $\mathbf{A} = \mathbf{a}$ with multiple limit state functions each with a probabilistic representation [Melchers, 1992].

As noted in Section 3.5.4.2, if the limit state expression $G(\mathbf{x}) = 0$ is known explicitly, $f_{S|A}(\ )$ can be evaluated directly by multiple integration along the radial direction S. As a practical alternative, when only the first two moments of the random variables $\mathbf{X}$ contributing to S are known, the first two moments of S can be estimated using second-moment algebra (Section A.11).

The situation becomes more complex if there are several limit state functions. In this case their probability distribution may overlap for any simulation direction $\mathbf{A} = \mathbf{a}$. The effective cdf $F_{S|A}(\ )$ can be obtained by enveloping all component $F_{S_i|A}(\ )$ for each limit state function (which is described in the load space as a probabilistic function, see Figure 3.13). This is shown schematically in Figure 5.13 and becomes:

$$F_{S|A}(\ ) = \sup_{i,S}[F_{S_i|A}(s)] \tag{5.30}$$

The evaluation of $f_{S|A}(\ )$ follows directly as

$$f_{S|A}(\ ) = f_{S_i|A}(\ )\Big|_{F_{S_i|A}(\ )>F_{S_j|A}(\ )} \quad \forall j \neq i \tag{5.31}$$

both of which can be used with little difficulty if numerical methods are used for integration of (3.45) or (3.46).

It might be noted that the possibility of solving structural reliability problems in the load space **Q** treated as a vector of random variables has been explored also in various ways other than directional sampling [Augusti and Baratta, 1973; Schwarz, 1980; Melchers, 1981; Moses, 1982; Gorman, 1984; Lin and Corotis, 1985; and Katsuki and Frangopol, 1994]. In most of these cases, simplified methods of numerical multi-dimensional integration were proposed.

As already noted briefly in Section 3.5.4, the concept of the load space formulation is attractive because it should be possible to include all types of structural behaviour, including non-linear effects, in the analysis. This has been demonstrated for certain complex structures [Moarefzedah and Melchers, 1996b] and for problems involving finite element analysis [Guan and Melchers, 1998]. However, a possible limitation of this approach is that it is assumed that the system limit states do not depend on the load path, that is, on the order in which the loads are applied to the structure [Ditlevsen and Bjerager, 1986; Ditlevsen and Madsen, 1996]. Of course, as discussed in Section 5.1 this limitation is not an issue in the case of a one-parameter load system. It also appears not to be a serious limitation for a range of framed structures. Where these limitations are not satisfied, the system reliability estimation problem becomes much more complex.

5.4   System Reliability Bounds

Rather than to attempt to proceed with the direct integration of expressions (5.9) and (5.14), an alternative approach is to develop upper and lower bounds on the probability of failure of a structural system. Consider a structural system subject to a sequence of loadings and which may fail in any one (or more) of a number of possible failure modes under any one loading in the loading sequence. The total probability of structural failure may then be expressed in terms of mode failure probabilities as (see Section A.1)

$$P(F) = P(F_1) \cup P(F_2 \cap S_1) \cup P(F_3 \cap S_2 \cap S_1) \cup P(F_4 \cap S_3 \cap S_2 \cap S_1) \cup \ldots \quad (5.32)$$

where F_i denotes the event 'failure of the structure due to failure in the i th mode, for all loading' and S_i denotes the complementary event 'survival of the i th mode under all loading' (and hence survival of the structure). Since $P(F_2 \cap S_1) = P(F_2) - P(F_2 \cap F_1) \ldots$, (5.32) may be written also as

$$\begin{aligned} P(F) = P(F_1) + P(F_2) - P(F_1 \cap F_2) + P(F_3) - P(F_1 \cap F_3) \\ - P(F_2 \cap F_3) + P(F_1 \cap F_2 \cap F_3) + \ldots \end{aligned} \quad (5.33)$$

where $(F_1 \cap F_2)$ is the event that failure occurs in both modes 1 and 2, etc.

5.4.1   First-Order Series Bounds

The probability of failure for the structure can be expressed as $P(F) = 1 - P(S)$, where $P(S)$ is the probability of survival. For independent failure modes, $P(S)$ can be represented by the product of the mode survival probabilities, or, noting that $P(S_i) = 1 - P(F_i)$, by

$$P(F) = 1 - \prod_{i=1}^{m} \left[1 - P(F_i) \right] \quad (5.34)$$

@Seismicisolation

where, as before, $P(F_i)$ is the probability of failure in mode i. This result can, by expansion, be shown to be identical with (5.33). Also, it follows directly from (5.33) that, if $P(F_i) << 1$, the terms $P(F_i \cap F_j)$ are negligible and (5.34) can be approximated by [Freudenthal et al., 1966].

$$P(F) \approx \sum_{i=1}^{m} P(F_i) \tag{5.35}$$

In the case where all failure modes are fully dependent, it follows directly that the weakest failure mode will always be the most likely to fail, irrespective of the random nature of the material strength. Hence

$$P(F) = \max_{i=1}^{m} \left[P(F_i) \right] \tag{5.36}$$

Equations (5.34) or (5.35) and (5.36) can be used to define relatively crude bounds on the failure probability of any structural system of the series type when the failure modes are somewhere between completely independent and fully dependent [Cornell, 1967]:

$$\max_{i=1}^{m} \left[P(F_i) \right] \leq P(F) \leq 1 - \prod_{i=1}^{m} \left[1 - P(F_i) \right] \tag{5.37}$$

It has been suggested that for many practical structural systems the series bounds (5.37) tend to be rather wide [*cf*. Grimmelt and Schuëller, 1982].

Example 5.6 For the rigid-plastic frame shown in Figure 5.10 the mode safety indices $\beta_a, \ldots, \beta_d$ were calculated in Example 5.4 as (4.32, 4.83, 6.44, 7.21). From Appendix D, the corresponding (nominal) failure probabilities are $(0.77 \times 10^{-5}, 0.70 \times 10^{-6}, 0.59 \times 10^{-10}, 0.28 \times 10^{-12})$, and from (5.37) the first order system failure probability is then bounded by

$$\max_{i=1}^{m}(p_i) \leq p_f \leq 1 - \prod_{i=1}^{4}(1 - p_i) \approx \sum_{i=1}^{4} p_i$$

or

$$0.77 \times 10^{-5} \leq p_f \leq 0.84 \times 10^{-5}$$

It is evident that modes c and d have negligible effect on the failure probability of the structure.

5.4.2 Second-Order Series Bounds

Second-order bounds are obtained by retaining terms such as $P(F_1 \cap F_2)$ in expression (5.33). For ease of exposition, (5.33) may be rewritten as

$$P(F) = P(F_1)$$

$$+ P(F_2) - P(F_1 \cap F_2)$$

$$+ P(F_3) - P(F_1 \cap F_3) - P(F_2 \cap F_3) + P(F_1 \cap F_2 \cap F_3)$$

$$+ P(F_4) - P(F_1 \cap F_4) - P(F_2 \cap F_4) - P(F_3 \cap F_4) + P(F_1 \cap F_2 \cap F_4)$$

$$+ P(F_1 \cap F_3 \cap F_4) + P(F_2 \cap F_3 \cap F_4) - P(F_1 \cap F_2 \cap F_3 \cap F_4)$$

$$+ P(F_5) - \ldots$$

$$= \sum_{i=1}^{m} P(F_i) - \sum \sum_{i<j}^{m} P(F_i \cap F_j) + \sum \sum \sum_{i<j<k}^{m} P(F_i \cap F_j \cap F_k) - \ldots \tag{5.38}$$

Because of the alternating signs as the order of the terms increases, it is evident that consideration only of first-order terms (i.e. $P(F_i)$) produces an upper bound on $P(F)$, consideration only of first- and second-order terms a lower bound, first-, second- and third-order terms again on upper bound, and so on [Bonferroni, 1936].

It should be clear also that consideration of an additional failure mode cannot reduce the probability of structural failure, so that each complete line in equation (5.38) makes a non-negative contribution to $P(F)$. Noting that $P(F_i \cap F_j) \geq P(F_i \cap F_j \cap F_k)$, a lower bound to (5.38) can be obtained if only the terms $P(F_i) - P(F_i \cap F_j)$ are retained, provided that each makes a non-negative contribution [Ditlevsen, 1979b]. This can be expressed as:

$$P(F) \geq P(F_1) + \sum_{i=2}^{m} \max \left\{ \left[P(F_i) - \sum_{j=1}^{i-1} P(F_i \cap F_j) \right], 0 \right\} \tag{5.39}$$

An alternative way of using the terms $P(F_i)$ and $P(F_i \cap F_j)$ is to select only those combinations of all such (k) terms in (5.38) which give the maximum value (of the lower bound) [Kounias, 1968]:

$$P(F) \geq P(F_1) + \max \left\{ \sum_{i=2, j<i}^{k \leq m} \left[P(F_i) - P\left(F_i \cap F_j \right) \right] \right\} \tag{5.40}$$

In both formulations the result depends on the order in which the various modes of failure are labelled. Algorithms for optimal ordering of events to obtain the best bounds have been proposed [Dawson and Sankoff, 1967; Hunter, 1977]; a useful rule of thumb is to order the modes in order of decreasing importance. For a given ordering, (5.39) may give a better bound than (5.40); both bounds are equal if all possible orderings are considered [Ramachandran, 1984].

An upper bound may be obtained by simplifying each line in (5.38). As noted, a typical line, such as line 5, makes a non-negative contribution to $P(F)$ and can be written, with P_{ijk} for $P(F_i \cap F_j \cap F_k)$ etc., as

$$U_5 = P_5 - P_{15} - P_{25} - P_{35} - P_{45} + P_{125} + P_{135} + P_{145} + P_{235} + P_{245} + P_{345}$$

$$- P_{1235} - P_{1245} - P_{1345} - P_{2345} + P_{12345} \tag{5.41}$$

Apart from the term P_5, the rest of the line can be written as

$$-V_5 = -P\left(E_{15} \cup E_{25} \cup E_{35} \cup E_{45} \right) \tag{5.42}$$

where E_{ij} represents the event ij. For any pair of events A, B, say, it is well known that $P(A \cup B) \geq \max [P(A), P(B)]$. It follows readily that

$$V_5 \geq \max \left[P(E_{15}), P(E_{25}), P(E_{35}), P(E_{45}) \right] \tag{5.43}$$

and, since V_5 makes a negative contribution to U_5 use of the bound (5.43) will increase the right-hand side of (5.41). Hence

$$U_5 \leq P_5 - \max_{j<5} \left(P_{j5} \right) \tag{5.44}$$

but, since $P_{j5} \equiv P(F_j \cap F_5)$ and since line 5 was a typical example, it follows that [Kounias, 1968; Vanmarcke, 1973; Hunter, 1976; Ditlevsen, 1979b]

$$P(F) \leq \sum_{i=1}^{m} P(F_i) - \sum_{i=2}^{m} \max_{j<i} \left[P(F_j \cap F_i) \right] \tag{5.45}$$

This result may also depend on the ordering of failure events F_i.

Bounds (5.39) and (5.45) have been compared with (crude) Monte Carlo simulation results for a series of rigid-framed, rigid-plastic frames [Grimmelt and Schuëller, 1982]. For a range of distribution types and a range of variances, it was found that the bounds were mainly quite close to the simulation results. However, the bounds are not necessarily always close [Ditlevsen, 1979b].

Example 5.7 Consider the three linear limit state functions shown in Figure 5.14(a) in two-dimensional y space. For simplicity, the safety indices β_1, β_2 and β_3 are shown of equal length. The probability contents enclosed by each pair of limit state functions have been denoted $a, b, \ldots, e$ and f, the last bounded by all three limit state functions. For three limit state functions, the lower bound (5.39) becomes

$$
\begin{aligned}
p^- &= p_1 + (p_2 - p_{21})^+ + (p_3 - p_{31} - p_{32})^+ \quad \text{with } (\ )^+ \equiv \max(\ , 0) \\
&= (b + c + d + f) + \left[(a + b + c) - (b + c) \right]^+ + \left[(c + d + e) - (c + d) - c \right]^+ \\
&= a + b + c + d + f + (-c + e)^+
\end{aligned}
$$
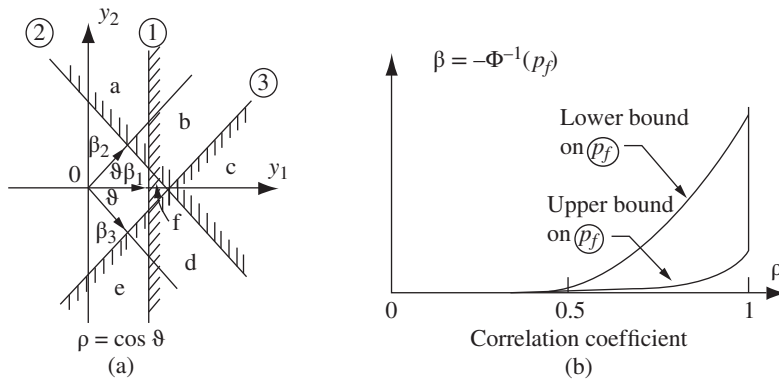
Figure 5.14 (a) Limit states for Example 5.5: (b) typical bounds for equi-correlated limit states [after Ditlevsen, 1979b].

while the upper bound (5.45) is

$$
\begin{aligned}
p^+ &= p_1 + p_2 + p_3 - \left[(p_{12})^+ + (p_{13}, p_{23})^+ \right] \\
&= (b + c + d + f) + (a + b + c) + (c + d + e) - \left[(b + c) + (c + d, c)^+ \right] \\
&= a + b + c + d + e + f
\end{aligned}
$$

In this case, the upper bound gives the correct result. As the limit states 1, 2, 3 become more correlated, i.e. as ρ increases and the angle ν becomes smaller (see Section C.1.3), the probability content of region c will increase and the bounds will diverge further. This is indicated schematically in Figure 5.14(b). When all three limit state functions coincide, they are perfectly correlated (dependent) so that (5.36) gives a unique result for p_f. This is responsible for the cut-off effect shown at the right of Figure 5.14(b).

5.4.3 Second-Order Series Bounds by Loading Sequences

The series bounds discussed so far consider failure events according to different modes of failure for all possible loadings. In some situations it may be desirable to consider a sequence of loadings, perhaps dependent in some way, and to determine the bounds on the probability of failure for the system. It may be shown that the bounds derived above are symmetric with respect to loading sequences with the failure event now defined over all modes of failure.

From expression (5.32) the probability of structural failure under a sequence of loading vectors $Q_1, Q_2, Q_3, \ldots$, may be expressed as

$$
P(F) = P(F_1) + P(F_2 \,|\, S_1)P(S_1) + P(F_3 \,|\, S_2 \cap S_1)P(S_2 \cap S_1) + \ldots \tag{5.46}
$$

where F_i denotes the event 'structural failure due to the i th loading', and S denotes the complementary event 'structure survival under the i th loading' $P(F_i) = 1 - P(S_i)$.

In general there will be dependence between failure under the i th loading and survival under previous loadings in the sequence; let this be denoted the 'transition' probability

$$
p_i = P(F_i \,|\, S_{i-1} \cap S_{i-2} \cap S_{i-3} \cap \ldots) \tag{5.47}
$$

Also, since

$$
P(S_3 \cap S_2 \cap S_1) = P(S_3 \,|\, S_2 \cap S_1)P(S_2 \cap S_1) = P(S_3 \,|\, S_2 \cap S_1)P(S_2 \,|\, S_1)P(S_1)
$$

and similarly for other corresponding terms in equation (5.32), it follows, upon using equation (5.47) and writing p_1 for $P(F_1)$, that

$$
P(F) = p_1 + p_2(1 - p_1) + p_3(1 - p_2)(1 - p_1) + p_4(1 - p_3)(1 - p_2)(1 - p_1) + \ldots \tag{5.48}
$$

or, for n loads in the loading sequence

$$
P(F) = \sum_{i=1}^{n} p_i - \sum \sum_{j<i}^{n} p_i p_j + \sum \sum_{k<j<i} \sum^{n} p_i p_j p_k - \sum \sum_{\ell<k} \sum_{<j<i} \sum^{n} p_i p_j p_k p_\ell + \ldots \tag{5.49}
$$

which is identical with equation (5.38) provided that $P(F_i)$ is interpreted as p_i, $P(F_i \cap F_j), j < i$ is interpreted as $p_i p_j$, $j < i$, etc. Hence, with this interpretation, the bounds

(5.39) and (5.45) can be interpreted as bounds on $P(F)$ for structural failure under load sequences.

5.4.4 Series Bounds by Modes and Loading Sequences

The series bounds (5.39) and (5.45) for failure modes can be generalized to include loading sequences. For failure in several modes, each of the bounds given by equations (5.39) or (5.45) can be interpreted as the probability $P(F_k)$ of failure under k th loading in a load sequence. To determine the total probability of failure, under the complete loading sequence, equations (5.39) and (5.45) are again applicable, but now interpreted for loading sequences as in Section 5.4.3 above.

In practice, however, it is not always easy to evaluate the terms $P(F_i \cap F_j)$ since F_i and F_j usually will be correlated (see Example 5.7). One approach is to then use a simpler result obtained by considering two limiting cases for the evaluation of the terms $P(F_i \cap F_j)$: complete independence of (F_i, F_j) or complete dependence. If the events (F_i, F_j) are completely independent, (A.4) applies and (5.33) reduces to (5.34).

Similarly, if (F_i, F_j) are completely dependent, then terms of form $P(F_1 \cap F_2 \cap F_3)$, …, reduce to $\max[P(F_1), P(F_2), P(F_3)]$, …, since the critical case will govern. As a result, (5.32) reduces to (5.36).

It is now possible to extend the first-order bounds (5.37) to consider the effect of both loading sequences and failure modes:

$$\max_i^m \left\{ \max_j^n \left[P(F_{ij}) \right] \right\} \le P(F) \le 1 - \prod_{ij}^{mn} \left[1 - P(F_{ij}) \right] \tag{5.50}$$

where $P(F_{ij})$ is the probability of failure in the i th mode under the j th load in the loading sequence. The right-hand bound may be replaced by a slightly looser bound, provided that $P(F_{ij}) << 1$ [Cornell, 1967]:

$$\max_i^m \left\{ \max_j^n \left[P(F_{ij}) \right] \right\} \le P(F) \le \sum_j^m \sum_i^n P(F_{ij}) \tag{5.51}$$

When it is known that either load sequences or failure modes are independent, the appropriate left-hand maximum operator can be replaced by a summation operator to improve the bounds; similarly, if it is known that either load sequences or failure modes are completely dependent, the appropriate right-hand summation operator can be replaced by a maximum operator.

If it is known that the load sequence consists of N successive, mutually exclusive independent loads having the same probability density function, it follows readily that the right-hand bound can be replaced by [Freudenthal et al., 1966]:

$$N \sum_i^m P(F_{ij}) \tag{5.52}$$

5.4.5 Improved Series Bounds and Parallel System Bounds

As demonstrated in Example 5.7, the second-order series bounds generally deteriorate as the correlation between (linear) limit state functions increases. One approach

to improving series bounds is to transform the problem to one resulting in lower correlation between limit state functions. This may be achieved using (C.13) to obtain a new set of variables [Ditlevsen, 1982b].

Alternatively, improved bounds for series systems may be obtained if higher-order terms are retained, for example, if terms of the form $P_{ijk} = P(F_i \cap F_j \cap F_k)$ are retained in (5.32) [Hohenbichler and Rackwitz, 1983a; Ramachandran, 1984; Feng, 1989; Greig, 1992; Zhang, 1993]. In this case the third-order series bounds become, with $F_i(i = 1, \ldots, m)$ denoting the m possible failure modes:

$$P_3^- \le P\left(\bigcup_{i=1}^{m} F_i \right) \le P_3^+ \tag{5.53}$$

with

$$P_3^- = \sum_{i=1}^{m} \left[P_i - \sum_{j<i} \left(P_{ij} - \max_{k<j} P_{ijk} \right) \right]^+$$

$$P_3^+ = \sum_{i=1}^{m} \left(P_i - \sum_{j<i} \left[P_{ij} - \sum_{k<j} P_{ijk} \right]^+ \right)$$

where $[\ ]^+$ indicates that the term is to be included only if the term $[\ ]$ is positive.

Again some ordering of failure events may be necessary to obtain the best bounds. However, the greatest difficulty is to evaluate the tri-section terms P_{ijk}. When the events F_i are all expressible as linear functions, a non-linear lower bound is given by [Ramachandran, 1984].

$$P_{ijk} \ge \frac{P(F_i \cap F_k)P(F_i \cap F_j)}{P(F_i)} \tag{5.54}$$

provided that $\rho_{kj} > \rho_{ik}\rho_{ij} > 0$ where ρ_{ij} is the correlation coefficient between the linear failure functions for events i and j, etc. An alternative but approximate approach for both P_{ij} and P_{ijk} based on the angle between the linear limit state functions has been proposed by Feng (1989).

For parallel systems the failure probability is given by (5.2) or (5.13). Bounds for this can be obtained from applying series bounds to the right-hand side of the identity:

$$P\left(\bigcap_{i=1}^{m} F_i \right) = 1 - P\left(\bigcup_{i=1}^{m} F_i \right) \tag{5.55}$$

The resulting bounds are poor since the second term on the right will be close to unity for high-reliability systems. In the special case of parallel systems with linear safety functions, a better approach is to apply the results given in Appendix C for the multi-normal integral with multiple linear limit state functions.

5.4.6 First-Order Second-Moment Method in Systems Reliability

Utilization of series bounds such as the second-order series bounds (5.39) and (5.45) requires evaluation of intersection terms of the form $P(F_i \cap F_j)$ where F_i denotes the event 'failure in limit state i'. In two dimensions the intersection terms refer to

odd-shaped domains such as D_1 in Figure 5.7 as obtained from the non-linear limit state functions $G_k(\mathbf{x}) = 0$ ($k = 1, 2, 3$).

In principle it would be possible to use Monte Carlo integration to evaluate the probability content of terms such as $P(F_i \cap F_j)$ for use with the bounds given above. This is seldom appropriate, however, since a direct Monte Carlo evaluation of the whole system is likely to be more efficient (than the use of system bounds together with Monte Carlo evaluation of the intersections).

The second-order series bounds are more useful in the special case of problems with linear limit state functions and therefore when used in conjunction with the FOSM methods of Chapter 4. The evaluation of the intersections $P(F_i \cap F_j)$ is then over regions such as D_1 in Figure 5.15 bounded by, for example, $g_{L1}(\mathbf{y}) = 0$ and $g_{L2}(\mathbf{y}) = 0$. The limit state functions can be linearized, once the checking points y_i^* have been identified, and the direction cosines are determined (see Section 4.3.2). The approximating linearized limit state functions $g_L(\ ) = 0$ are then given by (4.7).

For linearized limit states given by $g_{L1}(\mathbf{y}) = 0$ and $g_{L2}(\mathbf{y}) = 0$, the probability content enclosed by these limit states is

$$P(F_1 \cap F_2) = P\left[\bigcap_{i=1}^{2} g_{Li}(\mathbf{y}) \leq 0\right] \tag{5.56}$$

which for the standardized Normal vector $\mathbf{y}$ can be evaluated using the bivariate Normal integral $\Phi_2(\ )$ [see (A.140b) and Appendix C]. In each case the correlation coefficient ρ between the two limit state functions (1 and 2, here) is required to be known. It can be obtained for two intersecting limit states 1 and 2 as follows.

In standardized independent Normal $\mathbf{y}$ space, a linear limit state function is given by (4.7):

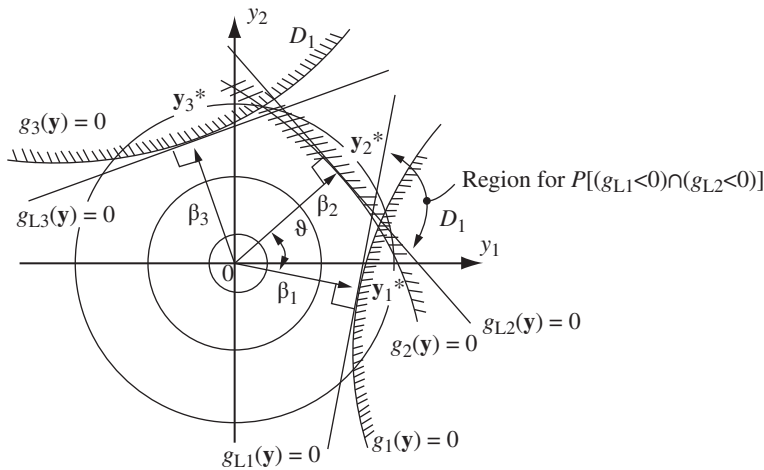$$g_{Li}(y) = \beta_i + \sum_{j=1}^{n} \alpha_{ij} y_j \tag{5.57}$$

Figure 5.15 Linearization of limit states in standard normal space.

For $g_1(\ )$ and $g_2(\ )$, the variance and covariance are then (A.162) and (A.163)

$$\sigma_i^2 = \sum_{j=1}^n \alpha_{ij}^2 \qquad i = 1, 2$$

$$\text{cov}(g_{L1}, g_{L2}) = \sum_j^n \alpha_{1j}\alpha_{2j}$$

and from (A.124)

$$\rho_{12} = \frac{\text{cov}(g_{L1}, g_{L2})}{\left(\sigma_1^2 \sigma_2^2\right)^{1/2}} = \frac{\sum_j^n \alpha_{1j}\alpha_{2j}}{\left(\sum_j^n \alpha_{1j}^2 \sum_j^n \alpha_{2j}^2\right)^{1/2}} \tag{5.58}$$

These expressions can be given a geometric interpretation when attention is restricted to the (y_1, y_2) plane, in **y** space (see Figure 5.16).

From elementary geometry, the unit outward normal vectors $\mathbf{n}_i$ $(i = 1, 2)$ to the hyperplanes $g_{L1}(\mathbf{y}) = 0$ and $g_{L2}(\mathbf{y}) = 0$ shown in Figure 5.16 are obtained from (5.57) [Ditlevsen, 1979b]

$$n_1 = \sum_{j=1}^n \alpha_{1j}\ \mathbf{e}_j \Big/ \left(\sum_{j=1}^n \alpha_{1j}\right)^{1/2} \tag{5.59a}$$

$$n_2 = \sum_{j=1}^n \alpha_{2j}\ \mathbf{e}_j \Big/ \left(\sum_{j=1}^n \alpha_{2j}\right)^{1/2} \tag{5.59b}$$

where the $\mathbf{e}_i$ represent the unit base vectors. The scalar product of these normals is given by $\mathbf{n}_1 \cdot \mathbf{n}_2 = n_1 n_2 \cos v = \cos v$, where v is the angle between the $\mathbf{n}_i (i = 1, 2)$ in the plane common to both (see Figure 5.16). It follows readily from expressions (5.59) that the scalar product is also equal to the right-hand side of expression (5.58) so that (*cf*. Section 3.2)

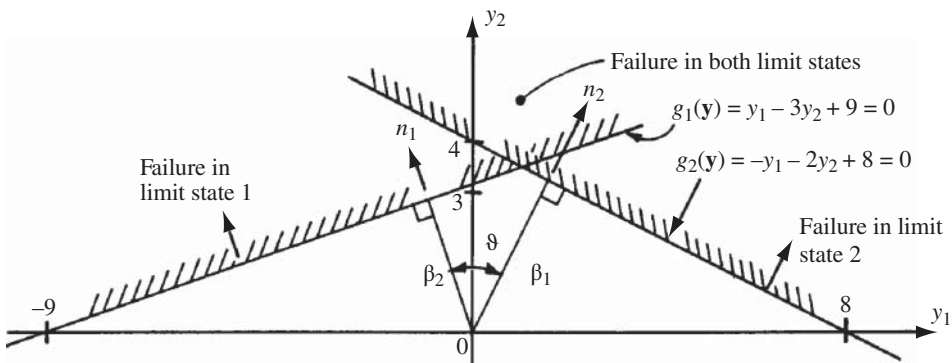$$\rho_{12} = \rho(y_1, y_2) = \cos v = \mathbf{n}_1 \cdot \mathbf{n}_2 \tag{5.60}$$

Figure 5.16 Intersection of linear limit states.

@Seismicisolation

Example 5.8   For the two linear limit state functions $g_1(\mathbf{y}) = 0$ and $g_2(\mathbf{y}) = 0$ shown in Figure 5.16 in standardized Normal space, it follows from (A.162) and (A.163) that $\sigma_1^2 = +10$, $\sigma_2^2 = +5$ and $\mathrm{cov}(y_1, y_2) = +5$ from which $\rho = 5/(10 \times 5)^{1/2} = 1/\sqrt{2} > 0$ so that $\nu \arccos(1/\sqrt{2}) = 45°$. Using (4.1), $\beta_1 = 9/\sqrt{10} = 2.85$ and $\beta_2 = 8/\sqrt{5} = 3.59$. Applying now (C.8) and (C.9) it follows that $h = \beta_1$, $k = \beta_2$, $a = (\beta_1 - \rho\beta_2)/(1 - \rho^2)^{1/2}$ and $b = (\beta_2 - \rho\beta_1)/(1 - \rho^2)^{1/2}$ so that $\Phi(-h) = 0.002186$, $\Phi(-k) = 0.000165$, $\Phi(-a) = 0.33264$ and $\Phi(-b) = 0.0135$. Substituting these values in (C.8) yields $0.000\,055 \leq P(g_1 \leq 0 \cap g_2 \leq 0) \leq 0.000\,084$.

Let the event $g_1 < 0$ be denoted F_1 and similarly for F_2. Expressions (5.39) and (5.45) for the probability bounds for a two-failure-mode structure then lead to

$$P(F_1) + P(F_2) - P(F_1 \cap F_2)^+ \leq P(F) \leq P(F_1) + P(F_2) - P(F_1 \cap F_2)^-$$

or $0.002\,26 < p_f < 0.002\,29$, where the choices for the intersections have been made to give the widest bounds.

Example 5.9   The nominal failure probability for the rigid-plastic frame of Example 5.4 will now be determined using second-order system bounds and the FOSM result for $P(F_i \cap F_j)$. Only the first three collapse modes of Example 5.4 will be considered. These are

$$
\begin{array}{llllll}
\text{mode 1:} \ +M_1 & & +2M_3 & +2M_4 & -H & -V = 0 \quad \text{(combined)} \\
\text{mode 2:} & +M_2 & +2M_3 & +M_4 & & -V = 0 \quad \text{(beam)} \\
\text{mode 3:} \ +M_1 & +M_2 & & +M_4 & -H & = 0 \quad \text{(sway)}
\end{array}
$$

Let each random variable be standardized to $N(0, 1)$, such that $x_i = (X_i - \mu_{X_i})/\sigma_{X_i}$. Noting that for all $X_i = (M_1, \ldots, M_4, H, V)$ the means and standard deviations are $\mu_{X_i} = 1.0$ and $\sigma_{X_i} = (0.15, 0.15, 0.15, 0.15, 0.17, 0.50)$ it follows that the limit state equations in standard Normal space are

$$
\begin{aligned}
g_1 &= 0.15m_1 + 0.30m_3 + 0.30m_4 - 0.17h - 0.5v + 3 = 0 \\
g_2 &= 0.15m_2 + 0.30m_3 + 0.15m_4 \qquad\quad - 0.5v + 3 = 0 \\
g_3 &= 0.15m_1 + 0.15m_2 + 0.15m_4 - 0.17h \qquad + 2 = 0
\end{aligned}
$$

Further, using (A.162) and (A.163)

$$
\begin{aligned}
\sigma_{g_1}^2 &= (0.15)^2 + (0.3)^2 + (0.3)^2 + (0.17)^2 + (0.5)^2 = 0.481 \\
\sigma_{g_2}^2 &= 0.385 \\
\sigma_{g_3}^2 &= 0.096 \\
\mathrm{cov}(g_1, g_2) &= (0 + 0 + 0.3 \times 0.3 + 0.3 \times 0.15) + 0 + (0.5)^2 = 0.385 \\
\mathrm{cov}(g_1, g_3) &= 0.096 \\
\mathrm{cov}(g_2, g_3) &= 0.045
\end{aligned}
$$

From (5.58) it follows that the correlation coefficients are

$$\rho_{12} = \frac{0.385}{(0.481 \times 0.385)^{1/2}} = 0.895$$

$$\rho_{13} = 0.447$$

$$\rho_{23} = 0.234$$

so that the angles $\nu = \arccos\rho$ are $\nu_{12} = 26.5°$, $\nu_{13} = 63.5°$ and $\nu_{23} = 76.5°$.

The β indices were calculated already in Example 5.4. They are given also by $\beta = \mu_g / \sigma_{gi}$ or

$$\beta_1 = \frac{3}{\sqrt{0.481}} = 4.32, \ \beta_2 = 4.83, \ \beta_3 = 6.44$$

since $\mu_{x_i} = 0$. From Appendix E the corresponding nominal probabilities are 0.77×10^{-5}, 0.70×10^{-6} and 0.59×10^{-10}.

It is now possible to calculate the terms $P(F_i \cap F_j)$ needed for the second-order bounds (5.39) and (5.45). This can be done by using the bounds given by (C.8) (see also Example 5.8). As before, let p_{ij} denote $P(F_i \cap F_j)$. Then for p_{12},

$$h = \beta_1 = 4.32, \quad k = \beta_2 = 4.83$$

$$a = \frac{\beta_1 - \rho_{12}\beta_2}{(1 - \rho_{12}^2)^{1/2}} = \frac{4.32 - 0.895 \times 4.83}{(1 - 0.895^2)^{1/2}} = -0.0064$$

$$b = \frac{\beta_2 - \rho_{12}\beta_1}{(1 - \rho_{12}^2)^{1/2}} = \frac{4.83 - 0.895 \times 4.32}{(1 - 0.895^2)^{1/2}} = 2.160$$

so that, according to (C.8), the bounds are

$$p_{12} = \left[\Phi(-h)\Phi(-b)^+, \ \Phi(-k)\Phi(-a) \right]$$
$$= \left[(0.77 \times 10^{-5})(0.01539)^+, \ (0.70 \times 10^{-6})(\sim 0.5) \right]$$
$$= \left[0.35 \times 10^{-6}, \ 0.47 \times 10^{-6} \right]$$

and for p_{13},

$$p_{13} = \left[0.317 \times 10^{-11}, \ 0.479 \times 10^{-11} \right]$$
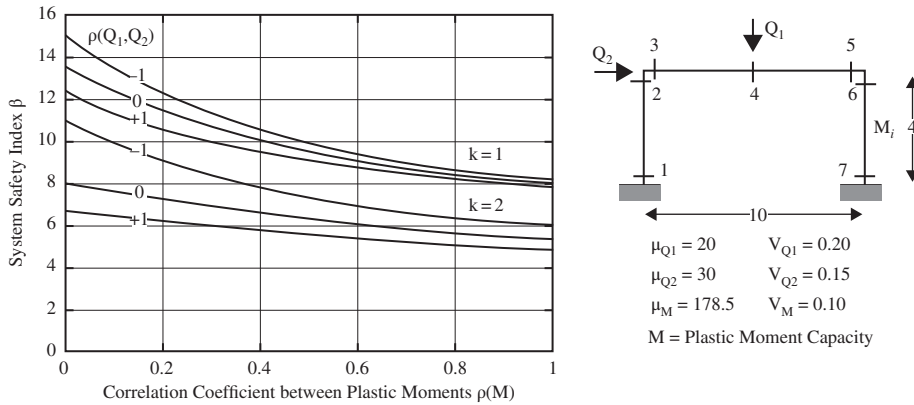
and, for p_{23}

$$p_{23} = \left[0.189 \times 10^{-13}, \ 0.374 \times 10^{-13} \right]$$

Substituting into (5.39) to obtain the lower bound on the system failure probability,

$$p_f^- = 0.77 \times 10^{-5} + \left(0.70 \times 10^{-6} - 0.47 \times 10^{-6} \right)^+$$
$$+ \left(0.59 \times 10^{-10} - 0.479 \times 10^{-11} - 0.374 \times 10^{-13} \right)^+$$
$$= 0.79 \times 10^{-5}$$

The upper bound is given by (5.45):

$$p_f^+ = \left(0.77 \times 10^{-5} + 0.70 \times 10^{-6} + 0.59 \times 10^{-10} \right) - 0.35 \times 10^{-6}$$
$$- \max \left(0.317 \times 10^{-5}, \ 0.189 \times 10^{-13} \right)$$
$$= 0.81 \times 10^{-5}$$

Figure 5.17 Effect of correlation on system safety index $\beta = -\Phi^{-1}(p_f)$.

In each case, the p_{ij} result giving the worst p_f^+ value has been chosen.

The bounds on the nominal probability of failure for the system coincide within the limit of accuracy of the calculations used here. As expected, the present result is contained within the first-order bounds determined in Example 5.6.

5.4.7 Correlation Effects

The above examples show that the failure modes are correlated if some or all of the resistance and load basic variables are shared between two or more of the limit state functions. This has important implications for the estimation of structural system failure probabilities, as was seen above in the calculation of bounds. It is also seen in the Monte Carlo techniques but is handled there automatically through the complete failure domain being defined as: $\bigcup\limits_{i=1}^{m} G_i(\mathbf{X}) \leq 0$ (see Figure 5.12).

Correlation also can arise from dependence between loads and, more commonly, from correlation between structural members and within individual members [Garson, 1980; Melchers, 1983a]. As has been noted already in Section 4.4.3, correlation of basic variables in second-moment reliability analysis is dealt with by transforming the correlated set to an uncorrelated set (see Appendix B).

A set of typical results showing correlation effects for a rigid-plastic portal frame, subject to two loads each applied once only and each having the statistical properties shown, is given in Figure 5.17 [Frangopol, 1985a]. Experimental data on actual strength (and load) correlation are, however, scarce. In practical problems conservative assumptions may need to be made.

5.4.8 Bounds by Matrix Operations and Linear Programming*

As noted earlier, the second-order series bounds (5.45) and the improved third-order series bounds (5.53) depend on the ordering of failure modes. Ideally the narrowest bounds are desired, but this requires computing all $n!$ possible sequences of the ordering of the failure modes, usually entailing lengthy calculations. An alternative is to use

matrix operations [Song and Kang, 2009] or linear programming to expedite the process [Song and Der Kiureghian, 2003] as described below.

Consider a system event E_{sys} whose i^{th} component, $i = 1, \ldots, n$, has two possible states: failure or survival. The sample space can be obtained by enumerating the $m = 2^n$ basic mutually exclusive and collectively exhaustive (MECE) events $e_j, j = 1, \ldots, m$. Then, any system event can be represented by an event vector **c** whose j^{th} element is 1 if e_j belongs to the system event, and 0 otherwise. Let $p_j = P[e_j], j = 1, \ldots, m$, denote the probability of basic event e_j. Since the e_j represent mutually exclusive events, the probability of the system event, $P[E_{sys}]$, is simply the sum of probabilities of basic MECE events contributing to the system event. Hence, the system probability can be computed by the inner product:

$$P\left[E_{sys}\right] = P_{sys} = \sum_{j:e_j \subseteq E_{sys}} p_j = \mathbf{c}^T \mathbf{p} \tag{5.61}$$

where $\mathbf{p} = \{p_j\}^T, j = 1, \ldots, m$ is the column probability vector of the components p_j. This formulation can be generalized to compute probabilities of multiple system events under multiple conditions on component failure by the matrix multiplication: $\mathbf{P}_{sys} = \mathbf{C}^T \mathbf{P}$, where $\mathbf{P}_{sys}$ is the matrix of system event probabilities, whose elements $(P_{sys})_{ij}$ are the probabilities that the ith system event occurs under the jth condition; $\mathbf{C} = [\mathbf{c}_1, \mathbf{c}_2, \ldots, \mathbf{c}_{n_{sys}}]$ is the matrix whose columns are event vectors, for n_{sys} possible system events; and $\mathbf{P} = [\mathbf{p}_1, \mathbf{p}_2, \ldots, \mathbf{p}_{n_{cond}}]$ is the matrix whose columns are the probability vectors for the n_{cond} different component conditions. This scheme has been called the matrix-based system reliability (MSR) technique [Song and Kang, 2009].

As an example, for the case of $n = 3$ component events, the $2^3 = 8$ basic MECE events are:

$$e_1 = E_1 E_2 E_3, \quad e_2 = \overline{E}_1 E_2 E_3, \quad e_3 = E_1 \overline{E}_2 E_3, \quad e_4 = E_1 E_2 \overline{E}_3,$$
$$e_5 = \overline{E}_1 \overline{E}_2 E_3, \quad e_6 = \overline{E}_1 E_2 \overline{E}_3, \quad e_7 = E_1 \overline{E}_2 \overline{E}_3, \quad e_8 = \overline{E}_1 \overline{E}_2 \overline{E}_3. \tag{5.62}$$

where $E_i E_j = E_i \cap E_j$. These events are listed in Table 5.1, together with coefficients c_i leading to the four system events $E_1 \cup E_2 \cup E_3$ (series system), $E_1 \cap E_2 \cap E_3$ (parallel system), $(E_1 \cap E_2) \cup E_3$ (mixed system), $(E_1 \cup E_2) \cap (\overline{E}_2 \cup E_3)$ (mixed system).

The advantages the MSR technique over other system reliability techniques include: (a) computation of system probabilities are performed by simple matrix operations, regardless of the complexity of the system event; (b) if there is incomplete information on component failure probabilities and/or on their statistical dependency, the MSR technique still yields the narrowest possible bounds for the given information (this leads to a linear programming problem, as shown below); and (c) the conditional probabilities and derivatives of system probabilities are easily calculated.

A drawback of the MSR technique is that the size of the problem increases exponentially with number of component events, although this is not necessarily a problem with modern personal computers.

For small-size systems, event vector **c** can be identified directly. For larger systems, event vectors can be constructed by simple matrix manipulations of component event vectors. Let $\mathbf{c}_E$ denote the event vector of the generic event E. The complementary event

Table 5.1 Basic MECE events and coefficients c_i for a three-component system.

System event	$e_1 = E_1 E_2 E_3$	$e_2 = \bar{E}_1 E_2 E_3$	$e_3 = E_1 \bar{E}_2 E_3$	$e_4 = E_1 E_2 \bar{E}_3$	$e_5 = \bar{E}_1 \bar{E}_2 E_3$	$e_6 = \bar{E}_1 E_2 \bar{E}_3$	$e_7 = E_1 \bar{E}_2 \bar{E}_3$	$e_8 = \bar{E}_1 \bar{E}_2 \bar{E}_3$
				Basic MECE events				
$E_1 \cup E_2 \cup E_3$	1	1	1	1	1	1	1	0
$E_1 \cap E_2 \cap E_3$	1	0	0	0	0	0	0	0
$(E_1 \cap E_2) \cup E_3$	1	1	1	1	1	0	0	0
$(E_1 \cup E_2) \cap (\bar{E}_2 \cup E_3)$	1	1	1	0	0	0	1	0

vector, the union and intersections can be obtained as:

$$\mathbf{c}_{\overline{E}} = \mathbf{1} - \mathbf{c}_E$$

$$\mathbf{c}_{E_1 E_2 \ldots E_n} = \mathbf{c}_{E_1} * \mathbf{c}_{E_2} * \ldots * \mathbf{c}_{E_n}$$

$$\mathbf{c}_{E_1 \cup E_2 \cup \ldots \cup E_n} = \mathbf{1} - (\mathbf{1} - \mathbf{c}_{E_1}) * (\mathbf{1} - \mathbf{c}_{E_2}) * \ldots * (\mathbf{1} - \mathbf{c}_{E_n}) \tag{5.63}$$

where $*$ denotes element-by-element multiplication. The event vector can be constructed from component and other system events using the matrix manipulations in (5.63).

The probability vector $\mathbf{p}$ can also be constructed by simple matrix manipulations. First, assume that all component probabilities are known, and that component events are statistically independent of each other. Each element of the probability vector can be computed as the product of the probabilities of the components and their complementary events. The following iterative procedure can be employed:

$$\mathbf{p}_{[1]} = \begin{bmatrix} P_1 & \overline{P}_1 \end{bmatrix}$$

$$\mathbf{p}_{[i]} = \begin{bmatrix} \mathbf{p}_{[i-1]} P_i \\ \mathbf{p}_{[i-1]} \overline{P}_i \end{bmatrix} \tag{5.64}$$

where P_i is the probability of the ith component. The final vector $\mathbf{p}_{[n]}$ is the probability vector $\mathbf{p}$ for a system of n components.

If some component probabilities are not known, or if only their bounds are known, system reliability cannot be computed by Eq. (5.61). However, system reliability bounds can still be computed by solving a linear programming problem, where the unknown vector of MECE event probabilities $\mathbf{p}$ is the vector of design variables, and where known element probabilities are used as constraints:

Find $\mathbf{p}^{MIN}$ which minimizes $\mathbf{c}^T \mathbf{p}$

subject to $\mathbf{A}_1 \mathbf{p} = \mathbf{b}_1$, $\mathbf{A}_2 \mathbf{p} \geq \mathbf{b}_2$, $\sum_{j=1}^{m} p_j = 1$, $\mathbf{p} \geq 0$, \hfill (5.65)

Find $\mathbf{p}^{MAX}$ which minimizes $\mathbf{c}^T \mathbf{p}$

subject to $\mathbf{A}_1 \mathbf{p} = \mathbf{b}_1$, $\mathbf{A}_3 \mathbf{p} \leq \mathbf{b}_3$, $\sum_{j=1}^{m} p_j = 1$, $\mathbf{p} \geq 0$, \hfill (5.66)

where $\mathbf{A}_1$, $\mathbf{A}_2$, and $\mathbf{A}_3$ are matrices whose rows are event vectors for which probabilities or bounds are known, $\mathbf{b}_1$ is the vector of known probabilities and $\mathbf{b}_2$, $\mathbf{b}_3$ are the lower and upper probability bounds. The system reliability bounds are obtained from the minimum and maximum objective function values found using Eqns. (5.65) and (5.66):

$$\mathbf{c}^T \mathbf{p}^{MIN} \leq P_{sys} \leq \mathbf{c}^T \mathbf{p}^{MAX} \tag{5.67}$$

The constraints in Eqns. (5.65) and (5.66) are obtained as follows. Due to the mutual exclusivity of basic MECE events, the probability of any subset of these events is obtained as the sum of probabilities of the constituent events. Taking the three-component event in Table 5.1 as an example, the single-mode probabilities

are:

$$P[E_1] = P_1 = p_1 + p_3 + p_4 + p_7$$
$$P[E_2] = P_2 = p_1 + p_2 + p_4 + p_6$$
$$P[E_3] = P_3 = p_1 + p_2 + p_3 + p_5 \tag{5.68}$$

This can be generalized to:

$$P\left[E_i\right] = P_i = \sum_{r:e_r \subseteq E_i} p_r \tag{5.69}$$

In a similar way, probabilities of intersection of events are given by:

$$P\left[E_i E_j\right] = P_{ij} = \sum_{r:e_r \subseteq E_i E_j} p_r \tag{5.70}$$

and

$$P\left[E_i E_j E_k\right] = P_{ijk} = \sum_{r:e_r \subseteq E_i E_j E_k} p_r \tag{5.71}$$

The probabilities in (5.69) to (5.71) are employed as linear equality constraints in (5.68), with $\mathbf{A}_1$ the matrix containing 0's and 1's and $\mathbf{b}_1$ the vector containing the known probabilities. If the probabilities in (5.69) to (5.71) are given as inequalities, they are employed as inequality constraints, such that $\mathbf{A}_2\mathbf{p} \geq \mathbf{b}_2$ and $\mathbf{A}_3\mathbf{p} \leq \mathbf{b}_3$. This is the case for conventional structural reliability problems, where bi-modal joint probability bounds are obtained from Eq. (5.56). In general, the tri-modal bounds (5.71) are difficult to evaluate in structural reliability, and need not be provided. If higher-order bounds are not provided in Eq. (5.67), the bounds will be wider, but still better than the second-order bounds (5.45). It has been shown that the bounds obtained by solving (5.67) are the narrowest-possible bounds for the information provided [Song and Der Kiureghian, 2003].

5.5 Implicit Limit States

5.5.1 Introduction

In many practical problems the equation (or equations) used to represent the limit state function may not be known explicitly. Instead, the limit state may be representable only at discrete points (in hyperspace) obtained, point-by-point, through a calculation or evaluation procedure, such as a finite element analysis. This means that the safe domain and the optimal sampling location(s) or the design point for FOSM and similar techniques can be defined only through point-by-point 'discovery' of where the implicit surface is located relative to the random variables. Obviously, one way of determining the location of the (implicit) limit state function is through conducting a number of repeated numerical analyses, each with a different vector of values of the random variables. These values could be random, as in Monte Carlo analysis, or specifically ordered. Irrespective of the precise procedure, it is clear that the FOSM and related methods are not immediately applicable, since they require a closed, and preferably differentiable,

@Seismicisolation

format for the limit state function $G(\mathbf{x}) = 0$. If Monte Carlo analysis is used for structural reliability evaluation and when one or more implicit limit state functions is defined by a Finite Element or other numerical procedure, a parallel problem arises. In this case many evaluations will be required to check the limit state function(s), and even more if gradients are required. In both cases the way forward is to construct an artificial limit state function, preferably closed form and differentiable and to use that as a surrogate (or meta-model) for the actual limit state function(s).

Several approaches have been proposed to construct surrogate limit states. These include (i) response surfaces, (ii) artificial neural networks, (iii) vector support machine techniques and (iv) Gaussian process modelling, also known as the Kriging technique. Because the notion of response surfaces underlies all the others, it is described in the next section. The others are described briefly subsequently.

5.5.2   Response Surfaces

5.5.2.1   Basics of Response Surfaces

A closed form, differentiable limit state surface can be constructed artificially, using a polynomial or other suitable function fitted to the results obtained from a limited number of discrete numerical analyses. Such a surface in (hyper-)space is termed a 'response surface'. Ideally the response surface should represent the structural response with most accuracy in the area around the checking point(s). Lower accuracy might be acceptable elsewhere. Provided the approximating response surface fits the point responses reasonably well, a fairly good estimate of structural failure probability is then likely to be obtained. Leonel et al. (2011) have provided an historical overview of response surface applications to structural reliability problems.

As before, let the structural response be represented by $G(\mathbf{X})$ and let it be an implicit function of the random variables $\mathbf{X}$. This means it can be evaluated only for discrete values of $\mathbf{X} = \mathbf{x}$. Let the vector $\overline{\mathbf{x}}$ represent such a discrete set of points in $\mathbf{x}$ space, and let $G(\mathbf{x})$ be evaluated at these points. The 'response surface' approach is then to seek a function $\overline{G}(\mathbf{x})$ which best fits the discrete set of values of $G(\overline{\mathbf{x}})$. Most commonly the format of the response surface adopted is to let $\overline{G}(\mathbf{x})$ be an n th order polynomial. The undetermined coefficients in this polynomial are then determined so as to minimize the error of approximation, particularly in the region around the checking point. As noted earlier, this point is known also as the point of maximum likelihood or the most probable point (MPP).

Theoretically the order n of the polynomial selected for fitting to the discrete point evaluations of $G(\mathbf{X})$ will affect the number of such evaluations required to be obtained. It also is related to the number of derivatives that are required to be estimated. Typically, for a well-conditioned system it is desirable for $\overline{G}(\mathbf{x})$ to be of equal or lower degree than $G(\mathbf{x})$. Higher-degree functions for $\overline{G}(\mathbf{x})$ are likely to lead to ill-conditioned systems of equations to be solved for the undetermined coefficients. This is known more generally to lead to solutions having erratic behaviour for small changes in the input values.

In practice, since the actual limit state function is known only through (some) discrete outcomes, its form and degree are not known a priori, nor can the checking point be estimated. This means there is little guidance for the selection of the approximating function $\overline{G}(\mathbf{x})$. However, most commonly a second order polynomial is employed for the response surface, with regression analysis to obtain the best fit [Faravelli, 1989; Bucher

and Bourgund, 1990; El-Tawil et al., 1992; Rajashekhar and Ellingwood, 1993; Maymon, 1993]. For this reason they are known also as 'polynomial regression' models.

Consider the limit state function approximated by a polynomial as follows:

$$\overline{G}(\mathbf{X}) = A + \mathbf{X}^T\mathbf{B} + \mathbf{X}^T\mathbf{C}\mathbf{X} \tag{5.72}$$

with undetermined (regression) coefficients defined by $A, \mathbf{B}^T = [B_1, B_2, \ldots B_n]$ and

$$\mathbf{C} = \begin{bmatrix} C_{11} & \cdots & C_{1n} \\ \vdots & & \vdots \\ sym & \cdots & C_{nn} \end{bmatrix}.$$

The (regression) coefficients can be obtained by conducting a series of numerical 'experiments', that is, a series of structural analyses with input variables selected according to some 'experimental design'. An appropriate experimental design takes into account that the objective lies in estimating, reasonably accurately, the probability of failure and this implies that the main interest is in the region of the maximum likelihood within the failure domain, that is in the region of the checking point. However, as noted, in practice it is unlikely that this will be known initially, and thus some trial and error may be required.

5.5.2.2   Fitting the Response Surface
Possibly the simplest approach for selecting input variables for the experimental design is to select them around the mean value of the variables. Thus points located along the axes are appropriate. A simple 2-D experimental design is shown in Figure 5.18. More complex designs are available in texts dealing with response surface methodology in general [e.g. Myers, 1971; Santner et al., 2003] and also have been discussed for structural reliability problems [Rajashekhar and Ellingwood, 1993].

Typically there will be a difference between the approximating function (the fitted response surface) and the actual response or the implicit limit state function. Usually this difference is the result both of intrinsic randomness and of 'lack of fit' contributed by using the simpler function (5.72) to represent the actual limit state surface. It is not
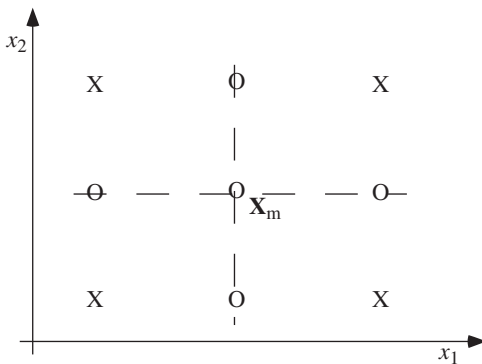

Figure 5.18 Simple experimental design for a two-variable problem with $\mathbf{X}_m$ as mean point.

possible to separate them without more refined and detailed analysis. The important practical step, however, is to try to select the (regression) coefficients such that the total error is minimized. This minimization can be formulated as follows.

Let the vector $\mathbf{D}$ represent the collection of regression coefficients A, $\mathbf{B}$, $\mathbf{C}$. Then (5.72) can be represented as $\overline{G}(\mathbf{D}, \mathbf{X})$. Also, for each point $\overline{\mathbf{x}}_i$ in the experimental design let ε_i represent the error between the evaluation of the actual (but implicit) limit state function $G(\overline{\mathbf{x}}_i)$ and the approximating (response) surface (5.72) given now as $\overline{G}(\mathbf{D}, \overline{\mathbf{x}}_i)$. This is repeated for each point in the experimental design. The total error is then minimized. One simple approach is to use a least-squares-fit method, with $\mathbf{D}$ selected to minimize the sum of squares of the errors:

$$S = \min_{\mathbf{D}} \left[\sum_{i=1}^n \varepsilon_i^2 \right]^{1/2} = \min_{\mathbf{D}} \left[\sum_{i=1}^n \left(\overline{G}\left(\mathbf{D}, \overline{\mathbf{x}}_i\right) - G\left(\overline{\mathbf{x}}_i\right) \right)^2 \right]^{1/2} \tag{5.73}$$

The above approach to obtaining an approximating limit state function (i.e. a response surface) is known also as polynomial regression, for obvious reasons. Another approach is to reduce the set of random variables $\mathbf{X}$ to the smaller set $\mathbf{X}_A$ describing their spatial averages. This can be done, for example, by using the same (i.e. spatial average) yield strength at every point on a plate under stress, rather than specifically allowing for the variation of yield strength from point to point (or from finite element to finite element).

A quite different approach is to simplify the error effect of random variables (or spatial averages) as having only an additive effect on the response, rather than some more complex relationship [Faravelli, 1989]. The enhanced expression (5.72) with additive error effects is then given by:

$$\overline{G}(\mathbf{X}) = A + \mathbf{X}^T \mathbf{B} + \mathbf{X}^T \mathbf{C} \mathbf{X} + \sum_j \left(e_j + \sum_k e_{jk} + \ldots \right) + \varepsilon \tag{5.74}$$

where the $e_j, e_{jk}, \ldots$ are the error terms due to spatial averaging (assumed here independent of the spatially averaged random variables) and ε represents the remaining errors (such as due to randomness) [Veneziano et al., 1983]. This format is useful if the $e_j, e_{jk}, \ldots$ can be obtained separately, such as through an analysis of variance of the effect of spatial averaging. The error to be considered for fitting $\overline{G}(\overline{\mathbf{x}})$ is then restricted only to the term ε.

A more complex but potentially more useful approach is to use an iterative solution scheme to obtain good points for fitting the approximating response surface to the actual (but implicit) limit state function [Bucher and Bourgund, 1990]. Let (5.72) have just sufficient undetermined coefficients to fit the evaluations $G(\overline{\mathbf{x}})$ exactly – a so-called 'fully saturated' experimental design – so that the surface fits exactly at the evaluation points $\overline{\mathbf{x}}$. Typically these might be at a mean point $\mathbf{x}_\mathrm{m}$ (see Figure 5.18) and at points given by $x_i = x_{\mathrm{m}i} \pm h_i \sigma_i$ where h_i is an arbitrary factor and σ_i is the standard deviation of X_i. Using these points, the approximating surface $\overline{G}(\overline{\mathbf{x}})$ for the assumed mean point $\mathbf{x}_\mathrm{m}$ can be determined exactly. If the approximating surface is located in the optimal position, the mean point $\mathbf{x}_\mathrm{m}$ would coincide with the point of maximum likelihood (the checking point), and the distance from this point to the origin would be a minimum in standardized Normal space (see Section 4.3.2).

If $\mathbf{x}_m$ is not the checking point, some other point, say $\mathbf{x}_D$, can be found on the approximating surface $\overline{G}(\overline{\mathbf{x}})$ which is closer to the origin and which is therefore the best estimate of the checking point. With $\mathbf{x}_D$ known, a new mean point $\mathbf{x}_m^*$ can be obtained by linear interpolation between $\mathbf{x}_m$ and $\mathbf{x}_D$, as:

$$\mathbf{x}_m^* = \mathbf{x}_m + (\mathbf{x}_D - \mathbf{x}_m)\frac{G(\mathbf{x}_m)}{\left[G(\mathbf{x}_m) - G(\mathbf{x}_D)\right]} \tag{5.75}$$

The speed with which this technique approaches a sufficiently accurate fit depends on the selection of h_i and the shape of the actual (but implicit) limit state function in the area being explored. It should be evident that the results are improved if the location of points is selected to correspond with points in the lower tail area for random variables representing resistances and in the upper tail area for random variables representing loads [Rajashekhar and Ellingwood, 1993]. Nevertheless, in general, convergence to all possibly relevant design points is not guaranteed [e.g. Beet et al. 2012]. It is possible to modify search algorithms to direct the search away from checking points already obtained [e.g. Der Kiureghian and Dakessian, 1998] or to add some error control to prevent oscillations about the checking point(s) being sought [Duprat et al., 2010]. Some of these issues are discussed in more detail in Leonel et al. (2011).

5.5.3 Applications of Response Surfaces

A number of example applications of response surfaces have been given in the literature [e.g. Faravelli, 1989; Bucher and Bourgund, 1990; Wu et al., 1990; Schuëller et al., 1991; El-Tawil et al., 1992; Rajashekhar and Ellingwood, 1993; Grandhi and Wang, 1997], and software has been developed [e.g. Schuëller and Bucher, 1991]. These developments suggest that the concept of a response surface works well provided the checking point (i.e. the point of maximum likelihood or the MPP) can be identified and that reasonable decisions can be made about the points to be used for fitting the response surface. This has led to the use of iteration [e.g. Liu and Der Kiureghian, 1991b; Liu and Moses, 1994; Kim and Na, 1997; Romero et al. 2004].

For linear and near-linear limit state functions the estimated probability is likely to be relatively insensitive to accurate fitting, but this may not be the case for highly curved limit state surfaces, or with intersecting limit state surfaces. In this context it might be noted that quadratic (parabolic) response surfaces tend to mirror those used in 'second order' second moment theory, with a quadratic (or parabolic) surface fitted either to a known non-linear limit state surface (see Section 4.5.1) or to known discrete points, as in response surfaces. It follows that there is a close parallel between these two approaches.

The gradients required at the point of maximum likelihood can be determined or estimated approximately using a finite difference–type approach, although at extra computational cost. Alternatively, the finite element analysis code might be modified to provide gradient [e.g. Lemaire et al., 1997].

An important application of response surfaces is for the representation of random fields that normally requires extensive finite element modelling. Applications with implications for structural reliability include the statistical variation of properties such as Young's modulus across a plate and the variability of soil properties in embankments. This is a rather specialized topic and various ways have been suggested for doing this

[e.g. Vanmarcke et al., 1986; Li and Der Kiureghian, 1993; Zhang and Ellingwood, 1995; Matthies et al., 1997].

5.5.4 Other Techniques for Obtaining Surrogate Limit States

Several techniques other than obtaining a response surface by polynomial regression have been explored. One of these is the use of machine learning techniques, such as artificial neural networks, sometimes portrayed as a universal approximating technique with wide application [Gurney, 1997]. However, it is not without its critics [e.g. Dewdney, 1997]. It has been proposed as applicable to generating an approximating limit state function, by iteration ('learning') for structural reliability problems [e.g. Hurtado and Alvarez, 2001]. Another machine learning approach is based on support vector machine techniques that construct a hyperplane or a set of such planes in n dimensional space such that each hyperplane best fits the individual points (realizations) with its perpendicular distance closest to the point of interest [Kecman, 2001]. Because this has a direct analogy to the linear limit state function in FOSM theory, it has been proposed as appropriate for use with structural reliability analysis [Bourinet et al., 2011].

A further technique is Gaussian process modelling (or Kriging). It works by predicting an appropriate continuous functional form between data points for the mean and for (Gaussian) variability. This is obtained as a realization of a random field described by the Gaussian process. Since this produces functional relationships that are smooth and continuous, interpolation between data points usually is more accurate than for simpler techniques. However, the computational costs tend to be high.

There is a wealth of literature dealing with Gaussian process modelling as a statistical tool for fitting a function to discrete data points in hyper-space [Cressie, 1993; Santner et al., 2003; Press et al., 2007]. It has its roots in attempts to simulate variability in 3-D situations such as for mineral ore deposit exploration [Matheron, 1973]. For structural reliability analyses the sign of the limit state function (that is, of the predicted surface) is the most important factor [Kaymaz, 2005], and this has allowed the procedure to be simplified specifically for Monte Carlo applications [Echard, et al. 2011]. Comparisons of these different techniques and their results for specific examples are available [e.g. Bucher and Most, 2008; Bichon et al., 2008; Dubourg et al., 2013; Gasper et al., 2014].

5.6 Functionally Dependent Limit States

5.6.1 Effect of Order of Loading

So far it has been assumed that the limit state functions, explicit or implicit, and the probability of failure, are not dependent on the manner, order or sequencing of the loads applied to the structure. For simple, statically determinate structural systems the estimate of the probability of failure usually does not depend on such sequencing but this is not always the case. For example, in a framed structure the first member to fail may affect the subsequent internal force distribution and thus affect the sequence of failure of subsequent members. So-called 'jacket' type offshore structures often are of this type. More generally the limit state functions (and thus most likely also the probability of failure) are load-sequence and failure-sequence dependent, that is, they are functionally dependent. This type of problem is considered in this section.

@Seismicisolation

In order not to limit discussion to any particular type of structure, let the term 'nodes' be used to denote members in trusses, or local regions in frames where failure may occur. Examples are the plastic failure modes with their localized 'plastic hinges' in ideal-rigid-plastic structural theory [Heyman, 1971], as discussed in Section 5.2.3.3 and Examples 5.3 and 5.4. In practical structures as distinct from their idealized 'plastic' equivalents, the generation of the failure modes for such structures is likely to come about through a sequence of formation of plastic hinges. More generally, this suggests that any failure mode for a structure is likely to consist of a sequential occurrence of failure, often confined mainly at discrete nodes. Considering the materials used for construction, it is likely also that there will be dependence in the (physical) properties of the nodes. This dependence must be taken into account in evaluating the system reliability.

5.6.2 Failure Mode Enumeration and Reduction

All modes of failure making a significant contribution to the failure probability must be identified (*cf.* Section 5.2.2); if this is not done, the probability calculated will be under-estimated. One approach to identify all structural failure modes is through exhaustive enumeration of all possible combinations of sequences of node failures, in each case following the notion of an event tree (Section 5.2.2.1). For all but the simplest structural systems this will be a major task even if done systematically. Thus, each node should be considered in turn and added to a sequence of failure of previous nodes. Each new sequence is examined to ascertain whether a valid structural failure mode has been attained; if not, a further node may be added. The concept is shown schematically in Figure 5.19.

When structural failure is defined as collapse of the structure or some part of it, as for example in plastic theory, each failure mode must be kinematically admissible (i.e. a valid collapse or failure mode must exist). In addition, of course, there must be correspondence everywhere between internal actions and local strains. Equilibrium also must be satisfied.

The probability that the k th failure mode, consisting of n nodes, will occur is given by

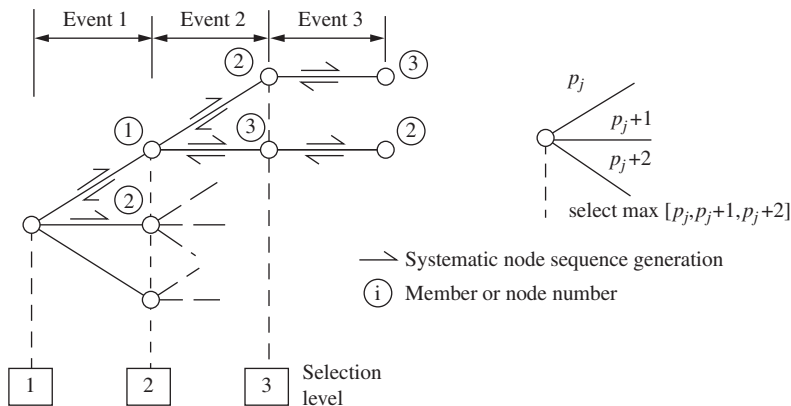$$p_{f_k} = P(E_1 \cap E_2 \cap \ldots \cap E_n) \tag{5.76}$$

Figure 5.19 Systematic enumeration procedure.

where E_i denotes the event 'resistance of the i th node exceeded'. In general a number of such sequences of failure modes exist. An example is shown in Figure 5.19 with the sequence of failure modes shown as 1, 2, 3. The probability of failure for this sequence may be evaluated by any of the methods described so far.

When a failure mode has been identified, enumeration of the next failure mode is achieved by 'back-tracking' until a new combination or ordering of nodes becomes possible. For complex node behaviour, unloading, stress reversal, loss of stiffness, etc. also may need to be considered, including as possibilities in the event tree. This will add greatly to computation effort and still presents a challenge for the probabilistic analysis of complex structures, even with the adoption of systematic procedures. For the special case of ideally rigid-plastic structures considerable simplifications are possible, since the precise order of failure of the nodes in a sequence of modes should not matter [Heyman, 1971].

Computational effort is likely to be considerably reduced if failure modes that contribute little to the structural failure probability could be identified before being included in the computational scheme. They could then be eliminated from further analysis if the error in so doing is not large [Ibrahim, 1992]. A number of techniques have been proposed to do this as early as possible in the enumeration procedure, and preferably before full calculation of mode failure probabilities [Moses, 1982; Murotsu et al., 1977, 1984; Guenard, 1984; Melchers and Tang, 1984; Thoft-Christensen and Murotsu, 1986; Ibrahim, 1992; Zimmerman et al., 1992]. Some of these are intuitive and empirical.

5.6.3 Reduction of Number of Limit States—Truncation

In addition to reducing the complexity of each failure mode (limit state), it would be computationally advantageous also to reduce the number of failure modes (limit states) that need be considered without significant compromise of the estimated probability of failure for the structure as a whole. One approach to do this is to eliminate all failure modes for which (see 5.76 above) the individual failure probability $p_{f_k} \leq \delta p_f$, where δ is an appropriately valued 'truncation criterion' and p_f is the estimated nominal failure probability for the whole structural system. With this criterion, all failure modes are evaluated if $\delta = 0$.

Unless a subjective estimate is available prior to the analysis, p_f may be approximated by the most significant (i.e. maximum) value of p_f so far estimated in the procedure, e.g. from an earlier estimation of a mode failure probability p_{fk}. Let this value be denoted p_f^*:

$$p_f^* = \max_{\ell=1}^{k-1} \left(p_{f_\ell} \right), \quad k \geq 2 \tag{5.77}$$

Since it always will be the case that $p_f^* \leq p_f$ the use of (5.77) is conservative, because fewer failure modes are discarded. Further, it is noted that the probability of failure for each individual failure mode included in (5.77) may be bounded by using a smaller number of nodes, $q \leq n$, as shown in the inequalities

$$p_{f_k} = P\left(E_1 \cap E_2 \cap \ldots E_n \right) \leq P\left(E_1 \cap E_2 \cap \ldots \cap E_q \right) \ldots \leq P\left(E_1 \cap E_2 \right) \leq P(E_1) \tag{5.78}$$

In principle the selection of the node(s) to be eliminated may be in any order. However, intuitively it is clear the approximation for p_{fk} and hence the probability of failure of the whole system may depend on the choice of which node(s) to delete. As noted in Section 6.5.2, an efficient algorithm will select the nodes of little consequence as early as possible. A reasonable strategy is to select the next node such that the probability of occurrence of the partial node sequence including the selected node is maximized. Working from the first to the q th node in a sequence, this means that the selections are made as

first node:
$$P\left(E_1\right) = \max_i \left[P_i(E_1)\right] \tag{5.79a}$$

second node:
$$P\left(E_1 \cap E_2\right) = \max_i \left[P_i(E_1 \cap E_2)\right] \tag{5.79b}$$

.
.

or in general for the q th node:

$$P\left(E_1 \cap E_2 \ldots \cap E_q\right) = \max_i \left[P_i(E_1 \cap E_2 \ldots \cap E_q)\right] \tag{5.79c}$$

where the maximization is over the set of all 'eligible nodes' at each selection level (see Figure 5.19). Thus, at the q th level, the events E_1 to E_{q-1} are held fixed and a decision is made about selection of event E_q from the remaining nodes. This strategy will achieve a reasonably good estimate p_f in (5.77).

For the evaluations of the failure probabilities in expressions (5.76, 5.78 and 5.79) any of the methods discussed in Chapters 3 and 4 and in Appendix C can be used. Then, with the probabilities p_{f_k} for the dominant failure modes known, the nominal failure probability for the structural system can be obtained, in principle, from (5.1) as

$$p_f = P\left(F_1 \cup F_2 \cup F_3 \cup \ldots \cup F_m\right) \tag{5.80}$$

where the event F_i $(i = 1, \ldots, m)$, represents failure in the i th mode. As noted in Section 5.2.2, considering only the dominant modes obtained by the simplifications described above will underestimate the system failure probability.

5.6.4 Applications

Although reasonably simple for single parameter loading or once-only loadings (i.e. time-invariant cases) and useful for determining failure modes of systems that are not too large [e.g. Xiao and Mahadevan, 1994], the detailed step-by-step analysis of systems through event tree analysis usually becomes very complex and highly computationally demanding. Some early efforts have been made to further simplify the analysis, but a critical analysis suggests that full or even reduced enumeration for complex systems is not particularly fruitful [Murotsu et al., 1977, 1983; Grimmelt et al. 1983; Thoft-Christensen and Sørensen 1982; Murotsu et al., 1985]. One possibility is to define the load combinations to be used in a reliability analysis in a manner analogous to that used in conventional structural design and for which only a limited number of combinations of loading is considered [Ditlevsen and Bjerager, 1984; Ditlevsen and Madsen, 1996]. Such an approach, whilst not fundamental, at least could give a conditional probability statement with clearly defined conditions. More generally,

however, how to deal with problems for which the failure probability is load-path dependent and for which the critical limit states change depending on the order and sequencing of multiple loads, remains an outstanding, unsolved problem for application of structural reliability.

5.7 Conclusion

The reliability analysis of structural systems follows the procedures outlined in Chapters 3 and 4 but with more complex formulation of limit states. For structural systems in which the limit states do not depend on previous loadings or events, the analysis can proceed directly with the use of the 'crude' Monte Carlo or with the efficient importance-sampling and directional sampling procedures. Classification of the system as one with series, parallel or more complex subsystems is helpful for the use of system reliability (probability of failure) bounding theorems, such as might be used in conjunction with the various first-order methods (FOSM, FOR).

The failure modes for the structure are not always known. These can be investigated to some extent using Monte Carlo simulation, or they may be enumerated either exhaustively or through simplified methods. Of particular interest are those failure modes that make the greatest contribution to the system failure probability. A systematic procedure to select these for one-parameter loading situations was described, together with various procedures for limit state definition and the calculation of the corresponding probabilities.

Except as noted in Section 5.6, the techniques described in this chapter have limitations regarding the sequencing of loading applied to the structure. They all have a further limitation, namely that applied loading is assumed a once-only application of an extreme value (one-parameter) loading system (i.e. the maximum for the lifetime of the structure). This limitation allows the basic reliability problem (1.31) to be invoked, but it cannot deal with time-variant loadings. This limitation can be removed, at least for simple structural systems, using the theory of Chapter 6.

6

Time-Dependent Reliability

6.1 Introduction

This chapter discusses so-called 'stochastic', 'time-dependent' or 'time-variant' random variables and the related failure probability calculations. Attention is confined initially to situations of the type considered in Chapter 1, that is, with the resistance measured in terms of material yield strength or some type of permissible stress. Later in this chapter some introductory comments are made about fatigue reliability and about problems involving dynamic structural behaviour.

As noted in Chapter 1, in general the basic variables $\mathbf{X}$ will be functions of time. This comes about, for example, because loading changes with time (even if it is quasi-static, such as is the case for most floor loading) and because material strength properties change with time, either as a direct result of previously applied loading or because of some deterioration mechanism. Fatigue and corrosion are typical examples of strength deterioration.

The elementary reliability problem (1.15) in 'stochastic' (i.e. time-variant) terms with a resistance $R(t)$ and a load effect $S(t)$, at time t becomes

$$p_f(t) = P[R(t) \leq S(t)] \tag{6.1}$$

If the instantaneous probability density functions $f_R(t)$ and $f_S(t)$ of $R(t)$ and $S(t)$ respectively are known, the instantaneous failure probability $p_f(t)$ can be obtained from the convolution integral (1.18). Schematically, the changes in $f_R(t), f_S(t)$ and $p_f(t)$ with time can be depicted as in Figure 1.7.

Strictly, (6.1) has meaning only if the load effect $S(t)$ increases in value at time t (otherwise failure would have occurred earlier) or if the random load (effect) is re-applied precisely at this time. Failure could not occur precisely at the very instant of time t (assuming, of course, that at time less than t the member or structure was safe). Thus, in general, a change in load or load effect is required; this is assured if:

(1) there are discrete load changes (as will be discussed in Section 6.2 below);
(2) for continuous time-varying-loads, an arbitrary small increment δt, in time, is considered instead of instantaneous time t.

With this interpretation, it follows that

$$p_f(t) = \int_{G[\mathbf{X}(t)] \leq 0} f_{\mathbf{X}(t)}[\mathbf{x}(t)] d\mathbf{x}(t) \tag{6.2}$$
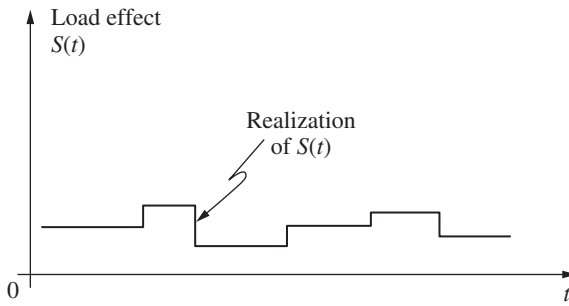
Figure 6.1 Typical realization of random process load effect.

which may be represented, in two-dimensional space, as in Figure 1.8 for any given time t. As before, $\mathbf{X}(t)$ is a vector comprised of the basic random variables.

In principle, the instantaneous failure probability given by (6.1) or (6.2) can be integrated over an interval of time $0 - t$ to obtain the failure probability over that period. In practice, however, the instantaneous value of $p_f(t)$ usually is correlated to the value $p_f(t + \delta t)$, $\delta t \to 0$, since typically the processes $\mathbf{X}(t)$ themselves are correlated in time. This may be seen in a typical 'sample function' or 'realization' of a random process load effect, as shown in Figure 6.1.

The classical approach is to consider the integration transferred to the load or load effect process, which is then assumed to be representable, over the total time period, by an extreme value distribution. This means the load or load effect has been turned from a process into a random variable. Also, the resistance is assumed to be time invariant. This approach formed the basis of discussion in the earlier chapters. It also is known as the 'classical' reliability problem [Freudenthal, 1961]. The theory underlying this approach will be outlined in Section 6.2.

A refinement is to consider shorter periods of time, such as the duration of a storm, or a year, and to apply extreme value theory within that period. Simple ideas akin to the concept of the return period (Section 1.3) then can be used to determine the failure probability over the lifetime of the structure. This approach, discussed in Section 6.3, historically has been popular for practical reliability analyses of major structures, such as offshore platforms, towers, etc., subject to definable and discrete loading events.

A somewhat different way of looking at the problem is to consider the safety margin associated with (6.1):

$$Z(t) = R(t) - S(t) \tag{6.3}$$

and to establish the probability that $Z(t)$ becomes zero or less in the lifetime t_L of the structure. This constitutes a so-called 'crossing' problem. The time at which $Z(t)$ becomes less than zero for the first time is called the 'time to failure' (Figure 6.2) and is a random variable. The probability that $Z(t) \leq 0$ occurs during t_L is called the 'first-passage' probability.

The corresponding situation in two-variable space is shown in Figure 6.3. The probability that the vector process $\mathbf{X}(t)$ will leave the 'safe' region $G(\mathbf{X}) > 0$ (i.e. the probability that an 'outcrossing' will occur) during the structural lifetime t_L is again the so-called
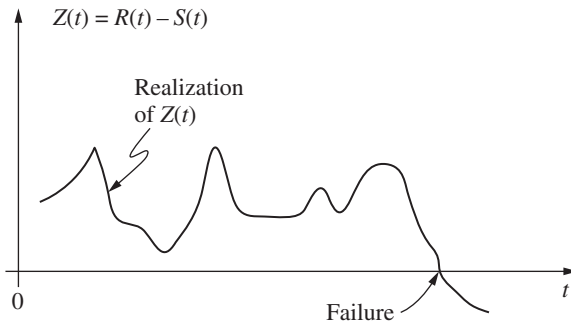
Figure 6.2 Realization of safety margin process $Z(t)$ and time to failure.
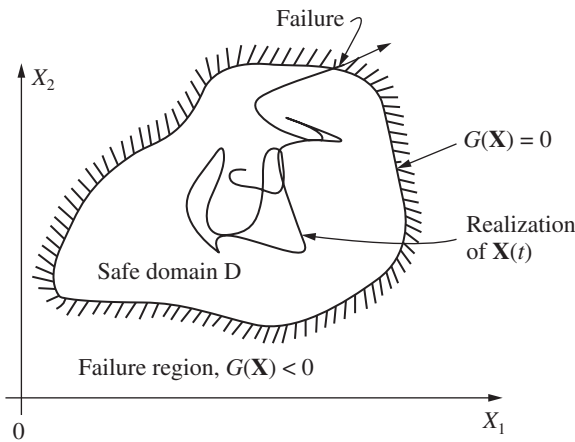
Figure 6.3 Outcrossing of vector process $\mathbf{X}(t)$.

'first-passage' probability. It is, of course, equal to the probability of failure of the structure since failure is defined by $G(\mathbf{X}) \leq 0$.

The first-passage concept is more general than the classical approaches. In particular, there is no restriction on the form of $G(\mathbf{X})$. However, the determination of the first-passage probability and a proper understanding of the concept do require some knowledge of stochastic processes. An introduction to this topic is given in Section 6.4. An introductory discussion of the time-dependent approach to reliability calculation follows in Section 6.5. If the elementary reliability problem (6.1) is to be made to cope with more than one load or load effect, as is required, for example, in design code applications, it is necessary to combine two or more load effects into one equivalent load effect. This may be achieved using the theory and methods of Sections 6.4 and 6.5 and is described in Section 6.6.

An important strength requirement for structures is fatigue strength. This has not so far been considered, as it is essentially a time-dependent problem. The essential probabilistic considerations for the analysis of fatigue reliability are outlined in Section 6.8, following brief comments in Section 6.7 about problems involving dynamic structural behaviour.

6.2 Time-Integrated Approach

6.2.1 Basic Notions

In the time-integrated approach, the whole lifetime $[0, t_L]$ of the structure is considered as a single unit, and all statistical properties of all random variables must relate to this lifetime. Thus the probability distribution of interest for loads is that for lifetime maximum loads. Similarly, the probability distribution of interest for resistance is the lifetime minimum. Simple comparison of the maximum load and the minimum resistance is, however, not appropriate since it is highly unlikely that the occurrence of the lifetime maximum load will coincide with the lifetime minimum resistance, as shown in Figure 6.4 for typical realizations of $R(t)$ and $S(t)$.

For many practical problems it is sufficient to assume, initially at least, that $R(t)$ is time independent. The typical realization of $R(t)$ is now a horizontal line (Figure 6.5). The actual location of this realization of R is, of course, governed by the probability density function $f_R(\ )$ if R is a random variable. With this restriction (6.1) becomes

$$p_f(t_L) = P[R \leq S_{\max}(t_L)] \tag{6.4}$$

where $S_{\max}(t_L)$ denotes the maximum load effect in the period $[0, t_L]$. It is of course possible, but unlikely in practice, to interchange the assumptions placed on R and S.

The probability distribution for $S_{\max}(\ )$ may be obtained directly by fitting an appropriate probability distribution function to observed extreme value data of past observations and assuming it will be applicable also to the future. Usually, however, data are not available for a sufficiently long period of time, and records for shorter periods generally must be used to synthesize the extreme value distributions. Probability distributions for loads and for resistances are discussed in Chapters 6 and 7.

The time-integrated approach is based on the concept of applying a (one-parameter) loading system Q to the structure at regular intervals in time. In this case the probability of failure of the structure may be considered simply a function of the number N of statistically independent loading applications to cause failure [Freudenthal et al., 1966]:

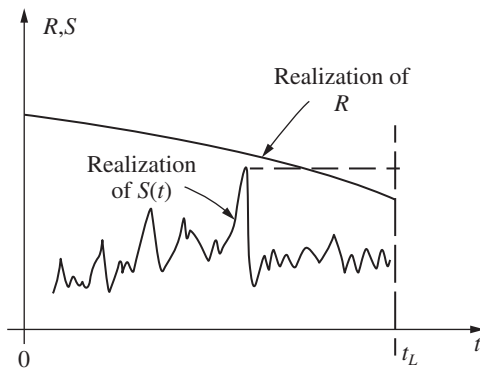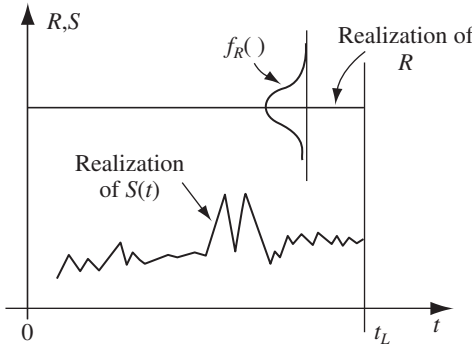$$P(N \leq n) \equiv F_N(n) = 1 - L_N(n) \tag{6.5}$$

Figure 6.4 Typical realizations of load effect $S(t)$ and resistance $R(t)$ when both are non-stationary.

Figure 6.5 Typical realizations of load effect $S(t)$ and resistance R, with R a time-independent random variable.

where n is some given number of load applications, $F_N(n)$ is the cumulative distribution function of N, and $L_N(n)$ is defined as the 'reliability function'. Since N is discrete, it follows that the probability mass function $f_N()$ is given by (*cf.* A9):

$$f_N(n) \equiv P(N = n) = F_N(n) - F_N(n - 1) \tag{6.6}$$

It is also possible to define the so-called 'hazard' function:

$$h_N(n) = P(N = n \,|\, N > n - 1) = \frac{f_N(n)}{1 - F_N(n - 1)} \tag{6.7}$$

It expresses the probability of failure under the n th loading ($N = n$) given that failure has not occurred under a previous loading ($N > n - 1$). It is more commonly expressed in terms of time (see Section 6.3.3 below).

It will be assumed that load applications are independent in time, i.e. there is no dependence between the i th and j th load application ($i \neq j$). It will be assumed also, for convenience, that the resistance R and the load effect S (associated with one application of Q) each have known probability density functions $f_R(), f_S()$ (and hence associated cumulative distribution functions). Both R and S (and therefore Q) will be assumed to be stationary random processes, i.e. $f_R()$ and $f_S()$ do not change with time.

Then, for a series of n (independent) loads applied to the structure, the probability that the maximum load effect S^* is less than some value x, say, is given by

$$F_{S^*}(x) = P(S^* < x) = P(S_1 < x).P(S_2 < x) \ldots = [F_S(x)]^n \tag{6.8}$$

If n is very large, (6.8) asymptotically approaches one of the extreme value distributions (see Sections A.5.11–A.5.13), which may then be used to describe S^*.

The justification for using extreme value distributions in the time-integrated approach can now be given directly. Using the same argument as in Section 1.4.2, the probability of failure, i.e. the probability that fewer than n load applications can be supported, is

$$P(N < n) = \int_0^\infty \{[1 - F_S(y)]^n\} f_R(y) dy \tag{6.9a}$$

$$= \int_0^\infty [1 - F_{S^*}(y)] f_R(y) dy \tag{6.9b}$$

and integrating by parts produces [see also (1.19)]

$$p_f = F_N(n) = \int_0^\infty F_R(y) f_{S^*}(y) dy \tag{6.10}$$

which is identical with (1.18) but with an extreme value distribution for the maximum applied load effect S^*. Note that (6.10) does not contain specifically the number of load applications; this has been absorbed into the derivation of the distribution for S^* (and is therefore assumed to be 'large'). Note also that the lower integration limit in (6.10) differs from that in (1.18)—the reason for this should be clear.

6.2.2 Conversion to a Time-Independent Format*

In practical situations, more than one load system may act. Usually the load systems are assumed independent (e.g. live load and wind load) but may not be (e.g. wave load and wind load). In addition, the peaks of different load processes usually do not coincide. Hence it would be rather conservative to use an extreme value distribution for each load system separately. The usual procedure is to derive one process to represent the combined effect of several load processes. This is the so-called 'load combination' problem, as discussed in Section 6.6. It has application also in design code calibration, as discussed in Chapter 9, in which case the equivalent load is converted to a time-independent equivalent for use in time-invariant reliability analysis (i.e. a 'time-integrated' approach).

Essentially the same approach can be used directly to convert a time-dependent reliability problem to a time-independent one [Bucher et al., 1988; Chen et al., 1988]. First it is necessary to evaluate the maximum combined load effect of the time-varying loads expected during the lifetime $[0 - t_L]$ of the structure. This can be expressed as a generalization of (6.4) with the probability of the limit state function being violated (i.e. ($G(\ ) < 0$) under the load effect, given by:

$$p_f(t_L) = P\left\{ G\left[\mathbf{R}, \max_{[0, t_L]} S(\mathbf{Q}(t))\right] < 0 \right\}$$
$$= P\{G[\mathbf{R}, S_{\max}(t_L)] < 0\} \tag{6.11}$$

where $S(\ )$ is the load effect resulting from the load processes $\mathbf{Q}(t)$ and $\mathbf{R}$ is the vector of structural resistances with the joint probability density function (pdf) $f_{\mathbf{R}}(\ )$.

Since (6.11) is difficult to solve directly, Wen and Chen (1987) proposed a conditioning scheme with $\mathbf{R}$ in (6.11) replaced by a realization $\mathbf{r}$ so that the probability given by (6.11) is the conditional failure probability $p_f(t_L|\mathbf{r})$. The total probability is then given

$$p_f(t_L) = \int_{\mathbf{r}} p_f(t_L|\mathbf{r}) f_{\mathbf{R}}(\mathbf{r}) d\mathbf{r} \tag{6.12}$$

For $\mathbf{R}$ independent of $\mathbf{Q}(t)$, the conditional probability can be written as

$$p_f(t_L|\mathbf{r}) = 1 - F_{S_{\max}}(t_L, \mathbf{r}) \tag{6.13}$$

where $F_{S_{\max}}(\ )$ is the cumulative distribution function of $S_{\max}$, the lifetime maximum effect of the combined load processes. Its evaluation is discussed in Section (6.6). Alternatively, Monte Carlo methods can be used [e.g. Chen, 1989].

A slightly different approach is to convert from a time-dependent to a lifetime time-independent problem through the introduction of an auxiliary random variable.

This allows an augmented limit state function to be written in time-independent reliability, which is then solved using FOSM theory or Monte Carlo simulation [see Wen and Chen, 1987; Madsen and Zadeh, 1987].

A possible difficulty with both these last two approaches is that the conditional failure probability $p_f(t_L|\mathbf{r})$ must be available for all realizations $\mathbf{r}$ of $\mathbf{R}$. Also, the use of an equivalent load effect as a substitute for the actual load processes is only valid in linear elastic structural systems (since the theory relies on superposition) or for ideal plastic systems (since the loading sequence is then irrelevant—see Chapter 5).

Despite the apparent simplicity of the time-integrated approach, for situations involving multiple load processes it is generally better to turn to stochastic process theory (Section 6.4) and the applications that follow from it (Section 6.5).

6.3 Discretized Approach

In the discretized approach to handling time-dependent structural reliability problems, the lifetime of the structure is divided into a number of units. These can be time periods such as one year, say, or they may be taken as the occurrence of a discrete event such as a storm of a particular duration. The reliability problem then becomes the calculation of the probability of failure given that n_L years or events occur during the lifetime t_L of the structure. For a given unit time period n_L is fixed, once t_L is decided. However, for storm events, n_L is not known *a priori,* although the average rate of occurrence of storms may be known.

The discrete time unit may be a day, a month, a year, etc., although a year is commonly adopted. The failure probability calculated using the method of the previous section then is the probability of failure per year. The corresponding resistance and load effect variables of interest are the extreme values per year, with appropriate probability density functions. Such distributions are obtained from observations (e.g. wind, waves) and are related to the particular time period used as the reference (e.g. one year). Thus the maximum wind force per year will have a different probability density function to (say) that of the maximum wind force per day. Only under particular assumptions is it possible to relate these distributions easily, as will be seen below.

The discretized approach can be justified along similar lines to that used in Section 6.2 for the time-integrated approach. As noted, two cases may be distinguished:

(1) n_L known deterministically;
(2) n_L a random variable.

6.3.1 Known Number of Discrete Events

Consider a set of n_L loads applied to the structure. If a given time period is now considered (e.g. one year) within which n_L may be considered 'large' and for which each load occurrence may be considered to be an independent event, then (6.8) may be used to obtain the extreme value distribution S_1^* for S for one year. The probability p_{f_1} of failure per year is then given by (6.10). However, the probability of failure for a life of n_L years is given by (6.9a), with S_1^* substituted for S and assumed independent between years [Freudenthal et al., 1966]:

$$p_f(n_L) = F_{N_L}(n_L) = \int_0^\infty \{1 - [F_S^*(y)]^{n_L}\} f_R(y) dy \tag{6.14}$$

@Seismicisolation

Noting that

$$[F(y)]^n = [1 - \overline{F}(y)]^n \approx 1 - n\overline{F}(y) + n(n-1)\frac{\overline{F}(y)^2}{2} - \dots$$

where $\overline{F}(\ ) = 1 - F(\ )$ and neglecting second-order terms, it follows easily that

$$p_f(n_L) \approx \int_0^\infty \{1 - [1 - n_L\overline{F}s_1^*(y)]\} f_R(y)dy \tag{6.15}$$

or

$$p_f(n_L) \approx n_L \int_0^\infty \overline{F}s_1^*(y)f_R(y)dy \tag{6.16}$$

$$\approx n_L p_{f_1} \tag{6.17}$$

where the alternate expression (1.19) has been used for p_{f_1}. The neglect of second-order terms in (6.15) is valid only for those values of y for which $n\overline{F} \ll 1$. It is easily shown that this implies high values of y and that as a consequence the approximation (6.15) and hence (6.16) and (6.17) are most accurate for situations in which the standard deviation for load effects is much greater than that for the resistances, i.e. $\sigma_S \gg \sigma_R$. Clearly these approximations are restricted also to small values of p_{f_1} and $p_f(n_L)$. Result (6.17) shows that the lifetime failure probability $p_f(n_L)$ can be determined (approximately) from the annual failure probability p_{f_1} simply by multiplying the latter by the number n_L of years in the designated lifetime t_L.

Rather than expressing the life of a structure in terms of the number of load applications, a more natural parameter is time T. The probability that a structure will fail during a time period $[0, t]$ may then be stated as

$$P(T < t) = F_T(t) = 1 - L_T(t) \tag{6.18}$$

where $F_T(\ )$ is the cumulative distribution function of T and $L_T(\ )$ is the 'reliability function' expressed in terms of time.

If now p_i is the failure probability for the i th time unit (*cf.* p_{f_1} above and 6.10), then, using the same arguments as for (6.8),

$$P(T < t) = 1 - \prod_{i=1}^{t}(1 - p_i) = 1 - (1 - p)^t \tag{6.19}$$

if $p_i = p$ for all i (as is the case for time-invariant R) and assuming independence of p between time units. If pt is sufficiently small, this may be approximated by

$$P(T < t) \approx 1 - \exp(-tp) \approx tp \tag{6.20}$$

which corresponds to (6.17) (and has the same limitations) provided that t and p are interpreted appropriately. This also shows clearly that the choice of time period is arbitrary, provided that it is consistent between t and p. Nevertheless the choice of one year is very common. The probability of failure for a lifetime $[0, t_L]$ is thus

$$p_f(t_L) = 1 - \exp(-t_L p) \approx t_L p \tag{6.21}$$

6.3.2 Random Number of Discrete Events

The failure probability p_i for the i th time unit depends on the number of load applications which occur during that time unit. If a time unit is considered to be an 'event' such as a storm, the actual number of load applications during the event might be ignored provided that an appropriate extreme value probability distribution is used to describe the maximum load effect S_e^* occurring during the event. The discretization is now over 'events' (of indeterminate duration) rather than periods of given duration as in Section 6.3.1.

The number of occurrences of the events, however, needs to be known to obtain the lifetime failure probability $p_f(t_L)$. Let this be given by $p_k(t)$, the probability of k events in time $[0, t]$. Then the probability of failure for a period $[0, t]$ may be expressed in time terms as (*cf.* 6.11):

$$p_f(t) = F_T(t) = \int_0^\infty \sum_{k=0}^\infty p_k(t) \left\{ 1 - \left[F_{S_e^*}(y) \right]^k \right\} f_R(y) dy \tag{6.22}$$

in which all possible values of the number of events are considered.

A common assumption is to take $p_k(t)$ as Poisson distributed (see Section A.5.4):

$$p_k(t) = \frac{(vt)^k e^{-vt}}{k!} \tag{6.23}$$

where v is the mean rate of occurrence of events. In view of the derivation of the Poisson distribution, this means that the events must be independent and non-overlapping. This is likely to be closely true if v is very low. If (6.23) is substituted into (6.22) and a series approximation similar to that used in deriving (6.15) is applied, it follows readily that

$$p_f(t) \approx 1 - \exp(-vt p_{f_e}) \tag{6.24}$$

where p_{f_e} is the probability of failure given the occurrence of a single event. It is given by (6.10) with S_e^* substituted for S^*. Further, expression (6.24) corresponds to (6.20) when it is recognized that $v p_{f_e}$ is the average failure probability per unit time. Again the same limitations regarding accuracy apply to (6.24) as apply to (6.16) and (6.20).

It should be noted that the calculation of the value of p_{f_e}, the probability of failure given that the event occurs, may well need to take account of some conditional information [e.g. Schuëller and Choi, 1977]. For example, if the event of interest is the occurrence of a storm at an offshore structure, then the maximum load effect S_e^* may depend on the occurrence of the 'characteristic' wave height H_k during that storm. Let $S_e^*|H_k$ represent the maximum load effect given the occurrence of a characteristic wave height H_k. It has a probability density function $f_{S_e^*|H_k}(\ )$. Then the probability density function $f_{H_k}(h)$ expresses the probability of occurrence of a characteristic wave height between h and $h + \delta h$ as $\delta h \to 0$. The conditional failure probability $p_{f_e}|H_k$ may then be calculated from (1.18):

$$p_{f_e}|(H_k = h) = \int_0^\infty F_R(y) f_{S_e^*|H_k}(y) dy \tag{6.25}$$

Table 6.1 Analyses of failure probability for Example 6.2.

Characteristic wave height H_k(m)	$f_{H_k}(). \Delta h$	$p_{f_e}\,\vert H_k$	$\sum p_{f_e\vert H_k} f_{H_k} \Delta h$
24	0.100	0.2×10^{-9}	0.020×10^{-9}
26	0.640	0.9×10^{-9}	0.576×10^{-9}
28	0.180	4.0×10^{-9}	0.720×10^{-9}
30	0.060	12.0×10^{-9}	0.720×10^{-9}
32	0.015	24.0×10^{-9}	0.360×10^{-9}
34	-0.005	50.0×10^{-9}	0.250×10^{-9}
$\Delta h = 2$ m	$\sum = 1.00$		$\sum = 2.65 \times 10^{-9}$

Further, assuming $H_k > 0$, it follows from (A.11) that the unconditional failure probability is given by

$$p_{f_e} = \int_0^\infty p_{f_e}\vert(H_k = h)\ f_{H_k}(h)\,dh \tag{6.26}$$

The probability density functions $f_{H_k}(\ )$ may be obtained directly from field observations. However, determination of $f_{S_e^*\vert H_k}(\ )$ will require both loading data for a given H_k and a structural analysis using the applied loading Q_e^* corresponding to S_e^*.

Example 6.2   An offshore platform is subject to an average of 2.5 storms/year. It has a planned design life of $t_L = 15$ years. Estimates of the probability of failure given a particular characteristic wave height during a storm are set out in Table 6.1. This also shows the estimated occurrence probabilities $f_{H_k}(\ )$. Δh for each characteristic wave height.

Expression (6.26) may be approximated as $\sum p_{f_e\vert H_k} f_{H_k} \Delta h$ to obtain $p_{f_e} = 2.65 \times 10^{-9}$. Using (6.24), the probability of failure in the period [0–15 years] is:

$$\begin{aligned}
p_f(t_L) &\approx 1 - \exp[(-2.5)(15)(2.65 \times 10^{-9})] \\
&\approx (-2.5)(15)(2.65 \times 10^{-9}) \\
&\approx 10^{-7}
\end{aligned}$$

6.3.3   Return Period

The return period was introduced in Section 1.3 as the mean time between defined probabilistic events, usually taken as the exceedance of some given level or load. This concept can be generalized by defining the events in terms of limit state violation, calculated using any of the methods of Section 1.4, and Chapters 3, 4 and 5. Thus the generalized return period may be defined as

$$\overline{T}_G = \frac{1}{p_{f_1}} \tag{6.27}$$

where p_{f_1} is the probability of limit state violation per unit time (often taken as 1 year) calculated from (1.18) or (1.31), and $\overline{T}_G$ is measured in similar time units (i.e. years). If

there are n_L time units in the design life t_L, and assuming, as before, independence of events between time units, (6.17) may be used to obtain the lifetime failure probability:

$$p_f(t_L) \approx \frac{n_L}{T_G} \tag{6.28}$$

Further, if there are m independent phenomena contributing to the failure probability, then (see Section A.2)

$$p_{f_T} = \sum_i^m p_{f_i} \tag{6.29}$$

or

$$\frac{1}{T_T} = \sum_i^m \frac{1}{T_i} \tag{6.30}$$

This shows that the reciprocals of return periods may be added, but only under the assumption of independence of events between time units.

6.3.4   Hazard Function

Another measure sometimes used in classical time-dependent reliability theory is the 'hazard function'. It may be expressed either in terms of the number of load applications (see also Section 6.2) or in terms of time. The latter will be used here.

From (6.18), the life of a structure expressed in terms of time as the parameter is given by $P(T < t) = F_T(t)$ while the probability density of the design life is

$$f_T(t) = \frac{d}{dt}[F_T(t)] \tag{6.31}$$

This is also called the 'unconditional failure rate', as it reflects the probability of failure in the time interval t to $t + dt$ as $dt \rightarrow 0$.

The hazard function (also called 'age specific failure rate' or 'conditional failure rate') expresses the likelihood of failure in the time interval t to $t + dt$ as $dt \rightarrow 0$, but now given that failure has not occurred prior to time t, i.e.

$$P(\text{failure } t \leq T \leq t + dt \,|\, \text{no failure } t \leq T) = \frac{P(t \leq T \leq t + dt)}{1 - P(T \leq t)}$$

or

$$h_T(t) = \frac{f_T(t)}{1 - F_T(t)} \tag{6.32}$$

It is immediately evident that, for $F_T(t)$ small, that is for systems with very low failure probability and thus very high reliability, i.e. $[1 - F_T(t)] \rightarrow 1$, the hazard function $h_T(t)$ is closely similar to $f_T(t)$. Some typical hazard functions are shown in Figure 6.6. Using (6.18) and (6.20) it is not difficult to show that (6.32) can be recast to

$$F_T(t) = 1 - \exp\left[-\int_0^t h_T(\tau)d\tau\right] \approx \int_0^t h_T(\tau)d\tau \tag{6.33}$$
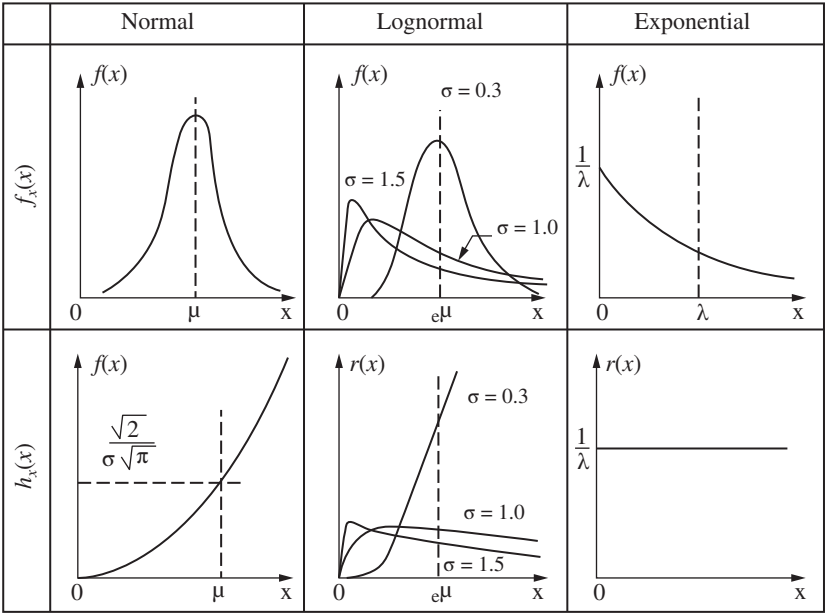
Figure 6.6 Typical hazard functions $h_T(t)$.

and

$$f_T(t) = h_T(t) \exp\left[-\int_0^t h_T(\tau)d\tau\right] \tag{6.34}$$

when it is noted that the integral term in [ ] represents the total probability of failure $P(T < t)$. It follows that knowledge of one of $f_T(t)$, $F_T(t)$ or $h_T(t)$ is sufficient to obtain the other two.

For a typical, realistic structure, the hazard function usually is more complex than the idealizations in Figure 6.6 and typically has the form of a 'bath-tub' curve (see Figure 6.7). This shows the initial high-risk phase during which the hazard rate reduces sharply as
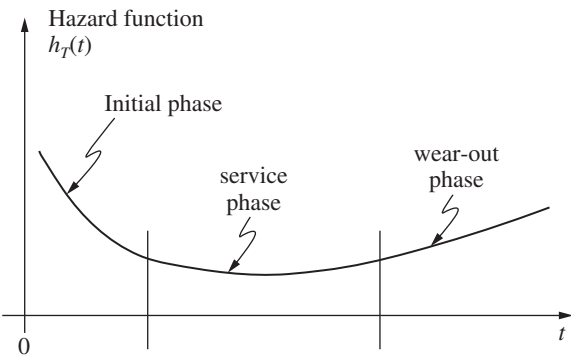
Figure 6.7 Typical variation of hazard function with age of structure.

experience is gained with loading the structure. This is essentially a proof-loading stage. As the design life is approached, the hazard rate increases owing to deterioration and wearing-out.

6.4 Stochastic Process Theory

Continuing with the discretization of the previous section to ever smaller time intervals produces, in the limit, what might be called the 'instantaneous' approach for dealing with time-dependent problems. Before proceeding to discuss this in detail it is necessary to introduce some basic ideas about stochastic processes. It is necessary also to describe some elementary processes used in later sections of this chapter. The discussion in the following section is based largely on Crandall and Mark (1963), Newland (1984), Papoulis (1965) and Parzen (1962).

6.4.1 Stochastic Process

A stochastic process $X(t)$ is a random function of time t. At any point in time t the value of $X(t)$ is a random variable governed by probability density function $f_X(x, t)$. As before, a specific realization of $X(t)$ at time t is denoted $x(t)$. More generally, the variable t may be replaced by any kind of finite or countable infinite set of values, such as the number of load applications (see Section 6.3). However, time is convenient.

For each value of t, the observed outcome of $X(t)$ may be plotted; the complete set of such values over a given time interval is called a 'realization' or 'sample function', such as shown in Figure 6.8. Since X is a random variable, the precise form of the realization cannot be predicted. However, statements can be made about its statistical properties. Thus, in direct correspondence to the definition (A.10) for a random variable, the mean of all possible realizations at any point in time is simply

$$\mu_X(t) = \int_{-\infty}^{\infty} x \, f_X(x, \, t) dx \tag{6.35}$$

where $f_X(x, t)$ is the probability density function at time t. The correlation between the realizations at two points in time t_1 and t_2 is termed the 'autocorrelation function' since
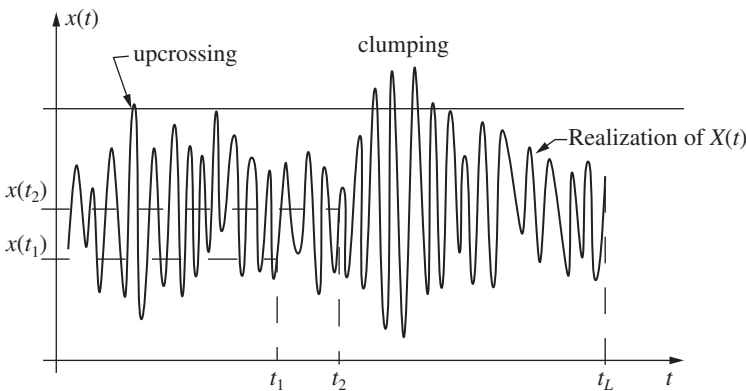
Figure 6.8 Realizations $x(t)$ of process $X(t)$ showing clumping effect and barrier crossing.

it relates to one realization (see Figure 6.8):

$$R_{XX}(t_1, t_2) = E[X(t_1)X(t_2)]$$

$$= \int_{-\infty}^{\infty} \int_{-\infty}^{\infty} x_1 x_2 f_{XX}(x_1 x_2; t_1 t_2) dx_1 dx_2 \tag{6.36}$$

where $f_{XX}(\ ) = \partial^2 F_{XX}(\ )/\partial x_1 \partial x_2$ is the joint probability density function. Here $F_{XX}(\ ) = P\{[X(t_1) \le x_1] \cap [X(t_2) \le x_2]\}$. It is also possible to define an (auto)covariance function analogous to (A.123):

$$C_{XX}(t_1, t_2) = E\{[X(t_1) - \mu_X(t_1)][X(t_2) - \mu_X(t_2)]\}$$

$$= R_{XX}(t_1, t_2) - \mu_X(t_1)\mu_X(t_2) \tag{6.37}$$

As might be expected, if $t_2 = t_1 = t$, the (auto)covariance function becomes the variance function $\sigma_X^2(t)$:

$$\sigma_X^2(t) = C_{XX}(t, t) = R_{XX}(t, t) - \mu_X^2(t) \tag{6.38}$$

analogous to (A.11) and with $\sigma_X(t) = D[X(t)]$ denoting the standard deviation function.

Just as higher 'moments' (see Section A.4) can be used to provide a description of an ordinary random variable, higher-order correlation functions also can be established. However, these are seldom of much practical interest.

In addition, the above concepts for the scalar process $X(t)$ may be generalized to the vector process $\mathbf{X}(t) = [X_1(t), X_2(t), \dots, X_n(t)]$ having covariance functions $C_{X_i X_j} = \text{cov}[X_i(t_1), X_j(t_2)]$. When $i = j$, these are autocovariance functions for X_i; when $i \ne j$, $C_{X_i X_j}$ is termed a 'cross-covariance' function. The collection of functions $C_{X_i X_j}$ is expressed in a covariance function matrix $\mathbf{C}_X$ analogous to the covariance matrix.

Finally, the correlation function (matrix) may be defined analogously to (A.124) as

$$\rho[X_i(t_1), X_j(t_2)] = \frac{\text{cov}[X_i(t_1), X_j(t_2)]}{D[X_i(t_1)]D[X_j(t_2)]}$$

where $D[\ ] = \mathbf{C}_X^{1/2}$ for $t_1 = t_2$, $X_i = X_j$.

Typically, $\rho[X_i(t_1), X_j(t_2)]$ might have the form $\rho = \exp[-k(t_1 - t_2)(x_1 - x_2)]$ where k is some defined constant. In this case ρ reduces with greater separation of time points t_1 and t_2, or component processes X_1 and X_2, as might be expected. Also, if $t_1 = t_2$, $X_1 = X_2$, then $\rho = 1$, as expected for correlation at a point in time of the same process component.

6.4.2 Stationary Processes

When the random nature of a stochastic process does not change with time, it is said to be a '(strictly) stationary' process. This means that all its moments also are independent of time. When only the mean $\mu_X(t)$ and the autocorrelation $R_{XX}(t_1, t_2)$ are independent of absolute time, the process is said to be 'weakly stationary' or 'covariance stationary'. Since the normal distribution is uniquely described by its first two moments, a weakly stationary normal process is also strictly stationary.

A direct consequence of stationarity is that for $C_{XX}(\ )$ and $R_{XX}(\ )$ only the relative difference $(t_1 - t_2) = \tau$, say, is of importance. Thus (6.36), for example, becomes

$$R_{XX}(\tau) = E[X(t)X(t + \tau)] \qquad (6.36a)$$

In particular, if $\tau = 0$, $R_{XX}(0) = E(X^2)$, which represents the 'mean-square' value of $X(t)$. Also note that $R_{XX}(\tau)$ is an even function in τ, i.e. $R_{XX}(\tau) = R_{XX}(-\tau)$, as is easily verified.

If a process is stationary, by definition it cannot start or stop. Each realization must, theoretically, extend over $-\infty \leq t \leq +\infty$. Usually this is ignored in practical applications. Often stationarity can be assumed to hold after a sufficient time from the start of the process. Even if the process is slowly changing with time, it may be acceptable to consider several shorter subprocesses each reasonably stationary over their respective durations.

6.4.3 Derivative Process

For the discussion to follow an important property of a process $X(t)$ is its derivative process $\dot{X}(t)$, defined for any realization $x(t)$ as

$$\dot{x}(t) = \frac{d}{dt}[x(t)] \qquad (6.39)$$

The existence of such a derivative implies certain regularity properties of $X(t)$; in particular $X(t)$ is differentiable only (a) if its autocorrelation function $R_{XX}(\tau)$ has a continuous second-order derivative $R''_{XX}(\tau) = \partial^2 R_{XX}(\tau)/\partial \tau^2$ and (b) if $R''_{XX}(0)$ exists. This may be examined by considering the limit as $\tau \to 0$ of the incremental form $[x(t + \tau) - x(t)]/\tau$ expressed in terms of $R_{XX}(\tau)$ and its derivatives. For details see Papoulis (1965) and also Ditlevsen (1981b).

If the second derivative exists, the first derivative $R'_{XX}(\ )$ must exist also. Then, since $R_{XX}(\tau)$ is an even function in τ (see previous section), it follows that at $\tau = 0$

$$\frac{\partial R_{XX}(0)}{d\tau} = 0 \qquad (6.40)$$

Further, it follows from the previous section that the derivative process $\dot{X}(t)$ will be a stationary process if its autocorrelation function $R_{\dot{X}\dot{X}}(t_1, t_2)$ can be expressed as $R_{\dot{X}\dot{X}}(\tau)$. To show this consider the cross-correlation between $X(t)$ and $\dot{X}(t)$ [Papoulis, 1965]:

$$R_{X\dot{X}}(t_1, t_2) = E[X(t_1)\dot{X}(t_2)] \qquad (6.41)$$

that can be written in limit form as

$$R_{X\dot{X}}(t_1, t_2) = \lim_{dt_2 \to 0} \left\{ E\left[X_1(t)\frac{X(t_2 + dt_2) - X(t_2)}{dt_2}\right] \right\}$$

$$= \lim_{dt_2 \to 0} \left[\frac{R_{XX}(t_1, t_2 + dt_2) - R_{XX}(t_1, t_2)}{dt_2}\right]$$

or

$$R_{X\dot{X}}(t_1, t_2) = \frac{\partial R_{XX}(t_1, t_2)}{\partial t_2} \qquad (6.42)$$

Also, using a similar procedure, it follows that

$$R_{X\dot{X}}(t_1, t_2) = \frac{\partial^2 R_{XX}(t_1, t_2)}{\partial t_1 \partial t_2} \qquad (6.43)$$

Further, if $X(t)$ is stationary, with $\tau = t_1 - t_2$, it follows immediately that

$$R_{X\dot{X}}(\tau) = \frac{dR_{XX}(\tau)}{d\tau} \qquad (6.44)$$

and

$$R_{\dot{X}\dot{X}}(\tau) = -\frac{d^2 R_{XX}(\tau)}{d\tau^2} \qquad (6.45)$$

from which it follows that the process $\dot{X}(t)$ is covariance stationary if $X(t)$ is covariance stationary (see Section 6.4.2).

Also using (6.40) in (6.44), it follows that for a stationary process $R_{X\dot{X}}(\tau) = E[X(t) \dot{X}(t + \tau)] = 0$ if $\tau = 0$, which has the useful property that there is no correlation between a stationary process and its derivative process at any point in time t. (This does not mean, however, that there is no correlation between $X(t_1)$ and $X(t_2)$ for $t_1 \neq t_2$.)

6.4.4 Ergodic Processes

The mean (6.35) and the correlation (6.36) were defined for a stationary process as averages over all realizations. If they can be defined equally well by the time average over a single realization of a stationary process, the process is 'weakly ergodic'. If the equality holds for all moments of a strictly stationary process, the process is 'strictly ergodic'. Ergodicity in the mean is defined as

$$\mu_X = \lim_{T \to \infty} \left[\frac{1}{T} \int_0^T x(t) dt \right] \qquad (6.46)$$

and ergodicity in correlation as

$$R_{XX}(\tau) = \lim_{T \to \infty} \left[\frac{1}{T} \int_0^T x(t + \tau) x(t) dt \right] \qquad (6.47)$$

This property clearly can hold only for stationary processes. It is of considerable practical value in estimating statistical parameters from one or a few sufficiently long records of the process. The accuracy obtained will depend on the duration T of available records. Often stationarity and ergodicity are assumed to hold in the analysis of stochastic process records unless (and until) there is evidence to the contrary.

6.4.5 First-Passage Probability

As noted in Section 6.1, for time-dependent reliability interest lies mainly in the time expected to elapse before the first occurrence of an excursion of the random vector $\mathbf{X}(t)$ out of the safe domain D, defined by $G(\mathbf{X}) > 0$ (see Figure 6.3). The probability of the first occurrence of such an excursion may be considered to be equivalent to the probability

$p_f(t)$ of structural failure during a given period $[0, t]$:

$$p_f(t) = 1 - P[N(t) = 0 | \mathbf{X}(0) \in D] \, P[\mathbf{X}(0) \in D] \tag{6.48}$$

where $\mathbf{X}(0) \in D$ signifies that the process $\mathbf{X}(t)$ starts in the safe domain D at zero time and $N(t)$ is the number of outcrossings in the time interval $[0, t]$.

In general, solutions of (6.48) are rather difficult to obtain owing to the need to account for the complete history of the process $\mathbf{X}(t)$ in the interval $[0, t]$. Usually solutions will depend on the nature of the process $\mathbf{X}(t)$. Series or other approximations have been suggested [e.g. Rice, 1944; Vanmarcke, 1975]. Fortunately, for reliability problems, outcrossings typically occur so rarely that often it is satisfactory for the individual outcrossings to be assumed independent events, and therefore independent of the probability of any earlier outcrossings, including one at $t = 0$. The probability of no outcrossings in $[0, t]$ may then be approximated using the Poisson distribution (A.30) with zero events [Cramer and Leadbetter, 1967]:

$$P[N(t) = 0] = \frac{(vT)^0}{0!} e^{-vt} = e^{-vt} \tag{6.49}$$

where v is the mean outcrossing rate from the domain D. (A similar approach was used in Section 6.3.2 when dealing with the random occurrence of events such as storms).

In expression (6.48), the term $P[\mathbf{X}(0) \in D]$ clearly is equivalent to $1 - p_f(0)$, where $p_f(0)$ is the probability of failure at time $t = 0$. Using also (6.49), expression (6.48) becomes [*cf.* Veneziano et al., 1977]

$$p_f(t) = 1 - [1 - p_f(0)] \; e^{-vt} \tag{6.50}$$

$$= p_f(0) + [1 - p_f(0)](1 - e^{-vt}) \tag{6.51}$$

but, since $vt > 1 - e^{-vt}$,

$$p_f(t) \le p_f(0) + [1 - p_f(0)]vt \tag{6.52}$$

This result is an upper bound on the failure probability. It is particularly useful in structural reliability work since it accounts for the initial probability of failure $p_f(0)$ (i.e. that on first loading) and also properly accounts for the subsequent rate of failure given by $[1 - p_f(0)]vt$. Only in the special case when vt is very close to zero and $p_f(0) \ll vt$ does the 'first passage' or failure probability become the more commonly quoted result

$$p_f(t) \approx 1 - e^{-vt} \approx vt \tag{6.53}$$

In both cases, a useful result is that if the vector process $\mathbf{X}(t)$ is smooth but non-stationary, vt may be replaced by the average outcrossing rate $\int_0^t v(\tau)d\tau$.

Other, perhaps more aesthetic, derivations are available [Leadbetter et al., 1983]. Various improvements to these expressions have been proposed, as reviewed by Engelund et al. (1995). As might be expected from the way the above expressions have been derived, results produced by these expressions are good for rare outcrossings but less so as the boundary moves closer to the origin (i.e. the outcrossings become increasingly not 'rare').

Simulation results support that (6.52) is an upper bound. They also show that excursions tend to occur in 'clumps' (see Figure 6.8) and obviously are not strictly

independent; these aspects will be ignored herein but can be important in certain problems [Lin, 1970; Yang, 1975; Leadbetter et al., 1983].

6.4.6 Distribution of Local Maxima

A local maximum of the scalar stochastic process $X(t)$ is defined as the value of $X(t)$ at which $\dot{X}(t) = 0$ and $\ddot{X}(t) < 0$, i.e. when $\dot{X}(t)$ has a zero crossing. Local maxima are therefore all the peaks in a typical realization of $X(t)$ (see Figure 6.8). Note that for a scalar process $X(t)$ outcrossings simply become 'upcrossings' of a barrier $x = a$ (see Figure 6.8).

The full distribution function for the local maxima can be obtained, in principle, from an extension of Rice's formula (6.72) as considered in Section 6.5.3 below; this approach really is tractable only for normal processes.

Fortunately, for typical structural reliability problems the mean upcrossing rate v for $X(t)$ usually is low to very low in value. As a result, the distribution of the local maxima can be approximated directly from the first-passage probability given by expression (6.50), using the assumption that the upcrossings follow a Poisson distribution

$$1 - F_m(a) = p_f(t) = 1 - [1 - p_f(0)] \; e^{-vt} \tag{6.54}$$

where $F_m(a)$ is the cumulative distribution function $P(X_m < a)$ for the maximum X_m in the time interval $[0, t]$. Simplifying, it follows that

$$F_m(a) \approx e^{-vt} = 1 - vt \tag{6.55}$$

where v is the mean upcrossing rate in $[0, t]$ out of the safe domain D, defined, for a scalar process $X(t)$, as $x \leq a$. This is known also as a 'level' crossing problem (see Section 6.4.8.1). Evidently, the Poisson assumption becomes less accurate at lower levels $x = a$, and hence $F_m( )$ is only well approximated by (6.55) for high values of $x = a$. Result (6.55) is of considerable importance for the discussions to follow.

6.5 Stochastic Processes and Outcrossings

In this section a number of stochastic processes commonly applied in structural reliability applications are described. This is followed by a discussion of the theory for barrier (or 'up-') crossings of stochastic scalar processes and its generalization to outcrossings for a vector process. An introduction is then given to available analytical and simulation solutions for outcrossing problems, including situations composed of multiple boundaries. All this is further preliminary information for the discussion in Section 6.6 of time-dependent reliability problems.

6.5.1 Discrete Processes

6.5.1.1 Borges Processes

One of the simplest discrete processes in time t is generated by a sequence Y_k of independent and identically distributed random variables each acting over a given (deterministic) length of time t_b (the so-called 'holding time'). A typical realization of this (stationary) process $w_b(t)$ is shown in Figure 6.9 [Ferry-Borges and Castenheta, 1971].
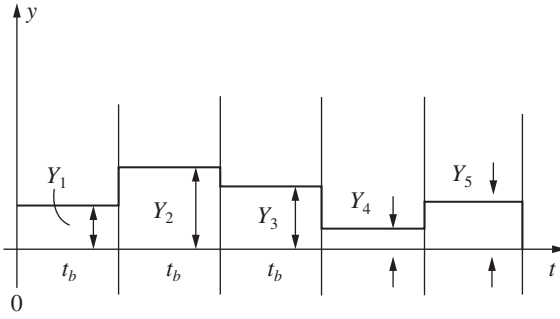
Figure 6.9 Realization of a Borges process.

In a given time interval $[0, t_L]$ the number of sequences of Y will be $r = t_L/t_b$ so that, owing to independence, the distribution of the extreme value of the sequence is given by

$$P\left\{ \max_{0 \leq t \leq t_L} [w_b(t; t_b, Y)] \leq a \right\} = P\left[\bigcap_{i=1}^{r} (Y_i \leq a) \right] = [F_Y(a)]^r \qquad (6.56)$$

The first occurrence of the level crossing $Y > a$ must be associated with a maximum value of Y in $[0, t_L]$. It follows therefore that, on average, the number of sequences before which $Y > a$ occurs is equal to r and that the probability that this occurs is given by

$$1 - P\left[\max_{0 \leq t \leq t_L} (w_b \leq a) \right] \text{ or}$$

$$p_f(t_L) = 1 - [F_Y(a)]^r = 1 - [F_Y(a)]^{t_L/t_b} \qquad (6.57)$$

6.5.1.2 Poisson Counting Process

If the time of occurrence of the event, rather than its magnitude, is a random variable, a different but still elementary type of process is obtained; the so-called 'Poisson counting process'. If $N(t)$ denotes the number of discrete events (or 'states') $n = 0, 1, 2, 3, \ldots$ in a given time interval $[0, t]$, then the number of events in $[0, t]$ is given by the Poisson distribution (A.30)

$$P(n, t) = \frac{(vt)^n e^{-vt}}{n!} \qquad (6.58)$$

where v is the mean rate of occurrence of events per unit time, also known as the 'intensity' of the process.

The application of the Poisson distribution in the time domain assumes (i) that the probability that an event occurs during any time increment t to $t + \Delta t$ is asymptotically proportional to Δt and (ii) that the probability of more than one event in any time interval is negligible as $\Delta t \to 0$. There is thus no overlap between events. Also $N(0) = 0$.

An important assumption is that the occurrence of events in time increments Δt_i, Δt_j, $i \neq j$, is independent. This means that, for any $t_o < t_1 < t_2 < \ldots < t_m$, the m random variables

$$N(t_1) - N(t_0), \ldots, N(t_m) - N(t_{m-1}) \qquad (6.59)$$
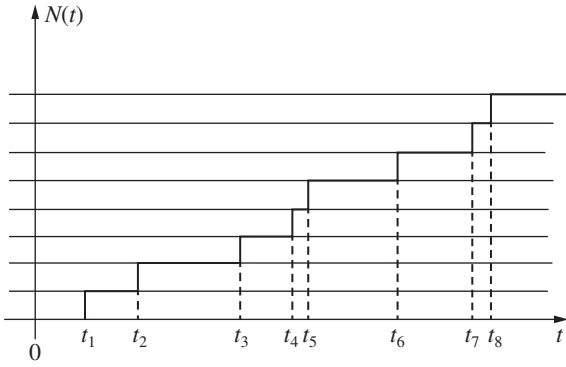
Figure 6.10 Realization of Poisson counting process.

are independent. Clearly, if (6.59) is independent also of t_i (but not of $t_{i+1} - t_i$) the process has stationary independent increments [Parzen, 1962].

A typical realization of a Poisson counting process is shown in Figure 6.10. If ν is constant, the process is termed 'homogeneous'. If $\nu = \nu(t)$, it is 'non-homogeneous', in which case νt in (6.58) must be replaced by $\nu(t) = \int_0^t \nu(\tau)d\tau$. In this case the time increments are no longer stationary, since $N(t)$ depends directly on t, rather than on some time increment.

The Poisson counting process is a case of so-called Markov (or memory-less) processes with discrete states $(0, 1, 2, \ldots)$ in continuous time t. It is 'memory-less' in the sense that each state is independent of previous states.

For Poisson processes, the cumulative distribution function $F_W(t)$ for the time W_n which must elapse before the occurrence of the nth event is obtained by considering all the possible number of events $N(t) < n$, or

$$F_W(t) = 1 - P(W_n > t) = 1 - P[N(t) < n]$$

$$= 1 - \sum_{k=0}^{n-1} \frac{(\nu t)^k e^{-\nu t}}{k!} \tag{6.60}$$

This expression represents a Gamma distribution (see A.40) with mean n/ν and variance n/ν^2.

Of particular interest is the waiting time before the occurrence of the first event $(n = 1)$ during the time period $[0, t]$. From (6.60) with $n = 1$, there is obtained:

$$p_f(t) = F_W(t) = 1 - e^{-\nu t} \tag{6.61}$$

This result will be recognized as equivalent to the first-passage probability (see 6.53).

6.5.1.3 Filtered Poisson process

If stochastic properties are now also attributed to the events (states) in a Poisson process, a so-called 'filtered Poisson process' is obtained. Typically it is defined as [Parzen, 1962]:

$$X(t) = \sum_{k=1}^{N(t)} w(t, t_k, Y_k) \tag{6.62}$$

@Seismicisolation

where $N(t)$ is a Poisson process of intensity v generating the time points t_k at which the events have a random magnitude Y_k. The Y_k are assumed independent and identically distributed. Also $w(t, t_k, Y_k)$ is a 'response function', which represents the response contributing (linearly) to $X(t)$ at time t, owing to the magnitude Y_k acting at time t_k. Generally, it is taken that $w(\ ) = 0$ for $t < t_k$.

A filtered Poisson process requires the specification of the intensity v governing $N(t)$, the distributional properties of Y_k and the form of the response function $w(t, t_k, Y_k)$.

Two forms of filtered Poisson processes have particular relevance to reliability studies. These processes are:

(1) Poisson 'spike' process;
(2) Poisson square wave process.

Both processes allow explicit evaluation of their stochastic properties and find application mainly in modelling of loading processes (see Chapter 7). However, many other Poisson processes can be postulated, depending on the choices F_{Y_k} and $w(\ )$ and by allowing the holding time also to be a random variable (so that pulse overlap can occur) [e.g. Grigoriu, 1975]. These more complex processes, however, are beyond the scope of this book.

6.5.1.4 Poisson Spike Process

A process having constant intensity v and rectangular pulses of height Y_k and length b may be described by a response function

$$w_S(t, t_k, Y_k) = Y_k, \qquad 0 < t - t_k < b$$
$$= 0, \qquad \text{otherwise} \tag{6.63}$$

A typical realization is shown in Figure 6.11. Here Y_k is a random variable, independent between pulses and defined by the cumulative distribution function $F_Y(\ )$.

The level crossing rate and the first-passage probability may be obtained directly from the limit as $b \to 0$. The probability that the process $Y(t)$ has a height greater than $a(t)$ is $1 - F_Y(a)$ and the probability that $Y(t)$ has a height less than $a(t)$ is $F_Y(a)$, so that the
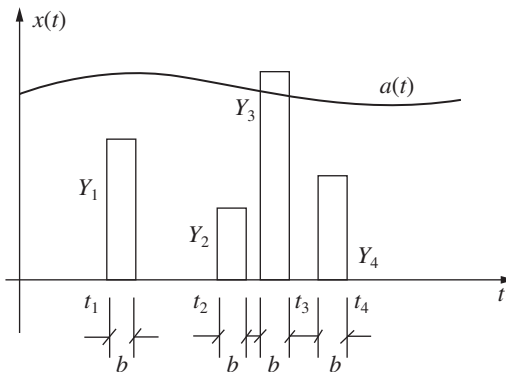
Figure 6.11 Realization and upcrossing of a Poisson spike process.

probability of an upcrossing v^+ of level $a(t)$ in time $\Delta t \to 0$ is

$$
\begin{aligned}
v_a^+(t) &= \lim_{\Delta t \to 0} \left\{ \frac{1}{\Delta t}[P(\text{upcrossing in } \Delta t)]v \right\} \\
&= \lim \left[\frac{1}{\Delta t}(P\{[Y(t) \le a(t)] \cap [Y(t + \Delta t) > a(t)]\}v) \right] \\
&= F_Y[a(t)]\{1 - F_Y[a(t)]\}v
\end{aligned}
\tag{6.64}
$$

where $v = v(t)$ is the rate of arrival of the pulses. If a is large and time invariant, (6.64) reduces to $v_a^+ \approx [1 - F_Y(a)]v$.

It should be evident that v_a^+ in (6.64) expresses the intensity of a Poisson process. It is then possible to use (6.61) to obtain the first-passage probability, since 'failure' is the occurrence of the first event (a spike greater than a); thus

$$
p_{f_1}(t_L) = 1 - \exp\{-[1 - F_Y(a)]v t_L\}
\tag{6.65}
$$

where t_L is the nominal lifetime of the structure. As before a, v_a^+ and v may each be considered to be functions of time with appropriate substitution of $\int_0^t v(\tau)d\tau$ for v and $a(t)$ for a in (6.65).

The cumulative distribution function for the maximum value of the process $X(t)$ may be obtained by considering $a(t)$ as time invariant. Then the first-passage probability (6.65) represents also the probability that the maximum value of $X(t)$ is greater than a since the first-passage point must be the same as the maximum value of $X(t)$. Hence

$$
F_{X_{\max}}(a) = P[X_{\max}(t) < a] = \exp\{-[1 - F_Y(a)]v t_L\}
\tag{6.66}
$$

6.5.1.5 Poisson Square Wave Process

When the length b of each rectangular pulse in Figure 6.11 is given by the random interval $t_n - t_{n-1}$, the square wave process of Figure 6.12 is obtained. The pulse height Y_k now stays constant until the next event at time t_{k+1} generates a new pulse height Y_{k+1}. As before, the Y_k are independent, identically distributed random variables. Proceeding exactly as for a Poisson spike process, and with a constant level a, the level crossing rate v_a^+ is given by (6.64) so that the first-passage probability for a time period $[0, t_L]$ is given by

$$
p_{f_1}(t_L) = F_{Y_0}(a)(1 - \exp\{-F_Y(a)[1 - F_Y(a)]\}v t_L)
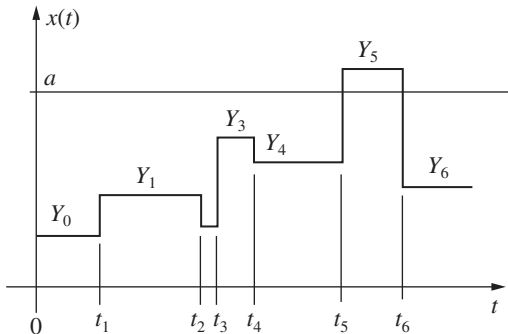\tag{6.67}
$$

Figure 6.12 Realization of Poisson square wave process.

where $F_{Y_0}(a)$ is the probability that $Y_0 < a$, an event independent of subsequent events because of the assumption on Y_k. Clearly, if a is large, then $F_{Y_0}(a) \approx F_Y(a) \approx 1$ and $p_{f_1} \to 0$.

It follows readily that the cumulative distribution function for the maximum value of $X(t)$ is derived in a manner similar to that for the Poisson spike process, as

$$F_{X_{\max}}(a) = P(X_{\max} < a) = F_{Y_0}(a)\exp\{-[1 - F_Y(a)]\nu t_L\} \tag{6.68}$$

6.5.1.6 Renewal Processes

The Poisson processes above are particular forms of a more general type of process in which events occur along a time axis. Such a process can be taken to define the potential beginning and end times of load events or pulses. The time between events in the case of Poisson processes is exponentially distributed, as is easily shown. More generally, 'renewal processes' are those for which the events along the time axis are governed by an appropriate probability law, not necessarily Poisson.

A further generalization is to employ pulse shapes more complex than the rectangles and spikes considered so far. For most of these more general cases, however, no theoretical results are available for up-crossing rates, although the results (6.64) for the Poisson processes above may be taken as an approximation.

It is also possible to define the cumulative distribution function of Y_k, the pulse height, such that there is a finite probability p that $Y_k = 0$. This might occur, for example, in some types of floor loading. A typical distribution of Y_k for such a case is shown in Figure 6.13 [Bosshard, 1975]. In this case (6.64) will be modified to

$$\nu_a^+ = [p + qF(a)]\{q[1 - F(a)]\}\nu \tag{6.69}$$

where $F(\ )$ is the 'improper' cumulative distribution function defined in Figure 6.13.
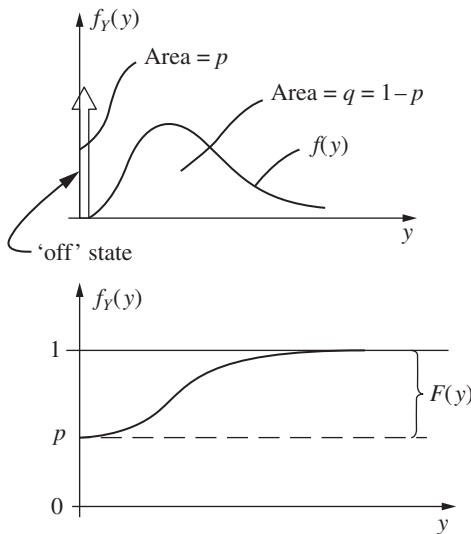
Figure 6.13 Probability density function and cumulative distribution function for 'mixed' renewal process.

Note that $q = 1 - p$ and that $F_Y(\ )$ is now $p + qF(\ )$ so that, by differentiation, the probability density function is given by $f_Y(y) = p\delta(y) + qf(y)$, where $f(\ )$ is defined in Figure 6.13 and $\delta(\ )$ is the Dirac delta function.

In expression (6.69) the first term represents the probability that $Y(t) \leq a(t)$ and the second term the probability that $Y(t) > a(t)$. If each pulse automatically returns to zero after it has been applied, the first term in (6.69) is obviously unity [Larrabee and Cornell, 1981]. Processes of this type have been called 'mixed processes'. Note that the mean arrival rate of pulses for the mixed process is qv, where v is the mean arrival rate of pulses for the unmodified process $Y(t)$.

6.5.2 Continuous Processes

Most natural phenomena do not change their characteristics at specific points in time but do so continuously. Thus, for example, wind velocity and wave height are not discrete processes in time but are continuous ones. A typical realization of a continuous process is shown in Figure 6.14.

There are many types of possible continuous processes $X(t)$ that can be postulated. Because of their mathematically tractable properties, the most common continuous process employed in stochastic process work is the Normal (or Gaussian) process $X(t)$. At any time t this is, of course, Normal distributed. This means that for any set of times $t_1, t_2, \ldots, t_n, X(t_i), (i = 1, 2, \ldots, n)$, is jointly Normal distributed, with a given correlation structure between the time points. As before, if the correlation structure does not change with time, the process is (strictly) stationary (see Section 6.4.2).

6.5.3 Barrier (or Level) Upcrossing Rate

As noted in Section 6.1, an important property in reliability studies is the rate at which a random process $X(t)$ 'upcrosses' a 'barrier' or 'level' $x = a(t)$ (Figure 6.14). If $X(t)$ represents a loading process, then $x = a(t)$ might represent a (time-dependent) resistance or, if $X(t)$ represents a safety margin, then $x = a(t) = 0$ might represent the limit state. For the present, a scalar process $X(t)$ only will be considered; the more general case for the vector process $\mathbf{X}(t)$ is described in Section 6.5.4 below.

Consider the segment of sample function $x(t)$, shown in Figure 6.15, between the times t_1 and $t_1 + dt$, where $dt \to 0$. Without loss of generality, the time $t_1 + dt$ may be

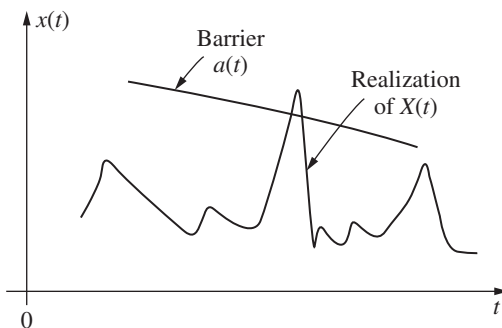**Figure 6.14** Typical realization and barrier crossing of continuous process $X(t)$.
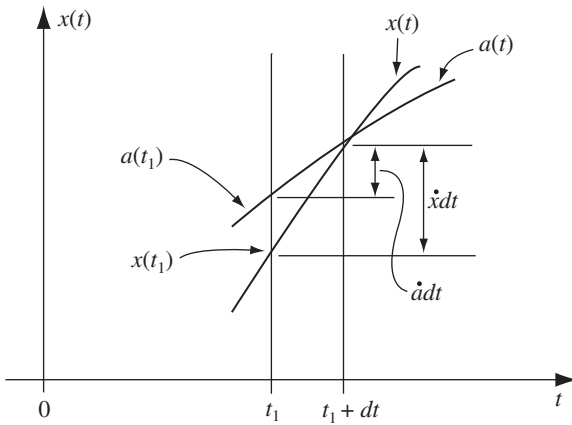
@Seismicisolation

Figure 6.15 Segment of sample function $x(t)$ crossing barrier $a(t)$ in dt.

considered to be the time at which the barrier crossing occurs. Also, for dt sufficiently small, the curves between t_1 and $t_1 + dt$ can be taken as straight lines.

The sample functions which cross $a(t)$ during dt must start below $a(t)$ at t_1 and have sufficient slope $\dot{x}(t)$ at t_1 to pass through $a(t)$ during dt. The limits on the slope $\dot{X}(t)$ are evidently

$$\dot{x}dt - \dot{a}dt \geq a(t) - x(t) \text{ as } dt \to 0 \text{ and } x(t_1) \leq a(t_1) \tag{6.70}$$

These limits are plotted in Figure 6.16 on orthogonal $(x, \dot{x})$ axes. From Section 6.4.3, $X(t)$ and $\dot{X}(t)$ are uncorrelated, so that this representation is straightforward. Now the probability that $X(t)$ is between x and $x + dx$ and that $\dot{X}(t)$ is between $\dot{x}$ and $\dot{x} + d\dot{x}$ is given by the joint probability density function $f_{X\dot{X}}(\ )$. The total number of barrier crossings in dt is given by the fraction of all possible realizations which satisfy the conditions (6.70); this is identical with the probability content contained above the shaded region (i.e. perpendicular to the page) in Figure 6.16, or

$$N = \int_{\dot{a}}^{\infty} \int_{a-(\dot{x}-\dot{a})dt}^{a} f_{X\dot{X}}(x, \dot{x}) dx d\dot{x} \tag{6.71}$$
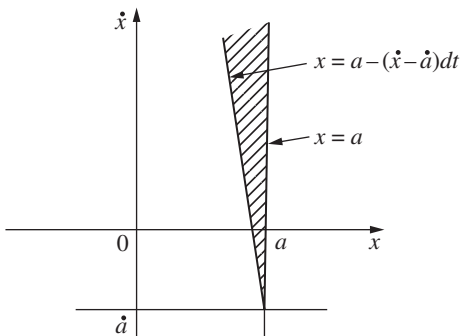
Figure 6.16 Integration limits in $(x, \dot{x})$ plane.

As $dt \to 0$, the shaded region in Figure 6.16 tends to reduce to a narrow strip, or, equivalently, $a - (\dot{x} - \dot{a})dt \to a$ in the lower integration limit in (6.71), so that upon dividing through by dt and integrating over x, the barrier upcrossing rate is given by [Rice, 1944]:

$$v_a^+ = \int_{\dot{a}}^{\infty} (\dot{x} - \dot{a}) f_{X\dot{X}}(a, \dot{x}) d\dot{x} \tag{6.72}$$

Evidently, if a is not time dependent, $\dot{a} = 0$. Also note that the barrier upcrossing rate v_a^+ is an ensemble average, i.e. it is the average over all realizations of $X(t)$ at time t. Only if the process is ergodic will v_a^+ also be the time average frequency of upcrossings of level $x = a$.

In the special case when $X(t)$ is a stationary normal process, $f_{X\dot{X}}(\,)$ is given by [*cf.* (A.125) with $\rho = 0$]

$$f_{X\dot{X}} = \frac{1}{2\pi \sigma_X \sigma_{\dot{X}}} \exp\left\{ -\frac{1}{2}\left[\left(\frac{a - \mu_X}{\sigma_X^2}\right)^2 + \frac{\dot{x}^2}{\sigma_X^2} \right] \right\} \tag{6.73}$$

in which $X(t)$ is Normal distributed $N(\mu_X, \sigma_X^2)$ and $\dot{X}(t)$ is $N(0, \sigma_{\dot{X}}^2)$. The mean of $\dot{X}(t)$ is zero for a stationary process. Noting that

$$\int_0^{\infty} \dot{x} \exp\left(-\frac{\dot{x}^2}{2\sigma_{\dot{X}}^2}\right) d\dot{x} = \sigma_{\dot{X}}^2$$

and substituting (6.73) into (6.72) and integrating produces (noting that a is time-invariant)

$$v_a^+ = \frac{1}{2\pi} \frac{\sigma_{\dot{X}}}{\sigma_X} \exp\left[-\frac{(a - \mu_X)^2}{2\sigma_X^2} \right] = \frac{\sigma_{\dot{X}}}{(2\pi)^{1/2}} f_X(\,) \tag{6.74}$$

with $f_X(\,) = (1/\sigma_X)\phi[(a - \mu_X)/\sigma_X]$, where $\phi(\,)$ is the standard normal density function (see Section A.5.7). Note also that σ_X is obtained from (6.38) as

$$\sigma_X^2(t) = R_{XX}(t, t) - \mu_X^2(t) \tag{6.75}$$

For a stationary process this becomes

$$\sigma_X^2 = R_{XX}(\tau = 0) - \mu_X^2 \tag{6.76}$$

By analogy, $\sigma_{\dot{X}}$ is obtained similarly from $\sigma_{\dot{X}}^2(t) = R_{\dot{X}\dot{X}}(t, t) - \mu_{\dot{X}}^2(t)$. Since $R_{\dot{X}\dot{X}}(t, t) = R_{\dot{X}\dot{X}}(\tau = 0)$ for a stationary process, using (6.45) and $\mu_{\dot{X}} = 0$ leaves the variance of $\dot{X}$ as

$$\sigma_{\dot{X}}^2 = -\frac{\partial^2 R_{XX}(0)}{\partial \tau^2} \tag{6.77}$$

For non-normal processes, the joint probability density function $f_{X\dot{X}}(\,)$ usually will be much less amenable to definition and integration. Such processes arise, for example, in river flows, mean hourly wind speeds and when Normal (i.e. Gaussian) processes

are transformed non-linearly. It is sometimes suggested that for such processes the upcrossing rate may be approximated by (6.74). However, this approximation can be seriously in error [Grigoriu, 1984].

The Gaussian process with $\mu_X = 0$ has special significance for dynamic problems (see Section 6.7) or those involving fatigue (see Section 6.8). The upcrossing rate v_a^+ for $a = 0$ then counts the number of loading cycles. For a standardized Gaussian process this is given by $v_0^+ = \sigma_{\dot{X}}/2\pi\sigma_X$.

Finally, all the above results, and in particular expression (6.72), may be extended to smooth non-stationary processes by interpreting v_a^+ and $f_{X\dot{X}}( )$ as time dependent.

6.5.4 Outcrossing Rate

6.5.4.1 Generalization from Barrier Crossing Rate

The above notion of a barrier crossing, involving the scalar process $X(t)$, can be generalized immediately to the outcrossing concept, now involving the vector process $\mathbf{X}(t)$. For the two-component process $\mathbf{X}(t) = [X_1(t), X_2(t)]$ a realization of $\mathbf{X}(t)$ might be as shown in Figure 6.17. The barriers $B_i(i = 1, 2, \ldots)$ indicated are limit state equations in $\mathbf{x}$ space defining the safe domain D_S [Veneziano et al., 1977].

To proceed, let the barriers to the safe domain D_S be described by $D_S : Z(t) = G[X(t)] \leq 0$. Then the scalar process Z(t) can be used in (6.72), provided that $f_{Z\dot{Z}}$ can be determined, since whenever $\mathbf{X}(t)$ outcrosses barriers $B_i(i = 1, 2, \ldots)$, $Z(t)$ upcrosses the level zero. Closed-form solutions are available only for a very limited range of problems. Of these, almost all deal with special types of two-dimensional Normal (i.e. Gaussian) processes, and with open or closed square or circular domains [Hasofer, 1974].

More generally in m dimensional space $\mathbf{x}$, the safe domain D_S is bounded by a series of q discontinuous hyper-surfaces $B_i(i = 1, 2, \ldots, q)$ forming the q limit state functions

$$D_S : G_i[\mathbf{X}(t)] \leq 0, \qquad (i = 1, \ldots, q) \tag{6.78}$$

This represents the type of problem of interest in structural reliability studies (see Section 6.1), but is not particularly amenable to closed-form solution. In most cases it is necessary to obtain approximate solutions even for Normal processes.
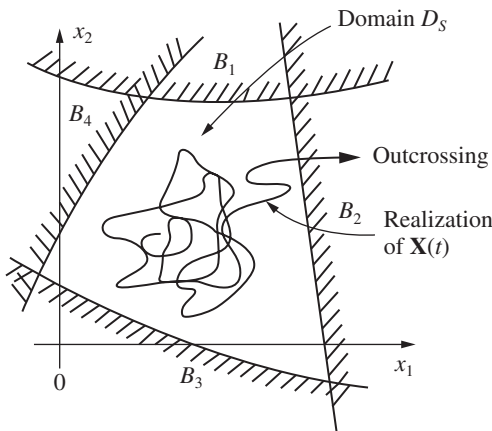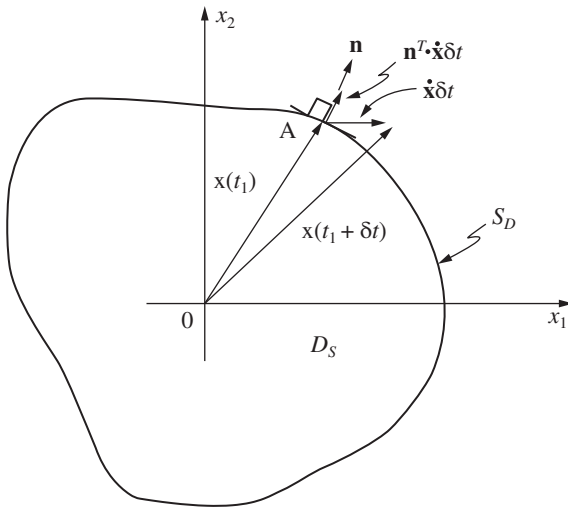

Figure 6.17 Outcrossing from safe domain D_S in two-dimensional space **x**.

Figure 6.18 Vector process realization $\mathbf{x}(t)$, its change in time increment δt and component normal to domain boundary S_D.

The first step is to generalize the Rice formula (6.72) to deal with a vector process $\mathbf{X}(t)$. For convenience of exposition consider a two-dimensional vector process $\mathbf{X}(t)$ and an arbitrary domain D_S (Figure 6.18). Let $\mathbf{x}(t_1)$ be on the limit state surface at A. For an outcrossing to occur, $\mathbf{x}(t_2)$ with $t_2 = t_1 + \delta t$ where $\delta t \to 0$, must be outside the domain D_S. The change in $\mathbf{x}(\ )$ over the time increment δt is shown by the vector $\dot{\mathbf{x}}\delta t$ where $\dot{\mathbf{X}}(t_1)$ is the random vector of time derivatives $[\partial X_1/\partial t, \partial X_2/\partial t]^T$ evaluated at time t_1. If $\mathbf{n}(t)$ represents a unit outward normal at A, then the component $\dot{\mathbf{x}}\delta t$ which contributes to outcrossing (rather than merely moving along the domain boundary) is the scalar product $n^T \cdot \dot{\mathbf{x}} \ \delta t > 0$ [i.e.$(n_1 \dot{x}_1 + n_2 \dot{x}_2 + \ldots)\delta t > 0$] as shown. For convenience, let this be called $\dot{x}_n$ (a scalar) as $\delta t \to 0$. Comparison with the one-dimensional process described in Section 6.5.3 and shown in Figure 6.15 shows that in this case $\dot{x}_n$ corresponds directly to $\dot{x}$. It seems entirely plausible, therefore, to suggest that (6.72) generalizes to the m-dimensional vector process as

$$v_D^+ = \int_{S_D} \left[\int_0^\infty \dot{x}_n f_{\mathbf{X}\dot{X}_n}(\mathbf{x}, \ \dot{x}_n)d\dot{x}_n \right] d\mathbf{x} \tag{6.79}$$

where the first integral is necessary to ensure that all points of the domain boundary S_D are considered. A formal proof is available [Belyaev, 1968; Belyaev and Nosko, 1969]; the result is not restricted to Normal (i.e. Gaussian) processes.

Noting (A.119), expression (6.79) may be rewritten by replacing $\dot{x}_n$ in the inner integral by the conditional expectation of the random scalar $\dot{X}_n$:

$$v_D^+ = \int_{S_D} E(\dot{X}_n|\mathbf{X} = \mathbf{x})^+ f_{\mathbf{X}}(\mathbf{x})d\mathbf{x} \tag{6.80}$$

where, in (6.79) and (6.80), $\mathbf{X} = \mathbf{X}(t)$ and $E(\dot{X}_n|\mathbf{X} = \mathbf{x}) = \dot{x}_n = \mathbf{n}(t)\dot{\mathbf{x}}(t) > 0$. The latter condition is denoted by $(\ )^+$; if $\dot{x}_n \le 0$, the expectation becomes $E(\ ) = 0$.

In (6.80) the outcrossing rate v_D^+ can be interpreted (somewhat non-rigorously) as follows. For any elemental point $\mathbf{x}(t)$ on S_D, $E(\ )$ in (6.80) represents the expectation that

an outcrossing will occur; this is then weighted by the 'probability' $f_{\mathbf{X}}(\mathbf{x})$ that such a value of $\mathbf{x}$ will occur. This process is repeated for all points on the domain boundary S_D and the results 'summed' (as represented by the integral). Comparison with (6.72) shows that the integrand in (6.80) might be seen as a one-dimensional solution, appropriately weighted.

The solution of (6.79) or (6.80), in general, is still not straightforward. A few theoretically exact solutions are available for simple time-invariant safe domains D_S under the assumption that $\mathbf{X}(t)$ and $\dot{\mathbf{X}}(t)$ at any time t are mutually independent [Veneziano et al., 1977; Hohenbichler and Rackwitz, 1986b]. However these solutions these tend to be too restrictive for use in structural reliability analysis. An approximate bounding technique is available for convex polyhedron safe domains and continuous Gaussian processes; this is discussed in Section 6.5.4.3.

In all the above it has been assumed that $\mathbf{X}(t)$ is stationary, although, as usual, the latter restriction may be removed for smooth non-stationary processes by appropriate substitution of $\int_0^t v_D^+(s)ds$ for v_D^+ and by modifying (6.80) appropriately in $f_{\mathbf{X}}(\ )$.

6.5.4.2 Outcrossings for Discrete Processes

Discrete processes, such as Poisson square wave processes (see Section 6.5.1.5), commonly are used to describe loads such as floor loadings, in offices, hospitals, car parks, etc. The outcrossing rate is now considered for the special case in which each of the n independent components $X_i(t)$ of the vector process $\mathbf{X}(t)$ is Poisson square wave.

Let the magnitude Y_i of the process be normal distributed, and let the arrival times t be Poisson distributed with a mean arrival rate v_i. A typical realization is shown in Figure 6.19.

The total outcrossing rate v_D^+ is the sum over all components of the probability that an outcrossing occurs for each component, weighted by the occurrence probability of that combination of components [Breitung and Rackwitz, 1982; Rackwitz, 1985a]. This may be expressed as

$$v_D^+ = \sum_{i=1}^n v_i \int_{-\infty}^{\infty} P(\text{outcrossing due to } Y_i) f_{\mathbf{X}^*}(\mathbf{x}) d\mathbf{x} \tag{6.81}$$
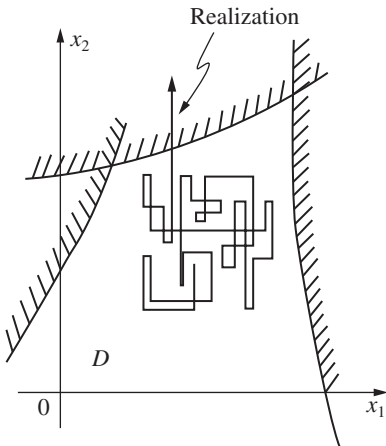

Figure 6.19 Typical realization of Poisson square wave vector process $\mathbf{X}(t)$ in two dimensions.

where $P(\ ) = P[(Y_i, \mathbf{x}^*) \in D_S]P[(Y_i, \mathbf{x}^*) \notin D_S]$. Here $\mathbf{X}^*$ is $\mathbf{X}$ without the ith component, evaluated at the time that the i th component has a renewal. The probability density function for $\mathbf{X}^*$ is:

$$f_{\mathbf{X}^*}(\ ) = \delta(x_i)\prod_{j=1}^{n} f_{X_j}(x_j), \qquad j \neq i \tag{6.82}$$

and $\delta(x_i)$ is the Dirac delta function, introduced to ensure that $f_{\mathbf{X}^*}(\ ) = 0$ unless the ith component is considered. The (multiple) integral in (6.81) extends over all the components of $\mathbf{X}$ and for any one component extends over all its values $-\infty < X_i < \infty$. Particular solutions depend on the shape of the domain. If this is defined as the hypercube $a_j \leq x_j \leq b_j$, and $\mathbf{X}$ is a vector with standard normal components, it follows that

$$P[(Y_i, \mathbf{x}^*) \in D_S] = P(a_i \leq Y_i \leq b_i) = \Phi(b_i) - \Phi(a_i) \quad \text{for } a_j \leq x_j \leq b_j; j \neq i$$
$$= 0 \quad \text{otherwise} \tag{6.83}$$

and

$$P[(Y_i, \mathbf{x}^*) \notin D_S] = P[(Y_i < a) \cup (Y_i > b_i)] = 1 - \Phi(b_i) + \Phi(a_i) \tag{6.84}$$

so that

$$v_D^+ = \sum_{i=1}^{n} \left\{ v_i \int_{a_1}^{b} \ldots \int_{a_n}^{b} [\Phi(b_i) - \Phi(a_i)][1 - \Phi(b_i) + \Phi(a_i)] \right.$$
$$\left. \times \prod_{j=1, j \neq 1}^{n} \phi(x_j)dx_1 \ldots dx_{i-1}dx_{i+1} \ldots dx_n \right\} \tag{6.85}$$

$$= \sum_{i=1}^{n} \left\{ v_i[\Phi(b_i) - \Phi(a_i)][1 - \Phi(b_i) + \Phi(a_i)] . \prod_{j=1, j \neq i}^{n} [\Phi(b_j) - \Phi(a_j)] \right\} \tag{6.86}$$

This expression has a direct interpretation. The first [ ] term represents the probability that the renewal Y_i of X_i is in the safe domain D_S, the second [ ] term represents the probability that Y_i is outside D_S and the $\prod$[ ] term is the probability that all the remaining components are in D_S, i.e. that X_i actually is the only component outcrossing at this time. Evidently (6.86) may be contracted to

$$v_D^+ = \prod_{j=1, j \neq i}^{n} [\Phi(b_j) - \Phi(a_j)] \sum_{i=1}^{n} \{v_i[1 - \Phi(b_i) + \Phi(a_i)]\} \tag{6.87}$$

in which the $\prod$[ ] term denotes the probability that all components are in the safe domain D_S and the summation term represents the sum of each component that is independently out of D_S.

By a parallel argument it may be shown that for a hyper-plane defined by $\beta + \mathbf{AX} = 0$ where $\mathbf{A} = [\alpha_1, \alpha_2, \ldots]^T$ is the vector of direction cosines of the normal to the hyper-plane and β the distance from the origin perpendicular to the plane

(*cf.* Section 4.3.2), the outcrossing rate is given by

$$v_D^+ = \sum_{i=1}^{n} \{v_i[\Phi(-\beta) - \Phi_2(-\beta, -\beta, \rho)]\} \tag{6.88}$$

where $\rho_i = 1 - \alpha_i^2$ and $\Phi_2(\ )$ is the bivariate standard Normal integral [Breitung and Rackwitz, 1982].

Extension of these analytical results to other forms of limit state functions is not necessarily easy since the formulation of the term $P(\ )$ in (6.81) generally is more difficult than for the above examples. An alternative is to use numerical methods for the evaluation of the integrals, as outlined in Section 6.5.5.

For the special case of linear addition of just two (independent) load processes $X_1(t)$ and $X_2(t)$ the range of analytic solutions for the mean outcrossing rate and hence the first-passage probability is somewhat greater. For Poisson square wave processes, exact solutions for the first-passage problem have been given by Bosshard (1975), Hasofer (1974) and Gaver and Jacobs (1981). An exact solution for the mean level upcrossing rate of rectangular renewal processes was given by Larrabee and Cornell (1979). Approximate solutions or bounds for the mean level crossing rate also are available for two additive renewal processes having more general pulse shapes [Larrabee and Cornell, 1981; Madsen et al., 1979; Waugh, 1977]. Because of their particular use in load combinations, consideration of these special results is deferred to Section 6.7.

6.5.4.3 Outcrossings for Continuous Gaussian Processes

Analytic solutions for outcrossing rates for continuous processes when the limit state functions have general forms are limited. Again, numerical solutions can be obtained rather more easily, as outlined in Section 6.5.5.

For Normal processes some analytic progress has been made, particularly when the safe domain is described by convex (hyper-)polyhedrals as limit state functions. In this case the failure domain consists of a set of linear limit state functions and, as might be expected, the problem of outcrossing rate determination has a close affinity with the first-order second-moment (FOSM) method. The possibility of extension of the results to non-Normal processes, in the manner of the first-order reliability (FOR) method of Chapter 4 is noted briefly in Section 6.5.4.4 below. First, however, normal processes with convex polyhedral limit state functions are considered.

Recall that for the safe domain D_S, bounded by S_D, the outcrossing rate v_D^+ of a vector process $X(t)$, is given by (6.80):

$$v_D^+ = \int_{S_D} E(\dot{X}_n | \mathbf{X} = \mathbf{x})^+ f_{\mathbf{X}}(\mathbf{x}) d\mathbf{x} \tag{6.89}$$

where, as before, $(\dot{X}_n | \mathbf{X} = \mathbf{x}) = \dot{x}_n = \mathbf{n}(t) \cdot \dot{\mathbf{x}}(t) > 0$ is the unit rate vector normal to S_D at $\mathbf{x}$ and $(\ )^+ \geq 0$ for $\dot{x}_n > 0$, and $(\ )^+ = 0$ otherwise. Also as before, the term $f_{\mathbf{X}}(\mathbf{x})$ denotes the probability density function for $\mathbf{X}(t)$.

Let it now be assumed that S_D consists of a set of time-invariant piecewise continuous convex (hyper-)planes. It then follows that on any one (hyper-)plane, the expectation term $E(\ )^+$ will be independent of the precise value of $\mathbf{X}$, since the unit normal $\dot{x}_n$ will have the same direction anywhere on the (hyper)plane. Also, as shown in Section 6.4.3,

X_i and $\dot{X}_i$ are independent, so that (6.89) may be rewritten as

$$v_D^+ = E(\dot{X}_n)^+ \int_{S_D} f_{\mathbf{X}}(\mathbf{x})d\mathbf{x} \tag{6.90}$$

where the integral over the domain surface S_D represents the probability that $\mathbf{X}$ lies on S_D and the expectation term $E(\ )$ that an outcrossing will occur for $\mathbf{X}$ on S_D. For any one (the l th) (hyper-)plane H_l, containing the partial domain surface ΔS_l, the partial outcrossing rate is then

$$v_{\Delta D_l}^+ = E(\dot{X}_{nl})^+ \int_{\Delta S_l} f_{\mathbf{X}}(\mathbf{x})d\mathbf{x} \tag{6.91}$$

In parallel to (6.90), the integral in (6.91) represents the probability that $\mathbf{X}$ lies on ΔS_l. This can be considered also in two parts: firstly, the probability that $\mathbf{X}$ lies on the (hyper-)plane H_l and, secondly, that $\mathbf{X}$ lies within ΔS_l given that $\mathbf{X}$ is on H_l. It should be noted that, for linear limit state functions, ΔS_l as projected on H_l is a (hyper-)polygon of dimension $n-1$; the probability content within ΔS_l may be obtained directly by integrating $f_{\mathbf{X}}^*(\ )$ over ΔS_l, where $f_{\mathbf{X}}^*(\ )$ is the $n-1$ probability density function obtained from $f_{\mathbf{X}}(\ )$ by integrating in the direction normal to H_l. Rather than determining $f_{\mathbf{X}}^*(\ )$ first, $f_{\mathbf{X}}(\ )$ may be integrated over the $n-1$ dimensions of ΔS_l, provided that the result is weighted by the probability that $\mathbf{X}$ lies on H_l. Hence the integral in (6.91) may be replaced by two terms:

$$v_{\Delta D_l}^+ = E(\dot{X}_{nl})^+ \int_{H_l} f_{\mathbf{X}}(\mathbf{x})d\mathbf{x} \int_{\Delta S_l, n-1} f_{\mathbf{X}}(\mathbf{x})d\mathbf{x} \tag{6.92}$$

where it is now understood that integration of $f_{\mathbf{X}}(\ )$ over ΔS_l is in $n-1$ dimensions and that the integral over H_l is in one dimension, perpendicular to H_l [Veneziano et al., 1977].

The second integral in (6.92) may be evaluated by using the system bounds for linear limit state function (see Chapter 5) but now used to determine the probability content p_l contained within ΔS_l rather than that outside ΔS_l. Clearly the probability content required is the complement of that obtained directly from the system bounds. Example 6.3 below will illustrate this.

The first integral in (6.92), which represents the probability that $\mathbf{X}$ lies on H_l, may be evaluated by considering what happens when the hyper-plane H_l is displaced laterally to itself.
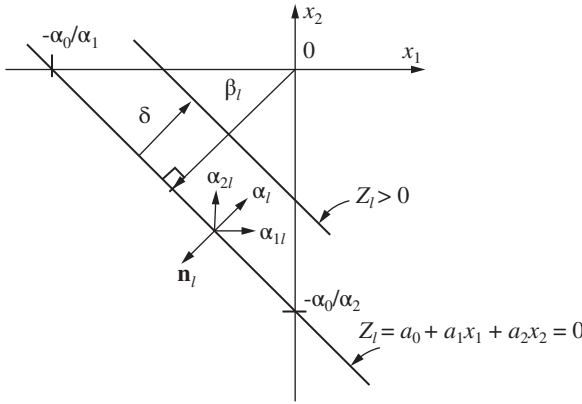
If the l th linear safety margin has the expression $Z_l = a_0 + a_1 X_1 + a_2 X_2 + \ldots + a_n X_n$, with $a_0 > 0$ and the a_i all constants, it follows from the discussion in Section 4.3 that the limit state $Z_l = 0$ has a normal on H_l defined by:

$$\mathbf{A}_l = (\alpha_{1l}, \alpha_{2l}, \ldots)^T \tag{6.93}$$

where

$$\alpha_{il} = \frac{a_i}{l} \tag{6.94}$$

Figure 6.20 Parallel shift of hyperplane H_l.

with

$$l = \left(\sum_{i=1}^{n} a_i^2 \right)^{1/2}$$

If the (hyper-)plane is displaced a distance δ in the direction of the normal $\mathbf{A}_l$, the change in the value of Z_l is (see Figure 6.20):

$$Z_l(>0) - Z_l(=0) = [a_0 + a_1(X_1 + \delta\alpha_1) + a_2(X_2 + \delta\alpha_2) + \ldots] - (a_0 + a_1 X_1 + \ldots)$$

which becomes, using (6.94):

$$Z_l(>0) - Z_l(=0) = \delta \sum_{i=1}^{n} a_i \alpha_{il} = \delta \left(\sum_{i=1}^{n} a_i^2 \right)^{1/2} \tag{6.95}$$

For linear limit state functions the reliability index is given by $\beta = \mu_Z/\sigma_Z = E(Z_l)/D(Z_l)$ and the corresponding change in the reliability index is:

$$\Delta\beta_l = \frac{E(Z_l > 0) - E(Z_l = 0)}{D(Z_l)} \tag{6.96}$$

Figure 6.20 makes clear that the probability content between the two hyperplanes is given by $\Delta\Phi(-\beta_l) = \Phi(-\beta_l) - \Phi[-(\beta_l - \Delta\beta_l)]$. It follows that the probability density $\int_{H_l} f_{\mathbf{X}}(\,)d\mathbf{x}$ is then the probability change as δ, the distance between the planes, approaches zero:

$$\int_{H_l} f_{\mathbf{X}}(\mathbf{x})d\mathbf{x} = \lim_{\delta \to 0} \left[\frac{\Delta\Phi(-\beta_l)}{\delta} \right] = \lim_{\delta \to 0} \left[\phi(\beta_l) \frac{\Delta\beta_l}{\delta} \right] \tag{6.97}$$

or, using (6.95) and (6.96),

$$\int_{H_l} f_{\mathbf{X}}(\mathbf{x})d\mathbf{x} = \frac{\phi(\beta_l)}{D(Z_l)} \left(\sum_{i=1}^{n} a_i^2 \right)^{1/2} \tag{6.98}$$

When all X_i are standard Normal random variables, it follows readily that (6.92) reduces to $\phi(\beta_l)$ [Veneziano et al. 1977].

The result (6.98) together with the expectation term $E(\ )^+$ in (6.92) may be seen as a correction term defined by

$$K_l = E(\dot{X}_{nl})^+ \int_{H_l} f_{\mathbf{X}}(\mathbf{x}) d\mathbf{x} \tag{6.99}$$

This term can be simplified by noting that the polyhedron ΔS_l may be defined on H_l by a series of linear limit state functions based on the (random variable) safety margin expressions:

$$Z_j = a_{0j} + \sum_{i=1}^{n} a_{ij} X_i \qquad j = 1, \dots, n; \ j \neq l \tag{6.100}$$

such that $Z_j > 0$ inside the safe domain defined on H_l, that is, within ΔS_l, and with $Z_l = 0$ elsewhere.

Noting that $\dot{Z}_l = \sum_{i=1}^{n} a_i \dot{X}_i$ and $\dot{X}_{nl} = n_l^T \cdot \dot{\mathbf{X}}$, where $\mathbf{n}_l$ is the outward normal vector to the plane H_l and therefore equal to $-\mathbf{A}_l$ (see Figures 6.18 and 6.20), it follows that, using (6.94):

$$\dot{X}_{nl} = -\mathbf{A}_l^T \cdot \dot{\mathbf{X}} = -\sum_{i=1}^{n} \alpha_{il} \dot{X}_i \tag{6.101}$$

$$= \sum_{i=1}^{n} a_i \dot{X}_i \Big/ \left(\sum_{i=1}^{n} a_i^2 \right)^{1/2} \tag{6.102}$$

$$= -\frac{\dot{Z}_l}{\left(\sum_{i=1}^{n} a_i^2 \right)^{1/2}} \tag{6.103}$$

Collecting terms (6.103) and (6.98) into (6.99) produces

$$K_l = E(-\dot{Z}_l) + \frac{\phi(\beta_l)}{D(Z_l)} \tag{6.104}$$

This expression can be simplified further by noting that Z_l and therefore $\dot{Z}_l$ are both Normal distributed (since $\mathbf{X}$ is Normal). Let the mean and standard deviation of $\dot{Z}_l$ be μ and σ respectively. Then the probability density function $f_{\dot{Z}_l}(\ )$ is also given by $(1/\sigma)\phi[(\dot{z} - \mu)/\sigma]$ while the expectation conditional terms on having $-\dot{Z}_l > 0$ is given by (A.10):

$$E(-\dot{Z}_l)^+ = -\int_{-\infty}^{0} v \frac{1}{\sigma} \ \phi\left(\frac{v - \mu}{\sigma}\right) \ dv \tag{6.105}$$

where the integration limits have been chosen to achieve the positive part of expectation. Integrating by parts and substituting into (6.104),

$$K_l = \phi(\beta_l) \frac{\sigma}{D(Z_l)} \left[\phi\left(\frac{\mu}{\sigma}\right) - \frac{\mu}{\sigma} \Phi\left(-\frac{\mu}{\sigma}\right) \right] \tag{6.106}$$

where $\mu = E(\dot{Z}_l)$, $\sigma = D(\dot{Z}_l)$. Here $\phi(\ )$ and $\Phi(\ )$ are the usual probability density function and cumulative distribution function for the standardized normal distribution respectively. In the important case when the limit states are time invariant, $\mu = E(\dot{Z}_l) = 0$ and noting that $\phi(0) = 1/\sqrt{2\pi}$ and $\sigma = D(\dot{Z}_l)$ (see above) it follows that (6.106) reduces to

$$K_l = \frac{\phi(\beta_l)}{(2\pi)^{1/2}} \frac{D(\dot{Z}_l)}{D(Z_l)} \tag{6.107}$$

The outcrossing rate v_D^+ for the whole domain is obtained as the sum of the outcrossing rate for each hyper-plane H_l, $l = 1, \ldots, k$, thus:

$$v_D^+ = \sum_{l=1}^{k} v_{D_l}^+ = \sum_{l=1}^{k} K_l p_l \tag{6.108}$$

where $p_l = \int_{\Delta S_l} f_{\mathbf{X}}(\mathbf{x}) d\mathbf{x}$ as described for equation (6.92). If p_l is bounded, then (6.108) also results in bounds, but now on v_D^+.

The above has been obtained assuming differentiability of each safety margin Z_l for all l. In particular, this implies that for the existence of the mean $E[\dot{Z}_i(t)]$ the mean value function $E[Z_i(t)]$ must be differentiable for all t and that for the existence of the standard deviation $D[\dot{Z}_i(t)]$ the covariance function $\text{cov}[Z_i(t_1), Z_j(t_2)]$ must be differentiable with $i = j$ and for $t_1 = t_2$, thus:

$$E[\dot{Z}_i(t)] = \frac{d}{dt}\{E[Z_i(t)]\}. \tag{6.109}$$

$$\text{var}[\dot{Z}_i(t)] = \text{cov}[\dot{Z}_i(t), \dot{Z}_j(t)] = \left. \frac{\partial^2}{\partial t_1 \partial t_2} \text{cov}[Z_i(t_1), Z_j(t_2)] \right|_{\substack{i=j \\ t_1=t_2}} \tag{6.110}$$

6.5.4.4 General Regions and Processes

When the safe region is not necessarily convex, the determination of the outcrossing rate becomes more difficult. If the unsafe region can be visualized or expressed mathematically in terms of unions and intersections of component planar (half-space) regions, some conceptual results for unions and intersections of unsafe regions may be useful [Rackwitz, 1984]. Alternatively, a simplified convex (or spherical) region boundary may be employed to produce bounds on the outcrossing rate [e.g. Veneziano et al., 1977]. However, these bounds may be extremely conservative.

A further complication arises with non-linear limit state functions. As in FOSM theory, these may be linearized. As might be expected and as has been shown by an asymptotic argument [Breitung, 1984; 1988], for an individual limit state surface an appropriate choice of expansion point is the point of greatest local outcrossing density, parallel in concept to the point having $f_X(\ )$ a maximum is used as expansion point in time-invariant theory (see also Chapter 4). Interestingly, some earlier results have suggested that the precise choice of linearization point usually is not critical to obtaining a reasonably accurate result [Breitung and Rackwitz, 1982]. Once linearization points have been chosen, and the limit state linearization carried out, the estimation of the mean outcrossing rate may follow the procedures outlined in the previous sections.

Another possibility is that the vector process $\mathbf{X}(t)$ is not Normal or completely continuous in all its components. In principle it is possible to separate the calculation of the outcrossing rate into that concerned with continuous processes, that concerned

with (various) discontinuous processes and that concerned with time-invariant random variables [Rackwitz, 1984]. The corresponding outcrossing rates from the time-variant components may be added provided that it is (reasonably) assumed that the different groups of component processes are independent.

Non-normal component processes may be transformed to equivalent Normal processes in the manner of Section 4.4.3, again using the point of maximum local outcrossing rate as expansion point, even in the general case of non-Normal vector process(es) and non-linear limit state function, as has been shown to be appropriate by Breitung and Hohenbichler (1989). In a simplified version, when each component is independently subject to a uni-variate non-linear transformation that ignores dependence between components, such a transformation has also been termed a 'translation' of the Normal process [Grigoriu, 1984].

6.5.5 Numerical Evaluation of Outcrossing Rates

The possibility of numerical evaluation of outcrossing rates is confined to numerical evaluation of the various functions given in the previous sections or the use of simulation techniques. Given the form of the outcrossing problem shown in Figure 6.18, it is natural that directional simulation has been proposed for numerical evaluation of outcrossing rates for arbitrary but convex region boundaries. It has been developed for the n-dimensional standard Normal (Gaussian) vector process $N(\boldsymbol{\mu}_X, \mathbf{C} = \mathbf{I})$ having continuous derivatives, where $\boldsymbol{\mu}_X$ is the vector of means and $\mathbf{C} = \mathbf{I}$ is the (diagonal) covariance matrix [Ditlevsen et al., 1987]. The simulation can be based on using the mean as the origin (see Section 3.5). The integral to be evaluated is (6.80) over the domain boundary S_D. The integral requires evaluation of the term $\dot{\mathbf{X}}_n \,|\, \mathbf{X} = \mathbf{x}$ where $\dot{x}_n = \mathbf{n}(t) \cdot \dot{\mathbf{x}}(t)$; this means that the outward normal $\mathbf{n}(t)$ is the critical matter for evaluation (see Figure 6.18). For the special case when the problem is reparameterized to the standard Normal space and when the limit state expressions are linear functions, this presents little difficulty since the expressions for the linear limit state functions directly yield the expressions for the Normal equivalents, for all t. An importance sampling technique, similar to that shown in Figure 3.9 is readily added.

These ideas for numerical integration to estimate outcrossing rates usually can be included directly in techniques for estimating time-dependent probability of failure, as is discussed in the following section. It will be sufficient, therefore, to not give further details simply for outcrossing evaluation at this stage.

Before continuing, however, it is important to observe that by focussing on the determination of an outcrossing rate, the time-dependent vector process crossing problem has been changed to one of determining a scalar measure, rather similar to the return period and the annual probability of failure of Section 6.2, or even the lifetime probability of failure of Section 6.1. The difference is essentially one of the time-scale used and the possibility to account for the effect of multiple components of the vector process. A more direct way to deal with these matters is possible only with the use of stochastic process theory, as described in the next section. It opens the way to handle time-dependent reliability estimation for multiple load processes in a rational manner.

6.6   Time-Dependent Reliability

6.6.1   Introduction

In the time-dependent reliability approach, the probability of failure of the structure is estimated directly from the first-passage probability. This is valid for high reliability systems. It is obtained from the probability that the process $S(t)$ leaves the safe domain D_S during the nominal life $[0, t_L]$ of the structure (see Figure 6.17). As noted in Section 6.1, this can be expressed as

$$p_f(t) = P[R(t) \leq S(t)] \qquad \forall (t \in [0 - t_L]) \tag{6.111}$$

where $[0, t_L]$ denotes the structural lifetime or other period of interest, $R(t)$ is the resistance of the structure at a point in time and as a function of time t and $S(t)$ is the load effect process, also a function of time. To make it operational and more general, in Section 6.2 this expression was conditioned on the resistance, expressed as a vector, which will now be considered also to be a function of time: $\mathbf{R}(t)$ with pdf $f_{\mathbf{R}}(\;)$. It then followed that:

$$p_f(t_L) = \int_{\mathbf{r}} p_f(t_L|\mathbf{r}) f_{\mathbf{R}}(\mathbf{r}) d\mathbf{r} \tag{6.112}$$

where the conditional failure probability $p_f(t_L|\mathbf{r})$ is a function of the vector of load processes $\mathbf{Q}(t)$ (or the vector of load effect processes $\mathbf{S}(t)$, depending on precisely how the problem is formulated). Importantly, it represents the failure probability conditional on the given realization $\mathbf{R} = \mathbf{r}$ of the structural resistance. This problem can now be seen to be the 'outcrossing' problem described above, with the resistance realization $\mathbf{R} = \mathbf{r}$ giving a deterministic 'boundary' and the load process $\mathbf{Q}(t)$ forming the process for which the probability of outcrossing is of interest. It follows that the results given above for outcrossing rates can be used directly, provided there is a relationship between $p_f(t_L|\mathbf{r})$ and outcrossing rates.

In general no simple relationship exists. The most useful approach is to rely on the stochastic process theory result (6.51, 6.52 or 6.53) that provides an upper bound relationship between the (conditional) failure probability and the mean outcrossing rate v_D^+:

$$p_f(t_L) \leq p_f(0) + [1 - p_f(0)]v_D^+ t_L \tag{6.113}$$

where $p_f(0)$ is the probability of the structure failing at time $t = 0$, i.e. typically on first load application. This result is valid for stationary vector load processes; if the vector load processes are smoothly nonstationary $v_D^+ t_L$ may be replaced by $\int_0^{t_L} v_D^+(\tau) d\tau$.

It should be clear that three matters are of interest in evaluating (6.113). The first is the evaluation of the term $p_f(0)$. It is not a time-dependent and can be evaluated directly using any of the methods discussed in Chapters 3, 4 and 5. The second matter is the evaluation of the outcrossing rate: for this the methods discussed in Section 6.5 are relevant. When these (conditional) terms have been collected what remains is the integration in (6.112) to obtain the unconditional failure probability. This is discussed in the sections to follow.

The third matter of interest is the closeness of the upper bound (6.113) to the correct result. As noted in Section 6.4.5 for narrow band load processes (such as for the responses of dynamically excited structures, see Section 6.8) it is possible for the out-crossings to occur in 'clumps'. In this case the upper bound expression will over-estimate the outcrossing rate, perhaps significantly. Conversely, if the load process vector is not a narrow band process, the bound is generally quite close (as 'clumping' is less likely).

A completely different approach for estimating time-dependent reliability is to by-pass the finding of outcrossing rates altogether and to estimate the probability of a multivariate vector process entering the deterministic failure domain through direct simulation of each continuous vector process [Hasofer et al., 1987]. To do this, it is convenient to let each multi-variate standard Gaussian vector process be represented by a trigonometric series with random coefficients [see also Shinozuka, 1987]. Directional simulation is then used to estimate the probability, using, for each directional sample, the lifetime maximum approach to estimate the probability of the vector process passing out of the domain. Although this is a very direct technique, it appears to have the disadvantage of high computational requirements, since it requires at least $s(t + 1)$ simulations, where s is the number of components of the random vector process and t is the number of random coefficients used to represent each random process. The optimal value for t does not appear to be well researched, and it could well be substantial in size. This technique for estimating time-dependent failure probabilities is not discussed further herein although it has been applied in practical cases for checking results obtained by methods discussed below [e.g. Moarefzedah and Melchers, 1996a].

6.6.2 Sampling Methods for Unconditional Failure Probability

As noted, generally the integration of (6.112) cannot be performed analytically. Also, (6.113) may not be available analytically either. For tackling this problem three possibilities have been proposed; these are associated with simulation and with FOSM/FOR/SOR methods respectively. They are described briefly below.

6.6.2.1 Importance and Conditional Sampling

In this scheme, evaluation of (6.112) is performed by Importance Sampling, and the evaluation of (6.113) is considered through conditional expectation (Section 3.6.1) [Mori and Ellingwood, 1993a]. The process starts with time-invariant importance sampling:

$$p_f = \int \ldots \int I[G(\mathbf{x}) \leq 0]\frac{f_X(\mathbf{x})}{h_V(\mathbf{x})}h_V(\mathbf{x})d\mathbf{x} \tag{3.17}$$

where the integration is, as usual, over the failure domain D. Also, if appropriate, the limit state function $G(\mathbf{x}) = 0$ can represent a collection of m individual limit state functions $\bigcup_{i=1}^{m} G(\mathbf{x}) = 0$. The multiple integral can be written in terms of conditional probabilities as

$$p_f = \int \ldots \int_{D_1} \frac{\left\{ \int \ldots \int_{D_2} I[G(\mathbf{x}_1, \mathbf{x}_2) \leq 0] f_{X_2|X_1}(\mathbf{x}_2|\mathbf{x}_1)d\mathbf{x}_2 \right\} f_{X_1}(\mathbf{x}_1)}{h_V(\mathbf{x}_1)} h_V(\mathbf{x}_1)d\mathbf{x}_1 \tag{6.114}$$

$$= \int \ldots \int_{D_1} \frac{p_{f|X_1=\mathbf{x}_1} \cdot f_{X_1}(\mathbf{x}_1)}{h_V(\mathbf{x}_1)} h_V(\mathbf{x}_1)d\mathbf{x}_1 \tag{6.115}$$

where the { } term in (6.114) has been replaced by the conditional probability $p_{f|\mathbf{X}_1=\mathbf{x}_1}$. In (6.115) $\mathbf{X}_1$ and $\mathbf{X}_2$ are subsets of the random vector $\mathbf{X}$, with $f_{\mathbf{X}_2|\mathbf{X}_1}(\ )$ the conditional pdf of $\mathbf{X}_2$ given $\mathbf{X}_1$ and D_1 and D_2 being the sample spaces for $\mathbf{X}_1$ and $\mathbf{X}_2$ respectively. Here D_1 and D_2 must be mutually exclusive and together must completely encompass D.

The next step is to recognize that (6.115) has the same form as the time-dependent reliability function (6.112) and that the m-fold integration over D_1 can be performed by Monte Carlo simulation (i.e. by importance sampling) with samples selected as usual from the importance sampling pdf $h_{\mathbf{V}}(\ )$ (see Section 3.4.2).

If the { } term in (6.114) can be evaluated numerically (or perhaps in closed form), it will be evaluated (i.e. given a conditional expectation result) for each sampling in the importance sampling scheme. In this way conditional expectation variance reduction is achieved (see also Section 3.6.1), thereby reducing the amount of Monte Carlo (importance) sampling required.

In practice this approach appears to be feasible only for simplified systems such as a weakest link (series) system subject to a limited form of random process, such as a Poisson spike process. For this the conditional expectation can be obtained reasonably efficiently, such as when the conditional failure probability for the strength of any link $R_i = a_i$ is given by (6.65) [Mori and Ellingwood, 1993a].

6.6.2.2 Directional Simulation in the Load Process Space

Directional simulation in the load process space follows rather directly from the outcrossing notions of Section 6.5.4.1, when, in Figure 6.18, the vector ($\mathbf{X}$) of random processes is interpreted as the (m-dimensional) vector of (stationary) load processes $\mathbf{Q}(t)$. It then follows that in the space $\mathbf{x}$ the domain boundary S_D can be interpreted as one realization of the structural resistance, denoted $\mathbf{R} = \mathbf{r}$. Further, the conventional limit state functions $G_i(\mathbf{q}, \mathbf{x}) = 0, i = 1, \dots, k$ are now interpreted as probabilistic 'boundaries', as shown schematically in Figure 3.12. The only difference between the ideas of directional simulation presented in Section 3.5.4 and those here is that the loads are now interpreted as load processes $\mathbf{Q}(t)$.

As in Section 3.5.4, let the resistance $\mathbf{R}$ of the system have the joint probability density function $f_{\mathbf{R}}(\ )$. Also, let it be a function of other random variables $\mathbf{X}$ such that $\mathbf{R} = \mathbf{R}(\mathbf{X})$ and where the components of $\mathbf{X}$ are not necessarily independent of time. They could be the resistances of structural members or of components or elements, or they could be material properties and their uncertainties. More generally, $\mathbf{X}$ could contain also any uncertainties in the specification of the load processes, and $\mathbf{Q}(t)$ could contain processes other than load processes. In that case the pdf of $\mathbf{Q}(t)$ also could reflect dependence between the load components.

The probability of failure for the structural system is given by (6.112) or (3.46). The conditional probability of failure $p_f(t_L|\mathbf{r})$ for a given resistance realization $\mathbf{R} = \mathbf{r}$ (and for the time period t_L of interest) can be estimated from the outcrossing rate v_D^+ and the initial failure probability $p_f(0)$ with the use of (6.51) or the upper bound (6.52) for high reliability systems:

$$p_f(s|\mathbf{a}) \le p_f(0, s|\mathbf{a}) + \{1 - \exp[-v_D^+(s|\mathbf{a})t_L]\} \tag{6.54}$$

where, as before, $p_f(0, s|\mathbf{a})$ is the failure probability at time $t = 0$ and v_D^+ is the outcrossing rate of the vector process $\mathbf{Q}(t)$ out of the safe domain D. Directional simulation in the

load process space, as in Section (3.5.4), may then be applied using (6.112) or (3.46) and the relationship $\mathbf{R} = S.\mathbf{A} + \mathbf{c}$:

$$p_f = \int_{\substack{\text{unit} \\ \text{sphere}}} f_{\mathbf{A}}(\mathbf{a}) \left[\int_S p_f(s|\mathbf{a}).f_{S|\mathbf{A}}(s|\mathbf{a})ds \right] d\mathbf{a} \tag{3.46}$$

where, as before, $\mathbf{A}$ is a vector of direction cosines having a pdf $f_{\mathbf{A}}(\ )$, S is a (scalar) radial distance representing the (conditional) structural strength, $\mathbf{c}$ is some point selected as the origin for directional simulation and $f_{S|\mathbf{A}}(\ )$ is the conditional pdf. The evaluation of $f_{S|\mathbf{A}}(\ )$ has been discussed in Section 5.3.4. The same principles apply in the case of time-dependent problems.

The directional simulation approach in the load space has been applied for Gaussian processes and for Poisson pulse processes [Melchers, 1992; 1994; 1995b; Moarefzedeh and Melchers, 1996a].

As before, the assumption underlying the use of the load-space formulation is that the limit states are independent of the realizations of the load processes, that is, the limit state functions have been assumed to be load-path independent (see discussion in Section 5.1).

6.6.3   FOSM/FOR Methods for Unconditional Failure Probability

For given realizations of the limit state function(s) $G_i[\mathbf{X}(t)] \geq 0$ with $i = 1, \ldots, n$, the safe domain D_S is fully described, and both $p_f(0)$ and v_D^+ can be determined by methods described already in Section 6.5 for FOSM/FOR techniques. An example is given below. The conditional failure probability $p_f(t_L | \mathbf{r})$ can then be evaluated, using the upper bound (6.54) for outcrossing rate for each (linearized) limit state function independently. Then, provided the load processes are purely normal vector processes, an upper bound to the first-passage probability can be obtained through the use of the second-order system bounds (5.39) and (5.45) of Chapter 5 and FOSM/FOR theory. Examples have been given by Ditlevsen (1983b) and Wickham (1985), and a further example is given below.

The main part of the problem now remaining is the integration over the resistance random variables $\mathbf{R}$. As was noted in Section 6.2, one approach is to introduce an auxiliary random variable. This converts the time-dependent problem to a time-invariant one. However, experience suggests that while the formulation using the auxiliary random variable is exact to the accuracy of the FOR/SOR method used, when the limit state function is time variant or the processes are non-stationary, computational times tend to become excessive [Rackwitz, 1993].

Alternatively, the problem can be reformulated to employ Laplace integral approximations [Breitung, 1984; 1994]. Unfortunately, this scheme appears to be effective only for small to very small variability in the components of $\mathbf{R}$.

It would appear that while classical FOSM/FOR/SOR methods are very effective for time-independent reliability analysis and for determination of outcrossing rates (see example below) they become difficult to apply for fully time-dependent problems, largely because of the integration required with respect to time-invariant random variables such as the structural resistance $\mathbf{R}$. For this purpose it has been suggested
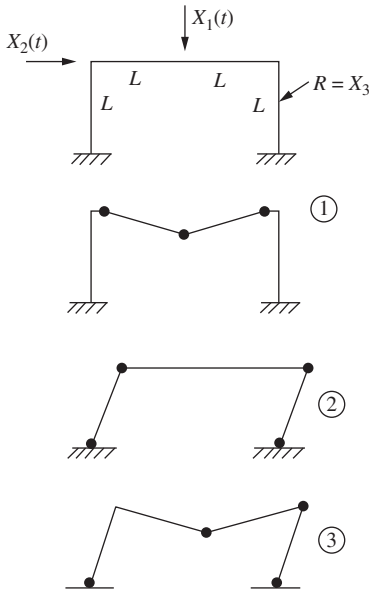
Figure 6.21 Rigid-plastic frame and plastic collapse modes.

that importance sampling and similar Monte Carlo techniques offer the most practical solution method [Rackwitz, 1993].

Example 6.3 [Adapted from Ditlevsen, 1983b] The rigid-plastic frame shown in Figure 6.21 is loaded by two stationary Gaussian stochastic load processes $X_1(t)$ and $X_2(t)$. Their expected values are $E[X_1(t)] = \mu$ and $E[X_2(t)] = 0.5\mu$. The covariance functions are $c_{11}(t_1, t_2) = c_{22}(t_1, t_2) = \sigma^2\rho(\tau)$ and $c_{12}(t_1, t_2) = c_{21}(t_1, t_2) = 0.5\sigma^2\rho(\tau)$. Because of stationarity these are functions only of the time difference $\tau = t_1 - t_2$. If $\tau = 0$, then $\rho = 1$. The resistance is given by random variable X_3 with mean or expected value $E(X_3) = \lambda\mu$ and negligible standard deviation. Further, let $\sigma = 0.25\mu$ and $L = 4$ units.

i) Preliminaries The first (preliminary) step is to determine the time-independent β indices for each failure mode. For the rigid-plastic collapse modes in Figure 6.21 the expressions for the corresponding safety margins are

$$\begin{bmatrix} Z_1 \\ Z_2 \\ Z_3 \end{bmatrix} = \begin{bmatrix} -4 & & +4 \\ & -4 & +4 \\ -4 & -4 & +6 \end{bmatrix} \begin{bmatrix} X_1 \\ X_2 \\ X_3 \end{bmatrix} \quad \text{or } \mathbf{Z} = \mathbf{A}.\mathbf{X} \tag{6.116}$$

from which the mean values of Z_i are $4\mu(\lambda - 1)$, $4\mu(\lambda - \frac{1}{2})$ and $6\mu(\lambda - 1)$ respectively. To determine the standard deviations of Z_i, expression (A.162) can be applied and (A.163) used to find the covariances between the Z_i. All the required results are more

easily obtained by matrix manipulation as given by (B.15)

$$\mathbf{C_Z} = \mathbf{A}\mathbf{C_X}\mathbf{A}^T \tag{6.117}$$

where $\mathbf{C_X}$ is the matrix of covariance functions c_{ij} between X_i and X_j. In the present case for only the two random processes X_1 and X_2 it is simply

$$\mathbf{C_X} = \sigma^2 \begin{bmatrix} \rho(\tau) & 0.5\rho(\tau) \\ 0.5\rho(\tau) & \rho(\tau) \end{bmatrix} = \sigma^2 \begin{bmatrix} a & b \\ b & a \end{bmatrix}, \text{ say.} \tag{6.118}$$

Substituting this into (6.117) together with the relevant part of (6.116) produces:

$$\mathbf{C_Z} = 16\sigma^2 \begin{bmatrix} -1 & 0 \\ 0 & -1 \\ -1 & -1 \end{bmatrix} \begin{bmatrix} a & b \\ b & a \end{bmatrix} \begin{bmatrix} -1 & 0 & -1 \\ 0 & -1 & -1 \end{bmatrix} \tag{6.119}$$

or

$$\mathbf{C_Z} = 16\sigma^2 \begin{bmatrix} a & b & a+b \\ b & a & a+b \\ a+b & a+b & 2(a+b) \end{bmatrix} \tag{6.120}$$

If $\tau = t_1 - t_2 = 0$ as is required to obtain the variances for Z_1, Z_2 and Z_3 according to (6.39) and (6.36a), then $\rho = 1$ and (6.120) becomes

$$\mathbf{C_Z} = 16\sigma^2 \begin{bmatrix} 1.0 & 0.5 & 1.5 \\ 0.5 & 1.0 & 1.5 \\ 1.5 & 1.5 & 3.0 \end{bmatrix} \tag{6.121}$$

The diagonal terms represent the variances, so that the standard deviations $D(Z_i)$ are 4σ, 4σ and $4\sqrt{3}\sigma$ respectively. The collapse mode reliability indices $\beta_i = E(Z_i)/D(Z_i)$ become $4(\lambda - 1)$, $4\left(\lambda - \frac{1}{2}\right)$ and $2\sqrt{3}(\lambda - 1)$.

(ii) Initial Failure Probability The probability of failure at time $t = 0$, given by $p_f(0)$ can now be calculated using the methods of Chapter 5. Here the bounds (5.39) and (5.45) together with the approximation (C.8) for the calculation of $P(F_i \cap F_j)$ will be applied. To use the latter, the correlations $\rho_{ij} = \rho(Z_i, Z_j)$ are required. These are obtained from (6.121) as

$$\rho_{12} = \rho_{21} = \frac{\text{cov}(Z_1, Z_2)}{\sigma_{Z_1}\sigma_{Z_2}} = \frac{16\sigma^2(0.5)}{(4\sigma)(4\sigma)} = 0.5$$

$$\rho_{13} = \rho_{31} = \frac{16\sigma^2(1.5)}{(4\sigma)(4\sqrt{3}\sigma)} = 0.5\sqrt{3}$$

$$\rho_{23} = \rho_{32} = \frac{16\sigma^2(1.5)}{(4\sigma)(4\sqrt{3}\sigma)} = 0.5\sqrt{3}$$

$$\rho_{11} = \rho_{22} = \rho_{33} = 1$$

@Seismicisolation

To use (C.8), the terms $(\beta_i - \beta_j \rho_{ij})/(1 - \rho_{ij}^2)^{1/2}$ need to be evaluated. It may be shown that these terms represent the 'conditional' values $\beta_{i|j}$ (see Example 6.4) below. The results are easily found to be:

$$\beta_{i|j} = \begin{bmatrix} 0 & \frac{4}{\sqrt{3}}\left(\lambda - \frac{3}{2}\right) & 2\lambda - 2 \\ \frac{4}{\sqrt{3}}\lambda & 0 & 2\lambda + 2 \\ 0 & -2\sqrt{3} & 0 \end{bmatrix} \tag{6.122}$$

Using the worst appropriate bound (i.e. additive bound) from (C.8) and ordering the reliability indices according to increasing values, produces the following lower bound on the initial failure probability:

$$\begin{aligned} p_f(0) > \Phi(-\beta_3) &+ \{\Phi(-\beta_1) - [\Phi(-\beta_1)\Phi(-\beta_{13}) + \Phi(-\beta_3)\Phi(-\beta_{31})]\}^+ \\ &+ \{\Phi(-\beta_2) - [\Phi(-\beta_2)\Phi(-\beta_{12}) + \Phi(-\beta_1)\Phi(-\beta_{21})] \\ &- [\Phi(-\beta_2)\Phi(-\beta_{32}) + \Phi(-\beta_3)\Phi(-\beta_{23})]\}^+ \end{aligned}$$

where $\{z\}^+$ indicates $\{\ \} = 0$ if $z \leq 0$. This bound is a function of the value assigned to the resistance random variable $R = r$. For example, if $\lambda = R/\mu = 2$ it can be shown easily that

$$p_f(0) > 2.797 \times 10^{-4} \tag{6.123}$$

From expression (5.45) an upper bound on $p_f(0)$ is given by

$$\begin{aligned} p_f(0) \leq \Phi(-\beta_3) &+ \Phi(-\beta_2) + \Phi(\beta_1) - \max[\Phi(-\beta_1)\Phi(-\beta_{31}), \Phi(-\beta_2)\Phi(-\beta_{32})] \\ &- \max[\Phi(-\beta_2)\Phi(-\beta_{32}), \Phi(-\beta_3)\Phi(-\beta_{23})] \end{aligned}$$

which becomes, for $\lambda = 2$ as before,

$$p_f(0) < 2.858 \times 10^{-4} \tag{6.124}$$

(iii) Conditional Probability on H_3, H_2 ***and*** H_1 The condition probability $\int_{\Delta S_i} f_{\mathbf{x}}(\mathbf{x})\,d\mathbf{x}$ contained in equation (6.91) for $l = 3$ requires the projection of the limit state functions 1 and 2 onto the plane H_3 representing the third limit state function. The projections of the reliability indices β_1 and β_2 are required also (see Figure 6.22(a)). It may be shown that the β projections are the conditional reliability indices $\beta_{i|j}$ already calculated above (see also Example 6.4 below). Also required are the conditional correlations $\rho_{ij|k}$, representing, typically, the angle $v_{12|3}$ shown in Figure 6.22(b), since $\rho = \cos v$ as in (5.58). It may be shown, either using a geometrical argument (see Example 6.4) or from a regression consideration [Ditlevsen, 1983b], that

$$\rho_{ij|k} = \frac{\rho_{ij} - \rho_{ik}\rho_{jk}}{[(1 - \rho_{ik}^2)(1 - \rho_{jk}^2)]^{1/2}} \tag{6.125}$$

which results in

$$\rho_{12|3} = -1, \quad \rho_{13|2} = \rho_{23|1} = +1 \tag{6.126}$$

@Seismicisolation

(a)

(b)
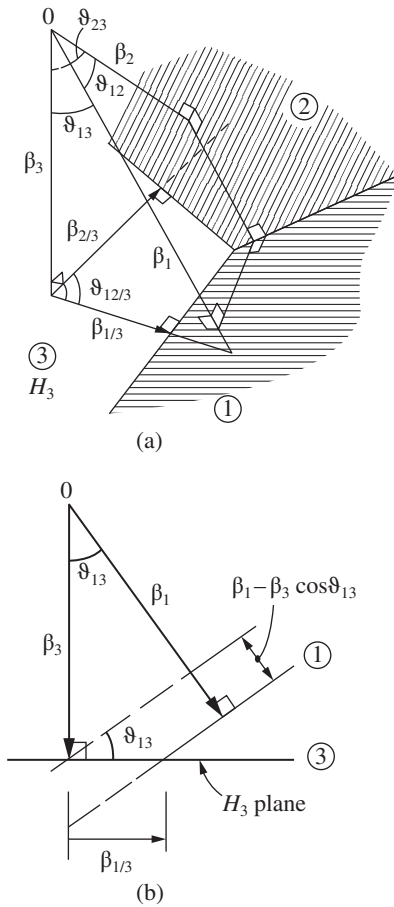
Figure 6.22 Projections of reliability indices and planes 1, 2 and 3.

The conditional probability content within ΔS_3 on the plane H_3 now can be bounded using (6.122) and (6.126) and using the most conservative combinations in (C.8). Noting that the bounds produce the probability content outside the region ΔS_3, it follows that the probability content within ΔS_3 is bounded by

$$1.0 - p_3 > \Phi(-\beta_{1|3}) + \{\Phi(-\beta_{2|3}) - [\Phi(-\beta_{2|3})\Phi(-A) + \Phi(-\beta_{1|3})\Phi(-B)]\}$$
$$1.0 - p_3 < \Phi(-\beta_{1|3}) + \{\Phi(-\beta_{2|3}) - \max[\Phi(-\beta_{2|3})\Phi(-A), \Phi(-\beta_{1|3})\Phi(-B)]$$

$$(6.127a)$$

with (see C.9)

$$A = \frac{\beta_{1|3} - (\rho_{12|3})\beta_{2|3}}{[1 - (\rho_{12|3})^2]^{1/2}} = \frac{(2\lambda - 2) - (-1)(2\lambda + 2)}{[1 - (-1)^2]^{1/2}} = \infty$$

$$(6.127b)$$

$$B = \frac{\beta_{2|3} - (\rho_{21|3})\beta_{1|3}}{[1 - (\rho_{21|3})^2]^{1/2}} = \frac{(2\lambda + 2) - (-1)(2\lambda - 2)}{[1 - (-1)^2]^{1/2}} = \infty$$

What these two results demonstrate in the present case is that the limit state functions are 180° 'apart' on the H_3 plane and that both conditional safety indices must be considered as contributing to the overall probability estimate. Such a specialized result would not, in general, be expected.

That the limit state functions are 180° apart on the H_3 plane follows from fact that in (6.126) it was found already that $\rho_{12|3} = -1$. However, following through the calculations for the bounds provides the same conclusion, as from (6.127a) the upper and lower bounds are clearly the same:

$$1 - p_3 = \Phi(-\beta_{1|3}) + \Phi(-\beta_{2|3})$$
$$= \Phi[-(2\lambda - 2)] + \Phi[-(2\lambda + 2)]$$

which follows directly from the bounding expressions when it is noted that $\Phi(-A) = \Phi(-B) = \Phi(-\infty) = 0$. Further, it follows readily that with $\lambda = 2$:

$$p_3 = 0.9772 \tag{6.127c}$$

For plane H_2 the correlation between the first and the third failure modes is $\rho_{13|2} = 1$ which means that the limit state equations for $\beta_{1|2}$ and $\beta_{3|2}$ are parallel (0° apart) and that the smallest β value is critical. Since $\beta_{3|2} = 2\sqrt{3} < \beta_{1|2} = \frac{4}{\sqrt{3}}\left(\lambda - \frac{3}{2}\right)$ for all λ, it follows that irrespective of the value of λ,

$$1 - p_2 = \Phi(-2\sqrt{3}) \quad \text{or} \quad p_2 = 0.99973 \tag{6.128}$$

Similarly, it can be shown that for the plane H_1, for all values of λ,

$$p_1 = 0.5 \tag{6.129}$$

(iv) Outcrossing Rate and First-Passage Probability   In this example the limit state expressions are time invariant: thus the correction factor K_l for the outcrossing rate through a plane (see 6.98 and 6.99) is given by (6.107). The terms $D(\dot{Z}_l)$ are obtained from the square root of the diagonals of var $(\dot{Z}_l)$ given by (6.110).

To carry out the differentiation required by (6.110), the general expression for $\mathbf{C}_Z$ given by (6.119) is used with τ replaced by $\tau = t_1 - t_2$ prior to differentiation, in turn, with respect to t_1 and t_2. Then, putting $\tau = t_1 - t_2 = 0$, produces the variance of $\dot{Z}_l$ on the diagonals $i = j$ (*cf.* Section 6.4.3). It is then found that $D(\dot{Z}_l) = 4\sigma\gamma(1, 1, \sqrt{3})$, $l = 1, 2, 3$ with $\gamma = [-\rho''(0)]^{1/2}$.

From (6.107) the factors K_l, $l = 1, 2, 3$ become

$$K_l = \frac{\gamma}{(2\pi)^{1/2}}\left[\frac{\phi(3.65)}{\sqrt{1.2}}, \frac{\phi(5.48)}{\sqrt{1.2}}, \frac{\phi(3.23)}{\sqrt{1.15}}\right] \tag{6.130}$$

and, according to equation (6.108), the mean outcrossing rate v_D^+ is then given by

$$v_D^+ = [0.364\gamma\,\phi(3.65)](0.5) + [0.364\gamma\,\phi(5.48)](0.99973)$$
$$+ [0.372\gamma\,\phi(3.23)](0.9772) \tag{6.131}$$

where the bounds have been ignored owing to their closeness. Evaluating (6.131) results in $v_D^+ = 9.0 \times 10^{-4} \gamma$. The first-passage probability $p_f(t_L) \le p_f(0) + v_D t_L$ is then bounded using (6.52, 6.123 and 6.124):

$$(2.797 + 9.0 \gamma \, t_L)10^{-4} < [p_f(0) + v_D^+ t_L] < (2.858 + 9.0 \gamma \, t_L)10^{-4} \tag{6.132}$$

where, as before, $[0, t_L]$ is the period of interest. In practice $\gamma = [-\rho''(0)]^{1/2}$ can be evaluated if an analytic expression is available for the correlation function, e.g. $\rho(\tau = t_1 - t_2) = A \exp[-B(t_1 - t_2)]$ where A and B are constants.

The numerical part of this example has been determined for $R = \lambda \mu = 2\mu$ where μ is the mean value of the load process X_1. Thus the (conditional) first passage probability obtained so far is for a deterministic resistance: specifically the result is conditional on $R = r = 2\mu$. If the resistance random variable properties are known, say if $f_R(\ )$ is known, then the result can be made unconditional by applying the theorem of total probability (A.6) or (A.118) or, equivalently, carrying out the integration over $\mathbf{r}$ in (6.112). This will require repeating the above calculations for different $R = r$ values (i.e. for different values of λ) sufficient to allow numerical integration or integration by simulation.

As noted at the beginning of this example, it is clear that the computational procedure outlined above is cumbersome even for this quite simple example.

Example 6.4 The reliability indices β_i have projections $\beta_{i|j}$, on the plane H_j as shown in Figure 6.22(b). These may be interpreted as conditional reliability indices in the sense of Example 6.3. The angles v_{ij} also are shown; by (5.60) these are related to the correlation coefficients through $\rho_{ij} = \cos v_{ij}$. Expressions for $\beta_{i|j}$ and $\rho_{ij|k}$ may be derived directly from the three-dimensional geometry in Figure 6.23 and in Figure 6.22(b); thus for $\beta_{1|3}$

$$\frac{E(Z_1|Z_3 = 0)}{D(Z_1|Z_3 = 0)} = \beta_{1|3} = \frac{\beta_1 - \beta_3 \cos v_{13}}{\sin v_{13}} = \frac{\beta_1 - \beta_3 \rho_{13}}{(1 - \rho_{13}^2)^{1/2}} \tag{6.133}$$

as also given in expression (C.9).
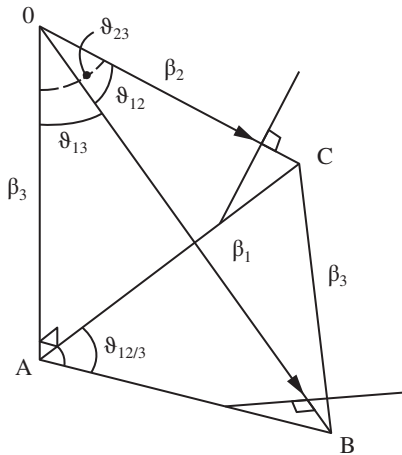
Figure 6.23 Geometry to determine conditional reliability indices and correlation coefficients.

To obtain $\rho_{12|3}$, the angle $v_{12|3}$ in Figure 6.23 must be calculated. This can be found by twice applying the cosine rule of trigonometry $a^2 = b^2 = c^2 - 2bc \cos A$ with angle A opposite side a:

$$BC^2 = OB^2 + OC^2 - 2(OB)(OC) \cos v_{12}$$

and

$$BC^2 = AB^2 + AC^2 - 2(AB)(AC) \cos v_{12|3}$$

With $AB = \beta_3 \tan v_{13}$, $AC = \beta_3 \tan v_{23}$, $OB = \beta_3 / \cos v_{23}$ and $OC = \beta_3 / \cos v_{23}$ and with $\rho_{ij} = \cos v_{ij}$, it follows readily that

$$\rho_{12|3} = \frac{\rho_{12} - \rho_{13}\rho_{23}}{[(1 - \rho_{13}^2)(1 - \rho_{23}^2)]^{1/2}} \qquad (6.134)$$

These results also apply, of course, to any three-dimensional subset of n-dimensional space. As used in Example 6.3 such a subset is sufficiently detailed for consideration of (hyper-)polyhedral safe regions.

6.6.4 Summary for Time-Dependent Reliability Estimation

The theory for time-dependent reliability assessment has developed rapidly, although in certain aspects it is not as fully developed as time-independent reliability. The various bases for it have been outlined above. It was seen that the simulation-based approaches became natural extensions of time-independent analysis once the outcrossing rate can be estimated efficiently.

However, the FOSM/FOR/SOR methods applied to time-dependent problems to determine probabilities of failure tend to be considerably more laborious than for time-independent problems. In applications resort often has to be made to numerical techniques to solve the resulting formulations. Even some early experience showed that for even relatively simple problems importance sampling was easier to apply and was the more satisfying numerical method [Rackwitz, 1993].

Unlike time-independent reliability techniques, for which there has been extensive discussion and comparison, often for a range of 'standard' cases, there has been relatively little comparison of the various approaches for solving time-dependent reliability problems. In part this could be because of the excessive computational times required for fundamental (e.g. crude Monte Carlo) comparisons when stochastic processes are involved. It also may be the strong focus in many application problems on the much simpler time-independent approaches, particularly FOSM and FOR, which are much more readily applied and easier to understand.

For many problems of practical significance, a fully time-dependent approach may not be needed. It is required, however, when the resistance basic variables are time dependent or when there is more than one loading case that must be considered as a time-variant loading. This is the usual case for structural design and for analysis, but it is clear that the methods described so far are much too complex for application in normal design and for specification in structural design codes. For these, simplified rules are required. However, in principle such simplified rules should be based on sound fundamentals and the above descriptions provide such a basis, particularly for the

difficult cases with more than one loading system applied. The development of design code rules on the basis of structural reliability principles is discussed in Chapter 9, but first consideration needs to be given to the matter of combination of time-dependent loading systems. This is the subject of the next section.

6.7 Load Combinations

6.7.1 Introduction

The load combination problem consists of finding an equivalent loading system to represent the effect of two or more stochastic load processes acting in combination or individually in a purely additive manner. This is a special case of the outcrossing problem considered in the previous sections.

The need for this result arises from code calibration work (see Chapter 9). Typically codes use simplified rules for load combinations. They are based on the application of the time-integrated approach (see Section 6.2). The simplified rules will be considered later in this section. First, as usual, it will be appropriate to consider some fundamentals.

If $X_1(t)$ and $X_2(t)$ represent stationary, mutually independent continuous load processes, the probability distribution in a time interval $[0, t_L]$ for the linear sum $X = X_1 + X_2$ can be obtained from a consideration of the upcrossing rate of $X(t)$ as a function of the barrier level $x = a$ (see 6.55). The main problem is thus the calculation of the upcrossing rate for X, for the barrier a or, equivalently, the outcrossing rate for (X_1, X_2) out of the domain bounded by the plane $x_1 + x_2 = a$.

If $X_1(t)$ and $X_2(t)$ are each Normal stationary processes, the sum $X = X_1 + X_2$ is also Normal and stationary, with mean and variance given by (A.160) and (A.162). The upcrossing rate for a stationary Normal process then follows directly from the result (6.74) for a single process $X(t)$.

Unfortunately not all load processes can be described adequately, even under instantaneous conditions, by a Normal process and, as noted in Section 6.5.3, the use of (6.74) for non-Normal processes is seldom sufficiently accurate.

6.7.2 General Formulation

In principle, the expected upcrossing rate may be determined using Rice's formula (6.72) for the sum process $X(t)$. To use it, the joint probability density function $f_{X\dot{X}}(\ )$ is required. This can be expressed in terms of $f_{X_1\dot{X}_1}(\ )$ and $f_{X_2\dot{X}_2}(\ )$ by means of the convolution integral

$$f_{X\dot{X}}(a, \dot{x}) = \int_{-\infty}^{\infty}\int_{-\infty}^{\infty}f_{X_1\dot{X}_1}(x_1, \dot{x}_1)f_{X_2\dot{X}_2}(a - x_1, \dot{x} - \dot{x}_1)dx_1 d\dot{x}_1 \tag{6.135}$$

noting that $\dot{x} = \dot{x}_1 + \dot{x}_2$, $x_1 = x - x_2$. Changing the order of integration, the resulting triple integral form for the upcrossing rate is given by (*cf.* 6.72):

$$v_X^+(a) = \int_{-\infty}^{\infty}\int_{-\infty}^{\infty}\int_{\dot{x}=-\dot{x}_1}^{\infty}(\dot{x} + \dot{x}_2)f_{X_1\dot{X}_1}(x, \dot{x}_1)f_{X_2\dot{X}_2}(a - x, \dot{x}_2)d\dot{x}_2 d\dot{x}_1 dx \tag{6.136}$$

This is seldom analytic. However, bounds can be established by changing the region of integration for $\dot{x}_1$ and $\dot{x}_2$. If the region of integration is increased to $0 \leq \dot{x}_1 \leq \infty$, $-\infty \leq \dot{x}_2 \leq \infty$ for the $\dot{x}_1$ component of (6.136), and to $-\infty \leq \dot{x}_1 \leq \infty$, $0 \leq \dot{x}_2 \leq \infty$ for the $\dot{x}_2$

component, an upper bound is obtained. Integrating over $\dot{x}_1$ and $\dot{x}_2$ leaves

$$v_X^+(a) \le \int_{u=-\infty}^{\infty} v_1(u) f_{X_2}(a-u)du + \int_{u=-\infty}^{\infty} v_2(u) f_{X_1}(a-u)du \tag{6.137}$$

where $v_i(u)$ is the upcrossing rate for the process $X_i(t)$. The rates $v_i(u)$ are evaluated readily using the results for a single variable. For some common processes they are given in Sections 6.5.1 and 6.5.2. The probability densities $f_{X_i}()$ are each a function of the relevant $X_i(t)$ for arbitrary time t. For obvious reasons they are known as the 'arbitrary-point-in-time' probability density functions.

Expression (6.137) is sometimes referred to as the 'point-crossing' formula. A lower bound can be obtained, and the results extended to more than two loads acting simultaneously for non-linear combinations and also extended to non-stationary load processes [Ditlevsen and Madsen, 1983].

For an important class of process combinations, (6.137) represents an exact solution. This class is largely that for which one of the two processes $X_1(t)$ or $X_2(t)$ has a discrete distribution, such as the square wave (Section 6.5.1.4) or is of the spike type (Section 6.5.1.4). More generally (6.137) is the exact result whenever the processes in the sum satisfy the following conditions [Larrabee and Cornell, 1981]:

$$P[\dot{X}_i(t) > 0 \ \text{and} \ \dot{X}_j(t) < 0] = 0 \tag{6.138}$$

for all processes i, j and at all times t. This condition ensures that one process does not cancel out the act of upcrossing of the other process, by decreasing in value at the same time. Typical processes that satisfy this condition are shown in Figure 6.24.

If $X_1(t)$ and $X_2(t)$ are each stationary Normal processes, with means μ_{X_1}, and μ_{X_2} and standard deviations σ_{X_1} and σ_{X_2} respectively, then, as usual

$$f_{X_i}(x_i) = \frac{1}{\sigma_{X_i}} \phi \left(\frac{x_i - \mu_{X_i}}{\sigma_{X_i}} \right)$$
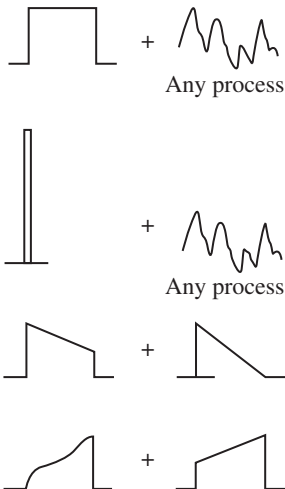
Figure 6.24 Combinations of random processes for which the 'point-crossing' formula is exact.

and, from (6.74), the upcrossing rate for each individual process $X_i(t)$ is

$$v_i^+(a) = \frac{1}{(2\pi)^{1/2}} \frac{\sigma_{\dot{X}_i}}{\sigma_{X_i}} \, \phi\left(\frac{a - \mu_{X_i}}{\sigma_{X_i}}\right)$$

When these are substituted into (6.137), the upper bound for the upcrossing rate for $X = X_1 + X_2$ becomes

$$v_X^+(a) \le \frac{1}{(2\pi)^{1/2}} \frac{\sigma_{\dot{X}_1} + \sigma_{\dot{X}_2}}{\sigma_X} \phi\left(\frac{a - \mu_X}{\sigma_X}\right)$$

with $\mu_X = \mu_{X_1} + \mu_{X_2}$ and $\sigma_X^2 = \sigma_{X_1}^2 + \sigma_{X_2}^2$. For the present case the exact result for the upcrossing rate for the combined process can be obtained from (6.74) with $\sigma_{\dot{X}}^2 = \sigma_{\dot{X}_1}^2 + \sigma_{\dot{X}_2}^2$. The error is thus indicated by the ratio $(\sigma_{\dot{X}_1} + \sigma_{\dot{X}_2})/(\sigma_{\dot{X}_1}^2 + \sigma_{\dot{X}_2}^2)^{1/2}$. This has a maximum of $\sqrt{2}$ when $\sigma_{\dot{X}_1} = \sigma_{\dot{X}_2}$. For most other combinations of load processes, the error is less [Larrabee and Cornell, 1981].

6.7.3 Discrete Processes

It will be instructive to consider the sum of two non-negative rectangular renewal processes of the 'mixed' type (see Section 6.5.1.6). Typical traces (realizations) are shown in Figure 6.25. From (6.69) the upcrossing rate for each process is

$$v_i^+(a) = v_i[p_i + q_i F_i(a)][q_i(1 - F_i(a))] \tag{6.139}$$

where the mean rate of arrival of pulses in the mixed process is $v_i q_i = v_{mi}$, say. Also the arbitrary-point-in-time distribution for a mixed process is $f_{x_i}(x_i) = p_i\delta(x_i) + q_i f_i(x_i)$, where $\delta(\ )$ is the Dirac delta function (see Figure 6.25) and $q_i = 1 - p_i$. Writing $G_i(\ ) = 1 - F_i(\ )$ and substituting into (6.137) for $v_i^+(\ )$ and $f_{X_i}(\ )$ with $i = 1,2$ and
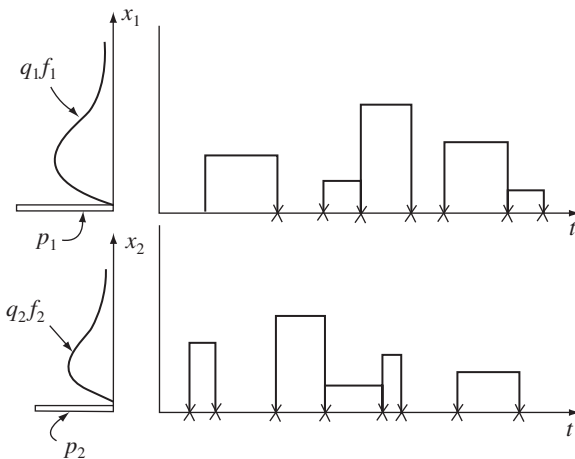
Figure 6.25 Typical realizations of mixed rectangular renewal processes with given probability density functions.

integrating will lead to

$$
\begin{aligned}
v_X^+(a) = {}& v_{m1}p_2[p_1 + q_1F_1(a)]G_1(a) + v_{m2}p_1[p_2 + q_2F_2(a)]G_2(a) \\
& + v_{m1}p_1q_2\left[\int_0^a G_1(a-x)f_2(x)dx\right] \\
& + v_{m2}p_2q_1\left[\int_0^a G_2(a-x)f_1(x)dx\right] \\
& + v_{m1}q_1q_2\left[\int_0^a F_1(a-x)G_1(a-x)f_2(x)dx\right] \\
& + v_{m2}q_1q_2\left[\int_0^a F_2(a-x)G_2(a-x)f_1(x)dx\right]
\end{aligned}
\tag{6.140}
$$

Fortunately, this rather fearsome-looking result has a simple explanation, as may be shown by looking at the problem from first principles.

For one process, the probability at each renewal that the process is active, i.e. that $X(t)$ has a non-zero value, is simply q (see Figure 6.25). Similarly, the probability that each renewal results in a zero (inactive) value of $X(t)$ is p, again not influenced by the value of $X(t)$ in the previous time increment. The process is therefore memory-less, or Markovian.

For two processes, the possible combinations of active and inactive states which allows the sum of the two processes to cross from below the barrier level a to above it are shown in Table 6.2 [Waugh, 1977; Larrabee and Cornell, 1979].

For each state change (i.e. the change of $X_1 + X_2 < a$ to the state $X_1 + X_2 > a$), the contribution to the upcrossing rate $v_X^+(a)$ is given by

$$
v_{(j)}^+ = \lim_{\Delta t \to 0}\left[P\left(\begin{array}{c}\text{up crossing}\\\text{of level }a\end{array}\middle|\begin{array}{c}\text{change of}\\\text{state in }\Delta t\end{array}\right)P\left(\begin{array}{c}\text{change of}\\\text{state in }\Delta t\end{array}\right)\right]
\tag{6.141}
$$

For state change (a) of Table 6.2, this becomes (with $\Omega = $ 'change of state in Δt'):

$$
v_{(a)}^+ = \lim_{\Delta t \to 0}(P\{[X_1(t) = 0] \cap [0 \le X_2(t) < a] \cap [X_2(t + \Delta t) > a]|\Omega\}P(\Omega))
$$

or

$$
v_{(a)}^+ = \{p_1[p_2 + q_2F_2(a)]G_2(a)\}v_2q_2
\tag{6.142}
$$

which corresponds to the second term in (6.140) noting that therein $v_2q_2 = v_{m2}$.

Table 6.2 Initial conditions and state changes for upcrossings.

State change	Process 1	Process 2	Upcrossing due to
(a)	Inactive	Active or inactive	Process 2
(b)	Active	Inactive	Process 2
(c)	Active	Active	Process 2
(d)	Active or inactive	Inactive	Process 1
(e)	Inactive	Active	Process 1
(f)	Active	Active	Process 1

For state change (b) of Table 6.2:

$$v^+_{(b)} = \lim_{\substack{\Delta t \to 0 \\ \text{all } x}} \langle P\{[0 < X_1(t)] \cap [X_2(t) = 0] \cap [X_2(t + \Delta t) > (a - x)|X_1 = x]|\Omega\}P(\Omega)\rangle$$

or

$$v^+_{(b)} = \left\{ q_1 p_2 \left[\int_0^a G_2(a - x)f_1(x)dx \right] \right\} v_2 q_2 \tag{6.143}$$

which corresponds to the fourth term in (6.140) with $v_2 q_2 = v_{m2}$. In a similar fashion it follows that the state change (c) is

$$v^+_{(c)} = \lim_{\substack{\Delta t \to 0 \\ \text{all } x}} (P\{[0 < X_1(t)] \cap [0 < X_2(t) < a - x] \cap [X_2(t + \Delta t) > (a - x)|X_1 = x]|\Omega\}P(\Omega))$$

$$\tag{6.144}$$

which is identical with the sixth term in (6.140). The other terms in (6.140) arise from state changes (d)-(f) of Table 6.2. If each pulse returns to zero prior to the commencement of the next pulse, the term $p_2 + q_2 F_2(a)$ in (6.142) is unity by definition, as is the term p_2 in (6.143). The fifth and sixth terms in (6.128) do not exist in this case.

With the upcrossing rate determined, the cumulative distribution function $F_X()$ for the total load $X = X_1 + X_2$ may be estimated using (6.55). The error in using (6.55) together with (6.140) has been investigated by comparison with the few known exact results for square wave processes [Hasofer, 1974; Bosshard, 1975; Larrabee and Cornell, 1979; Gaver and Jacobs, 1981] and found typically to give about a 20% overestimate for high barrier levels a, and about a 60% overestimate for lower levels of a. These are not insignificant errors, but at least they are conservative when translated to prediction of the probability of failure.

6.7.4 Simplifications

6.7.4.1 Load Coincidence Method

For impulse type loading with the pulses returning to zero, (6.140) may be considerably simplified (see above). Noting, for example, that $\int_0^a G_1(a - x)f_2(x)dx = G_{12}(a) - G_2(a)$, with $G_{12}() = 1 - F_{12}()$, where $F_{12}()$ is the cumulative distribution function for the total height of the two pulses, allows (6.140) to be simplified to

$$v^+_X(a) = v_{m1}(p_2 - v_{m2}\mu_1)G_1(a) + v_{m2}(p_1 - v_{m1}\mu_2)G_2(a) + v_{m1}v_{m2}(\mu_1 - \mu_2)G_{12}(a) \tag{6.145}$$

Here $v_{mi}\mu_i$ has been substituted for q_i. As before, v_{mi} is the mean pulse arrival rate of the process $X_i(t)$ (see 6.139). The terms μ_i are the mean durations of the pulses of $X_i(t)$. If the pulses are of short duration, $\mu_i \to 0$ while, if they are of relatively infrequent occurrence, $p_i \to 1$. Hence, a reasonable approximation for the upcrossing rate of the total process $X = X_1 + X_2$ is

$$v^+_X(a) \approx v_{m1}G_1(a) + v_{m2}G_2(a) + v_{m1}v_{m2}(\mu_1 + \mu_2)G_{12}(a) \tag{6.146a}$$

or

$$v^+_X(a) \approx v_{m1}G_1(a) + v_{m2}G_2(a) + v_{m1}v_{m2}G_{12}(a) \tag{6.146b}$$

where

$$v_{m1m2} = v_{m1}v_{m2}(\mu_1 + \mu_2) \tag{6.146c}$$

a result first given by Wen (1977a) using rather different reasoning. The first and second terms of (6.146a,b) each represent the upcrossing of one of the processes acting alone, while the third term represents upcrossings when both processes are active, i.e. when the pulses overlap. When the pulses are of very low rate of occurrence (i.e. the $v_i \to 0$), the third term may be neglected.

It has been found from comparisons with simulation results that expression (6.146) yields surprisingly good estimates of the upcrossing rate $v_X^+(a)$, even when the active fraction for each process is as high as 0.2, and for reasonably high levels of barrier a [Larrabee and Cornell, 1979]. Pulse shapes other than rectangular also have been considered, as has dependence between pulse renewals [Wen, 1977b, 1981, 1990].

6.7.4.2 Borges Processes

Borges processes (Section 6.5.1.1) are of particular interest in relation to code calibration work because their combination provides a sufficiently good estimate of the maximum combined load probability distribution [Turkstra and Madsen, 1980].

When each process $X_i(t)$ in the sum $X = X_l + X_2 + X_3 + \dots$ is represented as a Borges process such that the duration of pulses is $\tau_1 \geq \tau_2 \geq \tau_3 \geq \dots$ respectively for each process, with $\tau_i = m_i\tau_{i+1}$ with m_i an integer value, as shown in Figure 6.26, the theory used in the previous sections can still be applied. The occurrence rates are now $v_i = n_i/t_L$ where n_i is the integer number of pulses of process X_i in the period [0, t_L]. With the upcrossing rate determined according to one of the formulae above, the cumulative distribution function of the maximum value of X may be obtained through the application of (6.55). However, another approach is possible and will be outlined below.

It may be shown that cumulative distribution function $F_{\max X}()$ for the maximum value of X is given by (the convolution integral) [Grigoriu, 1975; Turkstra and Madsen, 1980]:

$$F_{\max X}(x) = \left\{ \int_{-\infty}^{x} F_{X_1}(v)[F_{X_2}(x - v)]^m dv \right\}^n \tag{6.147}$$
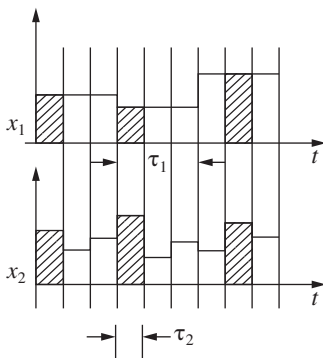
Figure 6.26 Realizations of two Borges processes, with $\tau_1 = m\tau_2$, where m is an integer.

for a two-component process with $\tau_2 = \tau_1/m$, m integer, and where there are n pulses of τ_1 in $[0, t_L]$. This integral becomes more complex for more than two loads, but it may be evaluated for such cases using an FOSM algorithm (Chapter 4).

The essential concept can be demonstrated using a linear combination of three loads. In this case the maximum in the period $[0, t_L]$ can be rewritten as

$$\max_{t_L} [X_1(t) + X_2(t) + X_3(t)] = \max_{t_L}[X_1(t) + Z_2(t)] \qquad (6.148)$$

where $Z_2(t)$ is another Borges process given by

$$Z_2(t) = X_2(t) + X_3^\circ(t, \tau_2) \qquad (6.149)$$

in which $X_3^\circ(\ )$ represents the maximum pulse of X_3 over the period τ_2 (there are τ_2/τ_3 such pulses; *cf.* Figure 6.26). $X_3^\circ(t, \tau_i)$ is also known as the τ_i duration envelope of $X(t)$.

The cumulative distribution function $F_{Z_2}(\ )$ of Z_2 is given by the convolution integral (6.147), now with $m = \tau_3/\tau_2$ and $n = 1$ since only the interval τ_2 is considered. The maximization can be rewritten as:

$$\max_{t_L}[X_1(t) + X_2(t) + X_3(t)] = \max_{t_L}[Z_1(t)] \qquad (6.150)$$

with

$$Z_1(t) = X_1(t) + Z_2^\circ(t, \tau_i) \qquad (6.151)$$

where $Z_2^\circ(\ )$ represents the total pulse of Z_2 over the time interval τ_1. Similarly, $F_{Z_1}(\ )$ can be obtained also from (6.147).

The above reformulation process can be extended to any number of loads in the sum provided that the $F_{Z_i}(\ )$ can be obtained and that the additions of the processes in $Z_i(t)$ can be carried out. Also FOSM theory can be applied [Rackwitz and Fiessler, 1978].

The procedure may be summarized as follows. Let the cumulative distribution functions $F_{X_i}(\ )$ of each process pulse be approximated by a Normal distribution (if X_i is not already Normal) on the basis of a set of trial 'checking points' $\mathbf{x}^*$. [Recall from Section 4.4 that in so doing the tail area $\{= F_{X_i}(\mathbf{x}^*)\}$ is preserved, and the same $f_{X_i}(\ )$ is ensured.] This transformation is carried out first for X_2 and also separately, using the same $\mathbf{x}^*$, for $F_{X_3^\circ}(x_3^\circ) = [F_{X_3}(x_3)]^m$. Recall that $m = \tau_2/\tau_3$ is the number of pulses of X_3 in an X_2 pulse.

As a result of the transformation, the mean $\mu_{X_2^*}$ and variance $\sigma_{X_2^*}^2$ for the equivalent Normal distribution for process X_2 are obtained, as well as $\mu_{X_3^\circ}$ and $\sigma_{X_3^\circ}^2$ for $X_3^\circ(\ )$. Hence the addition of (6.149) can be performed, to obtain the mean μ_{Z_2} and variance $\sigma_{Z_2}^2$ for $Z_2(t)$ as $\mu_{Z_2} = \mu_{X_2^*} + \mu_{X_3^\circ}$ and $\sigma_{Z_2}^2 = \sigma_{X_2^*}^2 + \sigma_{X_3^\circ}^2$. It is now possible to determine $Z_2^\circ(t, \tau_i)$ and to find the equivalent Normal distribution for $X_1(t)$ and $Z_2^\circ(\ )$ in (6.151) and hence the equivalent Normal distribution for $Z_1(t)$. This is, of course, the result sought, but it depends on the initial choice of the checking point $\mathbf{x}^*$. The complete distribution function $F_{\max X}(x)$ is obtained by systematically choosing different values of $\mathbf{x} = \mathbf{x}^*$ and repeating the above process. In direct correspondence to the concepts of Chapter 4, the individual checking point values $\mathbf{x}^*$ for the variables $X_i(t)$ are selected so as to

maximize the local joint probability density $f_{X_1}(x_1^*) f_{X_2}(x_2^*) f_{X_3}(x_3^*) \ldots$ The equivalent normal probability density functions $f_{X_i^*}(\ ) = f_{X_i}(\ )$ can be used for this purpose.

The use of this algorithm for deriving load combination rules for design codes has been described by Turkstra and Madsen (1980).

6.7.4.3 Deterministic Load Combination—Turkstra's Rule

The procedures described in the previous sections are, despite various simplifications, still too complex for use in design codes. These currently have simple additive rules for load combination. The most primitive form consists simply of adding stresses due to different loads without regard to different load uncertainties; others make some allowance for this with an appropriate set of multipliers. The question of interest here is the justification for such multipliers.

A deterministic load combination rule may be derived from a consideration of Borges processes [Turkstra and Madsen, 1980; Ostlund, 1993] or, as will be seen, directly from the 'point-crossing' formula (6.137) [Larrabee and Cornell, 1981].

If the approximation $G_{\max X}(a) = 1 - F_{\max X}(a) \approx v_X^+(a)t$ given by (6.55) is substituted in (6.137) there is obtained

$$G_{\max X}(a) \approx \int_{-\infty}^{\infty} G_{\max X_1}(x) f_2(a-x) dx + \int_{-\infty}^{\infty} G_{\max X_2}(x) f_1(a-x) dx \qquad (6.152)$$

where, as before, the maxima are taken over the time interval of interest, usually the life of the structure $[0, t_L]$. Noting that, if $Z = W + V$, with W, V independent, the complementary cumulative distributive function $G_Z(\ )$ is given by the convolution integral

$$G_Z(z) = \int_{-\infty}^{\infty} G_W(z-v) f_V(v) dv = \int_{-\infty}^{\infty} G_W(w) f_V(z-w) dw \qquad (6.153)$$

so that the two integrals in (6.152) represent, respectively, $\max X_1 + \overline{X}_2$ and $\overline{X}_1 + \max X_2$, with $\overline{X}_i$ representing the 'arbitrary-point-in-time' value of X_i. Similarly, if $Z = \max(W, V)$, then it may be shown that

$$G_Z(a) = G_W(a) + G_V(a) - G_W(a) G_V(a) \qquad (6.154)$$

where, for high barrier levels a, the last term may be ignored. Thus using (6.153) to represent each integral in (6.152) and then applying (6.154) it follows, loosely, that

$$\max X \approx \max[(\max X_1 + \overline{X}_2); (\overline{X}_1 + \max X_2)] \qquad (6.155)$$

This result is known as 'Turkstra's rule'. It states: 'design for (i) the largest value of the lifetime maximum of load 1 plus the value of load 2 when the maximum of 1 occurs or (ii) the lifetime maximum of load 2 plus the value of load 1 when the maximum of 2 occurs' [Turkstra, 1970]. The rule is readily extended to more than two loads. It can also be applied to load effects. For n loads,

$$\max X \approx \max \left(\max X_i + \sum_{j=1}^{n} \overline{X}_j \right), \ j \neq i; \ i = 1, \ldots, n \qquad (6.156)$$

In this form the rule is seen as being similar in form to the load combination rules in many existing code formats; it is also evident that it has some affinity with the

probabilistic requirements for load combination. However, Turkstra's rule does not fix the load levels to be used with the rule; these have to be selected separately. As will be seen in Chapter 9, the value of [max X_i] is commonly selected as the 95 percentile value of the load, while $\overline{X}_i$, the arbitrary-point-in-time value, may be taken as the mean value, provided that the process $X_i(t)$ is stationary.

Although a simple and convenient rule for code calibration work and sometimes other situations, Turkstra's rule is not really suitable for accurate computation of probabilities. This is because expression (6.152) is not an upper bound, as was (6.137), and because the ( ) terms in (6.156) are not independent, as implicit in (6.154) [Larrabee and Cornell, 1981].

6.8 Ensemble Crossing Rate and Barrier Failure Dominance

6.8.1 Introduction

Both the evaluation of crossing rates in the space of load variables and the integration required over time and over resistance random variables become computationally demanding for all but the simplest problems, particularly when resistance degradation or non-stationary load processes are involved. To ease the computational burden one possibility is to include the random resistance variables in the computation of (out)crossing rates. This results in *ensemble* crossing rates. In principle using these for integration in time would violate the (Poisson) assumption of independent crossings and also result in (perhaps grossly) approximate solutions.

Intuitively, the error involved in using ensemble crossing rates should depend on the relative contribution of load processes and of resistance variables towards failure probabilities. Indeed, there are some problems for which an up- or outcrossing event is more likely to occur due to a small variation of the barrier, rather than due to the occurrence of an exceptionally large load peak. For these, the concept of *barrier failure dominance* was introduced, as described briefly below.

6.8.2 Ensemble Crossing Rate Approximation

For all but the simplest combinations of limit states and for Gaussian load processes the computation of the upcrossing (6.72) and outcrossing (6.80) rates requires numerical evaluation. Rephrasing the discussion in Section 6.5.3, an outcrossing occurs when the limit state *process* changes from positive to negative in the load space:

$$v_D^+(\mathbf{r},\ t) = \lim_{\Delta t \to 0} \frac{1}{\Delta t} P[(g(\mathbf{r}, \mathbf{S}, t) > 0) \cap (g(\mathbf{r}, \mathbf{S}, t + \Delta t) < 0)], \qquad (6.157)$$

where $g(\mathbf{r}, \mathbf{S}, t)$ is a generic limit state function. Note that $v_D^+(\mathbf{r}, t)$ is conditional on one realization of the vector of random variables ($\mathbf{R} = \mathbf{r}$), as required in (6.112). One way of computing the above numerically is by means of the sensitivity of a parallel system reliability problem [Hagen and Tvedt, 1991]; a solution constructed based on Figure 6.16, with ($x, \dot{x}$) replaced by ($-g, -\dot{g}$) and with $a = 0$.

As noted above, inclusion of resistance degradation, or non-stationary load processes will produce crossing rates that are functions of time and thus need to be re-evaluated in any iterative computation scheme that allows, for example, for the effect of time. This

adds considerable computational requirements, especially in the case of multiple load processes crossing out of general-shaped safety domains (*cf.* 6.5.5).

To simplify matters, one approach is to use so-called *ensemble crossing rates*. For these the crossing rates are averaged over the resistance [Andrieu et al., 2002; Beck, 2003]. From (6.72), (6.80) or (6.157) this produces:

$$v_{ED}^+(t) = E_R[v_D^+(\mathbf{r}, t)]$$
$$= \lim_{\Delta t \to 0} \frac{1}{\Delta t} P[(g(\mathbf{R}, \mathbf{S}, t) > 0) \cap (g(\mathbf{R}, \mathbf{S}, t + \Delta t) < 0)]. \tag{6.158}$$

Of course, integrating the ensemble crossing rates over time is inconsistent with the Poisson assumption of independent events [Pearce and Wen, 1984; Wen and Chen, 1989; Schall et al., 1991]. The solutions so obtained also are approximate, with errors up to several orders of magnitude [Beck, 2003]. These errors are proportional to (i) the height of the random barrier, (ii) to the relative magnitude between variances (of the load process and of resistance variables), and (iii) to the mean number of zero crossings. They are not necessarily proportional to failure probabilities.

An estimate of these errors can be obtained by comparing with results obtained using the standard case of a single stationary Gaussian load process $S(t) \sim N(\mu_S, \sigma_S)$ crossing a scalar time-invariant Gaussian barrier $R \sim N(\mu_R, \sigma_R)$, for which a closed form solution is available for $v_{ED}^+(t)$ [Owen, 1980]. Compared to this case the ensemble crossing rate error is proportional to [Beck and Melchers, 2004a]:

$$error = -\log_{10} \left[\frac{v_{ED}^+(t)}{v_D^+(t)} \right] \propto e_p = \frac{1}{\sigma_S} \frac{\sigma_R^2 + \sigma_S^2}{(\mu_R - \mu_S)} \tag{6.159}$$

where, with $\mu = (\mu_R - \mu_S)/\sigma_S$ and $\sigma = \sigma_R/\sigma_S$, the error parameter e_p is given by:

$$e_p = \frac{\sigma^2 + 1}{\mu} \tag{6.160}$$

The error parameter e_p in (1.160) also applies for a standard Gaussian load process crossing a random barrier $R \sim N(\mu, \sigma)$ and for narrow-banded $S(t)$ and for broad-banded (first-order Markov) load processes [Beck and Melchers, 2004a]. Further, the *ensemble crossing rate* error in Eq. (6.160) is greater than one order of magnitude after just one or two zero crossings ($v_0 t \approx 1 - 2$) for large values of the error parameter ($e_p \gtrsim 1$). The error is less than one order of magnitude for $e_p \lesssim 0.5$, for up to about 200 zero crossing events [Beck, 2008].

6.8.3   Application to Turkstra's Rule and the Point Crossing Formula

To give some idea of the error involved in using the ensemble crossing rate, consider now a limited comparison with the use of Turkstra's rule and with the point crossing formula for the sum of three stationary standard Gaussian load processes X_i $i = 1,2,3$, crossing a Gaussian random barrier R [Beck and Melchers, 2005]:

$$G(R, \mathbf{S}, t) = R - (X_1(t) + X_2(t) + X_3(t)), \tag{6.161}$$

This is the load combination problem described in Section 6.7. For it, Turkstra's rule (6.156) yields an approximate distribution for the extreme value in a given time interval.

@Seismicisolation

On the other hand, the point crossing formula (6.137) yields an approximation (upper bound) for the crossing rate of the vector process $X(t) = X_1(t) + X_2(t) + X_3(t)$.

To estimate the errors in use of Turkstra's rule and use of the point crossing approach for (6.161), it is noted that both can be represented by the error parameter in (6.159). To do so requires standardization by the variance of the sum of the standard Gaussian processes ($\sigma_X = \sqrt{3}$). Then (6.159) reduces to (6.160) [Beck and Melchers, 2005]. The error trends for the two cases are opposing, however, as should be expected. When e_p given by (6.160) increases, the error in the ensemble crossing rate increases. However, for the same change in e_p the errors in using either Turkstra's rule or the load combination formula decrease. More generally, this suggests that there are some problems and a range of e_p values for which error in using the ensemble crossing rate approximation is smaller than errors of load-based approximations (Turkstra's rule or the load combination formula).

Continuing with the above comparison, consider now the following numerical example. Let the total process X be a broad-band process (e.g. a first order Markovian process with irregulatory factor $\alpha = 0.4$). Then, for a fixed number of load cycles characterized by, say 260 zero crossings, there will be 650 load peaks. For an error parameter (*cf.* 6.160) valued at $e_p \lesssim 1.1$ the error (*cf.* 6.159) of the ensemble crossing rate approximation is smaller than the corresponding error for Turkstra's load combination rule. However, both errors are very large over a wide range of the error parameter: $0.25 \lesssim e_p \lesssim 4$ [Beck and Melchers, 2005].

For high error parameter values, say $e_p \gtrsim 4$ (that is, for high standard deviations or low means—see 6.160), a study of the sensitivity factors obtained using an FOR solution of the resulting Turkstra load combination problems shows that the crossing problem is dominated by barrier (resistance) uncertainties. This means that in this case the Turkstra's load-based approximation is satisfactory. For the same example, the error of ensemble crossing rate approximation is smaller than the error of the point-crossing formula for $e_p \lesssim 0.27$, whereas the maximum point-crossing error $\log_{10}(\sqrt{3})$ *cf* Section 6.7.2) is obtained for $e_p \approx 0.22$.

How the above errors vary for other load processes, for different number of load cycles (zero crossings) and for different load combinations in (6.161) remains to be established. The ensemble crossing rate error increases very quickly with increasing number of load cycles [Beck, 2008], but the influence of numbers of load cycle or of integration time on Turkstra's load combination rule or the point-crossing formula remain areas for further investigation.

6.8.4 Barrier Failure Dominance

Extensive simulations have shown that for many time-variant reliability problems, (out-) crossings are more likely to occur due to a low realization of the random barrier, than to an exceptionally high load peak realization [Beck, 2003]. This phenomenon is known as *barrier failure dominance* [Beck and Melchers, 2005]. As indicated by the above examples, typically, it characterizes problems for which load-based approximations, such as the time-integrated approach (or Turkstra's rule) and the point-crossing formula, are appropriate.

At the other end of the spectrum, there are problems for which the load peak and the barrier realizations make a balanced contribution to (out-)crossing rates or,

equivalently, to first-passage failures. The transition between these behaviours can be tracked by the error parameter in (6.160). At the limit with $\sigma \to 0$, the ensemble crossing rate error is proportional to $1/\mu$ that is, it goes to zero asymptotically with $\mu \to \infty$. This is a well-known result for independent crossings and is consistent with the Poisson approximation.

6.8.5 Validity

The above discussion and examples have provided a different insight into how time-variant reliability problems might be handled, albeit in an approximate manner. Importantly, the results given herein and in the referenced literature must be interpreted with care and are valid only for the particular problems addressed, that is, crossings of a scalar stationary Gaussian process over a scalar Gaussian barrier, and crossings of the sum of three standard first-order Markov Gaussian processes over a scalar Gaussian barrier, for a fixed number of load cycles. Nevertheless, it might be expected that these results will have a degree of validity, even if only approximately, for problems not departing too much from the above scenarios (smoothly non-Gaussian load processes and barriers, other auto-correlation structures, smoothly non-stationary problems and vector-valued resistance variables). A further discussion of some such cases, including for non-Gaussian barriers, and for smoothly non-stationary problems, is available [Beck, 2003].

6.9 Dynamic Analysis of Structures

6.9.1 Introduction

A dynamic structural analysis is necessary when the structure interacts with the time-dependent loading acting on it in such a way as to affect the structural response to the loading. Usually both deformations and stresses are affected.

The traditional approach to the dynamic analysis of a structure is to work in the so-called 'time domain', which means that the equations of motion for the structure are integrated with respect to time. The loading must, of course, be specified in terms of its variation with time. The response calculated for the structure is in terms of stresses and deformations as a function of time. This procedure is very accurate and can be applied to quite complex structures. Material and structural properties may be non-linear, although in such cases the analysis is usually iterative and hence time consuming. Details of the procedure are outside the scope of this book, but excellent treatments exist [e.g. Clough and Penzien, 1975].

If the loading (or the structure, or both) has random properties, the 'time domain' solution scheme is of limited usefulness since a unique description of the loading as a function of time is of course not available. Naturally a realization (see Section 6.4.1) for the loading can be generated and the structural response analysed for this load system; such a procedure might be repeated many times and the statistics of the response determined. This means that one or more limit state functions $G(\mathbf{x}) = 0$ can be generated, provided of course, that a criterion such as maximum allowable stress or maximum allowable deformation also is specified. Further, it suggests that it should be possible to use a Monte Carlo technique to determine structural reliability. In practice such an approach requires a large number of time domain analyses to be performed.

Unfortunately, these are each already computationally very demanding, and this may render the Monte Carlo approach impractical, even with high-powered computers, unless it is possible to simplify the problem with the use of stochastic process theory. Largely for this reason the time domain method of solution has received relatively limited treatment in structural reliability theory and application [e.g. Schuëller, 1997; Wu, 2013].

6.9.2 Frequency Domain Analysis

When the structural behaviour is linear, i.e. for elastic structures under small-deflection assumptions, or more generally when the 'transfer function' between input (e.g. loads) and output (e.g. stresses) is linear, an alternative procedure termed the 'frequency domain' method may be employed. It has been used extensively in the analysis of the random vibration of mechanical systems [e.g. Newland, 1984] despite the limitations to linear systems. While the theory is essentially outside the scope of this book, it is useful to review briefly some aspects of the method since it has application in structural reliability analysis for systems such as dynamically sensitive large towers and offshore structures, particularly in relation to their fatigue life (see also Section 6.10).

One way in which a stationary stochastic process $X(t)$ can be analysed is by decomposing it into an infinite series of sine and cosine waves, each occurring with random magnitude but with their own constant frequency ω of oscillation. Such a representation is known as a Fourier integral representation. The coefficients for the cosine terms are obtained from integration of the product of the stochastic process $X(t)$ and cos ωt, and similarly for the sine terms. Each such term is a Fourier transform of $X(t)$. Since the random properties of $X(t)$ depend on its (auto-)correlation function $R_{XX}(\tau)$ (see Section 6.4.1), it might be imagined that the Fourier transform of $X(t)$ can be expressed as a function of $R_{XX}(\tau)$. Indeed the infinite number of cosine coefficients can be represented by a continuous function of ω:

$$S_x(\omega) = \frac{1}{2\pi} \int_{-\infty}^{\infty} R_{xx}(\tau) \cos \omega\tau d\tau \tag{6.162}$$

Since $R_{XX}(\tau)$ is a symmetric function, the equivalent to (6.162) for the sine terms is zero; also $S_X(\omega)$ is symmetric [Figure 6.27(a)]. Commonly $S_X(\omega)$ is known as the (mean-square) spectral density. Evidently, if $X(t)$ is completely chaotic, $R_{XX}(\tau)$ given by (6.36), is zero (except at $\tau = 0$!), and it follows that $S_X(\omega)$ is a constant for all ω. This situation is known also as 'white noise', since no particular frequency predominates over any other [see Figure 6.27(b)]. Similarly, if the stochastic process has a dominant frequency, around ω_0, say, the spectral density takes the form shown in Figure 6.27(c). This is known as a 'narrow-band' process, and it is of major interest in dynamic structural analysis because most structures have only one dominant mode of vibration. Typically this mode is associated with the (lowest) natural frequency of the structure. (Lesser modes of vibration are associated with higher natural frequencies, typically the resonant frequencies for the structure [e.g. Clough and Penzien, 1975]).

If in (6.162) τ is put to zero and both sides integrated over the range $-\infty$ to $+\infty$, it may be shown that $R_{XX}(0) = \int_{-\infty}^{\infty} S_X(\omega)d\omega$. Using also (6.36) and (6.76) and taking $u_X = 0$ produces:

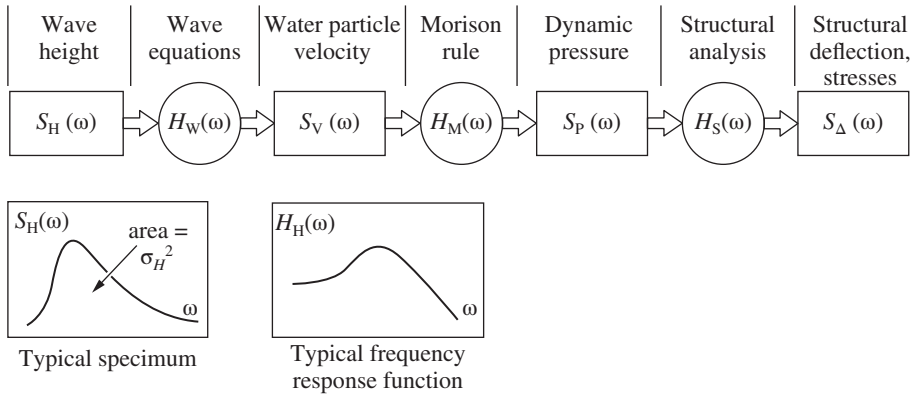$$\sigma_X^2 = E[X(t)^2] = \int_{-\infty}^{\infty} S_X(\omega)d\omega \tag{6.163}$$
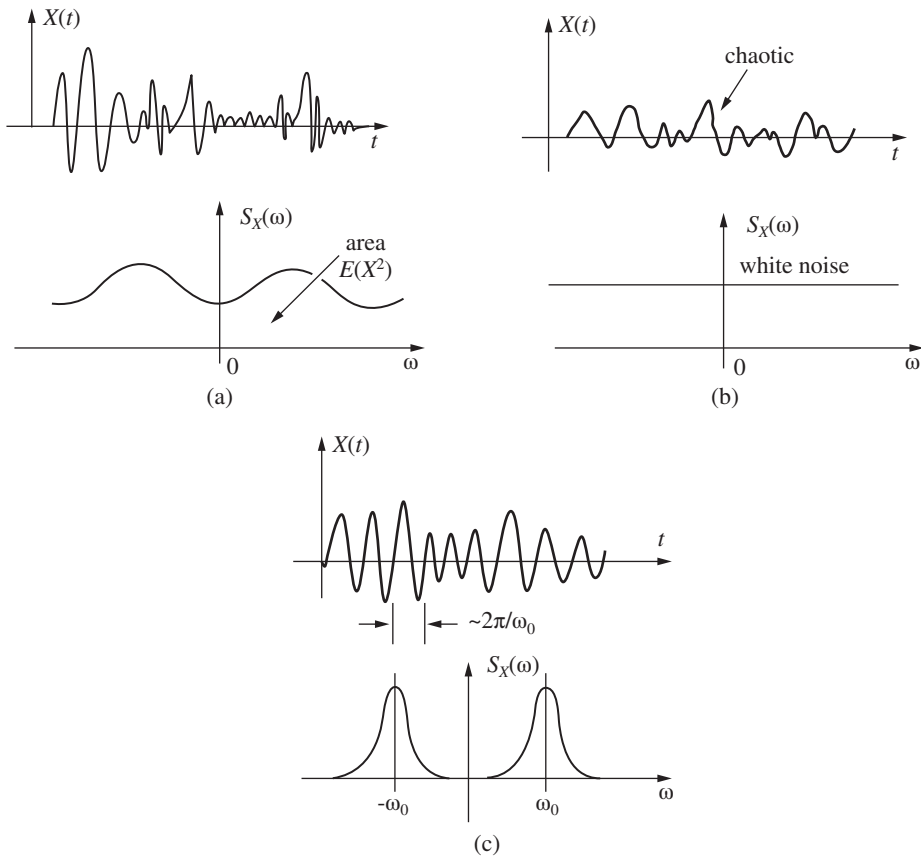
Figure 6.27 Realizations of and spectral densities for (a) wide-band, (b) white noise and (c) narrow-band random process.

This shows that the area under the curve $S_X(\omega)$ is the mean-square value of the stationary stochastic process $X(t)$ and is also equal to its variance (see Figure 6.27(a)). The requirement that $\mu_X = 0$ merely indicates that here the stochastic part of the problem is of interest. A separate structural analysis for the steady state condition $\mu_X \neq 0$ can be superimposed on the results from a stochastic analysis with $\mu_X = 0$.

The solution of (6.163) requires the availability of the spectral density of the structural deflections or of the stresses at some point in the structure. This may be obtained from consideration of the excitation-response relationship(s) for linear structures when working in the frequency domain. For a single input or load process $X(t)$ generating a single output (e.g. stress) $Y(t)$, this relationship is given, in essence, by

$$S_Y(\omega) = |H(\omega)|^2 S_X(\omega) \tag{6.164}$$

where the function $H(\omega)$ is known as the frequency response function. Expression (6.164) may be generalized for multiple independent inputs simply by (linear) superposition, although more complex relationships may need to be used when the inputs are

Wave height	Wave equations	Water particle velocity	Morison rule	Dynamic pressure	Structural analysis	Structural deflection, stresses
$S_H(\omega)$	$H_W(\omega)$	$S_V(\omega)$	$H_M(\omega)$	$S_P(\omega)$	$H_S(\omega)$	$S_\Delta(\omega)$

$S_H(\omega)$ area = σ_H^2 ω

Typical specimum

$H_H(\omega)$ ω

Typical frequency response function

Figure 6.28 Relationship between input and output spectral density functions for an example case of an offshore structure subject to hydrodynamic wave loading.

correlated [Newland, 1984]:

$$S_Y(\omega) = \sum_{i=1}^{n} |H_i(\omega)|^2 \; S_{X_i}(\omega) \tag{6.165}$$

The principles involved in (6.163) and (6.164) in using frequency response functions to obtain an output spectral density from input spectral information are illustrated schematically in Figure 6.28 for an offshore structure subject to wave loading. Ideally the spectral input is determined by analysis directly from actual observations of the physical process(es), that is, the wave processes in this case. Where such information is not available, it often is taken from previous analyses for similar structures. The frequency response function $H(\omega)$ depends on the system being analysed, and, for example, may be obtained by integrating the response of a structure to a given impulse [Clough and Penzien, 1975]. These details are outside the scope of the present discussion.

6.9.3 Reliability Analysis

For the structural reliability analysis involving structural dynamics using the frequency domain approach, the main item of interest is the probability distribution of the peaks of the output random process. As noted, the most straightforward case is for narrow-banded processes. Also the analysis is simplified by the use of extreme value distributions. To progress the discussion, let the probability distribution of the peaks be denoted $F_P(a)$, i.e. the probability that the peaks of $X(t)$ lie below the level $X(t) = a$, with $\mu_X = 0$. Use may be made immediately of the results in Section 6.5.3, for narrow-banded processes sufficiently smooth to have maxima only above $X = 0$. Then the proportion of cycles for which $X > a$ is simply v_a^+/v_0^+, where v_a^+ is the upcrossing rate given by (6.74) and v_0^+ is the rate at which cycles occur (i.e. the rate at which $X(t)$ upcrosses $x = 0$). It follows directly that, for $0 \le a \le \infty$,

$$1 - F_P(a) = \frac{v_a^+}{v_0^+} = \exp\left(-\frac{a^2}{2\sigma_X^2}\right) \tag{6.166}$$
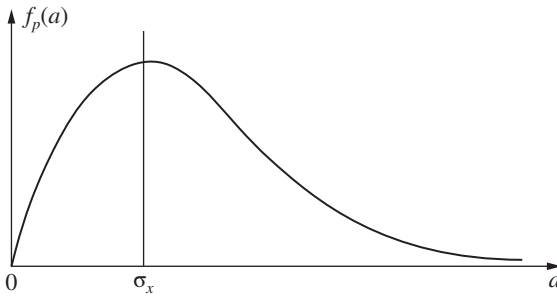
Figure 6.29 Probability density function for Rayleigh distribution.

and, by differentiation with respect to the level $x = a$,

$$f_P(a) \quad \frac{a}{\sigma_X^2} \exp\left(-\frac{a^2}{2\sigma_X^2}\right) \tag{6.167}$$

Expressions (6.166) and (6.167) represent the Rayleigh distribution (Figure 6.29). It is a special case of the Weibull (or EV-III) extreme value distribution (see A.102a). Evidently the maximum value of $f_P(a)$ is at $a = \sigma_X$ which is the magnitude of the majority of peaks. No peaks occur below $a = 0$.

If the process is not completely smooth, e.g. if more than one maximum may occur per zero crossing, or if the stochastic process $X(t)$ is not a Normal process, or does not have an exponential 'tail', the (more general) Weibull extreme value distribution may be more appropriate than Rayleigh to describe the probability distribution of the peaks of the process.

In both cases the probability density function can be used as input, as load cases, to a reliability analysis. Most applications have considered narrow-banded processes and have been confined to the use of the FOSM reliability estimation technique. Processes that are not narrow-banded represent a more difficult scenario for solution. One approach is to consider the actual structural dynamic response as an ensemble of narrow-banded responses and sum these in a weighted fashion. This ignores any correlation effects. A second is to use response surfaces based on repeated dynamic analyses of the structure, together with FOSM. This is still a major task, and difficulties with nonlinearity of the response surface and with convergence and accuracy have been reported [Wu, 2013]. It has been proposed to use response surfaces based on a perturbation approach, followed by a limited amount of Monte Carlo simulation [e.g. Huh and Haldar 2002] or by subset simulation [Au and Beck, 2003] (cf. Section 3.6.2).

6.10 Fatigue Analysis

6.10.1 General Formulation

A very important case of time-dependent reliability analysis concerns fatigue. It is also typical of limit states that are governed by the number of load applications (and their intensities) rather than by extreme events. A brief review of procedures for dealing

with fatigue in a reliability analysis is therefore of interest [Sobczyk and Spencer, 1992; Wirshing, 1998].

The safety margin or limit state function (1.15) can be re-expressed as

$$Z = X_a - X_r \tag{6.168}$$

where X_a represents the actual performance or strength of the structure and where X_r represents the required performance during the life of the structure. Thus, if fatigue life is expressed in terms of the number of cycles of stress, X_a becomes the number of cycles required to cause failure of the material and X_r the required number of cycles to satisfy design requirements for a given lifetime. A corresponding situation exists if fatigue life is measured in terms of crack size or in terms of a damage criterion. In general both X_a and X_r are uncertain quantities. Their precise description depends on the form of fatigue model employed.

6.10.2   The S-N Model

The traditional model to describe the 'fatigue life' N_i of a component or simple structure under constant-amplitude repeated loading is given by [e.g. ASCE, 1982]:

$$N_i = KS_i^{-m} \tag{6.169}$$

where K and m conventionally are taken as 'constants', and N_i is the number of stress cycles at constant stress amplitude S_i. Typically the 'constants' m and K are estimated from test results, and this implies that they will have a degree of uncertainty attached to them. In addition, it is known that different laboratories may produce somewhat different mean and standard deviations for these parameters under what are meant to be standard conditions. For this reason it has been conventional practice to assign conservative values to them in an effort to ensure that (6.169) produces a safe estimate of fatigue life N_i. However, in the context of reliability analysis, the model (6.169) must be a realistic rather than a conservative predictor, so that the typical values for m and K quoted in the literature may not be appropriate. Expected values need to be used, together with an analysis of the influence of the uncertainty in these parameters. Such an analysis can follow conventional structural reliability procedures.

The safety margin (6.168) may be written as

$$Z = KS_i^{-m} - N_0 \tag{6.170}$$

where N_0 is the number of cycles the structure must be able to sustain for satisfactory performance. N_0 may be subject to uncertainty.

In practice the amplitude of the stress cycles is not constant but is a random variable. If the number of cycles which occur at each amplitude level can be measured or estimated, the empirical Palmgren-Miner hypothesis

$$\sum_{i=1}^{l} \frac{n_i}{N_i} = \Delta \tag{6.171}$$

usually is adopted with the S-N model. Here n_i represents the actual number of cycles at the stress amplitude S_i and N_i is the fatigue limit (i.e. number of cycles to failure) for S_i for $1 < i < l$ where l denotes the number of cycle groups adopted for the analysis.

If the stress amplitudes caused by the applied loading are all different (6.171) reduces to

$$\sum_{i=1}^{N} \frac{1}{N_i} = \sum_{i=1}^{N} K^{-1} S_i^m = \Delta \tag{6.172}$$

where N is the total number of (random) variable-amplitude cycles. In practice the data is likely to be wide- or broad-band data (*cf.* Figure 6.27) and thus some regularity of cycles is likely. To deal with this it is conventional to divide the data into, say, l range groups. For each of these the number of cycles N_i must be determined, together with the corresponding probability distribution for S_i. Expression (6.172) written as a limit state now becomes

$$Z = \Delta - X_0 \sum_{i=1}^{l} K^{-1} N_i S_i^m \tag{6.173}$$

where Z is the safety margin as before and the random variable X_0 has been introduced to allow for model uncertainty, such as when there is difficulty in measuring S_i accurately.

The damage parameter Δ conventionally is taken as unity but typically lies in the range 0.9–1.5. Hence Δ reflects the (large) uncertainty arising from the empirical nature of (6.166); a Lognormal distribution with unit mean and a coefficient of variation of about 0.4–0.7 has been proposed as appropriate [Madsen, 1982; ASCE, 1982].

To use (6.173) the wide- or broad-band data (*cf.* Figure 6.27) must be divided into range groups, and the number of cycles N_i in each range $1 < i < l$ must be determined. Also, for each the corresponding stress range S_i is required, together with its uncertainty. To obtain estimates of the means of these variables, various so-called 'cycle-counting techniques' are available. The most well known are the rain-flow and the range-counting techniques. These are described in detail in the fatigue literature [e.g. Wirshing, 1998]. For each range group it is then possible to estimate both the mean and the variance of the stress range S_i. These can be combined with (6.173) to obtain the mean and variance of Z.

6.10.3 Fracture Mechanics Models

An alternative approach to fatigue modelling is to consider crack growth under repeated or random load systems [ASCE, 1982; Schijve, 1979; Provan, 1987; Bolotin et al., 1998]. Based on experimental evidence, the crack growth rate da/dN may be related to the range of stress intensity factor Δk (at the crack tip) by

$$\frac{da}{dN} = C(\Delta K)^m \tag{6.174}$$

where a is the current crack size (depth, length), N the number of stress cycles, and C and m are experimental 'constants', which depend, usually, on cycling frequency, the mean

stress and the environmental conditions, including the precise procedures followed for fatigue testing in the test laboratories where the experiments are conducted. Both C and m should be treated as uncertainties in a reliability analysis. The range of stress intensity factor ΔK, for situations in which the conventional stress intensity factor $K(a)$ does not change significantly with stress level, may be obtained from

$$\Delta K = K(a)\Delta S(\pi a)^{1/2}, \ \Delta K > K_{th} \tag{6.175}$$

where ΔS represents the range of applied stress and where $K(a)$ is a function of current crack length a, local geometry and the nature of the stress field, such as the possible extent of plastic flow at the crack tip. Also, ΔK_{th} is the threshold level of ΔK; below it $\Delta K = 0$.

The variation of crack length a with the number N of applied stress cycles can be obtained in principle from integration of (6.174) and using (6.175):

$$a(N) = a[a_0, \ K(a), \ \Delta S, \ C, \ m, \ \Delta K, \ \Delta K_{th}, \ N] \tag{6.176}$$

where a_0 is the initial crack length. Expression (6.176) can be used to obtain the mean and variance of $a(N)$ given that statistical parameters are known for the parameters involved. For variable-amplitude loading ΔS will depend on the loading sequence, and it will be a random variable. Methods for dealing with this include application of (6.176) in an incremental manner, or using an 'effective' ΔK approach [ASCE, 1982]. In any case, the limit state function (6.168) may be written as

$$Z = a_a - a(N) \tag{6.177}$$

where a_a is the performance requirement on crack length given a lifetime t_L in which N cycles of loading are expected to occur. An alternative limit state formulation is in terms of the crack-tip-opening displacement, a parameter influenced by the material 'toughness' [ASCE, 1982].

Examples have been given of the integration of dynamic analysis and fatigue, an important area of practical application, for example in offshore structure reliability assessment [Karadeniz et al., 1984, 2001; Baker, 1985; Yu et al. 2009]. However, the reader should consult the literature for many other examples.

6.11   Conclusion

This chapter has been concerned with including random processes as distinct from random variables in structural reliability analysis. The traditional time-integrated and discrete time approaches were reviewed. An overview of stochastic process theory was given in order to introduce the fully time-dependent approach to structural reliability. The procedures for problem solution using simulation approaches and using the FOSM/FOR/SOR methods were then outlined. An example application of the latter was given.

Three further topics were introduced. The discussion of load combinations was necessary to introduce simplified procedures for load combination rules currently employed in design codes and for the discussion of code calibration (see Chapter 9). This was followed by an outline of spectral methods as used for the analysis of dynamically sensitive structures, and it was indicated how results so obtained can be used in reliability calculation procedures. Finally, an overview of the reliability formulation for fatigue problems was given.

7

Load and Load Effect Modelling

7.1   Introduction

The loads that may act on a structure can be divided broadly into two groups: those due to natural phenomena, such as wind, wave, snow and earthquake loading, and those due to man-imposed effects, such as dead loads and live loads (e.g. floor loading).

The magnitude of most loads varies with time and with location. This means that loads can be represented as stochastic processes, such as those discussed in Chapter 6. In addition, dynamic effects may occur as a result of load–structure interaction. Because of these possibilities, the modelling of load processes can be quite difficult. As always, perfect models are not possible owing to insufficient data, imperfect understanding and the necessity to predict future loading. Appropriate models are therefore sought, particularly since loading is often the most uncertain factor in a structural reliability analysis. Efforts spent on loading data collection and on load modelling may be more productive than refinement of the reliability estimation techniques.

In the discussions to follow, usually only single load processes will be considered, since in principle at least, loading combinations can be treated, if required, using the methods already described in Section 6.7.

The process of constructing a probabilistic model for a particular load is as follows:

(1) identification and definition of the random variables to be used to represent the uncertainties in loading description (this depends on the understanding of the load process);
(2) selection of appropriate probability distributions for each random variable;
(3) selection or estimation of the distribution parameters using available data and standard parameter estimation techniques such as (a) method of moments, (b) method of maximum likelihood and (c) order statistics.

The main emphasis in the present chapter will be on items (1) and (2). Standard statistics texts may be consulted for item (3).

If observations of a physical load phenomenon are available over a period of time, the statistical properties of the load can be estimated directly from data records, and yearly maxima and daily maxima can be extracted to produce extreme value distributions for use in time-integrated analysis. If continuous records are available, the (approximately) instantaneous probability density function may be hypothesized, and a complete time-dependent reliability analysis (see Section 6.5) may be possible. Obviously, the level

of discernment and accuracy of the recording instrumentation available to measure such loads or load effects will influence the quality of the data and thus also the quality of the load modelling.

For man-imposed loads, such as live loads on building structures, only seldom are there sufficient long-term data to form a probabilistic model. Usually, probabilistic descriptions of loading must be derived mathematically, using whatever data are available (for calibration) together with appropriate and plausible physical models and assumptions. Largely to reflect the different aspects of load modelling, only three types of loading are discussed in this chapter; wind loading in Section 7.2, wave loading in Section 7.3 and floor loading in Section 7.4. For these loadings only limited attention will be given to the physics involved; attention will be focussed mainly on their probabilistic description. Loadings resulting from snow, earthquake, fire and impact or blast are important in many geographical locations and in some particular circumstances—for these the reader should consult the specialist literature. A brief summary of many models is given in the JCSS (2001) report. For traffic loads on highway bridges reference might be made to Nowak (1993) and Reid and Caprani (2014).

7.2 Wind Loading

Wind loading can be derived from statistical data for wind speeds. Relatively few data exist for direct wind force (or even localized wind pressure) although generally it is considered that wind is a chaotic phenomenon, at least in the micro–time scale. In principle, the most appropriate probabilistic model for 'instantaneous' wind speed at a point is a Normal process [Davenport, 1961]. In practice, departures from the idealized model have been noted [e.g. Melbourne, 1977; Holmes, 2007].

A complete description of wind action on structures to generate localized and overall wind forces requires consideration of the variation of wind speeds and hence wind pressures from point to point on the structure, and the response of the structure itself. However, these are matters for wind mechanics and will not be considered here [e.g. Simiu and Scanlan, 1978; Holmes, 2007].

To convert instantaneous wind speed $V(t)$ to wind pressure $W(t)$, acting on a particular part of a structure, use is made often of the standard hydro-dynamic relationship:

$$W(t) = \frac{1}{2} \rho C V(t)^2 \tag{7.1}$$

where ρ is the density of air (about $12 \, \text{N} / \text{m}^3$) and C is the 'wind pressure coefficient', a quasi-static quantity which depends on the size and orientation of the structure.

Expression (7.1) for the instantaneous wind pressure $W(t)$ can be used directly with the fully time-dependent reliability calculation approach of Section 6.6 if the dynamic response of the structure is not significant. However, for flexible structures, account will have to be taken of dynamic effects. In this case, the conventional procedure is to use a spectral analysis (see Section 6.8). Because (7.1) is non-linear, it must be linearized before it can be used in a spectral analysis to relate wind speeds, modelled as a normal process, to wind forces. The conventional approach is to consider the wind speed $V(t)$ to be composed of a time-independent mean value $\overline{V}$ and an additive stationary fluctuating component $v(t)$, assumed to be much smaller than $\overline{V}$. Then (7.1) can be linearized

to [Davenport, 1961; Holmes, 2007]:

$$W(t) \approx \tfrac{1}{2} \rho C[\overline{V}^2 + 2\overline{V}v(t)] \tag{7.2}$$

where $v(t)^2$ has been ignored. If there is more than one wind velocity component, $\overline{V}$ and $v(t)$ should be replaced by vectors in (7.1) and (7.2); when the structure also responds with a velocity of its own, $v(t)$ would be replaced by the relative velocity. The spectral density for $v(t)$, which represents the frequency components present in the random process $v(t)$, (see Section 6.8), and knowledge of which is required for a spectral analysis, has been given in different forms by Davenport (1967), Harris (1971) and Kaimal et al. (1972). Details are outside the scope of this book; readers are urged to consult specialist literature [e.g. Simiu and Scanlan, 1978; Holmes, 1998].

The output from the spectral analysis, such as the spectrum of forces, or deflections, is then converted to statistical properties for these quantities as outlined in Section 6.8.

For use with the time-integrated and the discrete time approaches of Sections 6.2 and 6.3, lifetime maximum and annual maximum wind speeds and their probability density functions are required. These can be derived either directly or indirectly from wind speed records. Wind speed records of reasonable reliability have, for many areas, been obtained as part of meteorological data collection.

Wind speed is measured either in terms of the '3 s gust' speed, i.e. the average speed over a gust of duration of about 3 seconds, or as the 'fastest-mile wind speed' (USA) which is the wind speed averaged over the passage of 1 mile of wind as measured by the anemometer propeller tips. Clearly the two are not equivalent, particularly at low wind speeds. These results may be converted to mean hourly wind speeds. Irrespective of the choice of basis of measurement, it is generally agreed that for non-cyclonic regions, the annual maximum wind speed as obtained from wind speed records can be described by an Extreme Value Type I (EV-I) distribution [Simiu et al., 1978; Simiu and Filliben, 1980; Harris, 1996]. This choice is consistent with the derivation of EV-I as the asymptotic distribution for maxima with the instantaneous wind speed described by a Normal process and if wind speed measurement readings are assumed independent (see Section A.5.11). Other distributions also offer a reasonable, but empirical, fit to the data, particularly at higher wind speeds. These include the Frechet (extreme value type II), Rayleigh and Weibull distributions [Thom, 1968; Davenport, 1983; Melbourne, 1977; 1998]. One (theoretical) difficulty is that the EV-I distribution permits negative $V(t)$ values; this is not the case with the Frechet distribution, which is also considered to be somewhat more conservative at high $V(t)$ values. However, negative and low values are of no interest for extreme wind scenarios, and the lower tails of all the distributions, extreme or otherwise, can be ignored. Only the upper tails of the distributions are of interest [*cf.* Galambos, 1987; Castillo and Sarabia, 1992].

The meteorological mechanism for generation of cyclones and hurricanes is entirely different from that of thunderstorms [Batts et al., 1980]. Data obtained for wind speeds measured for cyclones and hurricanes therefore represent a different statistical population from the data for wind speeds from thunderstorms. It is fundamental in statistic analysis, including for extreme value analysis, that the population must be homogeneous and therefore data from these two types of events should not be mixed. Evidence for the considerable difference in extreme value representation can be seen in some typical
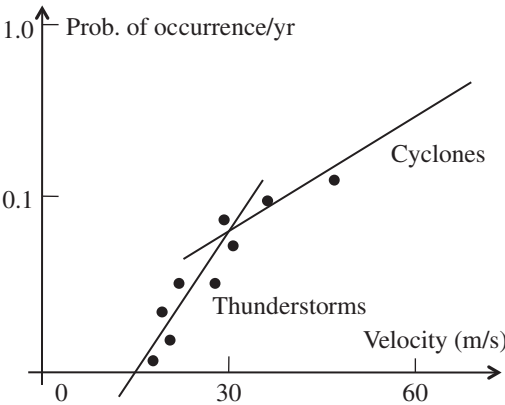
Figure 7.1 Typical wind gust speeds for cyclones and thunderstorms plotted on a Gumbel (EV) plot [based on data from Gomes and Vickery, 1976].

recorded data for wind speeds in the Gumbel plot of Figure 7.1. It shows two distinctly different Gumbel lines.

For the cyclonic wind speed there is some doubt whether long-term predictions can be made on the basis of the relatively short-term records available. Limited experience (e.g. El Nino phenomenon and also climate change aspects) suggests that longer-term atmospheric processes may exist to throw doubt on the usual assumptions that the processes are sufficiently stationary for application of EV theory. Nevertheless, it has been proposed that the most suitable model for the annual maximum wind speeds of cyclonic winds is an EV-I distribution [Russell and Schuëller, 1974; Gomes and Vickery, 1976; Simpson and Riehl, 1981], as indeed Figure 7.1 suggests.

The annual maximum wind speeds for cyclonic and non-cyclonic winds, referred to above, are suitable for use with the discrete time reliability calculation procedure (see Section 6.3). The lifetime maximum is also of importance, particularly for the time-integrated approach of Section 6.2. If $F_V(\ )$ denotes the cumulative distribution function of the velocity V, then, for independent annual maxima, $F_{VL} = [F_V(v)]^L$ where L is the lifetime in years. If V has the EV-I distribution, then $F_{VL}(\ )$ also will be EV-I distributed (see Appendix A). Some typical values and parameters are shown in Table 7.1. It is seen that, for $L = 50$ years, the ratio of annual mean to 50-year mean wind speed is roughly 0.7.

The daily maximum wind speed is of interest in determining daily maximum wind loads. These can be considered to be good approximations for the 'average-point-in-time' loadings. Wind speed data of this type can be obtained from meteorological centres. An EV-I distribution again appears appropriate.

The wind pressure loading W may be obtained from wind speed using the standard hydrodynamic relationship (7.1), which can be rewritten for particular structures or surfaces of structures, as [Holmes, 2007]:

$$W = kC_p V^2 \tag{7.3}$$

where C_p is the pressure coefficient (which may be a function of V) and $k = cEG$ is a 'constant' for a given structure (c is a 'constant', E an exposure coefficient and G the 'gust

Table 7.1 Typical average values of mean hourly wind speed data.

	Annual maximum			50-year maximum		
	Mean speed		Coefficient of variation	Mean speed		Coefficient of variation
	(m/s)	(miles/h)		(m/s)	(miles/h)	
USA[a)]	15.5	(34.7)	0.12–0.17	24.1	(18.6)	0.11–0.14
Australia[b)]	14.9	(33.3)	0.12	24.7	(55.2)	0.12
Cardington, UK[c)]	15.5	(34.7)	0.24	23	($\approx$ 52)	0.12

a) Converted from 'fastest-mile' wind records [Simiu and Filliben, 1980].
b) Converted from '3-sec.' wind records [Pham et al., 1983].
c) Converted from '3-sec.' wind records [Shellard, 1958].
Mean hourly speeds $\approx 0.77 \times$ fastest-mile speeds
Mean hourly speeds $\approx (1/1.55 - 1/1.7) \times 3$- sec. gust speeds.

factor', which depends on wind turbulence and the dynamic interaction of the wind and the structure) [Solari, 1993].

Standard wind engineering texts [e.g. Simiu and Scanlan, 1978; Holmes, 2007] or recommendations [JCSS, 2001] should be consulted for appropriate mean values for the above coefficients, which depend on structure size, orientation with respect to wind direction, structure geometry, surface roughness, etc.

Expression (7.3) may be used directly in a limit state function without formally deriving the statistical parameters and distribution of W. However, if these are nevertheless required, such as in code calibration work, it must be noted that the probability distribution for W cannot be obtained in closed form (since the square of EV-I has no simple distribution). Instead techniques such as Monte Carlo simulation must be used to determine an appropriate distribution [Dorman, 1983]. With inclusion of the data for the other parameters, it has been found that the EV-I distribution yields a good empirical fit for loads greater than the 90 percentile [Ellingwood et al., 1980]. Distributions and data for C_p, G and E must be estimated; however, it is by no means clear that C_p, for example, is a constant as commonly assumed; a Lognormal distribution has been suggested. As noted, typically the mean values for these parameters can be obtained from wind loading codes. Estimates for the coefficients of variation V_{C_p}, V_G and V_E are of the order 0.12–0.15, 0.11 and 0.16 respectively [e.g. Ellingwood et al., 1980; Schuëller et al., 1983; Davenport, 1987]. These results are suitable for use in code calibration (see Chapter 9).

For dynamically sensitive structures, annual or lifetime maximum probability density functions for loads are not obtainable directly. Recourse must be made to spectral analysis to convert instantaneous results to equivalent annual or lifetime maxima [Simiu and Scanlan, 1978]. Under resonant dynamic response, as may occur, for example, for bridge decks in suspension bridges, expression (7.3) is not valid. For these special treatment is required [e.g. Kareem, 1988; Holmes and Pham, 1994].

As noted above, directional effects may be important [Cook, 1983; Wen, 1983, 1984; Holmes, 2007]. Wind is a turbulent phenomenon and hence will change direction locally, as well as having an overall direction. Meteorological data can be used for overall directionality statistics; it is not uncommon to assume a uniform distribution for wind direction for locations for which records are insignificant.

Model recommendations for modelling wind loads for code writing purposes are given in the report by the Joint Committee on Structural Safety (2001).

7.3 Wave Loading

As might be imagined, the determination of statistical descriptions for wave loads has many features in parallel with that for wind loads, since both involve structure-fluid interaction. It is not proposed to discuss the physics of the problem in detail here; reference might be made, for example, to Sarpkaya and Isaacson (1981) for an extensive treatment of wave forces. Only a very brief account will be given here, with emphasis on statistical properties [see also Schuëller, 1981].

As a first approximation, the instantaneous velocity $\mathbf{U}(t)$ and the acceleration $\dot{\mathbf{U}}(t)$ of a water particle in a wave (see Figure 7.2) can be represented by independent Normal processes. The velocity has a mean equal to the current [Borgman, 1967]. If records for $\mathbf{U}(t)$ and $\dot{\mathbf{U}}(t)$ are available, e.g. from current measurements, σ_U and $\sigma_{\dot{U}}$ can be estimated directly. Where this is not the case μ_U, σ_U and $\sigma_{\dot{U}}$ can be calculated from wave theory and knowledge of the frequency components of wave height (i.e. the wave spectrum). The latter must be obtained from measurements, but now of wave height, wave period and wind speed.

Wave loading is of most interest during storm conditions. More generally, loadings during individual sea-states are of interest. These usually are taken as 3-hour events during which conditions are assumed constant. During a sea-state or a storm event it may be assumed that the sea elevation $\eta(t)$ is a stationary Normal (Gaussian) stochastic process, composed of only a small range of frequencies, i.e. it is assumed to be a 'narrow band' process (see Section 6.8). These assumptions allow the sea elevations to be related to the wave spectrum $S_\eta(\omega)$, where ω is the wave frequency ($\omega = 2\pi/T$, where T is the period). The spectrum obviously depends on the local conditions, such as fetch, for the development of wind-generated waves and water depth. As a result, various spectra have been proposed. For limited fetch conditions such as occur
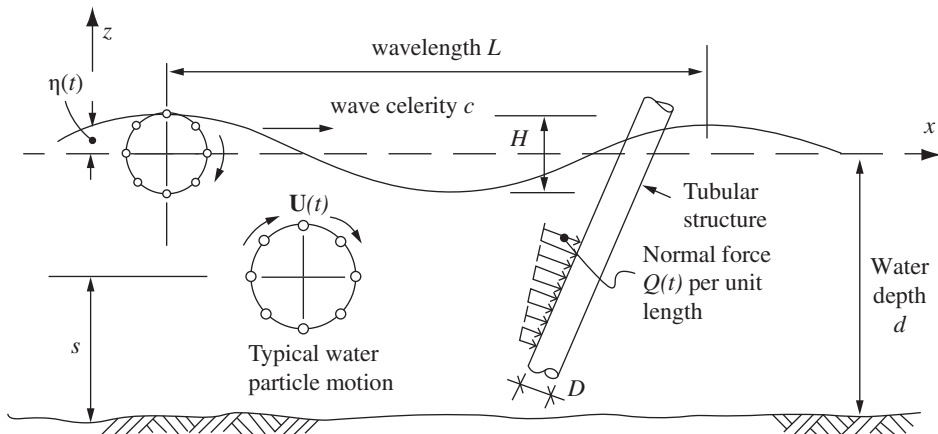
Figure 7.2 Schematic representation of water particle motion, wave shape and force exerted on a tubular structural member.

in the North Sea, the JONSWAP spectrum has been developed [Hasselmann et al., 1973]. Pierson and Moskowitz (1964) developed a spectrum for fully developed sea states. The typical shape of such spectra is shown as $S_H(\omega)$ in Figure 6.29. Typically the parameters describing the spectrum $S_H(\omega)$ are the significant wave height H_Z and the zero upcrossing period T_Z. Because of the assumption of stationary conditions during a sea-state, these parameters are constant during the sea-state. Usually they are estimated from observations during a particular sea-state, thereby allowing estimates to be made of probability distributions for H_Z and T_Z. Together with the wave spectrum this allows the statistical properties of the probability distribution of wave height to be estimated. For sinusoidal waves, the mean is at the mean water depth, so that $\mu_H = 0$; the variance can be estimated from (6.158) as $\sigma_H^2 = \text{var}[\eta(t)] = \int_0^\infty S_\eta(\omega)d\omega$. In principle this means that, for a fully developed sea, for which independence between successive wave heights usually is assumed, the Rayleigh distribution (see Section A.5.13) is considered to be the most appropriate for wave height [Longuet-Higgins, 1952; Holmes et al., 1983]. However, the other extreme value distributions (EV-I and EV-II) (see Sections A.5.11 and A.5.12) also have been proposed as suitable (but empirical) fits to data for different geographical locations. Note that in all cases these extreme value probability distributions should be considered conditional, in the sense that they apply provided that a storm event or a particular sea-state occurs. They also may be direction-dependent.

Water particle velocities $\mathbf{U}(t)$ are obtained from knowledge of wave height H and wave length L (see Figure 7.2). Many different theories have been proposed for wave height [Sarpkaya and Isaacson, 1981] but usually it is sufficient for wave force calculations to employ the so-called linear theory due to Airy [Lighthill, 1978]. This theory also can be used easily in spectral calculations.

According to Airy theory, the water surface elevation is given by a sine wave:

$$\eta(x, t) = \frac{H}{2} \sin(\omega t - kx) \tag{7.4}$$

where $\omega = 2\pi/T$ is the wave frequency, $T = 2\pi/\omega$ is the wave period, t is the time, H is the wave height, L is the wave length (distance between crests), $k = 2\pi/L$ is the wave number and x is the horizontal distance. The wave celerity is given by $c = \omega/k = L/T$ (see Figure 7.2). The horizontal components of velocity $\mathbf{U}$ and acceleration $\dot{\mathbf{U}}$ are given by [e.g. Lighthill, 1978; Weigel, 1964]:

$$U_h = \omega \frac{H}{2} \frac{\cosh[k(z + d)]}{\sinh(kd)} \sin(\omega t - kx) \tag{7.5a}$$

$$\dot{U}_h = \frac{dU}{dt} = \omega^2 \frac{H}{2} \frac{\cosh[k(z + d)]}{\sinh(kd)} \cos(\omega t - kx) \tag{7.5b}$$

where d is the water depth and z is the location of $\mathbf{U}$, $\dot{\mathbf{U}}$ below water surface.

The vertical component of velocity has a similar form, with sinh( ) for cosh( ) and cos( ) for sin( ). The acceleration component follows directly.

With known statistical properties for H, those for the components of water particle velocity $\mathbf{U}$ and water particle acceleration $\dot{\mathbf{U}}$ can be determined directly from expressions such as (7.5a) and (7.5b). As noted earlier, usually it is assumed that these may be represented by a Normal process, with the mean for U_h being the steady (horizontal) current, and the mean for $\dot{U}_h$ being zero.

Once the water particle velocity and acceleration are known at any depth z (Figure 7.2), the normal force per unit length exerted at a particular location of a slender cylinder such as typical in steel offshore structures is given by [Morison et al., 1950]

$$\mathbf{Q}(t) = k_d \mathbf{U}_n |\mathbf{U}_n| + k_m \dot{\mathbf{U}}_n \tag{7.6}$$

where $\mathbf{U}_n$ is the vector of incident water particle velocities normal to the cylinder. This expression originally was proposed for vertical piles but commonly is assumed to be valid for any pile orientation and also more generally. The first term in (7.6) relates to the drag force exerted by the wave on the pile; the second term relates to the influence of the mass of the water displaced by the cylinder on its oscillatory behaviour. For a circular cylinder of diameter D, and water of density ρ, the coefficients k_d and k_m are given by

$$k_d = \frac{C_d \rho D}{2}, \qquad k_m = \frac{C_m \rho \pi D^2}{4} \tag{7.7}$$

where the dimensionless drag and mass coefficients C_d and C_m have been extensively experimentally investigated, including for oscillating flows of given frequency [e.g. Morison et al., 1950; Tickell, 1977; Holmes and Tickell, 1979]. The results show a large degree of scatter, particularly for cylinders not oriented in a vertical direction. Some typical values are shown in Table 7.2.

The probability density function for Q at a particular location (x, z) can be determined from (7.6) and the known properties for $\mathbf{U}$ and $\dot{\mathbf{U}}$ using convolution or by Monte Carlo simulation. The mean and variance can be approximated by (A.178) and (A.179) respectively. Usually it is found that the probability density function for Q has more extensive upper and lower tails than a Normal distribution with the same mean and variance, so that approximation by a Normal distribution would be non-conservative for higher wave load estimation. Nevertheless, a common assumption [Borgman, 1967] is that the extreme cylinder force is Rayleigh distributed (see Section A.5.13), which implies the further assumption of a narrow-band process (see Section 6.8). This also tends to underestimate the probability of occurrence of higher wave loads. Other probability distributions have been examined for representing the response of the structure, for example, using Monte Carlo simulation. This suggests that a mixture of Generalized EV and Generalized Pareto distributions provide an appropriate empirical fit [e.g. Wang et al. 2013].

The extreme value distribution for $Q(t)$ can be obtained also from calculation of the upcrossing rate through the use of (6.54). The upcrossing rate can be found, in principle, from Rice's formula (6.72). However, this requires the existence of the fourth moment of the velocity spectrum, a rather restrictive requirement [Borgman, 1967].

Table 7.2 Indicative values for coefficients C_d and C_m for smooth clean cylinders.

Coefficient	Mean	Typical range	Coefficient of variation
C_d	0.65	0.6–0.75	≈ 0.25
C_m	1.5	1.2–1.8	$\approx 0.20-0.35$

In most cases 'jacket'-type offshore structures are sufficiently flexible for dynamic effects to be important. The usual approach is to employ spectral analysis (see Section 6.8). The procedure starts from the wave height spectrum $S_H(\omega)$ and requires linear relationships to convert wave height successively to velocities and accelerations [(7.4a) and (7.4b)], wave forces and structural load effects (see Figure 6.29). Linearization of Morison's equation (7.6) in the velocity term is required, a considerable approximation since the mean of the velocity is either zero or equal to the (generally small) current, unlike the linearization required for wind velocities (see Section 7.1). Details of the spectral analysis and the required simplifications are described in the classic paper by Borgman (1967), where correlation between wave forces at different locations also is considered.

In general, the resulting load effects are assumed to be Normal distributed, with variance obtained from the load effect spectrum through (6.158). Mean values must be obtained from a mean value analysis.

In order to refine the analysis outlined so far, second order wave theory has been proposed as more suitable to describe wave crest distributions [e.g. Forristall, 2000; JCSS, 2006]. However, even with such refinement, it is not possible to predict the so-called 'rogue' or 'freak' waves that have been observed from time to time [Haver and Andersen, 2000]. The postulated causes for these extreme waves range from what are considered to be instabilities in otherwise uniform groups of waves to unusual meteorological conditions [Bitner-Gregersen and Toffoli, 2011]. It is possible, for example, to compare this with the differences in the maximum wind speeds caused by thunderstorms and cyclones (Figure 7.1)—both of which may, in turn, affect wave height. Clearly, improved understanding of the 'rogue' wave height phenomena is required in order to overcome the considerable theoretical difficulties currently associated with their prediction [Olagnon and Prevosto, 2008].

7.4 Floor Loading

7.4.1 General

Live loading on floors must be modelled, since long-term records are not available, and since there are many possible parameters that may influence it. Attention will be confined herein mainly to office live loads, but similar considerations apply to other types of loading, such as self-weight, domestic and crowd floor loading and also car-park floor loading [JCSS, 2001].

Originally data used in design consisted of estimates of dense crowd loading. Thus, in 1883, UK floor loads were set at 140 lbf / ft^2 (approximately 7 kPa) for domestic dwellings and 170 - 225 lbf / ft^2 (8.3–11.0 kPa) for public areas. This was based on a typical man (weight, 170 lbf) occupying about 1 ft^2 in a crowd situation. For multi-storey buildings it is unlikely that all floors will be subject to crowd loading at the same time in corresponding locations. This led to the concept of 'live load reduction', a probabilistic concept that allows a reduction in load per unit area as the area under consideration increases. Such a rule was already in evidence in New York in the early 1900s.

Later work, directed mainly at setting design loadings rather that complete probability distributions, identified additional particular features of floor live loading [e.g.
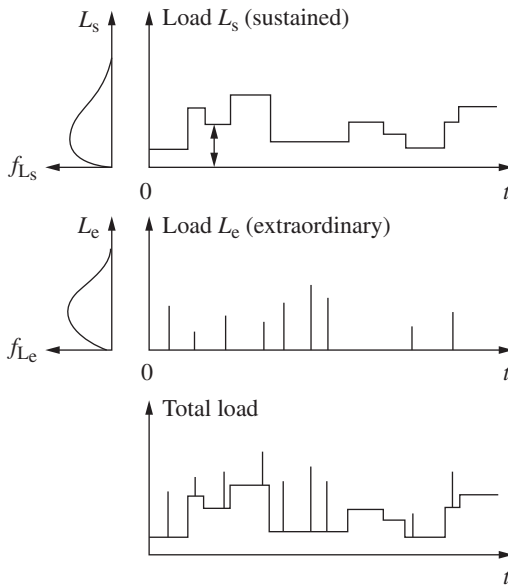
Figure 7.3 Schematic time histories of typical live loads.

Mitchell and Woodgate, 1971a; Lind and Davenport, 1972; Culver, 1976; Sentler, 1976; Choi, 1991, 1992]:

(a) typically loading consists of sustained plus short-term transient effects (Figure 7.3);
(b) changes in occupancy produce changes in the sustained loading (Figure 7.3);
(c) variation of loading exists within rooms, see Figures 7.4(a) and 7.4(b);
(d) variation of loading also exists between rooms, but there usually is some correlation;
(e) a degree of correlation usually exists between loadings on different floors (Figure 7.5);
(f) different uses of office spaces produces quite different 'arbitrary-point-in-time' (e.g. mean) loadings, which vary somewhat with floor area, see Figure 7.4(c).

In addition, there is the area dependence effect already mentioned (Figure 7.6). Ideally, all these factors must be accounted for in a model of floor loading. In order to make progress, sustained loading will be discussed first, followed by transient loads. These will then be combined using an appropriate load combination procedure.

7.4.2 Sustained Load Representation

The approach adopted below is to derive an expression for the floor load intensity at some arbitrary location in a building and then to convert this to an equivalent uniformly distributed loading. This fits in with conventional design loads and simplifies application in reliability analyses. Allowance is then made for tenancy changes before the complete probabilistic model is developed.

The 'arbitrary-point-in-time' load intensity $w_{ij}(x,y)$ on an infinitesimal area ΔA at location (x,y) on the ith floor of the jth building can be modelled in a simplified way as [Pier and Cornell, 1973]

$$w_{ij}(x,y) = m + \gamma_{bld} + \gamma_{flr} + \varepsilon(x,y) \tag{7.8}$$
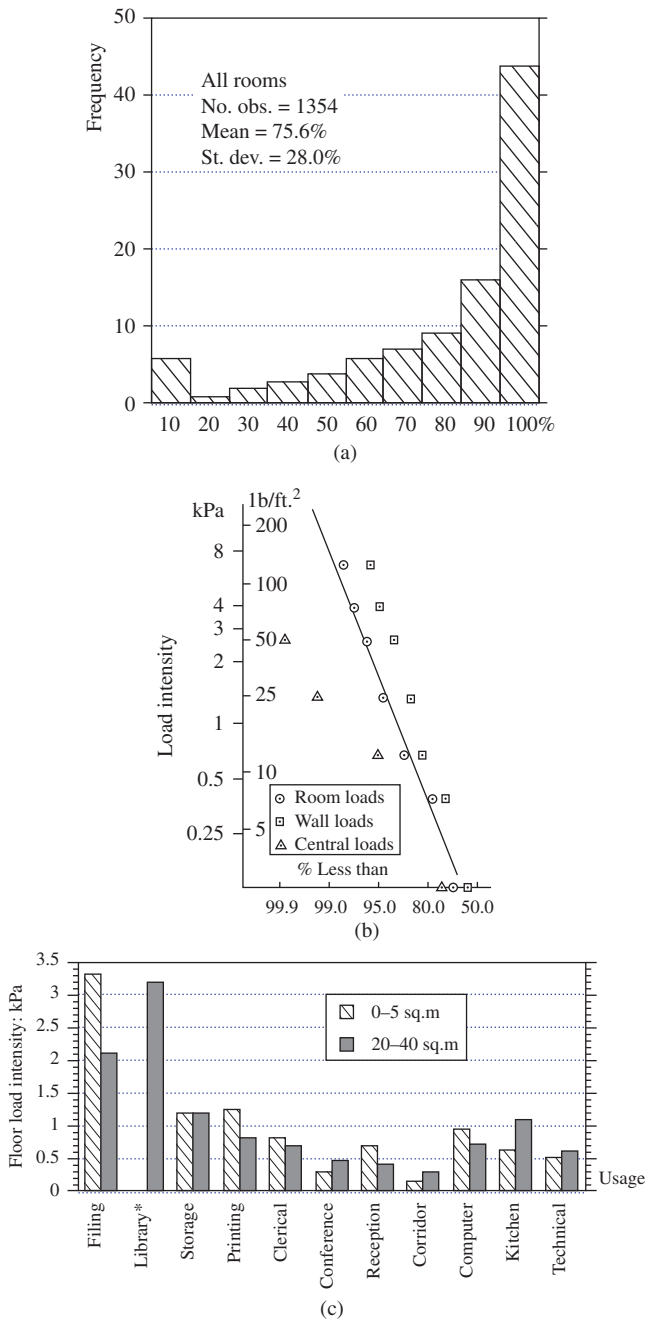
Figure 7.4 (a) Percentage of live load within 600 mm (2 ft) of walls [based on Culver, 1976]. (b) Observed distributions of floor loads on $600\,\mathrm{mm} \times 600\,\mathrm{mm}(2\,\mathrm{ft} \times 2\,\mathrm{ft})$ squares [based on Lind and Davenport, 1972]. (c) Floor load intensity for different usages, showing also the effect of area [based on data reported in Choi, 1992].
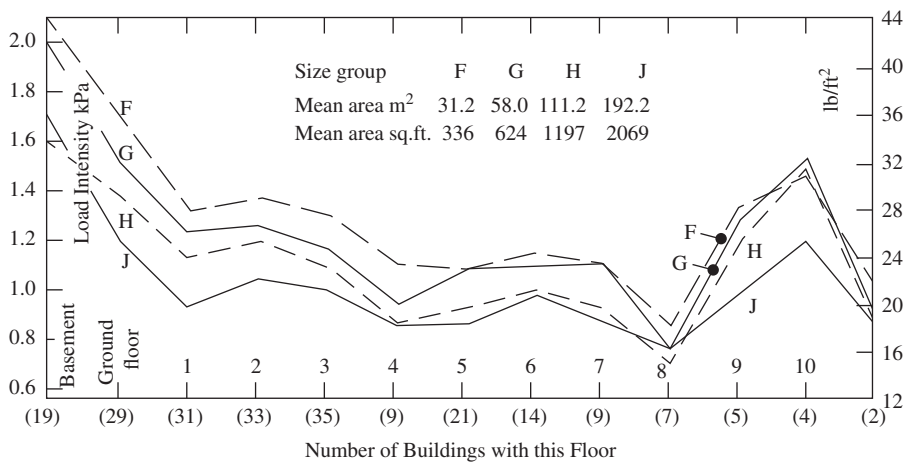
Figure 7.5 Variation of 95% level of occupancy loading with floor level number; one occupation only (i.e. 95% loads < values plotted) [Mitchell and Woodgate, 1971a]. Reproduced from Current Paper CP 3/71, Building Research Station, by permission of the Controller, HMSO. Crown copyright.
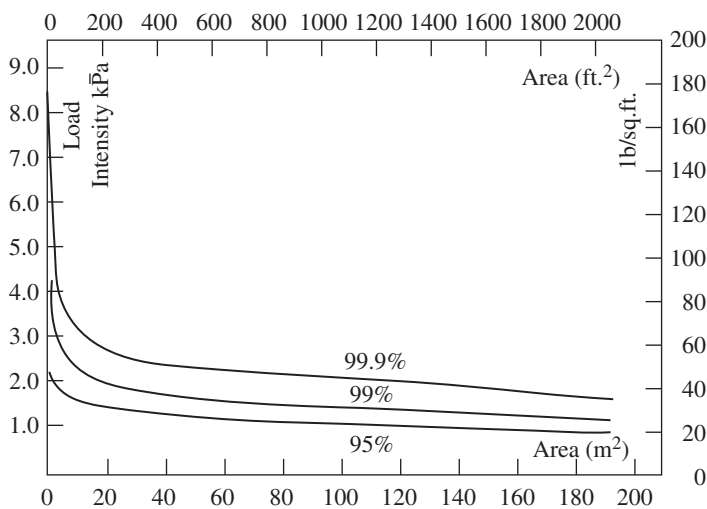
Figure 7.6 Variation of loading intensity probabilities with tributary area; floors other than lowest basements and ground floors; after one occupancy only [Mitchell and Woodgate, 1971a]. Reproduced from Current Paper CP 3/71, Building Research Station, by permission of the Controller, HMSO. Crown copyright.

where m is the 'grand' mean load intensity, γ_{bld} the deviation of floor load intensity from m for building j, γ_{flr} the deviation of floor load intensity from m for floor i for all buildings and ε the spatial uncertainty of floor loading for a given floor (also termed a zero mean 'random field' [see Arnold, 1981; Vanmarcke, 1983]).

The parameters γ and ε are random variables with zero means and are assumed independent, although obviously this is not always the case. The term $m + \gamma_{bld}$ represents the variation of average floor load from building to building; survey data such as those

of Mitchell and Woodgate (1971a) or Choi (1992) would allow γ_{bld} to be evaluated if the data were sufficiently extensive. A similar argument applies to γ_{flr}. Given the uncertainty in the model, a 'second-moment' representation is sufficient, so that the mean w_{ij} is simply $\mu_w = m$ and its variance is

$$\sigma_w^2 = \sigma_{bld}^2 + \sigma_{flr}^2 + \sigma_\varepsilon^2 \tag{7.9}$$

In order to use model (7.8), σ_{bld}, σ_{flr} and σ_ε must be evaluated. This can be done from survey data. Consider a floor of given area A, of size $a \times b$. The total load on this area is given by

$$L(A) = \int_0^a \int_0^b w(x, y)\, dx\, dy \tag{7.10}$$

with mean and variance:

$$E[L(A)] = \int_0^a \int_0^b E[w(x,y)]dx\, dy = \iint m\, dx\, dy = mA \tag{7.11}$$

$$\mathrm{var}[L(A)] = \int_0^a \int_0^a \int_0^b \int_0^b \mathrm{cov}[w(x_1, y_1),\, w(x_2, y_2)]dx_1\, dx_2\, dy_1\, dy_2$$
$$= \int_0^a \int_0^b \int_0^b \int_0^b \{\sigma_{bld}^2 + \sigma_{flr}^2 + \mathrm{cov}[\varepsilon(x_1 y_1),\, \varepsilon(x_2 y_2)]\}dx_1\, dx_2\, dy_1\, dy_2 \tag{7.12}$$

The latter expression can be evaluated if cov[ ] is known [*cf.* Vanmarcke, 1983]. One approach is to recognise that the covariance is likely to be inversely proportional to the distance between two points such as 1 and 2, thus

$$\mathrm{cov}[\ ] = \rho_c \sigma_\varepsilon^2 e^{-r^2/d} \tag{7.13}$$

where $r^2 = (x_1 - x_2)^2 + (y_1 - y_2)^2$, d is a constant, ρ_c is a correlation coefficient to allow for the so-called 'stacking effect' vertically between floors (the tendency for occupants to load floors in a similar pattern) and σ_ε^2 is the variance in ε.

Clearly r represents a horizontal and ρ_c a vertical spatial parameter. In general ρ_c would vary from location to location, but this is ignored here for simplicity. The constant d and the parameters ρ_c and σ_ε^2 may be evaluated from observations. For one floor, $\rho_c = 1$, and hence (7.12) may be shown to reduce to [Pier and Cornell, 1973]

$$\mathrm{var}[L(A)] = (\sigma_{bld}^2 + \sigma_{flr}^2)A^2 + A\pi d\ \sigma_\varepsilon^2 K(A) \tag{7.14}$$

where

$$K(A) = \left[\mathrm{erf}\left(\frac{A}{d}\right)^{1/2} - \left(\frac{d}{A\pi}\right)^{1/2}(1 - \exp(-A/d))\right]^2$$

and erf( ) is the error function.

The load $L(A)$ can be converted to an average load per unit area by dividing through by A, so that $L(A)/A \equiv U(A)$, with mean $E[U(A)] = m$ and variance

$$\mathrm{var}[U(A)] = \sigma_{bld}^2 + \sigma_{flr}^2 + \pi\ d\sigma_\varepsilon^2 \frac{K(A)}{A} \tag{7.15}$$
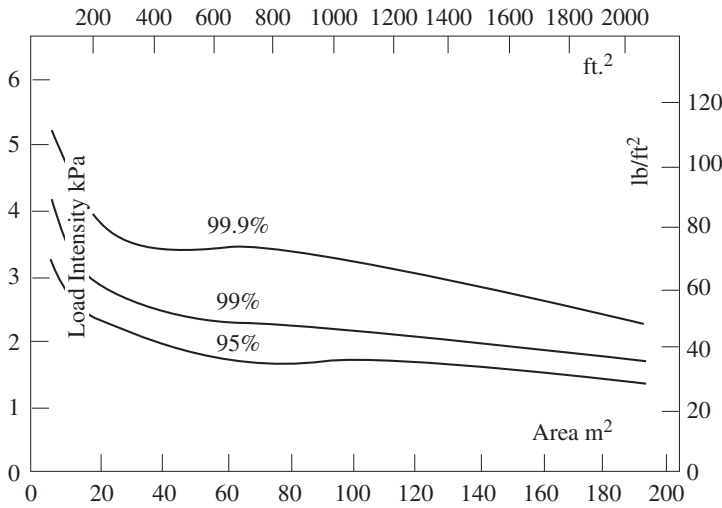
Figure 7.7 Variation of loading intensity probabilities with tributary area; floors other than lowest basements and ground floors; after 12 occupancies [Mitchell and Woodgate, 1971a]. Reproduced from Current Paper CP 3/71, Building Research Station, by permission of the Controller, HMSO. Crown copyright.

For n floors of equal area A the variance becomes

$$\text{var}[U(nA)] = \sigma_{bld}^2 + \frac{\sigma_{flr}^2}{n} + \pi \; d\sigma_\varepsilon^2 \frac{K(A)}{nA} + \rho_c \sigma_\varepsilon^2 \frac{(n-1)K(A)}{nA} \tag{7.16}$$

Survey data such as those shown in Figures 7.5–7.7 [Mitchell and Woodgate, 1971a] now may be used to estimate the parameters in (7.15) and (7.16). For example $\sigma_{bld}^2 + \sigma_{flr}^2$, σ_ε^2 and d may be obtained from the relationship between the coefficient of variation $\{\text{var}[U(A)]\}^{1/2}/m$ and area A, while ρ_c and σ_{bld}^2 may be obtained from the relationship between the coefficient of variation for the column load $\{\text{var}[U(A)]\}^{1/2}/m$ and n, the number of storeys supported [Pier and Cornell, 1973].

7.4.3 Equivalent Uniformly Distributed Load

With the estimation of the variances in (7.9), the load intensity $w(x, y)$ given by (7.8) is defined completely (in second-moment terms). However, often it is the equivalent uniformly distributed load (EUDL) which produces the same particular internal action (or load effect) as $w(x, y)$ that is desired. This is the type of loading specified in structural design codes. The fact that most loading codes also specify pattern loading, with alternate bays loaded and unloaded to somehow represent a worst condition, will be ignored in the discussion to follow. Clearly, to take it into account will require probabilistic considerations and the notion of an equivalent pattern load (EPL) [Reid, 1997].

A typical 'realization' of the actual loading $w(x)$ along the length x of a beam is shown in Figure 7.8(a). What is sought is the equivalent uniformly distributed load (EUDL), shown in Figure 7.8(c), such that, for example, the reaction R is estimated correctly.
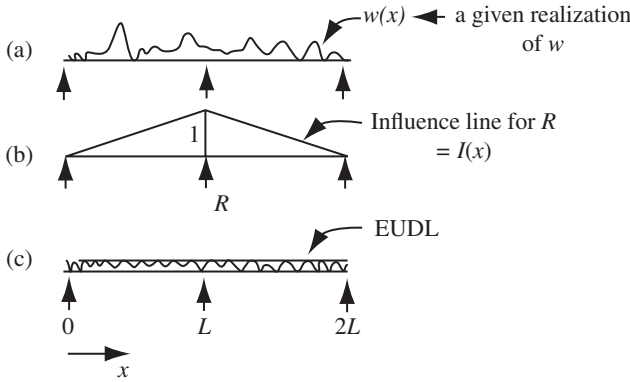
Figure 7.8 Equivalent uniformly distributed load EUDL related to actual load realization.

To proceed, let use be made of the influence line $I(x)$ shown in Figure 7.8(b). The reaction R can then be given both in terms of $w(x)$ and in terms of EUDL as

$$R = \int_0^{2L} w(x) I(x)\, dx = \int_0^{2L} (\text{EUDL}) \quad I(x) \quad dx \tag{7.17}$$

but, since (EUDL) is not a function of x,

$$(\text{EUDL}) = \frac{\int_0^{2L} w(x)\, I(x)\, dx}{\int_0^{2L} I(x)\, dx} \tag{7.18}$$

By using other appropriate influence lines, similar expressions can be derived for other actions (or load effects) while, in two dimensions, influence surfaces take the place of influence lines. By direct analogy, for a EUDL over an area

$$(\text{EUDL}) = L = \frac{\int_{A_I} \int w(x, y)\, I(x, y)\, dx\, dy}{\int_{A_I} \int I(x, y)\, dx\, dy} \tag{7.19}$$

where A_I is the so-called 'influence area'. It corresponds directly to the total beam length, or 'influence length' $2L$ in Figure 7.8, which is seen to be twice that of the tributary length (equal to L), for a reaction (half-span length for each span). Similarly, the influence area A_I is not, in general, identical with the tributary area A_T commonly used with live load reduction formulae for floor loadings in structural design codes. Some typical influence lines and surfaces are shown in Figure 7.9.

It follows readily that the mean for L is $E(L) = m$ and is unchanged from the arbitrary-point-in-time value, but the variance becomes larger:

$$\text{var}(L) = \frac{\int_{A_I} \int \int_{A_I} \int I(x_1, y_1) I(x_2, y_2) \text{cov}[w(x_1, y_1),\, w(x_2, y_2)] dx_1\, dy_1\, dx_2\, dy_2}{\left[\int_{A_I} \int I(x, y)\, dx\, dy\right]^2} \tag{7.20}$$

@Seismicisolation

(a) Midspan moment   (b) Midspan shear   (c) Interior column load

(d) End moment   (e) End shear   (f) Exterior column load

Influence area = $2l \times 2w$ Influence area = $2l \times 2w$

(g) Midspan moment   (h) Single storey column load
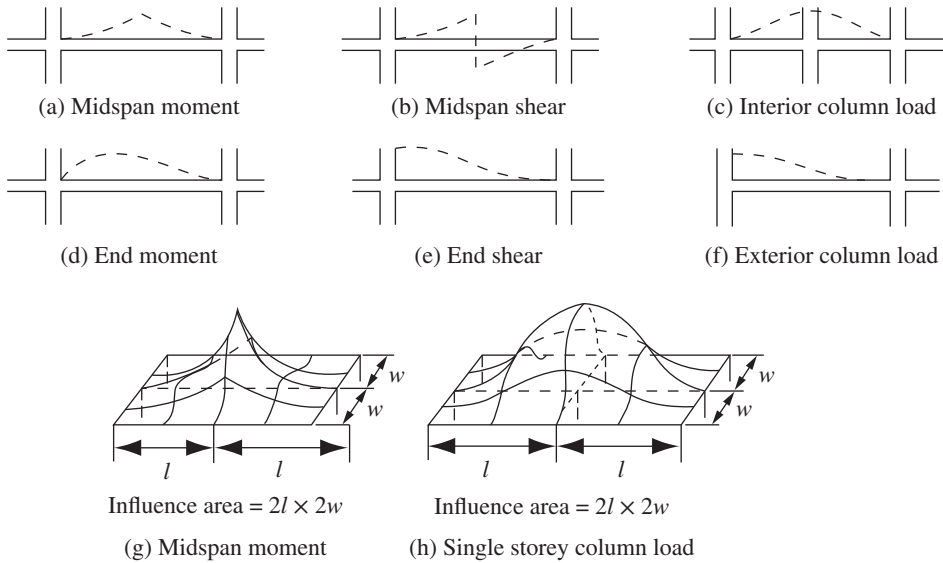
Figure 7.9 Typical influence lines (in plane frames) and typical influence surfaces [Reproduced from McGuire and Cornell (1974) by permission of the American Society of Civil Engineers].

Expression (7.20) can be bounded by assuming, conservatively, that the $w(x, y)$ are independent, from which it may be shown, using (7.15), that:

$$\text{var}(L) \leq \sigma_{bld}^2 + \sigma_{flr}^2 + \pi d \sigma_\varepsilon^2 \frac{K(A)}{A} k \tag{7.21a}$$

where

$$k = \frac{\int_{A_I} \int I^2(x, y) \ dx \ dy}{\left[\int_{A_I} \int I(x, y) \ dx \ dy \right]^2} \tag{7.21b}$$

Provided that appropriate influence areas A_I are used, the value of the equivalent uniformly distributed load L is relatively insensitive to the action being considered. This can be seen in the value k in (7.21) [McGuire and Cornell, 1974; Ellingwood and Culver, 1977]:

end moments in beams: $k = 2.04$
column loads: $k = 2.2$
midspan beam moments: $k = 2.76$

It follows that, in general, the variances of calculated EUDL will be approximately similar if both the influence areas are approximately similar and the influence surface shapes are approximately similar. The only exception is the EUDL value for mid-span shear, which, as expected, becomes comparable only if half the influence area is used [McGuire and Cornell, 1974].

Expressions (7.14–7.16 and 7.21) can be simplified further by assuming that the spatial correlation between loadings at different points on a floor is completely random, that is,

it is uncorrelated for any finite distance apart (also known as assuming the correlation is governed by 'white-noise'). Then $K(A)$ becomes a constant and (7.21a) is now given by:

$$\text{var}(L) \leq \sigma^2_{bld} + \sigma^2_{flr} + \frac{\sigma^2_S k}{A} \tag{7.22}$$

where the parameter σ^2_S is a constant obtained from fitting to observations [*cf.* Ellingwood and Culver, 1977; McGuire and Cornell, 1974].

7.4.4   Distribution of Equivalent Uniformly Distributed Load

By taking live load survey data and converting them directly to EUDL, it is possible to produce histograms showing the relative occurrence of different levels of equivalent loadings. This is shown in Figure 7.10 for increasing floor areas [Pier and Cornell, 1973].

As expected, the probability density function required to model these results changes from highly skewed to approximately Normal as the contributing floor area is increased (see Section A.5.8). An appropriate model is the Gamma distribution:

$$f_L(x) = \frac{\lambda(\lambda x)^k e^{-\lambda x}}{\Gamma(k)} \qquad x \geq 0 \tag{7.23}$$
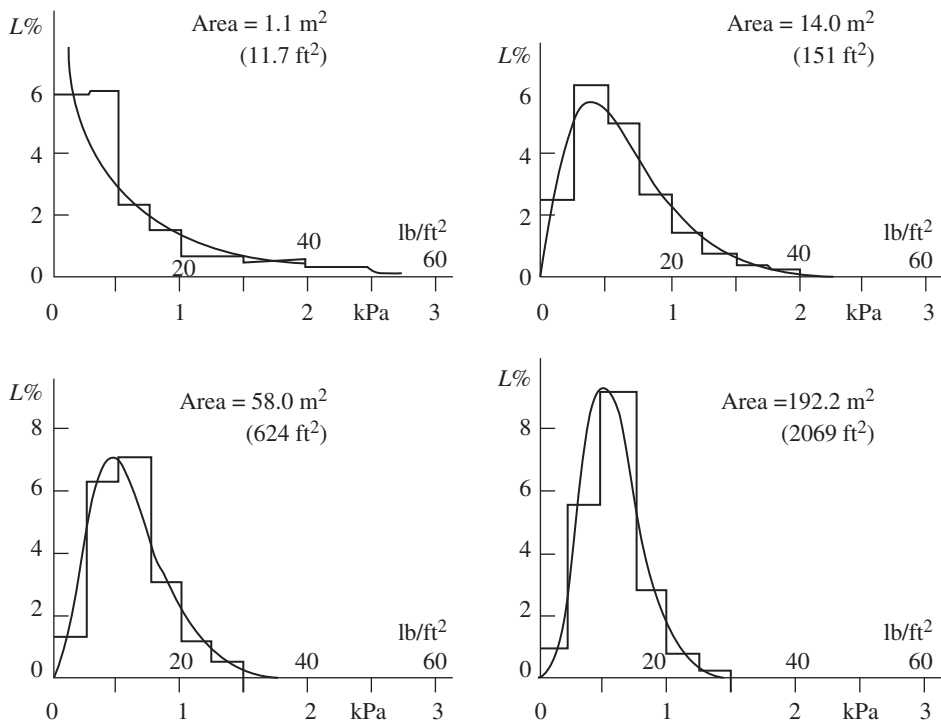
Figure 7.10 Histograms of floor load intensity as modelled by distribution functions. Reproduced from Pier and Cornell (1973) by permission of the American Society of Civil Engineers.

The parameters λ and k can be obtained from the mean and variance of L (see Section A.5.6). The Gamma distribution (7.23) appears to fit the observed data better than the Normal distribution or the Lognormal distribution in the > 90 percentile range [Corotis and Doshi, 1977]. The Extreme Value type I distribution is another possibility and is appropriate on physical grounds since the EUDL value reflects the maximum loading for a time interval.

As already noted in Section 6.5.1.6, it would be expected that for any structure there will be periods of zero live load and hence the probability density function strictly should have a probability 'spike' at the origin (see Figure 6.13). However, this is often (conservatively) ignored in modelling live loading.

The fact that the value of the EUDL is relatively insensitive to the type of internal action (stress resultant) is illustrated by plotting the load values at a given percentile of, say, the Gamma distribution against the influence area. A typical plot is given in Figure 7.11 in terms of the 90% fractiles ('design' values) for maximum sustained load (see Section 7.4.5) and maximum total load (see Section 7.4.7).

Typical values of parameters for arbitrary-point-in-time sustained floor loads are given in Table 7.3 for various floor loading types, including, for comparison, one set of information for domestic floors, one for retail spaces and one for car park floors (see also JCSS, 2001, 2006]. The differences in the mean m for office loads have been
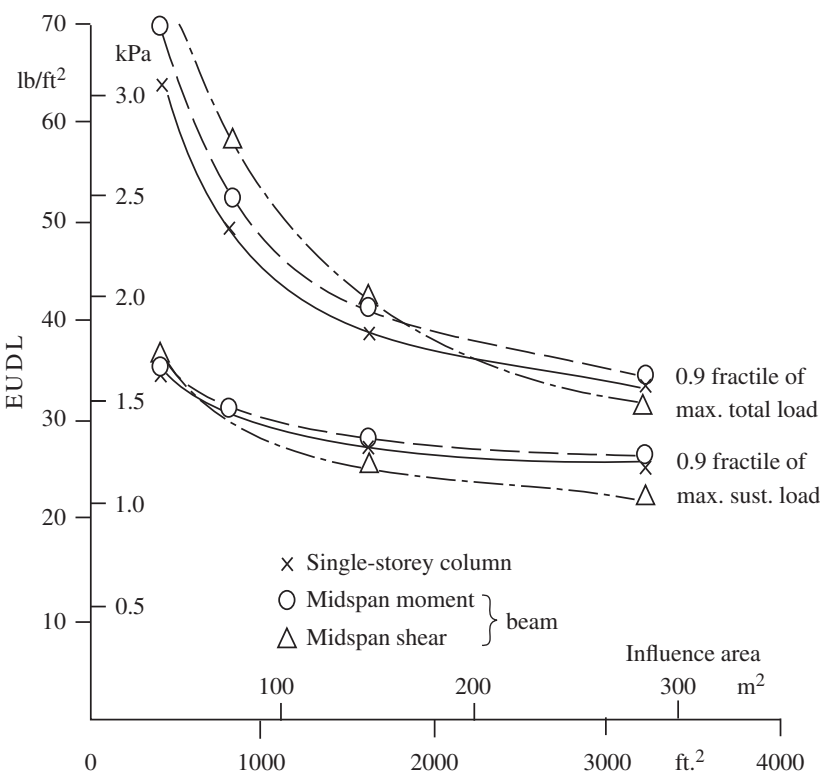
Figure 7.11 Single-storey beam and column fractiles as function of influence areas. Reproduced from McGuire and Cornell (1974) by permission of the American Society of Civil Engineers.

Table 7.3 Typical parameters for sustained floor loads (arbitrary-point-in-time values).

Occupancy	Mean m (kPa)	$\sigma^2_{bld} + \sigma^2_{flr}$	σ^2_S	Mean occupancy T years	Reference
Office UK	0.60	0.053	1.57	8	Mitchel and Woodgate (1971a)
Office USA	0.53	≈ 0.06	1.39	8	Chalk and Corotis (1980)
Office Australia	0.52	0.133	0.8	14.8	Choi (1992)
Office Sweden	0.364	0.038	0.29	10	Sentler (1974)
Apartments Sweden	0.285	0.001	0.28	5	Sentler (1976)
Domestic UK	0.59	0.077	0.635	10	Mitchell and Woodgate (1977)
Retail UK	0.75	0.249	0.458	7	Mitchell and Woodgate (1971b)
Carpark UK	0.66	–	1.61	0.000 8	Konig et al. (1985)

attributed (Choi, 1992) to differences in survey methodology, with, for example, room partitions etc. not being included in the US survey data. This accounts for about 0.04 kPa. Further, the Australian survey was performed some 10–20 years after the US and UK studies and includes (paper) filing and other storage areas. This is thought to account for the greater variation ($\sigma^2_{bld} + \sigma^2_{flr}$) evident in the Australian results. The low variability of floor loads in apartments has been attributed to the quite consistent way people use domestic apartments, resulting in only minor variations in floor loading (Sentler, 1975). This is unlike offices in more recent times for which (paper file) storage areas and equipment adds significantly to the variability. Data for open-plan office spaces and large areas with light-weight computer equipment and little or no paper storage appear not yet available. However, the older values are conservative.

7.4.5 Maximum (Lifetime) Sustained Load

For conventional structural design code work and when the time-integrated approach to structural reliability is used (see Section 6.2), it is desired to know the distribution of the lifetime maximum sustained load L_S. This is the maximum load that can be expected to act during the life of the structure.

It is clear from Figure 7.3 that L_S will depend on the changes in the occupancy and/or use of the floor during its lifetime. In formulating a model for L_S, let it be assumed that the loadings relevant to each occupancy are independent. Thus the maximum sustained load L_S during the lifetime t_L of the structure is

$$L_S = \max_t [L(t)], \qquad 0 < t < t_L \tag{7.24}$$

where the cumulative distribution function of L_S is given by $F_{L_S}(x) = P(L_S \leq x)$, also given in terms of the level crossing concept (Section 6.5.3) by

$$F_{L_S}(x) = P[L(0) \leq x]P[\text{no 'upcrossing' by } L(t) \text{ of } x, \text{ in } 0 \leq t \leq t_L] \tag{7.25}$$

Here $P[L(0) \leq x]$, which is equal to $F_L(x)$, denotes the probability that the initial sustained load is less than or equal to x. It is assumed in (7.25) that the maximum sustained

load is not caused by the first time the structure is loaded (as, for example, by the first tenant) and therefore the probability $P[L(0) > x]$ has been ignored. Subsequent changes in loading, as likely to be caused by a change in occupancy, could cause the occurrence of an 'upcrossing' event (Section 6.1) for the floor being considered (Figure 7.3). However, a change of occupancy need not always cause an upcrossing event. To model this, data [Mitchell and Woodgate, 1971a; Harris et al., 1981] suggest that changes of occupancy can be approximately (and asymptotically) represented by a Poisson counting process (cf. Section 6.5.1.2). This means the cumulative distribution function for L_S is:

$$F_{L_S}(x) = F_L(x)e^{-v_x t} \tag{7.26}$$

where v_x is the average rate of upcrossings. It is now necessary to relate the rate of upcrossings to the rate of occupancy changes. During a small interval of time Δt, the probability that an upcrossing occurs is given by

$$
\begin{aligned}
v_x \Delta t &= P(\text{one upcrossing in time } t \text{ to } t + \Delta t) \\
&= P(\text{upcrossing in this } \Delta t | \text{occupancy change in this } \Delta t)v_o
\end{aligned}
\tag{7.27}
$$

where v_o is the rate of occupancy changes. Expression (7.27) may be written also as

$$v_x \Delta t = P\{[L(t) < x] \cap [L(t + \Delta t) \geq x] \text{ occupancy change in this } \Delta t\} v_o \, \Delta t \tag{7.27a}$$

Cancelling Δt, and assuming that successive loads L are independent, leaves (*cf*. Sections 6.5.1.4 and 6.5.3)

$$v_x = F_L(x)[1 - F_L(x)]v_o \tag{7.28}$$

Substituting into (7.26) produces the cumulative distribution function for L_S in terms of that for the arbitrary-point-in-time load L as

$$F_{L_S}(x) = F_L(x)\exp\{-F_L(x)[1 - F_L(x)]v_o t\} \tag{7.29}$$

For extreme loads, $F_L(x) \to 1$ so that (7.29) may be approximated as

$$F_{L_S}(x) \approx \exp\{-v_o t[1 - F_L(x)]\} \tag{7.30}$$

Survey data suggest that there is a large degree of uncertainty about the rate of occupancy changes v_o. This is shown in Table 7.3 where T denotes the mean duration of occupancy. Assuming ergodicity (see Section 6.4.4) it follows that for typical US or UK office occupancy, $v_o = 1/T = 0.125$.

The magnitude of the maximum lifetime sustained load L_S is well described by either the Type I Extreme Value distribution or the Gamma distribution in the region of high load values. Methods for selecting the distribution and for fitting the distributions are available in the extreme value literature (e.g. Harris et al., 1981; Galambos, 1987; Castillo, 2012).

With multiple zones (floors, bays, etc.) contributing to the total load effect, such as in column loads, it is unlikely that all zones change tenancy at the same time [Chalk and Corotis, 1980]. However, data for the necessary correlation does not appear to be available. Ignoring this effect is obviously conservative.

7.4.6 Extraordinary Live Loads

Extraordinary live loads are those resulting from groups of people and from crowds. Such loads may result also from furniture stacking, repair work and emergency crowding. Usually they are not considered in live load surveys. For obvious reasons it is difficult to collect data about extraordinary live loads. Most available information has been gathered using questionnaires. It follows that there is considerable uncertainty about such 'data' and hence about the derived extraordinary loading.

Extraordinary live loads may be modelled as clusters of loads (e.g. persons) acting within a series of load cells randomly distributed over the floor area of interest. If a single occurrence of an extraordinary live load is denoted by E_1, then a plausible model might be [McGuire and Cornell, 1974; Ellingwood and Culver, 1977]

$$E_1 = QN\lambda \tag{7.31}$$

where Q is the weight of a single person, (typically $\mu_Q = 0.67$ kN or 150 lbf, $\sigma_Q \approx 0.11$ kN or 25 lbf, N is the number of loads (i.e. persons) per cell and λ is the mean number of cells per specific area A.

For offices and retail spaces typical values for N are $\mu_N \approx 4$ and $\sigma_N \approx 2$ while for domestic situations, Madsen and Turkstra (1979) suggested $\mu_N \approx 1$ and $\sigma_N \approx 0.67$. For car parks extraordinary live loads probably can be ignored.

The load E_1 reasonably may be assumed to be EV-I or Gamma distributed. Using second-moment concepts, the equivalent uniformly distributed load denoted L_{e1}, has mean and variance given by (A.167) and (A.169):

$$\mu_{e1} = \mu_Q \ \mu_N \frac{\lambda}{A} \tag{7.32}$$

and

$$\sigma_{e1}^2 = (\mu_Q^2 \sigma_N^2 + \mu_N^2 \sigma_Q^2 + \sigma_Q^2 \sigma_N^2)\frac{\lambda k}{A^2} \tag{7.33}$$

The parameter k is the influence area parameter given by (7.22) and has here been assumed to be identical for each load Q; this needed not be so in general.

The maximum extraordinary live load will consist of the contribution of a number of extraordinary loads (perhaps of different types). Typically there will be a random number of such occurrences of these loads during a given (reference) period t_L. Since the detailed probability distributions for each of these various types of extraordinary live loads is not generally available, let the probability distribution $F_{e1}(\ )$ for the instantaneous extraordinary live load be used as a surrogate for all these various load effects. Further, it is reasonable to assume that the arrival of each extraordinary live load is governed by a Poisson counting process (*cf*. Section 6.5.1.2). Then, following a derivation parallel to that for expression (7.30), the cumulative probability distribution function for the maximum extraordinary live load acting over a period t_L may be approximated by:

$$F_{L_e}(x) \approx \exp\{-\nu_e t_L[1 - F_{e1}(x)]\} \tag{7.34}$$

Although data are scarce, it seems reasonable to assume that ν_e, the average rate of extraordinary live load arrivals, is about one per year, and that λ which is a function

Table 7.4 Typical parameters for (multiple) extraordinary live loads[a].

Occupancy	μ_Q kPa	σ_Q kPa	μ_N	σ_N	T years	Reference
Office US						Harris et al. (1981)
• normal crowding	0.67	0.11	4	2	2.5	
• emergency crowding	0.67	0.11	10	5	50	
• remodelling	2.27	0.68	1	1	4	
Retail US	0.67	0.11	4	2		Madsen and Turkstra (1979)
Domestic US	0.67	0.11	1	0.67		Madsen and Turkstra (1979)
Office[b] Australia						Choi (1991)
• normal crowding	0.66	0.11	17.2	23	1	
• emergency crowding	0.66	0.11	30.2	33.1	50	
• remodelling	9.42	9.66	1	0	5	

a) These parameters are closely similar for single loads (*cf.* McGuire and Cornell, 1974; Ellingwood and Culver, 1977).

b) The values for N are higher due to Choi's use of a greater cell area (mean 23.8 m^2 *cf.* 16 m^2).

of area A, lies in the range 2 cells per 17 m^2 for 'small' areas, to an average of 1 cell per 17 m^2 for 'large' areas, with a 'small' area defined as 17 m^2 (180 ft^2). An empirical relationship $\lambda = (1.72A - 24.6)^{1/2}, A > 14.4$ m^2 (or $\lambda = (0.16A - 24.6)^{1/2}, A > 155$ ft^2) has been suggested to relate λ to the total floor area A [McGuire and Cornell, 1974]. Table 7.4 summarizes some typical data for extraordinary live loading as obtained from several surveys.

7.4.7 Total Live Load

To obtain a total live load it is necessary to consider the combined effect of the component loadings. The combination of a sustained live load modelled, for example, as a Poisson square wave process and an extraordinary live load modelled as, say, a Poisson spike process is not necessarily an easy matter, as noted in Chapter 6. However, some progress can be made with a simplified time-integrated approach, developed specifically for floor live loads and verified against field data. As described briefly below, it is based on earlier work in which the main emphasis was placed on deriving design loadings (i.e. upper fractiles) rather than complete probability distributions [McGuire and Cornell, 1974].

In accordance with Turkstra's rule (6.155), the total live load L_t during the lifetime of the structure can be considered as $L_t = \max_i(L_{ti})$. Intuitive argument suggests that the L_{ti} terms are likely to be one of the following:

$$\text{Case I:} \quad L_{t1} = L_S + L_{e1} \tag{7.35a}$$

$$\text{Case II:} \quad L_{t2} = L + L_e \tag{7.35b}$$

$$\text{Case III:} \quad L_{t3} = L_S + L_e \tag{7.35c}$$

Here L and L_S are interpreted as the arbitrary-point-in-time sustained live load and the maximum lifetime live load respectively, L_e as the maximum lifetime extraordinary

live load and L_{e1} as the maximum extraordinary live load during one sustained loading period. Each case therefore consists of a maximum load and an arbitrary-point-in-time load (*cf*. 6.155). In each case the loads are equivalent uniformly distributed loads. Although Turkstra's rule assumes that each load case is independent, simulation has shown that often case I and case II provide similar L_{ti} values and occur together. Case III was found to have a small probability of occurrence. The probability that a maximum total load occurs when neither component load process is at a lifetime maximum was found to be negligible [McGuire and Cornell, 1974; Chalk and Corotis, 1980].

With this method of load combination, a probability distribution for L_t can be derived only at the expense of some (conservative) simplifications. Thus, case II can be simplified by assuming that L is given approximately by the deterministic mean value m of sustained load in (7.8) and that $\sigma_{t2} \approx \sigma_e$, since $L_e >> L$ in general. Further, if $E(\tau)$ is the average or expected duration of L_S, and t_L is the expected structural lifetime, then the probability that L_S and L_e do not occur at the same time is $p = [t_L - E(\tau)]/t_L$. Assuming now that cases I and II are independent, the cumulative distribution function of the total load is given approximately by

$$F_{L_t}(x) = P(L_t < x) \approx P(L_S + L_{e1} < x)\, P(m + L_e < x)\, p + P(L_S + L_e < x)(1 - p) \quad (7.36)$$

Since both case I and case III represent lifetime maxima, it is reasonable to model them by Extreme Value type I distributions. For case II, L_e was already represented by the Extreme Value type I distribution. With these representations (7.36) becomes [Chalk and Corotis, 1980]:

$$F_{L_t}(x) = \exp[-\exp(-w_1)]\exp[-\exp(-w_2)]p + \exp[-\exp(-w_3)](1 - p) \quad (7.37)$$

where the $w_i = \alpha_i(x - \beta_i)$ represent the reduced variate forms for the Extreme Value type I distribution. Here $i = 1$, $i = 2$, $i = 3$ correspond to cases I, II and III respectively. The parameters α_i and β_i as used here are distribution parameters (*cf*. Appendix A). Hence the cumulative distribution function $F_{L_t}(\ )$ can be determined if the moments of each term in (7.36) are known.

A summary of some basic load parameters, load process statistics based on the models given above and the relative importance of cases I–III [see (7.35) above] is given in Table 7.5 for office floor loading. It is based on data reported by Corotis and Doshi (1977), Chalk and Corotis (1980) and Harris et al. (1981). For the maximum sustained load and the lifetime maximum extraordinary load the theoretically derived values are closely similar to results obtained by simulation (Monte Carlo) analysis. Parallel results are available for other occupancy classes.

7.4.8 Permanent and Construction Loads

Permanent loads are those that do not vary significantly through the life of the structure, even though their actual value may be uncertain. Dead loads are typically of this type. They result from the self-weights of the materials used in construction and from permanent installations. Because these individual permanent loadings are additive, the variability of the total permanent load is less than that of the individual items (as measured by the variance); it also suggests that the central limit theorem applies. Hence dead loads commonly are assumed approximated closely by the Normal distribution,

Table 7.5 Example of typical basic loads for office floors, the parameters derived for the load models and the results of load combinations (see text).

Basic Loading Parameters	Unit		kPa	lbf / ft^2
• Typical influence area (m^2)	A_I	20		
• Typical design life (years)	T	50		
Typical instantaneous uniformly distributed sustained load (arbitrary-point-in-time load)	L			
• Mean	μ_L		0.53	10.9
• Standard deviation	σ_L		0.37	7.6
• Average number of occupancy changes per year	ν_o	0.125		
• Expected occupancy duration (years)	$E(\tau) = 1/\nu_o$	8		
Typical instantaneous uniformly distributed extraordinary live load	L_{e1}			
• Mean	μ_{e1}		0.39	8
• Standard deviation	σ_{e1}		0.40	8.2
• Average number of extraordinary live load occurrences per year	ν_e	1		
Derived (simulated) Loads and Load Parameters				
Maximum sustained load L_s	L_S			
• Mean	μ_{L_S}		1.21	24.9
• Standard deviation	σ_{L_S}		0.33	6.9
Lifetime maximum extraordinary load	L_e			
• Mean	μ_{L_e}		1.79	36.7
• Standard deviation	σ_{L_e}		0.41	8.4
Simulated values for combinations				
• Case I $\quad L_S + L_{e1}$ (occurrence rate, 30%)	Mean		2.50	51.2
• Case II $\quad L + L_e$ (occurrence rate, 41%)	Mean		2.40	49.1
• Case III $\quad L_S + L_e$ (occurrence rate, 17%)	Mean		2.79	57.2
• Other (occurrence rate, 12%)	Mean		2.15	44.2

$1 \text{ kPa} \equiv 1 \text{ kN/m}^2 \approx 20.5 \text{ lbf/ft}^2$.

typically with a mean equal to the nominal load, and a coefficient of variation of 0.05–0.10. However, there is some evidence that dead loads are underestimated [Ellingwood et al., 1980] and a mean somewhat greater (say 5%) than the nominal may be appropriate. The variability in total dead load often appears to be due mainly to non-structural claddings, services and permanent installations rather than to the variability of the load-bearing materials themselves. A Lognormal distribution also has been suggested as appropriate [Pham, 1985]. A comprehensive summary of loads generated by self-weight of a wide range of materials is available [JCSS, 2001, section 2.1]. Generally the mean values are similar to the nominal values and the coefficients of variation small, < 0.1 for steel, 0.01–0.03 for most high-quality concretes, and 0.1 for various timbers.

Loads acting on a structure during construction have had little attention from a probabilistic point of view. Such loads include the placing of high-density loads temporarily on the structure (e.g. cranes, building materials such as bricks) and also formwork loads including loads due to freshly placed concrete. Due to obvious difficulties in data collection, the data that have been published typically show rather high variability because many different construction techniques are involved [Stewart, 2001; Juocevicius and Kadzys, 2009]. For example, for construction loads placed on newly-cast concrete slabs, the loading includes the live loads due to workmen, equipment and machinery and material storage. Survey results show large areas of slab with very little or zero loads and others with high loading intensity. This suggests a mixed distribution for the EUDL load (see Figure 6.13). For this, the mean value was estimated at 0.3 kPa (6.3lb / ft^2) with a standard deviation of 1.65 kPa (34.4lb / ft^2). A Gamma or Weibull distribution was found adequate to describe the non-zero part of the distribution [Karshenas and Ayoub, 1994].

7.5   Conclusion

Three different types of loading were discussed in this chapter, mainly to indicate the thinking involved in their modelling. If observations over a suitably long time period are available, load statistics may be deduced directly such as was outlined for wind loading (perhaps through a hydrodynamic relationship and/or a spectral analysis). Wave, snow and earthquake loadings are often considered to be in this category, depending on the geographical location.

Floor loading is of a special nature since it is influenced by many factors including the possibility of human intervention. This, and the fact that relatively few observations are available, tends to produce greater uncertainty than typical for most natural loadings.

In principle, the concepts and methodology used for modelling floor loading could be applied also to other man-imposed loads. In practice the modelling approaches adopted have attempted to deal with the unique features of the load being considered. For example, for traffic loads on bridges, the modelling approaches used include numerical simulation of moving traffic flows using observed data as a starting point, in a manner analogous to stream flow generation [e.g. Vrouwenvelder and Waarts, 1992; Crespo-Minguillon and Casas, 1997], simulation of static traffic configurations [e.g. Nowak, 1993; Reid and Caprani, 2014] and more theoretical approaches using stochastic process theory, including Markov models [e.g. Ghosn and Moses, 1985a]. Overall, it should be clear that the study of load modelling has become rather specialized, and reference to the appropriate literature is recommended.

8

Resistance Modelling

8.1 Introduction

The uncertainties associated with strength properties (and some stiffness properties) will be considered in this chapter to complement the discussion of loading given in the previous chapter.

To describe adequately the resistance properties of structural elements, information about the following is required:

(1) statistical properties for material strength and stiffness;
(2) statistical properties for dimensions;
(3) rules for the combination of various properties (as in reinforced concrete members);
(4) influence of time (e.g. size changes, strength changes, deterioration mechanisms such as fatigue, corrosion, erosion, weathering, marine growth effects);
(5) effect of 'proof loading', i.e. the increase in confidence resulting from prior successful loading;
(6) influence of fabrication methods on element and structural strength and stiffness (and perhaps other properties);
(7) influence of quality control measures such as construction inspection and in-service inspection;
(8) correlation effects between different properties and between different locations of members and structure.

Only relatively little information is available in statistical terms, mostly for items (1)–(3). Time-independent statistical properties for structural steel, reinforcing steel, concrete, masonry and timber have been summarized [Ellingwood et al., 1980; JCSS, 2000]. Because of space limitations, and to illustrate the essential ideas, the present chapter will be confirmed mainly to a review of the statistical properties of structural steel and reinforced concrete.

8.2 Basic Properties of Hot-Rolled Steel Members

8.2.1 Steel Material Properties

Steel material properties data have long been available from tests taken on billets produced at steel mills [e.g. Johnston and Opila, 1941; Julian, 1957; Alpsten, 1972] and

from more recent test programs [e.g. Simões da Silva, et al. 2009]. There are also data from more specialist individual research projects such as those conducted for naval and marine applications [e.g. Dandola and Basar, 1980].

The applicability of such data in reliability assessment must be evaluated. Thus mill test data are often considered unsuitable since the tests are performed at a loading rate greater than that likely in real structures. Further, the steel tested is not necessarily typical of the 'as supplied' steel. It is a practice, in some cases, to sell rejected higher grade steel as the next lower grade, and this tends to cause a possible second peak in the probability density function for the yield strength. This is clearly observed in the probability densities for the data reported by Simões da Silva et al. (2009), in some cases with a considerable peak at steel strengths much higher than the nominal strength. A further difficulty is that mill test samples are commonly taken from the webs of rolled sections, whereas in practice the (usually lower strength) properties of the (thicker) flanges are of more interest. Finally, there is evidence that (probably unintentioned) bias is present in mill test results as a result of the effect of different mills [Lay, 1979]. For steel weight and plate thickness it has been noted that steel plate supplied by manufacturers may be biased toward the higher limit in thickness if paid for by weight and biased towards the lower limit on thickness if paid for by piece supplied. Also a slight bias may be introduced by the technique employed to measure plate thickness [Hess et al. 2002].

8.2.2 Yield Strength

The strength of steel is dependent on the material properties of the alloy, and hence statistical properties must be related closely to the specified steel type. It is normal practice to sample each billet of steel and only if a specified minimum strength is achieved is the steel accepted for further processing. The data so obtained are extensive but, as already noted, have certain flaws if they are to be used for statistical properties of complete steel members.

Older, typical summaries of mill test data for steel hot-rolled shapes and derived from about 4000 samples are given in Table 8.1 for ATSM A7 steel from US mills. Both sets of data cover a number of steel mills, many shapes of section and a time span of more than 40 years prior to 1957. The specified yield strength of these steels varied from 200–275 MPa (30–40 ksi), but the bias ratios and COVs given in Table 8.1 are typical. There is no overlap between these data sets [Galambos and Ravindra, 1978].

Table 8.1 US yield stress F_y data.

Steel type	Nominal F_y (MPa)	Mean mill F_y / specified F_y	Est. mean static F_y / specified F_y	COV	Reference
ASTM A7*	200–275	1.21	1.09	0.087	Julian (1957)
ASTM A7*	200–275	1.21	1.09	0.078	Tall and Alpsten (1969)
Ordinary grade	230	1.3		0.124	Hess et al. (2002)
HSLA**	550	1.19		0.083	Hess et al. (2002)

* Data apply to samples taken from webs of hot-rolled sections.
** High-strength low alloy steels.

Table 8.2 British yield stress F_y data [Adapted from Baker, 1969].

Type of steel	Plate thickness (mm)	Mill	Mean mill F_y specified F_y	Estimated mean static F_y specified F_y	Coefficient of variation
Structural	10–13	Y	1.15	1.04	0.09
carbon steel	10–13	W	1.14	1.03	0.05
plates	37–50	Y	1.03	0.92	0.12
	37–50	W	1.07	0.96	0.05
High-strength	10–13	M	1.11	1.03	0.08
steel plates	10–13	K	1.11	1.03	0.04
	37–50	M	1.06	0.98	0.06
	37–50	L	1.15	1.17	0.05
Structural	10–13	Q	1.20	1.09	0.05
carbon steel	16–20	L	1.19	1.10	0.12
webs of shapes					
High-strength	6–10	N	1.19	1.11	0.06
steel	37–50	L	1.06	0.98	0.05
webs of shapes					
Structural	3.7	--	1.27	1.16	0.05
carbon steel	6.4	--	1.32	1.21	0.08
tubes					
High-strength	5.9	--	1.18	1.10	0.05
steel tubes	6.4	--	1.15	1.07	0.08

Nominal F_y: structural, 250 MPa (36 ksi); high-strength, 360 MPa (50 ksi).
Note: 25.4 mm = 1.0 in.

Table 8.2 summarises British mill test data given by Baker (1969) for both plates and structural sections to BS 15 and BS 968. A summary of Swedish mill test data is given in Table 8.3. More recent analyses [Hess. et al. 2002; Simões da Silva et al, 2009] based on much larger sample sizes from several different sources that include samples from rolled and from welded sectional shapes and from shipbuilding steels, show slightly higher bias and generally comparable COVs.

As noted, mill tests are invariably conducted at a higher strain rate than is usual for conventional 'quasi-static' loads on structures. This leads to an overestimate of the yield strength. An empirical correlation factor to obtain a static stress F_y from a test producing a higher strain rate stress F_{yh} is given by [Rao et al., 1966]

$$F_{yh} - F_y = 22 + 6900\varepsilon \quad \text{(MPa)}$$
$$= 3.2 + 1000\varepsilon \quad \text{(ksi)} \tag{8.1}$$

@Seismicisolation

Table 8.3 Swedish yield stress F_y data [Adapted from Alpsten, 1972].

Nominal F_y (MPa)	Mean mill F_y / specified F_y	Estimated mean static F_y / specified F_y	Coefficient of variation	Number of samples
220	1.234	1.11	0.103	19 857
260	1.174	1.06	0.099	19 217
360	1.108	1.03	0.057	11 170
400	1.092	1.02	0.054	2 447

Note: 1.0 MPa = 1.0 N / mm^2 = 0.145 ksi.

where ε is the strain per second, with $0.0002 \leq \varepsilon \leq 0.0016$. The difference $F_{yh} - F_y$ is approximately Normal distributed with a mean of about 24 MPa (3.5 ksi) and coefficient of variation of 0.13 [Mirza and MacGregor, 1979b]. This information allows mill test data to be converted to static stress values.

Using an upper range value for ε, Galambos and Ravindra (1978) suggested that, as a first approximation, the mill F_y can be reduced by 28 MPa (4 ksi). The effect on the coefficient of variation might be ignored. Where required, this approach has been used to obtain the adjusted ratios $F_y/F_{y\ specified}$ given in the tables above. The resulting values can be compared with those given in Table 8.4 obtained by Galambos and Ravindra (1978) for individual components rather than mill sample data, from limited numbers of experimental projects. It is seen that there is reasonable agreement for corresponding sample types. Generally similar COVs have been reported for data including shipbuilding steels [Hess et al., 2002] but with slightly higher range in bias factors (1.03–1.2).

The early work of Alpsten (1972) and Baker (1969) suggested that the Extreme Value Type I distribution, the Lognormal distribution, and, to a lesser degree, the truncated Normal distribution all fit the experimental data (see Figure 8.1). More recent reviews suggest the Lognormal distribution more often fits the data [Hess et al. 2002]. These distributions are all positively skewed as would be expected since the minimum value of the yield strength is zero and the distribution would be affected in the lower (left) tail by rejection of steel which does not pass mill tests. The distribution types that fit the data do not appear to be affected by mill or testing laboratory, nor by whether the tensile or compressive yield strength is considered [Johnston and Opila, 1941].

Table 8.4 Static yield stress data [Adapted from Galambos and Ravindra, 1978].

Location	Specified F_y (MPa)	Estimated mean static F_y / specified F_y	Coefficient of variation	Number of samples
Flange	228	1.00	0.12	34
Flange	345	1.08	0.08	13
Flange	24, 345, 448	1.08	0.09	6
Web and flange	379	1.00	0.05	24
Web	238	1.05	0.13	36
Box	248	1.06	0.07	80

Note: 1.0 MPa = 1.0 N / mm^2 = 0.145 ksi.
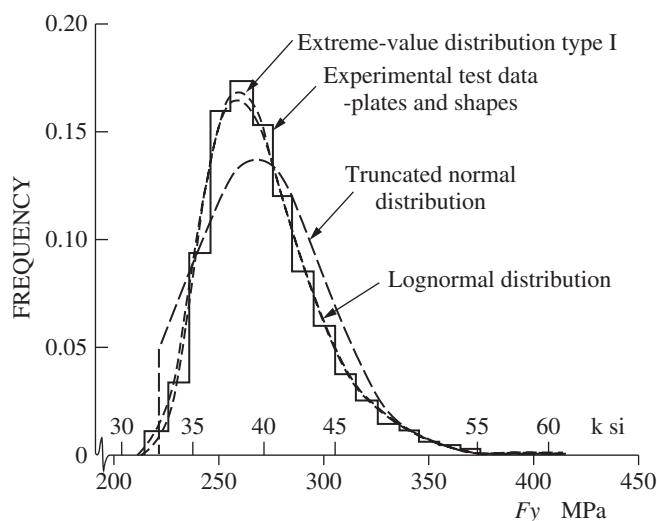
Figure 8.1 Typical histogram for yield strength of mild steel plates and shapes together with three fitted probability density functions [Adapted from Alpsten (1972) with permission from ASCE].

8.2.3 Moduli of Elasticity

A summary of collated data for the elastic moduli E (elastic modulus in tension or compression), v (Poisson's ratio) and G (shear modulus) is given in Table 8.5. The older data cover a period of more than 20 years and had at least 2 different (US) steel mills involved. The number of specimens tested did not permit estimation of the best probability distribution. However, for E the more recent, extensive, data suggest a Normal distribution [Hess et al. 2002]. This more recent work did not consider v or G.

Table 8.5 Elastic moduli of structural steel.

Property	Mean / Specified	Coefficient of variation	Number of tests	Type of test	Reference
E	1.01	0.010	7	Tension coupon	Lyse and Keyser (1934)
E	1.02	0.014	56	Tension coupon	Rao, et al. (1966)
E	1.02	0.01	67	Tension coupon	Julian (1957)[a]
E	1.02	0.01	67	Compression coupon	Julian (1957)[a]
E	1.03	0.038	50	Tension and compression coupon	Johnston and Opila (1941)
E	1.08	0.060	94	Tension coupon and stub column	Tall and Alpsten (1969)
E	0.99	0.076	many	Tension coupon	Hess et al. (2002)
v	0.99	0.026	57	Tension coupon	Julian (1957)[a]
v	0.99	0.021	48	Compression coupon	Julian (1957)[a]
G	1.08	0.042	5	Torsion coupon	Lyse and Keyser (1934)

Typical specified values: $E = 200\,000$ MPa ($\approx 29\,000$ ksi); $v = 0.03$; $G/E = 0.385$.

a) As attributed by Galambos and Ravindra (1978), but no data are given in report as published.

8.2.4   Strain-Hardening Properties

For reasons discussed by Alpsten (1972) the strain-hardening properties for steel, and thus the determination of their uncertainty, is difficult and has had relatively little attention, perhaps because it is seldom used for conventional design purposes. Investigations by Doane, quoted in Galambos and Ravindra (1978), suggest a value of the strain-hardening modulus E_{ST} = 3900 MPa (570 ksi) in tension and 4600 MPa (670 ksi) in compression, and that a coefficient of variation of 0.25 might be assumed.

8.2.5   Size Variation

Typical distributions of the cross-sectional dimensions of hot-rolled section shapes are given in Figure 8.2 [Alpsten, 1972]. Height and width variation appear to be quite small, typically with a coefficient of variation of 0.002. There is somewhat greater (but still small) variation in member and in plate thickness, with COVs typically around 0.02 [Hess et al. 2002].

Of somewhat more importance for strength is the variation in section properties such as cross-sectional area A, second moments of area I, weight W per unit length and elastic section modulus Z (S in US terminology). Some typical histograms are
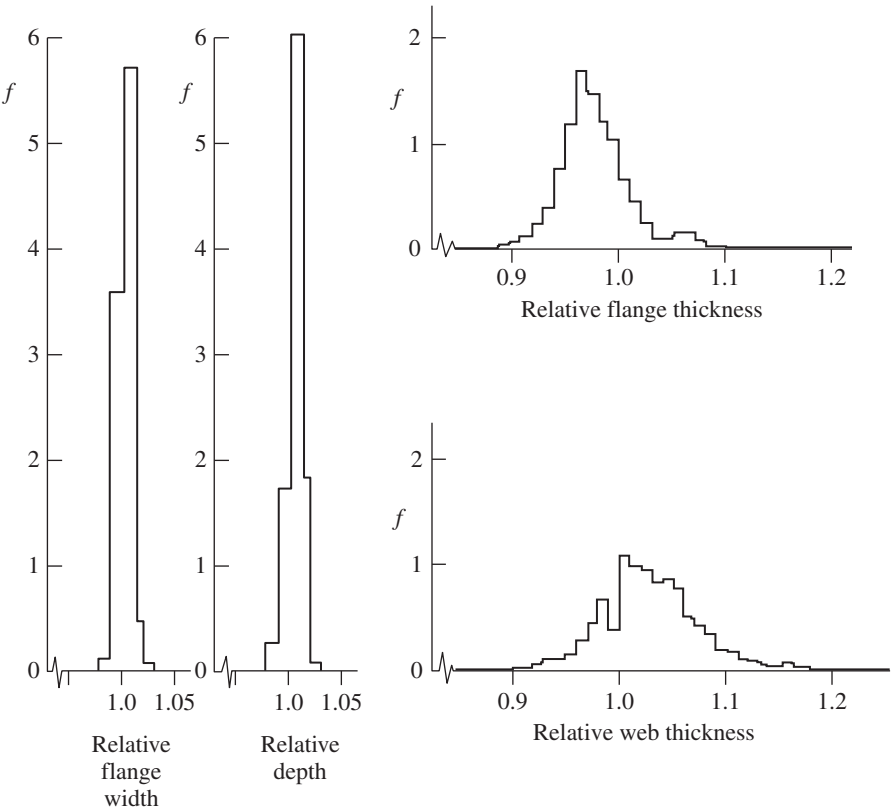
Figure 8.2 Typical histograms of cross-sectional dimensions for hot-rolled sections [Adapted from Alpsten (1972) with permission from ASCE].
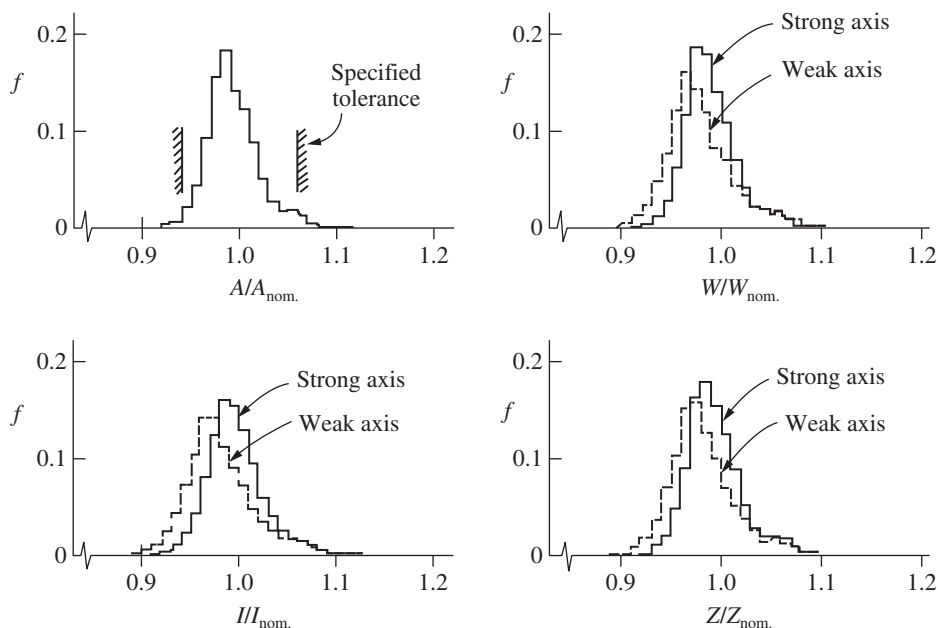
Figure 8.3 Typical histograms for section properties for hot-rolled mild steel sections [Adapted from Alpsten (1972) with permission from ASCE].

shown in Figure 8.3 [Alpsten, 1972]. Most of the variation is due to flange thickness variation. Overall, a value of unity for the ratio of mean/specified geometric properties is considered appropriate, with an average COV around 0.05 [Ellingwood et al., 1980]. For different and more modern data sets both for general and for marine grade steels, that included several Japanese steel grades [Dandola and Basar, 1980], generally similar values are appropriate [Hess et al., 2002].

8.2.6 Properties for Reliability Assessment

Some of the material and dimensional properties described above relate to 'as-milled' properties from a number of mills in aggregate (e.g. Table 8.1) while other data appear to cover results from just one mill (e.g. Table 8.2). It would be expected that there is greater variability in results as the data included in the database expands from:

(1) a billet of steel;
(2) all billets from one grade of steel and one mill;
(3) several mills;
(4) steel delivered to site, without guarantee that it is from one mill;
(5) steel of different sizes and strength grades.

For a reliability assessment, appropriate statistical properties must be used. This implies knowledge of sources of material supplies, and their quality. If such knowledge is not available or is limited to national or regional averages, rather conservative estimates for the coefficient of variation (and perhaps the probability density functions) must be made. Such a situation applies, for example, to structural code calibration

activities. Care must be taken, however, that data are from what can be considered to be homogeneous sources for the analysis at hand. For example, with good controls and supply from one source, items (1) and (2) might be appropriate. When data are from different disparate sources, such as when item (3) also applies, or when considerably different quality controls and quality assurance are involved, the COV is likely to be much higher. It follows that a reliability analysis must consider not just typical strength and related properties but also the quality assurance and related matters (*cf.* section 2.2.8).

8.3   Properties of Steel Reinforcing Bars

The sources of variability and the physical properties of interest for reinforcing bars are generally similar to those for hot-rolled steel shapes. The statistics for these properties have been overviewed by Mirza and MacGregor (1979b) and also by Bournonville et al. (2004).

There is negligible variation of yield or ultimate strength within the length of a typical reinforcing bar. Thus strength correlation can be taken as unity. For bars of the same size and in the same job lot it is likely that the bars will originate from the same (but unknown) steel mill, in which case the coefficient of variation is about 1–4% and the correlation coefficient between yield strengths of individual bars is around 0.9 (Rackwitz, 1996). Overall variability (COV) for bars from different sources and in different locations in the structure is likely to be around 4–7%.

Variability of bar sizes typically is small, with the ratio of actual area to nominal area having a mean of 1.00 and a COV of around 2%. There is an effect on yield and ultimate strength resulting from the rate of specimen testing, similar to that noted for structural steel.

After adjustment for rate of testing, and after allowing for nominal cross-section areas of bars, the probability density function for the yield strength of steel has variously been assumed to follow a Normal, Lognormal or Extreme value distribution [Alpsten, 1972; Mirza and MacGregor, 1979b] but none appears to be a particularly good fit away from the mean region. Mirza and McGregor (1979b) suggested the use of the Beta distribution for the yield strength:

$$ f_{F_Y} = A \left(\frac{F_y - a}{c} \right)^B \left(\frac{b - F_y}{c} \right)^C \tag{8.2} $$

where the constants (A, B, C, a, b, c) were obtained from fitting the distribution to the available data. Table 8.6 shows typical data for 300 and 410 MPa steels, in each case with a range of validity $a \leq F_y \leq b$. Generally similar values apply for high-strength reinforcing steels (e.g. 500MPA (75ksi) yield strength). Typically for these the COV is similar to those in Table 8.6 but reducing with increase in bar diameter (Mirza and MacGregor, 1979b, Bournonville, et al. 2004).

Generally similar results have been obtained for the statistical properties and probability distributions for the ultimate strength of reinforcing bars, their elongation and the cross-sectional areas of the bars (Bournonville et al., 2004). As noted for steels, the modulus of elasticity is very similar for all steels and tends to have very low variability,

Table 8.6 Coefficients for probability density function for yield strength of various grades of reinforcing bars [based on Mirza and McGregor, 1979b and Bournonville, et al., 2004].

Grade	Units	Mean	COV	A	B	C	a	b	c
300	MPa	≈ 310	≈ 0.11	4.106	2.21	3.82	228	428	200
40	ksi	≈ 45					33	62	29
410	MPa	461	≈ 0.08	7.587	2.02	6.95	372	703	331
60	ksi	66.8					54	102	48
500	MPA	≈ 560	0.04-0.11*	4.61	2.34	6.95	606	1150	545
75	ksi	≈ 80					88	167	79

*Reduces with increase in bar diameter.

and the expected value is close to the nominal value. Similarly, for steel reinforcing bars the expected value usually is very close to $E = 2.01 \times 10^5$ MPa ($\approx 29\,000$ ksi) with a low coefficient of variation of 0.033.

8.4 Concrete Statistical Properties

Although the statistical distribution of concrete compressive strength has been of interest for a long time [e.g. Julian, 1957; Freudenthal, 1956] it often has a much smaller influence on structural strength and behaviour than do reinforcement properties. This is due entirely to the conventional design philosophy of attempting to achieve ductility in the structure. Nevertheless, it is important for estimating reliability of reinforced columns and for serviceability investigations [e.g. Stewart, 1997].

Based on many test results for cast 'on-site' concrete test (or control) cylinders and cubes [e.g. Entroy, 1960; Murdock, 1953; Rüsch et al., 1969; Mirza et al., 1979], the values of the coefficient of variation or standard deviation given in Table 8.7 are appropriate for between-batch variation (i.e. considering concretes from all sources) for medium-strength concretes.

For these the bias (mean/nominal strength) is around 1.0. For high-strength concretes the COV is roughly halved, but the bias is greater [Tabsh and Aswad, 1995; Hueste et al.,

Table 8.7 Variation of 'on-site' concrete compressive strength for control cylinders and cubes (between-batch).

Concrete	Control	Bias	Coefficient of variation ($F'_c < 28$ *MPa*)	Standard deviation ($28 \leq F'_c \leq 45$ *MPa*)
Normal (< 45 MPa)	Excellent	≈ 1	0.07–0.10	2.8 MPa
	Average	≈ 1	0.15	4.2 MPa
	Poor	≈ 1	0.20	5.6 MPa
High-strength (55 MPa)	Good	≈ 1.3	0.09	
High-strength (70 MPa)	Good	≈ 1.1	0.09	

Note: 28 MPa ≈ 4 ksi.

2003; Nowak et al., 2012] – see Table 8.7. Similar results have been observed for modern light-weight concretes [Rakoczy and Nowak, 2012]. It appears that the lower COVs can be attributed to better quality control for the more modern concretes.

The coefficients of variation are roughly halved for within-batch variation (i.e. for concrete from one source). As before, it is evident that quality control is an important parameter (*cf.* section 2.2.8).

The above investigations confirmed that a Normal distribution is appropriate for the compressive strength of good quality, medium-strength, concrete. The Lognormal distribution and the Gumbel distribution also have been proposed [Drysdale, 1973; Silvestri et al., 2008], but it is clear the data are only slightly (positively) skewed and there is little to distinguish between the three distributions, except, and importantly, in the extreme tails, particularly the right (high-strength) tail. It has been suggested that the (slightly skewed) non-Normal distributions are more appropriate where concrete control is poor [Drysdale, 1973]. On the other hand, limited data for the strength of high strength (45 + MPa) concretes shows a distribution skewed towards the right (negative skew), better represented by a Beta distribution [Kolisko, et al. 2012].

In the assessment of existing structures and for reliability assessments, the in-situ concrete strengths are of most interest, rather than the results for field (control) cylinders. For concrete compressive strength the relationship between in-situ strength f_{cis} and the characteristic (or specified design) strength F_c' may be taken as [Mirza, et al., 1979]:

$$\bar{f}_{cis} = 0.675 F_c' + 7.7 \leq 1.15 F_c' \; MPa \tag{8.3}$$

$$V_{cis}^2 = V_{ccyl}^2 + 0.0084 \tag{8.4}$$

where $\bar{f}_{cis}$ is the mean in-situ strength, V_{ccyl} is the coefficient of variation for results for control cylinders taken on-site and the constant 0.0084 arises from variation between control cylinder strength and in-situ strength and from variation within cylinder tests.

Relationships (8.3) and (8.4) can be broken down by examining the influences between F_c' and the in-situ strength. Based on Canadian field investigations, Bartlett and McGregor (1996) suggested that (8.3) and (8.4) should be modified to:

$$f_{cis}' = F_2 \cdot F_1 \cdot F_c' \tag{8.5}$$

$$V_{cis}^2 = V_{F_2}^2 + V_{F_1}^2 \tag{8.6}$$

where $F_1 \cdot F_c'$ is the strength of concrete f_{ccyl}' (as measured by standard cylinders under laboratory control—'control cylinders') produced by concrete manufacturers. It allows for variation in materials, batching etc. and depends on the manufacturer's willingness to risk having low-strength concrete rejected. Typically, for cast in-situ concrete, $\bar{F}_1 = 1.25$ and $\sigma_{F_1} = 0.13$ while for precast concrete these become $\bar{F}_1 = 1.19$ and $\sigma_{F_1} = 0.06$ respectively. Both Normal and Lognormal distributions have been considered suitable.

The factor F_2 converts the control cylinder strength to the average in-place concrete strength. At 28 days it has a mean value of 0.95 for elements less than 450mm deep and 1.03 for deeper elements. At one year, these values are about 25% greater. The coefficient of variation in all cases is about 0.14. A Lognormal distribution appears

Table 8.8 Statistical parameters for k_{cp} and k_{cr} [Stewart, 1997].

| | k_{cp} | | k_{cr} for minimum curing times: | | | |
| | | | 3 days | | 7 days | |
Performance	Mean	COV	Mean	COV	Mean	COV
Poor	0.80	0.06	0.66	0.05	0.66	0.05
Fair	0.87	0.06	0.84	0.05	1.00	0.00
Good	1.00	0.00	1.00	0.00	1.00	0.00

to be the best probabilistic description for F_2. Using earlier published data, generally similar observations were made by Stewart (1995).

The strength estimate for control cylinders given by $f'_{ccyl} = F_1 \cdot F'_c$ can be considered in more detail, noting that it is a function of curing (k_{cr}) and compaction (k_{cp}) of the concrete [Stewart, 1995]:

$$f'_{ccyl} = k_{cp} \cdot k_{cr}(F'_c + 1.65 \ \sigma_{cyl}) \tag{8.7}$$

where the term ($F'_c + 1.65 \ \sigma_{cyl}$) represents the mean compressive strength of perfect control cylinders, σ_{cyl} is the standard deviation of the between-batch concrete strengths (see Table 8.6) and k_{cp} and k_{cr} are the compaction and the curing coefficients respectively. They are functions of workmanship and quality control, shown as 'performance' in Table 8.8.

The spatial variation of strength within a given structure, that is, the variation from point to point, also is of interest. For Canadian practice it was found to have a coefficient of variation of about 7% for one member cast from a single batch of concrete to about 13% for many members cast from a number of concrete batches. The coefficient for in-situ concrete strength, for yet-to-be-placed concrete (e.g. the design estimate of uncertainty), was estimated at about 23% [Barlett and McGregor, 1996].

The tensile strength of concrete and its modulus of elasticity have had some attention [Mirza et al., 1979], while probabilistic descriptions of creep and shrinkage properties have been discussed by Madsen and Bazant (1983).

Of particular interest in reinforced concrete construction is dimensional variability [Mirza and MacGregor, 1979a]. In most cases it has been found that the actual thickness of slabs is greater than the nominal thickness by ratios varying up to about 1.06, with a coefficient of variation up to about 0.08, but with corresponding values 1.005 and 0.02 for high quality bridge decks [Hueste et al., 2003; Nowak et al., 2012]. Similar values apply to precast slabs [Rakoczy and Nowak, 2012].

In contrast, the effective depth to the reinforcement for in-situ slabs appears to be generally less than specified, in the range (actual/nominal) 0.93–0.99 with a coefficient of variation of around 0.08. There is some evidence that these values are considerably better in good-quality work and that in precast slabs the deviation and variability is almost negligible [Mirza and MacGregor, 1979a]. Considerably fewer data are available for other concrete elements.

@Seismicisolation

8.5 Statistical Properties of Structural Members

8.5.1 Introduction

The probabilistic description for the strength or other properties of structural members depends on the probabilistic description of component properties for the member(s), such as the cross-sectional dimensions and material strengths. When probabilistic properties for the members are derived using mathematical relationships, differences between the derived result(s) and field or experimental results would be expected. In part this is due to inherent variability in experimental techniques and observations. The greater part of the difference, however, is the result of the simplification(s) introduced by the mathematical model used to relate material and geometric parameters to structural element behaviour. For example, in deriving an expression for the ultimate moment capacity of a reinforced concrete beam section, it is well known that assumptions are made about the concrete compressive stress distribution, about the form of the stress–strain relationships for the reinforcement, about the concrete tensile strength, etc. These assumptions usually are conservative. However, they add a degree of uncertainty to the transition from individual parameters to member strength. This variability is known variously as the 'modelling' uncertainty or the 'professional factor' (see also Chapter 2). It does not arise, of course, if the statistical properties of a structural member are obtained directly from 'extensive' experimental observations on the member itself. However, such tests are not always practical, and recourse may have to be made to modelling the member behaviour mathematically and using as input data information about the material and geometric probabilistic properties. These aspects are discussed further below.

8.5.2 Methods of Analysis

Let R represent the random variable strength of a structural member. It can be expressed in terms of material and geometric properties as a functional relationship:

$$R = \text{fn}(P, \mathbf{D}, \mathbf{R}_m) \tag{8.8}$$

where $\mathbf{R}_m$ is a vector of random variable material strengths, $\mathbf{D}$ a vector of random variable dimensions, cross-sectional areas, etc. (including those due to workmanship) and P is a so-called 'professional' or 'modelling' factor, a random variable which accounts for the accuracy of the model (expression) used to predict the actual strength from experimental observations, etc. If the relationship (8.8) is known explicitly and is of simple form, R can be evaluated rather easily using second-moment techniques. Otherwise simulation might be necessary to obtain the probability distribution of R. These approaches are outlined below.

8.5.3 Second-moment Analysis

In converting from parameter to member statistical properties, second-moment analysis can be used if the relationship between member strength and parameter properties is of simple form. For steel members, for example, this is the case for a number of important resistance properties. Thus, relationship (8.8) between test strength R and

nominal strength R_n (as determined from a code rule, say) can be expressed in a simple multiplicative form made up of random variables [Cornell, 1969a]:

$$R = \text{P.M.F.}R_n \tag{8.9}$$

where P is the professional factor as before but now used to allow for the difference between the actual strength and the nominal strength, M represents the material properties, such as yield strength, and F is the so-called 'fabrication' factor, representing sectional properties such as area and section moduli and including the effect of fabrication variability. The relationship between R and R_n will depend on how R_n is defined. The modelling factor P can account for this, but only if the multiplicative form of (8.9) is reasonably closely representative of reality. This is likely to be the case, for example, for beam bending but unlikely for columns subject to bending (see Section 8.4.5).

Typically, P, M and F are ratios of actual to nominal values and will have their own distributional properties. If it is assumed that each can be represented in second-moment format, then it follows that the estimated mean and coefficient of variation of R are (see A.166 and A.169):

$$\overline{R} \approx \overline{\text{P}}.\overline{\text{M}}.\overline{\text{F}}.R_n \tag{8.10}$$

and

$$V_R^2 \approx V_P^2 + V_M^2 + V_F^2 \tag{8.11}$$

where ( ) denotes the mean of the quantity and the V_i are coefficients of variation.

The nominal resistance R_n can be obtained directly from codes of practice, while the distributional properties of M and F have been discussed in the previous sections. The second-moment representation (8.10) and (8.11) usually is not strictly valid to represent all member properties, but it may be an acceptable approach, even for more complex member behaviour.

To apply the simplified approach of expressions (8.9)–(8.10), information is required about the professional or modelling factor P. For example, for the tensile strength of an element, no modelling error term is needed as this situation corresponds directly to the experimental observations used to derive the probability distribution for the material strength. On the other hand, for compact beam sections, with adequate lateral bracing, the resistance is given by the plastic stress and the modelling factor. The latter can be obtained directly from tests on beams for which simple plastic theory [Heyman, 1971] was the basis for analysis [e.g. Yura et al., 1978]. For example, in direct correspondence to (8.10):

$$R_{test} = \left(\frac{\text{test capacity}}{\text{nominal capacity}} \right)_{mean} \frac{\overline{F}_y}{F_{yn}} \frac{\overline{S}}{S_n} R_n \tag{8.12}$$

where $\overline{S}$ is the mean plastic section modulus, $\overline{F}_y$ is the mean yield stress, and S_n and F_{yn} are the corresponding nominal values. R_n is the nominal plastic moment. Typically, $\overline{\text{F}} = \overline{S}/S_n = 1.0$, $V_F = 0.05$, $\overline{\text{M}} = \overline{F}_y/F_{yn} = 1.05$ and $V_M = 0.10$ (see Tables 8.2–8.4).

Table 8.9 Typical ratios (of test to nominal resistance) for beams in the plastic range [Yura et al., 1978].

Beam type and moment type	Mean of test / nominal resistance: $\overline{P}$	Coefficient of variation: V_P	Number of tests
Determinate; uniform	1.02	0.06	33
Determinate; gradient	1.24	0.10	43
Indeterminate (also frames)	1.06	0.07	41

Table 8.10 Modelling statistics (Professional factor P) [Ellingwood et al., 1980].

Element type	$\overline{P}$	V_P	Remark
Tension member	1.00	0 00	
Compact wide flange beams			
Uniform moment	1.02	0.06	
Continuous beams	1.06	0.07	mechanism
Wide flange beams			
Elastic lateral torsional buckling	1.03	0.09	
Inelastic lateral torsional buckling	1.06	0.09	
Beam-columns	1.02	0.10	SSRC[a] column curves

a)   Structural Stability Research Council.

Beam test results show that resistance depends, among other things, on the moment gradient; typical values of $\overline{P}$ can be obtained from the ratio of mean test resistance to nominal resistance as shown in Table 8.9. The coefficients of variation V_P calculated from these ratios also are shown in Table 8.9. The value of V_P was obtained using (8.11) with V_R known from the scatter in the test results.

Generally similar but rather more complex analyses can be performed for beams laterally unsupported (for which elastic or inelastic buckling load is critical) for beam-columns, for plate girders, etc. The models that could be used in conjunction with the present approach to predict actual strength and the relevant model errors have been described in the literature [e.g. Yura et al., 1978; Bjorhovde et al., 1978; Cooper et al., 1978], including using more modern models for strength properties [e.g. Nowak et al., 2012]. Ideally these are then calibrated against actual detailed observations, such as described by Byfield and Nethercot (1998) for steel members subject to lateral-torsional buckling, a case of member behaviour not readily built up from more elemental information. Some typical values for $\overline{P}$ and V_P are shown in Table 8.10 [Ellingwood et al., 1980].

The main limitation of the above approach is that a purely second-moment interpretation is taken of all the parameters. As shown earlier, this is not necessarily sufficient for properly modelling steel yield strength or for modelling other parameters. Further, the probability distribution of the modelling or professional factor is not necessarily well

described simply in second-moment terms, and separable as in equation (8.9). For these and other reasons it may be necessary to turn to simulation.

8.5.4 Simulation

For the derivation of member properties from (non-Normal) dimensional and material properties or when there are complex relationships between them, simulation may be the only viable approach. Consider, for example, the strength of reinforced concrete beam-columns. It is well known that according to ultimate strength theory the strength of a beam-column can be represented in terms of a locus of points in the $N - M$ plane, where N represents axial thrust and M bending moment. The implicit relationship between N, M and various parameters is given, in conventional reinforced concrete theory notation, by [Ellingwood, 1977]:

$$N = \frac{M}{e} = 0.85 f'_C b(\beta_1 c) + A'_S(f'_S - 0.85 f'_C) - A_S f_S \tag{8.13a}$$

$$M = 0.85 f'_C b(\beta_1 c) \left(\frac{h}{2} - \frac{1}{2}\beta_1 c \right) + A'_S(f'_S - 0.85 f'_C) \left(\frac{h}{2} - d' \right) + A_S f_S \left(d - \frac{h}{2} \right) \tag{8.13b}$$

where e is the eccentricity measured from the centroid, c is the depth to neutral axis, $\beta_1 c$ is the depth to the resultant of compression stress 'block', h is the depth of the section, b is the breadth of section, d and d' are the concrete covers for the tensile and compressive reinforcements, A_S and A'_S are the areas of the tensile and compressive reinforcements, and f_S and f'_S are the stresses in tensile and compressive reinforcement respectively.

Because there are two strength terms, N and M, the resistance of a beam-column may be expressed in a variety of ways including:

(1) fixed N;
(2) fixed M;
(3) fixed eccentricity e;
(4) any other combination with variable N and M.

Approach (1) may be appropriate for earthquake-type situations, whereas approach (3) is probably appropriate for the usual design situation where axial thrust and moment increase roughly in proportion owing to the nature of the applied loading. For any particular analysis it is necessary to make the most appropriate choice consistent with the expected desired outcomes [Frangopol et al., 1997a]. Since the aims of a design or an analysis depend in part on the characteristics of each individual project or case, the choice may be difficult in code calibration work. Approach (4) may be relevant in complex structures but may not always be tractable or even feasible (*cf.* Section 5.1).

With known statistical properties for each of the variables in (8.13), conventional Monte Carlo simulation can be used to generate a sample distribution of resistance values. A typical result is shown in Figure 8.4 for the case of fixed eccentricity [Ellingwood, 1977]. The simulation procedure is shown schematically in Figure 8.5; it is evident that since the distribution of the resistance is desired with most interest over the whole region rather than only the tails, relatively few Monte Carlo simulations are required to obtain reasonable results, typically 100–500. However, simulation may need to be
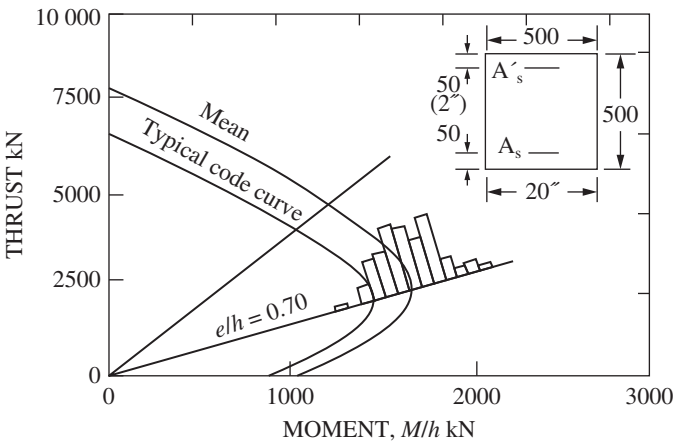
Figure 8.4 Typical member strength simulation results for reinforced concrete beam-columns [reproduced from Ellingwood (1977) by permission of American Society of Civil Engineers].
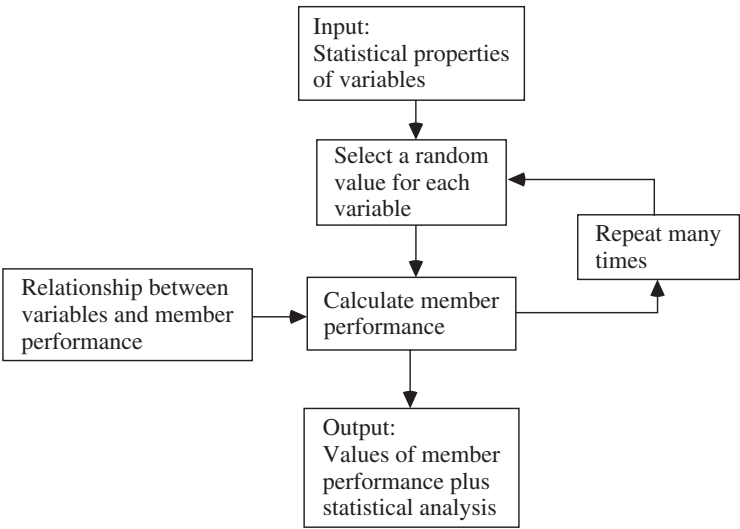
Figure 8.5 Simulation procedure for member strength statistical properties.

more extensive if good-quality modelling of the tails is required, such as is typical in reliability calculations.

Unfortunately, Expressions (8.13) do not predict the actual (or experimental) strength of beam-columns very accurately since they are nominal relationships used for code (or nominal) strength determination. If strengths predicted by (8.13) are compared with experimental data, it would be possible to obtain the ratio of test strength to calculated strength for each Monte Carlo sample and hence the mean and standard deviation for this ratio. Thus the 'professional' factor of the previous section would be found. However, owing to the poor predictability of (8.13), there would be much scatter in the ratio, i.e. its coefficient of variation would be high. If it is desired to get good prediction of expected

strength, better-quality relationships describing material and structural behaviour are necessary.

For example, a better relationship between N, M and e can be obtained by integrating the stress-strain curves for the steel and concrete to obtain the moment-curvature relationships for a given N and hence noting that failure occurs at the peak of the curve. This is a standard procedure for calculating beam-column strength [e.g. Tall, 1964; Frangopol et al., 1997b] and generally has been found to agree reasonably well with experimental observations. Grant et al., (1978) found that for reinforced beam-columns the theoretical approach slightly underestimated the available test data. The mean value of the ratio R_T/R_S (i.e. test strength to simulated strength) was found to be 1.007 with a coefficient of variation of 0.064. This factor can be further subdivided into:

(1) error due to the theory used to find the simulated strength;
(2) errors due to the test procedures used to determine the test strength;
(3) errors due to in-batch variability of concrete strength, of reinforcement strength and of dimensional variability.

For simplicity, the relationship might be expressed as

$$\frac{R_T}{R_S} = C_{T/S} = C_{\text{model}} C_{\text{testing}} C_{\text{in-batch}} \tag{8.14}$$

and, if a second-moment approach is used [see(A.169)],

$$V_{T/S}^2 \approx V_{\text{model}}^2 + V_{\text{testing}}^2 + V_{\text{in-batch}}^2 \tag{8.15}$$

From these expressions C_{model} and V_{model} can be determined if estimates for the other correction factors are available. Typically V_{testing} is in the range 0.02–0.04 and $V_{\text{in-batch}}$ is about 0.04. (These could be determined experimentally or by Monte Carlo simulation.) The respective means are approximately unity. It follows readily that $C_{T/S}$ has a mean of approximately 1.00 and a coefficient of variation $V_{T/S}$ of 0.03–0.046, the latter value corresponding to good-quality testing ($V_{\text{testing}} = 0.02$) [Mirza, 1996]. A general similar correction factor was found to be appropriate for other reinforced (and prestressed) concrete elements, such as beams [Allen, 1970; Ellingwood et al., 1980].

With an accurate procedure to predict actual (i.e. test) results, the ratio of actual to nominal strength, for an element, can be determined. For this, the nominal values of all the various parameters (stresses, dimensions, etc.) are substituted into the code rules to obtain a nominal resistance. Then by using Monte Carlo simulation, and the probability distributions for each parameter, accurate theoretical predictions of strength are obtained, each of which is then modified by the correction factor, $C_{T/S}$, to predict actual strengths. The ratio R_T/R_n (i.e. test strength to nominal strength) is found for each prediction, and, after a sufficient number of Monte Carlo trials, the mean and coefficient of variation are determined. Hence $\overline{R}/R_n$ and V_R are available. Note that, by directly determining predicted test strength and nominal strength, no explicit mention need be made of the 'professional factor' of Section 8.5.3. Some typical values of $\overline{R}/R_n$ and V_R for normal reinforced concrete elements are given in Table 8.11 based on US data and design codes [Ellingwood et al., 1980].

Table 8.11 Typical resistance statistics for reinforced concrete elements ($F'_C = 34\ MPa \approx 4800\ ksi$).

Action	Description	$\overline{R}/R_n$	COV = V_R
Bending	Continuous one-way slabs	1.22	0.15
Bending	Two-way slabs	1.12-1.16	0.14
Bending	Beams	1.05-1.16	0.08-0.14
Bending and axial	Short columns, compression failure	0.95	0.14
Bending and axial	Short columns, tension failure	1.05	0.12
Axial load	Slender columns, compression failure	1.10	0.17
Axial load	Slender columns, tension failure	0.95	0.12
Shear	No stirrups	0.93	0.21
Shear	Minimum stirrups	1.00	0.19

For steel structures similar analyses can be performed [e.g. Nadolski and Sykora, 2015] and calibrated against detailed test results and comparisons to models [e.g. Byfield and Nethercot, 1998; Rebelo et al., 2009].

8.6 Connections

The data available for structural connections in both steel and reinforced concrete construction are rather limited [Nadolski and Sykora, 2015]. Data quoted by Fisher et al. (1978) for fillet welds in tension, in which the welding electrodes were matched to the parent steel, indicate that the actual strength is on average about 1.05 of that specified, with a coefficient of variation of 0.04.

For fillet welds in shear, the ratio of fillet weld shear strength to weld electrode tensile strength typically is about 0.84, with a standard deviation of 0.09 and coefficient of variation of 0.10 (whichever is maximum). The ratio of fillet weld shear strength to specified strength is then $0.84 \times 1.05 = 0.88$, with a coefficient of variation given by $V = (0.1^2 + 0.04^2)^{1/2} = 0.11$. For this simple situation, there is little need to have a factor to account for modelling. However, fabrication of the weld will produce additional variability. $V_F = 0.15$ has been suggested [*cf.* Fisher et al., 1978].

Butt or 'groove' welds may be considered to develop the strength of the parent metal provided that they are adequately fabricated and correctly specified [Fisher et al., 1978].

Data and probabilistic models for the strength of high-strength bolts in tension, in shear and in friction grip configuration have been described by Fisher and Struik (1974) and Fisher et al. (1978).

8.7 Incorporation of Member Strength in Design

Because rolled steel sections and reinforcing bars are available only in discrete sizes, generally it will be the case that a greater section, or more bars, is provided at the end of the design process than strictly is required according to the calculations. Therefore the actual resistance of elements usually will be greater than that determined thus far. Occasionally designers will select downwards, for example if the error is less than, say, about 5%, but generally an upward selection to the next largest section of next whole number of bars is made. Thus the ratio of strength provided to strength required,

called the 'discretization factor', would be expected to have a mean greater than 1.0 and the corresponding probability distribution function would be expected to be skewed. Figure 8.6 shows a typical relationship for reinforced concrete columns [Mirza and MacGregor, 1979a]; similar graphs can be drawn for structural steel sections.

A typical probability density function obtained by simulation and not limiting over-design, is shown in Figure 8.7. Table 8.12 indicates a size effect for the discretization factor for reinforced concrete elements; this is greatest for flexural reinforcement
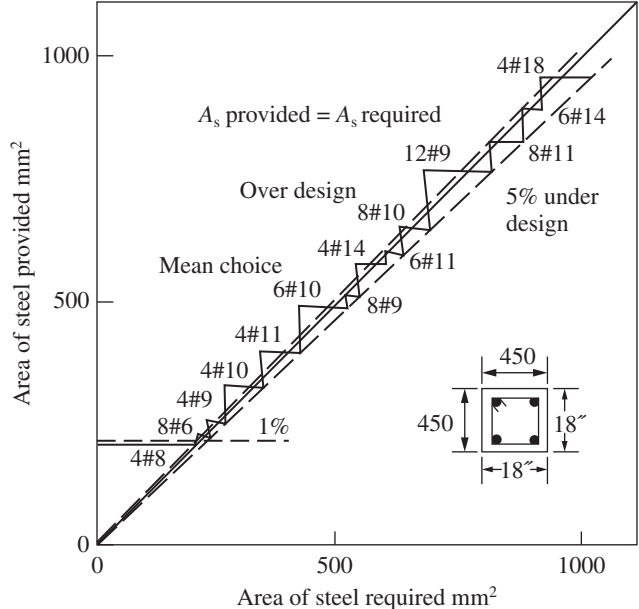
Figure 8.6 Effect of discrete sizes on actual strength provided for reinforced concrete columns [based on Mirza and MacGregor (1979a) with permission from ASCE].
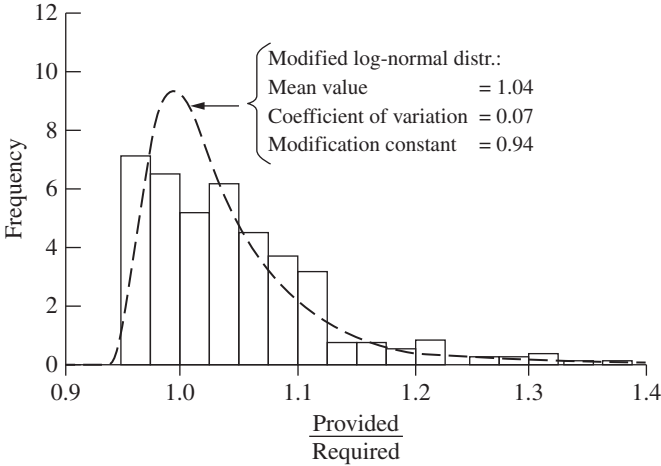
Figure 8.7 Typical probability density function for ratio of provided to required capacity for reinforcement concrete beams [reproduced from Mirza and MacGregor (1979a) with permission of ASCE].

Table 8.12 Typical statistical properties for discretization.

Element	Size mm × mm (in × in)	Mean of (provided/required)	Coefficient of variation	Remarks
Flexural reinforcement in	250 × 375 (10 × 30)	1.04	0.07	LN: c = 0.94
reinforced concrete beams	500 × 750 (20 × 30)	1.00	0.03	LN: c = 0.90
Stirrups (reinforced)		1.03	0.06	LN: c = 0.93
Vertical steel	300 × 300 (12 × 12)	1.03	0.06	LN: c = 0.93
Reinforced concrete columns	900 × 900 (36 × 36)	1.01	0.04	LN: c = 0.91
Steel beam-columns*		1.05	0.07	

LN = modified Lognormal distribution in which [log(provided / required) − c] is normally distributed.
Source: Mirza and MacGregor (1979a), * Lind (1976a).

in beams for the parts of the probability distribution away from the lower tail. Since the lower tail of strengths usually is of interest in reliability calculations, size effects often may be ignored. For reinforced concrete design generally, however, a discretization factor with modified Lognormal distribution, $c = 0.91$, a mean of 1.01 and coefficient of variation of 0.04 appears a reasonable choice.

It is important to note that the discretization factor does not take into account possible human error in the design process, nor does it consider self-checking or other checking. It is based entirely on assumptions of reasonable under-design (and over-) design.

8.8 Conclusion

Typical resistance properties for use in a structural reliability analysis were reviewed in this chapter, with particular reference to properties for steel members, concrete strength properties and structural element dimensions.

Usually the properties for structural members as distinct from those for samples are required for a reliability analysis. These can be obtained directly from experiments but also from the combination of the statistical properties of material strength, dimensions and design models. This combination can be done using a second-moment or a Monte Carlo analysis and thus to arrive at the member statistical properties and hence plausible probabilistic models for member behaviour. Comments on connections and on systematic overdesign due to discrete sizing close this chapter.

9

Codes and Structural Reliability

9.1 Introduction

The design of structures using a structural design code, or an equivalent regulation, may be described as 'structural proportioning by delegated professional authority' [Lind, 1969]. All designers required to use a particular design code are forced to follow one algorithm (usually) to achieve 'their' design. Key steps in the structural proportioning process have been predetermined for the designer by the rules in the design code. Thus any structural design for which a particular code was used reflects the 'design' of the code itself. It follows that the formulation of a structural design code directly influences the bulk detailed proportioning of all structures that will be designed using that code. The individual designer is left free to model the structure and to determine layout, main dimensions, connection types, support and loading conditions, etc., largely independent of the structural design code, but once such decisions have been made, the detail design in most cases is prescribed by code rules. Of course, where (parts of) the design code is not applicable or when there are no relevant code rules or one or more rules are known to be incorrect, designers have no choice but to use their discretion, guided by the best available practice and understanding at the time. This chapter is not concerned with these latter situations but only with the application of probability notions for the development of the rules in structural design codes.

The objective of structural engineering design may be taken, reasonably, to be the maximization of the total expected utility of the structure, given a prescribed reference data set and availability of materials and labour. There are then two complementary aspects of the design task that must be considered:

(a) optimization of the total expected utility of the structure (by the designer);
(b) optimization of the structural design code (by code-writing committee).

The aim of the main part of this chapter will be to consider item (b), i.e. how a code should be formulated to be optimum for the range of structures for which it is likely to be used. In particular, attention will be confined to:

(1) safety-checking rules in code theory;
(2) likely formats for so-called limit state design codes;
(3) relationship of these codes to the theoretical reliability concepts introduced in the previous chapters.

Practical matters such as proper wording of requirements, interpretation, etc., will not be discussed. It will be assumed that physical models, such as those describing column strength, etc., are given and not subject to optimization, although clearly that would be a possibility. Fundamental aspects of code-writing philosophy have been discussed by Lind (1969, 1972), Legerer (1970), Veneziano (1976), Turkstra (1970), Ditlevsen (1997) and Brown et al. (2008). An overview of the earlier developments in design code formulation and the challenges in code writing is available [Ellingwood, 1994].

The dates on the above references span the period during which there was most interest in design code development underpinned by probability arguments and structural reliability theory. Most subsequent developments of practical national and international structural design codes are based on these principles and have followed similar trends. For this reason much of the remainder of this chapter is focussed on the principles involved in design code development rather than attempting to account for the current state of play of code development in various countries and by international groups.

9.2 Structural Design Codes

A structural design code can be viewed as a predictive tool, in the sense that the designer, having followed the requirements of the code, expects, like others such as his client(s), that the resulting structure to be sufficiently safe and sufficiently serviceable during the period of its expected life. However, at the design stage, some matters are not known with any degree of certainty and can only be predicted (see Section 2.2). The way that a code is structured to allow for these uncertainties will affect the expected utility of any structure designed using it.

The degree of optimality of the expected utility of a code will depend on the interests of those affected by it. The various requirements a particular structure is expected to satisfy will depend on whose viewpoint is considered. Interested parties usually include the builder, the owner, the eventual user and various regulatory authorities. Since these parties are unlikely to have identical requirements the structure must meet, there is the potential for conflict (see below).

Regulatory authorities and structural engineers tend to rate structural safety as a very important requirement. However, from the point of view of the other parties, safety might be seen as 'necessary but not sufficient' [Bosshard, 1979]; other matters such as serviceability and costs also are important. Mostly, in countries with well-established rules and traditions and a legacy of successful engineering, structural safety for other than major or unusual structures is seldom the governing criterion, even though it superficially may appear to be so in the rules given in a structural design code. Other requirements such as serviceability and performance often are hidden behind what appear to be safety requirements. The reason is that generally it is difficult to write specific performance and serviceability requirements or codified rules, despite increasing interest in so doing. It should be clear that the role of structural design codes is rather more complex than simply addressing structural safety. Their overall role might better be seen as one in terms of national economic competitiveness and structural decision-making.

A further complication is that structural design codes must be applicable to whole families of structures, each with details and with requirements at which a code-writing

committee can only guess on the basis of the experience of its members and advisors. Again, prediction is involved. It is unlikely that in a single Code the differing requirements of the many structures and the many interested parties within its scope can be reconciled completely. It follows, intuitively, that a code is likely to be more suited or optimal for some types of structures than it is for others (*cf.* Ditlevsen, 1997). As a result, it is very unlikely that theoretical notions of optimisation of a code *ab initio* will be successful.

The practical, alternative approach used by code committees is:

(1) recognise that many structural design codes have been in existence for some considerable time;
(2) assume that these codes represent the collective wisdom of the profession and reflect a degree of consensus arrived at over many years;
(3) unless there is contrary evidence accept that the existing design code rules have produced satisfactory outcomes including by implication the expectations of society; and
(4) develop the new generation codes and code rules around the implied safety and serviceability of previous generation codes.

Following through this process can be viewed as representing an alternative form of code optimization, now through refinement, or the gradual improvement of code provisions (and, perhaps, their presentation and complexity) through accumulated experience and trade-offs.

It follows that changes to a design code should be introduced only gradually. Not all possible direct and side-effects of a change may be apparent, except in the long term. Changes also should be sufficiently small so as not to cause uncertainty and anxiety to code-writing committees, to code users and to other interested parties within the scope of the code. It has been proposed that code revisions resulting in safety-level changes greater than about 10% are likely to alarm practitioners [Sexsmith and Lind, 1977].

Code changes that do not involve safety levels also should be treated carefully. Even without technical changes, the complexity of a code may be perceived to have increased with the introduction of changes of philosophy (e.g. change in format from permissible stress to limit state design without significant changes to safety levels). Complexity also can be perceived to increase with the introduction of more comprehensive rules. At one time such changes were made in Britain's CP110 reinforced concrete code at the same time as the change of measurement units, with the result that 'limit state design', rather than all the changes combined, was commonly held to be responsible for making design much more complex.

The major inconsistency in traditional (allowable stress or non–limit state design) codes was in dealing with safety checking, particularly as expressed in the rules for load combinations. For a long time it has been typical for there to be different structural design codes, each dealing with only one material or form of construction, such as steel, reinforced concrete, prestressed concrete and timber structures. Traditionally, each of these codes had a different set of load combination requirements. These were seldom consistent between codes.

The overall aim of design code reformulation has been to reduce or eliminate inconsistencies, to try to achieve uniformity for structural code safety levels, and to employ more rational rules for safety and serviceability checking. Such rules should require the

designer to check all relevant limit states explicitly (rather than implicitly as was the case in many older, allowable stress codes). A further, and important, aim is to make all code requirements as clear as possible to the code user, so that it is obvious which limit state is actually being checked and the logic behind that checking rule.

Finally, it is noted that while codes usually are labelled 'design' codes, in fact they are seldom suited for direct design. Instead they consist of rules for checking whether a proposed design complies with accepted rules. Strictly, therefore, the discussion here is about the format of rules for checking the expected safety (and performance) of proposed structures against standards that have been accepted by experienced structural engineering professionals (and by implication accepted by society).

9.3   Safety-Checking Formats

9.3.1   Probability-Based Code Rules

In principle, structural 'design' codes could employ refined probabilistic approaches to design checking, based on Level 3 procedures (see Table 2.11). Such codes might be termed 'probabilistic' codes. At first sight this might appear to be a natural, fundamental choice, if only designers had sufficient background and experience with them. However, there are some interesting matters to be addressed to make such codes acceptable in practice.

As noted in Chapter 2, the choice of probability distributions can affect the estimated probability of failure (see Section 2.3.5). If this choice is left to individual designers, quite different outcomes might result from the use of some particular part of the code (e.g. checking rules for reinforced concrete columns) by different individuals. This would not be a satisfactory outcome. Evidently, there is need for consensus about the probability density functions to be adopted. This applies for all loads and for all structural properties. It applies also to the formulation of limit state functions and even the various design conditions to be considered and checked.

Further, in developing a probabilistic design code, consensus is needed on the acceptance criteria applicable to different structural failure conditions. Thus the criterion for beam bending failure might be different from that for beam shear failure, simply because for most beams impending bending failure usually involves a degree of warning whereas shear failure does not, and these two scenarios are likely to have different consequences. Clearly, structural failure has economic and social consequences, and these cannot be isolated from acceptance criteria (see also Chapter 2). Further, as international trade in engineering services grows, it is becoming increasingly desirable, including economically, that there be greater consensus in structural design code rules and requirements across regional areas and national boundaries. Major efforts in this direction have been made within (and around) the European Community by the Joint Committee on Structural Safety (Vrouwenvelder, 1997; JCSS, 2008).

Existing safety-checking formats for use in practical structural design largely are developments of existing deterministic formulations, rather that having been developed from fully probabilistic codes. They are all at Level 1 (see Table 2.11), involve no obvious probability calculations for the code user (although some selection of a nominal 'return period' might be required) and are essentially similar in appearance to the traditional

safety-checking formats long used for reinforced concrete design. The only difference is that the partial factors (and capacity reduction factors) are derived from probabilistic data rather than being selected (perhaps rather arbitrarily) by a code committee. A number of possible safety-checking formats have been proposed. These are outlined in the sections to follow.

In principle it should be possible to relate the Level 1 safety-checking formats to the fully probabilistic codes when they are developed. This aspect is discussed briefly in Section 9.4. Rather more attention is devoted to the relationship between nominal probability of failure (Level 2) and Level 1 safety-checking formats. Sections 9.5 and 9.6 deal with the selection of safety levels and the concept of code calibration, that is, the process of relating the Level 1 safety-checking format to the implied safety of previously, perhaps already long-existing, older design rules. Section 9.7 gives an example of code calibration. This is followed, in Sections 9.8 and 9.9, by discussion of some of the fundamental and applied issues. Finally it is noted here that much of the development outlined below took place in the period 1970–1985 and that therefore there is a certain historical flavour to the presentation. Since that time there has been much application of the principles established in that period but little new theoretical development.

9.3.2 Partial Factors Code Format

The Partial Factors code format is the one adopted for European structural design codes. It was developed from earlier code formats. It is formulated in the space of the load effects (stress resultants) and has the following general form [CEB, 1976]:

$$g_R \left(\frac{f_k}{\gamma_{m1}\gamma_{m2}\gamma_{m3}} \right) \geq g_S(\gamma_{f1}\gamma_{f2}\gamma_{f3}Q_k) \tag{9.1}$$

where g_R and g_S are resistance and load effect functions that convert the ( ) terms to resistance and load effects respectively, f_k and Q_k are characteristic material strengths and loads respectively (see Section 1.4.4), and γ_{mi} and γ_{fi} are the respective partial factors.

The partial factors γ_{mi}, on material strength, take account of the following possibilities [CEB, 1976]:

(a) unfavourable deviations of the strengths of materials or elements from the specified characteristic value;
(b) differences between the strength of the material or element in the structure from that derived from control test specimens;
(c) local weaknesses in the structural material or element arising principally from, or in, the construction process;
(d) inaccurate assessment of the resistance of elements derived from the strength of materials, including the variations of the dimensional accuracy achieved in construction as they affect the element resistance.

The partial factors γ_{fi} on actions take account of the following possibilities:

γ_{f1} deviation of actions from their characteristic values;
γ_{f2} reduced probability that all actions are at their characteristic value (see load combination factor below);
γ_{f3} inaccurate assessment of the action effects, including dimensional inaccuracies.

In addition, either γ_m or γ_f may be modified to allow for low consequences of failure and/or the possibility of brittle failure.

A particular form of (9.1) adopted by CEB (1976) is

$$g_R \left(\frac{f_{k1}}{\gamma_{m1}}, \frac{f_{k2}}{\gamma_{m2}}, \dots \right) \geq g_S \left[\gamma_{f1_{max}} \gamma_{f3} \sum Q_{max} + \gamma_{f1_{min}} \gamma_{f3} \sum Q_{min} + \gamma_{f1_{mean}} \gamma_{f3} \sum Q_{mean} \right.$$
$$\left. + \gamma_{f1} \gamma_{f3} \left(\psi_{p1} Q_{k1} + \sum_{1=2}^{n} \psi_{pi} Q_{ki} \right) \right] \tag{9.2}$$

where $\psi_{pi} \leq 1$ are load combination factors with $\psi_{p1} Q_{k1}$ denoting the most unfavourable loading. Up to three load combination factors $\psi_{pi} \leq 1 \, (i = 1, 2, 3)$ may be involved.

The ψ_{pi} may be considered as the ratio of the arbitrary-point-in-time loading (see Chapter 7) to the characteristic value of that loading. Here Q_{max} and Q_{min} denote the dead load action (and other permanent actions) acting in the most unfavourable manner for the limit state being considered. Values for the parameters in (9.2) for various limit states are given in Tables 9.1 and 9.2. In this particular implementation, γ_{f3} has been incorporated into γ_{f1}.

Table 9.1 Partial factors for CEB code format (CEB, 1976).

Limit state	Load	Partial factors in limit state					
		$\gamma_{f1\,max}$	$\gamma_{f1\,min}$	$\gamma_{f1\,mean}$	γ_{f1}	ψ_{p1}	$\psi_{pi}, i \geq 2$
Ultimate	Fundamental	1.2	0.9	0	1.4	1.0	A
	Accidental	1.0	1.0	0	1.0	B	C
Serviceability	Infrequent	0	0	1.0	1.0	1.0	B
	Quasi-permanent	0	0	1.0	1.0	C	C
	Frequent	0	0	1.0	1.0	B	C

Note: table shows the coefficients for each limit state equation.

Table 9.2 Load combination factors for CEB code format.

	Load combination factors ψ_p		
	A	B	C
Domestic buildings	0.5	0.7	0.4
Office buildings	0.5	0.8	0.4
Retail premises	0.5	0.9	0.4
Parking garages	0.6	0.7	0.6
Wind	0.55	0.2	0
Snow	0.55		
Wind and snow	0.55 and 0.4		

Source: CEB, 1976.

Values for the material partial factors γ_{mi} are fixed by the code committee dealing with that specific material. For reinforced concrete, for example, typical values are $\gamma_m = 1.5$ for concrete and $\gamma_m = 1.15$ for steel reinforcement, given normal control, average inspection and 'normal' consequences of failure.

The characteristic values of the loads and resistances are considered as their 95 or 5 percentile values as appropriate, or as their currently accepted code values in lieu.

9.3.3   Simplified Partial Factors Code Format

A somewhat less complex safety-checking format is that adopted for use in Canadian building codes [NRCC (1977); CSA (1974); Allen (1975)]. It takes the form

$$\phi R \geq g_S[\gamma_D D_n + \psi(\gamma_L L_n + \gamma_W W_n + \gamma_T T_n + \ldots)] \tag{9.3}$$

The left-hand side represents factored resistance, composed of a single resistance R, derived from characteristic strengths and characteristic material properties, dimensions, etc., and a single partial factor ϕ. The right-hand side consists of (a number of) factored load effect(s), where the function $g_S[\ ]$ converts the loads to load effects.

The partial factors γ_D, γ_L, γ_W and γ_T apply to the nominal dead load D_n, live load L_n, wind load W_n, etc. The partial factors are related to an 'importance factor' γ_I which is a measure of the consequences of failure. For most ordinary structures, $\gamma_I = 1.0$. For structures, such as hospitals, which must survive a natural or other disaster γ_I is set at greater than unity. The partial factors are then related to γ_I, e.g. $\gamma_D = 1.25$ γ_I normally, and 0.85 γ_I when D_n counteracts L_n, etc. For structures of lesser importance, or for structures subject mainly to dead load, γ_I is in the range 0.8–1.0.

The load combination factor ψ accounts for the reduced probability that L_n, W_n and T_n reach their nominal values simultaneously. Typically ψ takes on values 1.0, 0.7 and 0.6 respectively for one, two or three loadings to which it applies acting concurrently.

The NBC safety-checking format is derived from the earlier (non-probabilistic-based) safety-checking format of the American Concrete Institute (ACI) [e.g. MacGregor, 1976]. It is similar to the CEB format for load combinations, although the numerical values are somewhat different. However, the major difference lies in the treatment of resistance calculations. Whereas the CEB format uses factored material strengths, factored dimensions, etc., to allow for the possibility that the material, dimensions, etc., may be less than anticipated, the NBC format (and the LRFD format of Section 9.3.4) combines all the member understrength and geometrical error terms into the factor ϕ. This factor is intended to reflect the probability that the member as a whole is understrength.

The main disadvantage of the NBC safety-checking format is that it does not always allow adequately for the strength variance of members composed of different materials. If the axial load and moment are calculated for a given eccentrically loaded column using a Monte Carlo approach, a spread of results will be obtained [Grant et al., 1978]. As can be seen from Figure 8.5, the spread of results is much smaller for columns failing in tension. This could be predicted using the CEB safety-checking format, but not the NBC format (or LRFD format). Other examples, indicating that partial factors on material strengths are preferable to those on member strength, have been given by Allen (1981b). However, the major advantage of the NBC safety-checking format is that of simplicity, i.e. ϕ needs to be considered only once in calculations.

9.3.4 Load and Resistance Factor Code Format

A slightly simpler code format is the 'load and resistance factor' design safety-checking format adopted for use in US codes (Ravindra and Galambos, 1978). It has a compact form:

$$\phi R_n \geq \sum_{k=1}^{i} \gamma_k S_{km} \tag{9.4}$$

where ϕ and R_n are the 'resistance factor' and 'nominal resistance' as used conventionally in US practice, such as in the earlier (non-probabilistic) ACI safety-checking format, the γ_k are the 'load factors' or partial factors, and S_{km} denotes the 'mean load effects'. Note that compared with (9.3), this format combines the load effects rather than the loads themselves. Where the relationship between loading and load effect is linear, such forms are, of course, equivalent.

From a series of calibration exercises involving only simple second-moment concepts (see also Section 9.6) it was found that four specific versions of (9.4) were sufficient for most design situations, i.e. only four load combinations need be examined [Ravindra and Galambos, 1978]. These are

$$\phi R_n \geq \gamma_D \ \overline{D} + \gamma_L \ \overline{L} \tag{9.5a}$$

$$\phi R_n \geq \gamma_D \overline{D} + \gamma_{apt} \overline{L}_{apt} + \gamma_W \overline{W} \tag{9.5b}$$

$$\phi R_n \geq \gamma_D \overline{D} + \gamma_{apt} \overline{L}_{apt} + \gamma_S \overline{S} \tag{9.5c}$$

$$\phi R_n \geq \gamma_W \overline{W} - \gamma_D \overline{D} \tag{9.5d}$$

where $\overline{D}$ is the load effect due to the mean dead load, and $\overline{L}$, $\overline{W}$ and $\overline{S}$ are the means of the maximum lifetime live load, maximum lifetime wind load and maximum lifetime snow load respectively; γ_D, γ_L, γ_W and γ_S (each > 1.0) are the corresponding load factors, and $(\ )_{apt}$ represents the arbitrary-point-in-time value (or 'sustained' values; see Chapter 7). The load factor $\gamma_D < 1.0$ refers to the minimum dead load effect $\overline{D}$.

Expression (9.5b) is equivalent to the CEB format with $\gamma_{apt} \ \overline{L}_{apt}$ equivalent to $g_s(\gamma_{f1} \gamma_{f3} \Psi_{pi} Q_{ki})$ in (9.2) for the case of wind and live and dead load, except that Q_{ki} refers to the characteristic load (a 'maximum'), whereas $\overline{L}_{apt}$ is in the nature of a mean load. Similar comparisons can also be made for the other formulations [Ellingwood et al., 1980]. Compared with the CEB format (9.1, 9.2), the LRFD format has the advantage of being very similar to safety-checking formats previously in use in many countries, as well as having fewer load combinations that need to be considered. Thus, for a situation with dead, live, wind and snow loading, the CEB safety-checking format (9.1) requires checking of 32 load combinations, the simplified (NBC) format (9.3) requires 14 and the LRFD format requires 4 (including in each case load reversal due to wind uplift).

9.3.5 Some Observations

The safety-checking formats sketched above show different complexities; this implies that code-writers have considerable freedom in choosing a format. If too many partial factors are chosen, it may not be possible to derive consistent values for them all; in

theory the ideal number of variables (in this case the number of partial factors) is equal to the number of degrees of freedom of the problem. Conversely, if for simplicity and practicality only a few partial factors are used, it must be expected that they will not be an ideal fit and thus not constant over all design situations. In this case the safety-checking format has to apply to too great a range of possibilities. In effect, each partial factor now includes a number of sources of uncertainty or variability. The net effect of simplicity is that conservative values for partial factors must be used in order to cover all likely design situations. While this may simplify the mechanics of the design-checking process, it is possible also that there may be an associated structural cost penalty in some situations.

As noted, it is usually considered desirable to have the same safety-checking format for all codes across all materials, in particular in terms of load combinations. In principle, therefore, the safety-checking format should be independent of the material used for the structure. Variation in material strength and behaviour would then be included in the ϕ or γ_{mi} factors only.

9.4 Relationship Between Level 1 and Level 2 Safety Measures

Traditionally safety factors were selected largely on the basis of intuition and experience [e.g. Pugsley et al., 1955]. However, the availability of Level 2 probability methods (see Table 2.11) has made it possible to relate probabilistic safety measures such as p_{fN} or β to the partial factors of the Level 1 safety-checking formats, provided that some simplifications and approximations are accepted. The relationships developed below are not strictly necessary for practical code calibration, but they are useful in illustrating that there is a reasonable link between Level 1 and Level 2 safety measures.

The discussion to follow will be in terms of the time-integrated approach of Section 6.2. This means that specific reference to time-dependent behaviour of loads and resistances, etc., may be neglected provided that the appropriate (extreme value) probability distributions are used for the variables, and an appropriate load combination rule is employed.

Also, as noted earlier, reliability assessments for code work are made without detailed knowledge of the specific loads, materials and workmanship likely to apply or to be used in the actual project. Thus all such properties are predictions of some possible future implementation. This means that reasonably conservative parameters and probability density functions should be used. In turn, this means that the nominal failure probability and the corresponding safety index so calculated do not necessarily bear a close relationship to the nominal failure probability and safety index that would be obtained on the basis of data for the completed structure. This is an important matter for the safety checking of existing structures as distinct from safety checking for proposed (new) structures.

In order to keep in mind that it is a predicted value on the basis of quite uncertain information, the nominal failure probability and the corresponding safety index used in this chapter for code calibration will be denoted p_{fC} and β_C respectively. The distinction between p_{fN} and p_{fC} (and β and β_C) normally is not made in the structural reliability literature. However, it might clarify the difference in the nominal failure probability as used in code work and that used more generally—see also Sections 2.5.

9.4.1 Derivation from FOSM / FOR Theory

Recall from Chapter 4 that a vector of basic (Normal) random variables $\mathbf{X}$ can be standardized to $\mathbf{Y}$ through (4.3) or $y_i = (x_i - \mu_{X_i})/\sigma_{X_i}$. Also, the coordinates of the checking point $\mathbf{Y}_i^*$ in $\mathbf{Y}$ space are given by $y_i^* = -\alpha_i\beta$ (see 4.6) with α_i defined in (4.5). From these two expressions it follows that the coordinates of the checking point in $\mathbf{X}$ space are $x_i^* = \mu_{X_i} - \alpha_i\beta\sigma_{X_i}$ ($i = 1, \ldots, n$). When the $\mathbf{X}$ space is non-Normal, expression (4.44) must be used instead. Hence

$$x_i^* = F_{x_i}^{-1}[\Phi(y_i^*)] = \mu_{X_i}(1 - \alpha_i\beta_C V_{X_i}) \tag{9.6}$$

with the second equality applying only for Normal random variables and with the sign convention as adopted in Chapter 4. Similarly, the limit state function evaluated at the checking point $\mathbf{x}^*$ is

$$G(\mathbf{x}^*) = G\{F_{\mathbf{X}}^{-1}[\Phi(\mathbf{y}^*)]\} = G[\mu_{X_i}(1 - \alpha_i\beta_C V_{X_i})_{i=1,\ldots,n}] = 0 \tag{9.7}$$

This limit state function in the basic variables (e.g. material strengths, dimensions, loads) must be compatible with the appropriate safety-checking format chosen.

Let the subset X_i, $i = 1, \ldots, m$ be the resistance basic variables. Converting from means to characteristic values by the use of (1.24), the second part of (9.6), for FOSM, becomes

$$x_i^* = \mu_{X_i}(1 - \alpha_i\beta_C V_{X_i}) = \frac{1 - \alpha_i\beta_C V_{X_i}}{1 - k_{X_i} V_{X_i}} x_{ki} \tag{9.8}$$

where k_{X_i} represents the appropriate coefficient corresponding to the characteristic fractile of the Normal distribution (e.g. Table 1.3). Equation (9.8) may be written also as

$$x_i^* = \mu_{X_i}(1 - \alpha_i\beta_C V_{X_i}) = \frac{x_{ki}}{\gamma_{mi}} \tag{9.9}$$

where $1/\gamma_{mi} = (1 - \alpha_i\beta_C V_{X_i})/(1 - k_{X_i} V_{X_i}) = x_i^*/x_{ki}$ is defined as the partial factor on the resistance random variables.

Similarly, let X_i, $i = m + 1, \ldots, n$ represent loading basic variables. Then, using (1.25):

$$x_i^* = \mu_{X_i}(1 - \alpha_i\beta_C V_{X_i}) = \frac{1 - \alpha_i\beta_C V_{X_i}}{1 + k_{X_i} V_{X_i}} x_{ki} \tag{9.10}$$

$$= \gamma_{fi} x_{ki} \tag{9.11}$$

where $\gamma_{fi} = x_i^*/x_{ki}$ is defined as the partial factor on the load random variables.

The limit state equation (9.7) now becomes

$$G\left(\frac{x_{ki}}{\gamma_{mi}}, \ldots, \gamma_{fj} x_{kj}, \ldots\right) = 0, \quad i = 1, \ldots, m, \quad j = m + 1, \ldots, n \tag{9.12}$$

This expression contains the partial factors γ_{kj}. It is in a format similar to that of the various limit state design safety-checking formats described above.

Since (9.12) is also given by $G(\mathbf{x}^*) = 0$, it follows directly that the general expressions for γ_i are

$$\gamma_{mi} = \frac{x_{kj}}{x_j^*} = \frac{x_{kj}}{F_{X_i}^{-1}[\Phi(y_i^*)]} \tag{9.13a}$$

$$\gamma_{fj} = \frac{x_j^*}{x_{kj}} = \frac{F_{X_j}^{-1}[\Phi(y_j^*)]}{x_{kj}} \tag{9.13b}$$

with, as is easily verified, the second equality being applicable when $\mathbf{X}$ consists of non-Normal random variables.

It is important to note that the γ_i values are not necessarily unique. In reduced variable space, selection of a point $\mathbf{y}^{(1)}$ different from the checking point $\mathbf{y}^*$ (see Section 4.2) will lead to different α_i and hence to different γ_i values. Selecting different mean values for the basic variables (but leaving σ_{X_i} unchanged) will give, in general, a new set $\mathbf{y}^{(1)}$ for the checking point in the $\mathbf{Y}$ space. As a result, the set $\{\gamma\}$ will not necessarily be constant but may be a function of the mean or characteristic values selected for the basic variables. (Such a set of values is called a 'calibration point' below). This is an important observation and highlights the need for clear definition and consistency in code calibration work.

9.4.2   Special Case: Linear Limit State Function

If the limit state function is linear, and attention is confined to just one load case, the above results are much simplified. In the notation of Section 1.4.3, the limit state function is now

$$G(\mathbf{X}) = Z = R - S \tag{9.14}$$

with

$$\mu_Z = \mu_R - \mu_S \tag{9.15}$$

and

$$\sigma_Z = (\sigma_R^2 + \sigma_S^2)^{1/2} \tag{9.16}$$

The latter can be linearized, approximately, to [Ravindra et al., 1969]:

$$\sigma_Z \approx \alpha(\sigma_R + \sigma_S) \tag{9.17}$$

where α, the 'separation' function, is approximately constant, with a value $\alpha = 0.75 \pm 0.06$ for $\frac{1}{3} \leq \sigma_R/\sigma_S \leq 3$ and with an error $< 10\%$ (Figure 9.1). From (1.22) it follows that $\mu_R - \mu_S = \beta(\sigma_R^2 + \sigma_S^2)^{1/2}$ so that using (9.17) yields

$$\mu_Z = \mu_R - \mu_S \geq \alpha\beta_C(\mu_R V_R + \mu_S V_S) \tag{9.18}$$

The 'central' safety factor λ_0 (see Section 1.4.4) is obtained by rearranging (9.18):

$$\lambda_0 = \frac{\mu_R}{\mu_S} \geq \frac{1 + \alpha\beta_C V_S}{1 - \alpha\beta_C V_R} \tag{9.19}$$

@Seismicisolation
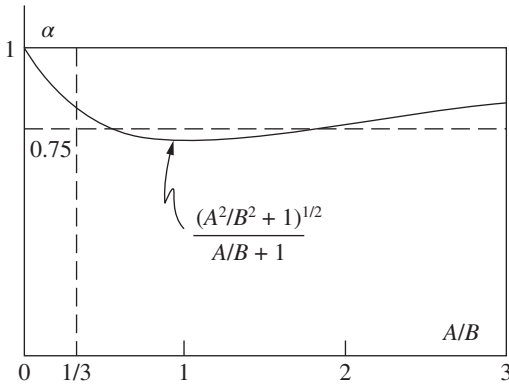
Figure 9.1 Variation in separation function α.

Using (1.24), (1.25) and (1.26) the 'characteristic' safety factor is then

$$\lambda_k = \frac{R_k}{S_k} = \frac{\mu_R(1 - k_R V_R)}{\mu_S(1 + k_S V_S)} \tag{9.20}$$

so that

$$\frac{R_k}{S_k} \geq \frac{(1 - k_R V_R)}{(1 - \alpha\beta_C V_R)} \frac{(1 + \alpha\beta_C V_S)}{(1 + k_S V_S)} \tag{9.21}$$

or

$$R_k \geq \gamma_R \gamma_S S_k \tag{9.22}$$

Evidently, (9.22) is in a partial factor format, and comparing with (9.20) and (9.21) it is seen that $\gamma_R = (1 - k_R V_R)/(1 - \alpha\beta_C V_R)$ is the partial factor for resistance, and that $\gamma_S = (1 + \alpha\beta_C V_S)/(1 + k_S V_S)$ is the partial factor for load effect. Comparing with the load and resistance factor format (9.4) it is seen immediately that $\phi = 1/\gamma_R$.

The partial factors γ may be assigned values by noting that, for agreed percentiles for the nominal (or 'design') resistance and the nominal (or 'design') loads, the values of k_R and k_S are known. It then remains to fix β_C to obtain γ_R and γ_S. The selection of an appropriate β_C value (or p_{fC}) is therefore central to the derivation of partial factors.

It will be seen that (9.9) and (9.11) for the resistance and loading partial factors respectively, are identical with the forms given in (9.21) when it is recognized that the separation function α (see 9.17) is a special case of the direction cosines (or sensitivity factors) α_i for the reliability problem with two basic variables. In fact, for two basic variables, $X_1 = R$, $X_2 = S$ with $G(\ ) = R - S = 0$, it is not difficult to show that $\alpha_R = \alpha$ and $-\alpha_S = \alpha$. [The sign change is necessary since $(\alpha_R, \alpha_S) = \alpha$ defined in Figure 4.2 is a vector, whereas α in (9.17) is a simple variable.]

9.5 Selection of Code Safety Levels

The selection of an appropriate value of β_C (or p_{fC}) in (9.21) is not an easy matter. As discussed in Chapter 2, appropriate *a priori* values for the structural probability of failure

@Seismicisolation

either over the planned life span, or per annum, are not readily available. Moreover, for codified safety-checking rules, it is not some external acceptable failure probability that is particularly relevant, for the reasons discussed in Chapter 2, but the notional failure probability p_{fC} (and the corresponding safety index β_C). As noted, this may bear very little relationship to any real or imputed p_f.

As discussed in Section 9.2, the approach usually adopted is that codes should be 'calibrated' against existing practice. This means they are calibrated against the implied accepted levels of structural safety. Thus, provided the safety levels implicit in existing design codes are perceived to be adequate, any new generation code should be framed in such a way that, for particular design situations, it has average safety levels not significantly different from those implicit in the previous generation code. Of course, there will be variation of β_C across different design situations, both in the existing code rules and in any new set of code rules. Such variation is likely to be somewhat different between generations of codes. In any case, a reasonable target is to design a new code so as to attempt to obtain a reasonably constant value of β_C across the code requirements most representative of practical design, and with relatively low variability.

The calibration approach to (structural) safety requirements outlined above has its limitations, particularly in the way it accounts for the probability of failure due to human variability and human error (Section 2.5). However, even without the presence of human error and variability it would be expected that β_C need not be constant over all designs, since, as also discussed in Chapter 2, a complete analysis should consider the risk and consequences of failure. Thus a cheap but critical component should have a relatively higher β_C value. In contrast, a load combination having very low probability of occurrence could have a relatively lower β_C value. Such allowances are difficult to consider and make in a rational manner owing to the impossibility of predicting the consequences of failure for every application of the structural design code rules. It could be expected that, in principle, codes can be written to allow a trade-off between expected consequences of failure and partial factors, but this appears to have been done so far only to a very limited extent (e.g. lower load factors for farm buildings, higher load factors for buildings with post-disaster functions).

9.6 Code Calibration Procedure

There is broad agreement on the procedure to be followed for code calibration, and this was used in a number of pioneering calibration efforts [e.g. Allen, 1975; Baker, 1976; CIRIA, 1977; Hawrenek and Rackwitz, 1976; Guiffre and Pinto, 1976; Skov, 1976; and Ravindra and Galambos, 1978]. However, probably the most influential document in practical and illustrative terms was the work for the American National Standard A58 (Minimum Design Loads in Buildings) [Ellingwood et al., 1980]. Most subsequent probabilistically-based code calibration work has followed a generally similar approach. The essential steps in the calibration process are [Lind, 1976b; Baker, 1976; Ellingwood et al., 1980]:

Step 1: Define Scope   Since it is unrealistic to expect one structural design code format to represent all design situations, it is convenient to limit the scope of the code to be

calibrated. Thus the material may be prescribed (e.g. steel structures), the structural type may be prescribed (e.g. building structures), etc.

Step 2: Select Calibration Points A design space, consisting of all basic variables, such as beam lengths, cross-sectional areas and properties, nominal permitted yield stresses, range of applied loads and loading types, continuity conditions, etc. is chosen. This is then divided into a set of approximately equal discrete zones (e.g. a simply supported 5m mild steel beam, supporting 25 m^2 precast concrete flooring of given dead load and to be designed for normal office loading). The resulting discrete valued points are used to calculate β_C values for the safety-checking format of the existing code (see below).

It is important that the effect of changes in the code format be considered for all possible designs for which the code will be used. This means that a range of realistic calibration points must be selected.

Step 3: Existing Design Code The existing structural design code(s) is now used to design the element (i.e. the 5 m beam). This is repeated for all appropriate combinations of calibration points within each discrete zone.

Step 4: Define Limit States Limit state functions are defined for each limit state, usually corresponding with those already explicit (or implicit) in existing codes. For example, in the case of steel beams, this might include limit states for bending strength, shear strength, local buckling, web buckling, flexural-torsional buckling, etc. Each of these limit states must be expressed in terms of the basic variables.

The definition of limit states may involve the use of appropriate strength models of the type described in Chapter 8 to convert strength basic variables to member strength, etc. These models should be realistic rather than code-based conservative approximations. See also the discussion in Section 8.5.

The definition of the limit states also requires a decision about the load combination model(s) to be employed (*cf.* Chapter 7). For most practical code calibration efforts to date, a simple load combination model, such as Turkstra's rule (6.144), has been used.

Step 5: Determine Statistical Properties Appropriate statistical properties (distributions, means, variances, average-point-in-time values) for each of the basic variables are required for the determination of β_C. Data such as given in Chapter 7 for loads and Chapter 8 for resistances can be used.

Step 6: Apply Method of Reliability Analysis Using an appropriate method of reliability analysis, assumed here to be the FOSM method, together with the limit state functions (Step 4) and the statistical data (Step 5), each of the designs obtained in Step 3 is analysed to determine β_C for each calibration point within each zone. The results could be arranged such that the applied loading becomes the chief independent parameter. Typical results, obtained for the American National Standard A58 (Minimum Design Loads in Buildings Code) [Ellingwood et al., 1980], using the FOSM/FOR algorithm (Section 4.4.4), are shown in Figures 9.2 and 9.3. For a given floor area supported ($A_T = 37m^2$) both different material combinations and loading situations are illustrated.

Figure 9.3 shows clearly that the existing code(s) safety-checking rules do not produce uniform β_C values even in the one design situation [e.g. reinforced concrete (RC) beam bending].
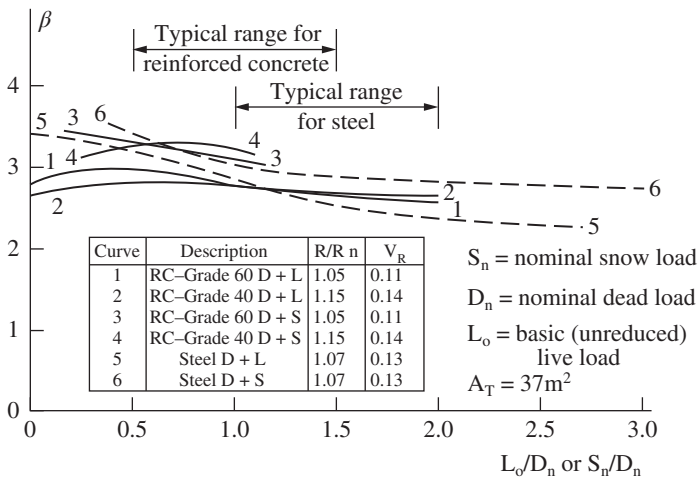
Figure 9.2 β index for steel and reinforced concrete beams in the existing code: gravity loads [Ellingwood et al., 1980].
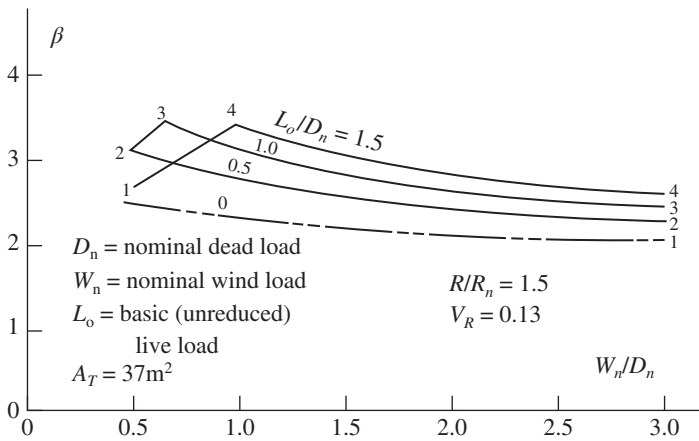
Figure 9.3 β index for steel beams in the existing code: gravity plus wind loads [Ellingwood et al., 1980].

As noted earlier, the β_C values obtained in this process depend very much on the probability models and the parameters chosen for the basic variables, and other calibration exercises may find β_C values considerably different from those shown in Figures 9.2 and 9.3. Provided the data used to obtain β_C are used consistently throughout the whole calibration process this should not be of concern (see Section 9.2).

Step 7: Select Target β_C Value From repeated analyses such as Step 6 above, the variation of β_C in the existing design practice becomes evident. In a purely internally consistent calibration exercise (i.e. developing a new code on the basis of the acceptable general level of safety of the old code) it would be appropriate to use this information to determine a weighted-average β_C. This would then be used as the target safety index β_T.

In principle, some allowance could be made for consequences of failure, with higher β_T values for high-consequence failures. In practice, this is seldom feasible, owing to the lack of appropriate information. One approach is simply to note the complexity of the issue and for the code committee to select β_T values semi-intuitively, such as on the basis of 'experience'. For example, for the ANS A58 work, $\beta_T = 3$ was selected for dead and live load (snow load) combinations, $\beta_T = 2.5$ for dead, live and wind and $\beta_T = 1.75$ under earthquake loads [Ellingwood et al., 1980]. These appear to correspond reasonably well with the range of values obtained from analysing the then existing (US) design codes, as illustrated in Figures 9.2 and 9.3. Exceptions are masonry structures, for which β_C ranges from 4 to 8, and for glue-laminated timber members, for which β_C ranges from 2.0 to 3.0 with a strong mean of 2.5. These divergences could (and should) be dealt with most appropriately by means of the partial factor(s) on material strength or resistance (e.g. through the ϕ factor).

For load combinations involving earthquake loading, β_T typically is significantly lower than for the more common load combinations. Although the consequences of structural failure caused by earthquakes usually are high, the forces involved in high reliability earthquake-resistant design are also high, suggesting that the value of β_T in this case reflects a trade-off between cost of initial construction and cost of failure consequences. As noted in Section 2.5, this is a complex issue, both for code calibration and philosophically.

Step 8: Observe Partial Factor Format Implicit in Existing Code   Although not essential, it is often useful to be able to see how the safety-checking format of the existing code converts to the partial factors in the safety-checking format of the new code, given that the β_T value has been set. The process to obtain these partial factors is essentially the reverse of the process of Step 7. For a given calibration point, the β_C value is calculated for a given limit state, using the existing code safety-checking format to determine the resistance. If $\beta_C < \beta_T$ the required resistance is suitably increased until $\beta_C = \beta_T$ is obtained. The checking point as well as the direction cosines α_i (of second moment theory) are then calculated. From these, the partial factors γ_i can be computed from (9.8) and (9.9). This process is then repeated for different calibration points and the variation in partial factors noted. Obviously, the partial factors would not be expected to be constant over all calibration points since β_C generally is not constant. For the revision of the A58 code, typical results are shown in Figure 9.4. Evidently, the ϕ factor (on resistances) is relatively constant over a wide range of L_n/D_n and W_n/D_n for a given material. (It is also rather insensitive to differences in material.) Although somewhat lower ϕ values occur for low L_n/D_n or W_n/D_n values, these are not in the design range commonly employed. Associated with these lower ϕ values are significant changes in γ_L and γ_W, although γ_D is much more uniform for wide ranges in applied loading.

It should be clear, therefore, that it is reasonable to uncouple the resistance and the loading partial factors as shown in Equation (9.22) and as discussed in Section 9.4.

The values of γ_D obtained from analysing US standards in this way are rather lower than expected, being around 1.1. In part, this is a result of the relatively lower variability in dead load. Further, the value of γ_L in Figure 9.4 is low since it applies to the average-point-in-time value of the live-load L_{apt} (*cf.* Chapter 7).

Step 9: Select Partial Factors   As seen above, the partial factors are not constant for a given code safety-checking format and given value of β_T. For normal design it is convenient for
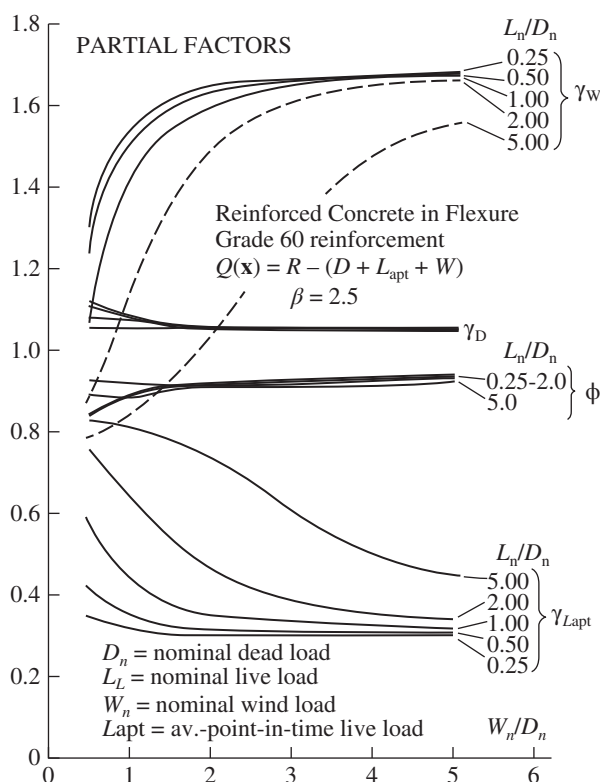
Figure 9.4 Variation of γ and ϕ factors for new safety-checking format for steel beam bending in the existing code rules [Ellingwood et al., 1980].

the partial factors in the code safety-checking format to be constant, at least over large groups of design-checking situations. To achieve this some deviation from β_T is to be expected. Hence, the selection of appropriate partial factors involves a certain amount of subjective judgement.

For a given range $1, \ldots, m$ of calibration points, the partial factors that best approximate the uniform target reliability can be obtained, in principle, by minimising the value of a measure of 'closeness' to the target reliability. In principle the approach that should be adopted is to minimize the weighted least-squares error in β_T:

$$S = \sum_{i=1}^{m} (\beta_T - \beta_{Ci})^2 w_i \tag{9.23}$$

where $p_{fCi} = \Phi(-\beta_{Ci})$ is the nominal probability of failure for a given calibration point i, $p_{fT} = \Phi(-\beta_T)$ is the target value and w_i is a weighting factor to account for the importance of the calibration point relative to design practice. The weighting factors sometimes must be selected subjectively but obviously $\sum_{i}^{m} w_i = 1$. In some cases $\log p_{fC}$ rather than β_C has been proposed for use in (9.23) in an attempt to make S relatively

@Seismicisolation
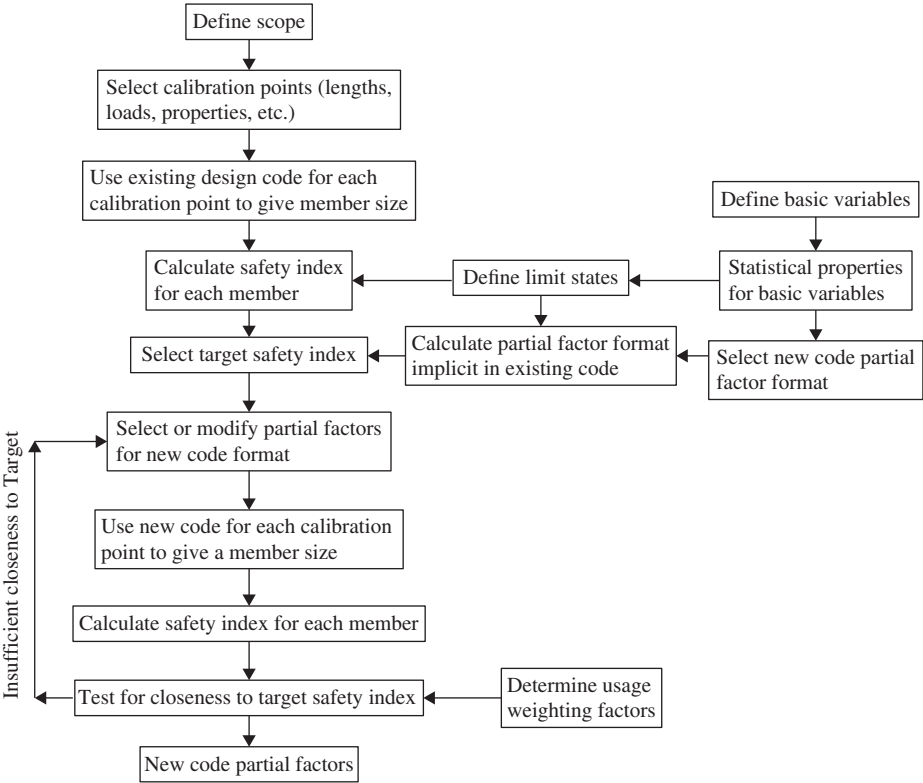
Figure 9.5 Flow chart for calibration of code safety-checking format.

more sensitive to very low values of the nominal failure probability. In principle, maximization of the socio-economic criterion using decision theory (see Section 2.4.2) would require that the most logical measure to use is p_f (or its surrogate $p_{fC} \approx p_{fN}$) since only p_f is compatible with costs [*cf.* Ditlevsen, 1997]. In addition, an upper limit such as $S \leq 0.25$ might be imposed so as to limit the deviation between target and calibration values.

To determine the partial factors for the new design code-checking format, trial values of the partial factors are used with the new generation code format to calculate β_C for each calibration point (*cf.* Steps 3–6 above). This result is substituted into (9.23). By repeated trial and error, and perhaps by (arbitrarily) assigning values to one or more partial factors, the set of partial factors minimizing (9.23) can be obtained. These values will then be the partial factors in the new generation code safety-checking format. The complete process for calibration is summarised in Figure 9.5.

9.7 Example of Code Calibration

To illustrate the calibration process, consider the following example for steel beam bending. This defines the scope (Step 1) for calibration. For simplicity, let it be assumed that the calibration is to be done in the load space and that no allowance

for live load reduction will be made. Also only dead load plus live load is considered and wind loading is ignored. Let the existing code safety-checking format for this situation be

$$R_n = (LF)(D_n + L_n) \tag{9.24}$$

where $(LF) = 1.7$ is the load factor, and all values are nominal values. By expressing L_n in terms of D_n, it will not be necessary to deal specifically with beam size, length, area supported, etc. Hence the calibration points have been selected. Equation (9.24) specifies the required resistance, given the nominal loads L_n and D_n which the resistance rules of the code must satisfy. In general, R_n will be a function of material and geometric properties as well as the resistance modelling rules selected by code committees.

Let the new code format be of the load and resistance factor design (LRFD) type (Section 9.3.4) given by $\phi R_n = \gamma_D D_n + \gamma_L L_n$ and let it be assumed, for simplicity, that the specification of D_n, L_n and R_n is not changed. This means that the code calibration exercise reduces essentially to one of finding a new load combination rule(s). It is now required to determine ϕ, γ_D and γ_L such that β_C is approximately constant and consistent with the existing code.

For beam bending, the limit state function formulated in the load space is (Step 4)

$$G(x) = R - D - L = 0 \tag{9.25}$$

where R is determined from codified beam-bending rules.

For Step 5, statistical properties for D, L and R are given in Chapters 7 and 8. For the present example let it be assumed that [*cf.* Ellingwood et al., 1980]

$$\frac{\mu_R}{R_n} = 1.18 \text{ (beam bending)}, \qquad V_R = 0.13$$

$$\frac{\mu_D}{D_n} = 1.05, \qquad V_D = 0.10$$

$$\frac{\mu_L}{L_n} = 1.00, \qquad V_L = 0.25$$

where, as before, the subscript n refers to 'nominal' values, i.e. values in the existing loading and resistance (or material) codes. These values correspond approximately to 'characteristic' values. For purposes of illustration in this example, each variable will be assumed Normal distributed. Of course, more generally R is often Lognormal, and L is extreme value type I; this can be treated easily using the first-order reliability (FOR) method but would destroy the simplicity of the example given here.

The reliability analysis, Step 6, may be performed using the FOSM method. Working in the original basic variable space (since (9.25) is linear):

$$\beta_C = \frac{G(\mu_{\mathbf{X}})}{\sigma_G}$$

where

$$G(\mu_{\mathbf{X}}) = \mu_R - \mu_D - \mu_L = 1.18\,R_n - 1.05\,D_n - 1.0\,L_n$$

and from (9.24)

$$R_n = (LF)\left(1 + \frac{L_n}{D_n}\right)D_n$$

so that

$$G(\mu_{\mathbf{X}}) = 1.18(LF)\left(1 + \frac{L_n}{D_n}\right)D_n - 1.05\,D_n - \frac{L_n}{D_n}D_n \tag{9.26a}$$

Further

$$
\begin{aligned}
\sigma_G^2 &= (\mu_R V_R)^2 + (\mu_D V_D)^2 + (\mu_L V_L)^2 \\
&= \left[1.18(LF)\left(1 + \frac{L_n}{D_n}\right)D_n \times 0.13\right]^2 + (1.05\ D_n \times 0.1)^2 + \left(0.25\frac{L_n}{D_n}D_n\right)^2 \\
&= D_n^2 \left\{ \left[0.153(LF)\left(1 + \frac{L_n}{D_n}\right)\right]^2 + (0.105)^2 + \left(\frac{0.25\ L_n}{D_n}\right)^2 \right\} \tag{9.26b}
\end{aligned}
$$

Consider now the case $L_n/D_n = 1.0$; then

$$\beta_C = \frac{2.36\,(LF) - 2.05}{[(0.306(LF))^2 + 0.0735]^{1/2}} \tag{9.27}$$

and if $(LF) = 1.7$ (the existing code value), then $\beta = 3.34$. The above process now may be repeated for a number of other L_n/D_n values (i.e. calibration points). A plot similar to Figure 9.2 would be obtained. On this basis, a target safety index can be selected (Step 7). Let this be $\beta_T = 3.0$ for purposes of illustration.

The partial factors implicit in the existing code formulation (9.24) may be determined as follows (Step 8). For $L_n/D_n = 1.0$ and for $\beta_T = 3.0$ it follows from (9.26) that, by trial and error, $(LF) = 1.7$.

Let the variables R, D and L be transformed to the 'reduced' variable space defined by (*cf.* Chapter 4)

$$r = \frac{R - \mu_R}{\sigma_R} = \frac{R - 1.18(LF)(1 + L_n/D_n)D_n}{1.18(LF)(1 + L_n/D_n)D_n V_R}$$

so that

$$\frac{R}{D_n} = 0.482r + 3.705$$

$$d = \frac{D - \mu_D}{\sigma_D} = \frac{D - 1.05D_n}{1.05D_n V_D}$$

giving

$$\frac{D}{D_n} = 0.105d + 1.05$$

$$l = \frac{L - \mu_L}{\sigma_L} = \frac{L - L_n}{L_n V_L}$$

or

$$\frac{L}{D_n} = 0.25l + 1.0$$

In reduced space the limit state equation $G(\mathbf{x}) = R - D - L$ now becomes

$$g(\mathbf{y}) = (0.482\ r - 0.105\ d - 0.25l + 3.705 - 1.05 - 1.0)D_n$$

The direction cosines α_i follow from (4.5):

$$c_r = \frac{\partial g}{\partial r} = 0.482\,D_n$$

$$c_d = \frac{\partial g}{\partial d} = -0.105\,D_n$$

$$c_l = \frac{\partial g}{\partial l} = -0.25\,D_n$$

and

$$l = \left[\sum_i \left(\frac{\partial g}{\partial y_i} \right)^2 \right]^{1/2} = 0.553\,D_n$$

so that

$$\alpha_r = \frac{0.482}{0.533} = 0.872$$

$$\alpha_d = -\frac{0.105}{0.533} = -0.190$$

$$\alpha_l = -\frac{0.25}{0.533} = -0.452$$

The partial factor for resistance is given by (9.9):

$$\phi = \frac{1}{\gamma_i} = \frac{(1 - \alpha_i \beta_C V_{X_i})}{(1 - k_{X_i} V_{X_i})} = \frac{x_i^*}{x_{ki}}$$

or

$$\phi = \frac{1}{\gamma_i} = (1 - \alpha_i \beta_C V_{X_i})\frac{\mu_X}{x_{ki}}$$

where x_k is the 'characteristic' value. This corresponds to the nominal value here. Substituting for R,

$$\phi = \frac{1}{\gamma_R} = [1 - 0.872(3)(0.13)](1.18) = 0.779$$

For loads the partial factors are given by (9.10) and substituting in a similar manner:

$$\gamma_i = \frac{x_i^*}{x_{ki}} = \frac{(1 - \alpha_i \beta_C V_{X_i})}{(1 + k_{X_i} V_{X_i})} = (1 - \alpha_i \beta_C V_{X_i})\frac{\mu_X}{x_{ki}}$$

@Seismicisolation

so that

$$\gamma_D = [1 + 0.19(3)(0.10)](1.05) = 1.11$$
$$\gamma_L = [1 + 0.452(3)(0.25)](1.0) = 1.34$$

Hence the partial factor format at $L_n/D_n = 1$ for $\beta_T = 3$, corresponding to the existing code format and the data given above, is

$$0.78 \, R_n \geq 1.11 \, D_n + 1.34 \, L_n$$

i.e. $\phi = 0.78$, $\gamma_D = 1.11$ and $\gamma_L = 1.34$. Again, the above process may be repeated for a number of other values of L_n/D_n (i.e. calibration points) and the results graphed (cf. Figure 9.4).

For purposes of illustration, let it now be decided that, for the adopted code format $\phi R_n = \gamma_D D_n + \gamma_L L_n$, the values for ϕ and γ_D are selected (arbitrarily) at $\phi = 0.80$ and $\gamma_D = 1.2$. The remaining γ_L is sought. A trial-and-error procedure is required.

Let the first trial be $\gamma_L = 1.4$. Then

$$R_n = \frac{1}{0.8}(1.2D_n + 1.4L_n)$$

so that, using (9.26a), the mean value of the limit state function is given by:

$$G(\mu_{\mathbf{X}}) = \mu_G = \frac{1.18}{0.8}\left(1.2 + 1.4\frac{L_n}{D_n}\right)D_n - 1.05D_n - \frac{L_n}{D_n}D_n$$

and the variance is given by (see 9.26b):

$$\sigma_G^2 = \left[\frac{1.18}{0.8}\left(1.2 + 1.4\frac{L_n}{D_n}\right)D_n \times 0.13\right]^2 + (1.05D_n \times 0.1)^2 + \left(\frac{L_n}{D_n} \times 0.25\right)^2 D_n^2$$

It follows that

$$\beta_C = \frac{\mu_G}{\sigma_G} = \frac{1.77(1 + 1.167L_n/D_n) - 1.05 - L_n/D_n}{[0.053(1 + 1.167L_n/D_n)^2 + 0.011 + 0.0625(L_n/D_n)^2]^{1/2}} \tag{9.28}$$

The solution of (9.28) in terms of β_C and p_{fC} values is given in Table 9.3 for various values of L_n/D_n (calibration points), together with an illustrative set of weighting factors and the calculation of S (Equation 9.23) using the $\log p$ version.

Table 9.3 Parameters for sample code calibration.

L_n/D_n	β_C	p_{fC}	$\log p_{fC}$	w_i	$S = (\log p_{fT} - \log p_{fC})^2 w_i$
1	3.14	0.84×10^{-3}	−3.07	0.2	0.0080
2	3.09	1.00×10^{-3}	−3.00	0.4	0.0068
3	3.05	1.14×10^{-3}	−2.94	0.3	0.0015
4	3.02	1.26×10^{-3}	−2.90	0.1	0.0001
$\beta_C =$	3.0	1.35×10^{-3}	−2.87	$\sum = 1$	$S = 0.0164$

@Seismicisolation

These calculations can be repeated for other trial values of γ_L; say $\gamma_L = 1.3$. In the expression for β_C the constant 1.167 is then replaced by 1.083 and a new value for S can be determined. Trial values for γ_L are chosen until the minimum value of S is found. The corresponding γ_L would be the value most consistent with $\beta_T = 3.0$. Naturally, the procedure could be repeated also for the partial factors ϕ and γ_D if desired.

9.8   Observations

9.8.1   Applications

The principles outlined above have been applied successfully for determining partial factor safety-checking formats for codes dealing with the design of the various elements of building structures. For these, many of the required statistical data have been collected and the necessary theoretical models constructed. However, most structures are more than the collection of their elements, and it is well known that there is considerable reserve capacity in many framed structures (see also Chapter 5). However, for various reasons, as indicated in Section 5.6, the application of probability and reliability analysis to structural systems has not yet been developed to the same intensity as for structural elements. The matter is largely unresolved and remains a challenge for research.

Calibration concepts for elements have been applied not only to building structure codes but also to bridge design codes [e.g. Nowak and Lind, 1979; Flint et al., 1981; Ghosn and Moses, 1985b]. The task appears to be more difficult owing to the nature of bridge loading, the influence of fatigue and the need to consider stability limit states, all of which are important for bridges. These phenomena also have been more difficult to quantify in probabilistic terms and, in some cases, do not easily allow the resistance to be separated from the load effects.

The application of code calibration has been extended also to other materials. It has been largely completed in various countries for timber structures [Ritter and Nowak, 1994; Mettem and Tietz 1999; Gauther, 2010] and for structural brickwork [e.g. Glanville, et al., 1996; Laird, et al., 2005] but also has raised some new issues to be resolved. Calibration exercises have revealed quite high, but varied, values for the safety index implied by current design codes. For example, for timber design, it is generally the case that the ratio μ_R/R_n (mean to nominal resistance) is much higher than for steel or reinforced concrete members. This appears to be due to the conservatism of existing timber design strength rules, largely to allow for the high variability in material properties and to allow for member and material imperfections [Ellingwood, 1977]. As a result, when reasonable target reliabilities are used with accepted loads for calibration purposes, the ϕ factor tends to be greater than unity (as R_n is so low). This is not a desirable result, and adjustment of the strength rules (i.e. R_n) to achieve $\phi \approx 0.8$ would be desirable. The ϕ factor can then be used as a parameter to express workmanship and quality of construction. An essentially similar situation exists for masonry structures.

The calibration referred to so far has been phrased in terms of 'ultimate' limit states. In principle, the calibration concept is also applicable to 'serviceability' (or any other) limit states. Serviceability limit states might include short- and long-term deflection, vibration, cracking and crack size. However, the situation is somewhat complicated

by the need to consider the implications or consequences of serviceability limit state violation and how this may influence the definition of serviceability failure. For example, in the case of deflection, there may be damage to other parts of the building, to partitions and to operating parts (e.g. lifts). There may be also a visual aspect (e.g. visible sag of floor) and a sensory aspect (e.g. sliding or unevenness of furniture). Thus, although criteria for maximum deflections have been set in many structural design codes, it is unclear how these relate to actual serviceability failure defined (Leicester and Beresford, 1977; Galambos and Ellingwood, 1986).

Despite these comments, the principal ideas of serviceability limit states are clear enough. For example, the limit state for deflection might be written as

$$G[\delta_L, \Delta(t)] = \delta_L - \Delta(t) \tag{9.29}$$

where δ_L is an allowable deflection limit and $\Delta(t)$ is the deflection at time t due to applied loading. Here $\Delta(t)$ can be obtained directly from structural analysis. Usually elastic analysis is sufficient. It would be an uncertain quantity as the loading (and the structural behaviour) is uncertain. However, since models for serviceability behaviour tend to be less developed than those for strength, the uncertainty in $\Delta(t)$ is likely to be higher.

The deflection criterion δ_L might be a constant or an uncertain quantity. The latter is possible since there are considerable difficulties with specification of serviceability criteria. This is because they are associated with subjective human reactions. Relatively few data are available in this area; in any case the variability is likely to be high, with coefficients of variation in the range 0.2–0.5.

As noted above, there are difficulties in defining appropriate criteria for the limit states for serviceability, as there is likely to be dependence between the criteria and the consequences of limit state violation. Some attempts have been made for simple systems such as simply supported reinforced concrete or steel beams in office and car-park construction (e.g. Stewart, 1996a,b).

The reference period for maximum sustained loading (see Section 7.4.5) for serviceability considerations typically is much lower than that for ultimate strength conditions and might be taken as one year if the serviceability state is recoverable (i.e. no permanent damage after removal of the load). Similarly, the target reliability index is likely to be lower than for ultimate strength. Values of $\beta_C = 1.6$ to 2.0 for an 8-hour reference period were obtained by Galambos and Ellingwood (1986) and $\beta_C = 2.0$ was used by Philpot et al. (1993) for timber beams. It has been suggested that the probability of serviceability failure typically should not exceed 0.10 during any one tenancy for irreversible damage and annually for reversible damage. This is roughly equivalent to $\beta_C = 1.28$ (Ellingwood, 1983).

9.8.2   Some Theoretical Issues

From the example given in Section 9.7 it should be clear that code calibration is by no means an objective exercise. The selection of the safety-checking format, the range of points used for calibration, the probability distributions employed for the variables in the calibration, the degree of linearization of the safety margin over the design space, the choice of minimum acceptable safety indices for various load combinations and materials, and the choice of minimum acceptable partial factors all require subjective assessment and choice.

Because the number of partial factors is limited even though the safety-checking format must cater for a wide range of structures, it is to be expected that the new code rules will be more conservative for some structural designs than for others and may even be un-conservative for some. This is clear from the minimization performed with expression (9.23). Moreover, if it is found that the residual S in (9.23) cannot be reduced to a sufficiently low value, it is likely that (i) the safety-checking format is too simple and will need more variables (partial factors), (ii) the range of structures or failure conditions being covered is too great or (iii) the range of the basic variables covered by the safety-checking format is too great. In principle, it is desired that the format chosen for safety checking be one that allows the smallest possible value of S to be obtained in calibration. Of course, in practice the safety-checking formats have been chosen for apparent convenience of designers and to minimize changes from existing practice. This is clear from the discussion in Section 9.3.

It follows from the above and also from the discussion of 'tail sensitivity' (Section 2.3.5) that comparison between β_C values obtained from different calibration exercises is meaningless without definition of the assumptions made in each calibration process. This applies also to a completely probabilistic code format.

Finally, philosophically the minimization of S only has meaning if it can be related to some over-riding optimization principle [e.g. Ditlevsen, 1997]. As discussed in Chapter 2, socio-economic optimization using net present value is widely accepted as appropriate. It then follows that S must relate to this criterion. As noted already in passing in Section 9.6, this can be the case only if p_f or its surrogate p_{fC} is used in (9.23).

9.9 Performance-Based Design

As noted in the earlier sections, robust methods for structural and other reliability analysis and estimation are available, together with a body of organized knowledge for loadings and resistances. This has opened up the possibility of adding other requirements, such as structural and other performance requirements, when probabilistic notions are used in a design process. This has been termed Performance-Based Design [SEAOC, 1995; Ghobarah, 2001; Augusti and Ciampoli, 2008; Ciampoli et al., 2011].

In Chapter 1 (*cf.* Section 1.1) it was noted that performance requirements for structures include limit states such as safety, functionality and comfort. More generally, the design of a structure must meet a broader range of requirements. These can be meeting damage measures such as loss of occupant comfort and damage to structural and nonstructural components in a building, due to excessive vibration or displacements. The likely number of casualties, economic losses or some threshold that represents the collapse or loss of serviceability during a hazard event also may be included.

To date the performance-based design concept has been used mostly for earthquake and wind engineering but is extending more widely. This has interesting implications. For traditional Codes, most decisions about the design specifications are made by individuals selected to sit on Code committees. However, since performance-based design focuses on wider issues, in principle many others ('stakeholders') could be involved.

The overall concept for performance-based design is shown, schematically, in Figure 9.6. The final design, say $g(\mathbf{d})$, can be considered to be a function of a vector of design or decision variables ($\mathbf{d}$) that have to meet, at some level of probability, a specified
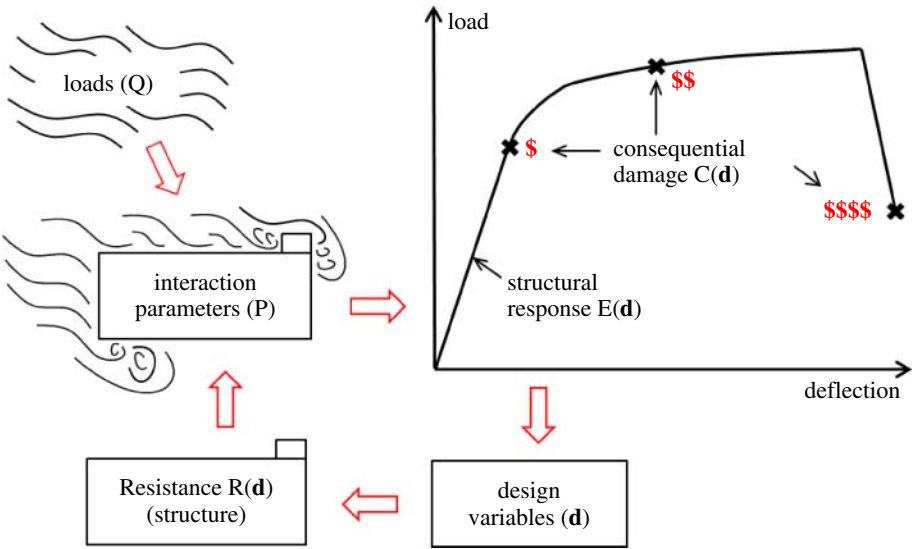
Figure 9.6 Schematic relationship between variables in performance-based design.

Table 9.4 Overview of variables and parameters in performance-based design.

Variable	Simple description	Examples	Performance-based design terminology
d	Design variables	sizes, heights, areas, location	Decision variables DV
C	Consequential damage	costs and other consequences of damage	Damage measures DM
E	Structural responses	deflections, stresses, accelerations, inter-story drift	Engineering demand parameters EDP
P	Parameters	aerodynamic coefficients (e.g. drag, inertia coefficients)	Interaction parameters IP
Q	Loads	mean wind velocity, turbulence intensity, direction, etc.	Intensity measures IM
R	Resistances	materials, strengths, geometry	structural parameters SP

set $\mathbf{d}^*$. Let this be denoted $P(\mathbf{d} > \mathbf{d}^*) > \delta$, a predefined probability of acceptance. In principle, δ must be decided prior to the performance-based design process. Table 9.4 shows the variables that are involved in $\mathbf{d}$ and gives typical examples for each variable. The (conditional) dependency structure between the variables is shown in Figure 9.6. Table 9.4 also shows the terminology used in the more specialized treatments of the subject [SEAOC, 1995].

@Seismicisolation

The main steps in the performance-based design process [Petrini and Ciampoli, 2012] are to select the relevant parameters as in Table 9.4 followed by the design process. The first step is to use structural mechanics to determine the structural responses and then assess whether the design constraints $\mathbf{d}^*$ are met. If not, the process is to refine the design through modification of some or all of the parameters and to repeat the process. This can be done, for example, using an optimization algorithm to do most or all of the repetitive work (Chapter 11). It is possible also to integrate the outcomes of the process as a set of conditional steps, as follows:

$$g(\mathbf{d}) = P(\mathbf{d} > \mathbf{d}^*)$$
$$= \iiint \iint g(\mathbf{d}|C) f(C|E) f(E|P, Q, R) f(P|Q, R) f(R) f(Q) dC\ dE\ dP\ dR\ dQ \quad (9.30)$$

The above integral looks complex, and it is indeed difficult to evaluate in practical problems. However, it conveys the main ideas of performance-based design. Starting from the outer integral, the idea is that the response of interest g(**d**) is integrated over:

1. the whole spectra of random load intensities (Q), instead of being computed only for one or two nominal values, corresponding to one or two mean return periods;
2. the uncertain parameters affecting structural resistance (R);
3. the uncertain interaction parameters (P), which depend on load intensity and structural (resistance) variables;
4. the whole spectra of structural responses (E), instead of just a serviceability and an ultimate limit state, as usual; this leads to a continuous transition between fully functional and completely failed;
5. the whole spectra of failure consequences (C) associated to structural responses (E).

Finally, it is noted that structural reliability analysis is concerned with whether the structural responses meet a given risk criterion. In probabilistic design the emphasis is on determining the structure (shape, sizes) to comply with a pre-set probabilistic criterion. This is discussed in more detail in Chapter 11.

9.10   Conclusion

This chapter has been concerned with applying the methods of reliability analysis outlined in the previous chapters to derive rational non-probabilistic safety-checking rules for use in so-called 'limit state design' codes. The format of the safety-checking rules adopted for such codes usually is of the partial factor format. This format was shown in Chapter 1 to be not necessarily mechanically invariant. However, provided that the method of application of the safety-checking rules is clearly set out in the structural design code, the problem of lack of invariance of the safety measure can be largely ignored.

To illustrate the code calibration procedure, the present chapter confined attention to the nominal failure probability for purposes of sizing structural members. Some of the justification for so doing was discussed by reference to Chapter 2. Further, a distinction was made between the nominal failure probability p_{fN} used elsewhere and p_{fC} used in the present chapter. This was considered to be appropriate because the latter probability is obtained to a large extent from predicted information. It therefore is likely to be subject

to a considerable amount of uncertainty. Also, it was noted, again, that the nominal failure probability implicit in the code-calibration work cannot be compared in a wholly rational manner with observed rates of failure of structures.

Finally, some brief remarks were made about performance-based design as a generalization of the traditional code based design approach. It allows a more general definition of what is required from the design process for a structure. This can have a direct input to optimization using a more direct application of a probabilistic framework rather than the traditional use of partial factors (see Chapter 11).

10

Probabilistic Evaluation of Existing Structures

10.1 Introduction

Once a structure has been designed, constructed and placed in service and perhaps has been in use for a long period of time, and perhaps suffered from deterioration, occasional overload, or misuse, the question may arise 'how safe is the structure?' It should be evident that this is quite a different question to that faced by designers of a new structure. Checking the structure against the code to which it was designed originally (or some more recent code) is not necessarily helpful since a design code needs to allow for uncertainties in the design and construction processes and these uncertainties will have been realized (i.e. they have been fully determined) in the finished structure. They are no longer uncertainties. However, determining what the actual values of various parameters might be for an existing, perhaps deteriorated, structure is not necessarily straightforward, and can introduce uncertainties of its own. An introduction to this matter is given in this chapter, together with a brief discussion of the criteria that might be used for decisions about the acceptability of an existing structure.

That the problem of assessment of existing structures is a major issue can be seen in some statistics. In 1996 it was estimated that, in the UK alone, more than 100,000 road bridges and some 25,000 railway under-bridges would need to be assessed, eventually, for remaining life and for load capacity [Menzies, 1996]. At about the same time, it was estimated that in the US about 50% of then-existing bridges were over 50 years old and that more than 100,000 bridges were rated as structurally deficient, and some 150–200 needed urgent attention each year [Dunker and Rabbat, 1993; Baboian, 1995]. These statistics have not changed much over the last few years, with the state (and safety) of national infrastructure increasingly causing concern. In 2013, of the more than 600,000 bridges in the US, with average age about 40 years, some 10% were considered likely to be structurally deficient. To bring them to satisfactory conditions will need an annual investment of some $US20 billion [ASCE, 2013]. Importantly, structures associated with buildings, ports, harbours and industrial facilities are not even included in these statistics.

Assessments of existing structures may be conducted for any one or more of the following reasons (Ellingwood, 1996):

(1) change of tenancy or use, including increased load requirements;
(2) concern about design or construction errors;
(3) concern about quality of building materials or workmanship;

(4) evaluation of effects of deterioration;

(5) assessment of damage following an extreme loading event (such as a wind storm or earthquake);

(6) concern about serviceability.

For buildings, changes of tenancy could bring about the need to support higher floor loadings. Thus increased ultimate strength and serviceability requirements must be met. For road and railway bridges there continues to be a world-wide demand for the limits on maximum bridge loading to be increased [Frangopol and Hearn, 1996].

In regions where the seismic risk is relatively high, there is pressure for older, existing structures to be up-graded to meet the higher seismic resistances demanded by newer-generation structural design codes. There may be very serious economic and social implications. Although less common, structural assessment of partially completed or existing buildings may be needed when there is concern about some aspect of the design or construction, including the quality of the materials used.

Many structural systems will have undergone some degree of deterioration. From a structural strength point of view, fatigue and corrosion are the main concerns. Spalling, cracking and changed appearance of concrete surfaces, while often superficial, also may indicate deterioration and require careful interpretation. For example, they may be due to corrosion of reinforcement, to sulphate attack or to microbiological attack. Similarly, the condition on steel structures with protective coatings such as paints or galvanizing tends to indicate the level of corrosion of the steel. Other indicators of possible deterioration include changes in natural frequency or damping and increased permanent deformations.

Deterioration effects are likely to be structure- and site-specific. For corrosion this is due to local climatic conditions, geographic features and structural form and orientation having an influence on deterioration agents such as rain, temperature and ultraviolet radiation. Similarly, environmental loading effects such as seismic loading also may have a degree of site specificity since ground-shaking may be amplified by local soil conditions. Thus structural assessments tend to be unique to the structure being considered. Although rather different approaches have been employed for structural assessments, there are some principal ideas involved.

The next section (10.2) provides a review of the assessment procedures for existing structures, including the use of proof loading and any knowledge of service performance. This shows that there are considerable uncertainties associated with assessment procedures, directly suggesting that probabilistic techniques are appropriate. The following section (10.3) describes how Bayes' rule (A.7) can be used to update an a priori (i.e. the already known, or computed) estimate of the probability of failure of a structure given additional information, irrespective of whether this is subjective or not. The primary focus is the effect of additional information gained through proof loading or the satisfactory service behaviour of a structure. The use of proof loading to gain information raises the question of the trade-off between the information gained and the possibility of damage caused by the proof loading and it effect on the probability of failure.

A more profound use of Bayes' rule is in up-dating the a priori probability density functions for the basic variables describing the structural reliability problem. This is described in Section 10.4. These can then be used in a reliability analysis to estimate the up-dated structural reliability.

@Seismicisolation

A different approach for the assessment of existing structures is to employ analytical modelling of the structure, including any modification of the probability density functions describing the random variables and including any deterioration effects and to re-assess its probability of limit state violation. It is similar to the analyses described in earlier chapters except for updated distributions and the inclusion of deterioration effects. Thus Monte Carlo analyses with different (i.e. updated) input variables and with sensitivity analysis can be used as well as the simplified methods of Chapter 4. In some cases more detailed modelling may be required for specific structural aspects, for example, a more detailed finite element analysis might be required in some area of the structure. In many respects this is the most comprehensive approach to dealing with existing structures. However, it may be feasible, in practice, only for complex structural systems with high consequential costs should failure occur. Section 10.5 provides an outline of these matters.

As noted earlier, the risk acceptance criteria for existing, service-proven, structures should not, in principle, be the same as those for the design of new structures. Conservatism in design rules for new structures generally incurs only a very small (and usually unknown) cost penalty in terms of structural costs. However, conservatism in acceptance criteria for an existing structure can have a major impact, with demolition (and possibly rebuilding), major repairs or upgrading or loss of business being the outcome of failure to meet criteria. This has resulted in strong pressures (commercial, social, heritage and others) to reduce the criteria where the socio-economic impact is likely to be severe. Section 10.6 discusses acceptance criteria for existing structural systems and also decision-theoretic applications, similar to those for new structures discussed in Chapter 2.

10.2 Assessment Procedures

10.2.1 Overall Procedure

Typically the assessment process for an existing structure will consist of the following steps:

(1) preliminary on-site inspection (to ascertain location, condition, loadings, environmental influences, special features, necessity for further testing);
(2) recovery and review of all relevant documentation, including loading history, maintenance and repair and alterations;
(3) specific on-site testing and measurements, including, perhaps, proof loading;
(4) analysis of collected data to refine (or 'up-date') the probability of failure estimate using Bayes' rule, or refining the probabilistic models for structural resistance (and perhaps loading) for analytical analysis;
(5) decision analysis to consider whether and how much extra data should be collected to achieve a cost-effective overall outcome.

Some of these are described in more detail below. At this stage attention will be confined to items (1)–(3). The first step is important in setting the framework for the subsequent analysis. It would determine the testing necessary to be carried out and the details desirable for performing the reliability analysis.

Information about the structure being assessed ought to be available, in principle, from the owner of the structure, its designer and local or state authorities charged with

approval processes. In practice, design information such as calculations and drawings often has been lost or cannot be traced, particularly for older structures. Thus a complete survey of the existing structure may be required, together with an analysis of member and system design strengths.

Almost certainly design code requirements for older buildings were different from those currently in force. Although there has been a general trend towards relaxing design code requirements [Ellingwood, 1996] concomitant with greater detail design needs, there are areas where design code requirements have become much more specific and older buildings are found not to comply, even for matters not specifically under scrutiny. Although the design and loading codes that would have applied to the original structure often are still available in archives, information about material specifications specific to the structure tends to cause the greatest difficulty, particularly for materials such as older concretes and wrought iron.

A further complication, particularly for older buildings, is that modifications may have been made to them and often these are poorly documented. Sometimes such modifications can have a negative influence on structural integrity or may hide significant defects. Similarly, maintenance practices are not always recorded. One area that can cause concern, for example for reinforced concrete structures, is the effectiveness of cathodic protection systems that have failed some (unknown) time in the past, leaving doubt about the actual state of reinforcement.

In the investigation of an existing structure, particularly for structural capacity, it is desirable to have as little negative influence caused by the investigation process. Thus the preference should be for the minimum of invasive techniques and, where possible and economic, non-invasive techniques. These include non-destructive techniques for material properties (e.g. rebound hammer, ultrasonic pulse techniques, deep penetration X-rays) and for element dimensions (e.g. electromagnetic cover meters, ultrasonics) as well as to detect defects (e.g. impact-echo techniques for large voids or delaminations) and for corrosion and deterioration (e.g. half-cell potential and resistivity measurements). Typically, such measurements provide only a partial and rather uncertain indication of the state of the structure [e.g. Silk et al., 1987; Paik and Melchers, 2008a].

Often the structural members requiring assessment are not accessible. Safety-critical structural members or components may be hidden by architectural finishes, by other structural components or by fire proofing materials or be otherwise inaccessible for inspection and testing. For these situations many of the existing non-destructive techniques are not wholly adequate—this remains an area in which further advances are urgently needed.

Probably the greatest challenge facing those assessing an existing structure is deciding what is to be assessed, where and how, and the extent and intensity of the assessment required to achieve sufficient confidence in the outcomes.

The most elementary level of assessment and decision consists of subjective classification systems, perhaps feeding into a condition matrix, from which subjective conclusions and recommendations can be made [e.g. Frangopol and Hearn, 1996]. More detailed assessments would supplement this approach with structural re-analyses and reference to existing design codes, or to codes for existing structures, if available. The latter have been developed in some specific cases but in general as yet without the benefit of a structural reliability code framework such as discussed in Chapter 9. These

simplified approaches are not the central focus of the present chapter. The discussion to follow will assume that some level of probabilistic assessment is of interest.

10.2.2 Service-Proven Structures

If a structure has been in service for a medium to a long period of time, and has not been altered or modified or deteriorated significantly during that time, and has performed satisfactorily during that time, it is likely that it remains satisfactory and, also, in most cases, safe. It can be said to be 'service-proven'. To some extent satisfactory performance may be an indicator also of adequate safety and of likely continuing safety, provided there is no evidence of significant on-going deterioration and the loadings are expected to remain substantially the same. Thus if a building is, say, 100 years old, this usually provides good evidence of satisfactory safety for dead and variable loads, provided these are not significantly different from those in the past. The reason is the general approach to structural design is to ensure sufficient structural and member ductility so as to provide sufficient resilience and gradual rather than sudden failures (Section 1.1). This means that for most structural systems, any unacceptable deformation, vibration, or local damage would have become evident to the users during normal operational service. This is irrespective of the details of serviceability criteria or safety requirements specified by a design code.

In using past service behaviour as an indicator of behaviour for assessing existing structures, attention must be given also to requirements that may exist or have existed on the structure during its service life, such as load limits for bridges. These may have the effect of modifying the upper (high load) tail(s) of the probability density function for applied loading (Figure 10.1). In this case there is a clustering of loadings just below the legal limit and a few rogue loadings beyond the legal limit. The precise distribution now depends also on the load limit enforcement regime and how this may or may not have varied over the service life.

Where loading events are infrequent, such as due to earthquake-induced ground motion, satisfactory past performance may not be a good indicator, since the infrequent loading event may not (yet) have occurred. A similar situation can apply for younger buildings and crowd loading (which is only very rarely applied to the magnitude specified in design codes).

In a sense service proof is better than a proof load test (see next section) in that the whole structure is 'tested' rather than some specific part of it and because the loadings are site-specific [Allen, 1991]. However, it is clear also that relying solely on past performance generally will not be sufficient (see comments in previous section).
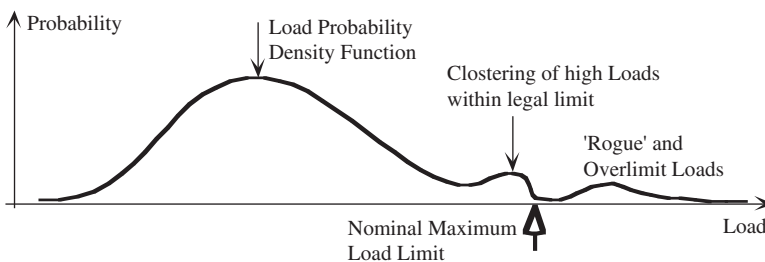
Figure 10.1 Schematic representation of the effect of legal limits and enforcement on the upper tail of the probability density function for applied bridge loading [Melchers, 2008a].

There are 'engineering' approaches to using satisfactory past performance in the evaluation of existing structures [ISE, 1980; OHBDC, 1983; Allen, 1991]. There also are efforts to formulate the concept in the context of structural reliability–based techniques. Hall (1988) proposed a Bayesian-based approach and Stewart and Val (1998) a simulation-based approach, including the effect also of structural deterioration. It should be clear that unless there is a high likelihood that the service period has included significant load levels, service-proof is less likely to be as informative as a proof-load test.

A special case of service-proof arises in relation to phenomenological uncertainty (see Section 2.2.2. For structural (and other) systems for which the critical limit state conditions perhaps are not fully understood or even known, phenomenological uncertainty may be an issue and an unrecognized and unformulated limit state may exist. Service-proof can increase the confidence that such a limit state is not critical, if it exists. The theory follows directly from Bayes' theorem (see above) [Riera and Rocha, 1997].

10.2.3   Proof Loading

The notion that further testing can provide additional information about a structure or its components is not new [e.g. Hall and Tsai, 1989]. In a sense proof-loading of an existing, in-service structure is the ultimate test of its performance, but what does such a test actually reveal about the structure?

If the proof load is highly correlated to the phenomenon of interest, such as measuring stiffness to make inferences about ultimate strength for reinforced concrete beams, a proof load test can be useful [Veneziano et al., 1984; Moses et al., 1994]. Also a proof load test can determine the minimum strength or capacity of a component, such as a reinforced concrete floor. The load supported by the floor then can be applied to the probability density function for its strength to truncate it below the proof load (see Figure 10.2). Typically, this increases the reliability index [Fujino and Lind, 1977; Fu and Tang, 1995; Moses, 1996]. But the test itself may (i) damage the structure or the material(s) of which it is composed [Kameda and Koike, 1975] and/or (ii) fail the structure. Generally, only higher levels of proof load have a significant effect on the predicted reliability, as is illustrated in Example 10.1 later in this chapter.
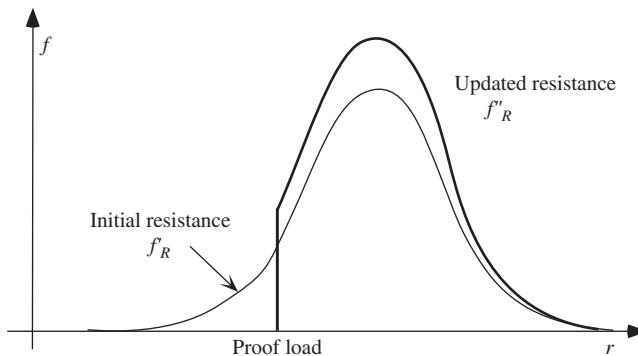
Figure 10.2 Truncation effect on structural resistance.

A typical proof load test consists of the following steps:

(1) slow application of loading in several approximately equal increments, allowing sufficient time between increments for the structural response to become reasonably steady (say about one hour);
(2) continued application of load steps until code specified proof load level is reached, provided that at each stage it is considered safe to continue loading;
(3) measurement of deformations at each stage and noting of cracking patterns and other signs of possible distress;
(4) at maximum load level holding the load for, say, 24 hours and continuing to monitor structural behaviour;
(5) slow unloading of the structure, monitoring deformations.

For steel and reinforced concrete structures the proof load test often is considered successful if the eventual deformations of the structure are less than about 25% of the maximum deformations expected under ultimate load, suggesting that inelastic behaviour of this magnitude is tolerable for the types of steel used. For reinforced concrete elements made with reinforcing steels that have less pronounced or short yield plateaus this may be optimistic. Importantly, the proof-load test says nothing about how close the proof-load might have been to the ultimate capacity of the structure, how much ductility remains, and whether structural or material damage has been caused by the proof test. Also, a proof load test result supplies little information about how the structure compares with the requirements of the relevant design code.

Load tests have been used also to estimate more accurately individual member forces, as demonstrated, for example, for truss bridges [Nowak and Tharmabala, 1988]. This is helpful in improving the theoretical analysis of a structure, such as through taking into account structural behaviour normally neglected by conventional analysis [Faber et al., 2000].

Most existing structural design codes provide only rather general guidelines for load testing. Typically, they require satisfactory performance under the test loads, and some specifications for what is deemed satisfactory behaviour. The test loads themselves typically correspond to the factored loads for gradual (bending) failure and to slightly higher load levels (e.g. 10% higher) for shear (brittle) failure [Allen, 1991].

10.3   Updating Probabilistic Information

10.3.1   Bayes Theorem

When additional information has been gathered about an existing structure or its components, the knowledge implicit in that information might be applied to improve any previous ('prior') estimate of the structural reliability of that structure. The framework for doing this is Bayesian statistics, which uses Bayes theorem (see Section A.2.2.4, Eqn. (A.7)):

$$P(A \,|\, E_c) = \frac{P(A \cap E_c)}{P(E_c)} \tag{A.7a}$$

where event A is conditional on event E_c. As noted in Appendix A, the latter can be expanded to the case where there are several conditioning events E_i, $i = 1, 2, \ldots, n$. Then (A.7a) becomes

$$
\begin{aligned}
P(A \mid E_1 \cap E_2 \cap E_3 \ldots E_n) &= \frac{P(A \cap E_1 \cap E_2 \cap E_3 \ldots E_n)}{P(E_1 \cap E_2 \cap E_3 \ldots E_n)} \\
&= \frac{P(E_1 \cap E_2 \cap E_3 \ldots E_n \mid A) P(A)}{P(E_1 \cap E_2 \cap E_3 \ldots E_n)}
\end{aligned}
\tag{A.7b}
$$

where the second equality shows the conditioning events E_i now being conditional on the original event A. To apply (A.7b) to a structural reliability problem, let the event A be the failure event $G(\mathbf{x}) < 0$ with, as before, the limit state function described by $G(\mathbf{x}) = 0$.

10.3.2 Updating Failure Probabilities for Proof Loads

A special case of (A.7b) is where the additional data available are the result of a single proof load applied to the structure. In this case $n = 1$. Let the structural limit state function for the proof load be denoted $H = 0$ and $H < 0$ denote failure under the proof load. Thus $H > 0$ denotes that the structure survived the proof load test. Then the updated probability of failure given that the structure survived under the proof loading can be expressed as [Madsen, 1987]:

$$
p_{fU} = P[G(\mathbf{X}) < 0 \mid H > 0] = \frac{P[G(\mathbf{X}) < 0 \cap H > 0]}{P[H > 0]}
\tag{10.1}
$$

In this expression the numerator on the right represents the probability of the structure failing even after it has survived the proof loading. It can be evaluated by the methods discussed in Chapters 3 and 4 and in Appendix C. The denominator represents the probability estimate of the structure surviving under the application of the proof load. This also can be estimated using the methods of Chapters 3 and 4. If required, the concept can be extended easily for multiple proof loads using (A7.b).

10.3.3 Updating Probability Density Functions

Instead of simply updating the estimate of the probability of failure with the use of one (or more) proof load tests (or information from service performance), Bayes' rule can be used to update probability density functions, provided sufficient extra (homogeneous and consistent) data is collected.

Consider first the concept of updating a probability density function. The idea is illustrated in Figure 10.3. If $f'_R(r)$ represents the (a priori) conditional probability density function (pdf) of, say, structural resistance R, and $f_V(\ )$ represents the (conditional) pdf of some new data (marked as the likelihood function), then the updated (*posteriori*) pdf $f''_R(\ )$ is likely as shown. Evidently, if the data has a lot of scatter, (i.e. if the likelihood function $f_V(\ )$ has a large variance, and thus has a flatter probability density function than that shown), it does not contain much information (i.e. it is 'non-informative'). Hence it does little to help in refining the original pdf. Conversely, if the data has very little scatter, then $f_V(\ )$ will be narrow, is highly 'informative' and will have a significant influence on $f''_R(\ )$. Similarly, if there is little understanding of the variable being considered, its a priori distribution $f'_R(\ )$ is highly uncertain (i.e. flat) and can be said to be 'non-informative'.
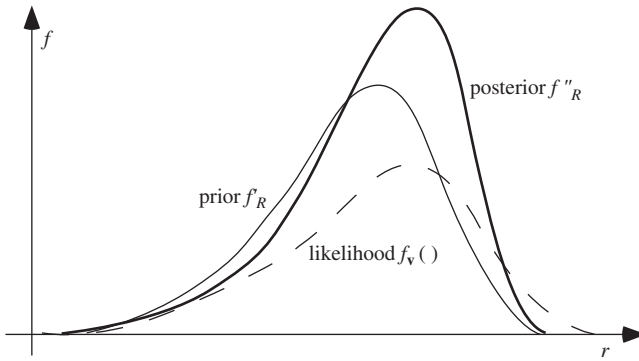
Figure 10.3 Known (a priori) pdf for resistance $f'_R(r)$ as modified by new information $f_V(\ )$ (likelihood function) and modified (*posteriori*) pdf $f''_R(\ )$.

The *posteriori* (or predictive) distribution will then be considerably influenced by the additional data.

From the numerator on the right-hand side of (10.1) it should be clear that θ a high degree of (negative) dependence between the structural failure event $G(\mathbf{X}) < 0$ and the successful proof-load event $H > 0$ will produce a tighter up-dated (*posterior*) distribution, giving more confidence about the estimated random vector $\mathbf{X}$ of interest. This means that the inspection and assessment procedures should be constructed so as to produce event outcomes $H > 0$ that are informative about $G(\mathbf{X})$. For example, measurements of beam stiffness can be used to make inferences about beam strength, provided the two are correlated highly, as is the case, for example, for reinforced concrete beams.

To make the concept of updating a probability density function operational, the parameters that define it, as in say vector θ, need to be updated. This can apply also to the situation when the parameters θ themselves are not known with a high degree of accuracy. In both scenarios it follows that the probability density function is dependent on θ. It can be stated as a conditional probability density function $f_{\mathbf{X}|\theta}(\mathbf{x}\,|\,\theta)$. Updating requires additional information and let this be considered obtained by making several (n) observations $\mathbf{x} = (x_1, \ldots, x_n)$ from which both the parameters θ can be updated and also the pdf $f_{\mathbf{X}|\theta}(\mathbf{x}\,|\,\theta)$ updated.

Let the initial knowledge about θ be represented by $f'_{\boldsymbol{\Theta}}(\theta)$, the prior distribution of θ, that is, the distribution which represents the information about θ before any observations are made. After the n observations $\mathbf{x} = (x_1, \ldots, x_n)$ have been made, the new (*posteriori*) distribution $f''_{\boldsymbol{\Theta}}(\theta)$ of θ, given $\mathbf{x}$ is given by [e.g. Rackwitz, 1985b]:

$$f''_{\boldsymbol{\Theta}}(\theta) = c.L(\theta\,|\,\mathbf{x})f'_{\boldsymbol{\Theta}}(\theta) \tag{10.2}$$

where $L(\theta\,|\,\mathbf{x})$ is the so-called 'likelihood' function as before and $c = \left[\int L(\theta\,|\,\mathbf{x})f'_{\boldsymbol{\Theta}}(\theta)\,d\theta\right]^{-1}$ is the normalizing factor. Here the likelihood function $L(\theta\,|\,\mathbf{x})$ represents the knowledge gained from the observations $\mathbf{x}$. It is the likelihood of observing the outcome $\mathbf{x}$ under the assumption that θ takes its current (set of) value(s)—it may be written also as $P(\mathbf{x}\,|\,\theta)$.

The likelihood function $L(\boldsymbol{\theta}|\mathbf{x})$ is proportional to the conditional probability of making the observations, thus

$$L(\boldsymbol{\theta}|\mathbf{x}) \propto \prod_{i=1}^{n} f_{\mathbf{X}|\boldsymbol{\Theta}}(x_i|\boldsymbol{\theta}) \tag{10.3}$$

where n is the number of samples (or observations).

Once $f_{\boldsymbol{\Theta}}(\boldsymbol{\theta})$ has been updated, it is possible to obtain the 'predictive' (or expected) distribution for $\mathbf{X}$, given that the sampling has been done and the probability density function for the parameters $\boldsymbol{\theta}$ has been refined, from

$$f_{\mathbf{X}}(\mathbf{x}) = \int_{\theta} f_{\mathbf{X}|\boldsymbol{\Theta}}(\mathbf{x}|\boldsymbol{\theta}) f_{\boldsymbol{\Theta}}''(\boldsymbol{\theta}) \, d\boldsymbol{\theta} \tag{10.4}$$

This is an expression of the total probability theorem (A.6). It might be compared also to (1.35).

Example 10.1 [adapted from Val et al., 1998a] A reinforced concrete column was suspected of deficient concrete strength. Core samples were taken. At first there were three such samples with core strengths (45.19, 39.95, 42.77 MPa) and a Bayesian analysis was performed. There was concern about the outcome, and three more samples were taken, with strengths (41.61, 43.39, 37.88 MPa). This was later followed by another four samples (46.11, 41.78, 43.93, 40.63 MPa). The mean and coefficient of variation for each total group of samples is shown in Table 10.1.

It is known from extensive experimental work that the relationship between the core strength $f_{c,core}$ and the in-situ strength $f_{c,is}$ of concrete is given by [Bartlett, 1997]:

$$f_{c,is} = K \cdot f_{c,core} \tag{10.5}$$

where K collects a number of factors (see Section 8.4). Here the core strength is the observed variable and is a function of the actual in-situ strength and the factor K which, in general, is known only as an uncertain relationship.

More generally, the relationship between the structural parameter x of interest (i.e. the in-situ concrete strength) and the parameter y actually observed, can be given as

$$y = ax^b \tag{10.6}$$

where a and b are calibration values. In the present example $a = K$ and will be assumed known, with known mean μ_a and known variance σ_a^2. These values could be obtained from repeated testing of the in-situ testing process or equipment when x is known (i.e. a calibration exercise). In the following, let b be a deterministic value (=1 in this example).

Table 10.1 Mean and standard deviation for samples.

No. of samples	Mean (MPa)	COV
3	42.58	0.062
6	41.73	0.063
10	42.26	0.059

Uncertainty in y can come about from (i) imprecision of the measurement instrument or process; (ii) model uncertainty, that is, how well (10.6) represents the relationship between x and y; and (iii) through limited sampling.

For convenience, let x and y be Lognormal in distribution. Then (10.6) becomes

$$Y = A + B.X \tag{10.7}$$

with $Y = \log y$, $A = \log a$ and $X = \log x$ each with a Normal distribution. Also, for these:

$$\mu_Y = \mu_A + b.\mu_X \tag{10.7a}$$

and

$$\sigma_Y^2 = \sigma_A^2 + b^2.\sigma_X^2 \tag{10.7b}$$

Evidently, x and a are independent random variables, and y is a dependent variable. Also, $\sigma_Y \geq \sigma_X$, $\sigma_Y \geq \sigma_A$ always. If enough observations of y are taken, it is possible to estimate the moments of the random variable Y (see Section A.5.9). The mean and variance for the Normal distributed X can then be estimated from $\mu_X = \frac{1}{b}(\mu_Y - \mu_A)$ and $\sigma_X^2 = \frac{1}{b^2}(\sigma_Y^2 - \sigma_A^2)$.

Thus in (10.3) the vector of (unknown) parameters θ becomes $\theta = (\mu_X, \sigma_X)$, and the likelihood function, given the vector of observations $\mathbf{Y'}$, is then proportional to:

$$L((\mu_X, \sigma_X)|\mathbf{Y'}) \propto \frac{1}{(\sigma_Y^2 - \sigma_A^2)^{n/2}} \exp\left\{ -\frac{b^2}{2(\sigma_Y^2 - \sigma_A^2)} \sum_{i=1}^{n} \left[Y_i - \frac{1}{b}(\mu_Y - \mu_A) \right]^2 \right\} \tag{10.8}$$

If it is assumed that the parameters μ_X and σ_X are independent a priori, their joint prior distribution is given by $f'_\Theta(\theta) = f_M(\mu).\ f_\Sigma(\sigma)$ where $f_M(\mu)$ and $f_\Sigma(\sigma)$ are marginal prior distributions of μ_X and σ_X respectively. The choice of these distributions depends on the information available about μ_X and σ_X a priori, as will now be discussed for the problem under consideration.

Let it be assumed that in the first analysis no attempt was made to look at the records to determine what might have been the specified concrete strength. Hence the prior knowledge is 'non-informative'. For this situation, the prior distribution is locally uniform on the mean μ_X [e.g. Box and Tiao, 1973]:

$$f_M(\mu_X) \propto \text{constant} \tag{10.9}$$

In this case the distribution of the standard deviation may be given by Jeffrey's rule [e.g. Box and Tiao, 1973], which leads to:

$$f_\Sigma(\sigma_X) \propto \frac{\sigma_X}{\sigma_Y^2 - \sigma_A^2} \tag{10.10}$$

with σ_A given above. Using these prior distributions in (10.4) produces the 'predictive' distribution for the compressive strength of concrete, assuming non-informative prior information. The resulting distributions for $n = 3$, 6, 10 are shown in Figure 10.4(a) [Val et al., 1998a].
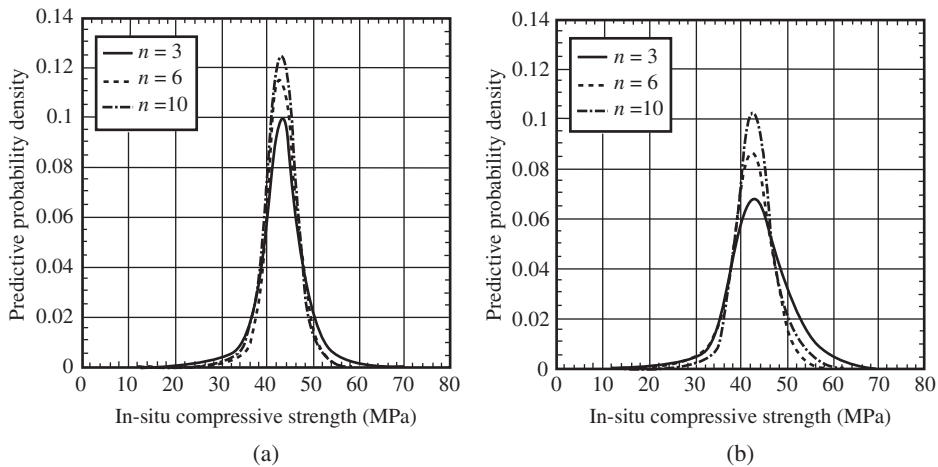
Figure 10.4 Predictive distributions for in-situ compressive strength of concrete (a) non-informative priors for μ and σ, (b) informative priors for both μ and σ.

If more information is known a priori, such as the characteristic compressive strength f_c' of the concrete used in the column, known relationships [Bartlett and MacGregor, 1996] (see Section 8.4) between this value and the mean of the in-situ strength and its variance can be used to derive the a priori distribution for μ. Similarly, generic data can be used to set an a priori distribution for σ [Val et al., 1998a]. If this is done, typical results such as shown in Figure 10.4(b) are obtained.

Evidently, in this example the non-informative prior, case (a), has a more peaked (narrower) distribution than case (b) and has a slightly lower mean. For a given value of compressive strength, say 50 MPA, the upper tail of the distribution (a) has a smaller probability content than for case (b). This indicates that there is a smaller probability that the actual strength of the concrete is 50 MPa or above.

Increasing the number of samples leads to a more peaked distribution in both cases, although the effect is slightly more pronounced for case (b). This demonstrates that case (a) is (of course) highly dependent on the samples. In case (b) the prior information is more important and there is less reliance on the sample information.

10.3.4 Pre-Posterior Analysis

The above examples have shown that additional information can be used to update the estimated probability of failure, either directly or through updated probability distributions to be used in a reliability analysis of the existing structure. Such additional information usually comes at some cost, including the actual cost of testing or additional investigations or both. A question that then arises is whether the cost of gaining the extra information is warranted in terms of the savings related to the updated estimate of the failure probability of the structure. The investigation of this can be done best through a decision framework (*cf.* Section 2.4.2) or similar, conducted before the estimation of the adjusted (*posterior*) failure probability. For that reason it has been termed *pre-posterior* decision analysis [Benjamin and Cornell, 1970; Diamantidis, 2001]. It may require the evaluation of different options for gaining information, each with its

own costs and likelihood of influencing the outcome probability estimate. The structural reliability estimation components of such a *pre-posterior* decision analysis are not significantly different from what has been outlined so far. Typically, only the decision framework itself (i.e. the event tree analysis) is somewhat more complex and requires cost estimates. The reader is referred to Diamantidis (2001) for more details about the fundamental issues involved. In addition, the literature now contains many example applications.

10.4 Analytical Assessment

10.4.1 General

Using analytical techniques to model the existing structure for evaluation has the advantage that known probabilistic information about materials and loadings relevant to the existing can be incorporated directly into the analysis. This information also can be up-dated and augmented with new information as it becomes available. Further, models for structural material deterioration can be incorporated easily, and these models can be updated, modified or replaced with better models as they become available. Also, sensitivity analyses can be performed at relatively low cost, irrespective of whether Monte Carlo methods or the simplified methods from Chapter 4 are employed. All this can be achieved more easily and with much less cost than can be achieved with tests such as proof loading.

A possible disadvantage of analytical techniques is uncertainty about how well the analytical model represents reality. While finite element and other structural modelling tools can be matched closely to represent the response of a structure (and in this sense a proof load test can be very useful for calibration), the modelling of the (most likely deteriorated) condition of the materials in the structure is likely to be less certain.

The damage caused by fatigue has had a considerable amount of study and, in general, can be modelled reasonably well. The main qualification is that particular care is required in the modelling of the details where fatigue cracking can commence, as these tend to dominate the subsequent behaviour.

On the other hand, damage mechanisms such as reinforcement corrosion, structural steel corrosion, sulphate and other chemical attack, frost damage and microbiological attack and the effect these have on structures generally are less well understood and therefore difficult to model convincingly for analysis. There also tends to be a rather high level of uncertainty associated with these various influences and their effects on the structure.

Within these constraints, modelling of the structure and its various influences allows appropriate probabilistic analysis to be performed. Particular care is required to use relevant data for the structure: while generic data (such as described in Chapter 8) is appropriate for the establishment of design rules as in Chapter 9, for the assessment of an existing structure it is better for the data to be directly relevant to that structure. Generic data must be used with great care. The next section gives a brief review of some deterioration models.

Once the models for the structure and the various deterioration and other models have been established, and probabilistic models for the various influences selected, the

reliability analysis follows a pattern similar to that described in the earlier chapters, using FOR/SOR methods, as demonstrated in some example applications [e.g. Micic et al., 1995; Enright and Frangopol, 1998]. Also, simulation techniques have been used for relatively simple structures [e.g. Mori and Ellingwood, 1993b; Stewart and Val, 2003; Akgul and Frangopol, 2005; Strauss et al., 2008]. It is likely that a full-scale probabilistic reliability analysis for an existing structure is feasible only for really major systems or those with very severe consequences should failure occur (e.g. nuclear facilities, nuclear waste storages, major oil and gas facilities).

10.4.2 Models for Deterioration

When the structure being assessed for remaining life and reliability has undergone some deterioration, the inspection process should attempt to ascertain the amount of deterioration that has occurred. Thus material loss due to corrosion might be estimated, and inspection might reveal fatigue cracking, but in general it will not be possible to obtain a complete picture of the deterioration of the structure. Some estimation from known fatigue mechanics and corrosion mechanics usually will be needed to supplement the visual and on-site inspection observations.

Inspection and observation itself introduces an element of uncertainty [e.g. Silk et al., 1987; Frangopol and Hearn, 1996], and this must be considered in the analysis [e.g. Moses, 1996].

As noted, apart from fatigue [Wirsching, 1998; Byers et al., 1997], the modelling of the mechanics of structural deterioration is not yet well developed. Simplified constant corrosion rate models have been used in some of the early work on the reliability assessment of ships [e.g. Piak et al., 1997] and steel pipelines [e.g. Ahammed and Melchers, 1997]. For atmospheric corrosion non-linear empirical curve-fitting approaches have been applied, as for example for steel bridge reliability [Albrecht and Naeemi, 1984; Hearn, 1996]. All these efforts showed that when compared to data, the uncertainty in material losses due to corrosion was very large. One issue is that some of the data sets used by investigators were not homogeneous, as would be required for valid probabilistic models. Data was simply 'opportunistic' and even for short-term exposures, when a 'rate' model might be expected to be reasonable, there are many cases in the literature with very high standard deviations [Guedes-Soares et al., 2006]. But even for well-controlled data it was found that the 'corrosion rate' or simple non-linear models are not sufficient to properly capture and thus represent corrosion behaviour for longer-term exposures. In particular, the parameters of such simple models are very sensitive to the period of exposure being modelled. All this suggests that the simpler models are not sufficiently discriminatory to capture longer term corrosion behaviour.

Much more detailed investigation has shown, initially for the marine corrosion of a variety of steels that the trend for corrosion loss versus exposure time is distinctly non-linear and, depending on the precise exposure conditions, such as water velocity, often exhibits bi-modal behaviour (Figure 10.5). This bi-modal behaviour is related to the development of the corrosion products on the metal surface and the changing conditions at the corrosion interface, denoted by the phases shown in Figure 10.5a [Melchers, 2008b]. Such behaviour also has been demonstrated for longer-term exposures of aluminium alloys and for copper alloys [Melchers, 2014a, 2015a]. In addition, for steels, much research activity has demonstrated that microbiologically influenced corrosion
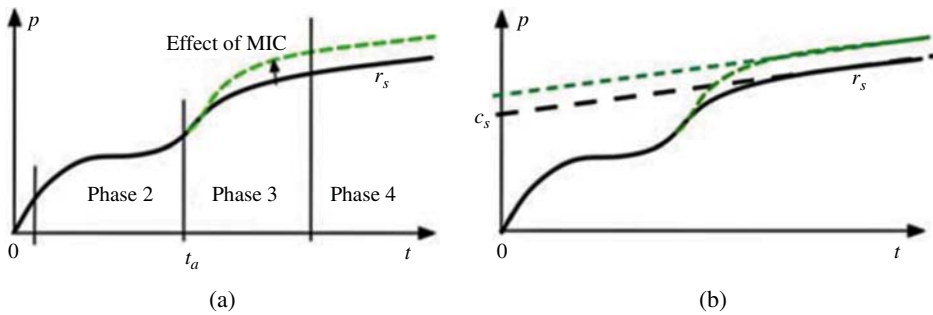
Figure 10.5 Typical bi-modal corrosion loss penetration p as a function of exposure period t showing (a) main phases in the early stages of corrosion and the effect of microbiologically influenced corrosion (MIC) and (b) the medium to longer-term linear bounding trend.

can be severe but only under particular circumstances [Melchers, 2014b]. These include unfavourable local conditions such as high nutrient loading and under-deposit corrosion, both important for some types of major steel marine infrastructure, including sheet piling, pipelines, welded zones, etc. [Melchers and Jeffrey, 2014; Melchers, 2015b; Comanescu et al., 2016; Chaves and Melchers, 2014]. Both the bi-modal characteristic and the influence of MIC can have significant influence on the statistical representation of maximum pit depth, for which the Gumbel extreme value distribution has long been considered the most appropriate representation [Galambos, 1987; Melchers, 2015b].

For reinforced concrete the most serious deterioration issue usually is reinforcement corrosion. In most coastal regions, where the significant infrastructure often is located, onshore and offshore, chloride diffusion to the reinforcement usually is considered the most critical issue, along with the ability for moisture to penetrate or be present at the reinforcement–concrete interface. Chlorides also may result from the application of de-icing salts to bridge decks [e.g. Hoffman and Weyers, 1994] and as air-borne particles in coastal inland regions. Cracking and spalling of concrete and loading intensity are other factors to be considered, although often these are the result of reinforcement corrosion [Gjorv, 2009].

A large number of papers have addressed these matters in a reliability context [e.g. Thoft-Christensen et al., 1996; Val and Melchers, 1997; Frangopol et al., 1997; Stewart and Rosowsky, 1998; Val, 2007; Strauss et al., 2008; Orcesi and Frangopol, 2011], most commonly using numerical models to simulate the physics of the situation, or interpretations from laboratory experiments. Unfortunately there has been remarkably little that relates the predictions of these models or experiments to observed behaviour of actual structures. In part this is because of the scarcity of systematic well-controlled, field observations over extended periods of time. However, there is now considerable evidence that the theory and the laboratory experimental results do not always relate well to field observations [Melchers and Li, 2009a,b; Angst et al., 2012]. This includes the threshold chloride content linked to the initiation of reinforcement corrosion [Angst et al., 2009; Melchers and Chaves, 2017], a factor most papers dealing with reliability analysis have assumed to be a random variable. However, the fact that the variability is so high indicates that the mechanisms and behaviours involved are not well understood, or simply that the conventional understanding of the factors involved is poor. Recent research and many field observations [as summarized by Angst et al., 2009; Melchers and
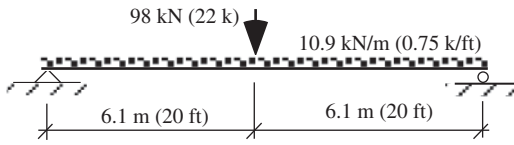
Figure 10.6 Beam in Example 10.2

Li, 2006; 2009b] suggests that high chloride content is not the critical issue for the initiation of reinforcement corrosion. A more sophisticated understanding is now beginning to be developed [Melchers and Chaves, 2016].

Example 10.2 [adapted from Ellingwood, 1996] Consider a $W24 \times 76$ wide-flange steel beam (610UB101 universal beam) simply supported over a 12.2 m span, as shown schematically in Figure 10.6. The nominal yield strength of the steel is 250 MPa (60 ksi). The loading is as shown. Assume that the design of the beam needs to comply with the LRFD format (see Section 9.3.4) given by

$$0.9 F_{yn} Z_{xn} = 1.2 M_D + 1.6 M_L \tag{10.11}$$

where F_{yn} and Z_{xn} are the nominal yield strength and plastic section modulus respectively and M_D, M_L are the moments due to dead and live loading. Usually the moment due to dead load, M_D, can be estimated reasonably accurately from careful measurements.

To assess the integrity of the beam under live load, it is subject to a proof load of magnitude q^*. This sets up a moment M_{q^*}. The event of withstanding the load test successfully can be expressed as

$$H = \left\{ F_{yn} Z_{xn} - M_D - M_{q*} > 0 \right\} \tag{10.12}$$

The updated probability of failure is then found from

$$p_{fn} = P[G(X) < 0 \,|\, H] \tag{10.13}$$

where the conditional probability term $P[\ ]$ is calculated according to (10.1).

Consider now the effect of the magnitude q^* of the proof load and the effect it has on the updated failure probability p_f'' for the above example [Ellingwood, 1996]. Assume it has a 50-year nominal service life. The variation in updated failure probability p_f'' as a function of q^* normalized with respect to the live load L is shown in Figure 10.7 for two cases of proof load, that is, applied at 10 years and at 25 years after construction. The functions are shown for two values of coefficient of variation of the resistance, namely for $V_R = 0.13$ and for $V_R = 0.18$.

It is seen that later application of the proof load in the life of the structure has a greater effect on the updated (*posteriori*) failure probability p_f''. This is as would be expected. Increasing the coefficient of variation of the resistance from $V_R = 0.13$ to $V_R = 0.18$ increases p_f'' significantly for lower magnitude proof loads. Also, proof loads of greater magnitude significantly reduce the value of p_f'' and that little information is gained for low proof loads, as shown with the curve $P(H < 0)$. In the present case a value of q^*/L less than about 1.2 provides little information.
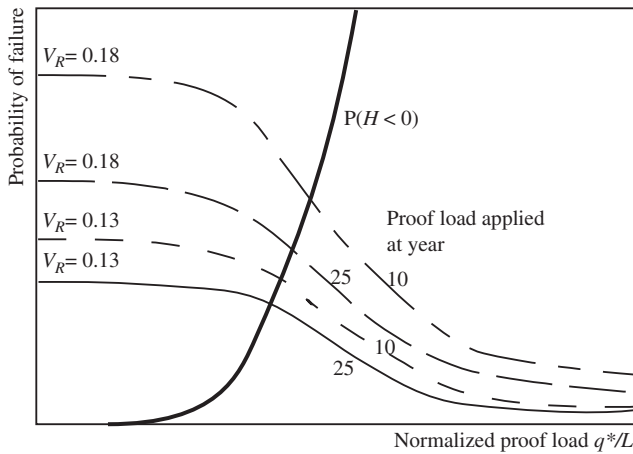
Figure 10.7 Posteriori failure probability p_f'' as a function of normalized proof load $q * /L$ and the probability of failure $P(H < 0) = 1 - P(H > 0)$ under the application of the proof load (schematic).

Table 10.2 Statistical data for Example 10.2.

Variable (Nominal value)	Mean/ Nominal	COV	Description
Dead load, D	1.05	0.10	Normal
Live load (50 years) L	1.00	0.25	EV-Type I
Live load (25 years) L	0.85	0.35	EV-Type I
Yield strength, F_y	1.05	0.11	Lognormal
Section modulus, Z_x	1.00	0.06	Normal
Flexural model bias, B	1.02	0.05	Normal

For higher proof loads it would be expected that there is an increased risk of structural failure under the application of increased levels of proof load. Indeed, this is shown on Figure 10.5 as $P(H < 0) = 1 - P(H > 0)$. Evidently, the probability of failure increases sharply as the estimate for p_f'' improves. From this notion arises the possibility of a decision analysis to determine the optimum proof load level based on the associated expected costs (including the costs of failure) [Diamantidis, 2001].

Continuing with the example, the matter of interest now is whether the service life of the beam can be extended by 50 years from the present. To assess this assume the governing limit state is the flexural limit state (10.11). The present safety can be assessed using the known or estimated statistical properties for the random variables, as shown in Table 10.2. Using these, the safety index is found to be $\beta_C \approx 2.6$.

To estimate whether the service life of the beam can be extended by 50 years from the present, some additional information was sought to try to reduce the COVs of some of the parameters. Thus, mill test reports for steel closely related to the steel in the structure indicated a mean yield strength of 345 MPa (50 ksi) with an estimated COV of 0.07. Using a rule such as given in Section 8.2.2 to estimate the static yield strength for use in design and analysis, indicated that a better estimate of the static yield strength is

300 MPa (44 ksi). No deterioration was observed so that the section modulus was taken as the original value. Observations and measurements of the dead load suggested that the original dead load was under-estimated by 10% on average, with a revised estimated COV of 0.05.

With this revised information the revised safety index becomes $\beta'_C \approx 3.4$. This shows that the beam is stronger than suggested by the original, nominal design procedure. In consequence, it would be possible to increase the applied live load L without violating code requirements. Specifically, L can be increased about 30% before β'_C decreases to the current safe value of $\beta_C \approx 2.6$.

10.5   Acceptance Criteria for Existing Structures

10.5.1   Nominal Probabilities

In setting acceptance criteria for the design of new structures a target acceptable β_T, or equivalently, a target acceptable probability of failure p_{fT} was used (see Chapter 9). As noted, this was based on back-calculation from the interpretation of the acceptability of existing good practice in structural engineering. The β_T or p_{fT} is then used to cal-ibrate the new rules for design. The process involved is now widely accepted for the development of code rules for the structural design of new structures (see Chapter 9).

It is important to recognize that within that process are hidden certain assumptions. These have to do with the translation of the design to the actual, constructed structure. The usual design procedure makes allowance, implicitly, for the uncertainties associ-ated with the documentation, interpretation and the various construction processes necessary to realize the structure. In terms of probability theory, the structure as built is just one realization of many possible outcomes. What is important is that once the realization has occurred, the uncertainties associated with the processes involved essentially have disappeared. What now replaces these uncertainties is our limited knowledge of the actual realization. In principle, given sufficient resources and ideal measurement and monitoring techniques, this lack of knowledge can be overcome. In practice this is possible only to a limited extent (as noted already earlier). But it should be clear that the nominal probability p_{fC} and corresponding safety index β_C used in the calibration process to obtain the target values p_{fT} or β_T in the development of design code rules for new structures cannot, in general, be directly translated to the verification of existing structures. As noted in Chapter 2, p_{fC} and β_C are surrogates for societal acceptable risk criteria even though the link between them is not necessarily clear. In the case of existing structures the link to societal acceptable risk criteria is likely to be different. For this reason we might define a nominal probability p_{fA} (and corresponding safety index β_A) for the assessment process.

The question now arises as to the values for p_{fA} or β_A which should be acceptable or which might be used as target values in any calibration process for a partial factor format for assessment of existing structures. This question has been addressed (i) using a simplified semi-probabilistic format, (ii) inferences from historical data and (iii) using decision theory and the various costs involved. The latter can be expanded to include broader utility indicators such as the Life Quality Index (see Section 2.4).

10.5.2 Semi-Probabilistic Safety Checking Formats

In the same way that semi-probabilistic safety checking formats such as LRFD (see Section 9.3.4) have been developed for the design of new structures, it has been proposed that rather similar formats can be developed for the safety assessment of existing structures. Clearly such formats would need to make allowance also for matters such as the quality of inspection, extent and quality of in-situ measurements, potential failure modes and possible consequences.

One possible format has been described by Allen (1991) for the Canadian National Building Code. In this approach the target reliability index β_T is adjusted by an amount $\Delta = \sum \Delta_i$ to allow for the above factors (see Table 10.3) to give β_A as $\beta_A = \beta_C - \Delta$. The standard code calibration processes are then applied to obtain the modified partial factors. Table 10.4 shows typical changes from the usual partial load factors (see also Section 9.3.2).

The resistances for use in the partial factor format would be taken as those measured or inferred for the structure being considered, modified to provide a lower fractile, conservative result. Where this is impractical, the nominal material strengths can be used together with measurements of the actual sizes installed. The partial factors are the same as for new design, except for some components where the current limit state design code is known to be excessively conservative, with higher β_T values. For these the partial resistance factors are modified (see Table 10.5 for some typical examples).

Table 10.3 Adjustments to reliability index β_C [Allen, 1991].

Assessment factor	Δ_i
Inspection performance Δ_1	
No inspection or drawings	−0.4
Inspected for identification/location	0.0
Satisfactory performance or dead load measured	0.25
System behaviour Δ_2	
Failure leads to collapse, personal injury likely	0.0
In between	0.25 (less under earthquake conditions)
Local failure, personal injury unlikely	0.50 (less under earthquake conditions)
Risk category Δ_3	
Very high	Use design code
High $n = 100-1000$	0.0
Normal $n = 10-99$	0.25
Low $n = 0-9$	0.50

n denotes the maximum number of people likely to be at risk on average during normal occupancy. The factors for Normal and Low are reduced by 0.25 for assembly occupancy and for timber (wood) structures.

Table 10.4 Typical changes to load factors for evaluation of existing buildings [Allen, 1991].

β_C adjustment	Load factor			Load
$\Delta = \sum \Delta_i$	Dead γ_D	Variable γ_L or γ_Q	Earthquake γ_Q	combination factor ψ
−0.4	1.35	1.70	1.40	0.70
0.0	1.25	1.50	1.00	0.70
0.25	1.20	1.40	0.80	0.70
1.00	1.08	1.10	0.40	0.80

Table 10.5 Typical resistance modification factors for bridges [after Allen, 1991].

Component or condition	Resistance modification factor
Steel bolts	1.5
Steel welds	1.3
RC compression members	1.2
RC shear (no stirrups)	0.84

10.5.3 Probabilistic Criteria

Target failure probabilities considered to encapsulate social aspects in a simplified form, the importance of historical buildings, some cost-benefit considerations and using preservation values inferred from current practice in Belgium and based on earlier formats (see Eq. 2.12) were proposed by Schueremans (2001):

$$p_f = S.T.A.C_f.N^{-1}.W^{-1} \times 10^{-4} \tag{10.14}$$

where:

S = social criterion factor (or preservation value)
T = residual service life (years)
A = activity factor
C_f = economic factor (costs or consequences of failure)
N = number of lives at risk (or likely to be in danger)
W = warning factor.

The factors in (10.14) are based in part on earlier work [Allen, 1991; CEB, 1976; CIRIA, 1977] (see Section 2.5.5) and are summarized in Table 10.6. Example applications are available [Schueremans and van Gemert, 2004]. As in other, similar, schemes [e.g. Stewart and Melchers 1988], the number of lives at risk is those at risk of death, rather than the risk of serious or other injuries.

10.5.4 Decision-Theory-Based Criteria

In principle, a more rational approach to selecting the values that might be adopted for p_{fA} or β_A for assessments of existing structures is to use decision-theoretical

@Seismicisolation

Table 10.6 Factors influencing target failure probabilities [based on Schueremans, 2001].

Social criterion factor	S	Warning factor	A
Places of public assembly, dams, internationally recognized historical buildings.	0.00	Fail-safe condition.	0.01
Domestic, trade, industrial, listed historical buildings.	0.05	Gradual failure with some warning likely.	0.1
Bridges.	0.5	Gradual failure hidden from view.	0.3
Towers, masts, offshore structures.	5	Sudden failure without warning.	1.0

Economic factor	C_f	Activity factor	A
- Not serious.	10	Post-disaster activity.	0.3
- Serious.	1	Normal activities: - buildings	1.0
		- bridges.	3.0
- Very serious.	0.1	High exposure structures.	10.0

(socio-economical) tools, similar to the approach used in Section 2.4.2 [Ditlevsen and Arnbjerg-Nielsen, 1989; Ang and De Leon, 1997]. In practice decisions from such an approach might be bounded by regulatory requirements, but the principle remains.

As noted before, in making decisions about existing structures, there are three main courses of action:

(1) leave the structure unchanged ('do nothing');
(2) strengthen the structure or change its use;
(3) demolish the structure and replace it with a new structure.

In cases (2) and (3) there may be a range of alternatives. Although these have an influence on the costs involved, they do not affect the essential discussion to follow.

Consider first the possibility of strengthening the structure as opposed to leaving it unchanged. After assessing the existing structure the probability of failure is estimated as p_{fA} (i.e. the *a posteriori* probability of failure). If c_{fail} is the sum of all the direct costs of failure associated with the structure and c_{new} is the estimated cost for creating a new structure if the existing one were to fail, the expected cost for option (1) is given by:

$$E_1 = (c_{fail} + c_{new})p_{fA} \tag{10.15}$$

If the structure were to be strengthened, a decision would be required as to the acceptable level of safety to be built into the new structure. Let this be p_f^*. Also, the cost of strengthening will be a function of this risk level: let this be given by $c_S(p_f^*) = a + b(1 - p_f^*) > 0$ where a is the initial cost of the strengthening work and $b(\ )$ is an increasing function as the probability of failure reduces. The expected total cost for option (2) is

then given by:

$$E_2 = (c_{\text{fail}} + c_{\text{new}})p_f^* + (a + b(1 - p_f^*)) \tag{10.16}$$

This will have a minimum, typically when $\partial E_2/\partial p_f^* = 0$. Let this minimum, if it exists, be E_{20} at p_{f0}. The decision is then made as follows. If $E_1 < E_{20}$ and $p_{f0} > p_{fA}$, no strengthening should be carried out (i.e. option 1 should be selected). If $E_1 \geq E_{20}$, strengthening the structure would be the most rational choice (i.e. option 2); this implies that $p_f^* > p_{fA}$.

The decision process to consider option (3) is only a little more complex. Recall that for new designs there is a nominal probability of failure considered the 'target' or code specified value, p_{fT} or safety index β_T (see Section 9.6). Clearly, if $p_{fA} >> p_{fT}$ there might be a case for demolition and rebuilding (option 3). In this case the new structure would have a nominal failure probability of p_{fT} and the expected total cost for this option would be

$$E_3 = c_{\text{demolition}} + c_{\text{new}} + (c_{\text{fail}} + c_{\text{new}})p_{fT} \approx c_{\text{new}} + (c_{\text{fail}} + c_{\text{new}})p_{fT} \tag{10.17}$$

where the approximation holds if, as is usually the case, $c_{\text{demolition}} << c_{\text{new}}$.

By decision-theory logic, if $E_3 > E_1$ option (3) is not a rational choice. Simplifying the inequality $E_3 > E_1$ then leads to the following decision rule:

$$\text{if } p_{fA} - \frac{1}{1 + c_{\text{fail}}/c_{\text{new}}} < p_{fT} \text{ then do nothing} \tag{10.18a}$$

$$\text{if } p_{fA} - \frac{1}{1 + c_{\text{fail}}/c_{\text{new}}} \geq p_{fT} \text{ then demolish and build new structure} \tag{10.18b}$$

Decision (10.18a) implies that a high value of p_{fA} could be acceptable provided that $c_{\text{fail}}/c_{\text{new}}$ in the second term of (10.17) is sufficiently large. However, it is likely that a decision outcome based on such logic usually would not be acceptable to society.

In practice the costs of failure c_{fail} is likely to be very high compared to the cost of a new structure c_{new}. Typically the ratio $c_{\text{fail}}/c_{\text{new}}$ is of the order of $10^4 - 10^6$ (CIRIA, 1977). This means that the second term in (10.17) is of the order of $10^{-6} - 10^{-4}$ and thus about an order of magnitude less than typical values for p_{fT}. Hence the second term can be neglected to obtain an approximate decision rule for option (1) as: $p_{fA} < p_{fT}$.

10.5.5 Life-Cycle Decision Approach

The above approach to making decisions about the acceptability of existing structures leads directly to the concept of optimal inspection and repair policies so as to minimize total expected costs, including repair and expected costs as consequences of failure. A number of investigators examined this issue in a variety of contexts [e.g. Thoft-Christensen and Sørensen, 1987; Sørensen and Faber, 1991; Nakken and Valsgard, 1995; Faber et al., 1996; Gomes et al., 2013; Gomes and Beck, 2014a, b], including for multiple limit state situations [e.g. Stewart and Val, 2003; Val, 2004; Akgul and Frangopol, 2005] and results from on-going monitoring processes [e.g. Orcesi and Frangopol, 2011]. Most have relied on mathematical modelling of the structural system of interest, implying that such analysis is representative of reality, such as, for example, cracking in concrete structures under elevated chloride environments [e.g. Vu and
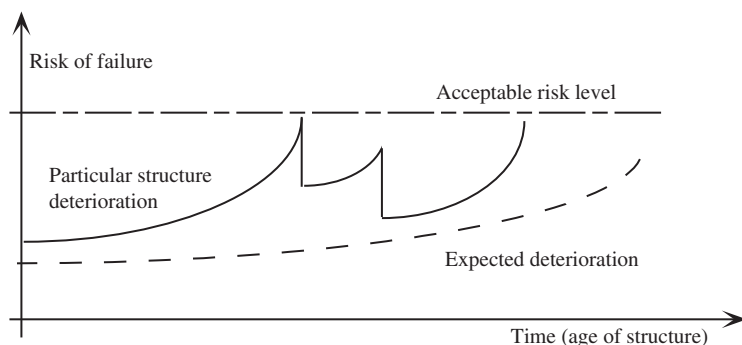
Figure 10.8 Life-cycle reliability and assessment, showing effect of appropriate repairs (schematic).

Stewart, 2005; Val, 2007; Strauss et al., 2008]. Most also have relied on strength issues, whereas serviceability also may be an important criterion for some structures.

It should be clear that reassessments are more likely to be necessary as the structure becomes older. For reinforced concrete structures aging can result in internal damage and interior deterioration, thereby increasing the rate of other influences such as chloride diffusion [Melchers et al., 2008]. Aging also raises the question as to the degree or intensity of the repairs that might be performed, given that further inspections and assessments might be made in the future. The process can be represented schematically as in Figure 10.8.

When the estimated reliability fails below an acceptable level, immediate action is required, such as closing road lanes or reducing the loads on a structure such as a bridge. Such action will bring with it various associated costs. If the estimated reliability lies only a little above the minimum acceptable, urgent action for repair or, worse, rebuilding might be warranted. This will also incur costs, and it may not be a useful medium-term solution, with further repairs etc. possible in the next few years (see Figure 10.8). The balance between possible courses of action and the associated costs if failure does occur can be addressed using a decision framework similar to the that discussed in the previous section and in Chapter 2. In each case the associated optimization criterion is the minimization of expected present value costs.

It is fair to note that life-cycle decision approaches are not necessarily always part of normal engineering practice owing to public works funding mechanisms and, in the private sector, possibly to lack of long-term commitment to a project.

10.6   Conclusion

This chapter has considered the main issues relevant for the probabilistic reliability assessment of existing structures. Many of the uncertainties which face designers of new structures are no longer an issue, as the structure has been 'realized' already. However, in making an assessment, many other uncertainties can arise, particularly if the data available for the original structure has been lost. In this case there are important matters, such as the amount and extent and detailing of reinforcement, for example, which must be inferred from field measurements, with concomitant high uncertainties and hence

penalties in terms of the safety and reliability assessment. It is important that owners, consultants and local authorities maintain adequate records, particularly for structures and buildings likely to be subject to re-use or life extension.

Finally it is noted that the decision-criteria approaches discussed herein may be supplemented by other considerations, including a possible need to preserve heritage values and to allow for architectural integrity in making structural engineering modifications when strengthening existing buildings and structures.

11

Structural Optimization and Reliability

11.1   Introduction

Structural design is primarily about technical issues: ensuring strength and serviceability, construction feasibility, safety, etc. But designers also must be cognizant of costs and maintenance issues. Increasing the safety of structural systems may add to costs, and cost savings sometimes can result in lower levels of structural safety. This chapter is primarily about design, that is the optimal sizing of a structure to meet predefined safety levels, considering explicitly the uncertainties in loads, strengths and engineering models and meeting some cost criterion. Thus the 'optimal' structure is sought under uncertainty conditions.

More specifically, the present chapter is about how to select the set of parameters, $\mathbf{d} = [d_1, d_2, \ldots, d_n]$ say, that define the optimal structure and meet a structural safety requirement $p_f < p_{fT}$ or safety index requirement $\beta > \beta_T$, when all properties and loads are defined, as usual, by the vector of random variables or processes $\mathbf{X}$. In contrast, the previous chapters were about analysis, without $\mathbf{d}$ as an independent set of variables, and the aim being to determine the value of p_f or β for given $\mathbf{X}$.

Some of the earliest works discussing structural reliability concepts recognized structural optimization as a possibility [Johnson, 1953, 1971; Ferry-Borges, 1954; Freudenthal, 1956; Benjamin, 1968; Cornell, 1969b; Turkstra, 1970; and Moses, 1977]. Algorithms explicitly addressing optimal design using reliability measures were proposed by Hilton and Feigen (1960), Liu et al. (1976) and Rosenblueth (1976a,b). Later, Enevoldsen and Sørensen (1994) employed classical decision theory for risk optimization of structural components and systems and also optimal inspection planning and sensitivity measures. Overviews of these developments are available [Moses, 1969; Frangopol, 1985b; and Beck and Gomes, 2012].

The next section (11.2) describes in more detail the type of problem of interest in the present chapter. Three types of optimization problems involving probabilistic information, indirectly or directly and with increasing complexity, are introduced. A simple example problem is used for each, using FOSM theory as the basis for probability calculations. Section 11.3 considers the most common reliability-based optimization problem (Reliability-Based Design Optimization—RBDO) coupled with FOR for probability estimation. To make the solution tractable, two simplifications are introduced, selected from a range of other possibilities proposed in the literature. An alternative is to try to decouple the reliability estimation from the optimization algorithm—a summary of some attempts to do this is provided. Section 11.4 turns to RBDO using system

reliability constraints. This allows free competition between failure modes but is also more difficult to solve. Monte Carlo methods for reliability estimation within optimization are addressed in Section 11.5. For these, the estimation of the gradient of the performance function (limit state function) is a critical issue, and the various approaches proposed for this are reviewed briefly. Finally, life-cycle cost and risk optimization (LCRO) algorithms are considered in Section 11.6. These are less well developed, and much scope for further work remains.

In the following, some familiarity with mathematical optimization theory is assumed. However, only relatively simple optimization problems are considered in this chapter—those that can be solved analytically, by graphical methods or by simple spread-sheet programming. For specialized numerical optimization algorithms, the reader is referred to Arora (2007, 2012), Haftka et al. (1990), Nocedal and Wright (2006) and Rao (2009).

11.2   Types of Reliability-based Optimization Problems

11.2.1   Introduction

Consider the vector $\mathbf{X} \in \mathbb{R}^{n_{RV}}$ that contains the n_{RV} random variables defining the structural dimensions, resistance properties of materials or structural members, loads and model errors. For simplicity, herein loads are modelled as random variables. They are, of course, derivable from random processes in time (Chapter 6).

For optimal design of a structure, however, there are other variables, termed 'design variables' $\mathbf{d}$, that usually are different from those in $\mathbf{X}$. They define the nominal member dimensions, partial safety factors, reinforcement ratio, design life, parameters of inspection and maintenance programs, etc. Let there be n_{DV} components of $\mathbf{d}$ collected in the vector $\mathbf{d} \in \mathbb{R}^{n_{DV}}$. Some components could be simply deterministic variables. Others might be variables such as the mean values of components in $\mathbf{X}$. The total number of variables (some or all random) in the definition of the structure is thus $n_{RV} + n_{DV}$.

As in the previous chapters, there are also limit state requirements to be met, but now these will depend also on $\mathbf{d}$. Also, in some cases, $\mathbf{d}$ may have to meet specific constraints. Let these be termed $g(\mathbf{d}) \leq 0$ and $h(\mathbf{d}) = 0$. Also, the components of the design vector $\mathbf{d}$ may be constrained, defined by $\{\mathbf{d}_{\min} \leq \mathbf{d} \leq \mathbf{d}_{\max}\}$.

The optimization problem now can be defined as finding the optimal vector of design variables $\mathbf{d}^* \in \mathbb{R}^{n_{DV}}$, that minimizes an objective function $f(\mathbf{d})$, subject to constraints, or:

> Find $\mathbf{d}^*$
>
> which minimizes the objective function $f(\mathbf{d})$
>
> subject to the following constraints:
>
> $$h_i(\mathbf{d}) = 0, \quad i = 1, \ldots, p\,;$$
> $$g_j(\mathbf{d}) \leq 0, \quad j = 1, \ldots, q\,;$$
> $$\mathbf{d} \in \mathrm{S} \subset \mathbb{R}^{n_{DV}}, \tag{11.1}$$

Here p is the number of equality constraints, q is the number of inequality constraints and $\mathrm{S} = \{\mathbf{d}_{\min}, \mathbf{d}_{\max}\}$. As before, the failure probability in terms of the random variables
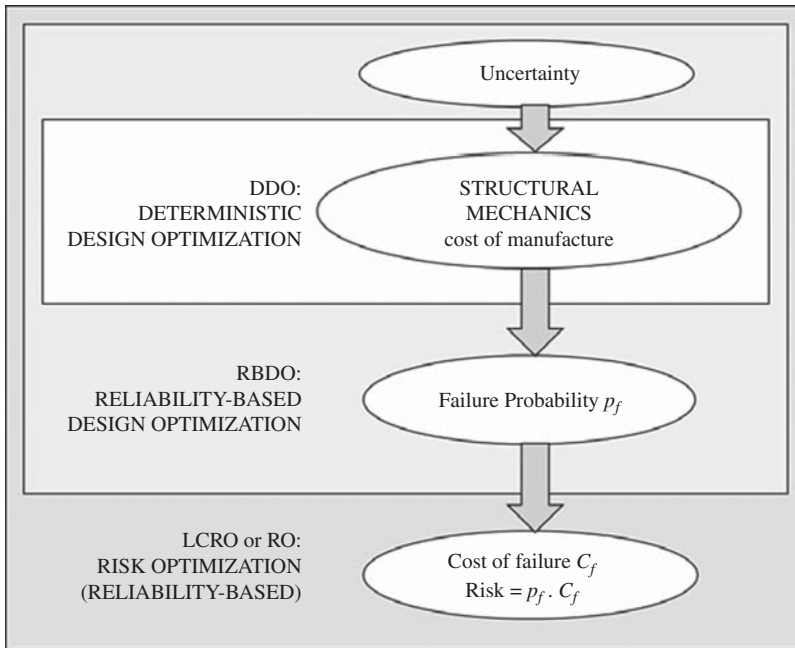
Figure 11.1 Conceptual relationship between structural uncertainties in design and the increasing complexity of optimization problems.

X can be expressed as in (1.31) for one limit state function and (5.9) more generally for the failure domain D. The objective function $f(\mathbf{d})$ in principle could be a complex combination of many factors but often is taken simply as the total volume of structural materials, or the cost of construction or manufacture.

The formal problem (11.1) can be reduced to a number of special cases (Figure 11.1). Starting from the uncertainties defining the structural reliability problem, it shows the increasing complexity that can be considered for probabilistic design optimization. However, mostly there are no simple (progressive) relationships between the types of problems as each relies on quite different formulations [Beck and Gomes, 2012]. These formulations are described below.

11.2.2 Deterministic Design Optimization (DDO)

11.2.2.1 Formulation

Deterministic Design Optimization (DDO) takes uncertainties into account only implicitly. Uncertainties in material strengths and in loads are considered only through partial safety factors. Formally DDO can be stated as:

Find $\mathbf{d}^*$ which minimizes $f(\mathbf{d})$

subject to: $\sigma(\mathbf{d}) \leq \sigma_{ALL},\ \mathbf{d} \in S,$ \hfill (11.2)

where, for example, σ denotes working stress and σ_{ALL} is an allowable stress, such as may be defined by the yield stress of the material, as in allowable stress design (*cf.* 1.1).

In terms of limit state (or LRFD) design:

Find $\mathbf{d}^*$ which minimizes $f(\mathbf{d})$

subject to: $\phi R(\mathbf{d}) \geq \gamma_D D_n + \gamma_L L_n + \gamma_W W_n, \ \mathbf{d} \in S,$ \hfill (11.3)

where ϕ and γ_i are partial safety factors on resistance and load variables, respectively, and $(\ )_n$ denotes nominal values for D, L, W, which refer to Dead, Live and Wind loads, respectively.

Since uncertainties in material strengths and loads are not considered explicitly, this formulation has the same limitations as discussed in Section 1.2. For example, optimization using the DDO formulation may lead to the conclusion that for a hyperstatic (statically indeterminate) structure one or more members are not loaded at all and thus could be removed. But considerations of uncertainty would indicate a finite probability that the members in question could be required to take some load at some time. Thus, the actual probability of failure would be underestimated. It follows that the results from DDO (deterministic design optimization) are not robust with respect to uncertainties. Efforts to improve robustness ('Robust Design Optimization') have focussed on adding factors, such as one or more statistics of structural behaviour or performance, to the objective function, or building a multi-objective optimization problem, with, say, mean system performance to be maximized and performance variance to be minimized [*cf.* Zang et al., 2005; Beyer and Sendhoff, 2007; Schuëller and Jensen, 2009; Beck et al., 2015].

11.2.2.2 Example of DDO Using FOSM

The essential features of DDO can be illustrated with a simple example, with the linear limit state function $g(\mathbf{d}, \mathbf{X}) = R - S = 0$ and with two independent Normal random variables $R \sim \mathrm{N}(\mu_R, \sigma_R), S \sim \mathrm{N}(\mu_S, \sigma_S)$ where R and S are resistance and load effect. As before, μ is the mean and σ is the standard deviation. This allows use of FOSM theory to estimate probabilities of failure. From Section 1.4.3 the failure probability is given by:

$$p_f = \Phi(-\beta), \ \text{with} \ \beta = \frac{\mu_R - \mu_S}{\sqrt{\sigma_R^2 + \sigma_S^2}}$$ \hfill (11.4)

where $\Phi(.)$ is the standard Normal distribution function and β is the safety index.

For this example, let the objective function be the mean μ_R of the structural resistance, and let there be a constraint on its value. Hence (11.2) is reformulated as:

Find μ_R^* which minimizes μ_R

subject to: $\mu_R \geq \gamma \mu_S,$ \hfill (11.5)

Here $\gamma \geq 1$ is a safety coefficient. The trivial solution $\mu_R = \mu_S = 0$, for which the structure vanishes, is avoided by requiring that $\mu_S > 0$. Using standard optimization notation (*cf.* 11.1), the problem is rewritten as:

Find μ_R^* which minimizes μ_R

subject to: $g(\mu_R) = \gamma \mu_S - \mu_R \leq 0$ \hfill (11.6)

Since this problem has a single design variable, a linear objective function and a linear inequality constraint, it follows immediately that the optimal solution occurs when $g(\mu_R) = 0$, which leads to $\mu_R^* = \gamma\mu_S$.

A more formal solution is obtained as follows. Since (11.6) represents a constrained optimization, use a Lagrangian multiplier u in (11.6) together with a slack variable s to produce the Lagrangian function:

$$\mathcal{L}(\mu_R, u, s) = \mu_R + u(\gamma\mu_S - \mu_R + s^2) \tag{11.7}$$

As is well-known, the condition for a minimum (formally the first-order Karush-Kuhn-Tucker (KKT) condition) is to have (11.7) stationary with respect to the design variable, the Lagrange multiplier and the slack variable. This produces:

$$\frac{\partial\mathcal{L}(\mu_R, u, s)}{\partial\mu_R} = 1 - u^* = 0, \qquad \therefore \qquad u^* = 1;$$

$$\frac{\partial\mathcal{L}(\mu_R, u, s)}{\partial s} = 2\,u^*s^* = 0, \qquad \therefore \qquad s^* = 0; \tag{11.8}$$

$$\frac{\partial\mathcal{L}(\mu_R, u, s)}{\partial u} = \gamma\mu_S - \mu_R^* + (s^*)^2 = 0, \qquad \therefore \qquad \mu_R^* = \gamma\mu_S.$$

The solution is obtained from the third condition. The other two (first two lines) refer to the constraint being active at the optimal point—the solution satisfies the first-order KKT necessary conditions and also the sufficiency conditions (for mathematical details see, for example, Nocedal and Wright, 2006; Arora, 2012). Hence, $\mu_R^* = \gamma\mu_S$ is the global minimum for this problem. Note that this result depends directly on the required safety factor γ, chosen as a constraint in this example.

11.2.3 Reliability-Based Design Optimization (RBDO)

11.2.3.1 Formulation

For Reliability-Based Design Optimization (RBDO) the objective function contains the design vector $\mathbf{d}$ as before, but the deterministic constraints in (11.2 and 11.3) are replaced by reliability constraints:

Find $\mathbf{d}^*$ which minimizes $f(\mathbf{d})$

subject to: $p_{fi}(\mathbf{d}) \leq p_{fTi}, i = 1, \ldots, n_{LS}; \mathbf{d} \in S$ \hfill (11.9)

where $p_{fi}(\mathbf{d})$ is the failure probability for the ith failure mode, $r_{Ti} = 1 - p_{fTi}$ is the target reliability for the ith failure mode, n_{LS} is the number of limit states and $S = \{\mathbf{d}_{\min}, \mathbf{d}_{\max}\}$ as in (11.1). The equivalent of (11.9) in terms of the reliability index β is:

Find $\mathbf{d}^*$ which minimizes $f(\mathbf{d})$

subject to: $\beta_i(\mathbf{d}) \geq \beta_{Ti}, i = 1, \ldots, n_{LS}; \mathbf{d} \in S$ \hfill (11.10)

Classical structural reliability methods such as FOSM, FOR or SOR methods or Monte Carlo simulation can be used to evaluate the p_{fi} and β_i in (11.9) and (11.10). However, the computational cost of evaluating these reliabilities may be significant, since the reliability analysis is now part of the computations for the optimization process.

This is discussed further in Sections 11.3 and 11.4. The example below uses the simplest approach—FOSM.

An alternative formulation in terms of system reliability $(1 - p_{fsys})$ is:

> Find $\mathbf{d}^*$ which minimizes $f(\mathbf{d})$
>
> subject to: $p_{fsys}(\mathbf{d}) \leq p_{fTsys}$; $\mathbf{d} \in S,$ (11.11)

where system reliability $(1 - p_{fsys})$ is a function of component reliabilities $(1 - p_{fi}, i = 1, \ldots, n_{LS})$ and where $r_{Tsys} = (1 - p_{fTsys})$ is the target system reliability. RBDO problems with system reliability constraints are significantly more difficult to solve; these problems are further addressed in Section 11.4.

11.2.3.2 Example of RBDO using FOSM

For the same example as above, the RBDO problem (11.10) can be stated as:

> Find μ_R^* which minimizes μ_R
>
> subject to: $\beta(\mu_R) \geq \beta_T,$ (11.12)

with the same notation as before and β_T the target reliability index. Assume, as usual for structural reliability, that $\beta_T \geq 0$, so that $p_f \leq 0.5$. Using (11.5) this becomes:

> Find μ_R^* which minimizes μ_R
>
> subject to: $g(\mu_R) = \beta_T - \dfrac{\mu_R - \mu_S}{\sqrt{\sigma_R^2 + \sigma_S^2}} \leq 0,$ (11.13)

In this case the Lagrangian function is:

$$\mathcal{L}(\mu_R, u, s) = \mu_R + u\left(\beta_T - \frac{\mu_R - \mu_S}{\sqrt{\sigma_R^2 + \sigma_S^2}} + s^2 \right). \tag{11.14}$$

and the stationarity conditions for an optimum (i.e. the first order KKT conditions) are:

$$\frac{\partial \mathcal{L}(\mu_R, u, s)}{\partial \mu_R} = 1 - \frac{u^*}{\sqrt{\sigma_R^2 + \sigma_S^2}} = 0, \quad \therefore \quad u^* = \sqrt{\sigma_R^2 + \sigma_S^2};$$

$$\frac{\partial \mathcal{L}(\mu_R, u, s)}{\partial s} = 2\,u^*s^* = 0, \qquad \therefore \quad s^* = 0;$$

$$\frac{\partial \mathcal{L}(\mu_R, u, s)}{\partial u} = \beta_T - \frac{\mu_R^* - \mu_S}{\sqrt{\sigma_R^2 + \sigma_S^2}} + (s^*)^2 = 0, \quad \therefore \quad \mu_R^* = \mu_S + \beta_T\sqrt{\sigma_R^2 + \sigma_S^2}.$$

$$\tag{11.15}$$

As before, the necessary KKT conditions are also sufficient. Therefore $\mu_R^* = \mu_S + \beta_T\sqrt{\sigma_R^2 + \sigma_S^2}$ is the global minimum. This shows that the optimal result depends directly on the chosen value of the target reliability index β_T.

11.2.4 Life-Cycle Cost and Risk Optimization (LCRO)

11.2.4.1 Formulation

Inclusion of costs of structural failure and consequential costs in the analysis requires a more comprehensive optimization (*cf.* Section 2.4.2). As in Eq. (2.7) each potential structural failure mode has an associated expected cost of failure (C_{EF}) and this depends on design decisions, i.e. $C_f(\mathbf{d})$, thus:

$$C_{EF}(\mathbf{d}) = C_f(\mathbf{d})p_f(\mathbf{d}) \tag{11.16}$$

where $p_f(\mathbf{d})$ is the probability of occurrence of that failure mode. Hence the total expected cost C_{ET} over the expected life of the structure (*cf.* Eq. 2.7) is a function of $\mathbf{d}$:

$$C_{ET}(\mathbf{d}) = C_c(\mathbf{d}) + C_o(\mathbf{d}) + C_{i\&m}(\mathbf{d}) + C_d(\mathbf{d}) + \sum_{i=1}^{n_{LS}} C_{fi}(\mathbf{d})p_{fi}(\mathbf{d}) \tag{11.17}$$

where C_c is the cost of construction, C_o is the cost of operation, $C_{i\&m}$ is the cost of inspection and maintenance, C_d is the cost of eventual disposal and C_{fi} is the cost of failure associated with the ith failure mode (limit state). As discussed in Section 2.4.2 there are likely to be costs associated with increasing safety—often, but not always, changes in $\mathbf{d}$ that reduce costs also could result in increased probability of failure and thus also an increase in expected cost of failure. In principle, reduction in expected failure costs can be achieved by targeted changes in $\mathbf{d}$, which generally increase costs. There are likely to be trade-offs between safety and economy and these should be considered, ideally, over the expected lifetime of the structure. This life-cycle problem can be formulated as Life-cycle Cost and Risk Optimization (LCRO):

> Find $\mathbf{d}^*$ which minimizes $C_{ET}(\mathbf{d})$
> subject to: $\mathbf{d} \in S$ $\tag{11.18}$

Compared to (11.9 and 11.10) for RBDO, expression (11.18) with (11.17) has the reliability constraints as part of the objective function. This is a crucial difference, not always made clear in the literature, with some works referring to (11.18) as an RBDO problem.

When there also are regulatory requirements on acceptable risk levels, the corresponding system reliability constraints can be included in (11.18) as:

> Find $\mathbf{d}^*$ which minimizes $C_{ET}(\mathbf{d})$
> subject to: $p_{fsys}(\mathbf{d}) \leq p_{fTsys}$; $\mathbf{d} \in S$ $\tag{11.19}$

or

> Find $\mathbf{d}^*$ which minimizes $C_{ET}(\mathbf{d})$
> subject to: $\beta_{sys}(\mathbf{d}) \geq \beta_{Tsys}$; $\mathbf{d} \in S$ $\tag{11.20}$

Whenever possible, the formulation in (11.18) should be preferred, as fewer constraints should result in more economical designs. For inactive constraints, (11.19) and (11.20) are equivalent to (11.18). The life-cycle risk optimization formulation is further discussed in Section 11.6.

11.2.4.2 Example of LCRO using FOSM

Using the same variables and FOSM reliability formulation as for the previous two examples, the Life-cycle Cost and Risk Optimization (LCRO) problem (11.18) becomes, for the special case with all lifetime costs neglected (*cf.* 11.17):

Find μ_R^* which minimizes $\mu_R + C_f\, p_f(\mu_R)$

subject to: $g(\mu_R) = \mu_S - \mu_R \leq 0.$ (11.21)

As before, it is required that $\mu_S > 0$ to avoid the trivial solution $\mu_R = \mu_S = 0$, for which the structure vanishes. Note that in (11.21) there is no safety constraint, but the probability of failure is part of the objective function. Assuming the cost of failure is proportional to μ_S ($C_f = k\,\mu_S$) and using the reliability index β (11.4), (11.21) becomes:

Find μ_R^* which minimizes $\mu_R + k\,\mu_S\,\Phi(-\beta)$

subject to: $g(\mu_R) = \mu_S - \mu_R \leq 0,$ (11.22)

As in the two previous examples, applying the Lagrangian multiplier u and the slack variable s, the Lagrangian function is:

$$\mathcal{L}(\mu_R, u, s) = \mu_R + k\,\mu_S\,\Phi(-\beta) + u(\mu_S - \mu_R + s^2).$$ (11.23)

The stationarity condition (first order KKT condition) for a minimum is:

$$\frac{\partial \mathcal{L}(\mu_R, u, s)}{\partial \mu_R} = 1 + k\,\mu_S \frac{\partial \Phi}{\partial \beta}\frac{\partial \beta}{\partial \mu_R} - u^* = 1 - \frac{k\,\mu_S\,\phi(\beta^*)}{\sqrt{\sigma_R^2 + \sigma_S^2}} - u^* = 0;$$

$$\therefore \quad u^* = 1 - \frac{k\,\mu_S\,\phi(\beta^*)}{\sqrt{\sigma_R^2 + \sigma_S^2}},$$ (11.24)

where β^* is the candidate optimum reliability index and ϕ is the standard normal probability density function. Without numerical values it is not possible to determine, from the above, whether the constraint is active or not. However, an active constraint in (11.22) would lead to very large failure probabilities, which is unusual in structural engineering. Hence, it is reasonable to assume the constraint is inactive, hence: $u^* = 0$ and $s^* > 0$. Then from (11.24) the optimal reliability index is given by:

$$\beta^* = \left[-2\,ln\left(\frac{\sqrt{2\pi}\sqrt{\sigma_R^2 + \sigma_S^2}}{k\,\mu_S} \right) \right]^{1/2}.$$ (11.25)

Note that this result is independent of μ_R^*. Eq. (11.25) also shows the minimal value of the failure cost multiplier k, for which a real solution is obtained: $k \geq k_0 = \sqrt{2\pi}\sqrt{\sigma_R^2 + \sigma_S^2}/\mu_S$. Note also that if the target reliability index β_T in (11.10) of the RBDO example (section 11.2.4.2) is set equal to the above (i.e. that given in 11.25)
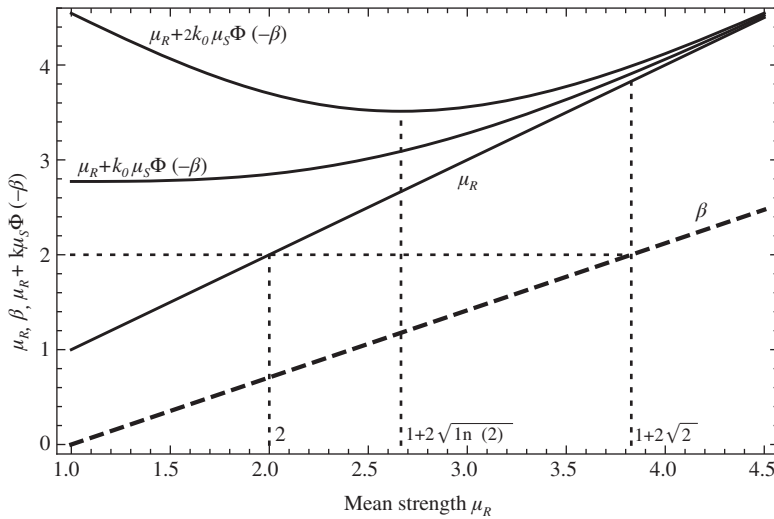
Figure 11.2 Solutions of DDO, RBDO and LCRO problems solved using FOSM.

the same result is obtained. In this case RBDO and LCRO provide the same optimal solution for the present example.

11.2.5 Comparison, Summary and Outlook

The solutions obtained by DDO, RBDO and LCRO for the three FOSM example problems considered above are compared in Figure 11.2, for the special case $\mu_S = \sigma_S = \sigma_R = 1$. The continuous heavy lines represent the objective functions for DDO and RBDO, as functions of mean strength μ_R, and for LCRO as a function of $(\mu_R + k\,\mu_S\,\Phi(-\beta))$, with $k = k_0$ and $k = 2k_0$).

The broken lines represent the optimum solutions for the problems considered above, based on setting $\gamma = 2$ for DDO and $\beta_T = 2$ for RBDO. The horizontal broken lines denote where the constraints become active (with $\gamma = \beta_T = 2$).

For the LCRO problem with failure cost multiplier $k = k_0$, the minimum of the objective function is obtained for an active constraint, with $\mu_R = \mu_S = 1$. For $k > k_0$, the objective function becomes convex, the constraint becomes inactive and the global minimum is inside the design domain. For $k = 2k_0$, the optimal strength is $\mu_R^* = 1 + 2\sqrt{\ln(2)} \cong 2.6651$.

The three examples given above were very simple and used the most elementary structural reliability theory (i.e. FOSM), including both probability of failure p_f and the safety index β. They showed the formulation of the objective function, of the constraints and also the optimization approach, in each case using Lagrangian multiplier formalism. Generally similar examples are available in the literature [Rosenblueth, 1976; Kanda and Ellingwood, 1991].

From here on, the discussion will focus largely on the formulation and solution of RBDO (Reliability-Based Design Optimization) problems, as these have had most attention in the literature. The next section considers RBDO with the use of the FOR method for estimating failure probabilities (and safety indices).

@Seismicisolation

11.3 Reliability Based Design Optimization (RBDO) Using First Order Reliability (FOR)

11.3.1 Introduction

Solving the reliability constraints in Eqs. (11.9) and (11.10) by the First Order Reliability (FOR) method leads to nested optimization loops. The outer loop involves design optimization; the inner loop involves search for the design point. The interactive solution of such nested loops is clearly computationally demanding. However, this classical approach is described here, before discussion of alternatives.

The First Order Reliability (FOR) method (*cf.* Section 4.4) consists of mapping the reliability problem from the original space $\mathbf{X}$ to standard normal (Gaussian) space $\mathbf{Y}$. This is accomplished by the transformation $\mathbf{y} = \mathrm{T}(\mathbf{x})$. The most probable point $\mathbf{y}^*$ is then found by solving a constrained optimization problem [*cf.* (4.4) and Section 4.4], restated here as:

Given $\mathbf{d}$, find $\mathbf{y}^*$ which minimizes $\beta(\mathbf{d}) = \|\mathbf{y}\| = (\mathbf{y}^T \mathbf{y})^{1/2}$

subject to: $g(\mathbf{d}, \mathbf{y}) = 0$ (11.26)

where $g(\mathbf{d}, \mathbf{y}) = g(\mathbf{d}, \mathrm{T}(\mathbf{x})) = 0$ is the limit state function, also mapped to the standard normal space. As before (*cf.* Section 4.3.4), the point $\mathbf{y}^*$ is known variously as the 'design' point, the point of maximum likelihood or the Most Probable Point (MPP). It is the point just on the edge or surface of the failure domain, possessing the highest likelihood (*cf.* Figure 4.5).

After $\mathbf{y}^*$ is found, a linear approximation to the limit state function is constructed, which yields [*cf.* (4.1)] $p_f(\mathbf{d}) \approx \Phi(-\beta(\mathbf{d}))$. This expression involves only the variables $\mathbf{d}$ since these only are permitted to be varied in the optimization process (*cf.* Section 11.1).

The minimization in (11.26) has to be carried out for every failure mode, and is solved for a candidate value of $\mathbf{d}$. This process must be performed repeatedly in the search for the optimal design $\mathbf{d}^*$. However, this process also is part of the optimization in (11.9 or 11.10) and if this is done by iteration, RBDO using FOR leads to nested optimization loops. This is computationally cumbersome and demanding. Further, typically the whole design space $\mathbf{d}$ is explored systematically during search for $\mathbf{d}^*$. As a result, (11.26) sometimes has to be solved for odd configurations, with the whole process possibly becoming unstable or even unsolvable. Therefore, alternative and robust ways of solving Eq. (11.26) are of interest.

11.3.2 Alternative Robust Solutions Schemes

One robust solution can be constructed by considering the cumulative distribution of the limit state function $G = g(\mathbf{d}, \mathbf{X})$, which is a random variable as a function of $\mathbf{d}$ and $\mathbf{X}$. In this context, it has been called the performance function [Youn et al., 2003]. The probability of failure as a function of the design parameters $\mathbf{d}$ is then:

$$p_f(\mathbf{d}) = P[g(\mathbf{d}, \mathbf{X}) \leq 0] = F_G(0) = \int_{g(\mathbf{d},\mathbf{x}) \leq 0} f_{\mathbf{X}}(\mathbf{x}) \, d\mathbf{x} \approx \Phi(-\beta(\mathbf{d})), \quad (11.27)$$

This expression can be solved in original space $\mathbf{X}$ or in standard Gaussian space $\mathbf{Y}$. For some values of $\mathbf{d}$, the reliability constraint will not become active; hence the limit state
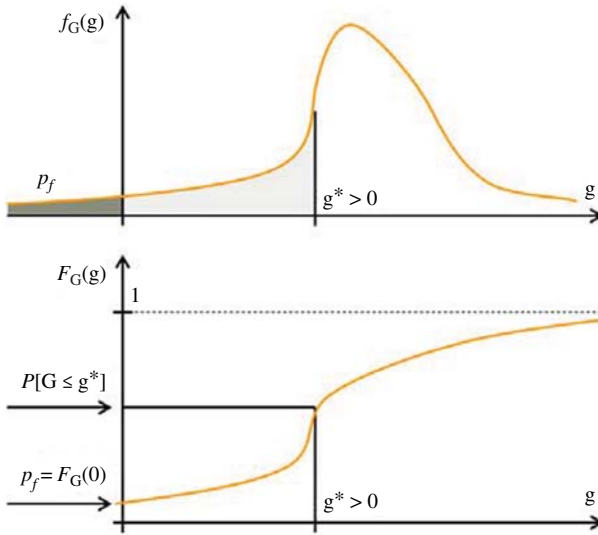
Figure 11.3 Probability density $f_G(g)$ and cumulative distribution $F_G(g)$ of the limit state function.

function will not become zero. Replacing the limit state 'zero' by value g^* produces:

$$F_G(g^*) = \int_{-\infty}^{g^*} f_G(z)\,dz = \int_{g(\mathbf{d},\mathbf{x})\leq g^*} f_{\mathbf{X}}(\mathbf{x})\,d\mathbf{x} \approx \Phi(-\beta_G) \tag{11.28}$$

which is valid for any $g = g^*$. These relations are sketched in Figure 11.3.

The last term in (11.28) involves a first-order approximation, equivalent to FOR, to the probability $F_G(g) = P[G \leq g]$. The original reliability constraint is recovered for $g = 0$, i.e., $p_f(\mathbf{d}) = F_G(0)$. The generalized reliability index β_G, which is a non-increasing function of g, is obtained from the equality [Madsen et al., 1986]:

$$F_G(g) = \Phi(-\beta_G) \tag{11.29}$$

This equality can be written in two alternative forms, using inverse transformations:

$$\beta_G(g) = -\Phi^{-1}[F_G(g)], \tag{11.30a}$$

$$g(\beta_G) = F_G^{-1}[\Phi(-\beta_G)]. \tag{11.30b}$$

The non-increasing $\beta_G \sim g$ relationship is obtained from the one-to-one mapping $F_G(g) \sim g$; it completely describes the cumulative distribution of the performance function. These relations are shown in Figure 11.4.

With this background, the reliability constraint in (11.26) can be written as:

$$F_G(0) \leq \Phi(-\beta_T), \tag{11.31}$$

which can be expressed in two alternative ways [Youn et al., 2003]:

$$\beta = -\Phi^{-1}[F_G(0)] \geq \beta_T, \tag{11.32a}$$

$$g_p^* = F_G^{-1}[\Phi(-\beta_T)] \geq 0, \tag{11.32b}$$
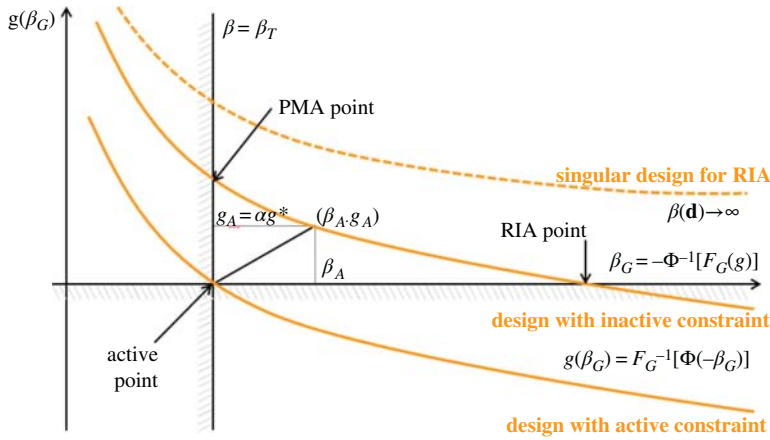
Figure 11.4 Interpretation of reliability constraint and generalized reliability index.

where β is the original, conventional reliability index, and g_p^* is called the 'target probabilistic performance measure'. Using (11.32b) to impose the reliability constraint:

$$g_p(\mathbf{d}) = F_G^{-1}[\Phi(-\beta(\mathbf{d}))] \geq 0, \tag{11.33}$$

where g_p is performance measure associated to reliability index β.

It follows from the above that there are two equivalent ways of expressing the RBDO constraint in (11.26). The first is the conventional form, which has been called the 'Reliability-Index Approach' (RIA) in this context:

Given $\mathbf{d}$, find $\mathbf{y}_{RIA}^*$ which minimizes $\beta(\mathbf{d}) = \|\mathbf{y}\|$

subject to: $g(\mathbf{d}, \mathbf{y}) = 0$. (11.34)

In this expression the point $\mathbf{y}_{RIA}^*$ was known also simply as $\mathbf{y}^*$ in Section 4.3. It was there known as the 'design' or 'checking' point or the Most Probable Point (MPP). It is the point of maximum likelihood within the failure domain, and usually located on its boundary (*cf.* Section 4.3).

Another way of expressing the RBDO constraint in (11.26) is the 'Performance-Measure Approach' (PMA), defined as:

Given $\mathbf{d}$, find $\mathbf{y}_{PMA}^*$ which minimizes $g(\mathbf{d},\ \mathbf{y})$

subject to: $\|\mathbf{y}\| = \beta_T$. (11.35)

where $\mathbf{y}_{PMA}^*$ is the 'Minimal Performance Point', herein abbreviated to MinPP. As shown in [Youn et al., 2003], Eq. (11.35) can be solved using the AMV algorithm [Tu et al., 1999]:

$$\mathbf{y}_{k+1} = -\beta_T \frac{\nabla g(\mathbf{d},\ \mathbf{y}_k)}{\|\nabla g(\mathbf{d},\ \mathbf{y}_k)\|} = -\boldsymbol{\alpha}_k \beta_T \tag{11.36a}$$

$$g(\mathbf{d}, \mathbf{y}_{k+1}) = g(\mathbf{d}, -\boldsymbol{\alpha}_k \beta_T) \tag{11.36b}$$

(a) Active reliability constraint: $\mathbf{y}^*_{RIA} = \mathbf{y}^*_{PMA}$ **(b) Inactive reliability constraint:** $\mathbf{y}^*_{RIA} \neq \mathbf{y}^*_{PMA}$
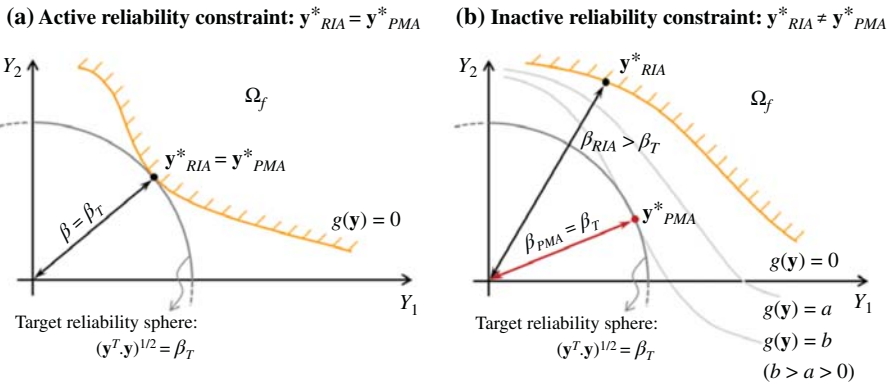
Figure 11.5 Comparison RIA x PMA: for active reliability constraint (left), points $\mathbf{y}^*_{RIA}$ and $\mathbf{y}^*_{PMA}$ are the same; for inactive constraint (right), these points are different.

11.3.3   Comparison Between RIA and PMA Solution Schemes

The differences between RIA and PMA and $\mathbf{y}^*_{RIA}$ and $\mathbf{y}^*_{PMA}$ are illustrated in Figure 11.5. The solutions $\mathbf{y}^*_{RIA}$ and $\mathbf{y}^*_{PMA}$ are the same if, at the end of an RBDO iteration, the constraint is active (see also Figure 11.4). At any other point and for a given design $\mathbf{d}$, the point $\mathbf{y}^*_{PMA}$ represents the point of *minimal* performance on the target reliability hyper-sphere.

The main difference between RIA and PMA is the type of optimization problem that is solved in each case. It usually is easier to minimize a complicated function subject to a simple constraint (as in (11.35) for PMA) than to minimize a simple function subject to a complicated constraint (as in (11.34) for RIA). It has been demonstrated by examples that PMA tends to be more robust and converge faster than RIA [Youn et al., 2003]. As a result it tends to be more effective when the probabilistic constraint is either very feasible or very infeasible [Youn et al. 2003]. One of the reasons for this is that in PMA only the direction vector needs to be determined and this can take advantage of the spherical equality constraint $\|\mathbf{y}\| = \beta_T$ to find the minimal performance point (MinPP) $\mathbf{y}^*_{PMA}$.

It appears from experience that iterative convergence schemes also favour PMA. Usually, a search using the conventional RIA uses the HLRF algorithm (Section 4.3.6) and requires several iterations to reach the failure surface given by $g(\mathbf{d}, \mathbf{y}) = 0$. In the process the optimal design parameter(s) $\mathbf{d}$ is obtained. Typically, also, for a large target value of β the number of iterations required to converge on the limit state function increases, as $\mathbf{y}^*_{RIA}$ is further away from the origin. In contrast, for PMA the target reliabilities β_T are defined from the outset, and the search starts already on the $\|\mathbf{y}\| = \beta_T$ hyper-sphere. Thus the PMA search is independent of β [Lee et al., 2002]. Experience also shows that PMA tends to have lower dependence on the distribution of the random variables, as it is less affected by non-linearities in the $\mathbf{y} = T(\mathbf{x})$ mapping [Youn and Choi, 2004b]. This means that PMA can handle different distributions without significantly increasing the number of function evaluations. On the other hand, RIA often diverges when strongly non-Gaussian random variables are employed. For some values of $\mathbf{d}$, the RIA solution cannot be found since $\beta \to \infty$ (see Figure 11.4). The PMA solution, however, is always obtainable.

11.3.4 Solution of Nested Optimization Problems

Solution of RBDO problems using FOR leads to nested optimization problems. The inner optimization loop for reliability constraints can be solved using the RIA or PMA approaches, as discussed above. Solution of the outer structural optimization loop can be achieved with any of a variety of iterative numerical algorithms [Arora, 2007, 2012; Haftka et al., 1990]. One approach is to use Sequential Linear Programming [Nocedal and Wright, 2006; Rao, 2009] after linearizing the objective function and the constraints, and application of the Lagrangian multiplier technique, in a manner similar to Sections 4.3.4 to 4.3.6. Linearizing the constraints is not equivalent to replacing FOR by FOSM, as illustrated in the example to follow. The example also illustrates solution by Sequential Linear Programming.

11.3.5 Example of RBDO Using RIA and PMA

Consider now the design of a metal beam against formation of a plastic hinge, based on Problem 4.4. The random variables are the steel yield stress (σ_y), the plastic modulus of the cross-section (S) and the external bending moment load (M). These are grouped in the vector $\mathbf{X} = \{\sigma_y, S, M\}^T = \{X_1, X_2, X_3\}^T$. Table 4.1 shows the corresponding statistical parameters. An additional safety factor $\gamma = d$ is introduced to construct the optimization problem. The limit state function becomes:

$$g_X(d, \mathbf{X}) = d\,S\sigma_y - M = d\,X_1 X_2 - X_3 = 0 \tag{11.37}$$

As in Problem 4.4, this limit state, transformed to standard Gaussian space ($\mathbf{y} = T(\mathbf{x})$), is:

$$g(d, \mathbf{y}) = g_X(d, T^{-1}(\mathbf{y})) = d(5y_1 + 40)(2.5y_2 + 50) - 200y_3 - 1000$$
$$= d(12.5y_1 y_2 + 100y_2 + 250y_1 + 2000) - 200y_3 - 1000 \tag{11.38}$$

Solution of Problem 4.4 is recovered for $d = 1$, with $\beta = 3.0491$ obtained by an interactive solution. In the present example, the smallest d which produces a target reliability index of $\beta_T = 4$ is sought. The **RIA** version of this problem is:

Find d^* which minimizes $-d$

subject to: $\beta_T - \beta(d, \mathbf{y}_{RIA}^*) \leq 0$ \hfill (11.39)

for which the reliability index $\beta(d)$ is obtained as the solution to the internal optimization problem in (11.34).

The **PMA** version of the same problem is:

Find d^* which minimizes $-d$

subject to: $-g(d, \mathbf{y}_{PMA}^*) \leq 0$ \hfill (11.40)

where the internal optimization problem is given by Eq. (11.35).

The external problems are solved using Sequential Linear Programming [Nocedal and Wright, 2006; Rao, 2009]. The objective function is already linear; hence only the constraints need to be linearized. Starting from an initial trial design d_0, for $k = 0$, the RIA problem becomes:

For $k = 0, 1, 2, \ldots$, until $|d_{k+1} - d_k| \le \varepsilon_f$, starting with trial d_0:

find d which minimizes $-d$

subject to: $\beta_T - \beta(d_k) - \dfrac{\partial \beta}{\partial d}(d_k)(d - d_k) \le 0$ (11.41)

where $\beta(d_k)$ is solved using the HLRF algorithm (Section 4.3.6).

To simplify the notation, the linearized constraint in (11.41) is written as:

$$a_k + b_k d \le 0; \text{ where } a_k = \beta_T - \beta(d_k) + \frac{\partial \beta}{\partial d}(d_k)d_k \text{ and } b_k = -\frac{\partial \beta}{\partial d}(d_k) \qquad (11.42)$$

The Lagrangian function for the linearized problem is:

$$\mathcal{L}(d, u, s) = -d + u(a_k + b_k d + s^2) \qquad (11.43)$$

where, as before, u is a Lagrangian multiplier and s is a slack variable. For d^* to be solution to the above problem, the KKT first order necessary conditions are:

$$\frac{\partial \mathcal{L}}{\partial d} = -1 + u\, b_k = 0 \qquad \therefore \qquad u = \frac{1}{b_k} \qquad (11.44a)$$

$$\frac{\partial \mathcal{L}}{\partial u} = a_k + b_k d^* + s^2 = 0 \qquad (11.44b)$$

$$\frac{\partial \mathcal{L}}{\partial s} = 2\, u\, s = 0 \qquad\qquad \therefore \qquad s = 0 \qquad (11.44c)$$

Eventually, from Eq. (11.44b):

$$d^* = d_{k+1} = -\frac{a_k}{b_k} = d_k + \frac{\beta_T - \beta(d_k)}{\frac{\partial \beta}{\partial d}(d_k)} \qquad (11.45)$$

The solution in (11.45) shows the linearized reliability constraint. Although the constraint is linearized, computation of $\beta(d_k)$ is still done by FOR. The solution also involves the gradient $\partial \beta / \partial d$, which can be obtained interactively by repetitive hand calculations, as in Problem 4.4. For the present solution, finite differences are used.

The Sequential Linear Programming formulation of the PMA problem is:

For $k = 0, 1, 2, \ldots$, until $|d_{k+1} - d_k| \le \varepsilon_f$, starting with trial d_0:

find d which minimizes $-d$

subject to: $-g(d_k, \mathbf{y}_{PMA}^*) - \dfrac{\partial g}{\partial d}(d_k, \mathbf{y}_{PMA}^*)(d - d_k) \le 0$ (11.46)

where $\mathbf{y}_{PMA}^*$ is found using the AMV algorithm [Wu et al., 1990] (Section 4.7).

As before, to simplify the notation, the linearized constraint in (11.46) is rewritten as:

$$a_k + b_k d \le 0; \text{ where } a_k = -g(d_k, \mathbf{y}_{PMA}^*) + \frac{\partial g}{\partial d}(d_k, \mathbf{y}_{PMA}^*)d_k$$

$$\text{and } b_k = -\frac{\partial g}{\partial d}(d_k, \mathbf{y}_{PMA}^*) \qquad (11.47)$$

Then the Lagrangian function for the linearized problem is:

$$\mathcal{L}(d, u, s) = -d + u(a_k + b_k d + s^2) \tag{11.48}$$

which is identical to the Lagrangian of the RIA solution (11.43). Hence, the same result is obtained, which leads to:

$$d^* = d_{k+1} = -\frac{a_k}{b_k} = d_k - \frac{g(d_k, \mathbf{Y}^*_{PMA})}{\frac{\partial g}{\partial d}(d_k, \mathbf{Y}^*_{PMA})} \tag{11.49}$$

Note that the PMA solution only involves the gradient of the limit state function (11.38) with respect to the design variable. It is given by:

$$\frac{\partial g}{\partial d}(d, \mathbf{y}) = 12.5y_1 y_2 + 100y_2 + 250y_1 + 2000 \tag{11.50}$$

The interactive solutions above can be implemented in a spread-sheet or other programing software, together with the HLRF (Eq. 4.24) and AMV (Eq. 11.36b) algorithms. In principle, hand calculations could be used for the external optimization loop. However, this is prohibitive for the nested interactive solution for the internal optimization. For that reason the results shown in Table 11.1 were obtained in Mathematica. An initial value $d_0 = 1$ was used, with tolerance of $\varepsilon_f = 10^{-4}$. All RIA and PMA runs were started from the mean point ($\mathbf{x}^{(0)} = \{40, 50, 1000\}^T$). The PMA step (11.49), however, needs to be computed at the MinPP point $\mathbf{y}^*_{PMA}$ found in the previous iteration.

Table 11.1 shows the distinctly different outcomes of the RIA and PMA solution strategies. For the RIA solution, the limit state constraint is always enforced, such that $g(\mathbf{y}) \approx 0$ at the end of each HLRF run. The target reliability is obtained only at convergence of the external optimization. In the PMA solution, the reliability constraint is always enforced, such that $\beta = \beta_T$ at the end of each AMV iteration. The limit state function is only zeroed at convergence of the external optimization. Since the reliability

Table 11.1 Interactive solution results of external optimization loop, shown at the end of each internal reliability loop.

	k	d	β	$g(\mathbf{y})$
RIA	0	1.0	3.0491	$-9.2 \ 10^{-5}$
	1	1.22189	3.8755	$-8.2 \ 10^{-4}$
	2	1.26151	3.9971	$-1.1 \ 10^{-3}$
	3	1.26151	4.0000	$-1.1 \ 10^{-3}$
PMA	0	1.0	4.0	-304.41
	1	1.25417	4.0	-8.3427
	2	1.26151	4.0	$-5.58 \ 10^{-3}$
	3	1.26151	4.0	$-2.93 \ 10^{-7}$

constraint is active at the end of the RBDO solution, the MPP and MinPP points coincide:

$$\mathbf{y}^*_{RIA} = \mathbf{y}^*_{PMA} = \{-3.269, -0.806, +2.160\}^T$$
$$\mathbf{x}^*_{RIA} = \mathbf{x}^*_{PMA} = \{23.657, 47.984, 1432.0\}^T \quad (11.51)$$

11.3.6   Decoupling Techniques for Solving RBDO Problems

11.3.6.1   Decoupling: Serial Single Loop Methods

In the numerical optimization literature the decoupling concept is to separate the computations of the outer (structural) optimization loop from the inner (reliability) loop and to use sequential iteration to attempt to achieve a pre-assigned convergence criterion. The efficiency of the techniques varies considerably [Yang and Gu, 2004; Yang et al., 2005].

One particularly efficient, accurate and robust technique is the Sequential Optimization and Reliability Assessment (SORA) [Du and Chen, 2004]. It uses the PMA approach and replaces the reliability constraint by a deterministic constraint, by shifting the boundaries of violated (or low reliability) constraints towards the feasible direction. The equivalence between reliability and deterministic constraints is obtained by means of shifting vectors, calculated from previous reliability analysis. The reliability analysis is only performed after convergence of a deterministic sub-optimization round. Details are available in the literature. The SORA and other techniques, such as the efficient, robust and accurate single-loop computational technique proposed by Liang et al. (2004, 2007), been reviewed by Aoues and Chateauneuf (2010) and Lopez and Beck (2012).

11.3.6.2   Decoupling: Uni-level Methods

So-called uni-level methods are obtained by eliminating the inner reliability loop, and replacing it by optimality criteria imposed as constraints in the outer design optimization loop. In this way, concurrent convergence is obtained, where optimal design and target reliability are obtained simultaneously in the same optimization loop. For the classical reliability computations (RIA), two slightly different approaches have been proposed [Kuschel and Rackwitz, 2000; Agarwal et al., 2004; 2007]. Both require second-order derivatives, which are costly and potentially inaccurate to compute.

11.3.6.3   Sequential Approximate Programming (SAP)

Sequential Approximate Programming (SAP) is a technique for solving conventional optimization problems. The original optimization problem is decomposed into a sequence of simpler sub-optimization problems for which solutions are obtained by finding the minimum of an approximate objective function subject to approximate constraints. Approximations are generally linear or quadratic. Applications to RBDO have been illustrated by Cheng et al. (2006) and Yi et al. (2008).

11.4   RBDO with System Reliability Constraints

11.4.1   Formulation of System RBDO

When a structure or structural system has more than one failure mode, which is usually the case, it is more consistent to use a single system reliability constraint rather than a set of component reliability constraints. This applies also to the RBDO formulation. Consider a compound system failure domain:

$$\Omega_f(\mathbf{d}, \mathbf{x}) = \left\{ \mathbf{x} \Big| \bigcup_k \bigcap_{i \in C_k} g_i(\mathbf{d}, \mathbf{X}) \leq 0 \right\} \tag{11.52}$$

where C_k is the index set for the components of the kth cut set, such that series, parallel and combined cut-set systems can be represented. Let p_{fsys} represent the system failure probability and $r_{Tsys} = (1 - p_{fTsys})$ the target system reliability, such that (*cf.* 1.31):

$$p_{fsys} = P[\mathbf{X} \in \Omega_f] = \int_{\bigcup_k \bigcap_{i \in C_k} g_i(\mathbf{d}, \mathbf{X}) \leq 0} f_{\mathbf{X}}(\mathbf{x})\, d\mathbf{x} \tag{11.53}$$

For a structural system the RBDO formulation then becomes:

> Find $\mathbf{d}^*$ which minimizes $f(\mathbf{d})$
>
> subject to: $p_{fsys}(\mathbf{d}) \leq p_{fTsys}$; $\mathbf{d} \in S$, $\qquad\qquad$ (11.54)

where the system reliability $(1 - p_{fsys})$ is a function of component reliabilities $(1 - p_{fi}, i = 1, \dots, n_{LS})$. The component reliabilities themselves are sub-products of the solution of (11.54). Using the generalized reliability index defined as

$$\beta_{sys} = -\Phi^{-1}(p_{fsys}) = \Phi^{-1}(1 - p_{fsys}) \tag{11.55}$$

the RBDO formulation becomes:

> Find $\mathbf{d}^*$ which minimizes $f(\mathbf{d})$
>
> subject to: $\beta_{sys}(\mathbf{d}) \geq \beta_{Tsys}$; $\mathbf{d} \in S$, $\qquad\qquad$ (11.56)

where, in parallel to the system failure probabilities, the system reliability (β_{sys}) is a function of component reliabilities $(\beta_i, i = 1, \dots, n_{LS})$. These are obtained as sub-products of the solution of (11.56).

The problems given by (11.54) and (11.56) are significantly more difficult to solve than (11.9) and (11.10). Solution involves evaluation of system reliabilities in (11.53), but, more importantly, there are infinite number of combinations of component reliabilities potentially leading to the same overall system reliability. In addition, the derivatives of unions of limit states (11.53) are sensitive only to the dominant failure modes [Aoues and Chateauneuf, 2008] whereas the sensitivity with regard to other modes is difficult to compute since they are hidden behind dominant modes. This could bring instabilities to the solution of problems in RBDO for structural systems.

On the other hand, the formulations given in (11.54) and (11.56) contain fewer constraints and hence more 'degrees of freedom'. In turn this leads to easier

reconciliation between failure modes that potentially are critical—in the sense that it may be cheaper (in terms of the objective function $f(\mathbf{d})$) to reduce reliability in one failure mode and compensate for it in one or more other modes, while at the same time respecting overall system reliability.

11.4.2 Structural Systems RBDO with Component Reliability Constraints

Some system RBDO solutions require that reliability of individual components also be included as constraints. In this case, target component reliabilities should be included explicitly as additional design variables:

Find $\{\mathbf{d}^*, \boldsymbol{\beta}_T^*\}$ which minimizes $f(\mathbf{d})$

subject to: $\beta_{sys}(\mathbf{d}) \geq \beta_{Tsys}, \beta_i(\mathbf{d}) \geq \beta_{Ti}, i = 1, \ldots, n_{LS}; \mathbf{d} \in S;$ (11.57)

where $\boldsymbol{\beta}_T^* \in \mathbb{R}^{n_{LS}}$ is the vector of component target reliabilities (β_{Ti}). However, including these may result in an over-constrained problem, and thus should be avoided if possible [Aoues and Chateauneuf, 2008]. In general, if the system reliability constraint is active at the optimum, some (or many) component reliability constraints may become inactive, leading to over-designed components. On the other hand, due to redundant constraint specification, if many component constraints become active, the system reliability constraint becomes inactive and useless.

11.4.3 Structural System RBDO—solution Schemes

Regarding computations for solving system reliability RBDO problems, generally the same general approaches as for components have been used. Early investigators [e.g. Feng and Moses, 1986; Kim and Wen, 1990; Enevoldsen and Sørensen, 1993] solved simple problems by a nested brute-force computation, in which the system reliability 'loop' was solved, by employing different approximations, within the design optimization loop. Such nested solutions are very costly to compute, and examples have been restricted to simple problems. More specialized algorithms have only been developed more recently. These include a decoupling with heuristic adjustment of component reliabilities [Royset et al., 2001], and extension of SORA to series system RBDO [Ba-abbad et al., 2006], an extension of the SLA method based on second-order system reliability bounds [Liang et al., 2004] and a methodology employing an additional internal loop to minimize differences between component reliabilities and their targets [Aoues and Chateauneuf, 2008]. A more comprehensive single-loop system RBDO approach for general systems, similar to (11.53), was presented by Nguyen et al. (2010).

11.5 Simulation-based Design Optimization

11.5.1 Introduction

Methods for solving general design optimization problems using Monte Carlo simulation of various types (*cf.* Chapter 3) are considered in this section. Generally these are applicable to RBDO (11.9) and to LCRO (11.18) type problems. The use of simulation eliminates some of the numerical and stability problems observed for some of the

methods discussed in Sections 11.3 and 11.4. Mostly, simulation can deal well with problems involving strongly non-linear limit state functions, strongly non-linear $\mathbf{y} = T(\mathbf{x})$ mappings, and general system reliability analysis. However, simulation itself introduces some new issues, including potential instability due to random sampling and the necessity for large sample sizes to evaluate small failure probabilities. As a consequence, simulation may become prohibitive when dealing with structural responses given implicitly by non-linear FE models with many degrees of freedom, or in the solution of MDOF stochastic dynamics problems.

The methods described in this section can be classified as general methods for solving design optimization problems in presence of uncertainties. Such problems are called stochastic optimization problems in the literature, and are found in broad areas such as finances, mathematics, logistics and general engineering. A general overview and detailed description of stochastic optimization methods can be found in Birge and Louveaux (1997), Kall and Wallace (1994), Ruszczynski and Shapiro (2003) and Spall (2003).

Stochastic design optimization problems can be solved by the Simplex method and by entirely heuristic methods including Genetic Algorithms, Particle Swarm Optimization and Simulated Annealing that do not require gradients of the failure probability to be computed. However, this has the disadvantage that large numbers of design candidates are required to form statistical populations; hence they require large numbers of limit state function calls.

Stochastic design optimization problems can be solved also by first-order methods requiring computation of the gradient of failure probabilities with respect to the vector of design variables. This can be done by simulation, but it presents computational difficulties. Standard deterministic optimization algorithms can be employed, using at any iteration a set of realizations of the random variables of the problem [Ruszczynski and Shapiro, 2003]. This still requires large numbers of samples, and attention is required to ensure that these are independent samples. This may require attention to be given to the process of generating random numbers and hence random variates (*cf.* Section 3.3).

A third approach to solving stochastic design optimization problems is through application of stochastic quasi-gradient iterative search methods together with sample average approximations [Royset and Polak, 2004]. They can handle LCRO problems with failure probabilities in the objective function, but not RBDO problems with their failure probabilities as constraints.

Sample average approximations are constructed by replacing failure probabilities in the original problem by corresponding Monte Carlo simulation estimates. Results become asymptotically exact as the number of samples tends to infinity ($n_S \to \infty$), and are associated with a sampling error $e_{n_S}(\mathbf{d}, \mathbf{\Omega}_{n_S})$ for finite n_S. This method of solution is described further below.

11.5.2 Problem Formulation

Reliability constraints in RBDO and objective function in LCRO can be evaluated by simulation using conditional failure probabilities:

$$p_f(\mathbf{d}) = P(F \mid \mathbf{d}) = \int_\Omega P(F \mid \mathbf{d}, \mathbf{x}) p(\mathbf{x} \mid \mathbf{d}) \, d\mathbf{x}$$
$$= \int_\Omega I_F(\mathbf{d}, \mathbf{x}) p(\mathbf{x} \mid \mathbf{d}) \, d\mathbf{x} \tag{11.58}$$

where F represents the failure event, $p(\mathbf{x}|\mathbf{d}) = f_X(\mathbf{x})$ is the joint probability density of the random variables, which will be explicit functions of $\mathbf{d}$ when random design variables are present. Also, $I_F(\mathbf{d}, \mathbf{x})$ is the indicator function for failure (*cf.* 1.36), here written directly in terms of the failure domain Ω or Ω_f:

$$I_F(\mathbf{d}, \mathbf{x}) = 1 \ \text{ if } \ \mathbf{x} \in \Omega_f$$
$$I_F(\mathbf{d}, \mathbf{x}) = 0 \ \text{ if } \ \mathbf{x} \notin \Omega_f. \tag{11.59}$$

As observed in Section 3.3.4, (11.58) represents the expected value of the indicator function. An unbiased estimator of this expected value is obtained, from a finite number of samples n_S, drawn from $p(\mathbf{x}|\mathbf{d})$, as:

$$\hat{p}_f(\mathbf{d}, \mathbf{\Omega}_{n_S}) = \frac{1}{n_S} \sum_{i=1}^{n_S} I_F(\mathbf{d}, \mathbf{x}_i), \tag{11.60}$$

where $\mathbf{\Omega}_{n_S} = [\mathbf{x}_1, \mathbf{x}_2, \ldots, \mathbf{x}_{n_S}]$ represents the set of samples and $\mathbf{x}_i$ is the ith sample of the random variable vector. The estimator in (11.60) is said to be unbiased if:

$$\lim_{n_S \to \infty} \hat{p}_f(\mathbf{d}, \mathbf{\Omega}_{n_S}) = p_f(\mathbf{d}). \tag{11.61}$$

In practice, only a finite number of samples n_S can be employed. Fortunately, in most cases a good approximation is obtained for sufficiently large n_S. However, it does mean that simulation provides only an approximate solution to the optimization problem.

The formulation of RBDO using simulation is:

Find $\mathbf{d}_{n_S}^*$ which minimizes $f(\mathbf{d})$

subject to: $\hat{p}_{fi}(\mathbf{d}, \mathbf{\Omega}_{n_S}) \leq p_{fTi}, i = 1, \ldots, n_{LS}; \mathbf{d} \in S. \tag{11.62}$

The formulation for LCRO may be written as:

Find $\mathbf{d}_{n_S}^*$ which minimizes $C_c(\mathbf{d}) + \cdots + \sum_{i=1}^{n_{LS}} C_{fi}(\mathbf{d})\hat{p}_{fi}(\mathbf{d}, \mathbf{\Omega}_{n_S})$

subject to: $\mathbf{d} \in S. \tag{11.63}$

11.5.3 Remarks About Solutions

In the above implied iterative simulation schemes, greater accuracy for the solution of (11.62) and (11.63) requires reduction of the sampling error $e_{n_S}(\mathbf{d}, \mathbf{\Omega}_{n_S})$. This can be achieved using more samples (*cf.* Section 3.3.5), but at a computational cost. If the sampling procedure is consistent, it can be expected that $\mathbf{d}_{n_S}^* \to \mathbf{d}^*$ as $n_S \to \infty$. The appropriate number of samples n_S for a given problem may be estimated from convergence plots (*cf.* Section 3.3.5); however, n_S needs to be large enough for all candidate $\mathbf{d}$, and this may be difficult to prove or verify. Greater accuracy of the Monte Carlo solutions can be achieved also by appropriate selection of the random samples, through the use of specific variance reduction techniques such as 'common random numbers' [e.g. Rubinstein, 1981].

For smoother convergence of the iterative solution schemes, it usually is helpful if there are no sudden changes in behaviour of the functions involved [Rockafellar and

Royset, 2010]. Thus, it is likely to be helpful if the indicator function (11.59) is modified slightly to be less sharp in its binary behaviour. Thus a continuous indicator function could be considered as an approximation. Use of such a continuous indicator function in (11.58), in combination with the conditional random numbers for random sampling will tend to smoothen any comparisons between nearby designs $\mathbf{d}_1$ and $\mathbf{d}_2$, thereby making the simulation-based search for $\mathbf{d}_{n_s}^*$ more stable.

As noted, the solution of stochastic optimization problems (11.62) or (11.63) requires evaluation of derivatives of failure probabilities with respect to the design variables $\mathbf{d}$. The use of finite differences or similar schemes would require large numbers of samples, and would add 'noise' to the simulation. To try to obviate this, it has been proposed that artificial random variables be introduced in the simulation to allow gradients to be obtained in a single simulation run. This also permits sensitivities to be obtained, even though the computational effort is still considerable [Au, 2005; Taflanidis and Beck, 2008a; 2008b; 2009].

In addition, a small number of rather specialized techniques have been proposed. To estimate gradients of failure probabilities with respect to the design variables, various approximations to the Dirac delta function, used instead of the indicator function above have been proposed [Lacaze et al., 2015].

A technique named Simultaneous Perturbation Stochastic Analysis (SPSA), a stochastic search method, is based on the observation that one properly chosen simultaneous random perturbation of all components of $\mathbf{d}$ provides, in the long run, as much information as a set of one-at-a-time perturbations of individual components [Spall, 2003].

A two-stage approach termed Stochastic Subset Optimization (SSO) that combines a number of the techniques was proposed by Taflanidis and Beck (2008a, 2009b). It uses global searches performed by subset simulation with design variables artificially assumed as random variables. The local search is performed using SPSA. It also uses 'common random numbers' and indicator function smoothening, while importance sampling is employed for those random variables identified as more relevant. Further developments from this approach [Jia and Taflanidis, 2013; Jia et al., 2015], while efficient, tend to be limited to a small number of design variables, due to the difficulty in identifying the subsets in higher dimensions.

Techniques have been proposed to try to make some of the evaluations of probabilities easier. For example, for evaluating the integral in (11.58) by Importance Sampling (*cf.* Section 3.4), it has been proposed that a uniform importance sampling function over the integration domain relevant to an individual random variable might be advantageous [Rashki et al., 2012; Xiaopeng et al., 2014], possibly modified by a heuristic weighting scheme [Rashki et al., 2014]. In this case only the weightings need to be changed as simulation proceeds [Rashki et al., 2014]. Hence, the large cost of evaluating limit state functions for different realizations $\mathbf{x}_i$ is avoided. However, in its crude form, the method is not very efficient for problems involving small failure probabilities. Alternative suggestions to achieve similar computational simplifications also have been made [e.g. Yuan and Lu, 2014; Okasha, 2016] but these, too, remain to be further investigated, particularly for their computational effectiveness in application to RBDO problems.

Finally, a completely different approach specifically targeted at solving risk optimization problems using Monte Carlo simulation, builds on the notion that it is easier (less computationally demanding) to first identify the failure domain over the whole

design space and for each sample [Gomes and Beck, 2016]. That information then allows the probability of failure to be computed for any point in the design space, with no need of further limit state function evaluations. This strategy has been shown to be efficient for problems involving up to a dozen design variables. However, the efficiency of the method reduces considerably for problems involving twenty or more design variables. Special schemes for the extension to multiple design variables are still needed.

11.6 Life-cycle Cost and Risk Optimization

11.6.1 Introduction

Problems addressing life-cycle cost and risk optimization can be classified broadly into two somewhat overlapping types: optimal design under stochastic loading, and optimal design considering inspection and maintenance activities. Most published solutions on these topics tend to be problem-oriented. There is relatively little about appropriate solution techniques. In both approaches, expected costs of failure are part of the objective function. In the following, such applications are briefly described, noting that the formulations usually are very problem-specific.

11.6.2 Optimal Structural Design Under Stochastic Loads

Optimal structural design under stochastic loads involves time-variant reliability approaches, such as those addressed in Chapter 6. One of the first approaches to the problem, by Kim and Wen (1990), addressed optimal design of frame structures under multiple stochastic loads, considering the effects of member and/or system reliability constraints. Wen and Kang (2001a) addressed minimal life-cycle cost design of buildings under environmental loading such as earthquake and hurricanes. As has been recognized in other areas of structural design (*cf.* Chapters 1 and 2), it was observed that optimal designs were controlled mainly by failure consequences, and by design life. As might be expected intuitively, for structures subject to multiple hazards, design is controlled by the hazard with the *worst* combination of large uncertainty and strong intensity or severe consequences. When costs and consequences are considered in the formulation of the optimal problem, it was found that requiring uniform reliability under multiple hazards is not optimal. This was demonstrated for the design of an office building subject to earthquake and wind hazards [Wen and Kang, 2001b].

The optimal design of reinforced concrete frames subject to earthquake loading was found to be dominated by total expected damage costs, consisting mainly of building damage repair costs and indirect losses [Ang and Lee, 2001]. The contributions of fatality and injury rates, using a willingness to pay criterion, were found of secondary importance. For the optimal design of general, renewable structures it has been proposed that failure could be measured in terms of failure rates instead of failure probabilities and that the criteria for risk acceptability could be considered in terms of efficiency of investment towards life-saving measures [Rackwitz, 2001]. This agrees with heuristic observations (*cf.* Section 2.4).

The optimal design of linear and non-linear MDOF dynamical systems, subject to stochastic excitations has been considered extensively [Jensen, 2006; Jensen et al., 2008; Jensen et al., 2009; Jensen et al., 2015]. In this work, a numerically intensive procedure is employed in which load processes are discretized into thousands of random variables, and the resulting high-dimensional reliability problems are solved using different Monte Carlo techniques. Also, various approaches have been investigated to attempt to reduce the computational burden of solving the resulting RBDO problems. Some further solution strategies are available [Valdebenito and Schuëller, 2011].

11.6.3 Optimal Structural Design Considering Inspections and Maintenance

A large number of investigations have been reported for optimal design with allowance for the potential influence of the costs and effectiveness of inspections, repairs, maintenance and failure. Many of these are of the case-study type. However, some efforts are based on stochastic notions, such as renewal theory. Thus, failure models have been proposed for minimal life-cycle cost design of ageing components, considering also the costs of inspections, repairs, maintenance and the cost of failure [e.g. Rackwitz and Joanni, 2009]. This reinforced earlier (perhaps more heuristic) findings that inspection-based (predictive or pro-active) maintenance was more effective in terms of overall expected life-time costs than conventional age-dependent (preventive) maintenance.

A number of efforts have focussed on multi-objective optimization of structural maintenance strategies incorporating system reliability, system redundancy and life-cycle costs. This can have interesting practical outcomes. For example, Okasha and Frangopol (2009) showed that system reliability and system redundancy have different impacts on optimal maintenance strategies and confirmed that different maintenance actions might be applied to different components of a structural system, thereby potentially avoiding unnecessary maintenance actions or reducing or delaying maintenance on non-critical components.

Some of the Monte Carlo simulation techniques for solving life-cycle cost and risk optimization problems (*cf.* Section 11.4) were employed in [Gomes et al., 2013; Gomes and Beck, 2014a] to find optimal wall thickness and optimal inspection and maintenance plans for pipelines subject to corrosion defects, and in [Gomes and Beck, 2014b] to general structures subject to fatigue. Results illustrate the different compromises that can be achieved when designing structures under uncertainty, in particular for systems for which structural failures are, ultimately, unavoidable. This is in contrast to conventional engineering thinking, where proper design, construction and operation are assumed to eliminate failures.

11.7   Discussion and Conclusion

A comprehensive example covering many of the aspects considered herein is available, for the case of a concrete gravity dam. It compares deterministic, reliability-based and life-cycle cost and risk optimization for the case of equilibrium limit state functions [Beck, 2013]. The example and the computations are too large to be reproduced here.

In this chapter structural design optimization under the explicit consideration of uncertainties in loads and in strengths was considered. Some level of probabilistic influence can be considered using code-specified partial factors in an optimal design (herein termed Deterministic Design Optimization). However, a more satisfactory approach is to replace the code-specified single-limit-state constraints by reliability constrains, as in Reliability-Based Design Optimization (RBDO). An optimization problem with more degrees of freedom, with no deterministic counterpart, is obtained by using only system reliability constraints in RBDO. Such formulation leads to optimal points of compromise between competing failure modes. When costs of failure can be quantified, the apparently conflicting goals of economy and safety in structural design can be resolved by using the more comprehensive Life-cycle Cost and Risk Optimization (LCRO) formulation framework to develop rational designs.

The main methods used for solving RBDO and LCRO problems using FOR or Monte Carlo simulation were reviewed. Problems with a single system reliability constraint were considered and shown to lead to a less-constrained problem, where individual failure modes can compete with each other. The RBDO problem with system-reliability constraints, however, was shown to be significantly more difficult to solve. The reliability constraints can be imposed by the conventional reliability-index approach (RIA), or by the so-called performance-based approach (PMA). Overall it appears that the PMA approach has advantages for optimization in RBDO problems.

It was noted that structural optimization problems using FOR usually lead to nested optimizations loops. These can be approached by different de-coupling strategies, briefly reviewed herein. Solution by Monte Carlo simulation also is possible, even though this introduces issues of its own, the most important being the compounding of computational effort and time-cost. Some techniques to alleviate this issue were reviewed. Finally it was noted that for life-cycle-based optimization most efforts have been case-studies and that there is still relatively little fundamental theory available.

A

Summary of Probability Theory

A.1 Probability

Probability can be considered as a numerical measure of the likelihood that an event occurs relative to a set of alternative events that do not occur. The set of all possible events must be known.

The determination of the probability that an event occurs can be based on:

(1) *a priori* assumptions about the underlying mechanisms governing events(s);
(2) relative frequency of empirical observations in the past;
(3) intuitive or subjective assumptions.

The probability of an event E is denoted $P(E|X)$ where P is the probability operator, and $|X$ denotes the condition 'subject to X', where X denotes whatever may be known or assumed in determining $P(E|X)$. Hence any probability depends on the state of knowledge (or ignorance) (or more generally 'the state of nature') at the time that the probability is calculated. Seen in this way, all probabilities are conditional (as indicated by X [e.g. Tribus, 1969]. In many cases $P(E|X)$ will be denoted simply $P(E)$, the state of nature X being understood.

A.2 Mathematics of Probability

A.2.1 Axioms

(a) The probability $P(E)$ of an event E is a real non-negative number: $0 \leq P(E) \leq 1$.
(b) The probability of an inevitable event C is $P(C) = 1.0$. Hence the probability $P(0)$ of an impossible event equals zero.
(c) Addition rule. The probability that either or both of two events E_1 and E_2 occurs is

$$P(E_1 \cup E_2) = P(E_1) + P(E_2) - P(E_1 \cap E_2) \tag{A.1}$$

Hence for two *mutually exclusive* events

$$P(E_1 \cup E_2) = P(E_1) + P(E_2) \tag{A.2}$$

A.2.2 Derived Results

A.2.2.1 Multiplication Rule The probability that events E_1 and E_2 both occur can be written as the conditional probability of one with respect to the other (i.e. there is symmetry in E_1 and E_2):

$$P(E_1 \cap E_2) = P(E_1 \,|\, E_2)P(E_2) = P(E_2 \,|\, E_1)P(E_1) \tag{A.3}$$

If E_1 and E_2 are *independent*,

$$P(E_1 \,|\, E_2) = P(E_1) \ \text{ and } \ P(E_1 \cap E_2) = P(E_1)P(E_2) \tag{A.4}$$

(These statements are used to provide the formal definition of *independent* events [e.g. Lindley, 1976]).

A.2.2.2 Complementary Probability If $\overline{E}$ is the event that E does not occur,

$$P(E \cup \overline{E}) = P(E) + P(\overline{E}) = P(C) = 1$$

Therefore

$$P(\overline{E}) = 1 - P(E) \tag{A.5}$$

A.2.2.3 Conditional Probability It follows directly from (A.3) that

$$P(E_1 \,|\, E_2) = \frac{P(E_1 \cap E_2)}{P(E_2)} \tag{A.3a}$$

A.2.2.4 Total Probability Theorem By virtue of the multiplication rule it follows that for events E_i, $i = 1, 2, \ldots, n$, mutually exclusive and collectively exhaustive (i.e. covering all possibilities without overlap),

$$P(A) = P(A \,|\, E_1)P(E_1) + P(A \,|\, E_2)P(E_2) + \ldots + P(A \,|\, E_n)P(E_n) \tag{A.6}$$

A.2.2.5 Bayes' Theorem Expression (A.3a) is also a formal statement of Bayes' theorem [Lindley, 1976]. For practical applications it can be rewritten, with the aid of the right-hand equality in (A.3), as:

$$P(A \,|\, E_c) = \frac{P(A \cap E_c)}{P(E_c)} = \frac{P(E_c \,|\, A)P(A)}{P(E_c)} \tag{A.7a}$$

where A is an event conditional on conditioning event E_c. The latter can be expanded to the case where there are several conditioning events E_i, $i = 1, 2, \ldots, n$. Then (A.7a) becomes

$$
\begin{aligned}
P(A \,|\, E_1 \cap E_2 \cap E_3 \ldots E_n) &= \frac{P(A \cap E_1 \cap E_2 \cap E_3 \ldots E_n)}{P(E_1 \cap E_2 \cap E_3 \ldots E_n)} \\
&= \frac{P(E_1 \cap E_2 \cap E_3 \ldots E_n | A)P(A)}{P(E_1 \cap E_2 \cap E_3 \ldots E_n)}
\end{aligned}
\tag{A.7b}
$$

where the second equality shows the conditioning events E_i now being conditional on the original event A. On the right-hand side of (A.7b) the term $P(E_1 \cap E_2 \cap E_3 \dots E_n | A)$ is known as the 'likelihood function'. The term $[P(E_1 \cap E_2 \cap E_3 \dots E_n)]^{-1}$ is the 'normalizing factor', necessary to ensure both sides of (A.7) are proper probabilities.

A.3   Description of Random Variables

In what follows, only the case of continuous random variables will be noted; for discrete random variables the results are analogous with integration being replaced by summation. The probability that the random variable X takes on a value less than or equal to x (a specific value) is given by:

$$P(X \leq x) \equiv F_X(x) = \int_{-\infty}^{x} f_X(\varepsilon)\, d\varepsilon \tag{A.8}$$

where $F_X(x)$ is defined as the cumulative distribution function of X, and $F_X(x)$ is the probability density function. Obviously $f_X(x) = dF_X(x)/dx$; thus $f_X(x)$ is not a probability, but its local derivative. Specific cases of $f_X(x)$ and $F_X(x)$ are considered in Section A.5. Any function satisfying $F_X(-\infty) = 0$, $F_X(+\infty) = 1.0$, $F_X(x) \geq 0$, $f_X(x) \geq 0$, and for which the derivative $f_X(x) = dF_X(x)/dx$ exists, is a possible cumulative distribution function. However, in practice, attention is restricted to a limited set.

By direct extension of (A.8)

$$P(a < X \leq b) = \int_{-\infty}^{b} f_X(x)\, dx - \int_{-\infty}^{a} f_X(x)\, dx = F_X(b) - F_X(a) \tag{A.9}$$

A distribution may be described by a number of derived properties, commonly called 'moments', without specific reference to either $f_X(x)$ or $F_X(x)$. Also, for discrete functions, the probability density function is replaced by the probability mass function p_X.

A.4   Moments of Random Variables

A.4.1   Mean or Expected Value (First Moment)

This is a 'weighted average' of all the values that a random variable may take:

$$E(X) \equiv \mu_X = \int_{-\infty}^{\infty} x\, f_X(x)\ dx \approx \sum_i x_i p_X(x_i) \tag{A.10}$$

The integral expression is for continuous variables and the last expression is its discrete approximation or is the expression for a discrete random variable. In both cases the result is called the 'first moment' since it is the first moment of 'area' of the probability density function about the origin. (The mean μ_X is analogous to the centroidal distance of the cross-section for a beam).

Other central tendency measures are the *mode,* which is the most probable value, i.e. the value of x for which p_X or f_X is greatest and the *median*, which is the value of x for which $F_X(x) = 0.5$, i.e. values above and below the mean are equally likely.

A.4.2 Variance and Standard Deviation (Second Moment)

The variance of a random variable is a measure of the degree of randomness about the mean:

$$E(X - \mu_X)^2 = \text{var}(X)$$
$$= \int_{-\infty}^{\infty} (x - \mu_X)^2 f_X(x)\, dx \tag{A.11a}$$

or

$$= \sum_i (x_i - \mu_X)^2 \; p_X(x_i)$$
$$= E(X^2) - (\mu_X)^2 \tag{A.11b}$$

where the alternative expression is for discrete random variables. The last expression is exact for both types of random variable and is a useful result. The standard deviation is defined as

$$\sigma_X = [\text{var}(X)]^{1/2} \tag{A.12}$$

and the coefficient of variation is defined as

$$V_X = \frac{\sigma_X}{\mu_X} \tag{A.13}$$

A.4.3 Bounds on the Deviations from the Mean

For all discrete and continuous random variables there are bounds on the relationship between the standard deviation and the mean. The most well-known is due to Bienayme and Chebychev. For a random variable X, with mean μ_X and standard deviation σ_X, this relationship is

$$P(|X - \mu_X| \geq k\sigma_X) \leq 1/k^2 \tag{A.14}$$

where $k > 0$ is a real number. This is a (weak) general bound on the amount of deviation $|X - \mu_X|$ from the mean relative to the standard deviation. If it is known that $f_X(x)$ has a single peak and has so-called 'higher order' contact with the x axis at $x = \pm\infty$, the right-hand side of expression (A.14) may be replaced by $1/(2.25k^2)$. This is the 'Camp-Meidall' inequality [Freeman, 1963].

A.4.4 Skewness γ_1 (Third Moment)

A measure of skewness or lack of symmetry of a distribution is given by the third central moment about the mean:

$$E(X - \mu_X)^3 = \int_{-\infty}^{\infty} (x - \mu_X)^3 f_X(x)\, dx$$
$$\text{or} = \sum_i (x_i - \mu_X)^3 p_X(x_i) \tag{A.15}$$

$E(X - \mu_X)^3$ will be positive if there is greater dispersion of values of $X \geq \mu_X$ than for values of $X < \mu_X$; the sign and magnitude of $E(X - \mu_X)^3$ governs the sign and degree

of 'skewness'

$$\gamma_1 = \frac{E(X - \mu_X)^3}{\sigma_X^3}$$

Positive skewness is indicated by the longer 'tail' of the distribution in the positive direction.

A.4.5 Coefficient γ_2 of Kurtosis (Fourth Moment)

A measure of the 'flatness' of a distribution is given by the fourth central moment

$$E(X - \mu_X)^4 = \int_{-\infty}^{\infty} (x - \mu_X)^4 f_X(x)dx$$
$$\text{or} = \sum_i (x_i - \mu_X)^4 p_X(x_i) \qquad \text{(A.16)}$$

The greater the moment, the 'flatter' (less peaked) is the distribution. The kurtosis is defined as

$$\gamma_2 = \frac{E(X - \mu_X)^4}{\sigma_X^4}$$

with $\gamma_2 = 3.0$ for a standard Normal distribution. The measure is used in statistics only for large samples.

A.4.6 Higher Moments

Higher-order moments can be developed. A systematic way of developing moments indirectly employs the 'moment-generating function' [e.g. Ang and Tang, 1975]. In general, the set of all moments of a probability density function describes the function exactly; any subset of moments represents an approximation to it. For some probability density functions, a limited set of moments is sufficient to describe the function completely. Thus, the Normal, or Gaussian distribution, is completely described by its first two moments.

A.5 Common Univariate Probability Distributions

A.5.1 Binomial $B(n, p)$

The Binomial distribution gives the probability of exactly x 'successes' in n trials. Its probability mass function is given by

$$P(X = x) = p_X(x) = \binom{n}{x} p^x (1-p)^{n-x} \qquad x = 0, 1, 2, \ldots, n \qquad \text{(A.17)}$$

and the cumulative distribution function by

$$P(X \leq x) = F_X(x) = \sum_y^x \binom{n}{y} p^y (1-p)^{n-y} \qquad x = 0, 1, 2, \ldots, n \qquad \text{(A.18)}$$

where

$$\binom{n}{x} = \frac{n!}{x!(n-x)!} \tag{A.19}$$

is the binomial coefficient. The parameters are the number n of independent trials and the probability p of success per trial (= constant).
The moments are

$$E(X) = \mu_X = np \tag{A.20}$$

$$\text{var}(X) = \sigma_X^2 = np(1-p) \tag{A.21}$$

The binomial distribution is applicable where there are only two discrete alternatives per independent trial, with probability p and $1-p$ respectively. A useful property is

$$B(n_1, p) + B(n_2, p) = B(n_1 + n_2, p) \tag{A.22}$$

The 'multinomial' distribution applies where there are more than two discrete outcomes possible.

A.5.2 Geometric *G(p)*

The geometric distribution gives the probability that the nth trial is a success given that the first $n-1$ trials were failures. Its probability mass function and its cumulative distribution function are

$$P(N = n) = p_N(n) = (1-p)^{n-1}p \qquad n = 1, 2, \dots \tag{A.23}$$

$$P(N \le n) = F_N(n) = \sum_{i=1}^{n} (1-p)^{i-1}p = 1 - (1-p)^n \tag{A.24}$$

The parameters are the number n of independent trials and the probability p of success per trial (= constant). The moments are

$$E(N) = \mu_N = \frac{1}{p} \tag{A.25}$$

$$\text{var}(N) = \sigma_N^2 = \frac{1-p}{p^2} \tag{A.26}$$

For applications, see those for the binomial distribution. It is assumed that the trials are independent. A case in which this is not so occurs in sampling without replacement. The corresponding distribution is the hypergeometric HG(p) [Ang and Tang, 1975; Freeman, 1963].

A.5.3 Negative Binomial *NB(k, p)*

This distribution gives the probability that the k th occurrence of a success occurs at the t th trial. It is also known as the Pascal distribution. The probability mass function is

$$P(T = t) = p_T(t) = \binom{t-1}{k-1}(1-p)^{t-k}p^k \qquad t = k, k+1, \dots \tag{A.27}$$

The parameters are the number k of successes, the probability p of success per trial (= constant) and the number t of trials before k successes ($t \geq k$). The moments are

$$E(T) = \mu_T = \frac{k}{p} \tag{A.28}$$

$$\text{var}\,(T) = \sigma_T^2 = \frac{k(1-p)}{p^2} \tag{A.29}$$

The number of trials can be interpreted also as the number of time units. Other forms also exist.

A.5.4 Poisson *PN(vt)*

This distribution gives the probability of a number of occurrences X_t of a random event in a given (time) interval t, given that the mean rate of occurrences is known. The probability mass function and the cumulative distribution function are:

$$P(X_t = x) = p_X(x) = \frac{(vt)^x}{x!} e^{-vt} \tag{A.30}$$

$$P(X_t \leq x) = F_X(x) = \sum_{r=0}^{x} \frac{(vt)^r}{r!} e^{-vt} \tag{A.31}$$

The parameters are the mean occurrence rate (per unit time or space units) v, the time or space interval t, the average number $\lambda(= vt)$ of events in t, and the number X_t of occurrences in t. The moments are

$$E(X) = \mu_X = vt \tag{A.32}$$
$$\text{var}\,(X) = \sigma_X^2 = vt \tag{A.33}$$

The Poisson distribution results from (approximates) the Binomial distribution $B(n, p)$ as $n \to \infty$ and p is small by replacing the number of trials in the Binomial by the time interval. The relationship is given by $np = vt$ in the limit as $n \to \infty$, $p \to 0$. In practice, this is satisfied if, say, $n = 50$ for $p < 0.10$, or $n = 100$ for $p < 0.05$. The Poisson distribution has wide application in its own right and not merely as an approximation for the binomial distribution. When the Poisson distribution is used in terms of time or space units, with independence of events, a Poisson process results (see Chapter 6). Note that $(vt)^0/0! = 1$. Also note that the Poisson distribution has the useful property

$$PN(\lambda_1) + PN(\lambda_2) = PN(\lambda_1 + \lambda_2) \tag{A.34}$$

A.5.5 Exponential *EX(v)*

For events occurring according to a Poisson process the Exponential distribution describes the probability of the time to the first occurrence of an event. Its probability density and the cumulative distribution functions are, respectively,

$$P(T = t) = f_T(t) = v e^{-vt} \qquad t \geq 0 \tag{A.35}$$
$$P(T \leq t) = F_T(t) = 1 - e^{-vt} \qquad t \geq 0 \tag{A.36}$$

so that $P(T \geq t) = e^{-vt}$.

The parameters of the Exponential distribution are the mean rate of occurrence v and the time or space interval t. The moments are

$$E(T) = \mu_X = \frac{1}{v} = \overline{\Delta t} \tag{A.37}$$

$$\text{var}\,(T) = \sigma_T^2 = \left(\frac{1}{v}\right)^2 = (\overline{\Delta t})^2 \tag{A.38}$$

where $\overline{\Delta t}$ is the average time between arrivals (or the mean life).

The exponential distribution is the continuous analogue of the Geometric distribution. Since a Poisson process is stationary by definition, any starting time can be used, and hence T can refer to 'inter-arrival time', which is therefore exponentially distributed.

A.5.6 Gamma $GM(k, v)$ [and Chi-squared $\chi^2(n)$]

For events occurring according to a Poisson process, this distribution describes the probability of the time T to the kth occurrence of an event taking on a given value, t say. The distribution is generalized when k is not an integer. The probability density (Figure A.1) and the cumulative distribution function are, respectively;

$$P(T = t) = f_T(t) = \frac{v^k(t)^{k-1}}{\Gamma(k)}e^{-vt} \qquad t \geq 0 \tag{A.39}$$

$$P(T < t) = F_T(t) = 1 - \sum_{x=0}^{k-1}\frac{(vt)^x}{x!}e^{-vt} \qquad t \geq 0,\ k \ \text{integer} > 0 \tag{A.40a}$$

$$= \frac{\Gamma(k, vt)}{\Gamma(k)} \qquad t \geq 0,\ \text{all}\ k > 0 \tag{A.40b}$$
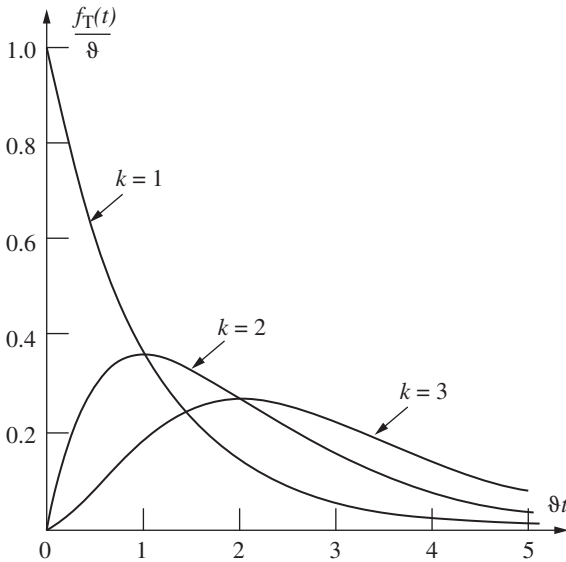
Figure A.1 Gamma probability density function.

where

$$\Gamma(k) = \int_0^\infty e^{-u} u^{k-1} du = (k-1)! \qquad \text{for } k \text{ integer} > 0 \tag{A.41}$$

and

$$\Gamma(k, x) = \int_0^x e^{-u} u^{k-1} \, du \tag{A.42}$$

The parameters are the mean occurrence rate v and the time or space interval t. The moments are

$$E(T) = \mu_T = \frac{k}{v} \tag{A.43}$$

$$\text{var}(T) = \sigma_T^2 = \frac{k}{v^2} \tag{A.44}$$

$$\gamma_1 = \frac{E(T - \mu_T)^3}{\sigma_T^3} = 2k^{-1/2} \qquad \text{(skewness coefficient)} \tag{A.45}$$

The gamma function $\Gamma(k)$ is the generalization of the factorial for non-integer k. It is tabulated as the 'incomplete gamma function' $\Gamma(k, vt)$ [e.g. Ang and Tang, 1975; Benjamin and Cornell, 1970]. For k integer, the distribution is known also as the 'Erlang' distribution, and is the continuous analogue of the negative binomial distribution.

The gamma distribution has the useful property that, if X_i is $GM(k_i, v)$, then

$$\sum_i^m X_i = GM\left(\sum_i^m k_i, v\right) \tag{A.46}$$

In the special case with $v = 1/2$ and $k = n/2$ expression (A.39) becomes

$$f_T(t) = 2^{-n/2} t^{n/2-1} e^{-t/2} / \Gamma(n/2) \tag{A.39a}$$

which is known as the **Chi-squared (χ^2) distribution** with $n = 1, 2, 3, \ldots$ degrees of freedom. It represents the probability density function for the sum of the squares of n independent Normal (i.e. Gaussian) random variables [Shiryaev, 1996].

A.5.7 Normal (Gaussian) $N(\mu, \sigma)$

The Normal distribution is one that arises frequently in practice as a limiting case of other probability distributions. It also is a reasonable model for observations of many physical processes or properties.
Its probability density function (Figure A.2) and its cumulative distribution functions are given by

$$f_X(x) = \frac{1}{(2\pi)^{1/2} \sigma_X} \exp\left[-\frac{1}{2}\left(\frac{x - \mu_X}{\sigma_X}\right)^2\right] \qquad -\infty \leq x \leq \infty \tag{A.47}$$

$$P(X \leq x) = F_X(x) = \frac{1}{(2\pi)^{1/2}} \int_{-\infty}^s e^{-\frac{1}{2}v^2} dv \qquad -\infty \leq x \leq \infty \tag{A.48}$$

where $s = (x - \mu_X)/\sigma_X$. There is no simple expression for $F_X(x)$. However, there are many approximations (see below).
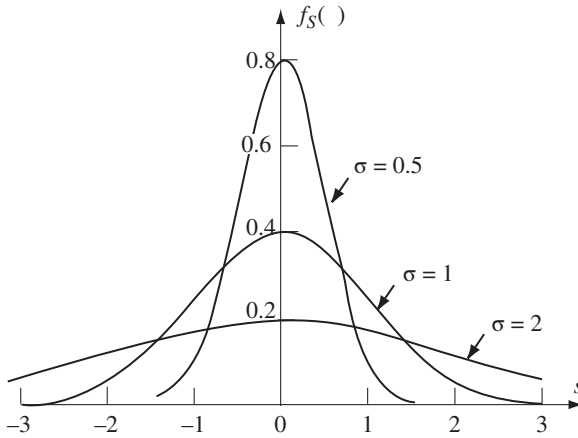
Figure A.2 Normal probability density function.

The parameters of the distribution are the mean value μ_X and the standard deviation σ_X. The moments are

$$E(X) = \mu_X \tag{A.49}$$
$$\text{var}(X) = E(X - \mu_X)^2 = \sigma_X^2 \tag{A.50}$$
$$E(X - \mu_X)^3 = 0 \quad \text{(no skewness)} \tag{A.51}$$
$$\frac{E(X - \mu_X)^4}{\sigma_X^4} = 3 \qquad \text{(coefficient of kurtosis)} \tag{A.52}$$

The standard Normal distribution $N(0, 1)$ usually is tabulated for both $f_X(x)$ and $F_X(x)$ (see Appendix D). The variate is then given by $s = (x - \mu_X)/\sigma_X$. Also $F_S(s)$ commonly is denoted $\Phi(s)$, while $f_S(s)$ usually is denoted $\phi(s)$. Note that, if X is $N(\mu_X, \sigma_X)$, then

$$f_X(x) = \frac{1}{\sigma_X} \, \phi\left(\frac{x - \mu_X}{\sigma_X}\right), \quad F_X(x) = \Phi\left(\frac{x - \mu_X}{\sigma_X}\right)$$

The Normal distribution has the following useful properties:

$$\Phi(-s) = 1 - \Phi(s) \tag{A.53}$$
$$s = \Phi^{-1}(p) = -\Phi^{-1}(1 - p) \tag{A.54}$$
$$P(a < x \le b) = \Phi\left(\frac{b - \mu_X}{\sigma_X}\right) - \Phi\left(\frac{a - \mu_X}{\sigma_X}\right) \tag{A.55}$$

If $Y = \sum_i X_i$ where X_i are independent $N(\mu_{X_i}, \sigma_{X_i})$, then (*cf.* Section A.11.1):

$$\mu_Y = \sum_i \mu_{X_i} \tag{A.56}$$
$$\sigma_Y^2 = \sum_i \sigma_{X_i}^2 \tag{A.57}$$

Approximate expressions are [Abramowitz and Stegun, 1966; Hastings, 1955]:

(i)

$$\Phi(-\beta) \approx \frac{1}{\beta(2\pi)^{1/2}} e^{-\frac{1}{2}\beta^2} \tag{A.58}$$

(ii)

$$\Phi(s) = P(S \le s) = 1 - \frac{1}{(2\pi)^{1/2}} e^{-\frac{1}{2}s^2} \left[\sum_{i=1}^{5} b_i t^i + \varepsilon(s) \right] \tag{A.59a}$$

where $t = (1 + 0.2316419s)^{-1}$ and the constants are b_i $(i = 1, \ldots, 5)$; (0.319 381 530; 0.356 563 782; 1.781 477 937; 1.821 255 978; 1.330 274 429). The error is $|\varepsilon(s)| < 7.5 \times 10^{-8}$.

(iii)

$$\Phi(s) = P(S \le s) = 1 - 0.5 \left(1 + \sum_{i=1}^{6} d_i x^i \right)^{-16} + \varepsilon(s) \tag{A.59b}$$

where the constants d_i $(i = 1, \ldots, 6)$ are: (0.049 867 3470; 0.021 141 0061; 0.003 277 6263; 3.800 36 ∞ 10^{-5}; 4.889 06 ∞ 10^{-5}; 0.538 30 ∞ 10^{-5}). The error is $|\varepsilon(s)| < 1.5 \times 10^{-7}$.

(iv)

$$\Phi(-\beta) \approx \left[\frac{\beta}{1 + \beta^2} + \left(\sum_{i=0}^{5} a_i \beta^i \right)^{-1} \right] \phi(\beta) + \varepsilon(\beta) \qquad \text{for} \quad \beta \ge 1 \tag{A.59c}$$

where $a_0 = (2/\pi)^{1/2}$ and the constants a_i $(i = 1, ., 5)$ have the following values: (1.280; 1.560; 1.775; 0.584; 0.427). The error is $|\varepsilon(\beta)| < 5 \times 10^{-5}$ [Rosenblueth, 1985b].

A.5.8 Central Limit Theorem

This famous theorem states that the probability distribution for the sum of a large number of random variables approaches the Normal distribution, irrespective of the individual distributions of the random variables [Freeman, 1963; Benjamin and Cornell, 1970 and many others].

A.5.9 Lognormal *LN*(λ, ε)

In the Lognormal distribution, the natural logarithm of the random variable X, rather than X itself, has a Normal distribution. The probability density function (Figure A.3) and the cumulative distribution functions are:

$$f_X(x) = \frac{1}{(2\pi)^{1/2} x \varepsilon} \exp\left[-\frac{1}{2} \left(\frac{\ln x - \lambda}{\varepsilon} \right)^2 \right] \qquad 0 \le x < \infty \tag{A.60}$$

$$F_X(x) = \int_{-\infty}^{x} f_X(u)\, du = \Phi\left(\frac{\ln x - \lambda}{\varepsilon} \right) \quad \text{(no explicit form)} \tag{A.61}$$

The parameters are

$$\lambda = E(\ln X) = \text{mean of } \ln(X) = \mu_{\ln x} \tag{A.61a}$$

$$\varepsilon^2 = \text{var}(\ln X) = \sigma^2_{\ln X} \tag{A.61b}$$
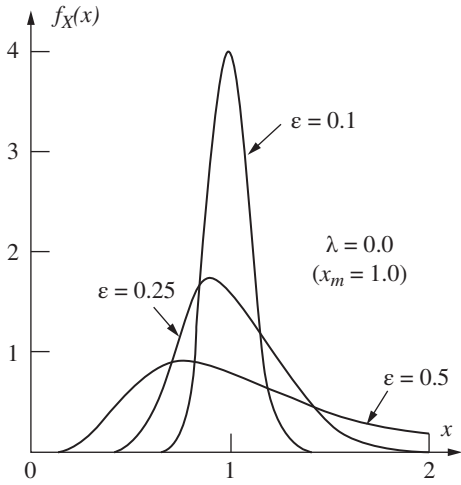
Figure A.3 Lognormal probability density function.

The moments are [e.g. Ang and Tang, 1975]:

$$E(X) = \mu_X = \exp\left(\lambda + \frac{1}{2}\,\varepsilon^2\right) \tag{A.62}$$

$$\text{var}\,(X) = \sigma_X^2 = \mu_X^2[\exp(\varepsilon^2) - 1] \tag{A.63}$$

Expression (A.61) allows probabilities to be evaluated using standard Normal tables when X is Lognormal. Further, the probability over an interval may be evaluated from

$$P(a < x \le b) = \Phi\left(\frac{\ln b - \lambda}{\varepsilon}\right) - \Phi\left(\frac{\ln a - \lambda}{\varepsilon}\right) \tag{A.64}$$

The Lognormal distribution has the following useful properties:

(1) From equation (A.62)

$$\lambda = \mu_{\ln X} - \frac{1}{2}\,\varepsilon^2$$

or

$$\lambda = \ln x_m = \ln\left[\frac{\mu_X}{(1 + V_X^2)^{1/2}}\right]$$

or

$$x_m = \mu_X \exp\left(\frac{1}{2}\,\varepsilon^2\right)$$

where x_m is the 'median' of x, defined as $P(X \le x_m) = 0.5$.

(2) From equation (A.63), with V_X defined as the coefficient of variation:

$$\varepsilon^2 = \sigma_{\ln X}^2 = \ln\left(1 + \frac{\sigma_X^2}{\mu_X^2}\right) = \ln(1 + V_X^2) \approx V_X^2 \qquad \text{for} \quad V_X \le 0.3$$

(3) Also $x_m = \dfrac{\mu_X}{(1 + V_X^2)^{1/2}}$ so that $x_m \le \mu_X$.

(4) If $Y = \displaystyle\prod_{i=1}^{n} X_i$ where the X_i are Lognormal, $LN(\lambda_i, \varepsilon_i)$, then

$$\mu_{\ln Y} = \sum_{i=1}^{n} \mu_{\ln X_i} \quad \text{or} \quad y_m = \prod_{i=1}^{n} x_{m_i} \quad \text{and} \quad \sigma_{\ln Y}^2 = \sum_{i=1}^{n} \sigma_{\ln X_i}^2 \tag{A.65}$$

Because of the relationship between the Normal and the Lognormal distributions, the central limit theorem extended to the Lognormal distribution states that the probability distribution for the *product* of a large number of random variables approaches a Lognormal distribution, irrespective of the individual distributions of the random variables.

A.5.10 Beta $BT(a, b, q, r)$

Although the Beta distribution may arise from physical considerations, its chief advantage is its great flexibility in fitting to data. It is given in various, essentially equivalent, forms. The probability density function is (Figure A.4):

$$\begin{aligned} f_X(x) &= \frac{1}{\beta(q, r)} \frac{(x - a)^{q-1}(b - x)^{r-1}}{(b - a)^{q+r-1}} \quad && a \le x \le b \\ &= 0 && \text{elsewhere} \end{aligned} \tag{A.66}$$
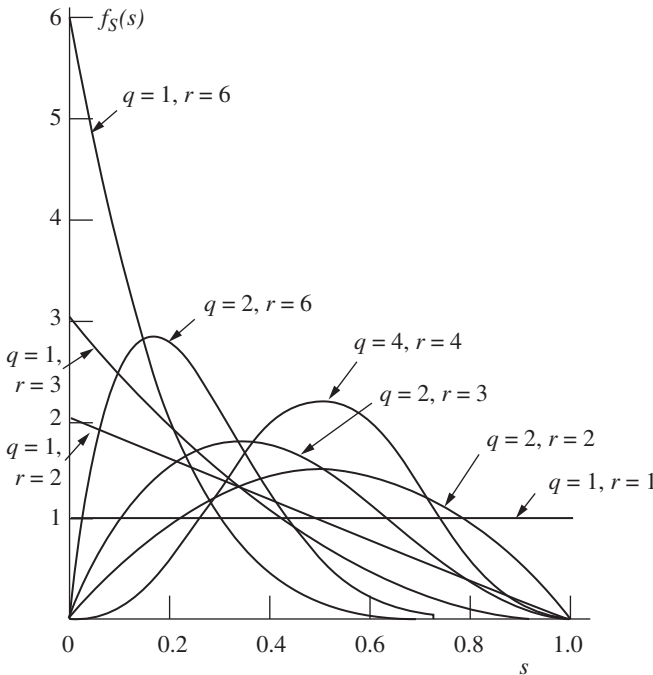
Figure A.4 Beta distribution probability density function for different parameters.

where the Beta function $\beta(q, r)$ is given by

$$\beta(q, r) = \int_0^1 x^{q-1}(1-x)^{r-1}dx = \frac{\Gamma(q)\Gamma(r)}{\Gamma(q+r)}$$

and, for q, r integer $= \dfrac{(q-1)!(r-1)!}{(q+r-1)!}$.

The parameters a and b describe the intervals for the general beta distribution. If $a = 0$, $b = 1$ the standard beta distribution is obtained:

$$
\begin{aligned}
f_S(s) &= \frac{1}{\beta(q, r)}s^{q-1}(1-s)^{r-1} & 0 \le s \le 1 \\
&= 0 & \text{elsewhere}
\end{aligned}
\tag{A.67}
$$

The cumulative distribution function is

$$F_S(s) = \frac{\beta_S(q, r)}{\beta(q, r)} \qquad 0 \le s \le 1 \tag{A.68}$$

where the incomplete Beta function is given by $\beta_S(q, r) = \int_0^S y^{q-1}(1-y)^{r-1}dy$.

The first two moments and the coefficient of skewness of the Beta distribution are:

$$E(X) = \mu_X = a + \frac{q(b-a)}{q+r} \tag{A.69}$$

$$\text{var}(X) = \sigma_X^2 = \frac{qr(b-a)^2}{(q+r)^2(q+r+1)} \tag{A.70}$$

$$\gamma_1 = \frac{2(r-q)}{(q+r)(q+r+2)\sigma_X} \quad \text{(skewness coefficient)} \tag{A.71}$$

The *incomplete Beta function ratio* $\beta_S(q, r)/\beta(q, r)$ has been tabulated [Pearson and Johnson, 1968]. If q, r are both integral, $BT(0, 1, q, r)$ is Binomially distributed such that

$$f_S(s) = (q+r-1)p_X(x) \tag{A.72}$$

where $p_X(x)$ is Binomially distributed as $B(q+r-2, s)$ with $x = q-1$.

A special case of the general Beta distribution is the *rectangular* or *uniform* distribution $BT(a, b, 1, 1) = R(a, b)$ with probability density function and cumulative distribution function given by:

$$
\begin{aligned}
f_X(x) &= \frac{1}{b-a} & a < x < b \\
&= 0 & \text{elsewhere} \\
F_X(x) &= \frac{x-a}{b-a} & a < x < b \\
&= 0 & x \le a \\
&= 1 & x \ge b
\end{aligned}
\tag{A.73}
$$

with moments

$$\mu_X = \frac{(a+b)}{2} \qquad \sigma_X^2 = \frac{(b-a)^2}{12} \tag{A.74}$$
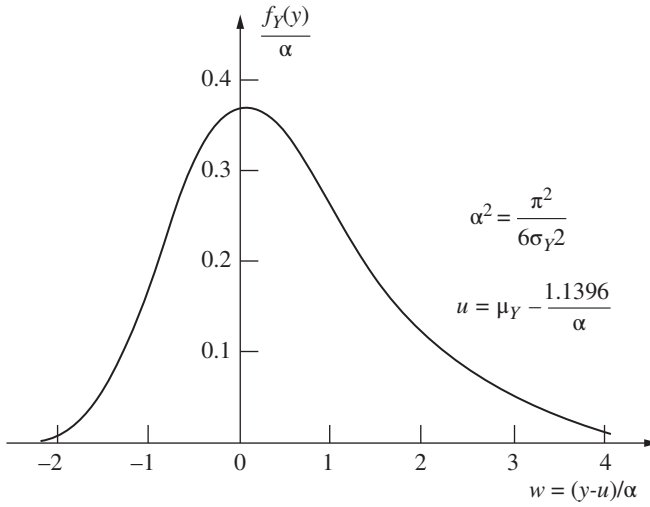
Figure A.5 Extreme value distribution type I (Gumbel).

A.5.11   Extreme Value Distribution Type I EV - $I(\mu, \alpha)$ [Gumbel distribution]

This is the limiting (asymptotic) distribution of the largest (smallest) of n random variables X_i as $n \to \infty$. The distribution of the X_i must be of the form $F_X(x) = 1 - \exp[-g(x)]$ or $f_X(x) = \exp[-g(x)]$ with $dg/dx > 0$. The Normal, Gamma and Exponential distributions are of this type. If Y is the *largest* of many independent random variables X_i then the probability density (Figure A.5) and cumulative distribution functions for Y are given, asymptotically, by [Gumbel, 1958]:

$$f_Y(y) = \alpha \, \exp[-\alpha(y - u) - e^{-\alpha(y-u)}] \qquad -\infty < y < \infty \tag{A.76}$$

$$F_Y(y) = \exp[-e^{-\alpha(y-u)}] \qquad -\infty < y < \infty \tag{A.77}$$

The parameters of this distribution are u, the mode of the distribution, and α, which is a measure of its dispersion. Usually α^{-1} is known as the 'slope' of the distribution (obtained when plotting the distribution on so-called 'Gumbel' paper). Both u and α can be obtained, using the moments of the distribution, from curve fitting to observed data. The moments are:

$$E(Y) = \mu_Y = u + \gamma/\alpha \tag{A.78}$$

$$\text{var}(Y) = \sigma_Y^2 = \frac{\pi^2}{6\alpha^2} \tag{A.79}$$

$$\gamma_1 = 1.1396 \qquad \text{(skewness)} \tag{A.80}$$

where $\gamma = 0.577\,215\,664\,9\ldots$ (known as Euler's constant). Expression (A.80) shows that the skewness is independent of the distribution parameters u and α. The following points might be noted in applications using this distribution:

(1) Although in theory the X_i of the underlying population should be completely independent and completely identical, in practice one or both these requirements may be relaxed [Gumbel, 1958], particularly in the case of large sample sizes [Leadbetter et al. 1983]. Also, it may be difficult in practice to determine the

appropriate underlying distribution of the X_i, and convergence to the asymptotic distribution may be slow. Nevertheless extreme value distributions are useful for fitting to experimental data even where the underlying mechanisms are not fully understood.

(2) The *EV-I* distribution usually is tabulated in terms of a reduced variate defined as $W = (Y - u)\alpha$ for which $u = 0$, $\alpha = 1$ and $F_W(w) = \exp[-e^{-w}]$ [NBS, 1953]. The probability density function and the cumulative distribution function in terms of Y are given by

$$f_Y(y) = \alpha \, f_W[(y - u)\alpha] \tag{A.81}$$

$$F_Y(y) = F_W[(y - u)\alpha] \tag{A.82}$$

(3) The *EV-I* distribution or Gumbel distribution is also known as the 'double exponential' or 'Fisher-Tippett Type I' distribution.

(4) The Gumbel (*EV-I*) distribution occurs as the limit of maxima of most standard (i.e. underlying) distributions, particularly the Normal distribution. It is considered the only possible limiting (asymptotic) distribution for the entire range of tail behaviour [Foureges et al. 2009].

In addition to the distribution of the largest value, a complementary distribution exists for the *smallest* value Y^S of many independent X_i. The corresponding probability density and cumulative distribution functions are:

$$f_{Y^S}(y^S) = \alpha \, \exp[\alpha(y^S - u) - e^{\alpha(y^S - u)}] \qquad -\infty < y^S < \infty \tag{A.83}$$

$$F_{Y^S}(y^S) = 1 - \exp[-e^{\alpha(y^S - u)}] \qquad -\infty < y^S < \infty \tag{A.84}$$

with moments

$$\mu_{Y^S} = u - \gamma/\alpha \tag{A.85}$$

$$\sigma_{Y^S}^2 = \frac{\pi^2}{6\alpha^2} \tag{A.86}$$

$$\gamma_1 = -1.1396 \tag{A.87}$$

The tabulated results for the reduced variable W described above can be applied since the distribution for Y^S is related to that for W by

$$f_{Y^S}(y^S) = \alpha f_W \; [-(y^S - u)\alpha] \tag{A.88}$$

$$F_{Y^S}(y^S) = 1 - F_W \; [-(y^S - u)\alpha] \tag{A.89}$$

The extreme value distribution for the minimum value has less practical application than that for the maximum value; the Weibull distribution (extreme value distribution type III) more commonly is used for smallest values.

A.5.12 Extreme Value Distribution Type II *EV-II(u, k)* [Frechet Distribution]

The EV-II distribution is the limiting distribution of the largest of n random variables X_i as $n \to \infty$. The distribution of the X_i must be of the form $F_X(x) = 1 - Ax^{-k}$, $x \geq 0$ where $A =$ constant [Gumbel, 1958]. Typical of this form are (1) the Pareto distribution and (2) the Cauchy distribution for $x \geq 0$. The probability density function (Figure A.6) and
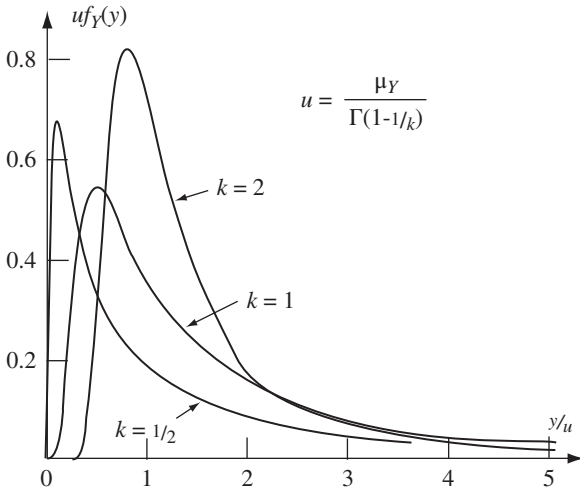
Figure A.6 Extreme value distribution type II (Frechet).

the cumulative distribution function are, respectively:

$$f_Y(y) = \frac{k}{y}\left(\frac{u}{y}\right)^k e^{-(u/y)^k} \qquad y \geq 0 \tag{A.90}$$

$$F_Y(y) = e^{-(u/y)^k} \qquad y \geq 0 \tag{A.91}$$

The distribution parameters are the characteristic value u (with median $> u >$ mode; median $\approx$ mode for $k > 4$) and $1/k$ which is a dimensionless measure of the dispersion of the distribution. The first two moments are:

$$E(Y) = \mu_Y = u\Gamma(1 - 1/k) \qquad k > 1 \tag{A.92}$$

$$\text{var}(Y) = \sigma_Y^2 = u^2\left[\Gamma(1 - 2/k) - \Gamma^2(1 - 1/k)\right] \qquad k > 2 \tag{A.93}$$

so that

$$V_Y^2 = \frac{\mu_Y^2}{\sigma_Y^2} = \frac{\Gamma(1 - 2/k)}{\Gamma^2(1 - 2/k)} - 1 \tag{A.94}$$

Moments of order $l \geq k$ do not exist; this complicates the estimation of u and k.

The following points should be noted in applications using this distribution.

(1) If it is known that $k > 2$, equation (A.94) may be used to evaluate k, and then u may be evaluated from (A.92).
(2) The type II distribution for Y [i.e. EV-II(u, k)], may be transformed to the type I distribution for Z [i.e. EV-I(u, α)], by letting $Z = \ln Y$. Then

$$f_Y(y) = \frac{1}{y} f_Z(\ln y) \tag{A.95}$$

$$F_Y(y) = F_Z(\ln y) \tag{A.96}$$

$$\alpha = k \tag{A.97}$$

Hence, in terms of the reduced variable W, which is tabulated (see Section A.5.11),

$$f_Y(y) = \frac{k}{y} f_W [(\ln y - \ln u)k] \tag{A.98}$$

$$F_Y(y) = F_W [(\ln y - \ln u)k] \tag{A.99}$$

(3) The above properties hold for $y \geq 0$. A more general result, for $y \geq \varepsilon$, $\varepsilon \neq 0$, can be obtained by linear transformation, writing $u - \varepsilon$ for u and $y - \varepsilon$ for y.
(4) The distribution for the smallest extreme value is of no practical interest.
(5) The underlying distributions X_i for the type II distribution typically have longer tails ($x \geq 0$) than those for the type I distribution.

A.5.13   Extreme Value Distribution Type III *EV - III(ε, u, k)* [Weibull]

The Weibull extreme value distribution represents the (asymptotic) distribution of the largest (smallest) value of n random variables X_i as $n \to \infty$, with X_i limited *in the tail of interest* to some maximum (minimum) value w (or ε), and X_i having a distribution of general form

$$F_X(x) = 1 - A(w - x)^k \qquad x \leq w, \, k > 0, \, A = \text{constant}$$

The rectangular ($k = 1$), triangular ($k = 2$) and the Gamma distribution ($\varepsilon = 0$) are of this form. The probability density function (Figure A.7) and the cumulative distribution function for the largest value Y^L of many independent X_i are given, respectively, by [Gumbel, 1958]:

$$f_{Y^L}(y^L) = \frac{k}{w - u} \left(\frac{w - y^L}{w - u} \right)^{k-1} F_{Y^L}(y^L) \qquad y^L \leq w \tag{A.100}$$

$$F_{Y^L}(y^L) = \exp\left[-\left(\frac{w - y^L}{w - u} \right)^k \right] \qquad y^L \leq w \tag{A.101}$$
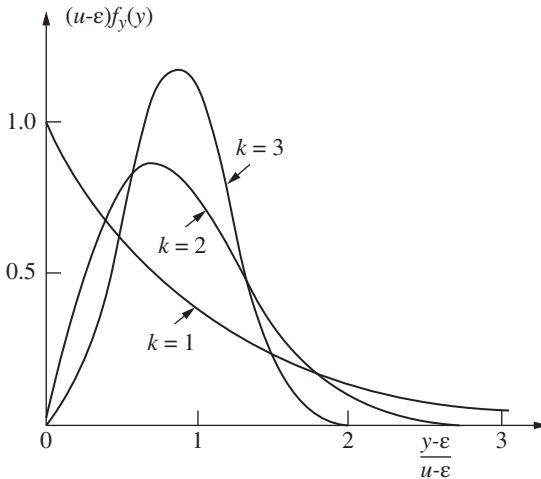
Figure A.7 Extreme value distribution type III (Weibull).

More useful is the distribution of the *smallest* value Y of many independent X_i. In this form it is commonly known as the Weibull distribution. The relevant cumulative distribution and the probability density functions are [Gumbel, 1958]:

$$F_Y(y) = P(Y \leq y) = 1 - P_Y(y) \qquad y \geq \varepsilon \tag{A.102}$$

where

$$P_Y(y) = \exp\left[-\left(\frac{y-\varepsilon}{u-\varepsilon}\right)^k\right] \qquad y \geq \varepsilon \tag{A.103}$$

which equals the probability of a value Y larger than y, i.e. $P(Y > y)$. Also,

$$f_Y(y) = \frac{\mathrm{d}F_Y(y)}{\mathrm{d}y} = \frac{k}{u-\varepsilon}\left(\frac{y-\varepsilon}{u-\varepsilon}\right)^{k-1} P_Y(y) \qquad y \geq \varepsilon \tag{A.104}$$

The parameters are the minimum value ε of X_i (and hence Y), the characteristic value u of the distribution (which converges to μ_Y as $k \to \infty$) and the 'scale parameter' $1/k$ (usually $k > 1$). The moments are

$$E(Y) = \mu_Y = \varepsilon + (u-\varepsilon)\Gamma(1 + 1/k) \tag{A.105}$$
$$\mathrm{var}\,(Y) = \sigma_Y^2 = (u-\varepsilon)^2\left[\Gamma(1 + 2/k) - \Gamma^2(1 + 1/k)\right] \tag{A.106}$$

The following points might be noted in application of this distribution:

(1) Estimation of the parameters ε, u and k generally is not straightforward. If the underlying distribution is known, k is known and ε and u can be estimated from the estimates for μ_Y and σ_Y^2. Otherwise, k may be estimated from sample skewness or u may be estimated from *order statistics* [Gumbel, 1958]. If the lower limit ε is known, or is zero, then u and k can be evaluated from equations (A.105) and (A.106) by writing y for $y - \varepsilon$ and hence

$$\mu_Y = u\Gamma(1 + 1/k)$$
$$\sigma_Y^2 = u^2\left[\Gamma(1 + 2/k) - \Gamma^2(1 + 1/k)\right]$$

and

$$1 + V_Y^2 = \frac{\Gamma(1 + 2/k)}{\Gamma^2(1 + 1/k)} \quad \text{or} \quad k \approx V_Y^{-1.09}$$

all of which can be estimated from sample data [Gumbel, 1958]. However, the procedure may be cumbersome [see also Mann et al., 1974].

(2) The distribution $F_Y(y)$ is pseudo-symmetric for $3.2 < k < 3.7$.

(3) If Y is $EV\text{-}III\ (\varepsilon, u, k)$ for smallest values, then $Z = \ln(Y - \varepsilon)$ is $EV\text{-}I\ [\ln(y - \varepsilon), k]$ for smallest values. This enables the third extreme value distribution to be evaluated using the tables for $EV\text{-}I$ (largest) in terms of the reduced variate W:

$$F_Y(y) = 1 - F_W\{-k[\ln(y - \varepsilon) - \ln(u - \varepsilon)]\} \qquad y \geq \varepsilon \tag{A.107}$$

$$f_Y(y) = \frac{k}{y - \varepsilon} f_W\left[-k \ln\left(\frac{y-\varepsilon}{u-\varepsilon}\right)\right] \qquad y \geq \varepsilon \tag{A.108}$$

(4) As noted, the distribution $P_Y(y)$ for the smallest values is commonly known as the Weibull distribution.

@Seismicisolation

(5) If $\varepsilon = 0$, $k = 2$ the distribution is also known as the Rayleigh distribution:

$$f_Y(y) = \frac{y}{\sigma_Y^2} \exp\left(-\frac{y^2}{2\,\sigma_Y^2}\right) \tag{A.102a}$$

$$F_Y(y) = 1 - \exp\left(-\frac{y^2}{2\sigma_Y^2}\right) \tag{A.103a}$$

A.5.14 Generalized Extreme Value distribution *GEV*

The generalized extreme value distribution is a combination of the above 3 extreme value distributions, with sufficient parameters to allow it to be fitted to almost any set of (continuous, homogeneous) extreme value data. Depending on the choice of parameters, each of EV-I, EV-II and EV-III can be recovered. It has a continuous, smooth cumulative probability function (CDF) given by [e.g. Leadbetter, et al. 1983; Kotz and Nadarajah, 2000; Coles, 2001]:

$$F_X(x) = P[X \le x] = \exp\left\{-\left[1 + \varepsilon\left(\frac{x-\mu}{\sigma}\right)\right]^{-1/\varepsilon}\right\} \quad \text{if } \varepsilon \ne 0 \tag{A.109a}$$

with $t(x) = 1 + \varepsilon\left(\frac{x-\mu}{\sigma}\right) > 0$, $\sigma > 0$

For $\varepsilon > 0$ (A.109a) can be shown to have the form of the Frechet (EV-II) distribution (A.91). For $\varepsilon < 0$ (A.109a) becomes the Weibull (EV-III) distribution. Expression (A.109a) is formally undefined for $\varepsilon = 0$. However, in the limiting case as $\varepsilon \to 0$ it defines the Gumbel distribution. Thus, (A.109a) becomes:

$$F_X(x) = \exp\left[-\exp\left(-\frac{(x-\mu)}{\sigma}\right)\right] \quad \text{if } \varepsilon = 0 \tag{A.109b}$$

which is the 'double exponential' form of the Gumbel EV distribution seen in (A.77).

While each of the original EV distributions (EV-I, EV-II and EV-III) are asymptotic distributions (for maxima or minima) relative to some underlying parent distribution, since the GEV distribution encompasses all three, it should be clear that there can be no single underlying (parent) distribution for which the GEV is the natural asymptotic EV distribution. In other words, while there might be some physical or other phenomenological reason for the choice of EV-I or II or III, this cannot be the case for the GEV distribution. It means there is no underlying logic or physical meaning and thus its application is entirely empirical. That means its application as an EV distribution is entirely as an empirical fit to EV data [Coles, 2001]. In turn this means that any extrapolation of data using the GEV distribution also is entirely empirical. Theoretically also, more data are required to obtain a satisfactory fit [Foureges et al. 2009].

A.6 Jointly Distributed Random Variables

A.6.1 Joint Probability Distribution

If an event is the result of two (or more) continuous random variables, X_1 and X_2 say, the (non-zero) probability that the event occurs for values less than (or equal to) x_1 and

x_2 is described by the joint cumulative distribution function

$$F_{X_1 X_2}(x_1, x_2) = P[(X_1 \leq x_1) \ \cap \ (X_2 \leq x_2)] \geq 0$$

$$= \int_{-\infty}^{x_1} \int_{-\infty}^{x_2} f_{X_1 X_2}(u, v) du dv \tag{A.110a}$$

where $f_{X_1 X_2}(x_1, x_2) \geq 0$ is the joint probability density function. Further, $f_{X_1 X_2}()$ can be given as follows, if the partial derivatives exist:

$$f_{X_1 X_2}(x_1, x_2) \equiv \lim_{\delta x_1, \delta x_2 \to 0} \{P[(x_1 < X_1 \leq x_1 + \delta x_1) \cap (x_2 < X_2 \leq x_2 + \delta x_2)]\}$$

$$= \frac{\partial^2 F_{X_1 X_2}(x_1, x_2)}{\partial x_1 \partial x_2} \tag{A.110b}$$

Also,

$$F_{X_1 X_2}(-\infty, -\infty) = 0 \tag{A.111}$$

$$F_{X_1 X_2}(-\infty, y) = 0 \ \text{ and vice versa in } (x_1, x_2) \tag{A.112}$$

$$F_{X_1 X_2}(\infty, y) = F_{X_2}(y) \ \text{ and vice versa in } (x_1, x_2) \tag{A.113}$$

$$F_{X_1 X_2}(\infty, \infty) = 1.0 \tag{A.114}$$

The last expression states that the volume under $F_{X_1 X_2}()$ is unity, as would be expected. For discrete random variables, analogous expressions apply.

A.6.2 Conditional Probability Distributions

If the probability that $(x_1 < X_1 \leq x_1 + \delta x_1)$ is a function of X_2, the following holds:

$$\lim_{\delta x_1, \delta x_2 \to 0} \{P[(x_1 < X_1 \leq x_1 + \delta x_1)|(x_2 < X_2 \leq x_2 + \delta x_2)]\} \equiv f_{X_1|X_2}(x_1|x_2) \tag{A.115}$$

According to (A.3), reading f as a probability over the infinitesimal region $(\delta x_1, \delta x_2)$:

$$f_{X_1|X_2}(x_1|x_2) = \frac{f_{X_1 X_2}(x_1, x_2)}{f_{X_2}(x_2)} \tag{A.116}$$

By analogy to (A.4), if X_1 and X_2 are independent,

$$f_{X_1 X_2}(x_1, x_2) = f_{X_1}(x_1) f_{X_2}(x_2) \tag{A.117}$$

A.6.3 Marginal Probability Distributions

A marginal probability density function may be obtained from the joint density function by integrating over the other variables, that is, by invoking the total probability theorem (A.6). Also making use of (A.116) produces:

$$f_{X_1}(x_1) = \int_{-\infty}^{\infty} f_{X_1|X_2}(x_1|x_2) f_{X_2}(x_2) \, dx_2 = \int_{-\infty}^{\infty} f_{X_1 X_2}(x_1, x_2) \, dx_2 \tag{A.118}$$

If X_1 and X_2 are *independent*, the conditional and marginal distributions are identical, so that $f_{X_1|X_2} = f_{X_1}$, $f_{X_1 X_2} = f_{X_1} f_{X_2}$, etc. In general, the relationship between $f_{X_1 X_2}$, $f_{X_1|X_2}$ and f_{X_1}, etc., takes the form shown in Figure A.8.
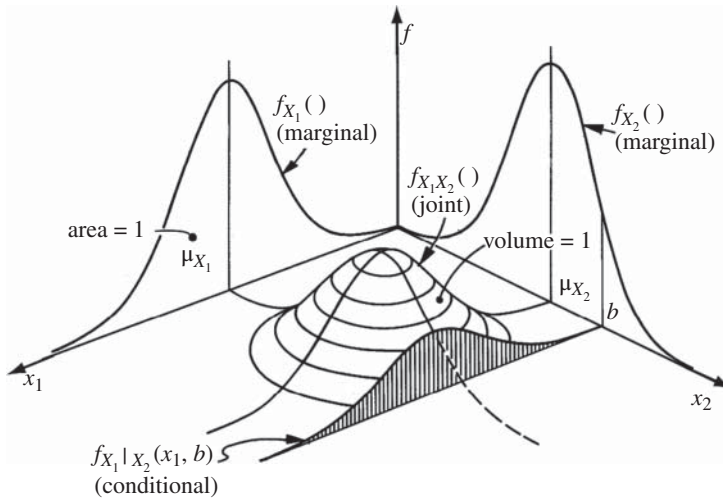
Figure A.8 Joint, marginal and conditional probability density functions.

Multivariate distributions and concepts follow directly by extending the above relationships.

A.7 Moments of Jointly Distributed Random Variables

The concept of moments may be extended to an event that depends on two (or more) random variables. Let the variables be the jointly distributed random variables X_1 and X_2.

A.7.1 Mean

$$
\mu_{X_1} \equiv E(X_1) = \int_{-\infty}^{\infty}\int_{-\infty}^{\infty} x_1 f_{X_1 X_2}(x_1, x_2)\ dx_1 dx_2
$$
$$
= \int_{-\infty}^{\infty} \mu_{X_1|X_2} f_{X_2}(x_2)\ dx_2 \tag{A.119}
$$

This is the first (marginal) moment of X_1, or, equivalently, the mean value of X_1 over all X_2. The fact that this is so can be seen also from the first double-integral term, which can be rewritten as

$$
\int_{-\infty}^{\infty} x_1 \left[\int_{-\infty}^{\infty} f_{X_1 X_2}(x_1, x_2) dx_2\right] dx_1 = \int_{-\infty}^{\infty} x_1 f_{X_1}(x_1) dx_1 = \mu_{X_1}
$$

since the term [ ] is the marginal distribution f_{X_1} according to (A.118). Also, the conditional mean of X_1, given that $X_2 = x_2$, is given by:

$$
\mu_{X_1|X_2} = E(X_1 | X_2 = x_2) = \int_{-\infty}^{\infty} x_1 f_{X_1|X_2}(x_1 | x_2) dx_1
$$

A.7.2 Variance

In a similar manner, extending the basic definition of the variance (A.11a):

$$\text{var}(X_1) \equiv E[(X_1 - \mu_{X_1})^2] = \int_{-\infty}^{\infty} \int_{-\infty}^{\infty} (x_1 - \mu_{X_1})^2 f_{X_1 X_2}(x_1, x_2) dx_1 dx_2 \qquad (A.120)$$

$$= \int_{-\infty}^{\infty} \text{var}(X_1 \,|\, x_2) f_{X_2}(x_2) dx_2 = \text{var}(X_1) \qquad (A.121)$$

Here the marginal variance of X_1, is

$$\text{var}(X_1 \,|\, X_2) \equiv \text{var}(X_1 | X_2 = x_2) \equiv E[(X_1 - \mu_{X_1 | X_2})^2 \,|\, X_2 = x_2]$$

$$= \int_{-\infty}^{\infty} (x_1 - \mu_{X_1 | X_2})^2 f_{X_1 | X_2}(x_1 \,|\, x_2) dx_1 \qquad (A.122)$$

A.7.3 Covariance and Correlation

The above expressions for the mean and the variance are symmetrical in (X_1, X_2). A further elementary moment exists involving both X_1 and X_2; this is the covariance. It has the same dimension as variance:

$$\text{cov}(X_1, X_2) \equiv E[(X_1 - \mu_{X_1})(X_2 - \mu_{X_2})]$$

$$= \int_{-\infty}^{\infty} \int_{-\infty}^{\infty} (x_1 - \mu_{X_1})(x_2 - \mu_{X_2}) f_{X_1 X_2}(x_1, x_2) dx_1 dx_2 \qquad (A.123)$$

Further, the correlation coefficient, defined as:

$$\rho_{X_1 X_2} = \frac{\text{cov}(X_1 X_2)}{(+)[\text{var}(X_1)\,\text{var}(X_2)]^{1/2}} = \frac{\text{cov}(X_1 X_2)}{\sigma_{X_1} \sigma_{X_2}} \qquad -1 \leq \rho \leq +1 \qquad (A.124)$$

is a measure of *linear* dependence between two random variables; if $\rho_{X_1 X_2} = 0$, it follows only that (X_1, X_2) are not *linearly* related, but they may be related in some other (non-linear) way. Correlation makes no statement about cause and effect [Benjamin and Cornell, 1970; Freeman, 1963]. A summary of the significance of ρ is given in Figure A.9. Higher-order moments also may be developed but these have little practical interest.

A.8 Bivariate Normal Distribution

The bivariate Normal distribution describes the joint probability density of two random variables for which the marginal distributions are Normal distributed. The probability density function usually is written as:

$$f_{X_1 X_2}(x_1, x_2, \rho) = \frac{1}{2\pi \sigma_{X_1} \sigma_{X_2}(1 - \rho^2)^{1/2}} \exp\left[\frac{-\frac{1}{2}(h^2 + k^2 - 2\rho hk)}{(1 - \rho^2)}\right] \qquad (A.125)$$
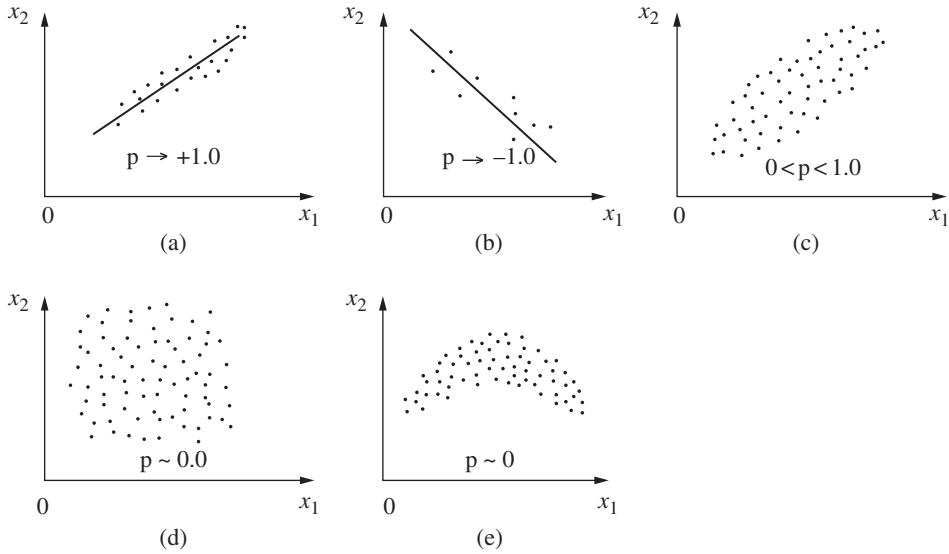
Figure A.9 Linear dependence between two variables as a function of correlation coefficient ρ.

with $-\infty < x_i < \infty$, $i = 1, 2$ and where $h = (x_1 - \mu_{X_1})/\sigma_{X_1}$ and $k = (x_2 - \mu_{X_2})/\sigma_{X_2}$. The 'standard' form, with zero means and unit standard deviations, is:

$$\phi_2(h, k, \rho) = \frac{1}{2\pi(1 - \rho^2)^{1/2}} \exp\left[\frac{-\frac{1}{2}(h^2 + k^2 - 2\rho hk)}{(1 - \rho^2)}\right] \quad -\infty < (h, k) < \infty \quad (A.126)$$

with h, k as before and $f_{X_1 X_2}(x_1, x_2, \rho) = \frac{1}{\sigma_{X_1} \sigma_{X_2}} \phi_2(h, k, \rho)$.

There is no explicit expression for the cumulative distribution function

$$F_{X_1 X_2}(x_1, x_2, \rho) = \int_{-\infty}^{\infty} \int_{-\infty}^{x_2} f_{X_1 X_2}(u, v, \rho) \, du dv$$

However, it may be evaluated by relating it the standard bivariate Normal function $\Phi_2(h, k, \rho)$ (which is extensively tabulated—see below) through:

$$F_{X_1 X_2}(x_1, x_2, \rho) = \Phi_2(h, k, \rho) = \int_{-\infty}^{h} \int_{-\infty}^{k} \phi_2(u, v, \rho) \, du dv \quad (A.127)$$

The parameters are the mean values (μ_{X_1}, μ_{X_2}) and the variances ($\sigma_{X_1}^2$, $\sigma_{X_2}^2$) and the correlation coefficient $\rho = \rho_{X_1 X_2}$.

The conditional moments (see Section A.7) are

$$E(X_2 \mid X_1 = x_1) = \mu_{X_2 \mid X_1} = \mu_{X_2} + \rho \frac{\sigma_{X_2}}{\sigma_{X_1}}(x_1 - \mu_{X_1}) \quad (A.128)$$

(this is known also as the 'regression function' of X_2 on X_1).

$$\text{var}(X_2 \mid X_1 = x_1) = \sigma_{X_2 \mid X_1}^2 = \sigma_{X_2}^2(1 - \rho^2) \quad (A.129)$$

$$\text{cov}(X_1, X_2) = \rho \sigma_{X_1} \sigma_{X_2} \quad (A.130)$$

where μ_{X_2} is the marginal mean and $\sigma_{X_2}^2$ is the marginal variance both defined in the marginal density functions [which are therefore $N(\mu_{X_i}, \sigma_{X_i}^2)$]:

$$f_{X_i}(x_i) = \int_{-\infty}^{\infty} f_{X_1 X_2}(x_1, x_2) dx_i \qquad i = 1, 2$$

$$= \frac{1}{(2\pi)^{1/2}\ \sigma_{X_i}} \exp\left[-\frac{1}{2}\left(\frac{x_i - \mu_{X_i}}{\sigma_{X_i}}\right)^2\right] \tag{A.131}$$

The properties of the bivariate Normal distributions are as follows [Owen, 1956; Johnson and Kotz, 1972]:

(1) The marginal distributions are Normal (see above). However, the converse may *not* be true; if $f_{X_1}(x_1)$ and $f_{X_2}(x_2)$ are Normal, the joint density function $f_{X_1 X_2}(x_1, x_2)$ is not necessarily bivariate Normal.
(2) If $\rho = 0$, i.e. if X_1 and X_2 are uncorrelated Normal random variables, they are also independent. Then $f_{X_1 X_2}(x_1, x_2) = f_{X_1}(x_1) f_{X_2}(x_2)$ with $f_{X_i}(x_i)$ Normal distributed.
(3) A common expression for the bivariate Normal is:

$$L(h, k, \rho) \equiv \frac{1}{2\pi(1-\rho^2)^{1/2}} \int_h^{\infty} \int_k^{\infty} exp\left[\frac{-\frac{1}{2}(u^2 + v^2 - 2\rho uv)}{(1-\rho^2)}\right] dudv \tag{A.132}$$

for which the following properties hold:

(a)
$$L(h, k, \rho) = L(k, h, \rho) \tag{A.133}$$

(b)
$$L(h, k, 0) = \frac{1}{4}[1 - \alpha(h)][1 - \alpha(k)] = [1 - \Phi(h)][1 - \Phi(k)] \tag{A.134}$$

(c)
$$\begin{aligned} L(h, k, -1) &= 0 && \text{if } h + k \geq 0 \\ &= 1 - \Phi(h) - \Phi(k) && \text{if } h + k \leq 0 \end{aligned} \tag{A.135}$$

(d)
$$L(h, k, 1) = \frac{1}{2}\ [1 - \alpha(t)] \quad \text{where } t = \max[h, k] \geq 0 \tag{A.136}$$

(e)
$$L(-h, k, \rho) = -L(h, k, -\rho) + \frac{1}{2}\ [1 - \alpha(h)] \tag{A.137}$$

(f)
$$L(-h, -k, \rho) = L(h, k, \rho) + \frac{1}{2}\ [\alpha(k) + \alpha(h)] = \Phi_2(h, k, \rho) \tag{A.138}$$

(g)
$$L(0, 0, \rho) = \frac{1}{4} + \frac{1}{2\pi}\ \arcsin\ \rho \tag{A.139}$$

(h)
$$L(h, k, \rho)$$
$$= \frac{1}{2\pi} \int_{\arccos\rho}^{\pi} \exp\left[-\frac{1}{2}(h^2 + k^2 - 2hk\ \cos\theta)\mathrm{cosec}^2\theta\right] d\theta \qquad h, k \geq 0 \tag{A.140}$$

(i)

$$\Phi_2(h, k, \rho) = \frac{1}{2\pi} \int_0^\rho \frac{1}{(1-z^2)^{1/2}} \exp\left[-\frac{\frac{1}{2}(h^2 + k^2 - 2hkz)}{(1-z^2)}\right] dz$$
$$+ \Phi(h).\Phi(k) \qquad h, k \geq 0 \tag{A.141}$$

where

$$\Phi_2(h, k, \rho) = 1 - L(h, -\infty, \rho) - L(-\infty, k, \rho) + L(h, k, \rho) \tag{A.141a}$$

$$\alpha(v) = \frac{1}{(2\pi)^{1/2}} \int_{-v}^{v} \exp\left(-\frac{1}{2}t^2\right) dt \tag{A.141b}$$

$$\Phi(v) = \frac{1}{(2\pi)^{1/2}} \int_{-\infty}^{v} \exp\left(-\frac{1}{2}t^2\right) dt \tag{A.141c}$$

$$\frac{1}{2}[1 - \alpha(v)] = 1 - \Phi(v) \tag{A.141d}$$

Charts for $L(h, 0, \rho)$, $0 \leq h \leq 1$, $-1 \leq \rho \leq 1$ and $L(h, 0, \rho)$, $h \geq 1$, $-1 \leq \rho \leq 1$ are given, for example, in Abramowitz and Stegun (1966). Using the relations (A.132) to (A.141) above, the probabilities over rectangular regions can be determined.

Regions of polygonal shape may be broken down into triangular regions. For these, tabulations exist [NBS, 1959] in terms of the circular Normal distribution, obtained by transforming the variables into an orthogonal set. Since triangles transform to triangles under rotation and scale change, the transformed variables can be used to obtain the required probability. Such a transformation is

$$\binom{u}{v} = \frac{\pm 1}{(2 \pm 2\rho)^{1/2}} \left(\frac{x_1 - \mu_{X_1}}{\sigma_{X_1}} \pm \frac{x_2 - \mu_{X_2}}{\sigma_{X_2}}\right) \qquad \rho \neq \pm 1 \tag{A.142}$$

or alternatively

$$u = \frac{1}{(1-\rho)^{1/2}} \left(\frac{x_1 - \mu_{X_1}}{\sigma_{X_1}} - \frac{\rho(x_2 - \mu_{X_2})}{\sigma_{X_2}}\right), \quad v = \frac{(x_2 - \mu_{X_2})}{\sigma_{X_2}} \qquad \rho \neq \pm 1 \tag{A.143}$$

A simpler function, defined by

$$V(h, k) = \frac{1}{2p} \int_0^h \int_0^{kx/h} \exp\left[-\frac{1}{2}(x^2 + y^2)\right] dy dx \tag{A.144}$$

could then be employed. It expresses the probability content (in the transformed circular Normal distribution) of the triangular region contained within the points $(0, 0)$, $(h, 0)$ and (h, k). It is tabulated extensively [NBS, 1959]. The relationship between $L(h, k, \rho)$ and $V(h, k)$ is

$$L(h, k, \rho) = V\left[h, \frac{k - \rho h}{(1 - \rho^2)^{1/2}}\right] + V\left[k, \frac{h - \rho k}{(1 - \rho^2)^{1/2}}\right] + \frac{\arcsin\rho}{2\pi}$$
$$+ \frac{1}{4}[1 - \alpha(h) - \alpha(k)] \tag{A.145}$$

with $\alpha(\ )$ as defined above.

A.9   Transformation of Random Variables

A.9.1   Transformation of a Single Random Variable

If $Y = g(X)$ and thus $X = g^{-1}(Y)$, where $g(\ )$ is a monotonic function, and X and Y are continuous random variables, it can be shown that the probability density function for the dependent variable Y in terms of that for X is given by [e.g. Ang and Tang, 1975; Freeman, 1963]:

$$f_Y(y) = f_X(x) \left| \frac{dx}{dy} \right| \tag{A.146}$$

where $x = g^{-1}(y)$. A physical meaning should be evident. In the case of x and y increasing monotonically, (A.146) is equivalent to

$$f_Y(y)dy = f_X(x)dx \tag{A.147}$$

This indicates that the infinitesimal area $f_X(x)dx$ under the f_X curve at x is equal to the corresponding infinitesimal area $f_Y(y)dy$ at $y(= g(x))$. Hence respective probabilities over dx and dy are maintained when f_Y is transformed from f_X by equation (A.146). See also Benjamin and Cornell (1970, p. 107) for a useful discussion of this situation.

If g is not a monotonic function, (A.146) does not apply, since y (or x) may take on more than one value. A general procedure, requiring adaptation to each individual problem, is to derive $F_Y(y)$ directly [Benjamin and Cornell, 1970, p. 110]:

$$F_Y(y) \equiv P(Y \leq y) = P[X \text{ has a value } x \text{ for which } g(x) \leq y]$$

$$= \int_{R_y} f_X(x)dx \tag{A.148}$$

where R_y is the region in which $g(x) \leq y$.

A particular transformation useful in Monte Carlo simulation work is that given by $y = F_X(x)$, $0 \leq y \leq 1$. If F_X is differentiable, $dy/dx = dF_X(x)/dx = f_X(x)$. Hence, substituting into (A.146) provides

$$f_Y(y) = f_X(x) \left| \frac{1}{f_X(x)} \right|, \qquad 0 \leq y \leq 1 \tag{A.149}$$

This is a Rectangular distribution, irrespective of the form of $F_X(x)$.

A.9.2   Transformation of Two or More Random Variables

Consider two random variables X_1 and X_2, with known joint density function $f_{X_1 X_2}(x_1, x_2)$ and which are related to two random variables Y_1 and Y_2 by known functions [Freeman, 1963]:

$$y_1 = y_1(x_1, x_2), \qquad y_2 = y_2(x_1, x_2)$$

having unique (i.e. one-to-one) inverses

$$x_1 = x_1(y_1, y_2), \qquad x_2 = x_2(y_1, y_2)$$

Then

$$f_{Y_1 Y_2}(y_1, y_2) = f_{X_1 X_2}(x_1, x_2) |\mathbf{J}| \tag{A.150}$$

where the Jacobian $\mathbf{J}$ is defined by

$$\mathbf{J} \equiv \begin{bmatrix} \dfrac{\partial x_1}{\partial y_1} & \dfrac{\partial x_2}{\partial y_1} \\[2mm] \dfrac{\partial x_1}{\partial y_2} & \dfrac{\partial x_2}{\partial y_2} \end{bmatrix} \equiv \dfrac{\partial(x_1, x_2)}{\partial(y_1, y_2)} \tag{A.151}$$

As in the case of the single random variable, an elemental volume defined by $f_{X_1 X_2}(x_1, x_2) dA(x_1, x_2)$ in the (x_1, x_2) variables remains invariant under the transformation (A.151), after which it is defined by $f_{Y_1 Y_2}(y_1, y_2) = dA(y_1, y_2)$.

Transformation (A.150) can be extended directly to more dimensions, provided the uniqueness of transformations remains valid. This is guaranteed 'locally' if $\mathbf{J}$ does not change sign with 'small' changes of X_i. The guarantee 'in the large' is less straightforward [Freeman, 1963].

A.9.3 Linear and Orthogonal Transformations

For the linear transformation

$$y_i = \sum_{j=1, n} a_{ij} x_j \qquad j = 1, 2, \ldots, n \tag{A.152}$$

the Jacobian is

$$\mathbf{J} = \begin{bmatrix} a_{11} & \cdot & a_{1n} \\ \cdot & & \cdot \\ a_{n1} & \cdot & a_{nn} \end{bmatrix} = \mathbf{A} \tag{A.153}$$

Here $\mathbf{A}$ is the transformation matrix, known from matrix theory to be orthogonal (i.e. the y_i are independent if $\mathbf{A}\mathbf{A}^T = 1$, the identity matrix. It follows readily that in this case $|\mathbf{J}| = |\mathbf{A}| = (\mathbf{A}\mathbf{A}^T)^{1/2} = \pm 1$ (see also Appendix B).

A.10 Functions of Random Variables

A.10.1 Function of a Single Random Variable

If $Y = g(X)$, the transformation results of Section A.9 apply directly, using (A.146) and (A.147) for monotonic functions, and (A.148) otherwise.

A.10.2 Function of Two or More Random Variables

If a function $Y = Y(X_1, X_2)$ is sought when the function Y and its inverse are unique in the sense of Section A.9, then the results of that section can be applied directly. Let

$Y = Y_1$ and let, say, $Y_2 = X_2$(or X_1), an entirely dummy relationship. From the joint density function $f_{Y_1 Y_2}$, the density function f_Y can be obtained by integrating over Y_2, using (A.118) but with the limits of integration changed, thus

$$f_Y(y) = f_{Y_1}(y_1) = \int_a^b f_{Y_1 Y_2}(y_1, y_2) dy_2 = \int_a^b f_{X_1 X_2}(x_1, x_2) \left| \frac{\partial(x_1, x_2)}{\partial(y_1, y_2)} \right| dx_2 \qquad (A.154)$$

This is an application of convolution to find what is essentially the marginal density function. The integration is seldom straightforward [for example, see Wadsworth and Bryan (1974)].

If the function $Y = Y(X_1, X_2)$ and its inverse are not unique in the sense of Section A.9, the above procedure is not valid. In parallel with the method of Section A.9, an appropriate procedure is to establish $F_Y(y)$ directly. In particular, we may write

$$F_Y(y) \equiv P(Y \leq y) = P[X_1, X_2 \text{ have values } (x_1, x_2) \text{ for which Y } (x_1, x_2) \leq y]$$

$$= \iint_{R_y} f_{X_1 X_2}(x_1, x_2) dx_1 dx_2 \qquad (A.155)$$

where R_y is the region over which $Y(x_1, x_2) \leq y$. The integration is again seldom straightforward. See Benjamin and Cornell (1970) for some examples.

A.10.3   Some Special Results

A.10.3.1 $Y = X_1 + X_2$
According to the convolution integral (A.154) and applying (A.117)

$$f_Y(y) = \int_{-\infty}^{\infty} f_{X_1}(x_1) f_{X_2}(y - x_1) dx_1 \qquad (A.156)$$

If X_1 and X_2 are statistically independent, and if f_{X_1} and f_{X_2} are Poisson distributions, then f_Y will be Poisson also (see A.34). Similarly, the sum of Gamma distributions is given by (A.46). If X_1 and X_2 are Normal distributed, then Y is Normal distributed also, with mean and variance given by

$$\mu_Y = \mu_{X_1} + \mu_{X_2} \qquad \text{var}(Y) = \text{var}(X_1) + \text{var}(X_2) \qquad (A.157)$$

A.10.3.2 $Y = X_1 X_2$
By convolution

$$f_Y(y) = \int_{-\infty}^{\infty} \left| \frac{1}{x_2} \right| f_{X_1 X_2} \left(\frac{y}{x_2}, x_2 \right) dx_2 \qquad (A.158)$$

If $Y = X_1 / X_2$ the same form holds with $|1/x_2|$ and y/x_2 replaced by x_2 and yx_2 respectively [Ang and Tang, 1975].

It is noted that an approximate method to combine random variables and to estimate the probability density function (pdf) of the combination can be based on the idea of using an exponential function with polynomial coefficients to represent the pdfs of the random variables. These can be then combined through their moments to yield the exponential function of the outcome random variable and hence its pdf [Er, 1998].

A.11   Moments of Functions of Random Variables

The joint probability density function for a function of several random variables usually is not easily obtainable. Fortunately, for many practical applications knowledge of the first and second moments may be sufficient.

The basic expressions for moments, equations (A.10) and (A.11), can be extended to a general function as follows

$$E(Y) = \int_{-\infty}^{\infty} \dots \int_{-\infty}^{\infty} Y(x_1, x_2, \dots, x_n) f_{X_1 X_2 \dots X_n}(x_1, x_2, \dots, x_n) dx_1 dx_2 \dots dx_2 \quad \text{(A.159)}$$

where $Y(x_1, x_2, \dots, x_n)$ is the function for which the moment is sought. Some special results are given below.

A.11.1   Linear Functions

If $Y = \sum_{i=1}^{n} a_i X_i$, then

$$E(Y) = \mu_Y = \sum_{i=1}^{n} a_i E(X_i) = \sum_{i=1}^{n} a_i \mu_{X_i} \quad \text{(A.160)}$$

$$E[(Y - \mu_Y)^2] = \text{var}(Y) = \sum_{i=1}^{n} a_i^2 \ \text{var}(X_i) + \sum_{j \neq i}^{n} \sum_{i=1}^{n} a_i a_j \text{cov}(X_i, X_j) \quad \text{(A.161)}$$

or, more compactly,

$$\text{var}(Y) = \sum_{j}^{n} \sum_{i}^{n} a_i a_j \rho_{ij} \sigma_{X_i} \sigma_{X_j} \quad \text{(A.162)}$$

where σ_{X_i} is the standard deviation of X_i and ρ_{ij} is the correlation coefficient between X_i and X_j, with $\rho_{ii} = 1$. If the X_i are *independent*, $\rho_{ij} = 0$ if $i \neq j$. Further, if there is a function $Z = \sum_{i=1}^{n} b_i X_i$, then [Ang and Tang, 1975]

$$\text{cov}(Y, Z) = \sum_{j}^{n} \sum_{i}^{n} a_i b_j \rho_{ij} \sigma_{X_i} \sigma_{X_j} \quad \text{(A.163)}$$

A.11.2   Product of Variates

If $Y = \prod_{i=1}^{n} X_i$, then three cases may be identified:

(a) If $n = 2$,

$$E(Y) = \mu_Y = E(X_1, X_2) = E(X_1)E(X_2) + \text{cov}(X_1, X_2) = \mu_{X_1} \mu_{X_2} + \rho \sigma_{X_1} \sigma_{X_2} \quad \text{(A.164)}$$

$$\text{var}(Y) = \sigma_Y^2 = [(\mu_{X_1} \sigma_{X_1})^2 + (\mu_{X_2} \sigma_{X_2})^2 + (\sigma_{X_1} \sigma_{X_2})^2](1 + \rho^2) \quad \text{(A.165)}$$

where ρ is the correlation coefficient between X_1 and X_2.

(b) If $n = 2$ and X_1, X_2 are *independent*, (i.e. $\rho = 0$), (A.165) reduces to

$$V_Y^2 = V_{X_1}^2 + V_{X_2}^2 @Seismicisolation \quad \text{(A.166)}$$

where $V_k = \sigma_k / \mu_k$ is the coefficient of variation. The last term in (A.166) is negligible if the coefficients of variation are small, say < 0.3. This result is of considerable practical importance.

(c) If $n \geq 2$ and the X_i are *independent*,

$$E(Y) = \mu_Y = E\left(\prod_{i=1}^{n} X_i\right) = \prod_{i=1}^{n} E(X_i) = \prod_{i=1}^{n} \mu_{X_i} \tag{A.167}$$

and from equation (A.1)

$$\text{var}(Y) = E(Y^2) - [E(Y)]^2 = \prod_{i=1}^{n} \mu_{X_i}^2 - \left(\prod_{i-1}^{n} \mu_{X_i}\right)^2 \tag{A.168}$$

An *approximate* result, that ignores second-order terms and that may be obtained using the methods of Section A.12, is [Benjamin and Cornell, 1970]:

$$\text{var}(Y) \approx \sum_{i=1}^{n} \left(\prod_{\substack{i=1 \\ j \neq i}}^{n} \mu_{X_i}^2\right) \sigma_{X_i}^2 \tag{A.169}$$

A.11.3   Division of Variates

An approximate result for $Y = X_1/X_2$ valid for random variables with reasonably small variance, is [Haugen, 1968] (excluding division by zero):

$$E(Y) = \mu_Y = \frac{\mu_{X_1}}{\mu_{X_2}} \left[1 + \frac{\sigma_{X_1}}{\mu_{X_1}}\left(\frac{\sigma_{X_1}}{\mu_{X_1}} - \rho\frac{\sigma_{X_2}}{\mu_{X_2}}\right)\left(1 + \frac{\sigma_{X_1}^2}{\mu_{X_1}^2} + \dots\right)\right] \tag{A.170}$$

or

$$E(Y) = \mu_Y \approx \frac{\mu_{X_1}}{\mu_{X_2}} \tag{A.171}$$

This is a first-order approximation. Also:

$$\text{var}(Y) = \sigma_Y^2 \approx \left(\frac{\mu_{X_1}}{\mu_{X_2}}\right)^2 \left(\frac{\sigma_{X_1}^2}{\mu_{X_1}^2} - 2\rho\frac{\sigma_{X_1}}{\mu_{X_1}}\frac{\sigma_{X_2}}{\mu_{X_2}} + \frac{\sigma_{X_1}^2}{\mu_{X_2}^2} + \text{higher order terms}\right) \tag{A.172}$$

$$\approx \left(\frac{\mu_{X_1}}{\mu_{X_2}}\right)^2 \left(V_{X_1}^2 - 2\rho V_{X_1} V_{X_2} + V_{X_2}^2\right) \tag{A.173}$$

A.11.4   Moments of a Square Root [Haugen, 1968]

If $Y = X^{1/2}$,

$$\mu_Y = \left(\mu_X^2 - \frac{1}{2}\sigma_X^2\right)^{1/4} \tag{A.174}$$

$$\sigma_Y^2 = \mu_X - \left(\mu_X^2 - \frac{1}{2}\sigma_X^2\right)^{1/2} \tag{A.175}$$

A.11.5   Moments of a Quadratic Form [Haugen, 1968]

If $Y = aX^2 + bX + c$, then using results already given

$$\mu_Y = a(\mu_X^2 + \sigma_X^2) + b\mu_X + c \tag{A.176}$$

$$\sigma_Y^2 = \sigma_X^2(2a\mu_X + b)^2 + 2a^2\sigma_X^4 \tag{A.177}$$

A.12   Approximate Moments for General Functions

The mean and variance of general functions usually are not obtained easily, owing to the integrations required in (A.159). Nor may information beyond that of the first two moments of each variable X_i be available. A useful approach is to calculate approximate moments by expanding the function $Y = Y(X_1, X_2, \ldots, X_n)$ in a Taylor series about the point defined by the vector of the means ($\mu_{X_1}, \mu_{X_2}, \ldots, \mu_{X_n}$) (or another appropriate point). By truncating the series at linear terms, the first-order mean and variance are

$$E(Y) \approx Y(\mu_{X_1}, \mu_{X_2}, \ldots, \mu_{Xn}) \tag{A.178}$$

$$\text{var}(Y) \approx \sum_i^n \sum_j^n c_i c_j \, \text{cov}(X_i, X_j) \tag{A.179}$$

where $c_i \equiv \left. \dfrac{\partial Y}{\partial X_i} \right|_{\mu_{X_i}, \mu_{X_2}, \ldots, \mu_{X_n}}$. If the X_i are independent, then $\text{cov}(X_i, X_j) = 0$ if $i \neq j$ and $\text{cov}(X_i, X_j) = \text{var}(X_i)$ if $i = j$. Similarly, the *second-order* approximation is given by

$$E(Y) \approx Y(\mu_{X_1}, \mu_{X_2}, \ldots, \mu_{X_n}) + \frac{1}{2} \sum_{i=1}^n \sum_{j=1}^n \frac{\partial^2 Y}{\partial X_i \partial X_j} \, \text{cov}(X_i, X_j) \tag{A.180}$$

with the $\partial^2 Y / \partial X_i \partial X_j$ evaluated at ($\mu_{X_1}, \mu_{X_2}, \ldots, \mu_{X_n}$). The second term is negligibly small if the coefficients of variation V_{X_i} are small and the function Y does not depart too much from linearity.

Reference might be made also to the approximate method noted at the end of Section A.10, since this is based on approximating the moments of general functions to obtain their probability density functions.

B

Rosenblatt and Other Transformations

B.1 Rosenblatt Transformation

A dependent random vector $\mathbf{X} = \{X_1, X_2, \ldots, X_n\}$ may be transformed to the independent Uniform distributed random vector $\mathbf{R} = \{R_1, \ldots, R_n\}$ through the Rosenblatt (1952) transformation $\mathbf{R} = T\mathbf{X}$ given by

$$
\begin{aligned}
r_1 &= P(X_1 \leq x_1) = F_1(x_1) \\
r_2 &= P(X_2 \leq x_2 | X_1 = x_1) = F_2(x_2 | x_1) \\
&\ \ . \\
&\ \ . \\
&\ \ . \\
r_n &= P(X_n \leq x_n | X_1 = x_1, \ldots, X_{n-1} = x_{n-1}) = F_n(x_n | x_1, \ldots, x_{n-1})
\end{aligned}
\tag{B.1}
$$

where $F_i()$ is shorthand for the conditional cumulative distribution function $F_{X_i | X_{i-1}, \ldots, X_1}()$.

If the joint probability density function $f_{\mathbf{X}}()$ is known, then $F_i()$ can be determined as follows. From Section A.6.2, the conditional probability density function $f_i()$ is given by

$$
f_i(x_i | x_1, \ldots, x_{n-1}) = \frac{f_{\mathbf{X}_i}(x_1, \ldots, x_i)}{f_{\mathbf{X}_{i-1}}(x_1, \ldots, x_{i-1})}
\tag{B.2}
$$

where $f_{\mathbf{X}_j}(x_1, \ldots, x_j)$ is a marginal probability density function, obtained from

$$
f_{\mathbf{X}_j}(x_1, \ldots, x_j) = \int_{-\infty}^{\infty} \ldots \int_{-\infty}^{\infty} f_{\mathbf{X}}(x_1, \ldots, x_n) dx_{j+1}, \ldots, dx_n
\tag{B.3}
$$

$F_i()$ is then obtained by integrating $f_i()$ given by (B.2) over x_i:

$$
F_i(x_i | x_1, \ldots, x_{n-1}) = \frac{\int_{-\infty}^{\infty} f_{\mathbf{X}_i}(x_1, \ldots, x_{i-1}, t) \, dt}{f_{\mathbf{X}_{i-1}}(x_1, \ldots, x_{i-1})}
\tag{B.4}
$$

With all the conditional cumulative distribution functions $F_i(\ )$ determined in this way, (B.1) may be inverted successively to obtain

$$x_1 = F_1^{-1}(r_1)$$
$$x_2 = F_2^{-1}(r_2|x_1)$$
$$\cdot$$
$$x_n = F_n^{-1}(r_n|x_1, \ldots, x_{n-1}) \tag{B.5}$$

It follows immediately that (B.5) can be used to generate the random vector $\mathbf{X}$ with probability density function $f_{\mathbf{X}}(\ )$ from $\mathbf{R}$. A practical difficulty is that, unless $F_i(\ )$ is simple in form, the inversion will need to be done numerically.

As noted by Rosenblatt (1952), there are $n!$ possible ways in which expressions (B.1) can be written, depending on the numbering adopted for the variables in $\mathbf{X}$. Equally, of course, there are $n!$ possible ways of conditioning the X_i in expression (B.1), as seen for the simple case $n = 2$ [Rubinstein, 1981]:

$$F_{X_1 X_2}(x_1, x_2) = F_{X_1}(x_1) f_{X_2|X_1}(x_2|x_1) = F_{X_2}(x_2) f_{X_1|X_2}(x_1|x_2)$$

It is probably obvious that this freedom can lead to considerable differences in the difficulty of solving for $\mathbf{X}$, i.e. in solving (B.5).

Unfortunately, the above method is not always useful for practical problems since $F_{\mathbf{X}}(\ )$, or the conditional probability density functions $f_i(\ )$ which characterize the dependence structure of the problem, are not always known. More commonly only some estimate of correlation may be available from the data. This case is discussed in Section B.2 below. A special case arises when the X_i are independent. All the conditional requirements in (B.5) then disappear and each transformation takes the form $x_i = F_i^{-1}(r_i)$ independent of all other $x_j(j \neq i)$.

The Rosenblatt transformation may be used to transform from one distribution to another by applying (B.1) twice, using $\mathbf{R}$ as a transmitter, e.g.

$$F_1(u_1) = r_1 = F_1(x_1)$$
$$F_2(u_2|u_1) = r_2 = F_2(x_2|x_1) \tag{B.6}$$
$$\text{etc.}$$

A particular case of interest is where $\mathbf{U}$ in (B.6) is standard Normal distributed, with $\mathbf{X}$, say, a vector of correlated random variables and $\mathbf{U}$ uncorrelated (independent). Then (B.6) may be written as

$$x_1 = F_1^{-1}[\Phi(u_1)]$$
$$x_2 = F_2^{-1}[\Phi(u_2)|x_1] \tag{B.7}$$
$$\text{etc.}$$

In practice, solution of (B.7) requires multiple integration [cf. (B.4)]. This technique is used in Section 4.4.3.1 to convert non-Normal distributed random variables to equivalent Normal random variables. Where both $\mathbf{U}$ and $\mathbf{X}$ are Normal vectors, an easier approach to finding the transformation implied by (B.7) is to make direct use of the special properties of the Normal distribution. This is considered in Section B.3.

This transformation usually is attributed to Rosenblatt (1952) but appears to have been given earlier by Segal (1938). It was first suggested for use in structural reliability by Hohenbichler and Rackwitz (1981).

B.2 Nataf Transformation

A dependent random vector $\mathbf{X} = (X_1, \ldots, X_n)$, for which the marginal cumulative distribution functions $F_{X_i}(\ ), i = 1, \ldots, n$ and the correlation matrix $\mathbf{P} = \{\rho_{ij}\}$ are known, may have assigned to it an approximate but completely specified joint probability distribution function $F_{\mathbf{X}}(\mathbf{x})$. It also may be transformed to the standardized Normal random variables $\mathbf{Y} = (Y_1, \ldots, Y_n)$ in $\mathbf{y}$ space, given by

$$Y_i = \Phi^{-1}[F_{X_i}(X_i)], \qquad i = 1, \ldots, n \tag{B.8}$$

where $\Phi(\ )$ is the standard Normal cumulative distribution function. Let $\mathbf{Y} = (Y_1, \ldots, Y_n)$ be n-dimensional standard Normal with joint probability density function $\phi_n(\mathbf{y}, \mathbf{P}')$ having zero means, unit standard deviations and correlation matrix $\mathbf{P}' = \{\rho'_{ij}\}$. Then, with the usual rules for transformation of random variables, the approximate joint density function $f_{\mathbf{X}}(\ )$ in $\mathbf{x}$ space is (Nataf, 1962):

$$f_{\mathbf{X}}(\mathbf{x}) = \phi_n(\mathbf{y}, \mathbf{P}') \cdot |\mathbf{J}| \tag{B.9a}$$

with

$$|\mathbf{J}| = \frac{\partial(y_1, \ldots, y_n)}{\partial(x_1, \ldots, x_n)} = \frac{f_{X_1}(x_1).f_{X_2}(x_2)\ldots f_{X_n}(x_n)}{\phi(y_1)\phi(y_2)\ldots\phi(y_n)} \tag{B.9b}$$

To solve for $\mathbf{P}' = \{\rho'_{ij}\}$ in (B.9) consider any two random variables (X_i, X_j) and the correlation between them as:

$$\rho_{ij} = \frac{\text{cov}[X_i X_j]}{\sigma_{X_i}\sigma_{X_i}} = E[Z_i Z_j] = \int_{-\infty}^{\infty}\int_{-\infty}^{\infty} z_i z_j \phi_2(y_i, y_j;\ \rho'_{ij})\, dy_i dy_j \tag{B.10}$$

with $Z_i = (X_i - \mu_{X_i})/\sigma_{X_i}$ and with y_i and y_j dummy variables. Here the correlation matrix $\mathbf{P}' = \{\rho'_{ij}\}$ can be obtained from the known $\mathbf{P} = \{\rho_{ij}\}$ iteratively from (B.10). This is readily programmed but is tedious to solve since the unknown is contained within the double integral. Empirical, approximating expressions for the ratio $R = \rho'_{ij}/\rho_{ij}$ are given in Tables B.1 to B.3 below for a selected set of distributions for random variables. A more complete set of approximating expressions is available in the literature (Liu and Der Kiureghian, 1986; Der Kiureghian and Liu, 1986).

Once the $\mathbf{P}' = \{\rho'_{ij}\}$ are obtained for any pair (X_i, X_j) expression (B.8) may be used to obtain the correlated standard Normal distribution in $\mathbf{y}$ space. For the two variables involved, an orthogonal transformation (see below) may be used to obtain independent standard Normal random variables for use in FOSM theory.

The Nataf transformation (B.9) relies on the following fundamental properties being valid for expression (B.10) [Liu and Der Kiureghian, 1986]:

(1) ρ_{ij} is an increasing function of ρ'_{ij};

(2) $\rho'_{ij} = 0$ for $\rho_{ij} = 0$ and vice versa;

(3) $R \geq 1$;

(4) If both marginal distributions are Normal, $R = 1$;

(5) If one of the marginal distributions is Normal, R is a constant;

(6) R is invariant to increasing linear transformations of X_i and X_j;

(7) R is independent of the parameters of the marginal distributions of Type 1 (those whose two-parameter distributions can be reduced to a parameter-free form by a linear transformation);

(8) R is a function of the coefficient of variation $V = \sigma / \mu$ for marginal distributions of Type 2 (those that cannot be reduced to a parameter-free form by a linear transformation).

Typical examples of the Type 1 and Type 2 distributions with cross-reference to their descriptions in Appendix A are given in Table B.1.

The approximate expressions for $R = \rho'_{ij} / \rho_{ij}$ are based on a polynomial of the form

$$R = a + bV_i + cV_i^2 + d\rho + e\rho^2 + f\rho V_i + gV_j + hV_j^2 + k\rho V_j + lV_iV_j$$

with the coefficients given in Tables B.2 and B.3. The maximum error in the approximations, given in Table B.2, generally is much below 1%. The exception is when the Exponential distribution is involved, in which case the maximum error can be up to about 2% or more when there is high negative correlation. This tends to be due to the shape of the Exponential distribution being considerably different from the Normal distribution used as the basis for the method. The maximum errors for the approximations in the formulae given in Table B.3 are shown in the last column of the table.

Table B.1 Selected two-parameters distributions.

Type & name	Reference (Appendix A)	Symbol	Standardized form
Type 1			
Normal	A 5.7	N	$\Phi(y)$
Uniform		U	$y, 0 \leq y \leq 1$
Shifted exponential	A 5.5	SE	$1 - \exp(-y), 0 \leq y \leq \infty$
Shifted Rayleigh	A 5.13	SR	$1 - \exp\left(-\frac{1}{2}y^2\right), 0 \leq y \leq \infty$
Extreme value I largest (Gumbel)	A 5.11	G	$\exp[-\exp(-y)]$
Extreme value I smallest	A 5.11	EVIS	$1 - \exp[-\exp(y)]$
Type 2			
Lognormal	A 5.9	LN	
Gamma	A 5.6	GM	
Extreme value II largest	A 5.12	EVIIL	
Extreme value III smallest (Weibull)	A 5.13	W	

Table B.2 Coefficients in formula for $R = \rho'_{ij} / \rho_{ij}$ for selected distributions.

X_j	X_i	a	b	c	d	e	f
				Coefficients			
N	N	1					
	SE	1.107					
	SR	1.014					
	G	1.031					
	LN	*note 1*					
	GM	1.001	−0.007	0.118			
	W	1.031	−0.195	0.328			
SE	SE	1.229			−0.367	0.153	
	SR	1.123			−0.100	0.021	
	G	1.142			−0.154	0.031	
	LN	1.098	0.019	0.303	0.003	0.025	−0.437
	GM	1.104	−0.008	0.173	0.003	0.014	−0.296
	W	1.147	0.145	0.010	−0.271	0.459	−0.467
SR	SR	1.028			−0.029	0	
	G	1.046			−0.045	0.006	
	LN	1.011	0.014	0.231	0.001	0.004	−0.130
	GM	1.014	−0.007	0.126	0.001	0.002	−0.090
	W	1.047	−0.212	0.353	0.042	0	−0.136
G	G	1.064			−0.069	0.005	
	LN	1.029	0.014	0.233	0.001	0.004	−0.197
	GM	1.031	−0.007	0.131	0.001	0.003	−0.132
	W	1.064	−0.210	0.356	0.065	0.003	−0.211

note 1: $= V_j / [\ln(1 + V_j^2)]^{1/2}$

B.3 Orthogonal Transformation of Normal Random Variables

Let **X** be a correlated vector of basic variables, with mean

$$E(X) = [E(X_1), E(X_2), \dots, E(X_n)] \tag{B.11}$$

and covariance matrix (*cf*. A.123)

$$\mathbf{C}_X = \text{cov}(X_i, X_j)_{n \times m} = (\sigma_{ij})_{n \times m} \tag{B.12}$$

Table B.3 Coefficients on formula for $R = \rho'_{ij} / \rho_{ij}$ for selected Type 2 distributions.

X_j	X_i	a	b	c	d	e	f
				Coefficients			
LN	LN	*note 1*					
	GM	1.001	0.004	0.223	0.033	0.002	−0.104
	W	1.031	0.052	0.220	0.052	0.002	0.005
GM	GM	1.002	−0.012	0.125	0.022	0.001	−0.077
	W	1.032	−0.007	0.121	0.034	0	−0.006
W	W	1.063	−0.200	0.337	−0.004	−0.001	0.007

g	h	k	l	Maximum Error
	Coefficients			
−0.016	0.130	−0.119	0.029	4.0%
−0.210	0.350	−0.174	0.009	2.4%
−0.012	0.125	−0.077	0.014	4.0%
−0.202	0.339	−0.111	0.003	4.0%
−0.200	0.337	0.007	−0.007	2.6%

note 1: $= \ln(1 + \rho V_i V_j) / [\rho \sqrt{\ln(1 + V_i^2) \cdot \ln(1 + V_j^2)}]$

with $\mathrm{cov}(X_i, X_i) = \mathrm{var}(X_i)$. The covariance matrix will be strictly diagonal if the **X** are uncorrelated. Recall that 'correlation' is a measure of linear dependence (see Section A.7.3). This is a sufficient measure of dependence for Normal distributions.

An uncorrelated vector **U**, and a linear transformation matrix **A**, is now sought, such that

$$\mathbf{U} = \mathbf{AX} \quad \text{or} \quad \mathbf{A}^{-1}\mathbf{U} = \mathbf{X} \tag{B.13}$$

It is clearly desirable that the transformation (B.13) is also orthogonal, i.e. the vector represented by **X** is unchanged in length under the transformation **A**. From well-known matrix theory this implies that $\mathbf{A}^T = \mathbf{A}^{-1}$. Further, the vector **U** will be uncorrelated if there exists a covariance matrix $\mathbf{C}_U$ which is strictly diagonal.

Under the linear transformation (B.13) the covariance matrix (B.12) is also transformed. It becomes the covariance matrix $\mathbf{C}_U$ for **U**:

$$\begin{aligned}
\mathbf{C}_U &= \mathrm{cov}(U_i, U_j) = \mathrm{cov}(\mathbf{U}, \mathbf{U}^T) \\
&= \mathrm{cov}(\mathbf{AX}, \mathbf{AX}) = \mathrm{cov}(\mathbf{AX}, \mathbf{X}^T\mathbf{A}^T) \\
&= \mathbf{A} \; \mathrm{cov}(\mathbf{X}, \mathbf{X}^T)\mathbf{A}^T
\end{aligned} \tag{B.14}$$

or

$$\mathbf{C}_U = \mathbf{A}\mathbf{C}_X\mathbf{A}^T \tag{B.15}$$

@Seismicisolation

To obtain **U** as an uncorrelated vector, the matrix **A** which makes (B.15) diagonal is sought. Thus, it is required that the off-diagonal terms (i.e. $i \neq j$) in $\mathbf{C}_U$ be zero. This can be done by finding the characteristic values (eigen-values) of $\mathbf{C}_X$ using well-known methods. In particular, consider a matrix **D**, having only diagonal coefficients λ_{ii}, defined by

$$\mathbf{C}_X \mathbf{A} = \mathbf{AD} \quad \text{or} \quad \mathbf{C}_X = \mathbf{ADA}^T \tag{B.16}$$

(provided that **A** is non-singular). Equation (B.16) may be written as a system of linear equations

$$\sum_i c_{ij} \; a_{jk} = a_{ik} \; \lambda_{ii}, \qquad i,k = 1, 2, \ldots, n \tag{B.17}$$

Equation (B.17) represents a system of n linear equations with $j = 1, \ldots, n$ terms of unknown coefficients a_{ij} on the left-hand side; typically

$$\begin{aligned}
c_{11} \; a_{11} + c_{12} \; a_{21} + c_{13} \; a_{31} + \cdots &= a_{11} \; \lambda_{11} \\
c_{11} \; a_{12} + c_{12} \; a_{22} + c_{13} \; a_{32} + \cdots &= a_{12} \; \lambda_{22}
\end{aligned} \tag{B.18}$$

$$\text{etc.}$$

This system of equations is homogenous and may be written using the Kronecker delta $\delta_{ij} (= 1 \; \text{if} \; i = j, \; \text{otherwise} = 0)$:

$$\sum_i (c_{ij} - \lambda_{ii}\delta_{ij})a_{jk} = 0, \qquad i,k = 1, \ldots, n \tag{B.19}$$

A system such as equations (B.19) has a non-trivial solution only if, for any value of k,

$$|c_{ij} - \lambda_{ii}\delta_{ij}| = 0 \tag{B.20}$$

or, more generally,

$$|\mathbf{C}_X - \lambda \mathbf{I}| = 0 \tag{B.21}$$

where **I** is the identity matrix. Equation (B.20) is the well-known 'characteristic' equation. Its solution, the 'characteristic values' $\lambda_{ii} \quad i = 1, \ldots, n$, of matrix **D** are obtained by expanding (B.20) and solving the determinant

$$\begin{vmatrix}
c_{11} - \lambda_{11} & c_{12} & c_{13} \\
c_{21} & c_2 - \lambda_{22} & c_{23} \\
c_{31} & c_{32} & c_{33} - \lambda_{33} \\
\cdot & \cdot & \cdot \\
\cdot & \cdot & \cdot
\end{vmatrix}_{n \times n} = 0 \tag{B.22}$$

There are standard procedures available to obtain λ.

For each λ_{ii}, Equations (B.18) have a solution $(a_{i1}, a_{i2}, \ldots, a_{ik}, \ldots, a_{in})$. This is termed the 'characteristic vector' and yields the ith row of matrix **A**. It represents the components of one of the uncorrelated vectors U_i in terms of the correlated vectors X_i, (and vice

versa since **A** is symmetric). Thus solution for all characteristic values λ_{ii} and hence the characteristic vectors produces the complete matrix **A**.

With **A** known, the uncorrelated vector **U** is then defined by

$$\mathbf{U} = \mathbf{A}\mathbf{X} \tag{B.13}$$

with

$$E(\mathbf{U}) = \mathbf{A}E(\mathbf{X}) \tag{B.23}$$

and using (B.15) there is obtained

$$\mathbf{C}_U^{1/2} = (\mathbf{A}\mathbf{C}_X\mathbf{A}^T)^{1/2} \tag{B.24}$$

where $C_U^{1/2}$ is the matrix of standard deviations of **U**. This comes as about as follows. Since **U** in uncorrelated, $\mathbf{C}_U$ is strictly diagonal. For a diagonal matrix, such as **D**, say, it is well known that $\{D_{ij}\}^2 = \{D_{ij}^{\,2}\}$. Hence $C_U^{1/2}$ consists only of terms $C_U^{1/2} = \sigma_{u_i} = \lambda_{ii}^{1/2}$ along the leading diagonal, where the λ_{ii} are the characteristic values.

A special case arises if the vector **U** consists of only one term, **Z**, say. Then (B14) is given by

$$\mathbf{Z} = \mathbf{A}\mathbf{X} \tag{B.25}$$

where the matrix **A** has become just one row of coefficients (see Sections 4.2 and A.11.1). The covariance matrix for **Z** is then one term (the variance) given by

$$\mathbf{C}_Z = \text{var}(\mathbf{Z}) = \mathbf{A}\mathbf{C}_X\mathbf{A}^T \tag{B.26}$$

Mathematical aside. The standard deviations $\lambda_{ii}^{1/2}$ of $\mathbf{C}_U$ must all be positive (or zero), since they have no physical meaning otherwise. This means that the transformation (B.15) must have special properties; in particular it is said that $\mathbf{C}_X$ must be a positive (semi-) definite matrix. In matrix terminology, this means that the determinant of any minor,

$$\det M_i = \begin{vmatrix} c_{11} & \cdot & \cdot & c_{i1} \\ \vdots & & & \vdots \\ c_{1i} & \cdot & \cdot & c_{ii} \end{vmatrix} \tag{B.27}$$

is defined as positive definite if $\det M_i > 0$ or positive semi-definite if $\det M_i \geq 0$. A matrix is non-negative definite if it is either of these.

B.4   Generation of Dependent Random Vectors

In some situations it may be necessary to generate dependent variables. As will be seen, with the exception of Normal distributed variables, this may not be easy in practice.

If the random variables in vector **X** are independent of each other, the joint probability density function can be decomposed as (*cf*. A.117)

$$f_{\mathbf{X}}(x) = \prod_{i=1}^{n} f_{X_i}(x_i) \tag{B.28}$$

where $f_{X_i}(x_i)$ is the marginal probability density function of the random variable X_i. The generation of the vector **X** follows directly from the inverse transform method (see Section **3.4.3**) for each random variable X_i separately.

If there is dependence between the random variables constituting **X**, (B.28) is replaced by (cf. (A.116) and A.3)

$$f_{\mathbf{X}}(\mathbf{x}) = f_{X_1}(x_1) f_{X_2|X_1}(x_2|x_1) \cdots f_{X_n|X_1,\ldots,X_{n-1}}(x_n|x_1,\ldots,x_{n-1}) \tag{B.29}$$

where $f_{X_k|X_i,\ldots,X_n}$ is the conditional probability density function of X_k given that $X_1 = x_1, \ldots$, and where $f_{X_1}(x_1)$ is the marginal probability density function of X_1.

Provided that the joint probability density function $f_{\mathbf{X}}(\mathbf{x})$ is known in terms of the conditional probability density functions as in (B.29), the inverse transform method of Section 3.3.3 can be extended to generate a sample vector $\hat{\mathbf{x}}$, such that $\hat{\mathbf{x}}$ is drawn from a distribution with mean vector $\mu_{\mathbf{X}}$ and covariance matrix $\mathbf{C}_X$ as defined by the joint probability density function $f_{\mathbf{x}}(\ )$ for the multivariate normal distribution (see also Appendix C):

$$f_{\mathbf{X}}(\mathbf{x}, \mathbf{C}_X) = \frac{1}{(2\pi)^{n/2}|\mathbf{C}_X|^{1/2}} \exp\left[-\frac{1}{2}(\mathbf{x} - \mu_{\mathbf{X}})^T \mathbf{C}_X^{-1}(\mathbf{x} - \mu_{\mathbf{X}})\right] \tag{B.30}$$

The vector **X** of correlated Normal (Gaussian) distributed random variables with given covariance matrix $\mathbf{C}_X$ can be generated from a vector of independent standardised Normal random variables such as $\mathbf{Y} = \{Y_i\}$ using either the orthogonal transformation of Section B.3 or the Rosenblatt transformation of Section B.1.

To be specific, let the n correlated random variables be **X**, with known mean vector $\mu_{\mathbf{x}}$, and known covariance matrix $\mathbf{C}_X$. Further, let **U** be the vector of independent random variables with strictly diagonal covariance matrix $\mathbf{C}_U$. Then the sample (i.e. generated) dependent values of **X** can be obtained from the sampled independent **U** by the orthogonal transformation (*cf.* B.14):

$$\mathbf{X} = \mathbf{A}^T\mathbf{U} \tag{B.31}$$

where, since $\mathbf{C}_X$ is positive definite and symmetric, the orthogonal transformation matrix $\mathbf{A}^T = \mathbf{A}^{-1}$ can be defined through the transformation of the covariance matrix (*cf.* B.15):

$$\mathbf{C}_U = \mathbf{A}\mathbf{C}_X\mathbf{A}^T \quad \text{or} \quad \mathbf{C}_X = \mathbf{A}^T\mathbf{C}_U\mathbf{A} \tag{B.32}$$

If **B** is substituted for $\mathbf{A}^T = \mathbf{A}^{-1}$ then

$$\mathbf{C}_X = \mathbf{B}\,\mathbf{C}_U\mathbf{B}^T \tag{B.33}$$

The elements b_{ij} of the square matrix **B** are given by

$$c_{ij} = \sum_{k=1}^{n} b_{ik}\, u_{kk}\, b_{jk} \tag{B.34}$$

where c_{ij} is known from $\mathbf{C}_X$. Also, $\mathbf{U} = \mathbf{Y}$ is the vector of independent standardized Normal variables, $u_{kk} = 1$ for all k, $u_{jk} = 0$, $j \neq k$,

The transformation (B.31) then becomes, after allowing for the normalization of the mean of **X**,

$$\mathbf{X} - \mu_\mathbf{X} = \mathbf{BY} \quad \text{or} \quad \mathbf{X} = \mathbf{BY} + \mu_\mathbf{X} \tag{B.35}$$

from which the correlated variables **X** can be generated for samples of **Y**. Further (B.32) reduces to

$$\mathbf{C}_X = \mathbf{BB}^T = \mathbf{A}^T\mathbf{A} \tag{B.36}$$

where the matrix **B** is square lower triangular and obtained directly from **A** as indicated for (B.33).

Alternatively, a recursive formula may be derived to obtain the elements b_{ij} of **B** (*cf.* Rosenblatt, 1952). Noting that **B** is lower triangular, consider for instance the following example of (B.36):

$$\begin{bmatrix} \sigma_{11} & \sigma_{12} & \sigma_{13} \\ \sigma_{21} & \sigma_{22} & \sigma_{23} \\ \sigma_{31} & \sigma_{32} & \sigma_{33} \end{bmatrix} = \begin{bmatrix} b_{11} & 0 & 0 \\ b_{21} & b_{22} & 0 \\ b_{31} & b_{32} & b_{33} \end{bmatrix} \begin{bmatrix} b_{11} & b_{21} & b_{31} \\ 0 & b_{22} & b_{32} \\ 0 & 0 & b_{33} \end{bmatrix} \tag{B.37}$$

from which

$$\sigma_{11} = b_{11}^2 \tag{B.38a}$$
$$\sigma_{22} = b_{21}^2 + b_{22}^2 \tag{B.38b}$$
$$\sigma_{33} = b_{31}^2 + b_{32}^2 + b_{33}^2 \tag{B.38c}$$

or generalizing

$$\sigma_{ii} = \sum_{k=1}^{n} b_{ik}^2 \quad k \le i$$

and

$$\sigma_{21} = \sigma_{12} = b_{21}b_{11} \tag{B.38d}$$

$$\sigma_{31} = \sigma_{13} = b_{31}b_{11} \tag{B.38e}$$

$$\sigma_{32} = \sigma_{23} = b_{31}b_{21} + b_{32}b_{22} \tag{B.38f}$$

or generalizing

$$\sigma_{ij} = \sum_{k=1}^{n} b_{ik}b_{jk} \quad k \le j < i$$

The recursive result now follows directly from (B.38a):

$$b_{11} = \sigma_{11}^{1/2}$$

from (B.38d)

$$b_{21} = \frac{\sigma_{21}}{b_{11}} = \frac{\sigma_{21}}{\sigma_{11}^{1/2}}$$

from (B.38b)

$$b_{22}^2 = \sigma_{22} - b_{21}^2$$

i.e.

$$b_{22} = \left(\sigma_{22} - \frac{\sigma_{21}^2}{\sigma_{11}} \right)^{1/2}$$

from (B.38e)

$$b_{31} = \frac{\sigma_{31}}{b_{11}} = \frac{\sigma_{31}}{\sigma_{11}^{1/2}}$$

from (B.38f)

$$b_{32} = \frac{\sigma_{32} - b_{31}b_{21}}{b_{22}}$$

etc. From thus it can be readily verified that the recursive formula

$$b_{ij} = \frac{\sigma_{ij} - \displaystyle\sum_{k=1}^{j-1} b_{ik}b_{jk}}{\left(\sigma_{jj} - \displaystyle\sum_{k=1}^{j-1} b_{jk}^2 \right)^{1/2}} \tag{B.39}$$

is valid provided that $\displaystyle\sum_{k=1}^{0}$ is interpreted as zero [Rubinstein, 1981].

Example B.1   It is desired to generate correlated Normal variates X_1 and X_2 having means 10 and 12, respectively, and a non-negative definite covariance matrix

$$\mathbf{C}_X = \begin{bmatrix} 2 & 2\sqrt{2} \\ 2\sqrt{2} & 7 \end{bmatrix}$$

From equations (B.38)

$$b_{11} = \sigma_{11}^{1/2} = \sqrt{2}$$

and

$$b_{21} = \frac{\sigma_{21}}{b_{11}} = \frac{2\sqrt{2}}{\sqrt{2}} = 2$$

and

$$b_{22} = \left(\sigma_{22} - \frac{\sigma_{21}^2}{\sigma_{11}} \right)^{1/2} = \left(7 - \frac{8}{2} \right)^{1/2} = \sqrt{3}$$

Hence

$$\mathbf{B} = \begin{bmatrix} \sqrt{2} & 0 \\ 0 & \sqrt{3} \end{bmatrix}$$

and, from (B.35),

$$X_1 = \sqrt{2}\, Y_1 + 10$$
$$X_2 = 2Y_1 + \sqrt{3}\, Y_2 + 12$$

where Y_1 and Y_2 are independent standardized normal variables (generated through a random number generator).

C

Bivariate and Multivariate Normal Integrals

C.1 Bivariate Normal Integral

C.1.1 Format

The bivariate Normal integral may be considered to arise as a special case of Equation (1.31) when the random vector $\mathbf{X}$ consists of just two components, X_1 and X_2, each normally distributed, and dependent through the correlation coefficient ρ (*cf.* A.124). Let the probability of interest and hence the failure region (and limit state equations) be defined by the region $X_1 > x_1, X_2 > x_2$, so that (1.31) becomes

$$p_f = \int_{X_2 > x_2}^{\infty} \int_{X_2 > x_1}^{\infty} f_{\mathbf{X}}(\mathbf{x}, \rho) d\mathbf{x} \tag{C.1}$$

The joint probability density function for $\mathbf{X}$ is given by (A.125):

$$f_{\mathbf{X}}(\mathbf{x}, \rho) = \frac{1}{2\pi \sigma_{X_1} \sigma_{X_2} (1-\rho^2)^{1/2}} \exp\left[-\frac{\frac{1}{2}(h^2 + k^2 - 2\rho h k)}{1-\rho^2} \right] \tag{C.2}$$

for $-\infty \leq x_i \leq \infty, i = 1,2$ and with $h = (x_1 - \mu_{X_1})/\sigma_{X_1}$ and $k = (x_2 - \mu_{X_2})/\sigma_{X_2}$.

The joint cumulative distribution function $F_{\mathbf{X}}()$ is obtained directly by integrating (C.2) (*cf.* A.127):

$$F_{\mathbf{X}}(\mathbf{x}, \rho) \equiv P\left[\bigcap_{i=1}^{2} (X_i \leq x_i) \right] \equiv \int_{-\infty}^{x_2} \int_{-\infty}^{x_1} f_{\mathbf{X}}(u, v, \rho) \, du \, dv \tag{C.3}$$

As in the univariate case, it is convenient to work with standardized Normal variables, $y_i = (x_i - \mu_{X_i})/\sigma_{X_i}$, $(\mu_{Y_i} = 0, \sigma_{Y_i} = 1)$. With these substitutions in (C.2) and (C.3):

$$f_{\mathbf{X}}(\mathbf{x}, \rho) = \frac{1}{\sigma_{X_1} \sigma_{X_2}} \phi_2(\mathbf{y}, \rho) \quad \text{and} \quad F_{\mathbf{X}}(\mathbf{x}, \rho) = \Phi_2(\mathbf{y}, \rho) \tag{C.4}$$

where $\phi_2()$ and $\Phi_2()$, respectively, are the joint probability density function and the joint cumulative distribution function for the standardized variables $\mathbf{y} = (y_1, y_2)$. The coordinates (h, k) in the reduced, but correlated, $\mathbf{y}$ space are shown in Figure C.1; the
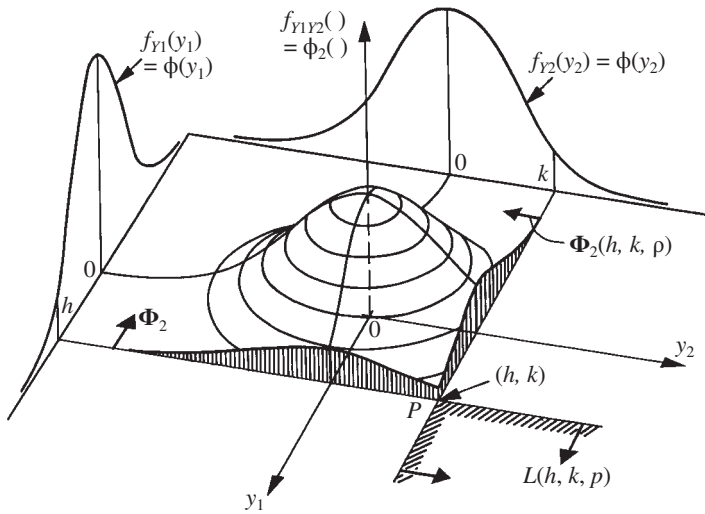
Figure C.1 Bivariate normal probability density function, marginal probability density functions and regions of integration $\Phi_2(\mathbf{y}, \rho)$ and $L(\ )$.
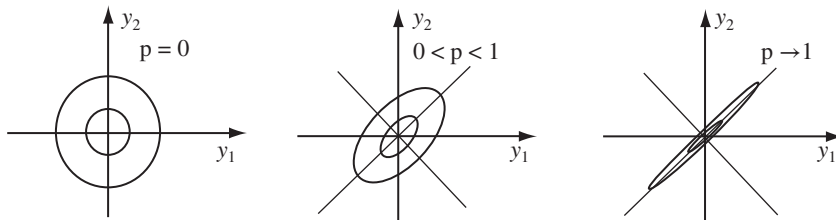
Figure C.2 Effect of correlation ρ between $\mathbf{y} = (y_1, y_2)$ on the form of the bivariate Normal probability density function $\Phi_2(\mathbf{y}, \rho)$.

probability content described by (C.3) is that to the upper left of the lines $y_1 = h$, $y_2 = k$, (i.e. the lines h, P, k). The actual shape of the distribution, and hence the probability content described by $\Phi_2(\mathbf{y}, \rho)$, depends on the correlation coefficient ρ, as indicated schematically in Figure C.2.

The region of interest for the calculation of p_f is that given by $y_1 < h, y_2 < k$ i.e. that lying to the lower right in Figure C.1. The probability content in that region is usually denoted by (A.132):

$$L(h, k, \rho) \equiv \frac{1}{2\pi}(1 - \rho^2)^{-1/2} \int_h^\infty \int_k^\infty \exp\left[-\frac{\frac{1}{2}(u^2 + v^2 - 2\rho uv)}{1 - \rho^2} \right] du\,dv \qquad (C.5)$$

It is not difficult to verify from Figure C.1 that $L(h, k, \rho) = \Phi_2(-h, -k, \rho)$ so that, if $L(\ )$ can be evaluated, so can $\Phi_2(\mathbf{y}, \rho)$ and vice versa. Tables for $L(\ )$ and other functions exist (see Section A.8). A particularly simple result is that $\Phi_2(y_1, +\infty, 0) = \Phi(y_1)$, the marginal distribution of y_1 as is easily verified (see also Figure C.1).

C.1.2 Reductions of Form

Although (C.5) can be integrated numerically, it also can be reduced to a single integral prior to numerical integration (Sheppard, 1900) (*cf.* A.140a with $\rho = \cos\theta$):

$$L(h, k, \rho) = \frac{1}{2\pi} \int_{\arccos\rho}^{\pi} \exp\left[-\frac{\frac{1}{2}(h^2 + k^2 - 2hk\cos\theta)}{\sin^2\theta}\right] d\theta, \qquad h, k \geq 0 \quad \text{(C.6)}$$

Expression (C.6) is obtained by substituting (C.2) into (C.3) and standardizing it to $\Phi_2(\ )$, and then successively:

(a) differentiating with respect to ρ
(b) integrating the result with respect to y_1 and y_2
(c) integrating that result with respect to ρ [Owen, 1956].

In addition, $\Phi_2(\ )$ can be reduced to a single integral, a result given by Owen (1956) (A.140b):

$$\Phi_2(h, k, \rho) = \frac{1}{2\pi} \int_0^\rho (1 - z^2)^{-\frac{1}{2}} \exp\left[-\frac{\frac{1}{2}(h^2 + k^2 - 2hkz)}{1 - z^2}\right] dz + \Phi(h)\Phi(k), \qquad h, k \geq 0$$

$$\text{(C.7)}$$

Other, equivalent, formulations exist [Johnson and Kotz, 1972], but (C.6) and (C.7) have particular simplicity, although they become less accurate as $\rho \to 1$.

C.1.3 Bounds

Rather than integrating (C.6) or (C.7) numerically, in some applications it may be sufficient to bound the probability content expressed by $\Phi_2(\ )$ or $L(\ )$. Consider first the relationship between the random variables Y_1 and Y_2 shown in Figure C.3(a) for a typical
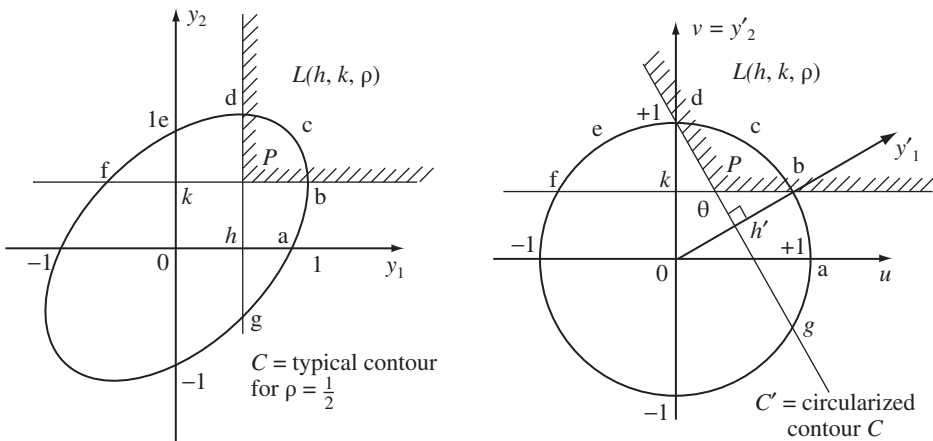
Figure C.3 (a) Integration region in original (correlated) standardized bivariate Normal space; (b) transformed integration region in transformed (independent) standardized bivariate Normal space.

probability density contour, say, $\rho = \frac{1}{2}$. It is more convenient to work in the circularized standard normal space (u, v), so that either of the transformations (A.142) or (A.143) must be applied. If the latter is used, the transformed contour C' (a circle) is obtained and the location of the y_1 axis is as shown in Figure C.3(b). Typical points (a)–(f) and the shaded zone $L(h, k, \rho)$ transform as shown. In the circularized normal space the axes y_1 and y_2 are at an angle $\theta < \pi/2$ to each other. The probability content $L(\ )$ enclosed by the lines $y_1 = h$ and $y_2 = k$ (lines dg, bf) in Figure C.3(a) is transformed to the shaded region shown in Figure C.3(b). It follows directly from (C.6) that the correlation coefficient and the angle shown in Figure C.3(b) are related by $\rho = \cos \theta$. Thus, if the random variables X_1 and X_2 are uncorrelated and independent, $\rho = 0$ (see Figure C.2) and $\theta = \pi/2$, which accords with Figure C.3.

Essentially the same information is seen in Figure C.4 with the (shaded) integration region shown as BPD. Let now CP be a perpendicular to PB and AP a perpendicular to DP. In the standardized normalized space (u, v) the probability in any right-angled region such as APD is given by the product of the probability contents $\Phi(-a)$ and $\Phi(-k)$ (see A.4). It then follows immediately that the probability content in the hatched region (i.e. in $L(h, k, \rho) = \Phi_2(-h, -k, \rho)$) is more than either that above BPC (i.e. the probability $\Phi(-b)\Phi(-h)$) or that to the upper right of APD (i.e. the probability $\Phi(-a)\Phi(-k)$) but less than that in these two components summed [Ditlevsen, 1979b]:

$$\max[\Phi(-b)\Phi(-h), \Phi(-a)\Phi(-k)] \leq \Phi_2(-h, -k, \rho) \leq \Phi(-b)\Phi(-h) + \Phi(-a)\Phi(-k)$$

$$(C.8)$$

It is not difficult to show that with $\rho = \cos \theta$:

$$a = \frac{h - \rho k}{(1 - \rho^2)^{1/2}} \qquad b = \frac{k - \rho h}{(1 - \rho^2)^{1/2}} \qquad (C.9)$$
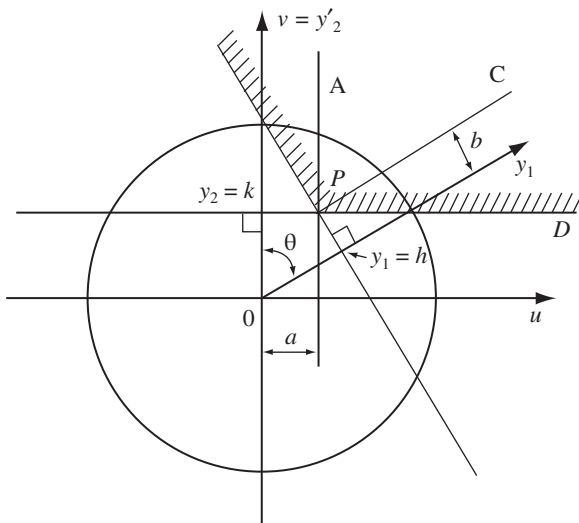
Figure C.4 Bounds BPC and APD for $\Phi_2(\ )$ over region BPD.

The above holds for $\rho \geq 0$, i.e. θ as shown. If $\rho < 0$, the y_1 axis is rotated clockwise and the bounds (C.9) become:

$$0 \leq \Phi_2(h, k, \rho) \leq \min[\Phi(b)\Phi(h), \Phi(a)\Phi(k)] \tag{C.10}$$

C.2 Multivariate Normal Integral

C.2.1 Format

Extending directly from the bivariate Normal distribution, it follows readily that the joint probability density function for the n-vector $\mathbf{X}$ is given by

$$f_{\mathbf{x}}(\mathbf{x}, \mathbf{C}_x) = (2\pi)^{-n/2} |\mathbf{C}_x|^{-\frac{1}{2}} \exp\left[-\frac{1}{2}(\mathbf{x} - \mu_{\mathbf{x}})^T \mathbf{C}_x^{-1}(\mathbf{x} - \mu_{\mathbf{x}})\right] \tag{C.11}$$

where $\mathbf{C}_X = (\sigma_{ij})$ is the covariance matrix of $\mathbf{X}$, with $\sigma_{ii} \equiv \sigma_{X_i}^2 = \text{var}(X_i)$, and for $i \neq j$, $\sigma_{ij} = \text{cov}(X_i, X_j)$ (cf. A. 124). Also $|\mathbf{C}_X|$ is the determinant of $\mathbf{C}_X$ and $\mathbf{C}_X^{-1}$ is its inverse. Further, $\mu_{\mathbf{X}}$ is the vector of mean values of $\mathbf{X}$. It is not difficult to verify that expression (C.11) reduces to (C.2) for $n = 2$.

For (C.11) the probability content defined by $X_i \leq x_i$, $i = 1, \ldots, n$ is given by the joint cumulative distribution function

$$F_{\mathbf{X}}(\mathbf{x}, \mathbf{C}_x) = P\left[\bigcap_{i=1}^{n}(X_i \leq x_i)\right] = \int_{-\infty}^{x_n} \cdots \int_{-\infty}^{x_1} f_{\mathbf{X}}(\mathbf{v}, \mathbf{C}_x)\,d\mathbf{v} \tag{C.12}$$

For use in actual applications, the equivalent standardized expressions are particularly useful since, if these can be evaluated, so can the original expressions. When the random variables are standardized (as usual according to $Y_i = (X_i - \mu_{x_i})/\sigma_{x_i}$), $\mathbf{C}_x$ becomes $\mathbf{R}$, the correlation matrix, and $F_{\mathbf{X}}(\mathbf{x}, \mathbf{C}_x) = \Phi_n(\mathbf{y}, \mathbf{R})$, where $\mathbf{Y}$ is the standardized Normal random variate vector, with zero mean, unit variance and correlation matrix $\mathbf{R}$.

C.2.2 Numerical Integration of Multi-Normal Integrals

Direct numerical integration of the multi-normal integral (C.12) is usually not practical if $n > 5$. Iterative reduction formulae are reviewed by Johnson and Kotz (1972) who describe them as somewhat laborious in practice when $\rho > 1/2$, even with the aid of computers. A procedure due to Milton (1972) uses the fact that the distribution of $X_1, X_2, \ldots, X_{r-1}$ conditional on X_r is itself multivariate Normal, so that computation from 2 to r dimensions can be applied iteratively. An improved procedure for bi- and trivariate integrals has been given by Daley (1974).

A number of numerical algorithms for the integration of the bivariate Normal integral have been proposed. The most common approach in practical use is still Owen's (1956), with a number of others being variants of it. A much simpler, but approximate algorithm is due to Grausland and Lind (1986). Both are best suited to wedge-shaped regions. The most accurate algorithm appears to be that suggested by Drezner (1978). It provides high accuracy for polygonal regions of integration but is slower in computation than other methods, such as direct integration algorithms that integrate over angular regions [Didonato, et al., 1980; Terza and Welland, 1991]. A further variant (Divgi, 1979)

was found to be only reasonably accurate but extremely efficient in computation time in an accuracy-speed trade-off. The only other comparison of some early algorithms is given in Johnson and Kotz (1972). Unfortunately, really useful comparisons between the various approaches do not appear to have been made.

C.2.3   Reduction to a Single Integral

When the correlation matrix $\mathbf{R} = \{\rho_{ij}\}$ has the special form $\rho_{ij} = b_i b_j (i \neq j)$ with $-1 \leq b_i \leq +1$, the n-dimensional integral (C.12) can be reduced to a single integral. Consider the transformation between the correlated standardized Normal n-vector $\mathbf{Y}$ and the $n + 1$ vector $(U_o, \mathbf{U})$ of independent standardized Normal random variables, given by

$$Y_i = b_i U_o + (1 - b_i^2)^{\frac{1}{2}} U_i, \qquad i = 1, \dots, n \tag{C.13}$$

It is a simple matter (using A.163) to show that the correlation between (Y_i, Y_j) is then given by $\rho_{ij} = b_i b_j (i \neq j)$ as desired.

The standardized multivariable joint cumulative distribution function can now be written as

$$\Phi_n(\mathbf{y}, \mathbf{R}) \equiv P\left[\bigcap_{i=1}^{n}(Y_i \leq y_i)\right] = P\left[\bigcap_{i=1}^{n}\left(U_i \leq \frac{y_i - b_i U_o}{(1 - b_i^2)}\right)\right] \tag{C.14}$$

which must hold for all U_0 values. Hence, integrating over U_0 (noting that U_0 is distributed as $\phi(u)$ and remembering that the $U_i, i = 1, \dots, n$ are statistically independent), it follows that [e.g. Dunnett and Sobel, 1955; Curnow and Dunnett, 1962]

$$\Phi_n(\mathbf{y}, \mathbf{R}) = \int_{-\infty}^{\infty} \left\{\prod_{i=1}^{n} \Phi\left[\frac{y_i - b_i u}{(1 - b_i^2)^{\frac{1}{2}}}\right]\right\} \Phi(u)du \tag{C.15}$$

Expression (C.15) represents the probability content contained in the hypercube $Y_i \leq y_i$. This is easily evaluated using one-dimensional numerical integration and is of particular interest for $y_i < 0$ since the 'tails' of the distribution are then evaluated. Evidently, numerical problems may arise if $\rho_{ij} \to 1$ as then $b_i \to 1$. Expression (C.15) can be applied also for negative correlations, although the integrand will then be complex [Johnson and Kotz, 1972].

C.2.4   Bounds on the Multivariate Normal Integral

For the standard Normal n-vector $\mathbf{Y}$ with correlation matrix $\mathbf{R}$, Slepian (1962) has shown that for the probability given by (C.14) the derivative with respect to the correlations ρ_{ij} in $\mathbf{R}$, is a non-decreasing function. This means that for another standard Normal n-vector, $\mathbf{V}$, say, with correlation matrix $\mathbf{K} = \{k_{ij}\}$ such that $k_{ij} \leq \rho_{ij}$ for all (i, j):

$$\Phi_n() = P_Y\left[\bigcap_{i=1}^{n}(Y_i \leq y_i)\right] \geq P_V\left[\bigcap_{i=1}^{n}(V_i \leq v_i)\right] \tag{C.16}$$

If $\mathbf{V}$ is selected to be identical with $\mathbf{Y}$, and $\mathbf{K} = \{k_{ij}\}$ selected such that $k_{ij} \leq \rho_{ij}$ for all (i, j), this inequality represents a lower bound on $\Phi_n(\;)$; by direct analogy an upper bound can be given [Gupta, 1963]. When these expressions are used in conjunction with (C.15), the bounds can be evaluated.

If the b_i values in (C.15) are chosen such that $b_i b_j < (>) \rho_{ij}$ then the lower and upper bounds respectively are obtained. Choosing $b_i^2 = \min_j(\rho_{ij})$, $b_i^2 = \max_j(\rho_{ij})$ results in wide bounds [Gupta, 1963]; an improvement is obtained by selecting, respectively, $b_i = \min_j(\rho_{ij} / b_j, 1)$ and $b_i = \max_j(\rho_{ij} / b_j, 1)$ for $i \neq j$ and $b_j \neq 0$ [Curnow and Dunnett, 1962]. Other choices of b_i are possible also; however, an appropriate selection is not straightforward. It follows that, in the case of negative correlation coefficients, replacing them with zero will produce a valid upper bound, without having to resort to complex integration (*cf.* Section C.1.2). In all cases care must be taken to ensure that the resulting correlation coefficient matrix is nonnegative definite (see Appendix B).

C.2.5 First-Order Multi-Normal (FOMN) Approach

C.2.5.1 Basic Method: B-FOMN

A special case of multi-Normal integration arises in structural reliability when there is one and only one limit state function for each basic variable in standard Normal (but not necessarily independent) space, i.e. $g(\mathbf{y}) = (y_i - \beta_i) = 0$. This means that each axis in basic variable space is intersected by only one limit state at $y_i = \beta_i$:

$$P\left(\bigcap_{i=1}^{n} Y_i \leq -\beta_i\right) = \Phi_n(-\boldsymbol{\beta}\,;\mathbf{R}) \tag{C.17}$$

where $\mathbf{Y}$ is the standard (correlated) Normal vector, $\mathbf{R}$ is the (positive definite) correlation matrix for $\mathbf{Y}$ and $\boldsymbol{\beta}$ is the vector of safety indices, with β_i the safety index in the y_i direction. Expression (C.17) was considered in (C.12) and (C.14) with the particular value Y_i rather than $-\beta_i$, but the latter will be retained here for convenience and to emphasize that the probability that Y_i is greater than β_i is sought (intersected for all directions).

Consideration will now be given as to how (C.17) can be approximated using only first-order second-moment (FOSM) concepts and the Rosenblatt transformation (see Appendix B). The result is of particular use in system reliability (see Chapter 5).

As usual, the original Normal random variables $\mathbf{X}$ may be reduced to $\mathbf{Y}$ using transformation (4.3). Then the correlated $\mathbf{Y}$ can be transformed to the uncorrelated standard Normal $\mathbf{U}$ by means of the inverse Rosenblatt transformation (see Appendix B):

$$\mathbf{Y} = \mathbf{B}\mathbf{U} \qquad \text{or} \qquad Y_i = \sum_{j=1}^{n} b_{ij} U_j \tag{C.18}$$

where the (lower triangular) elements b_{ij} are given by (B.33).

The dimension of (C.17) may be reduced by one, by first substituting (C.18) into (C.17) and then conditioning on $U_1 \le -\beta_1$ as follows [Hohenbichler and Rackwitz, 1983a]:

$$
\begin{aligned}
\Phi_n() &= P\left(\bigcap_{i=1}^{n} Y_i \le -\beta_i \right) \\
&= P\left(\bigcap_{i=1}^{n} \left(\sum_{j=1}^{n} b_{ij}U_j + \beta_i \right) \le 0 \right) \\
&= P\left[\bigcap_{i=2}^{n} \left(\sum_{j=1}^{i} b_{ij}U_j + \beta_i \le 0 \right) \middle| U_1 \le -\beta_1 \right] P(U_1 \le -\beta_1)
\end{aligned}
\tag{C.19}
$$

It is now desired to replace the first probability statement in (C.19) by one unconditioned on U_1;

$$
P\left[\bigcap_{i=2}^{n} \left(b_{i1}\tilde{U}_1 + \sum_{j=2}^{i} b_{ij}U_j + \beta_i \le 0 \right) \right]
\tag{C.20}
$$

where $\overline{U}_1$ is required to be constrained to $\overline{U}_1 \le -\beta_1$. Since all variables U_i are independent of each other, the conditioning on U_1 does not affect $U_2, U_3, \ldots$ etc.

The conditional distribution function of U_1 given that $\overline{U}_1 \le -\beta_1$ is

$$
\begin{aligned}
F_1(u) &= P(U_1 \le u \,|\, U_1 \le -\beta_1) \\
&= \frac{\Phi(u)}{\Phi(-\beta_1)} \quad \text{if} \quad U \le -\beta_1 \\
&= 1 \qquad\quad \text{if} \quad U > -\beta_1
\end{aligned}
$$

so that

$$
\tilde{U}_1 = \Phi^{-1}\left[\Phi(-\beta_1)F_1(\tilde{U}_1) \right] \qquad\qquad \tilde{U}_1 \le -\beta_1
\tag{C.21}
$$

In (C.21), almost any continuous distribution function, say $F_X(x)$, may be equated to $F_1(\tilde{U}_1)$, without really affecting the outcome of $\tilde{U}_1$. Let such a distribution be

$$
F_1(\tilde{U}_1) = F_X(x)
\tag{C.22}
$$

For first-order reliability (FOR) theory to be applicable, equation (C.20) must contain only Normal variables. Hence, replacing $F_1(\tilde{U}_1)$ by a Normal distribution function $\Phi(U_1)$ rather than by $F_X(x)$, it follows that (C.21) becomes

$$
\tilde{U}_1 = \Phi^{-1}[\Phi(-\beta_1)\Phi(U_1)]
\tag{C.23}
$$

Here the new standard Normal variable U_1 is not conditional, as is the original U_1 in (C.19). The reuse of the U_1 is permissible since all U_i are independent (Tang and Melchers, 1987a). Noting that $P(U_1 \le -\beta_1) = \Phi(-\beta_1)$, and using (C.20) and (C.23), expression

(C.19) can now be written as

$$\Phi_n(\ ) = P\left(\bigcap_{i=2}^{n}\left\{b_{i1}\Phi^{-1}[\Phi(-\beta_1)\Phi(U_1)] + \sum_{j=2}^{i}b_{ij}U_j + \beta_i \leq 0\right\}\right)\Phi(-\beta_1) \quad \text{(C.24)}$$

$$= P\left\{\bigcap_{i=2}^{n}[g_i(\mathbf{U}) \leq 0]\right\}\Phi(-\beta_1) \quad \text{(C.25)}$$

where $g_i(\mathbf{U}) \leq 0$ is the non-linear limit state term in { } in (C.24). According to (4.7) in Section 4.3.2, the approximating hyperplane, and hence the linearized limit state function, becomes

$$g_i(\mathbf{U}) \approx g_{Li}(\mathbf{U}) = \beta_i^{(2)} + \sum_{j=1}^{i}\alpha_{ij}U_j$$

It follows that expression (C.25) is linearized as

$$\Phi_n(\ ) \approx P\left\{\bigcap_{i=2}^{n}\left(\sum_{j=1}^{i}\alpha_{ij}U_j + \beta_i^{(2)} \leq 0\right)\right\}\Phi(-\beta_1) \quad \text{(C.26)}$$

where α_{ij} are the direction cosines $\mathbf{U}^*$ (a 'checking point') and $\beta_i^{(2)}$ is the shortest distance to the approximating plane

$$g_{Li}(\mathbf{U}) = \beta_i^{(2)} + \sum_{j=1}^{i}\alpha_{ij}U_j$$

The intersection of the $n-1$ approximating hyperplanes in $\mathbf{U}$ space can now be recast in the original correlated $\mathbf{Y}$ space:

$$\Phi_n(\ ) \approx P\left\{\bigcap_{i=2}^{n}Y_i^{(2)} \leq -\beta_i^{(2)}\right\}\Phi(-\beta_1) \quad \text{(C.27)}$$

$$\approx \Phi_{n-1}(-\beta^{(2)}; \mathbf{R}^{(2)})\Phi(-\beta_1) \quad \text{(C.28)}$$

where $\mathbf{R}^{(2)}$ now represents the matrix of correlation coefficients for the linear approximating hyperplanes and $\beta^{(2)}$ is the vector of $\beta_i^{(2)}$, $i = 2, \ldots, n$.

Repetition of the whole process in equation (4.43) eventually produces

$$\Phi_n(-\beta, \mathbf{R}) \approx \Phi(-\beta_1)\Phi(-\beta_2^{(2)}) \ldots \Phi(-\beta_n^{(n)}) \quad \text{(C.29)}$$

which has been found to produce excellent accuracy even for quite high n [Hohenbichler and Rackwitz, 1983a; Tang and Melchers, 1987a; Pandey, 1998], provided that the linearization of limit states $g_i(\mathbf{U})$ in (C.25) can be carried out efficiently. For comparison purposes below this will be termed the basic or B-FOMN approach.

C.2.5.2 Improved Method: I-FOMN

Fortunately, each limit state $g_i(\ )$ in (C.25) is only non-linear in U_1. If the linear space $(U_2, U_3,\ldots, U_i)$ is condensed into V space, an equivalent limit state function in two-dimensional (U_1, V) space may be written as

$$g_i(U_1, V) = b_{i1}\Phi^{-1}[\Phi(-\beta_1)\Phi(U_1)] + b_2 V + \beta_i = 0 \qquad (C.30)$$

where $b_2 = (1 - b_{i1}^2)^{1/2}$ and $V = \sum_{j=2}^{i} b_{ij}U_j / b_2$, $i = 2, 3,\ldots, n$. The b_{ij} are defined by (B.33).

This non-linear limit state function can be used directly to estimate $\beta_i^{(2)}$ and α_{ij}. To do this, the iteration routine of Section 4.3.6 can be used by approximating $g_i(U_l, V)$ with a hyperplane, as in changing (C.25) to (C.26), but with the hyperplane translated such that the enclosed probability content is equal to the more accurate estimate of $\beta_i^{(2)}$ [Hohenbichler and Rackwitz, 1983a]. This hyperplane can be obtained through first determining the direction cosines $\alpha_{E,i}$ (see Section 4.3.3). This is done by differentiating the functional expressing $\beta_E = -\Phi^{-1}[p_{fk}]$ (since $\beta_E = \beta_E(\mathbf{U})$, where $\mathbf{U}$ is the vector of (independent, standardized) Normal variables). Then, using (4.5): $c_{E,i} = \partial\beta_E / \partial U_i$, $\ell_{E,i}^2 = \sum_i c_{E,i}^2$ and $\alpha_{E,i} = c_{E,i} / \ell_{E,i}$. The main difficulty is to express β_E as a function of $\mathbf{U}$; generally a numerical solution procedure must be adopted [Gollwitzer and Rackwitz, 1983]. This improved approach might be termed the I-FOMN approach.

Example C.1 Consider the intersection $E_1 \cap E_2$ in standardized Normal space and the limit states L_1 and L_2 shown in Figure C.5(a). The dominant limit state is L_1; $\beta_1 < \beta_2$. The direction cosines for each are shown.

Using the approximate technique, the equivalent (hyperplane) limit state L_E is then defined by β_E and the direction cosines $\alpha_{E,i} = \alpha_{1,i}$ as shown. Also, the safety index for the equivalent limit state is given by $\beta_E = -\Phi^{-1}[P(E_1 \cap E_2)]$, which can be evaluated if $P(E_1 \cap E_2)$ can be evaluated.

(a)

(b)
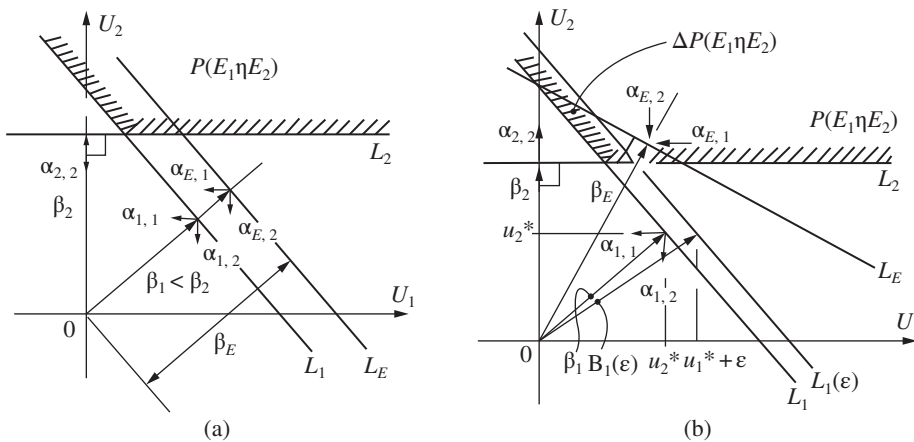
Figure C.5 (a) Approximate and (b) reoriented equivalent limit state functions.

The more accurate procedure finds a limit state L_E as shown in Figure C.5(b), with β_E as before, but with the orientation changed to that defined by the direction cosines $\alpha_{E,i}$. From (4.5) these are defined as $c_{E,i} / \ell$ where $c_{E,i} = \partial \beta_E / \partial u_i$. The change in β_E due to a small change ε in u_1 for β_1, say, can be visualized as in Figure C.1(b); the checking points u_i^* for both limit states are changed to $(u_1^* + \varepsilon, u_2^*)$. The concomitant change in each β_i $(i = 1, 2)$ is as shown; these changes also change the intersection probability by $\Delta P(E_1 \cap E_2)$. Clearly β_E changes also. It follows that

$$c_{E,i} = \frac{\partial \beta_E}{\partial u_1} = \lim_{\varepsilon \to 0} \left(\frac{\Delta \beta_E}{\varepsilon} \right)$$

$$= \lim_{\varepsilon \to 0} \left(\frac{(-)\Phi^{-1} P[\beta_1(\varepsilon), \beta_2(\varepsilon)] - (-)\Phi^{-1} P(\beta_1, \beta_2)}{\varepsilon} \right)$$

where $\beta_1^2(\varepsilon) = (u_1 + \varepsilon)^2 + u_2^2$ and $\beta_2(\varepsilon) = \beta_2$ in this case, since the change in u_1 does not affect β_2 for ε small.

C.2.5.3 Generalized Method: G-FOMN

An improved estimate of $\beta_i^{(2)}$ may be obtained by applying a reverse Rosenblatt transformation to each conditional probability content in (C.28) [Tang and Melchers, 1987a]. The conditional probability P_i for each term $\sum_{j=1}^{i} b_{ij} U_j + \beta_i \leq 0$ implicit in (C.28) is

$$P_i = P\left(\sum_{j=1}^{i} b_{ij} U_j + \beta_j \leq 0 \,|\, U_1 \leq -\beta_1 \right) \tag{C.31}$$

$$= P(Y_i + \beta_i \leq 0 \,|\, Y_1 \leq -\beta_1) \tag{C.32}$$

since $Y_1 = U_1$ and $Y_i = \sum_{j=1}^{i} b_{ij} U_j$ from (C.18) and b_{ij} is as defined in (B.33).

Using (A.3) this becomes

$$P_i = \frac{P[(Y_i \leq -\beta_i) \cap (Y_i \leq -\beta_1)]}{P(Y_1 \leq -\beta_1)} \tag{C.33}$$

$$= \frac{\Phi_2(-\beta_1, -\beta_i; \rho_{i1})}{\Phi(-\beta_1)}, \qquad i = 2, 3, \dots, n \tag{C.34}$$

$\Phi_2(\ )$ may be evaluated from (A.140b) or (C.7). Equation (C.34) then becomes

$$P_i = \Phi(-\beta_i) + \frac{1}{\Phi(-\beta_1) 2\pi} \int_0^{\rho_{i1}} \frac{1}{(1 - u^2)^{1/2}} \exp\left[\frac{-(\beta_1^2 + \beta_i^2 - 2\beta_1 \beta_i u)}{2(1 - u^2)} \right] du \tag{C.35}$$

and $\beta_i^{(2)} = -\Phi^{-1}(P_i)$ would be a better estimate for use in expressions (C.26) and (C.27) than the previous $\beta_i^{(2)}$. This more general approach has been termed the G-FOMN approach [Pandey, 1998].

Both the original method (I-FOMN) and its extension (G-FOMN) have been programmed using direct minimization of β rather than iteration [Tang and Melchers, 1987a].

@Seismicisolation

Example C.2 Consider a 20-dimensional multi-Normal integral with equi-correlation structure $r_{ij} = 0.9$ and equal intercepts $x_i = c$ along each axis, $i, j = 1, \ldots, 20$. For this problem it is possible to use the G-FOMN routine as well as numerical integration to compare the accuracy of the above approaches. The results of the G-FORM routine are almost identical to the results from numerical integration, while those for I-FOMN and B-FOMN are similar to these at zero fractile and about 70% and 30% of the multi-Normal probability estimated by numerical integration at normal fractile $c = -3$. Other results are described by Pandey (1998).

C.2.6   Product of Conditional Marginals (PCM) Approach

An alternative and sometimes simpler approach which appears to give results generally comparable in accuracy to G-FOMN is based on the notion that the m-dimensional multi-Normal integral can be represented as a product of m conditional probability terms.

The procedure can be illustrated for the trivariate Normal integral $\Phi_3(\mathbf{c}, \mathbf{R})$ where $x_i = c_i$ is the intercept of the i th plane on the x_i axis and $\mathbf{R} = \{r_{ij}\}$ is the correlation matrix, with $i, j = 1, 2, 3$. This integral can be represented in terms of conditional probability terms as:

$$\Phi_3(\mathbf{c}, \mathbf{R}) = P[(X_3 \leq c_3)\,|\,(X_2 \leq c_2) \cap (X_1 \leq c_1)]$$
$$\times P[(X_2 \leq c_2)\,|\,(X_1 \leq c_1)] \times \Phi_1(c_1) \tag{C.36}$$

The last term is readily evaluated. Evaluation of the second conditional term $P[(X_2 \leq c_2)\,|\,(X_1 \leq c_1)]$, requires evaluation of the marginal distribution of X_2 after truncation to $X_1 \leq c_1$. This marginal has a probability density function given by [Chou and Corotis, 1984] (*cf.* A.116):

$$f_{X_2|X_1 \leq c_1}(x_2) = \frac{1}{\Phi(c_1)} \int_{-\infty}^{c_1} \phi_{X_1 X_2}(x_1, x_2, r_{12})\, dx_1 \tag{C.37}$$

where $\phi_{X_1 X_2}(\ )$ is a bi-Normal density function. Clearly, the conditional marginal is not a Normal distribution. However, its mean $\mu_{2|1}$ and the standard deviation $\sigma_{2|1}$ can be expressed as [Birnbaum, 1950]:

$$\mu_{2|1} = -r_{12}A_1 \quad \text{with} \quad A_1 = \phi(c_1)/\Phi(c_1)$$
$$\sigma_{2|1} = (1 - r_{12}^2 B_1)^{1/2} \quad \text{with} \quad B_1 = A_1(c_1 + A_1)$$

These can be used to construct a Normal distribution with mean $\mu_{2|1}$ and standard deviation $\sigma_{2|1}$ to be used as a simple approximation for (C.37):

$$P[(X_2 \leq c_2)\,|\,(X_1 \leq c_1)] \approx \Phi\left(\frac{c_2 - \mu_{2|1}}{\sigma_{2|1}}\right) = \Phi(c_{2|1}), \text{ say} \tag{C.38}$$

where

$$c_{2|1} = \frac{c_2 - \mu_{2|1}}{\sigma_{2|1}} = \frac{c_2 + r_{12}A_1}{(1 - r_{12}^2 B_1)^{1/2}} \tag{C.39}$$

@Seismicisolation

Turning now to the evaluation of the first conditional term in (C.36), it is possible to employ expressions for the moments of truncated Normal distributions [Tallis, 1961]. However, it is also possible to express this term as [Terada and Takahashi, 1988]:

$$P[(X_3 \leq c_3) | (X_2 \leq c_2) \cap (X_1 \leq c_1)]$$
$$= P[\{(X_3 \leq c_3) | (X_1 \leq c_1)\} | \{(X_2 \leq c_2) | (X_1 \leq c_1)\}] \approx \Phi(c_{3|2}), \text{ say.}$$

This has a structure similar to (C.28) and therefore, by analogy to (C.39), the fractile $c_{3|2}$ of the conditional normal can be expressed as

$$c_{3|2} = \frac{c_{3|1} + r_{23|1}A_{2|1}}{(1 - r_{23|1}^2 B_{2|1})^{1/2}} \tag{C.40}$$

with $A_{2|1} = \phi(c_{2|1}) / \Phi(c_{2|1})$, $B_{2|1} = A_{2|1}(c_{2|1} + A_{2|1})$ and $r_{23|1} = r_{23|X_1 \leq c_1}$ given by the analytical expression [Johnson and Kotz, 1972]:

$$r_{23|1} = \frac{r_{23} - r_{12}r_{13}B_1}{(1 - r_{12}^2 B_1)^{1/2}(1 - r_{13}^2 B_1)^{1/2}} \tag{C.41}$$

Expression (C.41) allows $c_{3|2}$ to be computed from (C.40). Also $c_{2|1}$ can be obtained from (C.39) so that the trivariate Normal $\Phi_3(\mathbf{c}, \mathbf{R})$ can be computed, for $m = 3$, from the generalized expression obtained by induction:

$$\Phi_m(\mathbf{c}, \mathbf{R}) \approx \prod_{k=1}^{m} \Phi(c_{k|k-1}) \tag{C.42}$$

Expressions (C.40) and (C.41) can be extended readily by induction, with subscripts replaced as $3 \to m, 2 \to k, 1 \to (k-1)$ and $B_1 \to B_{(k-1)|(k-2)}$.

It is evident that the PCM method for approximating the multi-Normal integral is relatively simple, involving only estimation of conditional Normal fractiles $c_{p|q}$ through formulae such as (C.40), and then the product of one-dimensional Normal integrals in (C.42). A comparison of evaluations for a range of correlation coefficients, probability ranges and number of dimensions has demonstrated that this method usually is very close in approximation to the G-FOMN results and that both are generally good approximations to the 'exact' results obtained by numerical integration [Pandey, 1998].

D

Complementary Standard Normal Table

Table D.1 $N(0, 1)$ distribution defined as $\Phi(-\beta) = 1 - \Phi(\beta)$.

β	$\Phi(-\beta)$	β	$\Phi(-\beta)$	β	$\Phi(-\beta)$
0.	0.5	0.4	0.344578	0.8	0.211855
0.01	0.496011	0.41	0.340903	0.81	0.20897
0.02	0.492022	0.42	0.337243	0.82	0.206108
0.03	0.488034	0.43	0.333598	0.83	0.203269
0.04	0.484047	0.44	0.329969	0.84	0.200454
0.05	0.480061	0.45	0.326355	0.85	0.197663
0.06	0.476078	0.46	0.322758	0.86	0.194895
0.07	0.472097	0.47	0.319178	0.87	0.19215
0.08	0.468119	0.48	0.315614	0.88	0.18943
0.09	0.464144	0.49	0.312067	0.89	0.186733
0.1	0.460172	0.5	0.308538	0.9	0.18406
0.11	0.456205	0.51	0.305026	0.91	0.181411
0.12	0.452242	0.52	0.301532	0.92	0.178786
0.13	0.448283	0.53	0.298056	0.93	0.176186
0.14	0.44433	0.54	0.294599	0.94	0.173609
0.15	0.440382	0.55	0.29116	0.95	0.171056
0.16	0.436441	0.56	0.28774	0.96	0.168528
0.17	0.432505	0.57	0.284339	0.97	0.166023
0.18	0.428576	0.58	0.280957	0.98	0.163543
0.19	0.424655	0.59	0.277595	0.99	0.161087
0.2	0.42074	0.6	0.274253	1.	0.158655
0.21	0.416834	0.61	0.270931	1.01	0.156248
0.22	0.412936	0.62	0.267629	1.02	0.153864
0.23	0.409046	0.63	0.264347	1.03	0.151505
0.24	0.405165	0.64	0.261086	1.04	0.14917
0.25	0.401294	0.65	0.257846	1.05	0.146859
0.26	0.397432	0.66	0.254627	1.06	0.144572
0.27	0.39358	0.67	0.251429	1.07	0.14231
0.28	0.389739	0.68	0.248252	1.08	0.140071
0.29	0.385908	0.69	0.245097	1.09	0.137857
0.3	0.382089	0.7	0.241964	1.1	0.135666
0.31	0.37828	0.71	0.238852	1.11	0.1335
0.32	0.374484	0.72	0.235762	1.12	0.131357
0.33	0.3707	0.73	0.232695	1.13	0.129238
0.34	0.366928	0.74	0.22965	1.14	0.127143
0.35	0.363169	0.75	0.226627	1.15	0.125072
0.36	0.359424	0.76	0.223627	1.16	0.123024
0.37	0.355691	0.77	0.22065	1.17	0.121
0.38	0.351973	0.78	0.217695	1.18	0.119
0.39	0.348268	0.79	0.214764	1.19	0.117023

(Continued)

Table D.1 (Continued)

β	$\Phi(-\beta)$	β	$\Phi(-\beta)$	β	$\Phi(-\beta)$
1.2	1.1507×10^{-1}	1.8	3.59303×10^{-2}	2.4	8.19754×10^{-3}
1.21	1.13139×10^{-1}	1.81	3.51479×10^{-2}	2.41	7.97626×10^{-3}
1.22	1.11232×10^{-1}	1.82	3.43795×10^{-2}	2.42	7.76025×10^{-3}
1.23	1.09349×10^{-1}	1.83	3.3625×10^{-2}	2.43	7.54941×10^{-3}
1.24	1.07488×10^{-1}	1.84	3.28841×10^{-2}	2.44	7.34363×10^{-3}
1.25	1.0565×10^{-1}	1.85	3.21568×10^{-2}	2.45	7.14281×10^{-3}
1.26	1.03835×10^{-1}	1.86	3.14428×10^{-2}	2.46	6.94685×10^{-3}
1.27	1.02042×10^{-1}	1.87	3.07419×10^{-2}	2.47	6.75565×10^{-3}
1.28	1.00273×10^{-1}	1.88	3.0054×10^{-2}	2.48	6.56912×10^{-3}
1.29	9.85253×10^{-2}	1.89	2.9379×10^{-2}	2.49	6.38715×10^{-3}
1.3	9.68005×10^{-2}	1.9	2.87166×10^{-2}	2.5	6.20967×10^{-3}
1.31	9.50979×10^{-2}	1.91	2.80666×10^{-2}	2.51	6.03656×10^{-3}
1.32	9.34175×10^{-2}	1.92	2.74289×10^{-2}	2.52	5.86774×10^{-3}
1.33	9.17591×10^{-2}	1.93	2.68034×10^{-2}	2.53	5.70313×10^{-3}
1.34	9.01227×10^{-2}	1.94	2.61898×10^{-2}	2.54	5.54262×10^{-3}
1.35	8.8508×10^{-2}	1.95	2.55881×10^{-2}	2.55	5.38615×10^{-3}
1.36	8.6915×10^{-2}	1.96	2.49979×10^{-2}	2.56	5.23361×10^{-3}
1.37	8.53435×10^{-2}	1.97	2.44192×10^{-2}	2.57	5.08493×10^{-3}
1.38	8.37933×10^{-2}	1.98	2.38518×10^{-2}	2.58	4.94002×10^{-3}
1.39	8.22644×10^{-2}	1.99	2.32955×10^{-2}	2.59	4.7988×10^{-3}
1.4	8.07567×10^{-2}	2.	2.27501×10^{-2}	2.6	4.66119×10^{-3}
1.41	7.92698×10^{-2}	2.01	2.22156×10^{-2}	2.61	4.52711×10^{-3}
1.42	7.78038×10^{-2}	2.02	2.16917×10^{-2}	2.62	4.39649×10^{-3}
1.43	7.63585×10^{-2}	2.03	2.11783×10^{-2}	2.63	4.26924×10^{-3}
1.44	7.49337×10^{-2}	2.04	2.06752×10^{-2}	2.64	4.1453×10^{-3}
1.45	7.35293×10^{-2}	2.05	2.01822×10^{-2}	2.65	4.02459×10^{-3}
1.46	7.2145×10^{-2}	2.06	1.96993×10^{-2}	2.66	3.90703×10^{-3}
1.47	7.07809×10^{-2}	2.07	1.92262×10^{-2}	2.67	3.79256×10^{-3}
1.48	6.94366×10^{-2}	2.08	1.87628×10^{-2}	2.68	3.68111×10^{-3}
1.49	6.81121×10^{-2}	2.09	1.83089×10^{-2}	2.69	3.5726×10^{-3}
1.5	6.68072×10^{-2}	2.1	1.78644×10^{-2}	2.7	3.46697×10^{-3}
1.51	6.55217×10^{-2}	2.11	1.74292×10^{-2}	2.71	3.36416×10^{-3}
1.52	6.42555×10^{-2}	2.12	1.7003×10^{-2}	2.72	3.2641×10^{-3}
1.53	6.30084×10^{-2}	2.13	1.65858×10^{-2}	2.73	3.16672×10^{-3}
1.54	6.17802×10^{-2}	2.14	1.61774×10^{-2}	2.74	3.07196×10^{-3}
1.55	6.05708×10^{-2}	2.15	1.57776×10^{-2}	2.75	2.97976×10^{-3}
1.56	5.93799×10^{-2}	2.16	1.53863×10^{-2}	2.76	2.89007×10^{-3}
1.57	5.82076×10^{-2}	2.17	1.50034×10^{-2}	2.77	2.80281×10^{-3}
1.58	5.70534×10^{-2}	2.18	1.46287×10^{-2}	2.78	2.71794×10^{-3}
1.59	5.59174×10^{-2}	2.19	1.42621×10^{-2}	2.79	2.6354×10^{-3}
1.6	5.47993×10^{-2}	2.2	1.39034×10^{-2}	2.8	2.55513×10^{-3}
1.61	5.36989×10^{-2}	2.21	1.35526×10^{-2}	2.81	2.47707×10^{-3}
1.62	5.26161×10^{-2}	2.22	1.32094×10^{-2}	2.82	2.40118×10^{-3}
1.63	5.15507×10^{-2}	2.23	1.28737×10^{-2}	2.83	2.3274×10^{-3}
1.64	5.05026×10^{-2}	2.24	1.25455×10^{-2}	2.84	2.25568×10^{-3}
1.65	4.94715×10^{-2}	2.25	1.22245×10^{-2}	2.85	2.18596×10^{-3}
1.66	4.84572×10^{-2}	2.26	1.19106×10^{-2}	2.86	2.11821×10^{-3}
1.67	4.74597×10^{-2}	2.27	1.16038×10^{-2}	2.87	2.05236×10^{-3}
1.68	4.64787×10^{-2}	2.28	1.13038×10^{-2}	2.88	1.98838×10^{-3}
1.69	4.5514×10^{-2}	2.29	1.10107×10^{-2}	2.89	1.92621×10^{-3}
1.7	4.45655×10^{-2}	2.3	1.07241×10^{-2}	2.9	1.86581×10^{-3}
1.71	4.36329×10^{-2}	2.31	1.04441×10^{-2}	2.91	1.80714×10^{-3}
1.72	4.27162×10^{-2}	2.32	1.01704×10^{-2}	2.92	1.75016×10^{-3}
1.73	4.18151×10^{-2}	2.33	9.90308×10^{-3}	2.93	1.69481×10^{-3}
1.74	4.09295×10^{-2}	2.34	9.64187×10^{-3}	2.94	1.64106×10^{-3}
1.75	4.00592×10^{-2}	2.35	9.38671×10^{-3}	2.95	1.58887×10^{-3}
1.76	3.92039×10^{-2}	2.36	9.13747×10^{-3}	2.96	1.5382×10^{-3}
1.77	3.83636×10^{-2}	2.37	8.89404×10^{-3}	2.97	1.489×10^{-3}
1.78	3.7538×10^{-2}	2.38	8.65632×10^{-3}	2.98	1.44124×10^{-3}
1.79	3.6727×10^{-2}	2.39	8.42419×10^{-3}	2.99	1.39489×10^{-3}

(Continued)

Table D.1 (Continued)

β	$\Phi(-\beta)$	β	$\Phi(-\beta)$	β	$\Phi(-\beta)$
3.	1.3499×10^{-3}	3.6	1.59109×10^{-4}	5.	2.86652×10^{-7}
3.01	1.30624×10^{-3}	3.61	1.53099×10^{-4}	5.05	2.20905×10^{-7}
3.02	1.26387×10^{-3}	3.62	1.47302×10^{-4}	5.1	1.69827×10^{-7}
3.03	1.22277×10^{-3}	3.63	1.41711×10^{-4}	5.15	1.30243×10^{-7}
3.04	1.18289×10^{-3}	3.64	1.36319×10^{-4}	5.2	9.96443×10^{-8}
3.05	1.14421×10^{-3}	3.65	1.3112×10^{-4}	5.25	7.60496×10^{-8}
3.06	1.10668×10^{-3}	3.66	1.26108×10^{-4}	5.3	5.79013×10^{-8}
3.07	1.07029×10^{-3}	3.67	1.21275×10^{-4}	5.35	4.39771×10^{-8}
3.08	1.035×10^{-3}	3.68	1.16617×10^{-4}	5.4	3.33204×10^{-8}
3.09	1.00078×10^{-3}	3.69	1.12127×10^{-4}	5.45	2.51849×10^{-8}
3.1	9.67603×10^{-4}	3.7	1.078×10^{-4}	5.5	1.89896×10^{-8}
3.11	9.35437×10^{-4}	3.71	1.0363×10^{-4}	5.55	1.42835×10^{-8}
3.12	9.04255×10^{-4}	3.72	9.96114×10^{-5}	5.6	1.07176×10^{-8}
3.13	8.74032×10^{-4}	3.73	9.57399×10^{-5}	5.65	8.02239×10^{-9}
3.14	8.44739×10^{-4}	3.74	9.20101×10^{-5}	5.7	5.99037×10^{-9}
3.15	8.16352×10^{-4}	3.75	8.84173×10^{-5}	5.75	4.46217×10^{-9}
3.16	7.88846×10^{-4}	3.76	8.49567×10^{-5}	5.8	3.31575×10^{-9}
3.17	7.62195×10^{-4}	3.77	8.16238×10^{-5}	5.85	2.45787×10^{-9}
3.18	7.36375×10^{-4}	3.78	7.84142×10^{-5}	5.9	1.81751×10^{-9}
3.19	7.11364×10^{-4}	3.79	7.53236×10^{-5}	5.95	1.34071×10^{-9}
3.2	6.87138×10^{-4}	3.8	7.2348×10^{-5}	6.	9.86588×10^{-10}
3.21	6.63675×10^{-4}	3.81	6.94834×10^{-5}	6.05	7.24229×10^{-10}
3.22	6.40953×10^{-4}	3.82	6.67258×10^{-5}	6.1	5.30342×10^{-10}
3.23	6.18951×10^{-4}	3.83	6.40716×10^{-5}	6.15	3.87415×10^{-10}
3.24	5.97648×10^{-4}	3.84	6.15172×10^{-5}	6.2	2.82316×10^{-10}
3.25	5.77025×10^{-4}	3.85	5.90589×10^{-5}	6.25	2.05226×10^{-10}
3.26	5.57061×10^{-4}	3.86	5.66935×10^{-5}	6.3	1.48823×10^{-10}
3.27	5.37737×10^{-4}	3.87	5.44177×10^{-5}	6.35	1.07657×10^{-10}
3.28	5.19035×10^{-4}	3.88	5.22282×10^{-5}	6.4	7.76885×10^{-11}
3.29	5.00937×10^{-4}	3.89	5.01221×10^{-5}	6.45	5.59251×10^{-11}
3.3	4.83424×10^{-4}	3.9	4.80963×10^{-5}	6.5	4.016×10^{-11}
3.31	4.6648×10^{-4}	3.91	4.61481×10^{-5}	6.55	2.87685×10^{-11}
3.32	4.50087×10^{-4}	3.92	4.42745×10^{-5}	6.6	2.05579×10^{-11}
3.33	4.3423×10^{-4}	3.93	4.24729×10^{-5}	6.65	1.46547×10^{-11}
3.34	4.18892×10^{-4}	3.94	4.07408×10^{-5}	6.7	1.0421×10^{-11}
3.35	4.04058×10^{-4}	3.95	3.90756×10^{-5}	6.75	7.39225×10^{-12}
3.36	3.89712×10^{-4}	3.96	3.74749×10^{-5}	6.8	5.23098×10^{-12}
3.37	3.75841×10^{-4}	3.97	3.59363×10^{-5}	6.85	3.69249×10^{-12}
3.38	3.62429×10^{-4}	3.98	3.44576×10^{-5}	6.9	2.60014×10^{-12}
3.39	3.49463×10^{-4}	3.99	3.30366×10^{-5}	6.95	1.82643×10^{-12}
3.4	3.36929×10^{-4}	4.	3.16712×10^{-5}	7.	1.27981×10^{-12}
3.41	3.24814×10^{-4}	4.05	2.56088×10^{-5}	7.05	8.94562×10^{-13}
3.42	3.13106×10^{-4}	4.1	2.06575×10^{-5}	7.1	6.23779×10^{-13}
3.43	3.01791×10^{-4}	4.15	1.66238×10^{-5}	7.15	4.33875×10^{-13}
3.44	2.90857×10^{-4}	4.2	1.33457×10^{-5}	7.2	3.01037×10^{-13}
3.45	2.80293×10^{-4}	4.25	1.06885×10^{-5}	7.25	2.08389×10^{-13}
3.46	2.70088×10^{-4}	4.3	8.53991×10^{-6}	7.3	1.43885×10^{-13}
3.47	2.60229×10^{-4}	4.35	6.80688×10^{-6}	7.35	9.90874×10^{-14}
3.48	2.50707×10^{-4}	4.4	5.41254×10^{-6}	7.4	6.81122×10^{-14}
3.49	2.4151×10^{-4}	4.45	4.29351×10^{-6}	7.45	4.66849×10^{-14}
3.5	2.32629×10^{-4}	4.5	3.39767×10^{-6}	7.5	3.19189×10^{-14}
3.51	2.24053×10^{-4}	4.55	2.6823×10^{-6}	7.55	2.17604×10^{-14}
3.52	2.15773×10^{-4}	4.6	2.11245×10^{-6}	7.6	1.48215×10^{-14}
3.53	2.0778×10^{-4}	4.65	1.65968×10^{-6}	7.65	1.00475×10^{-14}
3.54	2.00064×10^{-4}	4.7	1.30081×10^{-6}	7.7	6.82787×10^{-15}
3.55	1.92616×10^{-4}	4.75	1.01708×10^{-6}	7.75	4.60743×10^{-15}
3.56	1.85427×10^{-4}	4.8	7.93328×10^{-7}	7.8	3.10862×10^{-15}
3.57	1.78491×10^{-4}	4.85	6.17307×10^{-7}	7.85	2.05391×10^{-15}
3.58	1.71797×10^{-4}	4.9	4.79183×10^{-7}	7.9	1.38778×10^{-15}
3.59	1.65339×10^{-4}	4.95	3.71067×10^{-7}	7.95	9.4369×10^{-16}

D.1 Standard Normal Probability Density Function $\phi(x)$

The standard normal probability density function $\phi(x)$ may be obtained, for low values of x from tables in standard statistics texts. For high values of x such tables generally are not helpful. A simple procedure may be used to estimate $\phi(x)$ from Table D.1 using the approximation:

$$\phi(x) \approx \frac{\Phi(-x + \Delta x) - \Phi(-x - \Delta x)}{2\,\Delta x}$$

For example, to evaluate $\phi(3.65)$:

$$\Phi(-3.64) = 0.1363E - 3$$
$$\Phi(-3.66) = \underline{0.1261E - 3}$$
$$\text{difference} = 0.0102E - 3$$
$$\phi(3.65) \approx (0.0102E - 3)/(0.02) = 0.51E - 3$$

@Seismicisolation

E

Random Numbers

Table E.1 gives a short list of random numbers generated for use with examples in the text only. Random numbers for use in realistic applications can be generated on a computer, or published tables may be used [Rand Corporation, 1955].

Table E.1

0.9311	0.4537
0.7163	0.1827
0.4626	0.2765
0.7895	0.6939
0.8184	0.8189
0.3008	0.9415
0.3989	0.4967
0.0563	0.2097
0.1470	0.4575
0.2036	0.4950
0.6624	0.8463
0.2825	0.2812
0.9819	0.6504
0.1527	0.8517
0.0373	0.0716
0.2131	0.8970
0.4812	0.1217
0.7389	0.2333
0.7582	0.6336
0.8675	0.5620

F

Selected Problems

Problems for Chapter 1

Problem 1.1 (Introduction to Poisson processes): Bus companies A and B have public concession to explore commercial transport between two cities. Each company runs one bus per hour, with buses of A leaving every hour and five minutes, buses of B leaving every hour and thirty-five minutes. Tickets can be sold on board or bought in advance. After some months of operation, a PhD student noticed that buses of company A were consistently departing five minutes late, whereas company B was respecting its schedule. The arrival rate of walk-in passengers (i.e., those that do not buy tickets in advance, but take the first bus leaving) changes during the day, and is given by $v(t)$ passengers per minute. Considering only the walk-in passengers, calculate the advantage that company A is making over company B by having its buses depart five minutes late.

Answer: The arrival of walk-in passengers during the day can be assumed to follow a Poisson process. Assuming the arrival rate to be constant over one hour ($v(t) \approx v$), the expected number of passengers for each company should be 30 v. The advantage of company A can be evaluated as:

$$\frac{35v}{25v} = 1.4$$

which is independent of v; hence also independent of $v(t)$ and approximately valid throughout the day.

Problem 1.2 (Poisson process): A PhD student travelled to France for a year of study abroad. He rented an apartment in a suburb, far from any bakeries but close to a tram station. Every morning he went to the station and picked the first tram, travelling south or north to the bakeries located in the next station. After a few weeks, he realized he was travelling more frequently south than north! Actually, he computed going to the north only once, for every 4 times he went south. Are there more trams going south than north?

Answer: The hypothesis of more trams going south than north for a generic tram line is unrealistic. The frequencies observed by the student can be explained by an hypothetical scheduling of the trams: for one tram scheduled every 10 minutes, for instance, the north-bound leaving every 02, 12, 22, … minutes of the hour, and the south bound

leaving every 00, 10, 20, … minutes of the hour will produce the observed frequencies, if the student takes the tram at random times every morning. If the student uses an alarm clock, then the explanation depends on the actual alarm and tram scheduling times.

Problem 1.3. (Return Period): A tower is required for 20 years of service such that the probability of failure as a result of wind loading during that time does not exceed 0.2. Assume that there is only one extreme event per year.

(a) Determine the return period for design purposes.
(b) What is the probability of failure during the first 10 years?
(c) Assume the tower can sustain, with repairs, just one extreme wind event without failure.

What is the probability of survival in the first 10 years (i.e. caused by further wind events)?

Answer:

(a) To determine the return period T_R, the annual probability of failure p_f is required. This implies that the probability of no failure per year is $(1 - p_f)$. To consider the combination of wind events to give just one failure in 20 years, the Geometric distribution (A.5.2) is relevant. It gives the probability that the nth trial is a success (i.e. tower failure in the present problem) given that the first n - 1 trials were failures (i.e. no structural failure in the present problem). This assumes independence between trials (i.e. between annual maximum wind loads).

$$P(N \leq n) = F_N(n) = \sum_{i=1}^{n} (1 - p_f)^{i-1} p_f = 1 - (1 - p_f)^n$$

which, for $n = 20$ years and the limit of 0.2 for the lifetime failure probability, becomes

$$0.20 = 1 - (1 - p_f)^{20} \text{ or } (1 - p_f) = (0.8)^{1/20} \text{ or } p_f = 0.0111$$

This is the probability of failure per year. The return period T_R is $1/p_f = 90.1$ years.

(b) The probability of failure in the first 10 years also can be determined using the Geometric distribution, since it can occur in any year. Assuming again that the probability of survival in any year is given by $(1 - p_f)$, the Geometric distribution becomes:

$$P(n \leq 10) = 1 - (1 - p_f)^{10} = 1 - (0.9889)^{10} = 0.106.$$

(c) In this case the probability of survival is sought given that one nominal failure is allowed. This can be computed as the probability there is just one event in 10 years and which can be repaired and then another, the one that causes failure. This can use the Binomial distribution (A.5.1, Eq. A.17). The probability of just two events is:

$$P(n = 2) = \binom{N}{2} p_f^2 (1 - p_f)^{N-2} = \frac{10 \times 9}{2} (0.0111)^2 (0.9889)^8 = 0.00507$$

Thus the probability of survival is 0.9949.

Problem 1.4. (Simple reliability): A beam is estimated to have a mean moment capacity (resistance) $R_{\text{mean}} = \mu_R = 200$ kNm with a coefficient of variation (V_R) = 0.1. The applied load sets up a moment (stress resultant) with a mean of $\mu_S = 100$ kNm. Its coefficient of variation (V_S) is estimated to be 0.3.

(a) estimate the central safety factor and then estimate the probability of failure if the loading is Extreme Value type 1 and the resistance Lognormal distributed.
(b) estimate the probability of failure if the loading is Normal distributed and resistance deterministic at the mean value,
(c) estimate the probability of failure if both loading and capacity are Normal distributed,
(d) if the strength given above is the 5% fractile and the resistance the 95% fractile, both Normal distributed, determine the mean load and resistance,
(e) for (d) what is the characteristic safety factor?

Answers:
(a) The central safety factor (see Eq. 1.23) is simply $200/100 = 2.0$. To estimate the probability of failure for the given CoVs and this central safety factor, see Figure 1.14, top, curve 6. It shows the p_f is about 10^{-2}.
(b) This case can be solved by referring to Figure 1.13, interpreting the loading there as the stress resultant here. Also, take a vertical line like the one marked $Q_{0.95}$ as $R = 200$. Then the probability of failure is the probability that lies to the right of $R = 200$. This can be from:

$$p_f = P(S > R) = F_S(S > 200) = 1 - F_S(S < 200) = 1 - \Phi\left(\frac{200 - \mu_S}{\sigma_S}\right)$$

with $\mu_S = 100$ and $\sigma_S = \mu_S \times V_S = 100 \times 0.3$. Using standard Normal tables to evaluate $\Phi(\ )$ produces $p_f = 4.2 \times 10^{-4}$.
(c) This case can be solved by substituting in Eq. (1.22), using the above means and (calculated) standard deviations. Note that $\sigma_R = 200 \times 0.1 = 20$. Then:

$$p_f = P(R - S < 0) = \Phi\left[\frac{-(\mu_R - \mu_S)}{(\sigma_R^2 + \sigma_S^2)^{1/2}}\right] = \Phi\left[\frac{-(200 - 100)}{(20^2 + 30^2)^{1/2}}\right] = \Phi(-2.77)$$

where the term $\Phi(-2.77) = \Phi(-\beta)$ which is read from Appendix D to correspond to a probability of failure of about 2.8×10^{-3}.
(d) For strength, Figure 1.12 shows the required information. Now $R_k = 200$ and μ_R is sought. As in Section 1.4.4, $k_{0.05} = 1.645$ (from Normal probability tables) and thus $R_k = 200 = \mu_R(1 - k_{0.05}V_R) = \mu_R(1 - 1.645 \times 0.1)$ from which $\mu_R = 239.4$.
For the stress resultant using Figure 1.13 it follows that: $S_k = 100 = \mu_S(1 + k_S V_S) = \mu_S(1 + 1.645 \times 0.3)$ from which $\mu_S = 66.96$.
(e) For the characteristic safety factor, see Eq. 1.26. It is $239.4/66.96 = 3.57$.

Problem 1.5 (Poisson process plus reliability): The strength of a structure against base accelerations caused by earthquakes was found to follow a Gaussian distribution with mean $\mu_R = 10$ m/s^2 and variance $\sigma_R^2 = 4$ m/s^2. A simplified seismic analysis is done by dividing the spectrum of possible earthquake intensities in three levels, as indicated in

the table below. The relative frequency of earthquakes of each level is also indicated in the Table.

(a) What is the expected number of earthquakes in a period of 100 years?
(b) What is the probability that at least one high-intensity earthquake happens in 100 years?
(c) What is the failure probability of the structure for a period of one year?
(d) What is the failure probability of the structure for a period of 100 years?

Intensity (i)	Acceleration a_i, (m/s^2)	Relative frequency v_i (earthquakes per year)
Low	4	0.0608
Medium	6	0.0150
High	8	0.0037

Answers:

(a) The expected number of earthquakes in 100 years is $100 (0.0608 + 0.0150 + 0.0037) = 7.95$.

(b) The probability that exactly n high-intensity earthquakes happens in 100 years is given by the Poisson distribution, *c.f.* A.30:

$$P[N = n] = \frac{(vt)^n}{n!}e^{-vt} = \frac{(0.0037t)^n}{n!}e^{-0.0037t}$$

The probability that at least one high-intensity earthquake happens in 100 years is given by:

$$\sum_{n=1}^{\infty} P[N = n] = 0.25557 + 0.04728 + 0.00583 + 0.00054 \ldots \approx 0.30927$$

(c) The conditional probability of failure of the structure, given an earthquake of intensity i, is given by:

$$p[f|i] = \Phi(-\beta_i) = \Phi\left(-\frac{10 - a_i}{2}\right)$$

which is evaluated as $\Phi(-3) = 0.00135$, $\Phi(-2) = 0.02275$ and $\Phi(-1) = 0.15866$ for the low, medium and high-intensity earthquakes, respectively. The failure probability of the structure for a one-year period becomes:

$$p_{f1} = \sum_{i=1}^{3} p[f|i]v_i$$

$$= 0.0608\Phi(-3) + 0.0150\Phi(-2) + 0.0037\Phi(-1) = 0.00101$$

(d) The conditional probabilities of failure are as given in item (c). The probability that at least one earthquake of each magnitude occurs in 100 years is evaluated following

item (b). Hence, the failure probability for 100 years becomes:

$$p_{f100} = \sum_{i=1}^{3} p[f|i] \left(\sum_{n=1}^{\infty} \frac{(v_i t)^n}{n!} e^{-v_i t} \right)$$

$$= 0.99771\Phi(-3) + 0.77687\Phi(-2) + 0.30927\Phi(-1) = 0.06809$$

Problems for Chapter 3

Problem 3.1 (Failure probability by integration): In an engineering problem, the strength or capacity has an uniform distribution between 2 and 3 units, $R \sim U(2, 3)$. The load or demand S has a triangular distribution between 1.2 and 2.2, with mode at 1.2 units. Assuming independence between R and S, determine the probability of failure $p_f = P[R \leq S]$.

Answer: From Eq. (1.17), the failure probability is evaluated as:

$$p_f = \int_{-\infty}^{+\infty} \int_{-\infty}^{y} f_S(y) f_R(x) \, dx \, dy = \int_{-\infty}^{+\infty} f_S(y) F_R(y) \, dy$$

$$= \int_{2}^{2.2} \left(\frac{22}{5} - 2y \right) (y - 2) \, dy = 0.002$$

Problem 3.2 (Simple Monte Carlo): Use the information given in Example 3.3 and write a computer code (or similar) to perform the computations. Use a computer-supplied random number generator instead of the numbers in Appendix E and then convert these to standard Normal variates using Eq. (3.5). Then convert these to the Normal random variables for stress resultant and resistance, with means and standard deviations as stated in Example 3.3, using, for example, Eq. (3.15). Carry-out a Monte Carlo analysis to estimate the probability of failure, for say 50, 100, 200, 500, and 1000 sample runs and plot the convergence of the result, to give a plot similar to Figure 3.3.

Problem 3.3 (Importance sampling with Monte Carlo analysis): Referring to Examples 3.4 and 3.5, write a computer program to represent the algorithm summarized in Table 3.1 for Importance Sampling. This shows outcomes for only 4 samples. Perform the same algorithm for, say 50, 100, 200, 500, and 1000 sample runs and plot the convergence of the result, to give a plot similar to Figure 3.3. Compare the results obtained with the estimated probability of failure of 0.0478 obtained with just 10 samplings.

Problem 3.4 (Directional simulation): Repeat the problem defined by the data in Examples 3.4 ad 3.5 but now using the directional simulation algorithm defined in Section 3.5.1. Perform the same algorithm for, say 50, 100, 200, 500, and 1000 sample runs and plot the convergence of the result (similar to Figure 3.3). Compare the results obtained with the estimated probability of failure so obtained with the result obtained in Problem 3.2.

Problems for Chapter 4

Problem 4.1 (Hasofer-Lind index): Determine the Hasofer-Lind reliability index β for a structure with a limit state function: $G(\mathbf{x}) = 0 = -x_1 + x_2 + 22$ where the independent random variables X_1 and X_2 have mean and standard deviations (20, 2) and (10, 1) respectively.

Answer: For this linear limit state function with Normal random variables, the simplest theory can be used to determine β. It is to use Eq. (1.21). This gives

$$\beta = \mu_G/\sigma_G = (-20 + 10 + 22)/(2^2 + 1^2)^{1/2} = 12/\sqrt{5} = 5.37.$$

More generally, using the formalism of FOSM theory, the first step is to seek the equivalent standard normal random variables. These are obtained using Eq. 4.3 as $Y_1 = (X_1 - 20)/2$ and $Y_2 = (X_2 - 10)/1$.
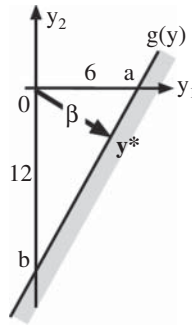
Next the limit state function is written in standard normal variables as:

$$g(\mathbf{y}) = -(y_1\sigma_{X1} + \mu_{X1}) + (y_2\sigma_{X2} + \mu_{X2}) + 22 = -2y_1 - 20 + y_2 + 10 + 22 = 0$$

i.e. $g(\mathbf{y}) = 0 = -2y_1 + y_2 + 12$

From Eq. (4.4) β is then the minimum distance from the origin to this limit state function in $\mathbf{y}$ space. In this simple case it can be obtained from geometry. The Figure at right shows the y axes and the limit state function, and also the distance β plus some notation. β is the shortest distance from the origin and this perpendicular to the limit state function at the point marked y^*, the checking point. From elementary geometry, by similar triangles, $\beta/0b = 0a/ab$ or $\beta/12 = 6/(12^2 + 6^2)^{1/2}$ from which $\beta = 5.37$.

As a third alternative, use the formalism in Section 4.4.2 to first determine the direction cosines for β as a vector and then use Eq. (4.6) to determine β. Consider Eq. (4.5a) for each vector, with λ as the arbitrary constant: $c_1 = \lambda\frac{\partial g}{\partial y_1} = -2$ and $c_2 = \lambda\frac{\partial g}{\partial y_2} = +1$ and

using Eq. (4.5b): $l = \left(\sum_i c_1^2\right)^{1/2} = ((-2)^2 + (+1)^2)^{1/2} = \sqrt{5}$

Then using Eq. (4.5c): $\alpha_i = -c_i/l$ produces the direction cosines $\alpha_1 = 2/\sqrt{5}$ and $\alpha_2 = -1/\sqrt{5}$. Applying Eq. (4.6) then gives the coordinates for $\mathbf{y}^*$ as: $\begin{Bmatrix} y_1^* \\ y_2^* \end{Bmatrix} = \beta \begin{Bmatrix} 2/\sqrt{5} \\ -1/\sqrt{5} \end{Bmatrix}$ and this must satisfy the limit state function $g(\mathbf{y}) = 0$ (see above). Substituting in produces:

$$g(\mathbf{y}) = 0 = -2y_1 + y_2 + 12 = -\left(\frac{2}{\sqrt{5}}\beta\right) + \left(\frac{-1}{\sqrt{5}}\beta\right) + 12 = \frac{-5}{\sqrt{5}}\beta + 12$$

from which $\beta = 5.37$ as before.

Problem 4.2 (linear limit state): A cantilever beam with rectangular cross-section (base $b = 30$ mm, height $h = 50$ mm) and length $L = 1$ m supports a concentrated load P of random intensity on its free end. The tip displacement is given by $y = -PL^3/(3EI)$, and the elasticity modulus is also random. Both random variables are Gaussian, with $P \sim N(\mu_P, \sigma_P) = N(1, 0.2)$ kN and $E \sim N(\mu_E, \sigma_E) = N(200, 10)$GPa. Evaluate the reliability index for an admissible tip displacement of $L/100$.

Answer: The problem formulation suggests a limit state function relating admissible with actual tip displacements:

$$g = \frac{L}{100} - \frac{PL^3}{3EI} = 0$$

As stated, this limit state is nonlinear in random variables P and E, which would require an iterative solution (*c.f.* Section 4.3.6). The iterative solution can be avoided by rewriting the limit state as:

$$g = 3EI - 100PL^2 = 0$$

Now the reliability index can be evaluated exactly as:

$$\beta = \frac{E[g]}{\sqrt{Var[g]}} = \frac{3I\mu_E - 100L^2\mu_P}{\sqrt{9I^2\sigma_E^2 + 100^2L^4\sigma_P^2}} = 3,96138$$

where $I = bh^3/12$ and $L = 10^3$ mm. An iterative solution using the non-linear limit state yields $\beta \approx 4.24$ in the first iteration.

Problem 4.3 (Non-linear limit state):

(a) Determine the Hasofer-Lind reliability index β for a structure with a limit state function: $G(\mathbf{x}) = 0 = \frac{1}{3}(20 - x_2)x_2 + \frac{1}{2}x_1 - 31\frac{1}{3}$ where the independent random variables X_1 and X_2 have mean and standard deviations (20, 2) and (10, 1) respectively. For the iterative solution assume a trial solution of $y_1^* = 0, y_2^* = +6$.

(b) If the mean point in the original $\mathbf{x}$ space is used as the first trial solution, that is if $y_1^* = 0, y_2^* = 0$ is used, does the iteration routine converge?

Answer:

(a) The standardized variables are as for Problem 4.1. Noting that, as before $x_i = \mu_{X_i} + y_i\sigma_{X_i}$ for $i = 1,2$, the limit state function in **y** space becomes:

$$g(\mathbf{y}) = 0 = \tfrac{1}{3}(20(\mu_{X_2} + y_2\sigma_{X_2}) - (\mu_{X_2} + y_2\sigma_{X_2})^2) + \tfrac{1}{2}(\mu_{X_1} + y_1\sigma_{X_1}) - 31\tfrac{1}{3}$$

and substituting for the values of the means and the standard deviations produces:

$$g(\mathbf{y}) = 0 = \tfrac{1}{3}y_2^2 + y_1 + 12$$

As before the direction cosines $\alpha_i = c_i/l$ can be obtained as:

$$c_1 = -\partial g/\partial y_1 = -1, \ c_2 = -\partial g/\partial y_2 = +\tfrac{2}{3}y_2 \ \text{and} \ l = \left((1)^2 + \left(-\tfrac{2}{3}y_2\right)^2\right)^{1/2}$$

Evidently, there are no explicit forms for the direction cosines until the checking point **y*** is located. The solution requires iteration using a trial solution or by minimization.

Trial solution 1: assume $y_1^* = 0, y_2^* = +6$. Then $\alpha_1 = -0.24, \alpha_2 = 0.97$ and, using Eq. (4.4) with the current **y** values the estimate for the reliability index is $\beta = 6$. With this value and the direction cosines Eq. (4.6) produces

$$\begin{Bmatrix} y_1^* \\ y_2^* \end{Bmatrix} = \beta \begin{Bmatrix} \alpha_1 \\ \alpha_2 \end{Bmatrix} = 6 \begin{Bmatrix} -0.24 \\ +0.97 \end{Bmatrix} = \begin{Bmatrix} -1.44 \\ +5.82 \end{Bmatrix}$$

which provides an updated set of **y** values. Two more cycles, in the same manner, produces $\beta = 5.84$ and

$$\begin{Bmatrix} y_1^* \\ y_2^* \end{Bmatrix} = \begin{Bmatrix} -1.51 \\ +5.64 \end{Bmatrix}$$

Geometrically the problem and solution in **y** space is as shown at right.
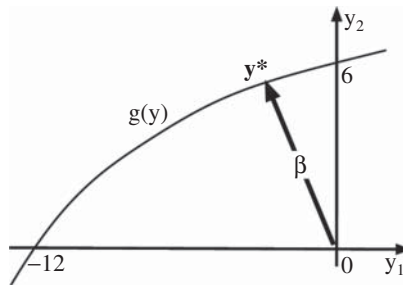
Problem 4.4: A uniform steel beam having yield strength f_y and a plastic modulus S is subject to an external bending moment M. Each is considered Normal (Gaussian) distributed with mean and standard deviation shown in the Table below. Estimate the reliability index β.

Variable		Distribution (mean, sd)	Unit
Steel yield stress f_y	X_1	$N(40, 5)$	kN/cm^2
Plastic cross-section modulus S	X_2	$N(50, 2.5)$	cm^3
Bending moment M	X_3	$N(1000, 200)$	kN cm

Answer: The (non-linear) limit state equation for this problem is:

$$g_X(\mathbf{X}) = Sf_y - M = X_1 X_2 - X_3 = 0 \tag{4.4.1}$$

with the second equality showing, for convenience, the random variables as collected in the vector $\mathbf{X} = \{X_1, X_2, X_3\}^T$. This limit state function is the same as that in Example 4.1 but in the following the problem is solved numerically, using the iterative scheme of Section 4.3.6. As noted (Section 4.4.5), there also are other ways of solving non-linear problems.

Start the solution by assembling the mean vector $\mathbf{M} = \{40, 50, 1000\}$ and the standard deviation matrix $\mathbf{D}$:

$$\mathbf{D} = \begin{bmatrix} 5 & 0 & 0 \\ 0 & 2.5 & 0 \\ 0 & 0 & 200 \end{bmatrix} \tag{4.4.2}$$

With this information it is possible to estimate the (Cornell) reliability index (*cf.* Section 1.4.3) as:

$$\beta = \frac{E[g(\mathbf{X})]}{\sqrt{Var[g(\mathbf{X})]}} = \frac{g(\mathbf{M})}{\sqrt{\nabla g^T \mathbf{D}^T \mathbf{D} \nabla g}} = \frac{40 \cdot 50 - 1000}{\sqrt{5^2 50^2 + 2.5^2 40^2 + 200^2}} \approx 2.9814 \tag{4.4.3}$$

Proceeding with the iterative solution scheme, in the original space $\mathbf{x}$ the gradient of the limit state function is:

$$\nabla g_X(\mathbf{X}) = \left\{ \frac{\partial g}{\partial X_i} \right\}_{i=1,2,3.} = \{X_2, X_1, -1\}^T \tag{4.4.4}$$

Next, the limit state function and other vectors need to be transformed to standard Gaussian space ($\mathbf{Y} = T(\mathbf{X})$), which is accomplished as:

$$\mathbf{X} = T^{-1}(\mathbf{Y}) = \mathbf{D}\,\mathbf{Y} + \mathbf{M} = \begin{bmatrix} 5 & 0 & 0 \\ 0 & 2.5 & 0 \\ 0 & 0 & 200 \end{bmatrix} \left\{ \begin{array}{c} Y_1 \\ Y_2 \\ Y_3 \end{array} \right\} + \left\{ \begin{array}{c} 40 \\ 50 \\ 1000 \end{array} \right\}$$

$$g(\mathbf{Y}) = g_X(T^{-1}(\mathbf{Y})) = (5Y_1 + 40)(2.5Y_2 + 50) - 200Y_3 - 1000$$
$$= 12.5 Y_1 Y_2 + 100 Y_2 + 250 Y_1 - 200 Y_3 + 1000$$

$$\nabla g(\mathbf{Y}) = \left\{ \frac{\partial g}{\partial Y_i} \right\}_{i=1,2,3.} = \{12.5 Y_2 + 250,\ 12.5 Y_1 + 100,\ -200\}^T \tag{4.4.5}$$

The first round of the interactive process, using the HLRF algorithm (Section 4.3.6, Eq. 4.24), with iteration counter $m = 0$, starts at the mean point:

$$\mathbf{x}^{(0)} = \mathbf{M} = \{40, 50, 1000\}^T; \ \mathbf{y}^{(0)} = \{0, 0, 0\}^T; \ \beta^{(0)} = 0;$$

$$g_X(\mathbf{x}^{(0)}) = g(\mathbf{y}^{(0)}) = 1000;$$

$$\nabla g(\mathbf{y}^{(0)}) = \{250, \ 100, -200\}^T;$$

$$\|\nabla g(\mathbf{y}^{(0)})\| = \sqrt{250^2 + 100^2 + 200^2} \approx 335.41 \tag{4.4.6}$$

From this information, the next candidate design point can be obtained by the next iteration ($m = 1$):

$$
\begin{aligned}
\mathbf{y}^{(1)} &= -\boldsymbol{\alpha}^{(0)} \left[\beta^{(0)} + \frac{g(\mathbf{y}^{(0)})}{\|\nabla g(\mathbf{y}^{(0)})\|} \right] \\
&= -\frac{1}{335.41} \{250, \ 100, -200\}^T \left[0 + \frac{1000}{335.41} \right] = \{0, 0, 0\}^T \\
&= \{-2.2222, \ -0.8889, \ +1.7778\}^T
\end{aligned}
\tag{4.4.7}
$$

The updated value of the reliability index is:

$$\beta^{(1)} = \|\mathbf{y}^{(1)}\| = 2.9814 \tag{4.4.8}$$

This is the same as the approximate solution obtained above (see Eq. 4.4.3). Repeating the iterations and re-evaluating Eqs. (4.4.6) to (4.4.8), gradual convergence of β is obtained as shown in the following Table.

m	y_1	y_2	y_3	β	$g(y)$	$\|\nabla g(y)\|$
0	0.0	0.0	0.0	0.0	1000.0	335.41
1	−2.2222	−0.8889	+1.7778	2.9814	24.691	319.82
2	−2.2779	−0.6887	+1.9071	3.0496	−0.1393	321.54
3	−2.2891	−0.6783	+1.8966	3.0491	−1.454 10^{-3}	321.60
4	−2.2898	−0.6768	+1.8962	3.0491	−1.385 10^{-5}	–

Adopting the stopping criteria $\beta^{(m+1)} - \beta^{(m)} \leq 10^{-4}$ and $g^{(m+1)} \leq 10^{-4}$ produces convergence to $\beta = 3.0491$ within five iterations. The reader can check this result by (admittedly lengthy) hand calculations. The reader can also verify that, for this particular problem, the same result is obtained for different starting points. This is because the limit state function can be considered 'well-behaved', or 'not excessively non-linear'.

Problem 4.5 (design of rectangular beam, linear limit states): A steel beam of rectangular cross-section (b, h) is subject to bending moment M and shear force V. These load effects, as well as normal (s_y) and shear (τ_y) yielding stresses are Gaussian random variables, whose parameters are given below. The maximum normal stress is $s = 6M/(bh^2)$, and the maximum shear stress is $\tau = 3V/(2bh)$.

(a) Using central safety coefficients $\gamma_s = \gamma_\tau = 2$, and considering $h = 2b$, determine the dimensions of the cross-section (b, h);

(b) Considering the cross-section found in (a), evaluate the reliability indexes for the normal and shear stress failure modes (β_s and β_τ);

(c) assuming a correlation of $\rho_{MV} = 0.5$, between load effect random variables, re-evaluate the individual reliability indexes.

$$M \sim N(\mu_M, \sigma_M) = N(40, 8).10^6 \text{ Nmm}, \quad S_y \sim N(\mu_S, \sigma_S) = N(10, 1.0) \text{ MPa},$$

$$V \sim N(\mu_V, \sigma_V) = N(150, 30).10^3 \text{ N}, \quad \tau_y \sim N(\mu_\tau, \sigma_\tau) = N(4, 0.4) \text{ MPa}.$$

Answers:

(a) The design problem is solved by requiring design strength to be equal to or larger than the design stress. Since a central safety factor is specified, design is based on mean values:

$$R_D \geq S_D$$
$$\mu_S bh^2 \geq 6\mu_M \gamma_s$$
$$2\mu_\tau bh \geq 3\mu_V \gamma_\tau$$

With $h = 2b$, the normal stress equation results $b^3 \geq 6\mu_M \gamma_s/(4\mu_S)$ or $b \geq 109.54$ mm, and the shear stress equation results in $b^2 \geq 3\mu_V \gamma_\tau/(4\mu_\tau)$ or $b \geq 237.17$ mm. Hence, the required cross-section is $(b, h) = (237.17, 474.34)$ mm.

(b) The limit state functions for normal and shear stress failure are:

$$g_S = S_y bh^2 - 6M$$
$$g_\tau = 2\tau_y bh - 3V$$

Note the similarity between these limit state equations and the design equations in item (a). The limit state equations above are linear in Gaussian random variables; hence the exact reliability indexes are obtained as:

$$\beta_S = \frac{E[g_S]}{\sqrt{Var[g_S]}} = \frac{bh^2\mu_S - 6\mu_M}{\sqrt{b^2h^4\sigma_S^2 + 36\sigma_M^2}} = 4.09$$

$$\beta_\tau = \frac{E[g_\tau]}{\sqrt{Var[g_\tau]}} = \frac{2bh\mu_\tau - 6\mu_V}{\sqrt{4b^2h^2\sigma_\tau^2 + 9\sigma_V^2}} = 3.54$$

(c) Solution to this item is better developed in matrix form. Vector $\mathbf{X}$ is assembled as: $\mathbf{X} = \{S_y, M, V, \tau_y\}$; such that the gradient vectors of the limit states become: $\nabla g_S = \{bh^2, -6,0,0\}$ and $\nabla g_\tau = \{0,0, -3,2bh\}$. The correlation between M and V is assembled in covariance matrix:

$$\text{cov} = \begin{vmatrix} \sigma_S^2 & 0 & 0 & 0 \\ 0 & \sigma_M^2 & 0.5\sigma_M\sigma_V & 0 \\ 0 & 0.5\sigma_M\sigma_V & \sigma_V^2 & 0 \\ 0 & 0 & 0 & \sigma_\tau^2 \end{vmatrix}$$

The reliability indexes become (*c.f.* A.179):

$$\beta_S = \frac{E[g_S]}{\sqrt{Var[g_S]}} = \frac{bh^2\mu_S - 6\mu_M}{\sqrt{\nabla_{g_S}^T \cdot \text{cov}.\nabla g_S}} = 4.09$$

$$\beta_\tau = \frac{E[g_\tau]}{\sqrt{Var[g_\tau]}} = \frac{2bh\mu_\tau - 6\mu_V}{\sqrt{\nabla_{g_\tau}^T \cdot \text{cov}.\nabla g_\tau}} = 3.54$$

Hence, correlation between M and V does not impact individual reliability indexes. It does impact, however, the correlation between limit states, and the system reliability, as can be verified by the reader.

Problems for Chapter 5

Problem 5.1 (Series system): For the rectangular beam solved in Problem 4.4, and considering the normal and shear stress failures as a series system, evaluate the system failure probability and system reliability index.

Answer:

(a) Since there are no common random variables, the limit state functions g_S and g_τ are independent. Hence the series system failure probability is (*c.f.* A.4):

$$p_{fsys} = \Phi(-\beta_S) + \Phi(-\beta_\tau) - \Phi(-\beta_S)\Phi(-\beta_\tau) = 2.24944 \ 10^{-4}$$

and the system reliability index is:

$$\beta_S = -\Phi^{-1}(p_{fsys}) = 3.51$$

Problem 5.2 (Series system): A statically determinate truss consisting of 3 independent members will fail if any one member fails. The probability of failure of each individual member has been estimated as:

member A: $p_{fA} = P(A) = 0.01$
member B: $p_{fB} = P(B) = 0.02$
member C: $p_{fC} = P(C) = 0.03$

Determine the probability of failure of the truss.

Answer: In general the probability of failure for a 3-member truss is the union of the three member failure events:

$$P(T) = P(A) \cup P(B) \cup P(C). \tag{5.2.1}$$

Expanding each term:

$$P(T) = P(A) + P(B) + P(C) - P(A \cap B) - P(B \cap C)$$
$$- P(C \cap A) + P(A \cap B \cap C) \tag{5.2.2}$$

But since the members are independent, the unions become multiplications, and substituting values:

$$P(T) = 0.01 + 0.02 + 0.03 - (0.01 \times 0.02) - (0.02 \times 0.03)$$
$$- (0.03 \times 0.01) + (0.01 \times 0.02 \times 0.03)$$
$$= 0.0589$$

An alternate solution is to work from the complementary probability of 'no-failure':

$$P(T) = 1 - P(\overline{A} \cap \overline{B} \cap \overline{C}) = 1 - P(\overline{A}).P(\overline{B}).P(\overline{C}) \tag{5.2.3}$$

where independence has been applied and $\overline{A}$ denoted the survival event for A and similarly for the others. Then, substituting $P(\overline{A}) = 1 - P(A)$ etc. produces

$$P(T) = 1 - (0.99)(0.98)(0.97) = 0.0589$$

Problem 5.3: For the same truss as in Problem 5.2, member C is now dependent on member B such that $P(C|B) = 0.6$ which is the probability of failure of C given that B has failed. Member A is independent of the other two. Determine an estimate of the probability of truss failure. Also what is the probability $P(B|C)$ and what meaning can be attached to this probability?

Answer: As before, the probability of truss failure is written as in Eq. (5.2.2). In the present case, the 5th term becomes $P(B \cap C) = P(C|B).P(B) = 0.6 \times 0.02 = 0.012$ while the last term in Eq. (5.2.2) becomes:

$$P(A \cap B \cap C) = P(A) \cap P(B \cap C) = 0.01 \times 0.012 = 0.00012.$$

The other terms in Eq. (5.2.2) are not changed, thus the failure probability is:

$$P(T) = 0.01 + 0.02 + 0.03 - (0.01 \times 0.02)$$
$$- 0.012 - (0.03 \times 0.01) + 0.00012 = 0.0476.$$

The alternate solution follows from the first part of (5.2.3), which may be written as:

$$P(T) = P(A \cup B \cup C) = 1 - P(\overline{A} \cap \overline{B \cup C}) \tag{5.3.1}$$

where, again, the over-bar denotes the non-failure event. The term $(\overline{B \cup C})$ in Eq. (5.3.1) can be written as $(\overline{B \cup C}) = 1 - P(B \cup C) = 1 - [P(B) + P(C) - P(C|B)P(B)] = 1 - (0.02 + 0.03 - 0.012)$ or $= 0.962$.

Substituting in Eq. (5.3.1), noting that event A is independent from the other two:

$$P(T) = 1 - P(\overline{A} \cap \overline{B \cup C}) = 1 - P(\overline{A}).P(\overline{B \cup C}) = 1 - (1 - 0.01).(0.962) = 0.0476.$$

The term $P(B|C)$ represents the probability that member B will fail given that C has failed. It is evaluated as follows. The term $P(B \cap C)$ can be written in two equivalent ways: $P(C|B).P(B)$ which is evaluated as before as $= 0.5 \times 0.03 = 0.015$. However, it also can be

written as $P(B|C).P(C)$. Equating the two and dividing gives $P(B|C) = P(B \cap C)/P(C) = 0.015/0.04 = 0.375$.

Problem 5.4: The probability that a reinforced concrete slab panel in a multi-storey building violates its deflection limit state is estimated at 0.1 for the building's anticipated 50-year life. This is the same for all panels. Because of continuity between slab panels it is estimated that there is a conditional probability of 0.7 that the deflection criterion for the adjacent slab also will be violated if the first one fails the deflection criterion. Determine the probability of violation of the slab deflection criterion for these cases:

(a) one or the other or both adjacent slab panels,
(b) one slab violates the criterion but not the other, and
(c) both slabs not meeting the criterion.

Answer: Despite the camouflage, this is a simple problem.

(a) Let A be slab one and B denote slab 2. Then the total probability of one or other or both, $P(F)$, is:

$$P(F) = P(A) + P(B) - P(A \cap B)$$

or

$$P(F) = P(A) + P(B) - P(A|B).P(B) = 0.1 + 0.1 - 0.7 \times 0.1 = 0.13$$

(b) This requires the occurrence of one or both of the following limit states: $A \cap \overline{B}$, $\overline{A} \cap B$. The probability is then:

$$P(F) = P(A \cap \overline{B}) + P(\overline{A} \cap B) = P(A).P(\overline{B}|A) + P(B).P(\overline{A}|B).$$

Since there is symmetry in A and B and thus in probability between the slabs this becomes

$$P(F) = 2[P(A)(1 - P(B|A))] = 2(0.1)(1 - 0.7) = 0.06$$

(c) This is given by $P(F) = P(A \cap B) = P(A|B).P(B) = (0.7)(0.1) = 0.07$.

Problem 5.5: A continuous beam consisting of two 4 m spans AB and BC is simply supported at A, B and C. Load Q_1 is applied at D (mid-span of AB) and load Q_2 at E (mid-span of BC). They loads both have the same mean and CoV (30, 0.3) and may be assumed Normal distributed. Ignore the potential that the actual load effect may be upward (although with very low probability). The mean plastic moment capacities are at D = 30, at B = 45 and at E = 25. All three may be assumed Normal distributed, with CoV = V = 0.1. Determine the upper and the lower bound on the probability of structural failure.

Answer: This is a structural system reliability problem. The first step is to define the modes of failure (which are plastic collapse modes) and the limit state equation for each mode.

The only collapse modes likely to occur are those shown below. In each case the angle θ at the plastic hinges can be cancelled out.
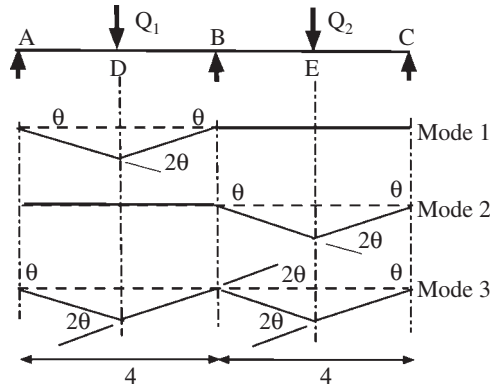
With vector **X** collecting all the random variables the limit state equations in the original space **x** are:

Mode 1: $G_1(\mathbf{X}) = 2M_D + M_B - 2Q_1 = 0$
Mode 2: $G_2(\mathbf{X}) = M_B + 2M_E - 2Q_2 = 0$
Mode 3: $G_3(\mathbf{X}) = 2M_D + 2M_B + 2M_E - 2Q_1 - 2Q_2 = 0$

These limit state equations are linear, so the most elementary approach to estimate β can be used:

$$\beta_1 = \frac{\mu_{G_1(\mathbf{X})}}{\sigma_{G_1(\mathbf{X})}} = \frac{2\mu_{M_D} + \mu_{M_E} - 2\mu_{Q_1}}{\left[2^2\sigma_{M_D}^2 + \sigma_{M_E}^2 + 2^2\sigma_{Q_1}^2\right]^{1/2}}$$

$$= \frac{2 \times 30 + 45 - 2 \times 30}{\left[2^2 \times 30^2 \times 0.1^2 + 45^2 \times 0.1^2 + 2^2 \times 30^2 \times 0.3^2\right]^{1/2}} = 2.31$$

$$\beta_2 = \frac{\mu_{G_2(\mathbf{X})}}{\sigma_{G_2(\mathbf{X})}} = \frac{\mu_{M_B} + 2\mu_{M_E} - 2\mu_{Q_2}}{\left[\sigma_{M_B}^2 + 2^2\sigma_{M_E}^2 + 2^2\sigma_{Q_2}^2\right]^{1/2}} = \frac{45 + 2 \times 25 - 2 \times 30}{\left[4.5^2 + 5^2 + 18^2\right]^{1/2}} = 1.82$$

$$\beta_3 = \frac{\mu_{G_3(\mathbf{X})}}{\sigma_{G_3(\mathbf{X})}} = \frac{2M_D + 2\mu_{M_B} + 2\mu_{M_E} - 2\mu_{Q_1} - 2\mu_{Q_2}}{\left[2^2\sigma_{M_B}^2 + 2^2\sigma_{M_B}^2 + 2^2\sigma_{M_E}^2 + 2^2\sigma_{Q_1}^2 + 2^2\sigma_{Q_2}^2\right]^{1/2}}$$

$$= \frac{2 \times 30 + 2 \times 45 + 2 \times 25 - 2 \times 30 - 2 \times 30}{\left[6^2 + 9^2 + 5^2 + 18^2 + 18^2\right]^{1/2}} = 2.846$$

Using Appendix D the respective equivalent failure probabilities are:

$$p_{f_1} = \Phi(-\beta) = \Phi(-2.31) = 0.01045, \ p_{f_2} = 0.0344, \ p_{f_3} = 0.00218.$$

The lower bound for the system probability of failure is obtained by assuming complete dependence between them and is given by (see Eq. 5.36) $p_{f_{system(lower)}} = \max_i \left(p_{f_i}\right) = 0.0344$

while the upper bund is obtained from assuming complete independence (see Eq. 5.35): $p_{f_{system(upper)}} = \sum_i \left(p_{f_i}\right) = 0.01045 + 0.0344 + 0.00218 = 0.0470$. The system probability bounds are thus: $0.0344 < p_{fS} < 0.0470$.

Problems for Chapter 6

Problem 6.1: A structure may fail in one or both of two independent failure mechanisms. From fitting to data, the two modes of failure have cumulative distribution functions given by: $F_{T_1}(t_1) = 1 - A\exp\left(-Bt_1\right)$ and $F_{T_2}(t_2) = 1 - \exp\left(-Ct_2^3\right)$ where A, B and C are constants and t_i denotes time (in years).

(a) What is the hazard function for each failure mechanism?
(b) Determine the hazard function for the whole structure.
(c) What is the probability of failure for a life of 20 years, given $B = 0.05$ and $C = 0.001$?

Answer:
(a) From Eq. (6.33), rewritten it follows that the hazard function h can be written as $h_T(t) = -\dfrac{d}{dt}\left[\ln(1 - F_T(t))\right]$ from which, after substitution and simplification:

$$h_{T1}(t_1) = -\frac{d}{dt}\left(\ln A - Bt_1\right) = +B \text{ and } h_{T2}(t_2) = -\frac{d}{dt}\left(-Ct_2^3\right) = +3Ct_2^2$$

(b) Because of independence the total hazard function is the sum of these two.
(c) Using Eq. (6.33) for the total hazard function, the cumulative probability is:

$$F_T(t = 20) = 1 - \exp\left[-\int_0^{t=20} h_T(\tau)d\tau\right]$$

$$= 1 - \exp\left[-\int_0^{20} + B + 3Ct_2^2\right] dt|_{t=20} = 0.99988$$

Problem 6.2: A structure is subject to pressure forces (in kPa) from dead, live and wind load effects as in the table below. Here 'apt' denotes the arbitrary-point-in-time value. The loads are denoted as components of the random vector **X**. Use Turkstra's rule to estimate the maximum value for the combination of these loads and the associated standard deviation.

Load	Dead (max)	Dead (apt)	Live (max)	Live (apt)	Wind (max)	Wind (apt)
Notation	X_1	$\overline{X}_1$	X_2	$\overline{X}_2$	X_3	$\overline{X}_3$
Distribution	Normal	Normal	Lognormal	Lognormal	Gumbel	Gumbel
Mean	0.9	0.8	6	2	1.6	1.2
SD	0.05	0.05	0.5	0.3	0.5	0.4

Answer: According to Eq. (6.156), the load combinations to be included for the maximum load are as follows, with values substituted:

$$\max X = \max \begin{pmatrix} X_1 + \overline{X}_2 + \overline{X}_3 \\ \overline{X}_1 + X_2 + \overline{X}_3 \\ \overline{X}_1 + \overline{X}_2 + X_3 \end{pmatrix} = \max \begin{Bmatrix} 0.9 + 2 + 1.6 \\ 0.8 + 6 + 1.6 \\ 0.8 + 2 + 1.2 \end{Bmatrix} = \max \begin{Bmatrix} 2.7 \\ 3.0 \\ 2.2 \end{Bmatrix} = 3.0 \text{ kPa}$$

Here the second load combination (involving the maximum live load) is critical. The uncertainty associated with this sum can be estimated using (A.162) for the sum of variances:

$$\sigma^2_{\max X} = \sum_{i=1}^{3} \sigma_i^2 = \sigma^2_{\overline{X}_1} + \sigma^2_{X_2} + \sigma^2_{\overline{X}_3} = (0.05)^2 + (0.5)^2 + (0.4)^2 = 0.41$$

or

$$\sigma_{\max X} = 0.64 \text{ kPa}.$$

Note that the probability distributions are not required for the solution by Turkstra's rule.

Problem 6.3: Two random load processes $Q_1(t)$ and $Q_2(t)$, both Normal (Gaussian) distributed with means and standard deviations given by (1.8, 0.4) kPa and (2.5, 0.5) kPa respectively can act on a structure. As functions of time the loads are Poisson pulse processes with arrival rates and mean durations of (2 per year, 1.5 days) and (5 per year, 1.1 days) respectively. (a) Estimate the probability that one or the other or a combination of both will exceed a total (barrier level) of 5.2 kPa in a 100-year design life. (b) What is the probability of just the combined loading ($Q_1(t) + Q_2(t)$) exceeding 6 kPa in a period of 50 years?

Answer:
(a) This problem can be solved by the 'load coincidence' approximation (Section 6.7.4). The first step is to determine the rate of occurrence of the two processes combined. From Eq. (6.146c):

$$\nu_{m1m2} = \nu_{m1}\nu_{m2}(\mu_1 + \mu_2) = (2)(5)(1.5 + 1.1)/365 = 0.055 \text{ per year.}$$

Since each load, $Q_1(t)$ and $Q_2(t)$, is Normal, the corresponding combined load $Q_1(t) + Q_2(t)$ also is Normal. It has a mean $(1.8 + 2.5) = 4.3$ and standard deviation $[0.4^2 + 0.5^2]^{1/2} = 0.64$. Using the standard Normal format, the probability of exceeding 5.2 kPa in any one year is then given by in Appendix D by $\Phi\left(\dfrac{4.3 - 5.2}{0.64}\right) = \Phi(-1.406) = 0.08$ per year. For each of the loads independently, the probabilities of exceeding 5.2 kPa are $\Phi\left(\dfrac{1.8 - 5.2}{0.64}\right) = \Phi(-5.3) = 5.77 \times 10^{-6}$ per year and $\Phi\left(\dfrac{2.5 - 5.2}{0.64}\right) = \Phi(-4.22) = 1.3 \times 10^{-3}$ per year. Both of these are very small compared with the combined load and are neglected.

The probability of exceeding the load level of 5.2 kPa in 100 years is calculated from Eq. (6.65): $p_{f_1}(t_L = 100) = 1 - \exp\left\{-[1 - F_Y(a)]vt_L\right\} = 1 - \exp\{-[0.08](0.055)(100)\} = 1 - 0.644 = 0.356$. This means there is a 36% chance in 100 years that the combined load will exceed 5.2 kPa.

(b) The probability of the combined load exceeding 6 kPa in any one year is given by $\Phi\left(\dfrac{4.3 - 6}{0.64}\right) = \Phi(-2.656) = 0.0039$ per year. Applying Eq. (5.65) for 50 years: $p_{f_1}(t_L = 50) = 1 - \exp\left\{-[1 - F_Y(a)]vt_L\right\} = 1 - \exp\{-[0.0039](0.055)(50)\} = 1 - 0.989 = 0.0107$ or a 1% chance of the combined load exceeding 6 kPa in a 50-year period.

Problems for Chapter 7

Problem 7.1 (Extreme values): From meteorological records for a given location, the annual maximum wind velocity was found to follow a Gumbel distribution with form parameter $\alpha = 0.6$ and location parameter $u = 11.64$ m/s. In order to build a high-rise building in this location, evaluate the 'nominal' wind speeds with mean return periods of 10 and 100 years.

Answer: The wind velocity with mean return period of n years, x_n, has a probability of $1/n$ of being exceeded in a single year. Hence:

$$P[X > x_n] = 1 - F_X(x_n) = \frac{1}{n} \text{ or } x_n = F_X^{-1}\left(1 - \frac{1}{n}\right)$$

Using Eq. (A.77), this becomes:

$$x_n = \frac{\log\left(-\log\left(1 - \frac{1}{n}\right)\right)}{-0.6} + 11.64$$

Solving the above for $n = 10$ and $n = 100$ yields: $x_{10} = 15.39$ and $x_{100} = 19.31$.

Problem 7.2 (Extreme values): An engineer wants to design a cistern to accumulate rain water. He gathers 100 readings of precipitation over 100 rainy days along one year, and finds out this data follows a Gaussian distribution with mean $\mu = 4$ mm and variance $\sigma^2 = 1$ mm.

(a) What is the distribution for the maximum precipitation in a single day, based on these yearly records?
(b) What is the probability that the maximum daily precipitation, in one year, is greater than 8 mm?
(c) Assuming the average of 100 rainy days per year is kept constant over the years, what is the probability that the maximum daily precipitation, in ten years, is greater than 8 mm?

Answers:
(a) The maximum precipitation in one year is the largest amongst 100 samples. Hence the cumulative distribution is:

$$F_{100}(x) = \left[\Phi\left(\frac{x - 4}{1}\right)\right]^{100}$$

(b) The probability that the maximum daily precipitation, in one year, is greater than 8 mm is:

$$p = 1 - F_{100}(8) = 1 - [\Phi(4)]^{100} = 0.00316$$

(c) The probability that the maximum daily precipitation, in ten years, is greater than 8 mm is:

$$p = 1 - F_{1000}(8) = 1 - [\Phi(4)]^{1000} = 0.03118$$

Problem 7.3 (Joint and marginal PDFs): A concentrated load P acting on a circular membrane of radius R can occupy any position over this membrane, with same probability (uniform distribution).

(a) Determine the joint probability density $f_{XY}(x, y)$ of the load position in terms of coordinates (x, y), for a coordinate system centered at the membrane centre $(x^2 + y^2 \leq R^2)$.

(b) From the joint density above, determine the marginal density $f_X(x)$. Is this marginal uniform?

Answers:

(a) The volume under the joint density function must be unitary, hence the height of the joint density is $h = 1/\pi R^2$. In order to express the joint density, we need to write y in terms of x: $y = \pm\sqrt{R^2 - x^2}$. The joint density becomes:

$$f_{XY}(x, y) = \begin{cases} 1/\pi R^2 & \text{if } (-R \leq x \leq +R, -\sqrt{R^2 - x^2} \leq y \leq +\sqrt{R^2 - x^2}) \\ 0 & \text{otherwise} \end{cases}$$

(b) The marginal density $f_X(x)$ is obtained by integrating $f_{XY}(x, y)$ over y (c.f. A.118):

$$f_X(x) = \int_{-\infty}^{+\infty} f_{XY}(x, y) dy = \begin{cases} \int_{-\sqrt{R^2 - x^2}}^{+\sqrt{R^2 - x^2}} \frac{1}{\pi R^2} dy = \frac{2\sqrt{R^2 - x^2}}{\pi R^2} \text{ if } (-R \leq x \leq +R) \\ 0 \text{ otherwise} \end{cases}$$

This marginal distribution depends on x, hence it is not uniform!

Problems for Chapter 10

Problem 10.1: In any one year, the probability of a truck exceeding the load limit on a particular wooden road bridge is estimated to be 0.10. If the truck is not overloaded by more than 10%, the probability of a cross member being subjected to the maximum wheel load is 0.05. The probability of the truck being overloaded by more than 10% is 0.3 and then the probability of the cross member being subjected to the maximum wheel load is 0.12.

Experiments on the cross members and experience have shown that the probability of failure under maximum wheel load is 8×10^{-4} and when not subjected to the maximum wheel load it is 4×10^{-5}.

Estimate the annual probability of failure of any one cross member if 1000 trucks use the bridge per year. Assume the probability of failure is negligible if the truck does not exceed the load limit.

Answer: To help untangle the information, let L denote the weight limit is exceeded, W denote the truck is overweight, M denote the maximum wheel load occurs on a cross beam and F denote the failure event. We can then write:

$$P(F) = P(F|L)P(L) + P(F|\overline{L})P(\overline{L})$$

in which the second term is negligible (see problem statement). It is ignored below. The conditional probabilities required are not known, but made up of component conditional events. Thus:

$$P(F) = P(F|L \cap W)P(L \cap W) + P(F|L \cap \overline{W})P(L \cap \overline{W})$$

$$P(F) = P(F|L \cap W \cap M)P(L \cap W \cap M) + P(F|L \cap W \cap \overline{M})P(L \cap W \cap \overline{M})$$

$$+ P(F|L \cap \overline{W} \cap M)P(L \cap \overline{W} \cap M) + P(F|L \cap \overline{W} \cap \overline{M})P(L \cap \overline{W} \cap \overline{M})$$

where the first term after the equality sign can be written as

$$= P(F|L \cap W \cap M)P(L \cap W \cap M) = P(F|L \cap W \cap M)(M|W \cap L)P(W|L)P(L)$$

and similarly for the other terms. Evidently this is very tedious. It is easier to use an event diagram as shown below. It shows all the conditional probabilities. Working through all the paths and adding the probabilities results in $P(F) = 0.00094$ per truck crossing. For 1000 crossings per year the annual estimated failure probability is 0.009 per year.

Total failure probability = 9.4×10^{-6}
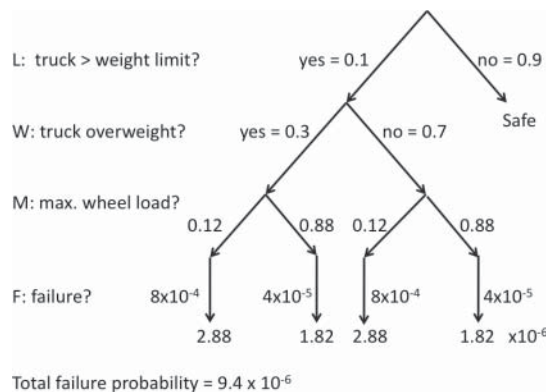
Problem 10.2. From tests on standard timber road bridges it has been estimated that 80% can safely support a 20-tonne truck loading, 10% can support a 15-tonne truck loading and the remaining 10% would fail under a loading less than a 15-tonne truck.

To assess the capacity of a similar bridge a proof load test was conducted with a 15-tonne truck. The bridge survived.

(a) Estimate the probability that this bridge will survive under 20-tonne truck loading,
(b) How does the answer to (a) change if the proof load test is only 90% reliable?
(c) Estimate the proof load T2 (90% reliable) to give a probability of 0.95 for survival under a 20-tonne load. To make this estimate, assume a linear relationship between 'the conditional probability that a proof load T2 will be supported given failure under a 20-tonne load' and 'the magnitude of the proof load T2'.

Answer:

(a) This problem requires the use of Bayes theorem.

Let S = bridge capacity > 20 tonne (i.e. survival) and $\bar{S}$ capacity < 20 tonne (the failure event).

Let T = bridge capacity > 15 tonne (i.e. test condition) and $\bar{T}$ capacity < 15 tonne.

$$\text{Bayes theorem: } P(S|T) = \frac{P(T|S)P(S)}{P(T|S)P(S) + P(T|\bar{S})P(\bar{S})} \tag{10.2.1}$$

Let it be assumed that the bridge will survive the test load if S is true. Thus $P(T|S) = 1$. Also $P(S) = 0.8$ from the data and thus $P(\bar{S})$. Further, the probability of survival under the 15-tonne proof load given the bridge would not support the maximum load of 20-tonne $= P(T|\bar{S}) = 0.1/(1 - 0.8) = 0.5$. Then:

$$P(S|T) = [1 \times 0.8]/[1 \times 0.8 + 0.5 \times 0.2] = 0.89.$$

(b) If the proof load test is 90% reliable, then $P(T|S) = 0.9$ and expression (10.2.1) becomes

$$P(S|T) = [0.9 \times 0.8]/[0.9 \times 0.8 + 0.5 \times 0.2] = 0.88. \tag{10.2.2}$$

(c) A probability of 0.95 is required for survival given the proof load T2 is successful: thus we need $P(S|T2) = 0.95$. This can be expressed again using Bayes theorem Eq. (10.2.1):

$$P(S|T2) = 0.95 = \frac{P(T2|S)P(S)}{P(T2|S)P(S) + P(T2|\bar{S})P(\bar{S})}$$

with $P(T|S) = 0.9$ and the result from (10.2.2.). All terms are known in Eq. (10.2.1) except $P(T|\bar{S})$. Thus:

$$P(S|T2) = 0.95 = [0.9 \times 0.88]/[0.9 \times 0.88 + P(T2|\bar{S}) \times 0.12]$$

from which $P(T2|\bar{S}) = 0.42$.

Index